



# International Journal of Environment Agriculture and Biotechnology

(IJEAB)

An open access Peer-Reviewed International Journal



DOI: 10.22161/ijeab.86

Vol.- 8 | Issue - 6 | Nov-Dec 2023

editor.ijeab@gmail.com | editor@ijeab.com | <https://www.ijeab.com/>

# International Journal of Environment, Agriculture and Biotechnology

(ISSN: 2456-1878)

DOI: 10.22161/ijeab

Vol-8, Issue-6

November - December, 2023

*Editor in Chief*

Dr. Pietro Paolo Falciglia

---

Copyright © 2023 International Journal of Environment, Agriculture and Biotechnology

Publisher

*Infogain Publication*

Email: [editor.ijeab@gmail.com](mailto:editor.ijeab@gmail.com) ; [editor@ijeab.com](mailto:editor@ijeab.com)

Web: [www.ijeab.com](http://www.ijeab.com)

## **International Editorial Board/ Reviewer Board**

- **Dr. Pietro Paolo Falciglia**, Environmental and Sanitary Engineering Group, University of Catania, Italy
- **Marcelo Huarte**, National Univ. of Mar del Plata. College of Agricultural Sciences, Balcarce, Argentina
- **Dr. Mehmet FiratBaran**, Department of Energy Systems Engineering, Altinsehir, Adiyaman /Turkey
- **Dr. Alexandra D. Solomou**, Hellenic Agricultural Organization "DEMETER", Institute of Mediterranean and Forest Ecosystems, Terma Alkmanos, Ilisia, 11528, Athens, Greece.
- **Dr. Barbara Molesini**, Department of Biotechnology, University of Verona, Italy
- **Dr. Krishnakumar Srinivasagam**, Vanavarayar Institute of Agriculture, Manakkadavu, Pollachi, Tamil Nadu, India
- **Prof. Guoju Xiao**, Environmental Ecology, Yinchuan, Ningxia, China
- **Dr. Adolf A. Acquaye**, University of York, Stockholm Environment Institute, York, United Kingdom
- **Dr. R. C. Tiwari**, Mizoram University, Tanhril Campus, Mizoram
- **Dr. Muhammad Majeed**, Kelappaji College of Agricultural Engg. & Technology, Kerala, India
- **Jiban Shrestha**, National Maize Research Program Rampur, Chitwan, Nepal Agricultural Research Council, Nepal
- **Dr. A. Heidari**, California South University (CSU), Irvine, California, USA
- **Dr. Mukesh Kumar Meena**, University of Agricultural Sciences, Raichur, Karnataka, India
- **Dr. M. Rajashekhar**, Gulbarga University, Gulbarga, Karnataka, India
- **Mr. B. A. Gudade**, Agronomy Indian Cardamom Research Institute, Tadong, Gangtok, Sikkim, India
- **Dr. S. K. Joshi**, Krishi Vigyan Kendra (KVK), Ganjam - 1, Orissa University of Agriculture and Technology, Bhanjanagar, Odisha, India
- **Heba Mahmoud Mohamed Afify**, Biomedical Engineering, Egypt
- **Denis Magnus Ken Amara**, School of Agriculture, Njala University, Private Mail Bag, Freetown, Sierra Leone.
- **Dr. Subha Ganguly**, Arawali Veterinary College, Sikar, India
- **Shoib A. Baba**, Indian institute of integrative medicine, Sanatnagar, Srinagar, India.
- **Elias kebede Hailu**, Natural Resource Research Directorate, EIAR, Werer, Ethiopia
- **Prof. Dr. Mirza Barjees Baig**, College of Food and Agriculture Sciences, King Saud University, Kingdom of Saudi Arabia,
- **Aliyev Zakir Hussein oglu**, Scientific direction: Agricultural sciences Region: Azerbaijan
- **Dr. Abd El-Aleem Saad Soliman Desoky**, Sohag University, Sohag Governorate, Egypt
- **Dr. Ghulam Abbas**, PhD (Poultry Nutrition), Riphah College of Veterinary Sciences, Lahore, Pakistan
- **Valter Luiz Maciel Júnior**, Universidade Estadual do Norte Fluminense, Laboratory of Animal Reproduction and Genetic Improvement – LRMGA, Rio de Janeiro, Brazil
- **Shahin Gavanji**, Faculty of Advanced Sciences and Technologies, University of Isfahan, Isfahan, Iran.
- **Neeraj Khare**, Amity Institute of Microbial Technology, Amity University, Jaipur-303002, Rajasthan, India
- **Javier Velasco Sarabia**, Investigator, National Institute of Fishing and Aquaculture, Avenida México No 190. Col. Del Carmen. CP. 04100. Del. Coyoacán, Ciudad de México.
- **Mr. Muhammad Usman**, Former Director General of Agricultural Research System, Government of Pakistan
- **Jaime Senabre**, Director and President of the International Scientific-Professional Committee of the National Symposium on Forest Fires (SINIF), Spain
- **Mohamed Ibrahim Mohamed**, Central labs, Egypt's Health Ministry, Department. of food bacteriology, zagazig, Egypt
- **Professor Jacinta A. Opara**, Centre for Health and Environmental Studies, University of Maiduguri, PMB 1069, Maiduguri-Nigeria
- **Dr. Josiah Chidiebere Okonkwo**, Nnamdi Azikiwe University, PMB 5025, Awka
- **Raga Mohamed Elzaki Ali**, College of Agricultural and Food Sciences, King Faisal University College of Agricultural and Food Sciences, Saudi Arabia
- **Engr. Aliyu Adinoyi**, International Crops Research Institute for the Semi-Arid Tropics Kano, Nigeria
- **Alireza Haghghi Hasanalideh**, Central and West Asian Rice Center (CWARice), Gilan Province, Iran
- **Dr. Lal Prasad Yadav (ARS)**, ICAR-Central Horticultural Experiment Station (CIAH), Godhra- 389340, Gujarat –India
- **Jogendra Singh**, Agricultural Research Institute (SKNAU, Jobner), Durgapura-Jaipur, India
- **Dr Rakesh Kumar Yadav**, Agricultural Research Station, Ummedganj, Agriculture University, Kota, Rajasthan, India.

# FOREWORD

I am pleased to put into the hands of readers Volume-8; Issue-6, November - December 2023 of “**International Journal of Environment, Agriculture and Biotechnology (IJEAB) (ISSN: 2456-1878)**”, an international journal which publishes peer reviewed quality research papers on a wide variety of topics related to **Environment, Agriculture and Biotechnology**. Looking to the keen interest shown by the authors and readers, the editorial board has decided to release issue with DOI (Digital Object Identifier) from CrossRef also, now using DOI paper of the author is available to the many libraries. This will motivate authors for quick publication of their research papers. Even with these changes our objective remains the same, that is, to encourage young researchers and academicians to think innovatively and share their research findings with others for the betterment of mankind.

I thank all the authors of the research papers for contributing their scholarly articles. Despite many challenges, the entire editorial board has worked tirelessly and helped me to bring out this issue of the journal well in time. They all deserve my heartfelt thanks.

Finally, I hope the readers will make good use of this valuable research material and continue to contribute their research finding for publication in this journal. Constructive comments and suggestions from our readers are welcome for further improvement of the quality and usefulness of the journal.

With warm regards.

Editor-in-Chief

Date: January, 2024

# Vol-8, Issue-6, November - December 2023

(DOI: 10.22161/ijeab.86)

---

1

[Effects of water stress and nutrient management on the performance of tomato](#)

Author(s): Md. Golam Rasul Miah, A. J. M. Sirajul Karim, Md. Moshiul Islam, Md. Dhin Islam, Mohammed Zia Uddin Kamal

 DOI: [10.22161/ijeab.86.1](https://doi.org/10.22161/ijeab.86.1)

Page No: 001-010

2

[South African legislation pertinent to building practice: A review in the context of inherent dolomite land hazard](#)

Author(s): S. Ngubelanga, J.L. Van Rooy


 DOI: [10.22161/ijeab.86.2](https://doi.org/10.22161/ijeab.86.2)

Page No: 011-019

3

[Analysis of Dynamic Changes of Winter Wheat in Xinye County, Henan Province Based on SVM Method](#)

Author(s): Yan Si, Bing-Yuh Lu, Yun-Shang Wang, Ruei-Yuan Wang

 DOI: [10.22161/ijeab.86.3](https://doi.org/10.22161/ijeab.86.3)

Page No: 020-028

4

[Analysis of Technical Efficiency and the Influence of Socioeconomic Factors on Oil Palm Farming in Muaro Jambi District - Indonesia](#)


Author(s): Yanuar Fitri, Saidin Nainggolan

Page No: 029-035

5

[Statistical analysis of recent rainfall variability and trend using a merged gauge and satellite time series data for the cotton zone of Mali](#)

Author(s): Souleymane Sidi Traore

 DOI: [10.22161/ijeab.86.5](https://doi.org/10.22161/ijeab.86.5)

Page No: 036-043

6

[Arsenic Content in Rice in Ghana: A Potential Health Hazard](#)

Author(s): Bartels Benjamin, Akua Nkuma, Gadzekpo Victor Patrick Yao

 DOI: [10.22161/ijeab.86.6](https://doi.org/10.22161/ijeab.86.6)

Page No: 044-047

7

[Adulteration of Honey on the Cape Coast Market in the Central Region of Ghana](#)

Author(s): Bartels Benjamin, Aggrey Ernestina, Gadzekpo Victor Patrick Yao

 DOI: [10.22161/ijeab.86.7](https://doi.org/10.22161/ijeab.86.7)

Page No: 048-054

**Research on Soil Erosion Intensity and Spatial Distribution Characteristics in Zhaoyang District of Zhaotong City Based on RS and GIS**

Author(s): Maohua Pan, Ruet-Yuan Wang, Bing-Yuh Lu

 DOI: [10.22161/ijeab.86.8](https://doi.org/10.22161/ijeab.86.8)

Page No: 055-068

**Proximate Composition, Energy and Nutritional Value of Local Malt (Asaana) Prepared from Maize in Ghana**

Author(s): Bartels Benjamin, Atakora Priscilla Ama, Gadzekpo Victor Patrick Yao

 DOI: [10.22161/ijeab.86.9](https://doi.org/10.22161/ijeab.86.9)

Page No: 069-072

**The Influence of Arbuscular Mycorrhizal Fungi (FMA) Dosage and Yomari Liquid Organic Fertilizer on the Growth of Seedlings of Agarwood-Producing Plants (Aquilaria malacensis Lamk.) on Former Gold Mining Soil**

Author(s): Benni Satria, Rachmad Hersi Martinsyah, Armansyah, Meisilva Erona, Warnita

 DOI: [10.22161/ijeab.86.10](https://doi.org/10.22161/ijeab.86.10)

Page No: 073-084

**The economic and environmental effects of gold panning in a zone of armed conflict in the circle of Gao**

Author(s): Abdoukadi Oumarou Toure, Fatoumata Maiga, Baba Faradji N'diaye, Issa Ouattara, Bamoussa Yalcouye

 DOI: [10.22161/ijeab.86.11](https://doi.org/10.22161/ijeab.86.11)

Page No: 085-093

**Lipases: Sources, immobilization techniques, and applications**

Author(s): Mudassar Hussain, Imad Khan, Bangzhi Jiang, Lei Zheng, Yuechao Pan, Jijie Hu, Azqa Ashraf, Aiman Salah Ud Din, Waleed AL-Ansi, Adil Khan, Xiaoqiang Zou

 DOI: [10.22161/ijeab.86.12](https://doi.org/10.22161/ijeab.86.12)

Page No: 094-121

**Laying and growth performance of local chicken (Gallus gallus domesticus) ecotype Konde in Burkina Faso**

Author(s): ZARE Yacouba, GNANDA B. Isidore, KERE Michel, TRAORE Boureima, HOUAGA Isidore, SANON F. Boris, ILBOUDO W. Fernand Ier jumeau, BOUGOUMA-YAMEOGO M. C. Valérie, REKAYA Romdhane, NIANOGO A. Joseph

 DOI: [10.22161/ijeab.86.13](https://doi.org/10.22161/ijeab.86.13)

Page No: 122-135

**The Impact of Technology-Enhanced Language Learning on English Proficiency: A Comparative Study of Digital Tools and Traditional Methods**

Author(s): Chandana US

 DOI: [10.22161/ijeab.86.14](https://doi.org/10.22161/ijeab.86.14)

Page No: 136-138

15

[Agro-Morphological Characters and PCR Based Markers for NEP NGU at Binh Dinh, Vietnam](#)

Author(s): Lang Thi Nguyen, Trân Khanh Thi Nguyen, Hieu Chi Bui, Khoa Anh Bien, Buu Chi Bui

 DOI: [10.22161/ijeab.86.15](https://doi.org/10.22161/ijeab.86.15)

Page No: 139-155

16

[Search for a suitable substrate for mass propagation of a local strain of Trichoderma harzianum \(ThTab\) isolated in Burkina Faso](#)

Author(s): Tobdem Gaston DABIRE, Masséni Yasmine OUOLOGUEME, Schémaéza BONZI and Irénée SOMDA

 DOI: [10.22161/ijeab.86.16](https://doi.org/10.22161/ijeab.86.16)

Page No: 156-166

17

[Extracting chromium-free protein hydrolysate from leather tanning wastes](#)

Author(s): Sameh Taha Kassem, Khaled Aly El-Shemy

 DOI: [10.22161/ijeab.86.17](https://doi.org/10.22161/ijeab.86.17)

Page No: 167-172

18

[Characterization, therapeutic applications, structures, and futures aspects of marine bioactive peptides](#)

Author(s): Azqa Ashraf, Aiman Salah Ud Din, Mudassar Hussain, Imad Khan, Farazia Hassan, Adnan Ahmad, Waleed AL-Ansi, Zaixiang Lou

 DOI: [10.22161/ijeab.86.18](https://doi.org/10.22161/ijeab.86.18)

Page No: 173-200

19

[Temperature and pH-sensitive chitosan-collagen hydrogels for antimicrobial and wound healing applications](#)

Author(s): Aiman Salah Ud Din, Azqa Ashraf, Mudassar Hussain, Adnan Ahmad, Imad Khan, Waleed AL-Ansi, Xiaoqiang Zou

 DOI: [10.22161/ijeab.86.19](https://doi.org/10.22161/ijeab.86.19)

Page No: 201-245

20

[The synergistic effect of non-thermal techniques and modified atmosphere packaging in food preservation](#)

Author(s): Farazia Hassan, Sehar Anwar, Mukesh, Hafiz Abdul Munam, Muhammad Arslan Asjad, Mudassar Hussain, Zahra batool, Nauman Khan, Muhammad Umair Khalid

 DOI: [10.22161/ijeab.86.20](https://doi.org/10.22161/ijeab.86.20)

Page No: 246-259

21

[The Effect of Eco Enzyme Concentration and NPK Fertilizer Dosage on the Growth and Yield of Sweet Potatoes \(Ipomoea batatas L.\) at the Urban Farming Planting System](#)

Author(s): Ferziana Nurmeilinda Dzirikrika, Sitawati, Nurul Aini, Dewi Ratih Rizki Damaiyanti

 DOI: [10.22161/ijeab.86.21](https://doi.org/10.22161/ijeab.86.21)

Page No: 260-263

22

*The Symbolism of Double Consciousness in the Works of W.E.B. Du Bois and its Evolution in Contemporary Black Literature*

Author(s): Neethu S

 DOI: [10.22161/ijeab.86.22](https://doi.org/10.22161/ijeab.86.22)

Page No: 267-269

23

*Cultural Hybridity in Focus: Exploring Globalized Identities Through Jhumpa Lahiri's The Namesake and Alejandro González Iñárritu's Babel*

Author(s): Arjun K Anil

 DOI: [10.22161/ijeab.86.23](https://doi.org/10.22161/ijeab.86.23)

Page No: 270-272

24

*Study of Biological Factors Likely to Influence Sensitivity to Dry Ball Disease of Rubber Tree in Three Rubber Production Zones of Cote D'ivoire*

Author(s): Zoh Olivia Dominique, Dolou Charlotte Tonessia, Éric Francis Soumahin, Kouamé Kouassi James Joseph, Amadou Doumbia

 DOI: [10.22161/ijeab.86.24](https://doi.org/10.22161/ijeab.86.24)

Page No: 273-283

25

*Pseudouridine in RNA: Enzymatic Synthesis Mechanisms and Functional Roles in Molecular Biology*

Author(s): Adil Khan, Yu Dong Hu, Salman Khan, Sahibzada Muhammad Aqeel, Imad Khan, Mudassar Hussain, Waleed AL-Ansi, Guochao Xu

 DOI: [10.22161/ijeab.86.25](https://doi.org/10.22161/ijeab.86.25)

Page No: 284-300

26

*Innovative Complex Coacervates of Gelatin and Sodium Carboxymethyl Cellulose for Cinnamaldehyde Delivery: Impact of Processing Conditions on Characteristics and Bioactivity*

Author(s): Mahran Abdulla, Shuqin Xia

 DOI: [10.22161/ijeab.86.26](https://doi.org/10.22161/ijeab.86.26)

Page No: 301-310





# Effects of water stress and nutrient management on the performance of tomato

Md. Golam Rasul Miah<sup>1</sup>, A. J. M. Sirajul Karim<sup>1</sup>, Md. Moshiul Islam<sup>2</sup>, Md. Dhin Islam<sup>1</sup>,  
Mohammed Zia Uddin Kamal<sup>1\*</sup>

<sup>1</sup>Department of Soil Science, Bangabandhu Sheikh Mujibur Rahman Agricultural University, Gazipur-1706, Bangladesh

<sup>2</sup>Department of Agronomy, Bangabandhu Sheikh Mujibur Rahman Agricultural University, Gazipur-1706, Bangladesh

\*Corresponding author: [zia@bsmrau.edu.bd](mailto:zia@bsmrau.edu.bd)

Received: 15 Sep 2023; Received in revised form: 21 Oct 2023; Accepted: 01 Nov 2023; Available online: 08 Nov 2023

©2023 The Author(s). Published by Infogain Publication. This is an open access article under the CC BY license

(<https://creativecommons.org/licenses/by/4.0/>).

**Abstract**— Management of nutrient and water scarcity are very important for getting higher yield of tomato specially in winter season in Bangladesh. The application of different fertilizer and manures increase the availability of nutrients which to stimulate plant growth that lead to enhance stress tolerance. Therefore, the main aim of this study is to investigate how different nutrients management practices improves growth by reducing impacts of water stress. Tomato plants were grown in field condition and different growth parameters such as height, root dry weight and shoot dry weight were measured. Yield and yield attributes of tomato were also determined. Recommended fertilizers along with organic manures application improve the growth and yield of tomato plants. On the other hand, growth and yield of tomato was lowest for no fertilization and manures treatment. This study improves our understanding about how nutrient management in water stress increase the growth and yield of tomato plant.



**Keywords**— tomato, nutrients, water stress, yield, manures

## I. INTRODUCTION

Climate change is recognized as a great threat to sustainable development of agricultural expansion thereby alarming for agricultural productivity. Global warming has direct impact on enhancement in evapotranspiration rates, and escalates water stress frequency and intensity with a rise from 1 to 30% in acute dry land by 2100 (Fischin *et al.*, 2007). The severity of water scarcity is unpredictable as it depends on many factors such as occurrence and distribution of rainfall, evaporative demands and moisture storing capacity of soils.

The aggressive exploitation of natural resources has endangered water resources, biodiversity and soil quality globally. Although it is notable that less than 1 % of the worlds fresh water (or about 0.007 % of all water on earth) is allowable for human consumption. It is anticipated that more than 1.8 billion peoples of the world will suffer absolute water scarcity and two thirds of the world community could be under water stress conditions by the year 2025 (Haji, 2011). Depletion of this valuable water

resource accelerates failure of water safeguard for world community and trigger poverty and malnutrition.

Arable lands are facing serious water scarcity due to climate change and available resources are depleting at an alarming rate, which necessitate efficient use of water for agriculture. Water deficit or drought is the most common stress condition globally and is increasingly of concern worldwide (Mahajan & Tuteja, 2005). Water scarcity has to be considered one of the major abiotic stresses that hinder the plant growth and development (Yang *et al.*, 2010). On an average drought and/or water scarcity instigate more than 50% crop yield loss worldwide (Bray *et al.*, 2000). Numerous alterations in morphological, metabolic, or/and physiological traits are induced by the water scarcity or drought stress in plant. At plant growth and development stage, water stress adversely affected plant elongation and growth expansion (Shao *et al.*, 2008). Water scarcity affected the leaf growth and leaf area and a greater root/shoot ration in several species (Jaleel *et al.*, 2009).

Severe water stress poses injurious effects on plant water relations, photosynthesis, ion uptake, and nutrient metabolism and assimilates partitioning (Jaleel *et al.*, 2009, Saud *et al.*, 2016). Stomatal closure and turgor losses under water stress are deemed to be the core cause of decreasing photosynthetic activity and crop production. (Farooq *et al.*, 2009). Under water stress plant response are extremely intricate and fluctuate among plant species and growth phases and water limitation duration (Fahad *et al.*, 2015).

During stress condition plant develop many adaptive strategies including escape, avoidance and tolerance mechanisms (Chaves *et al.*, 2003). Morphological plasticity, water physiological integration or gene regulation of plants could be possible acclimation mechanism at water stress condition (Jackson *et al.*, 2000). Under water scarcity conditions, plants alter metabolic and physiological function to minimize negative impacts and maximize survival (Thapa *et al.*, 2011). However, application of nutrition through fertilization increases the availability of limited nutrients, and then could alter system properties, which might be a potentially practical way to stimulate plant growth, enhance stress tolerance.

Like, optimal nitrogen application plays a crucial role in combating water stress (Marschner, 1995). N nutrition and drought tolerance are interrelated, with increased external N supply improving physiological status and growth in response to low soil water availability (Drenovsky *et al.*, 2012). Nitrogen is an essential structural constituent of protein, rubisco, nucleic acid, chlorophyll and some hormones and its application in the form of fertilizer accelerated the agronomic responses of crops (Ata-ul-Karim *et al.*, 2016). Nitrogen addition drives proper photosynthetic activity of the leaf (Brennan, 1992). Effective plant nutrition levels have also alleviated drought stress damage by sustaining the metabolic activities under water-restricted condition and at reduced leaf water potential. Thus, an adequate evaluation of water scarcity stress on the morpho-physiological traits under nitrogen fertilizer might deliver valuable understanding of tomato performance (Abid *et al.*, 2016).

However, organic manure might be another way for altering water stress (Forouzandeh *et al.*, 2015) and the storehouse of both micro and macronutrients and also act as natural mulch for conserving soil moisture and reducing moisture stress of soil. The soil-based application of organic amendments added humic substances to soil might have an ameliorating effect on water stressed to field grown crops (Zhang and Ervin, 2004). Thus, nutrient conservation through organic and inorganic fertilizer might be an approach for restoration of dry land agriculture to combat drought stress.

Tomato is most susceptible horticultural plant to drought stress because of its wide range of transpiring leaf surface, high stomatal conductance, having a shallow root system (Mohammed *et al.*, 2018). In Bangladesh tomato is grown mainly during the dry season (October-March) of the year, when the evapotranspiration is very high. Thus, understanding drought stress impact and searching its alleviating ways become urgent for dry land agriculture. However, a very little attempts was taken to combat the dry land tomato cultivation for future food security of Bangladesh. Based on the importance of dry land agriculture and combat to climate change induced food scarcity the present study is investigate the effects of water stress and nutrient management on the growth and yield of tomato.

## II. MATERIALS AND METHODS

### Study site and soil properties

The experiment was conducted at the research field of Bangabandhu Sheikh Mujibur Rahman Agricultural University (BSMRAU), Gazipur, Bangladesh. The experimental soil is terrace soils, which is nearly equivalent to Ochrept sub-order under the order Inceptisol of USDA Soil Taxonomy and belongs to the general soil type Shallow Red Brown Terrace Soil (Brammer, 1971; Saheed, 1984). The soil is friable clay loam with acidic in nature. The physico-chemical properties of studied soil are shown in Table 1.

Table 1 Physico-chemical characterization of experimental terrace soil surface layer (at the depth of 15 cm)

Soil Characteristics	Analytical Value	Soil Characteristics	Analytical Value
Physical properties		Chemical properties	
Particle size distribution		Soil pH	5.34
Sand	17.30%	Total N (%)	0.07
Silt	45.80%	Organic C (%)	0.63
Clay	36.90%	C: N ratio	9.0
Textual class	Silty clay loam	Available P (ppm)	9.3

Bulk density	1.38g/cm <sup>3</sup>	Exchangeable K (meq/100g)	0.09
Particle density	2.63 g/cm <sup>3</sup>	Exchangeable Ca (meq/100g)	5.34
Porosity (%)	47.4	Exchangeable Mg (meq/100g)	1.45
Hydraulic conductivity (cm sec <sup>-1</sup> )	4.6 x 10 <sup>-4</sup>	Exchangeable Na (meq/100g)	0.58
Field capacity (% by weight)	30.7	Available Sulphur (ppm)	13
-	-	Zinc content (ppm)	0.97
-	-	Boron content (ppm)	0.16

### Planting materials

Seedlings of 30 days of BARI Tomato-9 (Lalima) were used as planting material. BARI Tomato-9, a high yielding prolific bearer and bacterial wilt tolerant variety was developed by the Bangladesh Agricultural Research Institute (BARI), Joydebpur, Gazipur, Bangladesh. The potential yield of the variety is 90-95 t/ha.

### Experimental Design and Treatments

The two factors experiment was laid out in factorial Randomized Complete Block Design (RCBD) with three replications. Three different water stresses were considered as Factor A and four different nutrient management practices were studied as Factor B.

The experiment consisted of two factors:

#### Factor A: Different levels of Water stress-

- D<sub>1</sub> = Irrigation at 90% Field capacity (FC) (control)
- D<sub>2</sub> = Irrigation at 70% Field capacity (FC)
- D<sub>3</sub> = Irrigation at 50% Field capacity (FC)

#### Factor B: Different nutrient managements-

- N<sub>0</sub> = Control (No nutrient application)
- N<sub>1</sub> = Soil test based fertilizers (STB) (N<sub>145.0</sub> P<sub>41.5</sub> K<sub>75.0</sub> S<sub>11.6</sub> Zn<sub>0.9</sub> B<sub>1.0</sub> kg ha<sup>-1</sup>)

$$\text{iii. } N_2 = \text{STB} + 50\% N,$$

$$\text{iv. } N_3 = \text{STB} + 6 \text{ t ha}^{-1} \text{ poultry manure.}$$

There were 12 (3 × 4) treatments combination such as: D<sub>1</sub>N<sub>0</sub>, D<sub>1</sub>N<sub>1</sub>, D<sub>1</sub>N<sub>2</sub>, D<sub>1</sub>N<sub>3</sub>, D<sub>2</sub>N<sub>0</sub>, D<sub>2</sub>N<sub>1</sub>, D<sub>2</sub>N<sub>2</sub>, D<sub>2</sub>N<sub>3</sub>, D<sub>3</sub>N<sub>0</sub>, D<sub>3</sub>N<sub>1</sub>, D<sub>3</sub>N<sub>2</sub> and D<sub>3</sub>N<sub>3</sub>.

The unit plot size was 1.5 m × 1.5 m and maintain a 0.5 m drainage to separate one plot to another plot. One-month-old (accumulated in a pit and collected after month) poultry manure was procured from local poultry farm. Physical and chemical properties of poultry manure are presented in Table 2.

### Raising of seedlings

Tomato Seedlings were raised in one seedbed on a relatively high land at the research field of the department of Soil Science, BSMRAU. The size of the seedbed was 3 m × 1 m. The soil was well prepared with spade and made into loose friable and dried mass to obtain fine tilth. All weeds and stubbles were removed and 5 kg well rotten cowdung was applied during seedbed preparation. Germination was visible at 3 days after sowing of seeds. Heptachlor 40 WP was applied @ 4 kg ha<sup>-1</sup> around each seedbed as precautionary measure against ants and worm. Necessary shading by banana leaves was provided over the seedbed to protect the young seedlings from scorching sun. Weeding, mulching and irrigation were done from time to time as and when required and no chemical fertilizer was used in this seedbed.

Table 2 Physioco-chemical characterization of poultry manure

Organic matter	Moisture (%)	pH (1/2.5)	Organic carbon (%)	Total N (%)	P (%)	K (%)	Ca (%)	Mg (%)	Zn (ppm)	Cu (ppm)
Poultry manure	37.43	8.22	34.20	2.22	0.97	1.18	1.51	0.51	178.10	31.1

### Land preparation

The land was prepared well by deep plowing with a tractor followed by harrowing and laddering. The weeds and stubbles were removed and the 36 plots were prepared according to the layout of factorial RCBD design. Drains were made around each plot and excavated soil was used

for making dikes around each plot for restricting the lateral runoff of irrigation water.

### Uprooting and transplanting of seedlings

Healthy and uniform 30 days old seedlings were uprooted separately from the seedbed and were transplanted in the experimental plots and maintaining two seedlings in each

hill and row to row and plant to plant spacing of (75 cm × 50 cm).

The seedbed was watered before uprooting the seedlings from the seedbed so as to minimize damage to roots with ensuring maximum retention of roots. The seedlings were watered after transplanting. Shading was provided using banana leaf sheath for three days to protect the seedlings from the strong sunlight. Shading and watering in moderate quantity were continued till the seedlings were established

properly. The dead and very weak seedlings were replaced by the fresh and healthy ones soon after detection.

#### Manure and Fertilization:

The crop was fertilized with 145.0 kg N, 41.5 kg P, 75.0 kg K, 11.6 kg S, 0.9 kg Zn and 1.0 kg B ha<sup>-1</sup> as a soil test based fertilizer from urea, TSP, MoP, Gypsum, zinc sulphate and boric acid respectively. The applied nutrient in the different nutrient management are presented in Table 3

Table 3 Applied amounts of nutrients (kg ha<sup>-1</sup>) in different management treatments

Nutrient management	N	P	K	S	Zn	B	Poultry manure
N <sub>0</sub> (control)	-	-	-	-	-	-	-
N <sub>1</sub>	145.0	41.5	75.0	11.6	0.90	1.0	-
N <sub>2</sub>	217.5	41.5	75.0	11.6	0.90	1.0	-
N <sub>3</sub>	145.0	41.5	75.0	11.6	0.90	1.0	6 t ha <sup>-1</sup>

Half of the poultry manure and full amount of phosphorus, sulphur, zinc and boron from urea, TSP, MoP, Gypsum, zinc sulphate and boric acid respectively were applied at final land preparation. The remaining poultry manure was applied in pits before planting the seedlings. Nitrogen and potassium were applied in two equal splits at 15 and 35 days after transplanting under moist soil condition and were mixed thoroughly immediately after application.

#### Application of water stress

Tomato plants were exposed to the different water stress treatment two weeks after the seedling transplantation. The amount of water applied at different water stress was applied considering the field capacity of the soil. Keeping the depletion of water, applied stress required amounts of irrigation water at 90% FC, 70%FC and 50% was calculated and administered at 7 days intervals by using measured water can along with sprinkler from 14 days after transplanting to harvest.

#### Physico-chemical characterization of soil

Soil sample from each plot were collected considering the 0-15 cm depth at before treatment exposure and after harvest. The physico-chemical properties of the initial and residual soil samples were done by following suitable standard protocols.

#### Harvesting

Fruits were harvested at 4 days interval during early ripe stage when they developed slightly red color.

#### Plant height (cm)

Five-plant height was measured from plant of each unit plot from the ground level to the tip of the longest stem and

mean value was calculated. Plant height was recorded at 50% flowering stages.

#### Shoot and root dry weight

After final fruit plucking, five pre-selected plants in each plot were uprooted, chopped with sharp knife for portioning shoot and root, air-dried in the laboratory and finally oven-dried for 72 hours at 65°C. The sample was then transferred into desiccators and allowed to cool down at room temperature. The final weight of the sample was taken.

#### Number of fruits plant<sup>-1</sup>

The number of fruits per plant was counted from five plants of each unit plot and the average number of fruits per plant was recorded.

#### Yield plant<sup>-1</sup> (kg)

Yield of tomato per plant was recorded as average value of the whole fruit per plant harvested in different time and was expressed in kilogram.

#### Yield (t ha<sup>-1</sup>)

Yield per hectare of tomato fruits was calculated by converting the weight of total plant yield into hectare on the basis of total plant population of tomato per hectare and expressed in ton.

#### Statistical analysis:

The data were statistically analyzed by using Statistix Version 10.0 software to find out the significance of variation between treatments. The differences between the treatment means were judged by least significance difference (LSD) Test.

### III. RESULTS AND DISCUSSION

#### Effects of water stress and nutrient management on the growth of tomato plant

Effects of water stress and nutrient management singly and or in combination on tomato plant growth parameters is represent in the table 4, 5 and 6.

#### Plant height

The results showed that water stress significantly affected the plant height at both flowering stages (50% and 90%) (Table 4). The tallest plant at both 50% and 100% flowering stage (64.12 and 86.65 cm, respectively) were recorded from D<sub>1</sub> treatment with watering at 90% field capacity (FC), which was statistically similar with D<sub>2</sub> at 70% of FC. The shortest plant at both 50% and 100% flowering stage (59.95 and 78.15 cm, respectively) were found from the most water deficit D<sub>3</sub> treatment with 50% of FC. Thus, deficit irrigation with 50% FC significantly decreased the plant height of tomato at 50% and 100% flowering stage by approximately 15.9% and 16.7% respectively. Data revealed that well watered plot exhibited the healthy growth but the drought stress reduced the morphological parameters such as plant height of tomato. The diminishment in plant height could likewise be credited to declining in the cell extension and more leaf senescence in the plant prone to stress (Manivannan *et al.*, 2007). Pervez *et al.* (2009) found that significant results toward water stress signifying drought effects were registered on plant height of tomato plant. Ubaidullah *et al.* (2002) also found the similar result.

Significant variation was recorded for different levels of nutrient management on plant height of tomato at 50% and

100% flowering stage (Table 5). Data revealed that at 50% and 100% flowering stage, the tallest plant (72.34 and 97.58 cm, respectively) was found from N<sub>3</sub> treatment of STB based fertilizer along with 6-t/ha poultry manure, which was statistically similar with N<sub>2</sub> treatment. While, the shortest plant at 50% and 100% flowering stage (45.45, and 58.25 cm, respectively) was recorded from N<sub>0</sub> treatment.

Combined effect of different levels water stress and nutrient management showed significant differences on plant height of tomato at 50% and 100% flowering stage (Table 6). The tallest plant at both 50% and 100% flowering stage (73.73 and 100.57 cm, respectively) was found from D<sub>1</sub>N<sub>3</sub> treatment combination that was statistically similar with D<sub>1</sub>N<sub>2</sub>, D<sub>2</sub>N<sub>2</sub>, D<sub>2</sub>N<sub>3</sub>, D<sub>3</sub>N<sub>2</sub> and D<sub>3</sub>N<sub>3</sub>. While, the shortest plant (41.66 and 53.73 cm, at 50% and 100% flowering stage respectively) was found from D<sub>3</sub>N<sub>0</sub> treatment combination, which was statistically similar with D<sub>1</sub>N<sub>0</sub> and D<sub>2</sub>N<sub>0</sub> treatments. The present data reveals that nutrient management with STB based fertilizer along with 6 t/ha poultry manure significantly ameliorate the adverse effects of moisture stress on plant height of tomato. Similar trends were also observed in the treatment combination of STB fertilizer along with 50% more nitrogen. This might be due to higher manure application rate improved soil physical, chemical, and biological properties (Farhad, 2018). Application of poultry manure might be improved the porosity and protect the soil moisture depletion favor the growth and development of tomato plant. Moreover, N addition encourages the plant growth, which helps to ameliorate the adverse effects of water stress (Arun *et al.*, 2012).

Table 4 Effect of water stress on the growth parameters of tomato plant

Treatments	Plant height (cm)	Root DW Plant <sup>-1</sup> (g)	Shoot DW Plant <sup>-1</sup> (g)
D <sub>1</sub>	64.12a	1.80a	12.38a
D <sub>2</sub>	61.29ab	1.79ab	11.37a
D <sub>3</sub>	59.95b	1.63b	9.33b
CV (%)	7.95	5.67	12.20
SE (±)	2.005	0.041	0.61
LSD (0.05)	4.15	0.085	1.27

Table 5 Effect of nutrient management on the growth parameters of tomato plant

Treatments	Plant height (cm) (50%F)	Root DW Plant <sup>-1</sup> (g)	Shoot DW Plant <sup>-1</sup> (g)
N <sub>0</sub>	44.45c	1.42d	7.05c
N <sub>1</sub>	61.90b	1.70c	12.627b
N <sub>2</sub>	68.46a	1.86b	14.16a
N <sub>3</sub>	72.34a	2.11a	15.62a
SE (±)	2.31	0.047	0.7111
LSD (0.05)	4.80	0.098	1.47

Table 6 Combined effects of water stress and nutrient management on the growth parameters of tomato plant

Treatments	Plant height (cm) (50%F)	Root DW Plant <sup>-1</sup> (g)	Shoot DW Plant <sup>-1</sup> (g)
D <sub>1</sub> *N <sub>0</sub>	47.50e	1.39e	7.32e
D <sub>1</sub> *N <sub>1</sub>	64.96bcd	1.66d	13.16cd
D <sub>1</sub> *N <sub>2</sub>	70.30ab	1.71d	14.11abcd
D <sub>1</sub> *N <sub>3</sub>	73.73a	2.06abc	16.20a
D <sub>2</sub> *N <sub>0</sub>	44.20e	1.28e	6.087e
D <sub>2</sub> *N <sub>1</sub>	61.16cd	1.71d	12.97cd
D <sub>2</sub> *N <sub>2</sub>	68.83abc	1.90c	13.27bcd
D <sub>2</sub> *N <sub>3</sub>	70.96ab	2.17a	15.75ab
D <sub>3</sub> *N <sub>0</sub>	41.66e	1.04e	5.53e
D <sub>3</sub> *N <sub>1</sub>	59.54d	1.73d	11.74d
D <sub>3</sub> *N <sub>2</sub>	66.26abcd	1.96bc	15.11abc
D <sub>3</sub> *N <sub>3</sub>	72.33ab	2.11ab	14.91abc
SE (±)	4.01	0.082	1.23
LSD (0.05)	8.316	0.17	2.55

### Root dry weight

Root dry weight was significantly affected by different moisture stress. Irrigation at 90% field capacity at D<sub>1</sub> treatment showed the maximum root weight (1.80 g), which was statistically similar with the D<sub>2</sub> treatment maintaining 70% FC (Table 4). Irrigation at 50% field capacity significantly reduced the root dry mass of the tomato plant. Thus, root dry mass was linearly decreased with decreased amount of irrigation water added to the trial.

Nutrient management was also significantly influencing the root dry mass of tomato plant. (Table 5). Significantly higher amount of root dry mass was found in the N<sub>3</sub> treatment of STB fertilizer along with 6-t/ha poultry manure (2.11g). The lower amount of root dry matter was detected in the control treatment (1.42g). Application of organic amendments improves the physical, chemical and biological properties of soil that helps proper root growth and development of tomato plants (Jones *et al.*, 2007).

The interaction effects of water stress and nutrient management had provided a significant response on the root dry weight production (Table 6). In the present study, the highest roots dry weight (2.17g) was found in the treatment combination of D<sub>2</sub>N<sub>3</sub>, which was statistically identical with D<sub>3</sub>N<sub>3</sub> and D<sub>1</sub>N<sub>3</sub>. Thus, the study summarized that nutrient addition of STB fertilizer along with 6 t ha<sup>-1</sup> poultry manure overcome the adverse effect of water stress on tomato roots. Addition of organic and inorganic amendment helps to

improve the nutrient uptake mechanisms and osmotic balance that may provide the ameliorative effects of water stress of tomato plant (Farhad *et al.*, 2018)

### Effects water stress and nutrient management on yield and yield attributes of tomato

Effects of water stress and nutrient management singly and/or in combination on reproductive stage traits of tomato plant is present in the Table 7, 8 and 9.

### Number of fruits plant<sup>-1</sup>

Significant variation was recorded in terms of number of fruits plant<sup>-1</sup> of tomato due to different levels of moisture under the present trial (Table 7). The highest number of fruits plant<sup>-1</sup> (39.54) was recorded from D<sub>1</sub>, which was statistically similar with D<sub>2</sub>. While, the lowest number (23.93) was found from D<sub>3</sub> (Table 7). Pervez *et al.* (2009) and Ubaidullah *et al.* (2002) also found the similar results and they showed significant results toward drought stress signifying drought effects on the number of fruits plant<sup>-1</sup> of tomato.

Number of fruit plant<sup>-1</sup> of tomato showed significant difference due to different nutrient management (Table 8). The highest number of fruits plant<sup>-1</sup> (51.60) was recorded from N<sub>3</sub> treatment administered with 6 t ha<sup>-1</sup> poultry manure along with the STB fertilizer. However, control treatment (N<sub>0</sub>) provided the lowest fruit number plant<sup>-1</sup> (10.99). Wu *et al.*, (2018) explained that nutrient uptake plays an important role on transfer of carbon assimilates and fruit settling.

Interaction effect of water stress and nutrient management significantly affected the fruit number plant<sup>-1</sup> (Table 9). The present data indicated that the maximum fruit number plant<sup>-1</sup> (53.41) was accredited against the treatment combination of D<sub>1</sub>N<sub>3</sub>, which was statistically identical with D<sub>1</sub>N<sub>2</sub>, D<sub>2</sub>N<sub>3</sub>, and D<sub>3</sub>N<sub>3</sub>. The lowest fruit number plant<sup>-1</sup> (7.75) production was subjected to the treatment combination upholding the irrigation with 50% FC along with no fertilization (D<sub>3</sub>N<sub>0</sub>) treatment which was statistically similar with the D<sub>1</sub>N<sub>0</sub> and D<sub>1</sub>N<sub>0</sub>. The data of the present study reveal that the adverse effect of water stress on fruit number plant<sup>-1</sup> in tomato plant might be due to the ameliorative effects of organic matter along with STB fertilizer. Wu *et al.*, (2018) found similar findings that the effects of the interaction between water and fertilization on fruit settling were significant. Liu *et al.*, (2019) also found that various soil moisture and potassium administration provides a significant impact on fruit settling of tomato. They also suggested that addition of potassium might play an important role on minimizing the impact of water stress on fruit settling. Forhad *et al.*, (2018) also found similar finding that composted poultry manure was able to partially alleviate the effect of water stress on maize.

#### Fruit weight plant<sup>-1</sup> (g)

Weight of plant<sup>-1</sup> of tomato varied significantly due to effects of different levels of moisture (Table 7). The highest fruit weight per plant (3.51kg) was found from D<sub>1</sub>, which was similar with the data of D<sub>2</sub>. On the other hand, the lowest (0.93) was observed from D<sub>3</sub> (Table 7). Significant variation was recorded for different levels of nutrient management on fruit weight of plant<sup>-1</sup> (Table 8). The highest fruit weight per plant (3.36 kg) was recorded from N<sub>3</sub>, whereas the lowest weight (0.46) was attained from N<sub>0</sub>. These results suggested that nutrient management contribute in the enrichment of fruit weight. Combined effect of water stress and nutrient management significantly affected the fruit weight of plant<sup>-1</sup> (Table 9). The present data signified that the maximum fruit weight of plant<sup>-1</sup> (3.51 kg) was attained in the treatment combination of D<sub>1</sub>N<sub>3</sub>, which was statistically identical with D<sub>1</sub>N<sub>2</sub>, D<sub>2</sub>N<sub>3</sub> and D<sub>3</sub>N<sub>3</sub>. The lowest fruit weight of plant<sup>-1</sup> (0.32kg) was D<sub>3</sub>N<sub>0</sub> treatment that was statistically similar with the D<sub>1</sub>N<sub>0</sub> and D<sub>1</sub>N<sub>0</sub>. Thus the data reveal that the adverse effect of water stress on single fruit weight in tomato plant might be due to the ameliorative effects of organic matter along with the STB fertilizer.

Table 7 Effect of water stress on yield and yield attributes of tomato

Treatments	Fruit No. plant <sup>-1</sup>	Fruit Weight (Kg plant <sup>-1</sup> )	Yield (t ha <sup>-1</sup> )
D <sub>1</sub>	39.54a	2.46a	65.63a
D <sub>2</sub>	35.48ab	2.22b	59.22b
D <sub>3</sub>	30.82b	1.93b	49.23c
(%) CV	14.77	12.24	12.24
SE (±)	2.16	1.12	3.44
LSD <sub>(0.05)</sub>	4.49	1.12	7.13

Table 8 Effect of nutrient management on yield and yield attributes of tomato

Treatments	Fruit No. plant <sup>-1</sup>	Fruit Weight (Kg plant <sup>-1</sup> )	Yield (t ha <sup>-1</sup> )
N <sub>0</sub>	10.99d	0.46d	12.39d
N <sub>1</sub>	36.91c	2.29c	60.99c
N <sub>2</sub>	44.28b	2.84b	75.60b
N <sub>3</sub>	51.60a	3.36a	89.63a
SE (±)	2.50	1.29	3.44
LSD <sub>(0.05)</sub>	5.19	2.68	7.13

Table 9 Combined effects of water stress and nutrient management on yield and yield attributes of tomato

Treatments	Fruit No. plant <sup>-1</sup>	Fruit Weight (Kg plant <sup>-1</sup> )	Yield (t ha <sup>-1</sup> )
D <sub>1</sub> *N <sub>0</sub>	13.79e	0.59f	15.83f
D <sub>1</sub> *N <sub>1</sub>	43.36bc	2.69cd	71.86cd
D <sub>1</sub> *N <sub>2</sub>	47.60ab	3.05abc	81.36abc
D <sub>1</sub> *N <sub>3</sub>	53.41a	3.51a	93.47a
D <sub>2</sub> *N <sub>0</sub>	11.45e	0.49f	12.94f
D <sub>2</sub> *N <sub>1</sub>	35.92cd	2.25de	59.98de
D <sub>2</sub> *N <sub>2</sub>	42.18bc	2.74bc	73.07bc
D <sub>2</sub> *N <sub>3</sub>	52.38a	3.41a	90.90a
D <sub>3</sub> *N <sub>0</sub>	7.75e	0.32f	8.40f
D <sub>3</sub> *N <sub>1</sub>	31.46d	1.92e	51.12e
D <sub>3</sub> *N <sub>2</sub>	43.07bc	2.71bc	72.38bc
D <sub>3</sub> *N <sub>3</sub>	49.02ab	3.17ab	84.52ab
SE (±)	4.33	0.223	5.96
LSD (0.05)	8.99	0.463	12.36

### Fruit yield (t ha<sup>-1</sup>)

Different level of water stress significantly the fruit yield of tomato (Table 7). The highest fruit yield of tomato (65.63 t ha<sup>-1</sup>) was found from D<sub>1</sub> irrigation at 90% FC. On the other hand, the lowest (49.23) was observed from D<sub>3</sub> treatment (Table 7). These results suggest that fruit yield of tomato was severely affected by water stress. Similarly, Ullah *et al.*, (2016), explained that water stress restricts the nutrient availability and cell division and nutrient translocation process which hinder the yield of tomato under water scarcity.

Significant variation was recorded for different levels of nutrient management on fruit yield of tomato (Table 8). The highest fruit yield of tomato (89.63 t ha<sup>-1</sup>) was recorded from N<sub>3</sub>, whereas the lowest weight (12.39 t ha<sup>-1</sup>) was attained in N<sub>0</sub>. These results suggested that nutrient management contribute in the fruit yield of tomato. Such finding might be explained that, nutrient availability provides a significant role on the photosynthetic activity and carbon assimilation and translocation in the fruit (Wu *et al.*, 2018).

Combined effect of water stress and nutrient management significantly affected the fruit yield of tomato (Table 9). The present data signified that the maximum fruit yield of tomato (91.47 t ha<sup>-1</sup>) was attained in the treatment combination of D<sub>1</sub>N<sub>3</sub>, which was statistically identical with D<sub>1</sub>N<sub>2</sub>, D<sub>2</sub>N<sub>3</sub> and D<sub>3</sub>N<sub>3</sub>. The lowest fruit yield 8.40 t ha<sup>-1</sup> was

recorded in D<sub>3</sub>N<sub>0</sub> treatment that was statistically similar with the D<sub>1</sub>N<sub>0</sub> and D<sub>1</sub>N<sub>0</sub>. Thus the data reveal that the adverse effect of water stress on single fruit weight in tomato plant might be due to the ameliorative effects of organic matter along with STB fertilizer. Under water stress condition, organic matter increased the water holding capacity (Wang *et al.*, 2016). Li *et al.*, (2012) and Mahama *et al.*, (2016) also reported that nitrogen and water required for photosynthesis and transpiration also increase the capacity of cereals to mobilize and translocate photosynthates for grain formation and fruit formation which significantly increased the fruit yield.

## IV. CONCLUSIONS

The maximum biomass and fruit yield of tomato plant was obtained from the treatment receiving irrigation at 90% FC. Irrigation at 70% FC also provided the similar trends. Water scarcity (irrigation at 50% FC) severely affected the plant growth, yield and yield attributes of tomato. The highest biomass and fruit yield of tomato plant was ensured in the treatment N<sub>3</sub> receiving STB fertilizer along with 6 t ha<sup>-1</sup> poultry manure. Nutrient deficient condition (N<sub>0</sub>; control) severely demolishes the plant growth and yield of tomato. Combined effects of irrigation at 90% FC and nutrient management by STB fertilizer + 6 t ha<sup>-1</sup> poultry manure (D<sub>1</sub>N<sub>3</sub>) showed greater biomass and fruit yield of tomato plant. Thus, nutrient management with STB fertilizer + 6 t



ha<sup>-1</sup> poultry manure might be ameliorating the adverse effects of water stress on growth and yield of tomato.

## REFERENCES

- [1] Abid, M., Tian, Z., Ata-Ul-Karim, S.T., Cui, Y., Liu, Y., Zahoor, R., et al. (2016). Nitrogen nutrition improves the potential of wheat (*Triticum aestivum* L.) to alleviate the effects of drought stress during vegetative growth periods. *Front. Plant Sci.* 7:981. doi: 10.3389/fpls.2016.00981.
- [2] Arun, T., Upadhyaya, S.D., Upadhyay, A. Preeti Sagar, N. (2012). Responses of moisture stress on growth, yield and quality of isabgol (*Plantago ovata* Forsk). *J. Agric. Technol.* 8, 2,563-570.
- [3] Ata-Ul-Karim, S.T., Liu, X., Lu, Z., Yuan, Z., Zhu, Y., and Cao, W. (2016). In- season estimation of rice grain yield using critical nitrogen dilution curve. *Field Crops Res.* 195, 1–8. doi: 10.1016/j.fcr.2016.04.027.
- [4] Brammer, H. (1971). Soil Resources. Soil Survey project Bangladesh AGL. SF/Pak.6. Technical Report 3. pp 320-340.
- [5] Bray, E.A.J., Bailey, S., and Weretilnyk, E., (2000). Responses to abiotic stresses. In: W. Gruissem, B. Buchnan and R. Jones (Eds.). 1158–1249.
- [6] Bray, R.H. and Kurtz, L.T. (1945). Determination of total, organic and available form of phosphorus in soils. *Soil Sci.*, 59: 39-45.
- [7] Bremner, J.M., (1965). Total nitrogen. In C.A. Black et al., (ed.) *Methods of Soil analysis. Part-2. Agronomy* 9: 1149-1178.
- [8] Chaves, M. M., Maroco, J. P., and Pereira, J. S. (2003). Understanding plant responses to drought from genes to the whole plant. *Funct. Plant Biol.* 30, 239–264. doi: 10.1071/FP02076
- [9] Drenovsky R.E., Khasanova A., James J.J. (2012) Trait convergence and plasticity among native and invasive species in resource-poor environments. *Am J Bot* 99:629–639.
- [10] Fahad, S., Nie, L., Chen, Y., Wu, C., Xiong, D., Saud, S., et al. (2015). “Crop plant hormones and environmental stress,” in *Sustainable Agriculture Reviews*, Vol. 15, ed. E. Lichtfouse (Geneva: Springer International Publishing), 371–400.
- [11] Farhad, W., Cheema, M.A., Hammad, H.M., Saleem, M.F., Fahad, S., Abbas, F., Khosa, I. and Bakhat, H.F., (2018). Influence of composted poultry manure and irrigation regimes on some morpho-physiology parameters of maize under semiarid environments. *Environ. Sci. Pollut. Res.* 25(20), pp.19918-19931.
- [12] Farooq, M., Wahid, A., Kobayashi, N., Fujita, D., and Basra, S. M. A. (2009). Plant drought stress: effects, mechanisms and management. *Agron. Sustain. Dev.* 29, 185–212. doi: 10.1051/agro:2008021.
- [13] Fischlin, A., Midgley, G.F., Price, J.T., Leemans, R., Gopal, B., Turley, C., et al. (2007). “Ecosystems, their properties, goods, and services. Climate change 2007: impacts, adaptation and vulnerability,” in *Proceedings of the Contribution of Working Group II to the Fourth Assessment Report of the Intergovernmental Panel on Climate Change*, eds M. L. Parry, O. F. Canziani, J. P. Palutikof, and C. E. Hanson (Cambridge: Cambridge University Press), 211–272.
- [14] Forozandeh, M., Karimian, M.A., Mohkami, Z., (2015). Effect of drought stress and different types of organic fertilization on yield of cumin components in sistian regions. *European J. Medicinal Plant* 5(1), 95-100.
- [15] Haji H.T. (2011) Impact of climate change on surface water availability. Department of Civil Engineering. Tshwane University of Technology.
- [16] Jackson, R.B., Sperry, J. S., and Dawson, T. E. (2000). Root water uptake and transport: using physiological processes in global predictions. *Trends Plant Sci.* 5, 482–488. doi: 10.1016/S1360-1385(00)01766-0.
- [17] Jaleel, C.A., Manivannan, P., Wahid, A., Farooq, M., Somasundaram, R., Panneerselvam, R., et al. (2009). Drought stress in plants: a review on morphological characteristics and pigments composition. *Int. J. Agric. Biol.* 11, 100–105.
- [18] Jones S.K., Rees R.M., Skiba U.M., Ball B.C. (2007) Influence of organic and mineral N fertilizer on N<sub>2</sub>O fluxes from a temperate grassland. *Agric Ecosyst Environ* 121:74–83.
- [19] Li G., Zhang Z.S., Gao H.Y., Liu P., Dong S.T., Zhang J.W. (2012) Effects of nitrogen on photosynthetic characteristics of leaves from two different stay-green maize varieties at the grain-filling stage. *Can J Plant Sci* 92:671–680.
- [20] Liu, J., Hu, T., Feng, P., Wang, L., & Yang, S. (2019). Tomato yield and water use efficiency change with various soil moisture and potassium levels during different growth stages. *PloS one*, 14(3), e0213643.
- [21] Mahajan, S., & Tuteja, N. (2005). Cold, salinity and drought stresses: An overview. *Archives of Biochemistry and Biophysics*, 444(2), 139-158.
- [22] Mahama G.Y., Prasad P.V.V., Roozeboom K.L., Nippert J.B., Rice C.W. (2016) Response of maize to cover crops, fertilizer nitrogen rates, and economic return. *Agron J* 108:17–31.
- [23] Manivannan P., Jaleel C.A., Sankar B., Kishore Kumar A., Somasundaram R., Alagu Lakshmanan G.M., Panneerselvam R. (2007). Growth, biochemical modifications and proline metabolism in *Helianthus annuus* L. as induced by drought stress. *Colloids Surf B.* 59:141–149.
- [24] Marschner, H. (1995). *Mineral Nutrition of Higher Plants*. San Diego, CA: Academic Press, 483–507. doi: 10.1016/B978-012473542-2/50015-8
- [25] Mohammed, H.N., Mahmud, T.M.M., and Puteri, Edaroyati, M.W. (2018). Deficit irrigation for improving the postharvest quality of lowland tomato fruits. *Pertanika J. Trop. Agric. Sci.* 41(2): 741-758.
- [26] Pervez, M. A., Ayub, C. M., Khan, H. A., Shahid, M. A. and Ashraf, I. (2009). Effect of drought stress on growth, yield and seed quality of tomato (*Lycopersicon esculentum* L) Pakistan J. Agri. Sci. 46(3): 75-80.
- [27] Saud, S., Chen, Y., Fahad, S., Hussain, S., Na, L., Xin, L., et al. (2016). Silicate application increases the photosynthesis and its associated metabolic activities in Kentucky bluegrass under drought stress and post-drought recovery. *Environ. Sci. Pollut. Res.* 23, 17647–17655. doi: 10.1007/s11356-016-6957-x

- [28] Shao, H.B., Chu, L.Y., Shao, M.A., Jaleel, C.A., and Hongmei, M. (2008). Higher plant antioxidants and redox signaling under environmental stresses. *C. R. Biol.* 331, 433–441. doi: 10.1016/j.crv.2008.03.011
- [29] Thapa, G., Dey, M., Sahoo, L., Panda, S.K. (2011). An insight into the drought stress induced alterations in plants. *Biol Plant* 55:603–613.
- [30] Ubaidullah, J., Muhammad, I., Muhammad, S., Naeem, N. and Muhammad, N. (2002). Effect of different mulching materials and irrigation intervals on growth, yield and quality of tomato cv. Peshawar local (Roma). *Sarad J. Agric.* 18(2): 167-172.
- [31] Ullah, U., Ashraf, M., Shahzad, S. M., Siddiqui, A. R., Piracha, M. A., & Suleman, M. (2016). Growth behavior of tomato (*Solanum lycopersicum* L.) under drought stress in the presence of silicon and plant growth promoting rhizobacteria. *Soil & Environment*, 35(1).
- [32] Wang X, Jia Z, Liang L, Yang B, Ding R, Nie J, Wang J (2016) Impacts of manure application on soil environment, rainfall use efficiency and crop biomass under dry land farming. *Sci Rep* 3:1–8.
- [33] Wu, Z. Z., Ying, Y. Q., Zhang, Y. B., Bi, Y. F., Wang, A. K., & Du, X. H. (2018). Alleviation of drought stress in *Phyllostachys edulis* by N and P application. *Scientific reports*, 8(1), 228.
- [34] Yang, S., Vanderbeld, B., Wan, J., and Huang, Y. (2010). Narrowing down the targets: towards successful genetic engineering of drought-tolerant crops. *Mol. Plant* 3, 469–490. doi: 10.1093/mp/ssq016
- [35] Zhang, X.Z., and Ervin, E.H., (2004). Cytokinin-containing seaweed and humic acid extracts associated with creeping bentgrass. *J. Am. Soc. Hort. Sci.* 128(4): 492-496.



# South African legislation pertinent to building practice: A review in the context of inherent dolomite land hazard

Ngubelanga S.<sup>1,2</sup>, Van Rooy J.L.<sup>2</sup>

<sup>1</sup>Infrastructure and Land Use, Council for Geoscience, South Africa

Email: [sngubelanga@geoscience.org.za](mailto:sngubelanga@geoscience.org.za)

<sup>2</sup>Department of Geology, University of Pretoria, South Africa

Email: [louis.vanrooy@up.ac.za](mailto:louis.vanrooy@up.ac.za)

Received: 14 Sep 2023; Received in revised form: 20 Oct 2023; Accepted: 02 Nov 2023; Available online: 09 Nov 2023

©2023 The Author(s). Published by Infogain Publication. This is an open access article under the CC BY license

(<https://creativecommons.org/licenses/by/4.0/>).

**Abstract**— Dolomite land occurs across five of the nine South Africa provinces and its vast occurrence and distribution makes it difficult to avoid when planning for building projects. Such terrains are generally associated with the formation of ground instability events (sinkholes & subsidences) causing widespread damage to infrastructure or loss of life. Under section 24 of the Constitution of South Africa, (Act 108 of 1996), safe environment and protection thereof has been elevated to a basic human right. In the context of safe land use planning and sustainable infrastructure development, more particularly post-1994, a series of statutes have been promulgated to provide a legislated framework for building practice in South Africa.

The National Building Regulations and Building Standards (Act 103 of 1977) as amended, and the current National Building Regulations (NBR's), have been promulgated to promote uniformity in the law relating to the erection of buildings in South Africa including prioritizing safe land for human settlement. A key principle is that if conditions of the land on which a building was or is being or is to be erected, shows signs of becoming dangerous to property and/ or life, such conditions must be investigated and secured. However, there seem to be challenges in the practical implementation.

This paper therefore presents a review into the legislation pertinent to building practice to identify possible gaps, implementation challenges and damaging effects due to inappropriate development of dolomite land. The research further scrutinizes an influence or lack thereof, of the technical requirements aimed at ensuring sustainable development on geologically hazard prone terrains.

**Keywords**— dolomite land, hazard, legislation, implementation, negative effects.



## I. INTRODUCTION

The local and international experience has demonstrated that advancement in scientific knowledge and strict implementation of legislated disaster mitigation measures have the potential to encourage safe development of geologically unsuitable areas like dolomite (karst) land.

In South Africa, the term “Dolomite Land” refers to areas underlain directly or at shallow depths (<100 m) by karst, e.g. dolomite rock of the Chuniespoort and Ghaap Groups of the Transvaal Supergroup. It includes areas where dolomite is covered by younger deposits of Pretoria Group

and Karoo Supergroup or unconsolidated deposits of the Cenozoic age (Buttrick et al, 2001). Dolomite land has a negative connotation due to its association with damaging effects of sinkhole and subsidence formation (Buttrick et al, 2001).

Random occurrence of these ground instability events in densely populated urban areas is costly and may result in damage to infrastructure and in extreme cases the forced relocation of communities or even loss of life (Brink, 1979). According to Guitierrez et al. (2014), impacts and hazards associated with karst are rapidly increasing as development expands upon these areas without proper

planning taking into account the inherent hazards associated with these environments. However, avoiding development on such land is practically impossible given its distribution across five of the nine provinces in South Africa. Buttrick et al. (2011), stated that between 4 and 5 million South Africans reside or work on dolomite land, and that the costs to repair karst features far exceeds the cost of implementing appropriate annual dolomite risk management and maintenance interventions.

It is in this context therefore, that this research considered a review into the South African legislation pertinent to building practice and its influence or lack thereof, to

sustainable development of cities on geologically hazard prone terrains like dolomite land.

## II. OCCURRENCE AND DISTRIBUTION OF DOLOMITE LAND

According to Ford and Williams (1992), sinkholes are the most diagnostic surface expression of karst landscapes and can be found extensively throughout the world (approximately 7–10% of the earth land surface has been classified as karst terrain).



Fig.1: The occurrence and distribution of dolomite land in South Africa (© CGS,2013)

Given the dolomite land distribution, therefore, avoiding it is not practically possible. However, undue acceptance of the risk is also not an option subject to the state's obligation in terms of the Constitution. This brings about a critical question of how the current South African building legislation has influenced the sustainable land use planning and infrastructure development on dolomite land including mandatory reporting of ground instability events.

## III. REVIEW OF THE BUILDING LEGISLATIVE FRAMEWORK

### 3.1 The Constitution – Protection of Basic Human Rights

Section 24 of the South African Constitution (Act 108 of 1996), affords all South Africans the right to an environment that is not harmful to their health or well-being, and to have the environment protected, for the benefit of present and future generations, through reasonable legislative and other measures. This is a legislative obligation of the state to its citizens. In the broader context of creating safer environment for the citizens, the local authorities (municipalities) have a mandate to deliver basic services (housing, roads, water, etc.) in a sustainable manner and ensure adherence to disaster risk reduction principles. A selected list of critical statutes is presented in Fig. 2.

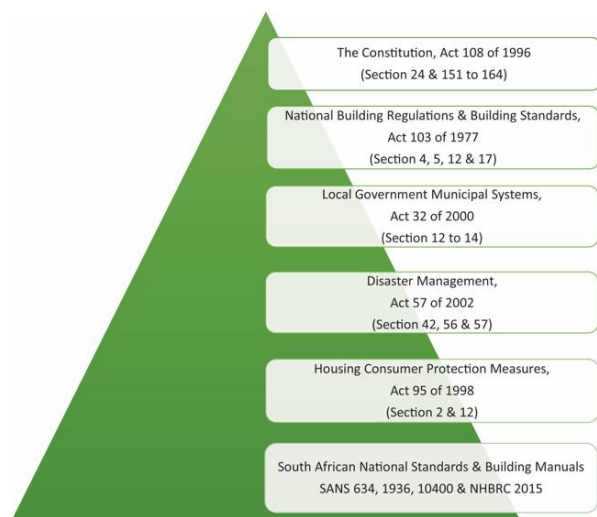


Fig.2: A selected list of critical statutes governing the building practice in South Africa.

In terms of Section 151(2), the executive and legislative authority of a municipality is vested in its Municipal Council and Section 151 (3) further state that a municipality has the right to govern, on its own initiative, the local government affairs of its community, subject to provincial and national legislation. Municipal status, objectives, duties and categories are prescribed in Section 151 to 164 of the Constitution. Therefore, municipalities have the executive and legislative authority to ensure that their communities are not exposed to an environment that is harmful to their health or well-being.

### 3.2 Supporting statutes to the Constitution

To give effect to the state constitutional obligation, a series of statutes have been promulgated to provide a legislative framework within which building practice operates in South Africa and their legislative intent are as follows:

- The National Building Regulations and Building Standards (Act 103 of 1977 – NBRBS), as amended is the principal building law in South Africa with a primary objective to promote uniformity in the law relating to erection of buildings.
- Local Government Municipal Systems (Act 32 of 2000 - LGMS), provide for the core principles, mechanisms and processes that are necessary to enable municipalities to move progressively towards the social and economic upliftment of local communities, and ensure universal access to essential services.
- Housing (Act 107 of 1997), provide for the facilitation of a sustainable housing development process; for this purpose to lay down general

principles applicable to housing development in all spheres of government.

- Disaster Management (Act 57 of 2002 – DM), provide for an integrated and co-ordinated disaster management policy that focuses on preventing or reducing the risk of disasters, mitigating the severity of disasters, emergency preparedness, rapid and effective response to disasters and post-disaster recovery.
- Housing Consumer Protection Measures (Act 95 of 1998 – HCPM), make provision for the protection of housing consumers; and to provide for the establishment and functions of the National Home Builders Registration Council; and to provide for matters connected therewith.
- Infrastructure Development (Act 23 of 2014 – ID), provide for the facilitation and co-ordination of public infrastructure development which is of significant economic or social importance to the Republic, to ensure that infrastructure development in the Republic is given priority in planning, approval and implementation.
- Standards (Act 8 of 2008), provide for the development, promotion and maintenance of standardization and quality in connection with commodities and the rendering of related conformity assessment services. This act provide the basis for the compilation and publication of national standards.

## IV. CHALLENGES FACING THE BUILDING LEGISLATION

### 4.1 The Building Legislation and Regulatory Process

Various sections of Act 103 of 1977, provide the basis for the establishment of regulatory process(es) in the building practice. In the context of regulating the building process, Section 4 stipulates that “no persons shall without prior approval by local authority, erect any building”, Section 5 states that “local authority shall appoint a person as building control officer”, Section 12 states that “if conditions of the land poses danger to life or property, such condition must be investigated and secured” and finally, Section 17 “provide for the establishment/publication of the National Building Regulations (NBRs)”.

The NBRs stipulates functional requirements that the proposed design or construction of the building must satisfy prior to approval by the local authority. According to the current deemed-to-satisfy standard for development of dolomite land, the South African National Standard

(SANS) 1936:2012, “An application for land use rights, made to any relevant authority, shall include a sufficient level of information to provide confidence in the presented determinations” and “The philosophy to be applied in the design of the foundations is that there shall be sufficient structural integrity and stability to allow occupants to safely escape in the event of sudden loss of support below the foundations of the structure”. This is based on the requirement to identify a hazard, determination of an Inherent Hazard Class (IHC), selection of permissible land use types and appropriate risk mitigation measures for each dolomite site to be developed.

South Africa’s past experience on the impact of sinkhole and subsidence formation has enabled the formulation of scientifically based building principles. These principles are detailed in scientific publications like Jennings et al. (1965), Brink (1979), Buttrick and van Schalkwyk (1995), Buttrick et al. (2001) and Buttrick et al. (2011), and have since been adopted into the relevant deemed-to-satisfy standards like SANS 1936 and SANS 10400. These are published under the Standards (Act 8 of 2008), giving them the mandatory status. In addition, the National Home Builders Registration Council (NHBRC) has been established under Section 2 of the Housing Consumer Protection Measures Act (Act 95 of 1998) to ensure added protection of housing consumers. Section 12 of this act states that the NHBRC must publish a Home Building Manual containing technical requirements and guidelines with which registered home builders shall comply, i.e. Part 13 of the NHBRC 2015 Home Building Manual.

The current South African building regulatory system is generally a “Performance-Based System” in nature and it prescribes a set of principles needed to satisfy the functional requirements. Deemed-to-satisfy standards define the technical requirements (investigation, analysis, mitigation measures and risk management, design and construction methods) for a building project to satisfy, which if enforced and complied with, will ensure adherence to functional requirements and ultimately, the protection of basic human rights. Watermeyer et al (2008) described a four level performance based regulatory system which has formed the basis for the development of a national standard for the development of dolomite land. A summary of the current performance-based building regulatory system in as far as it relates to building on dolomite land is presented in Fig. 3.

The challenge is however that not all areas are the same in terms of the geological, geotechnical, hydrological or climate conditions that may influence impact of sinkholes and subsidence formation, and neither are all areas equal in terms urbanisation or development density. Accordingly, Section 4 and 12 of the Act 107 of 1977 establish a single

building approval authority (the local sphere of government) aimed at ensuring consistent compliance to the functional requirements to investigate dangerous ground conditions. Furthermore, Section 5 gives only the local sphere of government the authority to a person “building control officer” to administer the NBRs functional requirements, and control the on-site activities on building projects within their area of jurisdiction. In this context, only the local sphere of government has the executive and legislative authority to approve building projects or enforce the NBRs.



Fig.3: Summary of a performance-based regulatory system (modified from Watermeyer et al., 2008)

However, other provincial and national departments including private entities may implement “Strategic Integrated Projects (SIPs)” under the Infrastructure Development (Act 23 of 2014) without prior consultation or approval by the local authority. Therefore, this duplication of responsibilities in the building regulatory process suggests that the current legislative framework contains some gaps and/ or conflicting legislative authority. In practice, this may lead to a dereliction of some building functional requirements as stipulated in the NBRs, which could potentially give rise to implementation challenges and negative effects due to inappropriate development on geologically hazard prone areas including dolomite land.

#### 4.2 The Building Legislation and Regulatory Gaps

Despite the constitutional intent in terms of Section 24 of the Constitution and Section 12 of Act 103 of 1977 to give effect to the constitutional principles as these relates to safe erection of buildings or a requirement to investigate dangerous land conditions, but there are problems in the

building practice. These problems are characterised by either inconsistent enforcement of the NBRs functional requirements at the decision making level and/ or the duplication of responsibilities in the building regulatory process.

For example, the deemed-to-satisfy rules like those stipulated in SANS 1936 or NHBRC 2015 Home Building Manual are generally not enforced during the formulation of Integrated Development Plans (IDPs) by the relevant state authorities. This often leads to the proclamation of townships on geologically hazard prone terrains without prior due considerations of the prevailing ground conditions. A review into the pertinent building legislation, therefore, suggests that there are gaps in the current building legislation and regulatory process as summarised in a schematic representation, Fig. 4.

In broad terms, the acceleration or exemption of the SIP's from the normal building regulatory process suggests possible omission of some functional requirements as stipulated in the principal building law. As such, the building practice is exposed to a risk of having building projects endorsed under the provisions of the Act 23 of 2014 and without prior due considerations of the possible dangerous ground conditions.

However, SIPs are not the only building projects implemented under an accelerated approach, subsidy housing built under the Reconstruction and Development Programme (RDP) are often exempted from adhering to the normal building regulatory process because political targets often supersede the legislative intent, especially during election periods.

Therefore, the dereliction of a legislative intent across all spheres of government based on economic, social or political importance has the potential to render NBRs functional requirements redundant. Such gaps in the regulatory process could mean that, although the pertinent building legislation prescribes necessary functional requirements for civil engineering or building projects, but in practice, infrastructure and human exposure to risks associated with development of geologically hazard prone terrains, including dolomite land, is not adequately addressed.

#### 4.3 The Building Legislation and Implementation Challenges

The past building legislation failed to force the state to invest into the geological or geotechnical studies aimed at reducing the impact of disaster risks on geologically hazard prone areas earmarked for development. In reality, the problem still persists today meaning that the current constitutional intent to articulate societal needs and

expectations is deferred. Geological unsuitable areas are being developed without prior due considerations of the prevailing ground conditions. This situation has created and continues to create hostile legacies for citizens to bear and the State to address. In the context of safe development of dolomite land, Buttrick et al. (2001), published a modified version of the "Method of Scenario Supposition", which has since been adopted into the SANS 1936 for development of dolomite land. This method requires that a hazard be identified, associated risk assessed and quantified, i.e. Inherent Hazard Class (IHC 1-8) and a D-Classification (D1-D4) be assigned prior to a decision on appropriate development types on dolomite land.

SANS 1936 demonstrates great scientific advancements which strive to bridge the gap between the existing scientific knowledge and the applicable legislation for consideration during the compilation of IDPs driving the spatial planning process.

According to SANS 1936 any organisation, department, state entity or individual owner that develops a parcel of dolomite land shall ensure compliance with the provisions of the relevant sections in Part 4.

Therefore, there is a need to discuss possible sources for non-compliance to functional requirements and to evaluate how these can be managed. As such, the capacity (fiscal & technical) of the approving organs of state and local authorities to implement NBRs functional requirements needs urgent attention and any identified capacity gaps must be addressed. As discussed above, building legislation in its current form is not particularly effective when used for decision making in land identification for development and is not responsive to pre- and post-developmental requirements for geologically hazard prone terrains.

This results in authorities identifying terrains like dolomite land unsuitable for certain land use types where risks cannot be economically mitigated years after a completed construction phase. However, avoiding dolomite land for development is also not an option. In practice, lack of consistent implementation of building legislation is considered to emanate from challenges set out in Table 1.

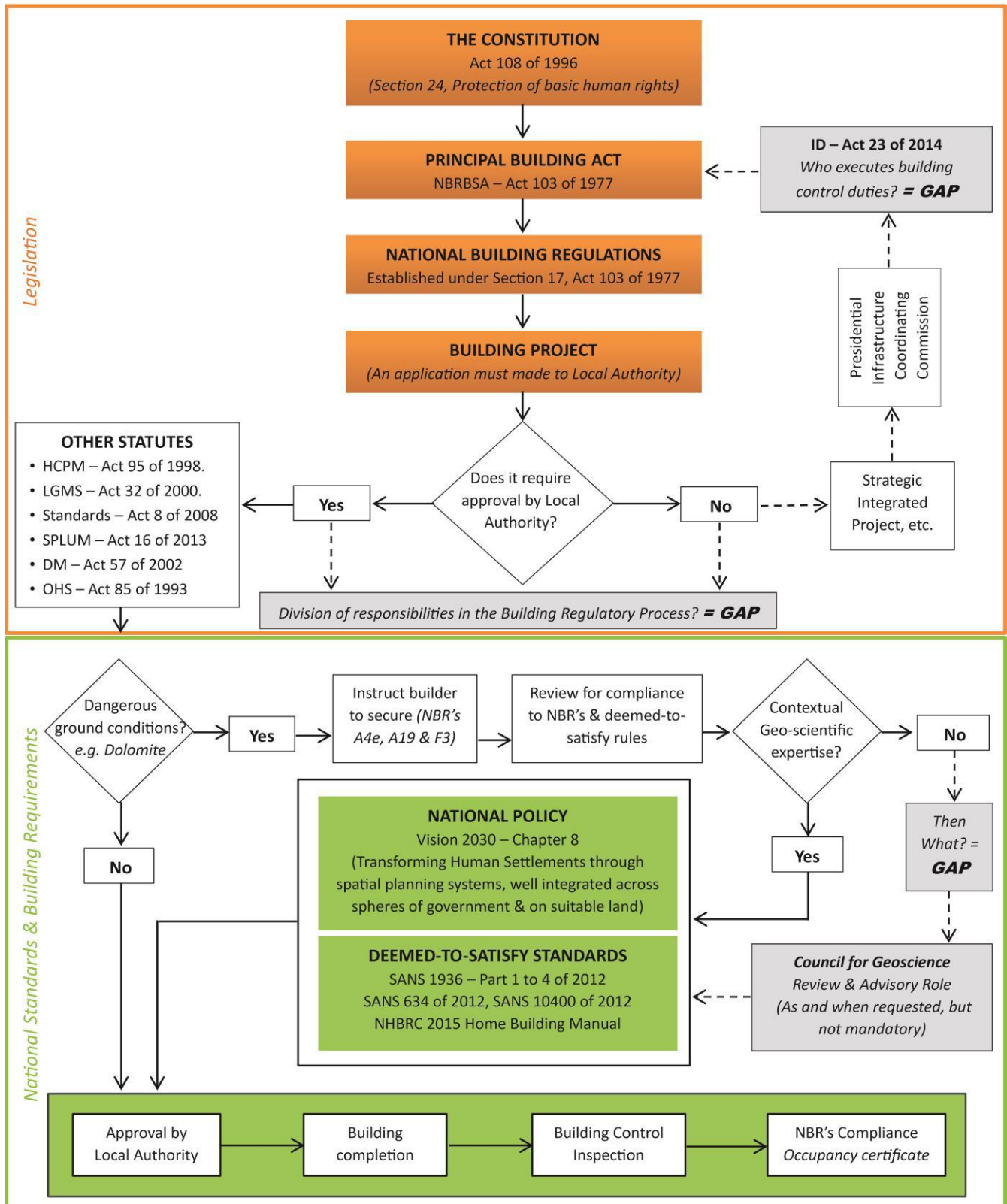


Fig.4: Summary of the building legislation and regulatory process

4.4 The Building Legislation and Damaging Effects

According to Buttrick et al. (2011), 4 to 5 million South Africans reside or work on dolomite land. In addition, South Africa has 46 of its 278 (17%) municipalities either

directly underlain by dolomite rock at surface or have a portion of dolomite land within their area of jurisdiction.

The latent danger of such terrain on infrastructure, including impact on the social well-being of citizens and



exposure to elevated frequency of ground instability events are well established in the scientific literature like Jennings et al, (1965), Bezuidenhout and Enslin (1969), Brink (1979), Kleywegt and Pike (1982), De Bruyn and Bell (2001) and Buttrick et al, (2001).

Buttrick et al, (2011), also refer to the relocation of a community of 30,000 households on dolomite land being relocated to safer ground in an area west of Johannesburg. Furthermore, South Africa should have gained adequate

experience from the sinkhole and subsidence catastrophes of the 1960's to 1970's as detailed in Brink (1979), Wolmarans (1984 & 1996) and Richardson (2013) to justify appropriate amendments to the current building legislative framework.

Identified gaps in the legislation and implementation challenges may have contributed to the continued destruction of infrastructure in particular, due to the formation of sinkholes as shown in Fig. 5.

Table.1: Challenges prohibiting the consistent implementation of building legislation.

No.	Description of Challenge	Comment
1	Silo Practice	Lack of a broad partnership across spheres of government, departments or state entities involved in building projects.
2	Capacity	Lack of capacity (fiscal & technical) at the local sphere of government, i.e. local authority responsible for administration of the NBR's requirements, control of the on-site activities and compliance to building regulatory process.
3	Division of Responsibilities	More than one state entity or department has the legislative authority to implement building projects using the provisions of different statutes, i.e. Act 103 of 1977 versus Act 23 of 2014.
4	Political and administrative Issues	Interference by executive authority on building processes and administrative instability at key organs of state like municipalities or implementing departments could lead to the dereliction of critical regulatory requirements.
5	Public Awareness	Lack of understanding of the dolomite land by the general public (planners, policy & decision makers, developers, etc.) often leads to difficulties in regulating a building process. Any effort to regulate dolomite impacts must begin with data collection and education.

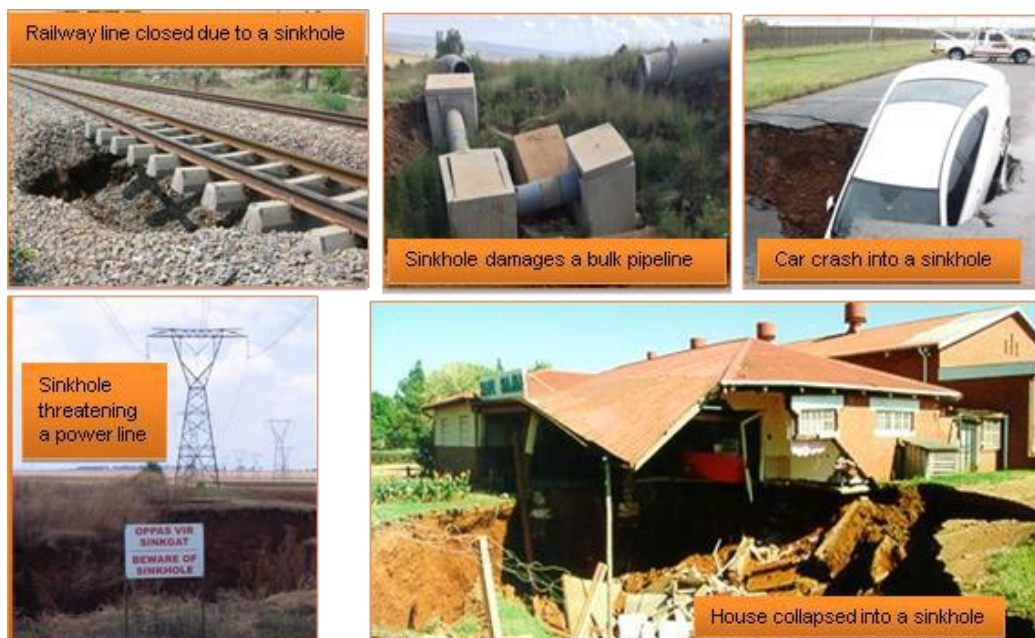


Fig.5: Examples of sinkhole impact associated with dolomite land in South Africa (© CGS Database)

V. CONCLUSION

A comprehensive legislative framework established to

regulate and promote uniformity in law relating to erection of buildings including the associated infrastructure exists

in South Africa. This is in accordance with the constitutional intent to protect basic human rights and to create an environment that is not harmful to the health or well-being of the citizens. Therefore, good legislation and policies have been promulgated in South Africa post-1994. However, it is also imperative to consider that without proper implementation good legislation serves no useful purpose.

A review of the applicable legislation in the context of building practice suggests that building legislative framework in its current form contains some gaps. These may have led to the implementation challenges and the continued damaging effects to property or infrastructure as summarised in Fig. 6. Buttrick et al. (2001), stated that sinkholes are generally of limited areal extent (diameter <100 m), but can manifest within minutes and without warning. In light of the identified gaps in the building legislation and implementation issues, it is concluded that communities residing on or cities built on dolomite land without due consideration of the pertinent functional requirements may be exposed to an unexpected risk of sinkhole formation. It is also crucial to consider that avoiding dolomite land for development is not practical and therefore, amendments to the current building law, promulgation of unambiguous policies and by-laws preventing approval of small (<1000 m<sup>2</sup>) residential stands within 50 m distance from high risk areas or known ground instability events is necessary.

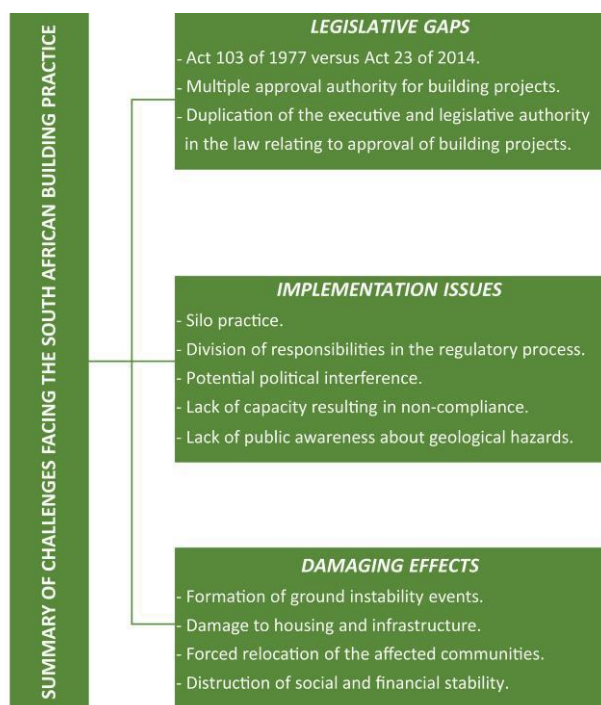


Fig.6: Summary of possible challenges facing the building industry in South Africa

In conclusion, a commitment to implement legislated functional requirements by decision makers, state organs, bulk service providers, contractors and individual site owners is central to the idea of sustainable development. Effective influence of the building legislation is also dependent on this commitment and failure by those involved to agree on the appropriate solutions could mean that the constitutional intent to protect basic human rights remains an academic concept. A closer interaction between geo-scientists and the decision makers (officials), more specifically at local sphere of government, is crucial in order to improve their mutual understanding of building regulatory processes and reduction of disaster risks on geologically hazard prone terrains. Furthermore, the interactions shall be aimed at improving the understanding of the link between spatial planning, sustainable infrastructure development, geohazards and disaster risk reduction.

Therefore, the recommendation is that, relevant sections in the Act 103 of 1977 be amended to stipulate that “no major development, expansion of existing development or township proclamation is permitted unless appropriate geohazard assessment studies have been conducted” and Act 57 of 2002 be amended to stipulate “guiding principles for funding of pre-disaster Geological Hazard Mitigation Plans” in response to the United Nations disaster risk reduction principles. The recommendations are made with an observation that the current building legislation has rather created a situation where the state responsibility to secure dangerous ground conditions has been relegated to an individual site developer. Relegating government functions to the private sector (property developers) and individual home/ site owners is dangerous.

## ACKNOWLEDGEMENTS

The authors acknowledge the data and monetary contributions by the South African Council for Geoscience towards this research.

## REFERENCES

- [1] Bezuidenhout, C. A. and Enslin, J. F., 1969. Surface subsidence and sinkholes in the dolomitic area of the Far West Rand, Transvaal, South Africa, in Proceedings of the First International Symposium on Land Subsidence, Tokyo. UNESCO Publication No 88, Paris, pp. 482 – 495.
- [2] Brink, A.B.A., 1979. Engineering Geology of Southern Africa. Volume 1. Building Publications, Silverton, 1979.
- [3] Buttrick, D.B. and Van Schalkwyk, A., 1995. The Method of Scenario Supposition for Stability Evaluation of sites on Dolomite Land in South Africa. South African Institution of Civil Engineering Journal. Fourth Quarter 1995, pp 9 – 14.

- [4] Buttrick, D.B., Van Schalkwyk, A., Kleywegt R.J. and Watermeyer, R., 2001. Proposed method for dolomite land hazard and risk assessment in South Africa. South African Institution of Civil Engineering Journal. Volume 43(2) 2001, pp. 27-36.
- [5] Buttrick, D.B., Trollip, N.Y.G., Watermeyer, R.B., Pieterse, N.D. And Gerber, A.G., 2011. A performance based approach to dolomite risk management. Environmental Earth Sciences, January 201. pp 1127-1138.
- [6] De Bruyn, I.A., Bell, F.G., 2001. The Occurrence of Sinkholes and Subsidence Depressions in the Far West Rand and Gauteng Province, South Africa and Their Engineering Implications. Environmental & Engineering Geoscience VII (3), 281-295.
- [7] Ford, D.C. and Williams, P.W., 1992. Karst Geomorphology and Hydrology. New York: Chapman and Hall.
- [8] Gutierrez, F., Parise, M., De Waele, J. And Jourde, H., 2014. A review on natural and human induced geohazards and impacts. Earth Science Reviews 138. August 2014, pp. 61-88.
- [9] Jennings, J.E., Brink, A.B.A., Louw, A. And Gowan, G.D., 1965. Sinkholes and subsidences in the Transvaal dolomite of South Arica. In; Proceedings 6th International conference of soil Mechanics and foundation engineering, Montreal, pp 51-54.
- [10] Kleywegt, R.J. and Pike, D.R., 1982. Surface subsidence and sinkhole caused by lowering of the dolomitic watertable on the Far West Rand Gold Field of South Africa. Annals of the Geological Survey of SA. Vol. 16, pp 77-105.
- [11] NHBRC, 2015. Home Building Manual and Guide – 2015. National Hpme Building Registration Council, Communications, Sunninghill, Johannesburg.
- [12] Oosthuizen, A.C., and Van Rooy, J.L., 2015. Hazard of sinkhole formation in the Centurion CBD using the Simplified Method of Scenario Supposition. Journal of the South African Institute of Civil Engineering, Volume 57 No.2, June 2015, pp 69-75.
- [13] Richardson, S., 2013. Sinkhole and subsidence record in the Chuniespoort Group dolomite, Gauteng, South Africa. Unpublished M. Sc. thesis, University of Pretoria, Pretoria, 2013.
- [14] South Africa, 1977. National Building Regulations and Building Standards Act – 103 of 1977, Government Printer, Pretoria.
- [15] South Africa, 1996. The Constitution of the Republic of South Africa Act – 108 of 1996, Government Printer, Pretoria.
- [16] South Africa, 1998. Housing Consumer Protection Measures Act – 95 of 1998, Government Printer, Pretoria.
- [17] South Africa, 2000. Local Government Municipal Systems Act – 32 of 2000, Government Printer, Pretoria.
- [18] South Africa, 2002. Disaster Management Act – 57 of 2002, Government Printer, Pretoria.
- [19] South African National Standard, 2012. Geotechnical Investigations for Township Establishment – SANS 634:2012. Edition 1 Published by SABS Standards Division, Pretoria 0001
- [20] South African National Standard, 2012. The Application of the National Building Regulations. SANS 10400:2012. Edition 3 Published by SABS Standards Division, Pretoria 0001.
- [21] South African National Standard, 2012. Development of dolomite land – SANS 1936:2012 – PART 1 to 4. Editions 1 Published by SABS Standards Division, Pretoria 0001.
- [22] South Africa, 2014. Infrastructure Development Act – 23 of 2014, Government Printer, Pretoria.
- [23] Watermeyer, R.B., Buttrick D.B., Trollip, N.Y.G., Gerber, A.A. and Pieterse, N. (2008). A performance based approach to the development of dolomite land. Proceedings of the Geotechnical Division of SAICE’s Conference on Problem Soils in South Africa. 3-4 November, Midrand.
- [24] Wolmarans, JF. 1984. Dewatering of the dolomite area on the Far Wes Rand: Events in perspective. Unpublished DSc thesis, University of Pretoria. (title translated from Afrikaans).
- [25] Wolmarans, J.F., 1996. Sinkholes and subsidences on the Far West rand. Seminar on the engineering geology of dolomite areas, university of Pretoria, Pretoria, 18 January 1996.



# Analysis of Dynamic Changes of Winter Wheat in Xinye County, Henan Province Based on SVM Method

Yan Si<sup>1</sup>, Bing-Yuh Lu<sup>2</sup>, Yun-Shang Wang<sup>3</sup>, Ruet-Yuan Wang\*<sup>4</sup>

<sup>1,4</sup>School of Science, Guangdong University of Petrochem Technology (GDUPT), China <sup>2</sup>Faculty of Automation, Guangdong University of Petrochemical Technology, China

<sup>3</sup>Graduate Institute, Fu Jen Catholic University

\*Corresponding author

Received: 13 Sep 2023; Received in revised form: 25 Oct 2023; Accepted: 05 Nov 2023; Available online: 11 Nov 2023

©2023 The Author(s). Published by Infogain Publication. This is an open access article under the CC BY license

(<https://creativecommons.org/licenses/by/4.0/>).

**Abstract**— *The guarantee of grain yield is an important issue for national security. Wheat is one of the main grain crops in China, and monitoring the spatio-temporal changes in its planting area and yield has important implications for decision-making support. With the development of remote sensing technology, estimating the long-term changes in the area of wheat planting has become a vital agricultural monitoring method. This article uses GF-1 satellite WFV sensor data to estimate the wheat planting areas in Xinye County, Henan Province in 2017, 2020, and 2023, mainly using SVM algorithm for calculation and comparison. After classification, the overall classification accuracy reaches over 95%, and the Kappa coefficient is above 0.95. The results show that the winter wheat planting area in Xinye County has shown an increasing trend over the past six years, from 34296.295 hm<sup>2</sup> in 2017 to 56914.662 hm<sup>2</sup> in 2023. By analyzing and summarizing the changes in regional crops, it has an important contribution to regional production and agricultural evaluation decision-making.*

**Keywords**— *Support Vector Machine (SVM), Winter wheat; Spatial and temporal distribution, Dynamic changes, Agricultural remote sensing*



## I. INTRODUCTION

Winter wheat is an important grain crop in China, and Xinye County, Henan Province, is a major grain producing county. Obtaining its agricultural spatial distribution information is of great significance for the local agricultural informatization and professional intelligent development. Traditional agricultural surveys require a significant amount of manpower, material resources, and time costs, and the final results cannot reflect spatial distribution information. The use of computer technology can further reduce costs, making survey results more

intuitive and improving efficiency through timeliness and visualization. Using remote sensing satellite data to detect crops in planting areas can meet the timely and long-term estimation needs of large areas. By analyzing data from multiple periods, resolutions, and sources, data on crop distribution, area, and yield estimation can be effectively obtained.

The research on grain estimation using agricultural remote sensing is to effectively distinguish monitored crop categories from other land features through algorithms and thresholds. The commonly used method is to establish

thresholds by normalizing vegetation indices to distinguish wheat from other land features. For example, Zhao et al. (2012) used the monthly normalized vegetation index to establish a linear model for winter wheat yield, which can effectively, quickly, and accurately estimate winter wheat yield [1]; Hao et al. (2017) used the normalized vegetation index as a threshold to segment and extract winter wheat, and calculated the area, achieving good results [2]; Liu et al. (2019) established a yield estimation model using normalized plant mean based on the annual average yield of rice, achieving remote sensing estimation of rice yield [3]; Ren et al. (2006) selected NDVI data ranging from 0.2 to 0.8 during the critical growth period of winter wheat and established their relationship with winter wheat yield, obtaining yield estimation data with an error of within 4%, which has high accuracy [4]. In addition, there are also methods for analyzing and identifying crops using multi-source data: for example, Feng et al. (2023) used multivariate remote sensing data to analyze Sentinel-1 SAR images and Sentinel-2 optical remote sensing images, and used SVM algorithm to achieve an overall classification accuracy of 94.3% [5].

Furthermore, different algorithms can also be used to better classify crops on the surface. For example, Sun et al. (2017) used different algorithms for supervised classification and compared the characteristics of six classification methods. The results showed that the producer and user precision of each classification method had different differences and could not be applied to all types of land objects. Each classification method had different advantages in different land object categories. Among them, the maximum likelihood classification (MLC), support vector machine (SVM) classification, and artificial neural network (ANN) classification have better overall classification accuracy and Kappa coefficient [6]. Many studies have shown that SVM has good advantages, for example, Sun et al. (2013) used SVM algorithm to monitor land use and cover changes in the Abihu Lake area in 1990, 2001, and 2011, and concluded that SVM classification method is the optimal classification method [7]; Guo et al. analyzed and evaluated six classification methods, including SVM, and concluded that the accuracy of SVM based classification methods is higher than other classification methods through comparative analysis of

classification experimental data; Chen et al. (2019) used multispectral images as the basis to train and effectively recognize landslide sample points in remote sensing images using landslide area SVM detection models [8]; Zu (2018) processed the remote sensing images of Zhuhai in Phase III, used SVM algorithm for land and water separation, and conducted cross processing on the results. The extracted coastline was analyzed to obtain the coastal construction changes of Zhuhai in the past decade [9]; Zhang et al. (2016) used SVM algorithm to classify wetland water bodies, and the results showed that SVM has higher accuracy in various aspects than traditional methods, making it very suitable for wetland information extraction and monitoring in arid areas [10]. In addition, the SVM classification method has been repeatedly tested as a mature and high-precision classification algorithm.

The selection of remote sensing data is mostly based on Sentinel and Landsat series satellites. However, in recent years, with the continuous improvement of domestic satellite level, high resolution series satellites have gradually been widely used. In terms of spatial resolution, medium and low resolution satellites have certain advantages in terms of breadth and temporal resolution, which have good benefits for large research areas. At the same time, they can compare the ground conditions of different years and the same time period, which can improve the requirements for temporal resolution. Based on this, this study is using the SVM classification algorithm, mainly using data from the GF-1 satellite WFV sensor with a spatial resolution of 16 meters. Xinye County is selected as the study area, and the distribution of winter wheat crops for three years is extracted and land use change statistics are conducted to analyze the area change of local grain crop cultivation, in order to obtain visual spatial information of crops.

## II. STUDY AREA AND DATA SOURCES

### 2.1 Study Area

Xinye County is located in the southwest of Henan Province ( $112^{\circ} 12' 44'' \sim 112^{\circ} 35' 42''$  E,  $32^{\circ} 19' 30'' \sim 32^{\circ} 49' 08''$  N), with a total administrative area of 1062km<sup>2</sup> (Figure 1). It belongs to the northern subtropical monsoon climate, with an average annual temperature of 16–17°C, an average annual precipitation of 800-900mm,

and an average annual frost-free period of 227 days. In summer, the temperature is high, precipitation is concentrated, and drought and flood disasters are frequent. In winter, it is dry and cold, with a small amount of rain and snow. Due to its location in the transitional zone between the north and south of China, the transition zone has obvious characteristics: a warm and humid climate, distinct seasonal changes, a long frost-free period, sufficient solar radiation, and being suitable for wheat growth, making it a key area for agricultural development in China. Xinye County is located in the hinterland of the Nanyang Basin, with a flat and vast terrain and an average elevation of around 100m. It is the only county in Nanyang City that does not have a mountainous distribution. There are two main rivers within the territory: the Bai River and the Tang River, as well as numerous tributaries. The river generally passes through the county town from north to south and finally enters the Han River in Hubei, returning to the Yangtze River basin.

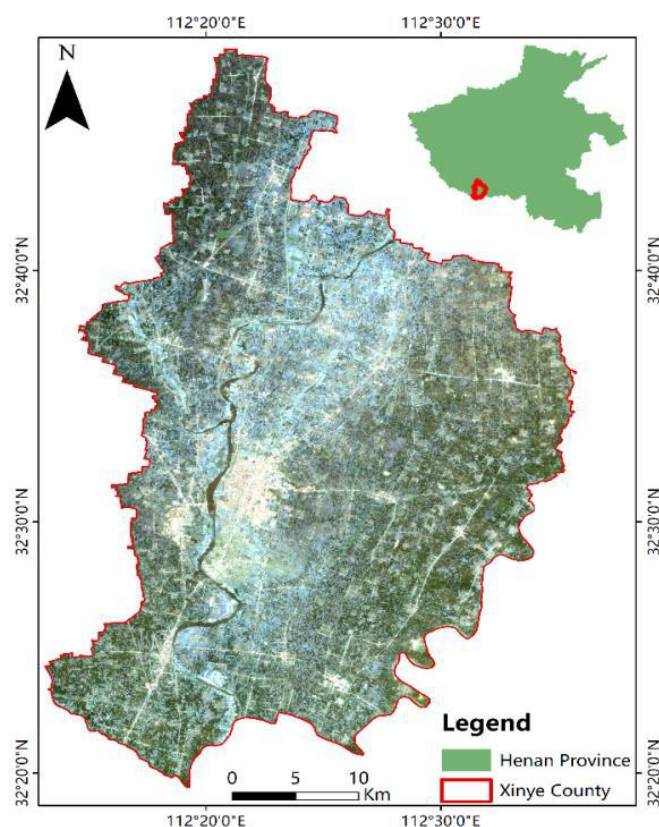


Fig.1 Regional Overview of Xinye County Prefecture

Under the influence of superior climate and hydrological resources, the perennial wheat planting area

of Xinye County can reach 533000 hectares, with a total yield of 3.25 billion kilograms, accounting for 11% of the yield in Henan Province and 1% of the national yield. It is truly a major grain county.

## 2.2 Data Sources

The remote sensing data source of this study is the GF-1 satellite WFV sensor data from the China Resources Satellite Application Center in 2017, 2020, and 2023 (<https://data.cresda.cn/#/home>). In the experiment, LANDSAT-8 L2 data was also used for geographic registration of images at different time resolutions, while ASTER GDEM 30M resolution DEM was used, which was sourced from the geospatial data cloud (<https://www.gscloud.cn/home>).

This article is based on ENVI software, after radiation correction, and uses the Atmospheric Correction Algorithm Tool (FLAASH) to produce available GF-1 series satellite data covering the Xinye County area in 2017, 2020, and 2023.

The ROI sample data is produced by combining the sample data with human visual interpretations of Google Earth high-resolution images. The classification of this study is divided into four types: water body, wheat, buildings, and bare land. Images at different times are compared and modified to avoid changes in the selected pixels at different times, which may affect the accuracy of the classification data.

## III. METHODOLOGY

The analysis image in this article is based on the GF-1/WFV satellite image with a 16m resolution spectral band as the main data source, assisted by Landsat-8 L2 level data. Sample data is constructed by identifying the spectral features of different land features, and SVM classification algorithm is used to conduct research using a human-machine interaction interpretation platform. The winter wheat planting information in the Xinye County area in 2017, 2020, and 2023 is obtained (Figure 2).

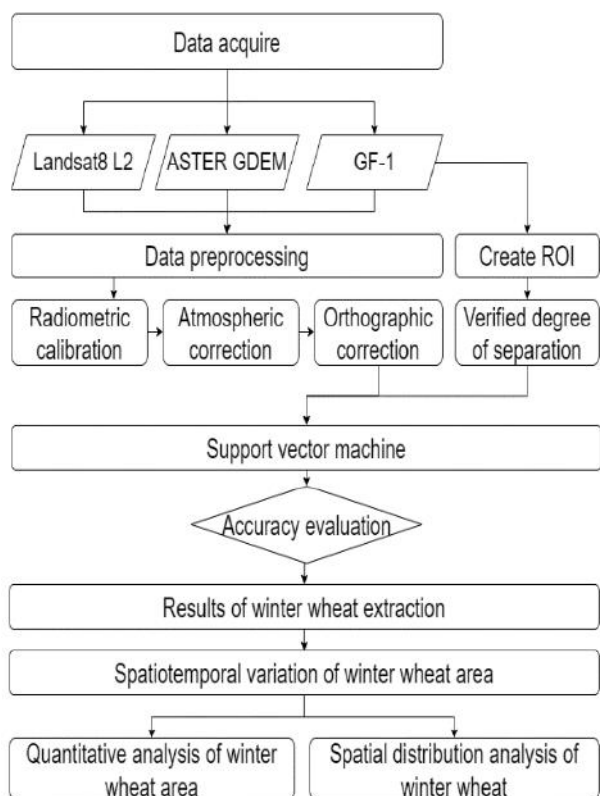
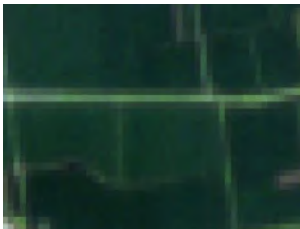
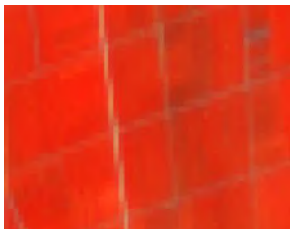

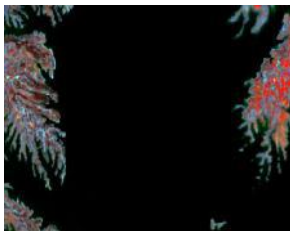
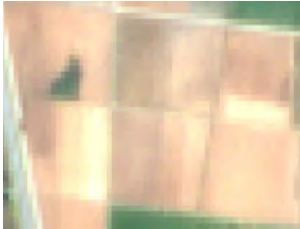
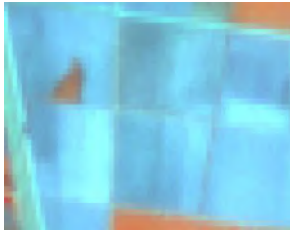


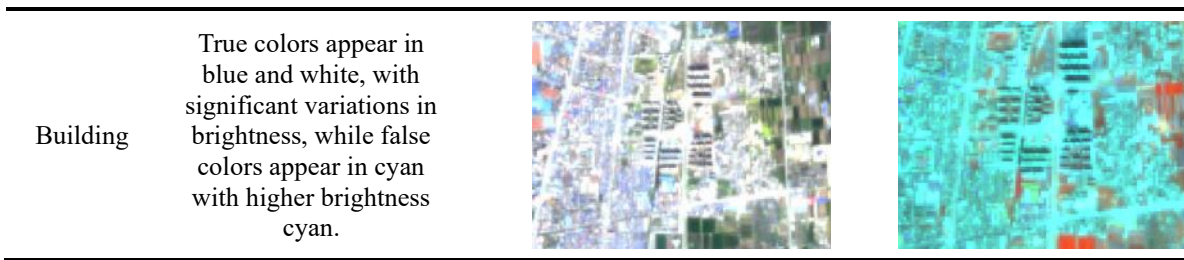
Fig.2 the Technology Roadmap of the Study

### 3.1 Obtaining ROI Sample Data

Due to the changes in the distribution of surface features in different years, except for rivers that have remained almost unchanged for six years, the planting of crops in different fields varies each year. The changes in bare land and wheat planting areas are significant, and manual sample data extraction is required for images from different years to establish training samples for subsequent interpretation. After repeated experiments and reference to other studies, a false color band combination of 432 was finally used for the production of ROI samples (Table 1). Under this band combination, the surface wheat showed a bright red color, while the bare ground showed a gray blue color, the buildings and roads were turquoise green, and the water body was black. Various objects can be distinguished well, which is helpful for the identification of objects and the production of sample areas, and can reduce the time cost of object identification.

Table 1 Ground Feature Characteristics of GF-1 Imagery in the False Color Band

Type	Characteristic	True color	False color
Wheat	Dark green or green appears in true colors, and red or orange red appears in false color combinations.		
Water body	The colors presented in true color and false color are similar, both being black.		
Bare land	True color appears in yellow, while false color appears in blue. There is a difference in brightness.		



The sample selection in the ROI area should cover the entire study area as much as possible, and the distribution of different types should also follow the principle of average distribution; Furthermore, the amount of image sample data in different time periods should be as close as possible to prevent significant differences in algorithm classification due to differences in sample data. Among them, the selection of water samples remained basically unchanged; The changes in buildings are also relatively small, with the addition of some roads and building areas in 2023; The selection of samples for bare land and wheat has relatively significant changes, and it can be observed from the images that the range of bare land has decreased, so the selection of samples has gradually decreased. The opposite is true for wheat samples (Table 2). The average separation degree of the sample pixels extracted based on the above principles is above 1.93, which meets the requirement of separation degree above 1.8.

Table 2 Sample Data Pixel Table (Unit: piece)

	2017	2020	2023
Water body	7108	7328	7012
Building	7746	5944	7852
Bare land	6230	5978	5630
Wheat	12420	13433	16513

**3.2 SVM Classification Algorithm**

Support Vector Machine (SVM) is a class of generalized linear classifiers that perform binary classification of data using supervised learning. Its decision boundary is the maximum-margin hyperplane that solves the learning sample. The algorithm logic is to transform the analyzed dataset into a high-dimensional new space through nonlinear algorithms, and in the new space, classify the dataset through algorithms to achieve nonlinear discrimination. The basic principle of SVM classification is to set  $x_i \in R^d$  as the input mode on a sample dataset, and  $y \in \{\pm 1\}$  as the output target. Let the

equation for the optimal decision surface be:

$$w^t x_i + b = 0 \dots \dots \dots (1)$$

The weight vectors  $w$  and  $b$  offset must satisfy constraint  $y_i(w^t x_i + b) \geq 1 - \xi_i$ . In the formula  $\xi_i$  is the slack variable of the sample under linearly indivisible constraints, and is the degree to which the pattern deviates from the ideal situation. The essence of SVM is to fit multiple hyperplanes into one, separate two types of data, and find a decision surface that minimizes the average classification error of all data. Based on this, the optimization formula is derived as follows:

$$\phi(w, \xi) = \frac{1}{2} w^T w + c \sum_{i=1}^n \xi_i \dots \dots \dots (2)$$

Among them,  $c$  represents a positive parameter specified by the user, which is used for SVM to support the punishment of sample correctness and error. It is a parameter that balances the complexity of the algorithm and the proportion of error samples. By balancing the complexity and learning cost of classification with limited samples, good classification results can be achieved [11-13].

**3.3 Precision Evaluation**

The confusion matrix is the commonly used method for evaluating the accuracy of remote sensing classification. The classification results are quantitatively rated based on classification accuracy, Kappa coefficient, and other specific values. The calculation formula for Kappa coefficient is as follows:

$$kappa = \frac{p_o - p_e}{1 - p_e} \dots \dots \dots (3)$$

Where  $p_o = \frac{\text{sum of diagonal elements}}{\text{sum of matrix elements}}$ , which is the consistency observed between the two sample data;

$$p_e = \frac{\sum_i \text{Sum of elements in the } i\text{-th row} * \text{Sum of elements in the } i\text{-th column}}{(\sum \text{All elements of the matrix})^2}$$

, which is the consistency of opportunities between two



samples.

The Kappa coefficient is obtained by combining different precision parameters, with values between [-1, 1]. The closer it is to 1, the higher the consistency of classification and the better the classification effect.

#### IV. ANALYSIS AND RESULT

##### 4.1 Winter Wheat Extracted by SVM Algorithm

Based on the requirements of average distribution in the study area, average number of sampling points, and average distance of sampling points, the sample data was created and classified using the SVM algorithm to obtain the classification of ground objects at different time resolutions (Figure 3). The water body has more obvious features in the false color image, and the overall separation degree is good, which is the blue part in the figure. However, the variation between buildings and bare land in the frequency band is relatively small, and there are bright

pixels in both the bare land and buildings in the false color, which affects the classification results of the algorithm, as are the white and orange parts in the image. Finally, winter wheat performs particularly well in the frequency band, making it relatively distinguishable from bare land and buildings, as shown in the green part of the image.

The accuracy verification part involves manually selecting test sample points and evaluating classification accuracy. Ultimately, the overall classification accuracy of images in 2017, 2020, and 2023 can reach over 95%, and the Kappa coefficient remains above 0.95. According to the quantitative rating system, it is closer to "1", indicating good overall classification performance. However, due to the optical resolution of the image, the classification results of smaller-scale features are not obvious, but their errors are still within an acceptable range, which has little impact on the overall research data.

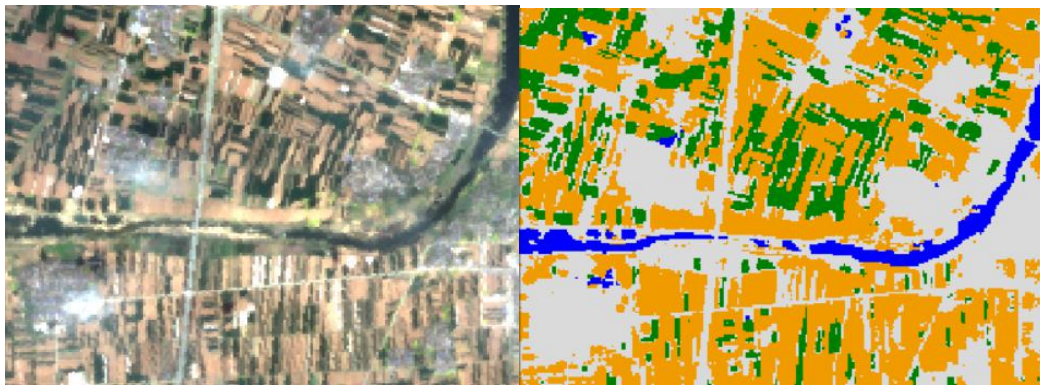


Fig.3 Comparison of Remote Sensing Images and Classification Results

##### 4.2 Analysis of Dynamic Changes in Winter Wheat

According to the classification results of the SVM algorithm, the distribution map of winter wheat planting areas in the study area was obtained, and it can be clearly observed that the winter wheat planting areas in Xinye County increased year by year from 2017 to 2023 (Figure 4). In 2017, there were also significant scattered patches in the wheat planting area, without a large-scale contiguous planting area. By 2023, it has been connected as a large-scale planting area. According to satellite image analysis,

the added area is the original bare land area. The central part of Xinye County is the county seat, and the overall area has not changed much. In 2017, there was a large amount of bare land in the north and south of the county town, and some wheat fields were interspersed among them, resulting in a large number of scattered wheat field areas. By 2023, a large amount of wasteland in the south and north will be reused, resulting in a significant increase in wheat cultivation areas.

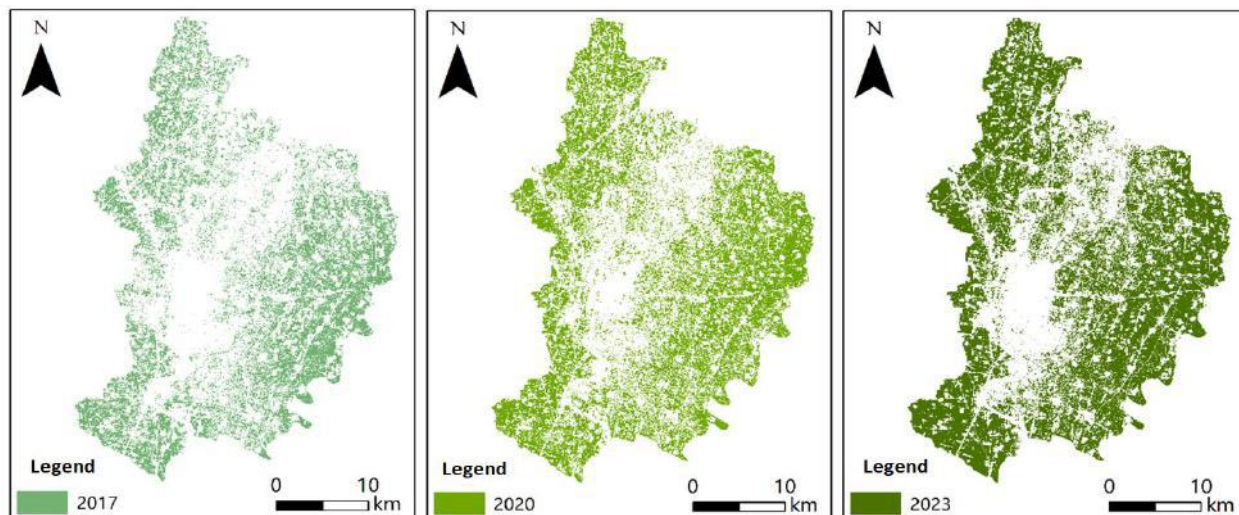


Fig.4 Temporal and Spatial Changes of Wheat Planting Areas in Xinye County

Using ArcGIS tool to conduct area statistics on the winter wheat planting areas in Xinye County for three years (Figure 5), the analysis shows that the total area of Xinye County is 106200 hm<sup>2</sup>, and the winter wheat area in April 2017 was 34296.295 hm<sup>2</sup>, accounting for 32% of the total area of the county; In April 2020, the winter wheat area was 46113.737 hm<sup>2</sup>, accounting for 43% of the county's total area; The winter wheat area in April 2023

was 56914.662 hm<sup>2</sup>, accounting for 54% of the entire county. The area of wheat planting areas has been increasing year by year, and the upward trend is obvious. At present, a circular surrounding planting area centered around the county town and river has been formed. The expansion of winter wheat cultivation in the future can develop into a large number of bare land near the river north of the central county town.

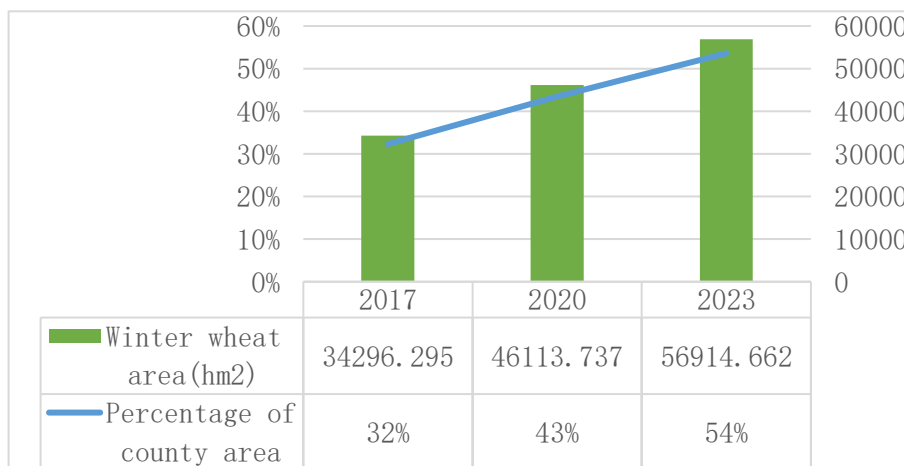


Fig.5 Changes in Winter Wheat Planting Area in Xinye County

**V. CONCLUSION**

This article uses the GF-1/WFV sensor image to extract the distribution information of winter wheat crops in Xinye County, Nanyang City, Henan Province in 2017, 2020, and 2023. High resolution satellite images are used as reference values to establish sample area (ROI), and accuracy verification is conducted to assist in dividing four

different types of feature pixels within the research area. SVM algorithm is used to classify and extract the distribution information of winter wheat crops from the WFV sensor, and the area is calculated. The final extraction effect meets the accuracy requirements. The main focus of this study is to verify the effectiveness of GF-1 imaging combined with SVM algorithm.

The overall classification accuracy of the SVM algorithm in this study is 95%. In the face of a small number of categories, moderate area, small terrain fluctuations, and relatively significant spectral differences of the research object, it has produced good results, and the visual effect is also relatively good. From the research process, the SVM algorithm has relatively high requirements for selecting research samples, and under better sample conditions, the classification effect will be better. In the study, the spectral differentiation between bare land and buildings was relatively low. As a result, the classification of the two types of features was unclear, but it did not affect the classification and extraction of winter wheat.

In terms of agricultural monitoring and analysis, the winter wheat planting area in Xinye County has been continuously increasing in the past six years, reaching 54% of the total county area in 2023. By utilizing a large amount of potential land, the planting area of food crops has been increased, ensuring food production.

This article obtained better classification results in a small scale, and in future research, it can be attempted to use SVM algorithm to study winter wheat in large areas and verify its effectiveness in large-scale space. Overall, this study utilizes remote sensing data sources and technology to monitor agricultural crop yields, which will help China achieve the goal of digitalization and intelligence in agriculture and move towards intelligent agriculture.

### ACKNOWLEDGEMENTS

The author is grateful for the research grants given to Ruei-Yuan Wang from GDUPT Talents Recruitment (No.2019rc098), in Guangdong Province, China, and Academic Affairs in GDUPT for Goal Problem-Oriented Teaching Innovation and Practice Project Grant No.701-234660.

### REFERENCES

[1] Zhao, W., He, Z., He, J., and Zhu, L. Remote sensing estimation for winter wheat yield in Henan based on the MODIS-NDVI data. *Geographical Research*, 2012, 31(12): 2310-2320. DOI:10.11821/yj2012120018.

[2] Hao, Z., Zhao, H., and Jiang, Y. Extraction of winter wheat

area information based on the improved NDVI density slicing method. *South to North Water Transfers and Water Science & Technology*, 2017, 15(3): 67272, 93.

[3] Liu, S., Niu, C., and Bian, L., Remote sensing estimation of rice yield based on NDVI. *Jiangsu Agricultural Sciences*, 2019, 47 (3): 193-198. doi:10.15889 / j.issn.1002—1302.2019.03.047

[4] Ren, J., Chen, Z., and Tang, H. Regional scale remote sensing-based yield estimation of winter wheat by using MODIS-NDVI data: A case study of Jining City in Shandong Province. *Chinese Journal of Applied Ecology*, 2006, 17(12): 2371-2375.

[5] Feng, Q., Ren, Y., Yao, X., Niu, B., Chen, B., and Zhao, Y. Identification of Winter Wheat in Huang-Huai-Hai Plain Based on Multi-source Optical Radar Data Fusion. *Transactions of the Chinese Society for Agricultural Machinery*, 2023, 54(2):160-168.

[6] Sun, K., and Lu, T. Comparison of Supervised Classification Methods in Remote Sensing Image Classification. *JIANGXI KEXUE*, 2017, 35(3):6.D0I:10.13990/j.issn1001-3679.2017.03.009.

[7] Sun, C., Li, X., and Meng, X. Analysis on Land Use and Land Cover Change and Driving Force of Ebinur Lake Region during the Past 20 Years Based on Support Vector Machine Classification. *Xinjiang Agricultural Sciences*, 2013, 50(7):1322-1329. DOI:10.6048/j.issn.1001-4330.2013.07.021

[8] Chen, S., Kang, Q., Shen, Z., and Zhou, R. Landslide Detection Based on Color Feature Model and SVM in Remote Sensing Imagery. *Spacecraft Recovery & Remote Sensing*, 2019, 40(6):10. DOI: 10.3969/j.issn.1009-8518.2019.06.011

[9] Zu, J. Coastal Line Extraction in Zhuhai City Based on Supervised Classification and Multi source Remote Sensing Data. *China Science and Technology Horizon*, 2018(22): DOI: 10.3969/j.issn.1671-2064.2018.22.087

[10] Zhang, X., and An, F. Research on Remote Sensing Classification for Ulungur Lake Wetlands Based on SVM. *HUBEI AGRICULTURAL SCIENCES*, 2016, 55(16):5. DOI:10.14088/j.cnki.issn0439-8114.2016.16.018.

[11] Zhang, F., Xue, Y., Li, Y., and Ding, X. Object-oriented building extraction of multi-source remote sensing imagery based on SVM. *Remote Sensing for Land & Resources*, 2008(2):27-29+47. DOI:10.6046/gtzyyg.2008.02.07.

- [12] He, D., Xiao, Y., Xiao, X., Huang, Y., and Zhou, Q. Application of the Support Vector Machine in Remote Sensed Image Processing. *Urban Geotechnical Investigation & Surveying*, 2006(3):4. DOI:10.3969/j.issn.1672-8262.2006.03.008.
- [13] Zhu, H., and Jia, Y. Remote Sensing Image Classification Based on Support Vector Machines. *Science Technology and Engineering*, 2010(15): 3659-3663. DOI:10.3969/j.issn.1671-1815.2010.15.023.



# **Analysis of Technical Efficiency and the Influence of Socioeconomic Factors on Oil Palm Farming in Muaro Jambi District - Indonesia**

Yanuar Fitri, Saidin Nainggolan

Department of Agriculture, Jambi University, Jambi, Indonesia  
Email: [yanuarfitri@yahoo.com](mailto:yanuarfitri@yahoo.com), [saidinnainggolan@yahoo.com](mailto:saidinnainggolan@yahoo.com)

Received: 03 Oct 2023; Received in revised form: 04 Nov 2023; Accepted: 11 Nov 2023; Available online: 20 Nov 2023  
©2023 The Author(s). Published by Infogain Publication. This is an open access article under the CC BY license (<https://creativecommons.org/licenses/by/4.0/>).

**Abstract**— *Technical efficiency and socioeconomic factors have a significant effect on the productivity of oil palm farming. Therefore, this study aimed to analyze technical efficiency and the influence of socioeconomic factors on oil palm farming. Sampling was conducted using the Simple Random Sampling method. The data used are primary data and secondary data. The analysis method used is descriptive analysis and Stochastic Frontier production function analysis with MLE method. The results showed that the average land area of farmers in oil palm plantations was 3.9 ha with an average productivity of 14,638 kg/ha. Production factors that have a significant effect on production are land area, NPK fertilizer, Urea fertilizer and Dolomite. While those that do not have a significant effect are labor and herbicides. The level of technical efficiency achieved was the lowest 0.81 and the highest 0.95 and with an average of 0.86 > 0.62 which means that farming is technically efficient. Socio-economic factors such as variables of age and distance from the farm to the farmer's house have the potential to reduce technical inefficiency but have no significant effect and variables that have a significant effect are variables of experience, education, and activeness in farmer groups while factors that increase technical inefficiency that have a significant effect are variables of land area.*



**Keywords**— *Self-help Pattern, Production Inputs, Production Response, Technical Efficiency, Socio-economic, Technical Inefficiency.*

## **I. INTRODUCTION**

Oil palm is a major export commodity that has many benefits for the Indonesian economy. The development of oil palm plantations began in 1969 when the Indonesian government established the State Plantation Company (PNP) with investment funding by the World Bank The Asian Development Bank. Since the beginning of the growth of oil palm in Indonesia, oil palm plantations are still dominated by large private and state plantations. However, over time smallholder plantations began to experience rapid growth.

Data (Ditjenbun, 2021) states that the productivity of smallholder oil palm plantations in 2019 was 3.24 tons/ha, this figure is still below the national average of 3.97

tons/ha. This means that smallholder plantations are still relatively low and still have the potential to further increase their productivity. Smallholder oil palm plantations in Indonesia still need more attention to be able to increase their productivity.

Jambi Province is the seventh largest palm oil producer in Indonesia with a total oil palm plantation area of 1,034,804 ha and produced 2,884,406 tons in 2019 (Ditjenbun, 2021). Based on the data, around 62.98 percent of oil palm plantations in Jambi Province based on control in 2019 were People's Plantations (PR), PBN was 1.97 percent, and PBS was 35.05 percent.

In 2019, Muaro Jambi Regency was one of the centers of oil palm farming in Jambi Province with the largest

total area of smallholder oil palm plantations in Jambi Province, which was 125,888 ha or 19.32 percent of the total area of smallholder oil palm plantations in Jambi Province, and occupied the second position for the area of Producing Plants (TM) of oil palm plantations with an area of 94,791 ha. Muaro Jambi Regency also has the largest number of oil palm farmers in Jambi Province with 57,714 families. However, oil palm productivity in Muaro Jambi is still low compared to other districts, reaching only 2,575 kg/ha. One of the sub-districts that has the largest smallholder oil palm area and the highest production in Muaro Jambi Regency is Sekernan Sub-district, but its productivity is still relatively low, reaching only 2,661 kg/ha. Judging from the Sekernan sub-district oil palm area, its productivity still has the potential to be increased again.

The low productivity of oil palm farming in Sekernan District can be caused by inefficient use of inputs. The use of production inputs such as land, seeds, fertilizers and labor should be carried out properly and efficiently so as to provide benefits to farmers because it will produce high productivity. Productivity is said to be high if the farm produces maximum production with a minimum combination of inputs. (Tajerin & Mohammad, 2005) states that studying technical efficiency is the same as studying productivity. A high level of technical efficiency will reflect high productivity because technical efficiency cannot be separated from the optimal combination of production factors.

Technical efficiency analysis is also carried out to determine technical factors that can affect the managerial ability of farmers to produce efficiently, which can increase the profit of the farmers themselves. Oil palm farming that is still not technically efficient is thought to occur because it is constrained by the risk of socio-economic uncertainty of farmers which causes technical inefficiency. Technical efficiency is closely related to technical inefficiency because technical inefficiency is the residue of technical efficiency. Not achieving technical efficiency is caused by sources of inefficiency both socially and economically.

## II. RESEARCH METHOD

This research was conducted in Sekernan District, Muaro Jambi Regency. This research location was chosen purposively with consideration of oil palm farming as a source of family income in the area. This research was conducted in Gerunggung Village. The village was selected with the consideration that it has a high area but low oil palm production. The objects used in this study were independent oil palm farmers. The number of samples used was 60 farmers with plant age groups based

on (Fauzi, 2012) namely 3-8 years, 9-13 years, 14-20 years, and 21-25 years. Sampling method using Simple Random Sampling. This study uses primary data obtained directly from independent oil palm farmers through a direct interview system using a questionnaire. The scope of this study is limited to determine the use of production inputs that affect the production produced. To analyze technical efficiency with the stochastic frontier method is done through two stages, namely the analysis of the actual production function and the analysis of the potential production function (frontier), then the ratio between actual production and potential production is the level of technical efficiency which ranges from 0 to 1.

The first stage is to analyze the actual production function using the Ordinary Least Squares (OLS) method. At this stage, estimating technology parameters and production inputs ( $\beta_m$ ) using the Ordinary Least Squares (OLS) method. Parameter estimation with the Ordinary Least Square (OLS) method is used to provide an overview of the average performance of the oil palm farming production process in Gerunggung Village at the existing technology level. The form of the actual production function with the OLS method is as follows:

The second stage is to analyze the frontier production function with the MLE Method. At this stage, the overall parameters of the production factor ( $\alpha$ ), intercept ( $\beta$ ), and variance of the two error components  $v_i$  and  $u_i$  are estimated using the Maximum Likelihood Estimation (MLE) method. The Maximum Likelihood Estimation (MLE) method is used to describe the best performance of the farm at the existing technology level. Mathematically, the stochastic frontier function is expressed in the following equation:

$$Y = X_i + ()$$

The transformation form of the Stochastic Frontier function is expressed as follows:

Description:

- Y : palm oil production (kg)
- $\beta_0$  : constant or intercept
- $X_1$  : land area planted with oil palm (ha)
- $X_2$  : amount of labor used (HOK)
- $X_3$  : amount of NPK fertilizer used (kg/year)
- $X_4$  : amount of Urea fertilizer used (kg/year)
- $X_5$  : amount of Dolomite fertilizer used (kg/year)
- $X_6$  : amount of Herbicide used (liter/year)
- $\epsilon_i$  : disturbance terms
- $\eta_i$  : technical inefficiency effect
- $i$  : indicates the i-th farmer

The analysis method to measure the level of technical efficiency of oil palm farming in the research area was

estimated using the equation formulated by (Tasman, 2008) as follows:

$$TE_i = \exp(-)$$

Description:

- TE<sub>i</sub> : technical efficiency achieved by the i-th farmer  
 : actual farm output  
 : potential output  
 : one-side error term ( )

The criteria for farmers who are classified as technically efficient in this study are if the efficiency index value  $\geq 0.62$  then the oil palm farm is technically efficient. Conversely, if the efficiency value is  $< 0.62$  then oil palm farming is still not technically efficient.

The method of analysis to answer the influence of socio-economic factors that cause the technical inefficiency of oil palm farming refers to the equation model developed by (Coelli et al., 2005). The estimation equation model used in this study is as follows :

It is suspected that the factors that negatively affect technical inefficiency are the age of farmers, farming experience, distance from the farm to the farmer's house, education, and activeness in farmer groups. While the factors that have a positive effect on technical inefficiency is the area of land because it is suspected that the wider the farm land, the more difficult it is for farmers to supervise their land and in carrying out garden maintenance.

### III. RESULT AND DISCUSSION

#### Characteristics of Respondent Farmers

Farmer characteristics are factors that influence farmers in managing their farms. Farmer characteristics studied were farmer age, farming experience, and land area.

Table 1. Characteristics of Farmer Respondents in the Study Area in 2022

Characteristics	Average	Percentage (%)
Farmer Age	44,2	25,00
Experience	17,68	33,33
Land Area	3,94	86,67

Table 1 shows that respondent farmers in the study area had ages ranging from 30 years old at the youngest and 59 years old at the oldest. The majority of farmers were between the ages of 45 and 49 years, which is about 25 percent of all sample farmers. The average age of respondent farmers in the study area was 44.2 years old. (Hernanto, 2018) stated that the productive age is between 15 - 50 years old, so the average farmer is still at a

productive age so that he is still able to cultivate the farm well to increase production.

The lowest farming experience of sample farmers in the study area is 5 years and the longest is 46 years. The most dominant farming experience is farming experience for 11 - 16 years, namely as many as 20 farmers with a percentage of 33.33 percent. The average farming experience in the study area is 17.68 years. According to (Hernanto, 2018) farming experience is one of the most determining factors for success, in the future farmers will be better at cultivating their farms because of their increasing experience.

The largest land area owned by the sample farmers was 20 ha and the smallest was 1.5 ha. The total land area of respondent farmers is 236.5 ha and the average land area is 3.9 ha. The most dominant land area is in the range of 1.5-5 ha with a frequency of 52 farmers or 86.67 percent. According to (Hernanto, 2018) The types of farmers based on the area of land cultivated are divided into four, namely (1) large farmers, those with land  $> 2$  ha, (2) medium farmers, those with land between 0.5 - 2 ha, (3) narrow farmers, those with land  $< 0.5$  ha, and (4) landless farm laborers. Sample farmers fall into the medium to large farmer groups.

#### Production Factor Usage

Production factors are very important factors in efforts to increase farm production. The production factors used should be in accordance with the recommendations in order to obtain the expected results. The use of production factors used by oil palm farmers in Gerunggung Village can be seen in the following table.

Table 2. Production Factor Usage in the Study Area in 2022

Production Factors	Total	Average
Herbicides	2.255	37,58
NPK fertilizer	16.320	272
Urea fertilizer	15.699	262
Dolomite	24.305	405

Table 2 shows that the average use of pesticides was at least 10 liters/ha, while the highest use was 60 liters/ha. The average herbicide use in the study area was 37.58 liters/ha. Herbicide use was most dominant in the range of 24 - 30 liters/ha, which was 20 percent of the sample farmers.

The lowest use of NPK fertilizer on oil palm farms in the study area based on sample farmers was 125 kg/ha and the highest was 420 kg/ha. The most dominant use of fertilizer is in the range of 125 - 167 kg/ha and 297 - 339 kg/ha which is about 20 percent. The average amount of NPK fertilizer used was 272 kg/ha. The use of NPK

fertilizer in the study area is still relatively low and not in accordance with recommendations by (Balitbang, 2013) which should be the average use of NPK fertilizer for oil palm farming is 350 kg/ha. The use of urea fertilizer for oil palm farming in the study area is most dominant in the range of 267 - 291 kg/ha around 36.67 percent of the sample farmers. The lowest amount of Urea fertilizer use was 167 kg/ha and the highest was 340 kg/ha. The average use of Urea fertilizer by sample farmers was 262 kg/ha. So the use of urea fertilizer in the study area is still not in accordance with the recommendations based on (Balitbang, 2013) of 300-375 kg/ha. The highest use of dolomite is 563 kg/ha and the lowest use is 125 kg/ha. Most farmers used dolomite in the range of 440 - 502 kg/ha which was 33 percent of the sample farmers. The average use of dolomite in oil palm farming in the study area was 405 kg/ha. The average use of dolomite in the study area has exceeded the number of recommendations by (Balitbang, 2013) which is 375 kg/ha for the use of dolomite.

#### Analysis of the Farm Production Function

Production function analysis was conducted with the aim of seeing how the influence of production factor variables affecting farm production. Before being analyzed, testing was carried out using the OLS (Ordinary Least Square) method. The results of the analysis obtained are the R<sup>2</sup> value of 0.99 and the variables that have a significant effect on production are land area, NPK fertilizer, Urea fertilizer, Dolomite and Herbicide. While the variable labor has no significant effect on production.

Table 3. Estimation of Palm Oil Farming Production Function in the Research Area with OLS Method in 2021

Variable	Parameter	Coefficient	t-statistic
Constant			
Land Area		7.0877	41,1611***
Labor		0.4683	13,2746***
NPK Fertilizer		-0.3071	-0,1234 <sup>ns</sup>
Urea Fertilizer		0.1621	4,4555***
Dolomite		0.1776	3,3478***
Herbicides		0.0892	2,7849***
		0.0260	1,2906 <sup>ns</sup>
<i>Sigma-squared</i>		0,0008	
$\Sigma\beta_i$		0.6163	
R <sup>2</sup>		= 0,9972	
t-tabel $\alpha$ (0,01), df : 54 = 2,6700			
t-tabel $\alpha$ (0,05), df : 54 = 2,0049			
t-tabel $\alpha$ (0,10), df : 54 = 1,6736			
Description: ***		= significant at $\alpha$ (0,01)	
**		= significant at $\alpha$ (0,05)	
*		= significant at $\alpha$ (0,10)	

ns = not significant

The estimation results of the oil palm production function with the OLS method are as follows:

$$\ln Y = 7.0877 (X_1^{0.4683} X_2^{-0.3071} X_3^{0.1621} X_4^{0.1776} X_5^{0.0892} X_6^{0.0260})$$

Table 3 shows the R<sup>2</sup> value of 0.9972, which means that the independent variables (land area, labor, NPK fertilizer, Urea fertilizer, Dolomite, and herbicide) together can explain the dependent variable (production) by 99.72 percent, while the remaining 0.28 percent is determined by other factors outside the model. The value of  $\Sigma\beta_i = 0,6163 < 1$ , meaning that the use of production factors in the study area is in region II of the production curve or the Decreasing Return to Scale area, which means that each additional unit of input produces a decreasing additional output. Variables that have a significant effect on production are land area, NPK fertilizer, Urea fertilizer and Dolomite which have a very significant effect at  $\alpha$  (0.01). While the variables that do not have a significant effect on production are labor and herbicide.

#### Analysis of the Farm Productivity Function

Estimation of the productivity function is carried out with the aim of knowing how the influence of variable production factors on farm productivity. Before being analyzed, testing is done using the MLE (Maximum Likelihood Estimation) method. From the analysis, it can be seen that the value of R<sup>2</sup> is 0,9537,  $\Sigma\beta_i$  is 0,8366 < 1, and the value of gamma is 0.9999. Variables that significantly affect productivity are labor, NPK fertilizer, Urea fertilizer, Dolomite, and Herbicide.

Table 4. Estimation of Palm Oil Farming Productivity Function in the Research Area with MLE Method in 2021

Variable	Parameter	Coefficient	t-statistics
Constant			
Labor		7,1480	55,5114***
NPK		0,0201	5,3946***
Fertilizer		0,1369	4,4577***
Urea		0,1840	4,8780***
Fertilizer		0,0834	3,6781***
Dolomite		0,4122	2,2209**
Herbicide			
<i>Sigma-squared</i>		0,0008	3,9758
<i>Gamma</i>		0,9999	51,7049
$\Sigma\beta_i$		0,8366	
<i>LR test of the one-sided error</i>			16,9181
<i>Log-likelihood function MLE</i>			137,4184
<i>Log-likelihood function OLS</i>			128,9594
R <sup>2</sup>		= 0,9537	
t-tabel $\alpha$ (0,01), df : 55 = 2,6682			



t-tabel  $\alpha$  (0,05), df : 55 = 2,0040

t-tabel  $\alpha$  (0,10), df : 55 = 1,6730

Description : \*\*\* = significant at  $\alpha$  (0,01)

\*\* = significant at  $\alpha$  (0,05)

The results of the estimation of the frontier productivity function of oil palm farming with the following equation:

$$\ln Y = 7,1480 (X_1^{0,0201} X_2^{0,1369} X_3^{0,1840} X_4^{0,0834} X_5^{0,4122})$$

Table 4 shows the  $R^2$  is 0,9537 which means that the independent variables (labor, NPK fertilizer, Urea fertilizer, Dolomite, and herbicide) together can explain the dependent variable (productivity) by 95.37 percent, while the remaining 4.63 percent is determined by other factors outside the model. The gamma value ( $\gamma$ ) indicates the presence or absence of inefficiency influence in the model. Statistically, the value of gamma ( $\gamma$ ) 0,9999 is close to 1, meaning that the error term is caused by technical inefficiency by 99.99 percent, and the remaining 0.01 percent is caused by external influences. The value of  $\sum \beta_i = 0,8366 < 1$ , meaning that the use of production factors in the study area is in region II of the production curve or the Decreasing Return to Scale area, which means that each addition of the same proportion of production inputs will result in a decreasing increase in output. Independent variables in the model that have a very significant effect on productivity at the  $\alpha = 0.01$  level are labor, NPK fertilizer, Urea fertilizer and Dolomite fertilizer, and herbicides have a significant effect at the  $\alpha = 0.05$  level.

The coefficient value of the labor variable of 0.0201 is positive with the value of  $t_{hit} = 5,3946 > t_{\alpha(0,01)} = 2,6682$  which means that the labor variable has a very significant effect on increasing FFB productivity. These results are in accordance with research studies (Thamrin, 2016), (Puruhito et al., 2019), and (Febriyanto, 2020) namely labor has a significant effect on increasing productivity. However, different results were obtained in (Asmara et al., 2011), (Ridho et al., 2014), (Sitanggang, 2018), and (Panjaitan et al., 2020) which stated that labor had no significant effect on increasing productivity.

The coefficient value of the NPK fertilizer variable obtained a value of 0.1369 with a positive sign with a value of  $t_{hit} = 4,4577 > t_{\alpha(0,01)} = 2,6682$  which means that the NPK fertilizer variable has a very significant effect on increasing FFB productivity, in line with research (Puruhito et al., 2019), and (Syuhada et al., 2022) which states that NPK fertilizer has a significant effect on increasing productivity.

The coefficient value of the Urea fertilizer variable was obtained at 0.1840 with a positive sign with a value of  $t_{hit} = 4,8780 > t_{\alpha(0,01)} = 2,6682$  which means that Urea fertilizer has a very significant effect on increasing FFB

productivity. These results are in accordance with research (Ridho et al., 2014) and (Napitupulu et al., 2020) which state that Urea fertilizer has a significant effect on increasing productivity, but different results are obtained (Nainggolan et al., 2019), and (Puruhito et al., 2019) that urea fertilizer has no significant effect on increasing the productivity of oil palm FFB.

Dolomite variable coefficient was obtained at 0,0834 with a positive sign with a value of  $t_{hit} = 3,6781 > t_{\alpha(0,01)} = 2,6682$  which means that the dolomite variable has a significant effect on increasing FFB productivity. This is in accordance with research by (Napitupulu et al., 2020) that dolomite has a significant effect on increasing productivity, but different results were obtained (Ridho et al., 2014) that dolomite has no significant effect on increasing FFB productivity.

The Herbicide coefficient value obtained is 0,4122 with a positive sign with the value of  $t_{hit} = 2,2209 > t_{\alpha(0,05)} = 2,0040$  which means that Herbicides have a significant effect on increasing FFB productivity with a confidence level of 95 percent. In accordance with research (Syuhada et al., 2022) that herbicides have a significant effect on increasing FFB productivity, but different results were obtained (Ridho et al., 2014) and (Puruhito et al., 2019) that herbicides have no significant effect on increasing the productivity of oil palm FFB.

#### Technical Efficiency Analysis of Oil Palm Farming

The measurement of technical efficiency is carried out with the aim of seeing how the achievement of production from the comparison of potential production with actual production. The value of technical efficiency is obtained by calculating actual production divided by potential production. Efficient farming if the value of technical efficiency  $> 0,62$ .

Table 5. Technical Efficiency of Independent Palm Oil Farming in the Research Area in 2021

	Technical Efficiency	Total Farmers (people)	Percentage (%)
	<b>0,81 – 0,83</b>	<b>7</b>	<b>11,67</b>
	<b>0,84 – 0,86</b>	<b>25</b>	<b>41,67</b>
	<b>0,87 – 0,89</b>	<b>22</b>	<b>36,67</b>
	<b>0,90 – 0,92</b>	<b>4</b>	<b>6,67</b>
	<b>0,93 – 0,95</b>	<b>1</b>	<b>1,66</b>
	<b>0,96</b>	<b>1</b>	<b>1,66</b>
<b>Total</b>	<b>-</b>	<b>60</b>	<b>100,00</b>
<b>Min</b>	<b>0,81</b>		
<b>Max</b>	<b>0,96</b>		
<b>Average</b>	<b>0,86</b>	<b>-</b>	<b>-</b>

The results of the measurement of technical efficiency obtained that the level of technical efficiency achieved by

independent oil palm farmers in the study area ranged from 0.81 to 0.96 with an average technical efficiency of 0.86. The average value of the actual technical efficiency of independent pattern oil palm farms in the study area is 0.86 which means that the average productivity achieved by oil palm farmers in the study area is about 86 percent of frontier production and can still be increased by 14 percent more. The average value of the technical efficiency level of oil palm farmers in the study area > 0.62 and the lowest technical efficiency value obtained is 0.81 > 0.62 which means that the overall independent pattern of oil palm farmers in the study area is technically efficient (ET > 0.62), but still needs to be improved again because the technical efficiency obtained by farmers can still be improved by 19 percent more. The technical efficiency figure obtained in this study is still below the technical efficiency in research (Harefa, 2021) which obtained an average technical efficiency of 0.86 with the lowest technical efficiency value of 0.63 and the highest 0.99.

**Influence of Socioeconomic Factors on Technical Inefficiency of Oil Palm Farms**

Technical inefficiency analysis was conducted to see how the influence of socioeconomic factors on technical inefficiency. The analysis was conducted using the OLS (Ordinary Least Square) method and the results showed that there was no violation of information on *Adj. R2*, *Prob (F-statistic)* and *Durbin Watson stat* related to classical assumption test.

Table 6. Results of Sources of Technical Inefficiency

Variable	Coefficient	Std. Error
Z1_LAHAN	0.002422	0.000689
Z2_UMUR	-0.000256	0.000421
Z3_PENGALAMAN	-0.001446	0.000305
Z4_JARAK	-0.000206	0.000990
Z5_PENDIDIKAN	-0.008695	0.002450
Z6_KEAKTIFAN	-0.016317	0.005900
C	0.269244	0.020744
R-squared	0.801999	Mean dependent var
Adjusted R-squared	0.779584	S.D. dependent var
S.E. of regression	0.013320	Akaike info criterion
Sum squared resid	0.009404	Schwarz criterion
Log likelihood	177.6935	Hannan-Quinn criter.
F-statistic	35.77921	Durbin-Watson stat
Prob(F-statistic)	0.000000	

Table 6 shows that the *Prob. (F-statistic)*  $0,000 < \alpha$  (0,05) shows that the results are simultaneously significant, meaning that the independent variables contained in the model together have a significant effect on the technical inefficiency of farming. Durbin Watson

stat value is  $1,585 < 2,00$  indicates that the model in the study is free from autocorrelation. Variables that have a significant effect on technical inefficiency in oil palm farming self-help pattern at the level of  $\alpha = 0,05$  are variables of land area, experience, education, and activeness in farmer groups. While the variables that do not have a significant effect on technical inefficiency are the variables of age and distance from the farm to the house.

Land area, experience, education, and activity in farmer groups have a significant effect on technical inefficiency with a positive land area coefficient, and the coefficient of experience, education, and activity in farmer groups is negative. In accordance with (Napitupulu et al., 2020) namely the land area has a significant effect on technical inefficiency with a positive coefficient value, and experience has a significant effect with a negative coefficient. However, different results were obtained (Syuhada et al., 2022) namely land area, experience and education had no significant effect on technical inefficiency

Variables that do not have a significant effect on technical inefficiency are age and distance from home. This result is consistent with (Syuhada et al., 2022) that age has no significant effect on technical inefficiency. However, it is inversely proportional to (Napitupulu et al., 2020) that the distance between the garden and the house has a significant effect on technical inefficiency with a positive coefficient, which means that the further the distance between the garden and the house, the more technical inefficiency will increase.

**V. CONCLUSION**

Farm management is still not as recommended, especially in the use of fertilizers. The use of NPK and Urea fertilizers is still below the recommendation, while Dolomite has exceeded the recommendation. The average production obtained by farmers is low compared to the national average production and is still below the potential production of oil palm based on the varieties used. Production factors of land area, NPK fertilizer, Urea fertilizer and Dolomite are production factors that can increase oil palm FFB production. The level of technical efficiency of independent pattern oil palm farming in the research area is technically efficient but still needs to be improved because technical inefficiency is still relatively high.

Socio-economic factors that have a significant effect on technical inefficiency in oil palm farming self-help patterns are land area, farming experience, education and activeness in farmer groups. While factors that do not have a significant effect on technical inefficiency are the age of

farmers and the distance of the plantation to the farmer's house.

### ACKNOWLEDGEMENTS

The authors would like to thank the field agricultural extension officers who participated in data collection and the Agriculture Office of Muaro Jambi Regency for providing secondary data references

### REFERENCES

- [1] Asmara, R., Hanani, N., & Irawati, N. (2011). The Analysis of Technical Efficiency with Frontier Approach in Business of Chips MOCAf (Modified Cassava Flour). *Habitat*, XXII(1), 52–59. <https://habitat.ub.ac.id/index.php/habitat/article/view/166>
- [2] Balitbang. (2013). *Rekomendasi Pemupukan N,P dan K pada Kelapa Sawit*.
- [3] Coelli, T. J., Rao, D. S. P., O'Donnell, C. J., & Battese, G. E. (2005). *An Introduction to Efficiency and Productivity Analysis* (2nd ed.). Springer Science & Business Media.
- [4] Ditjenbun. (2021). Statistik Perkebunan Unggulan Nasional 2019-2021. *Direktorat Jendral Perkebunan Kementerian Pertanian Republik Indonesia*, 1–88. <https://ditjenbun.pertanian.go.id/template/uploads/2021/04/BUKU-STATISTIK-PERKEBUNAN-2019-2021-OK.pdf>
- [5] Fauzi, Y. (2012). *Kelapa Sawit*. Penebar Swadaya.
- [6] Febriansyah, Ebi; Saad Murdy; Saidin Nainggolan. (2021). *Analisis Efisiensi Teknis, Inefisiensi Teknis dan Risiko Produksi Usahatani Padi Sawah di Kabupaten Tanjung Jabung Barat (dengan Pendekatan Maximum Likelihood Estimation)*. *JALOW* 4(1) : 65-73. <https://online-journal.unja.ac.id/JALOW/article/view/13324>
- [7] Febriyanto, A. T. (2020). *Analisis efisiensi teknis usahatani bawang merah di kabupaten demak*. <http://lib.unnes.ac.id/41883/>
- [8] Harefa, S. N. (2021). *Analisis Pendapatan dan Efisiensi Teknis Usahatani Kelapa Sawit Mandiri di Desa Markanding Kecamatan Bahar Utara Kabupaten Muaro Jambi*. <http://repository.unbari.ac.id/756/1>
- [9] Hernanto, F. (2018). *Ilmu Usahatani*. Penebar Swadaya.
- [10] Nainggolan, S., Fitri, Y., & Kurniasih, S. (2019). *Study of Technical Efficiency and Farmers' Production Risk Preferences in the Context of Increasing Paddy Rice Farming Productivity in Bungo Regency, Jambi Province - Indonesia*. 2(1), 13–23. <https://doi.org/10.22437/jalow.v2i1.7885>
- [11] Napitupulu, D. M. T., Nainggolan, S., & Murdy, S. (2020). Kajian Efisiensi Teknis, Sumber Inefisiensi dan Preferensi Risiko Petani Serta Implikasinya pada Upaya Peningkatan Produktivitas Perkebunan Kelapa Sawit di Provinsi Jambi. *JALOW | Journal of Agribusiness and Local Wisdom*, 3(2), 2621–1297. <https://doi.org/https://doi.org/10.22437/jalow.v3i2.11614>
- [12] Pahan, I. (2018). *Panduan Teknis Budidaya Kelapa Sawit untuk Praktisi Perkebunan*. Penebar Swadaya. Jakarta.
- [13] Panjaitan Edward, Ujang Paman, & Darus. (2020). *Analisis Pengaruh Faktor Produksi Terhadap Produktivitas Usahatani Kelapa Sawit Pola Swadaya Di Desa Sungai Buluh Kecamatan Kuantan Singingi Hilir, Kabupaten Kuantan Singingi*. *Dinamika Pertanian*, 36(1), 61–68. [https://doi.org/10.25299/dp.2020.vol36\(1\).5371](https://doi.org/10.25299/dp.2020.vol36(1).5371)
- [14] Puruhito, D. D., Jamhari, J., Hartono, S., & Irham, I. (2019). Faktor Penentu Produksi pada Perkebunan Rakyat Kelapa Sawit di Kabupaten Mamuju Utara. *Jurnal Teknosains*, 9(1), 58. <https://doi.org/10.22146/teknosains.38914>
- [15] Ridho, Z., Hadi, S., & Yusri, J. (2014). Efisiensi Produksi Kelapa Sawit Pola Swadaya di Desa Senama Nenek Kec Tapung Hulu Kabupaten Kampar. *JOMFAPERTA*, 1(1). <https://jom.unri.ac.id/index.php/JOMFAPERTA/article/view/2574/2506>
- [16] Sitanggang, Y. F. (2018). Analisis Efisiensi Teknis Usahatani Cabai Merah Keriting Menggunakan Stochastic Frontier Analysis (SFA) di Desa Mojorejo, Kecamatan Wates, Kabupaten Blitar. *Bitkom Research*, 63(2), 1–3. <http://repository.ub.ac.id/id/eprint/12338/>
- [17] Soekartawi. (2003). *Teori Ekonomi Produksi Dengan Pokok Analisis Fungsi Cobb Douglas*. Rajawali Press. Jakarta.
- [18] Suhada, F., Hasnah, H., & Khairati, R. (2022). Analisis Efisiensi Teknis Usahatani Kelapa Sawit: Analisis Stochastic Frontier. *Jurnal Ekonomi Pertanian Dan Agribisnis*, 6(1), 249–255. <https://doi.org/10.21776/ub.jepa.2022.006.01.24>
- [19] Tajerin, & Mohammad, N. (2005). Analisis Efisiensi Teknik Usaha Budidaya Pembesaran Ikan Kerapu dalam Keramba Jaring Apung di Perairan Teluk Lampung: Produktivitas, Faktor-faktor yang Mempengaruhi dan Implikasi Kebijakan Pengembangan Budidayanya. *Economic Journal of Emerging Markets*, 10(1), 95–105. <https://journal.uui.ac.id/JEP/article/view/608>
- [20] Tasman, A. (2008). *Analisis Efisiensi dan Produktivitas*. Penerbit Chandra Pratama.
- [21] Thamrin, S. (2016). Efisiensi Teknis Usahatani Kopi Arabika di Kabupaten Enrekang. *Ilmu Pertanian (Agricultural Science)*, 18(2), 92. <https://doi.org/10.22146/ipas.9090>
- [22] Wijoyo, Budi Sastro. (2019). Efisiensi Penggunaan Faktor-Faktor Produksi Pada Usahatani Kelapa Sawit Rakyat (Studi Kasus: Desa Lama Baru, Kecamatan Sei Lapan, Kabupaten Langkat). Medan: Universitas Muhammadiyah Sumatera Utara (UMSU). <http://repository.umsu.ac.id/handle/123456789/304>



# Statistical analysis of recent rainfall variability and trend using a merged gauge and satellite time series data for the cotton zone of Mali

Souleymane Sidi Traore

Department of Geography, Faculty of History and the Geography, University of Social Sciences and Management of Bamako, Campus of Badalabougou, Bamako, Mali

Joint GIS and Remote Sensing Unit, LaboSEP, Institute of Rural Economy, CRRRA-Sotuba, Bamako, Mali.

Corresponding Author: [sstraore@yahoo.fr](mailto:sstraore@yahoo.fr)

Received: 03 Oct 2023; Received in revised form: 04 Nov 2023; Accepted: 11 Nov 2023; Available online: 29 Nov 2023

©2023 The Author(s). Published by Infogain Publication. This is an open access article under the CC BY license

(<https://creativecommons.org/licenses/by/4.0/>).

**Abstract**— *The variability of rainfall patterns has a significant impact on people's livelihoods especially in areas where rain-fed agriculture predominates. The temporal variability and trend of rainfall was analysed using a newly rainfall time series created from the fusion with ground measurement and satellite data for ten met stations for the period 1983-2021. Mann Kendall's (MK) non-parametric test was used to verify the rainfall trend, the variability was analysed using the Coefficient of Variation (CoV), the annual distribution of precipitation was checked using the precipitation concentration index (PCI) and finally the synchronicity between stations was tested with an Kruskal Wallis (KW) test. The MK-test shows an increasing trend in precipitation for all stations even if this trend is not significant. This increase resulted in a general increase in the amount of rain received in the area. The analysis of rainfall data revealed a moderate intra and inter annual variability (CoV±20%). The PCI also revealed an irregularity of rainfall due to its high seasonality. The analysis of variance highlighted an asynchrony of the stations. These results provide an in-depth understanding of the recent rainfall variation and trend in the cotton zone of Mali.*



**Keyword**— *Rainfall, variability, trend, PCI, Cotton production zone of Mali*

## I. INTRODUCTION

Rainfall is one of the most key climate parameters which regulate and determine farming activities and production worldwide (Bekele et al. 2017; Mesike and Agbonaye, 2016). Agricultural boost in terms of high yield is based on sufficient amount and distribution of rainfall all through the seasons in any region (Zachariah et al. 2020). Consequently, in most African countries whose farming activity is mostly rainfed, robust and accurate estimation of the spatial and temporal distribution of rainfall including its trend are vital input parameters in order to secure sustainable agricultural activities (Ayalew et al. 2012). The change in rainfall regime can't be assessed easily due to meteorological processes but long-term rainfall could scale up the planning of agriculture in the rainfed region (Pradhan et al. 2020).

Located in West Africa (WA), Mali is a landlocked country located populated with about 22.6 million of habitants (World Bank, 2022). The country is large with 1 245 000 km<sup>2</sup> and shares a border with seven countries (Algeria, Mauritania, Senegal, Guinea, Côte d'Ivoire, Burkina Faso and Niger). The country spans with four climatic zones from north to south (Sahara Desert, Sahelian, Sudanian and pre-Guinean). Agricultural activities including farming, herding and fishing, are the main activities and employ about 80% of the population and contribute about 36% to the GDP (Maiga et al. 2019). Given the fact that Malian agricultural activities are largely dependent on rainfed-agriculture, analysis of long-term historical rainfall data is imperative. These analyses will provide robust information on the distribution of precipitation on one hand and better prepare

farmers on extreme events mitigation to avert agricultural losses on the second hand.

The high inter-annual rainfall variability in space and time is one of the most relevant characteristics of West Africa in general and the southern zone of Mali in particular. This is exhibited by variable onsets of the rainy season, somewhat more predictable endings, and droughts or excess water occurrence at any time during the growing season. A number of studies on the contemporaneous debate (e.g. Traore *et al.* 2021; Sanogo *et al.* 2015; Giannini, 2015) show that rainfall increased in the Sahel following the severe drought of the 1980s. Conversely, other researchers believe that the Sahel experienced drought throughout the 1990s (L'Hote *et al.* 2003; Nicholson *et al.* 2000). It is required to understand rainfall variability and trend at the temporal characteristics at local scale in order to gain a clear understanding of rainfall patterns. In this regard, long term study of rainfall pattern and its variability is imperative. Specially, in agricultural regions such as CPZ alteration in the rainfall patterns may have a major impact on the life and livelihood of people. With rapid climate change it becomes more imminent to study the trends in rainfall especially for those parts of the country which have higher dependability on agriculture. In this line, the present study seeks to investigate the recent variability and trend of rainfall and its distribution using 39-years (1983-2021) rainfall time series data for 10 selected weather stations in the cotton production zone (CPZ) of Mali.

## II. MATERIAL AND METHODS

### 2.1. Site description

The cotton production zone (CPZ) of Mali is located between 3°59'02" and 10°36'09" West longitude and 10°09'45" and 14°23'13" North latitude (Figure 1) with a coverage of 150,000 km<sup>2</sup> and an estimated population of 8 million habitants in 2017 (Soumare and Traore, 2019). The CZ extends from the Sahelian (300-700 mm) in the north, Sudanian (700-1200 mm) in the centre to the Sudano-Guinean (1200-1600 mm) eco-climatic zone in the south.

The spatial distribution of vegetation is largely related to cumulative (annual) rainfall and the length of the rainy season, which varies along the eco-climatic gradient. Vegetation patterns on a landscape scale are determined by localised climatic variations and human activities such as bush clearing and deforestation for agricultural or energy purposes, overgrazing and gold mining. The cotton production in the area is led by the Malian Company for the Development of Textiles (CMDT), spatially organised into 4 subsidiaries, 41 sectors and 520 zones of agricultural production involving more than 4,000 villages. Smallholder farming is the most common agricultural practice in the region. Millet, sorghum and cotton are primarily cultivated, whilst pastoralism (bovines, goats and sheep) is practised throughout the area. Cotton occupies about 30% of the cropping area, 60% for cereals (maize, sorghum and millet), and only 10% of the land is given over to small crops (cowpeas, soybeans, groundnuts, etc.).

### 2.2. Data description

The World Meteorological Organization (WMO, 2018) recommends an observation period of more than 30 years to ensure the independence of climate data time series to cope with natural climate variability. This fact is because shorter time series are more sensitive to the values at the start and end of the series. Therefore time-series data of rainfall from 1983 to 2021 for ten (10) meteorological stations in the cotton production zone were created. These data were derived from a fusion of satellite rainfall estimates from African Rainfall Climatology version 2 (ARC-2) adjusted with weathers stations data using the period of overlap of the two data sources then extended over the study period. Calibration procedures are described in Traore, 2024; Traore *et al.* (2022). Table 1 presents the general geographic information of the selected weather stations. These stations called reference weather stations in this study are those among the 54 stations listed in the area with no more than two (04) years of missing data. This is the criterion that motivated their choice for the present work.

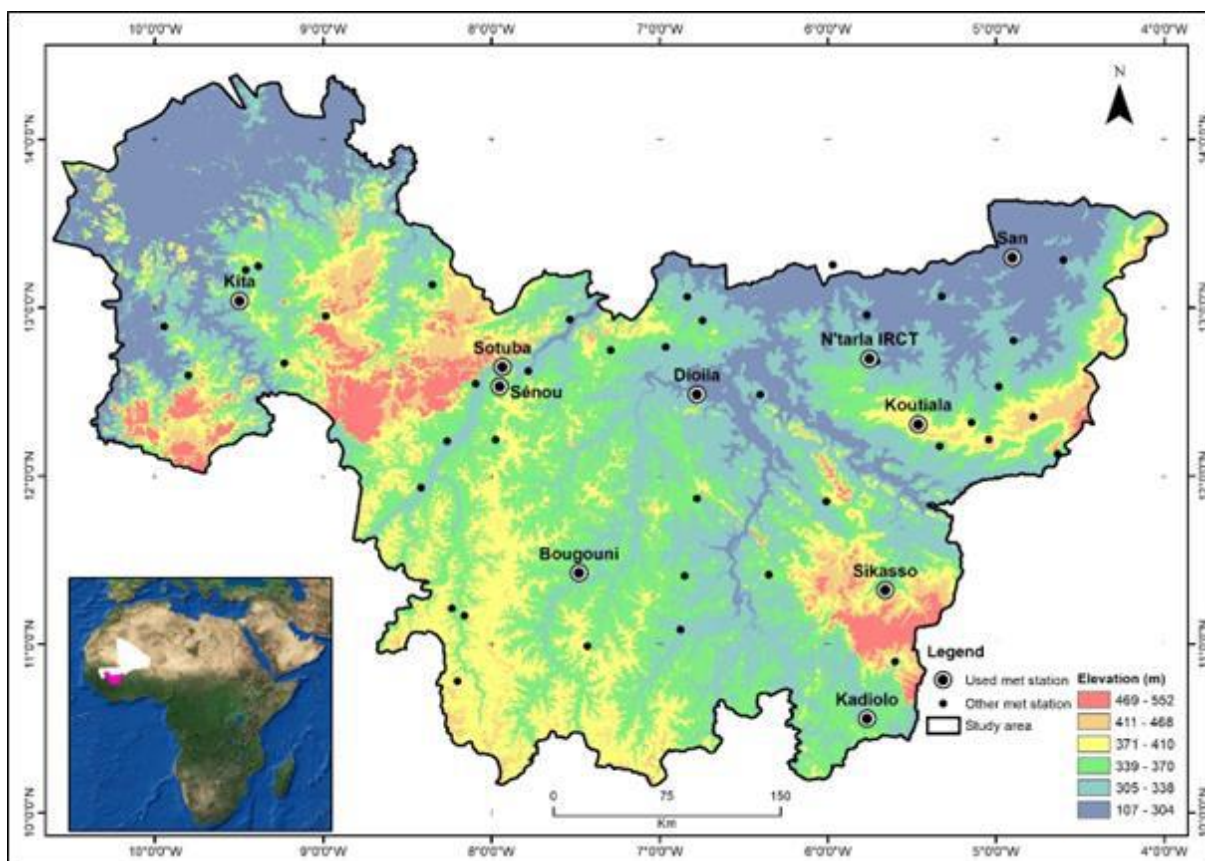


Fig.1: Relief map of cotton zone with selected weather station's location within the cotton zone of Mali (Source: Traore et al. 2022)

Table 1: Selected weather stations of the cotton zone and their general geographic information.

Code	Station name	AEZ*	Long (°W) DDMMSS	Lat (°N) DDMMSS	Altitude (m)
270131	Senou	PK	7°57'00"	12°31'59"	373
270162	Bougouni	HBN	7°28'35"	11°25'34"	350
270141	Dioila	PK	6°46'32"	12°29'14"	309
270178	Kadiolo	HBN	5°45'50"	10°33'34"	353
270107	Kita	PM	9°29'43"	13°02'34"	349
270144	Koutiala	PK	5°27'38"	12°18'35"	411
270121	N'tarla IRCT	PK	5°45'00"	12°42'00"	327
270100	San	BH	4°54'03"	13°18'03"	284
270165	Sikasso	PK	5°39'26"	11°19'25"	355
270130	Sotuba	PM	7°55'589"	12°39'00"	315

AEZ: Agro-ecological zone; PK: Plateau of Koutiala, HBN: Haut Bani Niger, PM: Mandingo Plateau, BH: Plateau of Bandiagara

## 2.3. Analyse procedures

### Normality test

Assessment of the normality of data is a prerequisite for selecting the best statistical methods for data analysis. In this regard, the available two main methods for assessing normality are graphical and numerical including statistical tests (Machin *et al.* 2007; Bland *et al.* 2015). This study applied a normality test using the Kolmogorov-Smirnov test (KS-test) method. KS-test is recommended when sample size is greater than 50 (Mishra *et al.* 2019). In such, daily, monthly and annual rainfall for all the stations were subjected to normality tests. The null hypothesis states that data are taken from a normal distributed population and when  $P > 0.05$ , null hypothesis is accepted and data are called as normally distributed.

### Coefficient of Variation (CoV)

The study uses CoV to examine the variability in rainfall. The higher value of CoV is an indicator of larger rainfall variability, and vice versa. The equation of CoV is as follows:

$$\text{CoV} = \frac{\theta}{\mu} \times 100 \quad (1)$$

Where CoV is the coefficient of variation;  $\theta$  is the standard deviation and  $\mu$  is the mean of rainfall over the studied period. CoV was computed to classify the degree of rainfall variability according to El-Mahdy, 2021 and Hael, 2021. CoV less than 20 indicate low variability, CoV greater than 20 and less than 30 indicate moderate variability; and CoV greater than 30 indicate high variability (Royé and Martin-Vide, 2017).

### Mann Kendall trend test

From the wide types of trend analysis methods, this study uses the non-parametric Mann-Kendall trend test (Mk-test) proposed by Mann (1945) and Kendall (1975). This test does not require the data to be normally distributed and has low sensitivity in abrupt breaks due to inhomogeneous time-series (Tabari *et al.* 2011) and have been widely employed to detect monotonic trends in the time series of hydrometeorological variables (Asfaw *et al.* 2018; Xu *et al.* 2018; Zakwan and Ara, 2018; Mohamed and El-Mahdy, 2021; Mohamed *et al.* 2022). The MK test is grounded on a null hypothesis ( $H_0$ ), which indicates that there is no trend-the data are independent and randomly ordered-and this is verified against the alternative hypothesis ( $H_a$ ), which supposes that there is a trend (Koudahe *et al.* 2018). In the calculation, the value of Z is the judgement criterion for the trend change (Xu *et al.* 2018). When  $|Z| \leq 1.96$ , the null hypothesis  $H_0$  is accepted, indicating that there is no significant trend at the 0.05 significance level.  $|Z| \geq 1.96$  demonstrates the trend of the time series is statistically

significant. It must be noted that a positive Z indicates that the sequence has an increasing trend, while a negative Z reflects a declining trend.

### Precipitation concentration index

Precipitation Concentration Index (PCI) was used to assess the monthly heterogeneity of rainfall amounts. PCI is a useful indicator to determine the precipitation changes of a specific region and defined as the ratio between sum of squared monthly rainfall to the square of annual rainfall (Bhattacharyya and Sreekesh, 2022). The PCI, proposed by Oliver (1980) and further modified by De Luis *et al.* (2011), is used for the calculation of the annual PCI following:

$$\text{PCI} = 100 \times \frac{\sum_{i=1}^{12} P_i^2}{(\sum_{i=1}^{12} P_i)^2} \quad (2)$$

PCI values of less than 10 indicate quite uniform annual distribution of rainfall, values between 11 to 15 denote a moderate rainfall distribution, 16 to 20 denote irregular rainfall distribution and above 20 represent a strong irregularity of rainfall distribution Asfaw *et al.* 2018 and Rahman *et al.* 2019, Pawar *et al.* 2022.

### Comparative analysis between stations

Comparison of several groups or independent samples requires the application of an appropriate statistical test. In this regard, the common statistical tests are ANOVA for normally distributed samples or groups and the Kruskal Wallis test (KW-test) for non-normally distributed samples or groups (Cabral Júnior and Lucena, 2019). In this study, the KW-test test was used since the hypothesis of the normality distribution of data was rejected at 1% of statistical significance, as verified by the KS-test (*p-value*: 0.5). As the KW-test compares (paired or unpaired) k samples based on the null hypothesis that the median differences within groups are not significant. In this research the groups were formed by daily/annual rainfall data for individual met stations to check the rainfall pattern' similarity and difference (synchronicity and asynchronicity) during the 39 years period. The null hypothesis is that there are no significant differences between the rainfall medians in the pattern in the study area.

## III. RESULTS AND DISCUSSION

### 3.1. Long-term rainfall temporal variability

Statistics of annual rainfall (1983-2021) show a comparatively higher rainfall amount for all the stations. The mean annual amount of rainfall varies from 1223.3 mm with a standard deviation of 272.6 at Sikasso to 745.4 mm with a standard deviation of 155 at San. The maximum rainfall at Sikasso was 1848.3 mm recorded in 2018 and the minimum was 781.0 mm recorded in 2002. In San, the maximum rainfall of the period was 1135.4 mm recorded in

2020 and the minimum was 480.9 mm recorded in 1992. The result of the normality test using KS revealed non-normality in the series for all the ten stations at a significance of 5%. Rainfall amounts show low variability

for Kadiolo station (18.8%) and Bougouni station (19.4%). Moderate variability in rainfall is observed in the rest of the stations.

Table 2: Summary statistics of annual rainfall (mm) of selected weather stations (1983-2021)

Station	Min	Median	Max	Average	Standard deviation	CoV (%)
Sikasso	781.0	1155.4	1848.3	1223.3	258.7	21.6
Bougouni	807.5	1151.7	1790.0	1187.7	227.8	19.4
Kadiolo	657.4	1115.5	1892.5	1192.5	218.7	18.8
Dioila	539.9	1024.7	1796.8	1074.1	271.3	25.7
Senou	577.9	986.5	1597.8	1017.7	207.1	20.4
Kita	630.2	978.9	1726.7	1033.4	226.2	22.7
N'tarla	557.4	957.5	1608.0	977.4	236.1	24.1
Sotuba	535.6	941.3	1562.3	982.9	199.5	20.5
Koutiala	588.8	912.0	1587.1	953.5	261.9	26.6
San	480.9	719.0	1135.4	745.4	153.4	20.7

### 3.2. Rainfall trend

The MK test and Sen's slope had been calculated for the trend analyses on the long period of rainfall data from 1983 to 2021 for the 10 meteorological stations in the zone. The results of trend analyses by the MK-test for the study stations were displayed in Table 2. In the Mann Kendall trend test, a p-value less than 0.05 means a significant trend and a p-value greater than 0.05 means is considered an insignificant or simply no trend (Di Leo et al. 2020; Amrhein et al. 2019). In general, all the stations showed a positive Sen's Slope (between S Slope= 3.99 and 19.67) indicating at least an increasing rainfall trend. Kita in western zone is the only station which exhibits a non-statistically significant trend (p-value of 0.345 greater than

0.05) with a positive Sen's slope value (Sen's slope = 3.99). The other stations show p-values between  $p=0.000$  and  $p=0.021$  ( $p < 0.05$ ) which makes the trends statistically significant upward trend of total rainfall amount. All the stations show either zero or positive values for Kendall's tau, Mann Kendall parameter (S), Variance (S) and this is a good sign of the increasing trend of rainfall. These results agreed with the rainfall recovery trend asserted by Lalou et al. 2019; Giannini, 2015; Sanogo et al. 2015 in West Africa. Indeed, the results are also in agreement with the analysis of Traore et al. 2021 who had noticed an increased rainfall trend for the period 1983-2018 using a rainfall time series from one meteorological station in the CPZ of Mali. With these results, one can assume that there is an increasing trend of rainfall amounts over the CPZ, significant at 99%.

Table 3: Mann-Kendal rainfall trend and Sen Slope for selected weather station (1983-2021)

Station	Kendall's tau	Sen Slope	S	Var(S)	P-value	Alpha	H0	Z Value
Sikasso	0.34	12.01	250	6832.7	0.003	0.05	Rejected	3.01***
Bougouni	0.26	8.45	192	6832.7	0.021	0.05	Rejected	2.31**
Kadiolo	0.32	10.44	238	6832.7	0.004	0.05	Rejected	2.87***
Dioila	0.58	19.67	432	6832.7	< 0.0001	0.05	Rejected	5.21***
Senou	0.46	12.04	338	6832.7	< 0.0001	0.05	Rejected	4.08***
Kita	0.11	3.99	79	6831.7	0.345	0.05	Accepted	0.94
N'tarla	0.57	15.44	420	6832.7	< 0.0001	0.05	Rejected	5.07***
Sotuba	0.34	8.43	250	6832.7	0.003	0.05	Rejected	3.01***
Koutiala	0.41	11.83	302	6832.7	0	0.05	Rejected	3.64***



San	0.43	8.58	320	6832.7	0	0.05	Rejected	3.86***
-----	------	------	-----	--------	---	------	----------	---------

Significance level: \*\*\* significant at 0.001; \*\* significant at 0.05

### 3.3. Precipitation Concentration Index (PCI) Analysis

The variation and distribution in seasonal rainfall signify a significant indicator to appreciate the concentration and sequential distribution of precipitation over a given year. Therefore, the variability and concentration of rainfall for seasonal rain was evaluated using annual PCI based on the monthly rainfall over a 39-year period (1983–2021) for 10 meteorological stations in the cotton zone of Mali. The

result shows that the rainfall at the 10 weathers stations falls under two classes of moderate and irregular precipitation concentration. Kadiolo station with a PCI value of 15 is the only station highlighting moderate rainfall distribution. A PCI value between 16 and 20 were observed in the reminder stations denoting an irregular rainfall distribution. These results corroborate with the results of Quenum *et al.* 2020 who had already proven an irregularity of rainfall in the savannah zone because of its more pronounced seasonality.

Table 4: PCI distribution for the ten stations used during 1983-2021 period

PCI distribution	PCI range	Annual
Uniform precipitation	< 10	NA
Moderate precipitation	11 to 15	Kadiolo
Irregular	16 to 20	Sikasso, Bougouni, Dioila, Senou, Kita, N'Tarla, Sotuba, Koutiala, San
Strong irregularity	> 20	NA

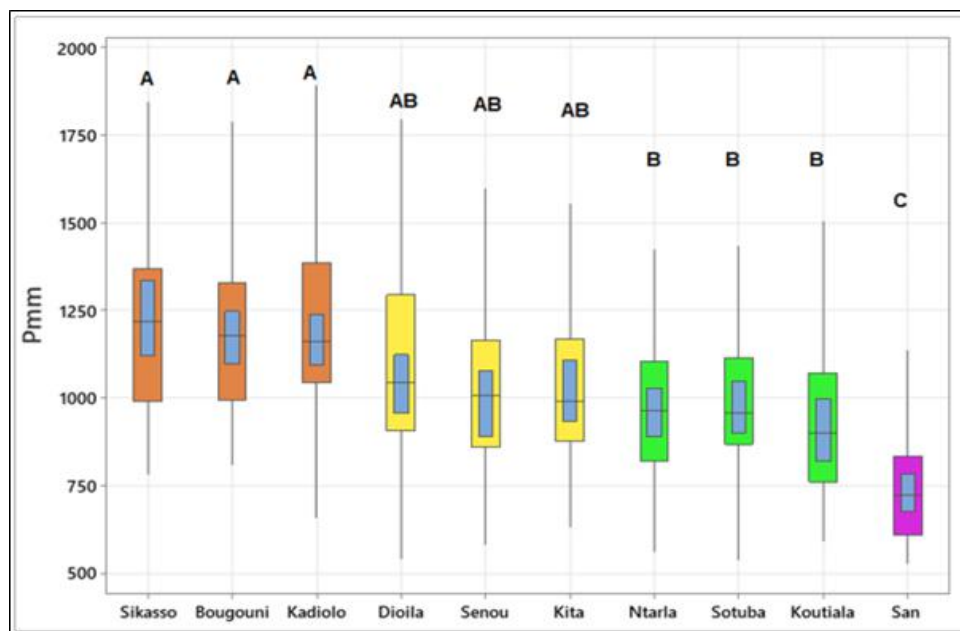


Fig.2: Boxplot classification of groups weather stations

### 3.4. Inter-station comparison of rainfall

Figure (3) shows the result of the comparison of the rainfall series of the 10 weather stations. Three homogeneous groups of stations were obtained whose medians are

different from each other. The group “A” consists of the stations of Sikasso, Bougouni and Kadiolo with a long-term average rainfall of around 1200 mm with a standard deviation of 253. The group “B” consists of the stations of

N'tarla, Sotuba and Koutiala with a long-term average rainfall of around 971mm with a standard deviation of 231. The "C" group consists only of the station of the station of San with a long-term average rainfall of 745 mm with a standard deviation of 155. The stations of Dioila, Senou and Kita, intermediate group "AB", present almost the same characteristics of the group "A" and the group "B" with a long-term average rainfall of about 1042 mm with a standard deviation of 252. Through this result, one can understand that there is local synchronicity between the stations and not zonal. This means that an increase or decrease in rainfall in any weather station is not widespread for all reminder weather stations in the same climatic zone or even all stations in the study area.

#### IV. CONCLUSION

In this paper, an investigation of the rainfall variability and trend in the CPZ of Mali has been performed by the means of daily to annual rainfall dataset from 1983 to 2021. Statistical analysis including CoV, Mann-Kendall non parametric trend test and PCI were carried out in order to detect variability, possible trend and concentration in the rainfall time series data. The rainfall amount showed moderate annual variability. A significant positive trend in total rainfall was observed over the study time period. The PCI showed an irregular rainfall variability in general that corresponds to the characteristic of the savannah zone. The comparison analysis used highlights a synchronicity between some weather stations. Finally, for improving precision and reliability of the application of the findings for practical use, increasing the number of study weather stations would be crucial. However, this research shows the importance of local level study in practical decision-making processes in agriculture and other water management programmes in the climate change adaptation context.

#### FUNDING

This research was conducted under AgrECO CML1430 project.

#### REFERENCES

- [1] Amrhein, V., Greenland, S., McShane, B. (2019). Scientists rise up against statistical significance. *Nature* 567:305-307 <https://doi.org/10.1038/d41586-019-00857-9>.
- [2] Asfaw, A., Simane, B., Hassen, A., & Bantider, A. (2018). Variability and time series trend analysis of rainfall and temperature in north central Ethiopia: A case study in Woleka sub-basin. *Weather and climate extremes*, 19, 29-41. <https://doi.org/10.1016/j.wace.2017.12.002>.
- [3] Ayalew, D., Tesfaye, K., Mamo, G., Yitafuru, B., & Bayu, W. (2012). Variability of rainfall and its current trend in Amhara region, Ethiopia. *African Journal of Agricultural Research*, 7(10), 1475-1486.
- [4] Bekele, F., Mosisa, N., & Terefe, D. (2017). Analysis of current rainfall variability and trends over Bale-Zone, South Eastern highland of Ethiopia. *Climate Change*, 3(12), 889-902.
- [5] Bhattacharyya, S., & Sreekesh, S. (2022). Assessments of multiple gridded-rainfall datasets for characterising the precipitation concentration index and its trends in India. *International Journal of Climatology*, 42(5), 3147– 3172. <https://doi.org/10.1002/joc.7412>
- [6] Bland, M. D., Whitson, M., Harris, H., Edmiaston, J., Connor, L. T., Fucetola, R., ... & Lang, C. E. (2015). Descriptive data analysis examining how standardised assessments are used to guide post-acute discharge recommendations for rehabilitation services after stroke. *Physical therapy*, 95(5), 710-719. <https://doi.org/10.2522/ptj.20140347>
- [7] Cabral Júnior, J., and Lucena, R. (2019). Analysis of Precipitation by Non-Parametric Test of Mann-Kendall and Kruskal-Wallis. *Mercator*, 19. doi:10.4215/rm2020.e19001.
- [8] De Luis, M., Gonzalez-Hidalgo, J.C., Brunetti, M. and Longares, L.A. (2011). Precipitation concentration changes in Spain 1946–2005. *Natural Hazards and Earth System Sciences*, 11(5), 1259– 1265. <https://doi.org/10.5194/nhess-11-1259-2011>.
- [9] Di Leo, G., Sardanelli, F. (2020). Statistical significance: p value, 0.05 threshold, and applications to radiomics-reasons for a conservative approach. *Eur Radiol Exp* 4, 18 <https://doi.org/10.1186/s41747-020-0145-y>.
- [10] El-Mahdy, M. E. S. (2021). Experimental method to predict scour characteristics downstream of stepped spillway equipped with V-Notch end sill. *Alexandria Engineering Journal*, 60(5), 4337-4346. <https://doi.org/10.1016/j.aej.2021.03.018>
- [11] Giannini, A. (2015). Climate change comes to the Sahel. *Nature Climate Change*, 5(8), 720-721. <https://doi.org/10.1038/nclimate2739>.
- [12] Hael, M. A. (2021). Modeling of rainfall variability using functional principal component method: a case study of Taiz region, Yemen. *Modeling Earth Systems and Environment*, 7(1), 17-27. <https://doi.org/10.1007/s40808-020-00876-w>
- [13] Kendall, M.G., (1975). Rank Correlation Methods, *ed. Charles Griffin, London*. Google Sch.
- [14] Koudahe, K.; Djaman, K.; Kayode, J.A.; Awokola, S.O.; Adebola, A.A. (2018). Impact of Climate Variability on Crop Yields in Southern Togo. *Environ. Pollut. Clim. Chang.* 2, 148.
- [15] L'Hote, Y.A.N.N., Mahe, G.I.L., & Some, B. (2003). The 1990s rainfall in the Sahel: the third driest decade since the beginning of the century. *Hydrological Sciences Journal*, 48(3), 493-496. <https://doi.org/10.1623/hysj.48.3.493.45283>.
- [16] Lalou, R., Sultan, B., Muller, B., & Ndonky, A. (2019). Does climate opportunity facilitate smallholder farmers' adaptive capacity in the Sahel? *Palgrave Commun* 5, 81.

- [18] Machin, D., Campbell, M. J., & Walters, S. J. (2007). *Medical statistics a textbook for the health sciences*. John Wiley & Sons, New York. google sch.
- [19] Maïga, O., Tounkara, M., Doumbia, S., & Sangho, H. (2019). Mali Political Economy Analysis. Report Research Technical Assistance Center, Washington, DC.
- [20] Mann, H. B. (1945). Nonparametric tests against trend. *Econometrica: Journal of the econometric society*, 245-259.
- [21] Mesike C.S., Agbonaye, O.E., (2016). Effects of rainfall on rubber yield in Nigeria. *Climate Change*, 2(7), 141-145.
- [22] Mishra, P., Pandey, C. M., Singh, U., Gupta, A., Sahu, C., & Keshri, A. (2019). Descriptive statistics and normality tests for statistical data. *Annals of cardiac anaesthesia*, 22(1), 67. doi: [10.4103/aca.ACA\\_157\\_18](https://doi.org/10.4103/aca.ACA_157_18).
- [23] Mohamed, M. A., and El-Mahdy, M. E. S. (2021). Impact of sunspot activity on the rainfall patterns over Eastern Africa: a case study of Sudan and South Sudan. *Journal of Water and Climate Change*, 12(5), 2104-2124. <https://doi.org/10.2166/wcc.2021.312>.
- [24] Mohamed, M. A., El Afandi, G. S., & El-Mahdy, M. E. S. (2022). Impact of climate change on rainfall variability in the Blue Nile basin. *Alexandria Engineering Journal*, 61(4), 3265-3275. <https://doi.org/10.1016/j.aej.2021.08.056>.
- [25] Nicholson, S. E., Some, B., & Kone, B. (2000). An analysis of recent rainfall conditions in West Africa, including the rainy seasons of the 1997 El Niño and the 1998 La Niña years. *Journal of climate*, 13(14), 2628-2640. [https://doi.org/10.1175/1520-0442\(2000\)013<2628:AAORRC>2.0.CO;2](https://doi.org/10.1175/1520-0442(2000)013<2628:AAORRC>2.0.CO;2)
- [26] Oliver, J.E. (1980). Monthly precipitation distribution: a comparative index. *Professional Geographer*, 32(3), 300–309. <https://doi.org/10.1111/j.0033-0124.1980.00300.x>.
- [27] Pawar, U., Karunathilaka, P., & Rathnayake, U. (2022). Spatio-temporal rainfall variability and concentration over Sri Lanka. *Advances in Meteorology*, 2022. <https://doi.org/10.1155/2022/6456761>.
- [28] Pradhan, A., Chandrakar, T., Nag, S. K., Dixit, A., & Mukherjee, S. C. (2020). Crop planning based on rainfall variability for Bastar region of Chhattisgarh, India. *Journal of Agrometeorology*, 22(4), 509-517.
- [29] Quenum, G.M.L.D., Klutse, N.A.B., Alamous, E.A., Lawin, E.A., Oguntunde, P.G. (2020). Precipitation Variability in West Africa in the Context of Global Warming and Adaptation Recommendations. In: Leal Filho, W., Oguge, N., Ayal, D., Adeleke, L., da Silva, I. (eds) *African Handbook of Climate Change Adaptation*. Springer, Cham. [https://doi.org/10.1007/978-3-030-42091-8\\_85-1](https://doi.org/10.1007/978-3-030-42091-8_85-1).
- [30] Rahman, M. S., & Islam, A. R. M. T. (2019). Are precipitation concentration and intensity changing in Bangladesh overtime? Analysis of the possible causes of changes in precipitation systems. *Science of the Total Environment*, 690, 370-387. <https://doi.org/10.1016/j.scitotenv.2019.06.529>.
- [31] Royé, D., and Martin-Vide, J. (2017). Concentration of daily precipitation in the contiguous United States, *Atmos. Res.* 196 (2017) 237-247. <https://doi.org/10.1016/j.atmosres.2017.06.011>.
- [32] Sanogo, S., Fink, A. H., Omotosho, J. A., Ba, A., Redl, R., & Ermert, V. (2015). Spatio-temporal characteristics of the recent rainfall recovery in West Africa. *International Journal of Climatology*, 35(15), 4589-4605.
- [33] Soumaré, M., Traoré, S. (2019). Présentation des zones cotonnières du Mali., Soumaré M. (éd), *Atlas des zones cotonnières du Mali, deuxième édition*, IER-CIRAD, pp 11.
- [34] Tabari, H., Marofi, S., Aeini, A., Talae, P.H., Mohammadi, K. (2011). Trend Analysis of Reference Evapotranspiration in the Western half of Iran. *Agricultural and Forest, Meteorology* 151, 128-136.
- [35] Traore, S.S. (2024). Validation des données d'estimation pluviométrique de « African Rainfall Climatology 2 » pour la zone cotonnière du Mali. *International Journal of Innovation and Applied Studies*, vol. 41, no. 3, pp. 889-896.
- [36] Traore, S.S., Soumare, M., Dembele, S., Ojeh, V. N., Guindo, S., & Diakite, C. H. (2021). Assessing Smallholder Farmers' Perception on Climate Variability in Relation to Climatological Evidence: A Case Study of Benguene in the Sudanian Zone of Mali. *East African Journal of Agriculture and Biotechnology*, 3(1), 24-34. <https://doi.org/10.37284/eajab.3.1.380>.
- [37] Traore, S.S., Guindo, S. Maïga, A.D., Sissoko, S. Soumaré, M. Diakité, C.H (2022). Evaluation et validation des données d'estimation pluviométrique de « African Rainfall Climatology 2 » pour la zone cotonnière du Mali. In : 13ème édition du Symposium Malien sur les Sciences Appliquées (MSAS 2022) ; 31 juillet au 05 août 2022 à Ségou, Mali – Acte en cours d'édition.
- [38] World Bank (2022). Country statistics “<https://data.worldbank.org/country/mali>” visited on 11/15/2023 at 15h31.
- [39] World Meteorological Organization; WMO, (2018) Guidelines on the Definition and Monitoring of Extreme Weather and Climate Events. Task Team Defin Extrem Weather Clim Events. <https://doi.org/10.1109/CSCI.2015.171>.
- [40] Xu, M., Kang, S.C., Wu, H., Yuan, X. (2018). Detection of Spatio-temporal variability of air temperature and precipitation based on long-term meteorological station observations over Tianshan Mountains, Central Asia. *Atmospheric Research*. 2018; 203:141–163. <https://doi.org/10.1016/j.atmosres.2017.12.007>.
- [41] Zachariah, M., Mondal, A., Das, M., AchutaRao, K. M., & Ghosh, S. (2020). On the role of rainfall deficits and cropping choices in loss of agricultural yield in Marathwada, India. *Environmental Research Letters*, 15(9), 094029.
- [42] Zakwan, M., & Ara, Z. (2019). Statistical analysis of rainfall in Bihar. *Sustainable Water Resources Management*, 5(4), 1781-1789. <https://doi.org/10.1007/s40899-019-00340-3>.



# Arsenic Content in Rice in Ghana: A Potential Health Hazard

Bartels Benjamin<sup>1</sup>, Akua Nkuma<sup>2</sup>, Gadzekpo Victor Patrick Yao<sup>3</sup>

<sup>1,2</sup>Department of Laboratory Technology, School of Physical Sciences, College of Agriculture and Natural Sciences, University of Cape Coast, Ghana

<sup>3</sup>Department of Chemistry, School of Physical Sciences, College of Agriculture and Natural Sciences, University of Cape Coast, Ghana

Received: 11 Oct 2023; Received in revised form: 20 Nov 2023; Accepted: 01 Dec 2023; Available online: 09 Dec 2023

©2023 The Author(s). Published by Infogain Publication. This is an open access article under the CC BY license

(<https://creativecommons.org/licenses/by/4.0/>).

**Abstract— Background and objectives:** Arsenic found mostly in rice and rice products is a carcinogen that affects the skin and internal organs. In recent times, concerns have been on the characteristic chronic concentration of this metal in rice even as FAO forecast increasing global production of rice. The aim of this study is to determine arsenic concentration in both local and imported rice patronized by consumers in the Central Region of Ghana. **Method:** A total of thirty-three samples comprising of seven locally produced rice and four imported brands were collected in three months from various outlets in Ghana. The samples were separately milled, digested and then filtered. The clear solution was used to run the arsenic test using A.A.S. **Results:** The local rice had concentration ranging from 0.256-0.420 mg/kg As, while the imported recorded 0.410-0.505 mg/kg As. The values obtained exceeded CODEX value of arsenic concentration in rice. **Conclusion:** Consumers of rice in Ghana are potentially at risk of arsenic related diseases.



**Keywords— Rice, arsenic, AAS, carcinogen**

## I. INTRODUCTION

Rice is one of the world's most important staple foods and supplies more than 50 % of the world's caloric intake (Clemens et al., 2013; Majumder & Banik, 2019)<sup>1,2</sup>. However, rice consumption poses a major health risk since the soils on which rice is normally grown are polluted with arsenic (As) (Zhao et al., 2014; Gonzalez et al., 2020; Oberoi et al., 2019)<sup>3,4,5</sup>. FAO's total world rice production for 2021 was 787,293,867 mt ([www.fao.org](http://www.fao.org))<sup>6</sup>. Rice plays a crucial role in ensuring global food security and cultivation provides employment for millions of farmers worldwide, supporting rural economies and livelihoods. In view of the gravity of health risks associated with As, different regulatory agencies like World Health Organization (WHO), Ghana Government, Vietnamese and China, have respectively legislated 300, 100-150, 200 and 200 -250µg/kg. (<https://www.sciencedirect.com/journal/heliyon>)<sup>7</sup>.

Recent rice surveys have shown that a significant amount of rice exceeded the WHO standard for arsenic (Zavala &

Duxbury, 2008; Rowell, 2014; Meharg et al., 2009)<sup>8,9,10</sup>. For instance, polished white rice in the American and French markets on average had 0.25 and 0.28 mg/kg As, respectively, while in Jamaica the white and brown rice samples had As ranging from 0.110 - 0.487 and 0.082–0.250 mg/kg, respectively (Meharg et al. 2009)<sup>10</sup>. A study in Vietnam reported a mean concentration of As in Vietnamese rice as 0.115mg/kg (Dinh Binh Chu et al., 2021)<sup>11</sup>.

In common with many other West African countries, the Government of Ghana conceived rice schemes as a major tool in improving food security and increasing rural incomes. To this end, Asian countries of all political stripes were encouraged to offer their expertise in the production of paddy rice. Ghana achieved the quite difficult feat of having experts from both North and South Korea, Taiwan and China all in the country simultaneously, working on isolated projects in remote areas (rice production in Ghana: country profile---AWS)<sup>12</sup>.

Ghana has relatively high rainfall compared with northern Nigeria and Mali and rice can be grown almost everywhere. Rice schemes are found right on the border with Burkina Faso, as in the case of Tono and down to the sea-coast. Rice production methods in Ghana can be divided into three types: Valley-bottom rice, Upland and Controlled flooding. (rice production in Ghana: country profile---AWS)<sup>12</sup>.

Ghana is 30% self –sufficient in rice production. The total rice demand is 600,000mt, the range of domestic production is 200,000 - 300,000 tons. The agro-ecological zones and production are respectively for irrigated, lowland/inland valleys and upland are 8, 77 and 15%. The contribution of the Northern, Volta and Upper East is 70% while Ashanti, Upper West, Brong Ahafo, Eastern, Central, Western, Greater Accra has 30% of the total production (Population Census, 2010; USDA/GSS/MOFA 2018-2019)<sup>13,14</sup>.

Rice research in Ghana has focused on the production of improved varieties with better production yields. While some attention has been given to rice macro-nutrient composition for purposes of both human and animal feeding (Amisshah et al., 2003, Adu-Kwarteng et al., 2003)<sup>15,16</sup>. There is little published data on the levels of potentially toxic elements (PTEs) in imported or locally produced rice from Ghana, the potential risk of As transfer to rice irrigated with mining-polluted surface waters has been highlighted (Adomako et al., 2010)<sup>17</sup>. In 2021, rice, paddy production for Ghana was 1.23 million tonnes. It increased from 70,100t in 1972 to 1.23mt in 2021 growing at an average annual rate of 8.85%. (<https://knoema.com/atlas>)<sup>18</sup>.

Given the significance of rice as a staple food and the potential health implications associated with As, this study aims to provide analysis of the arsenic content in local and imported rice in Ghana. The finding shall augment the empirical baseline data on rice in Ghana.

## II. MATERIALS AND METHOD

### 2.1 Procedure

#### 2.1.1 Collection of samples

The samples were collected during July to September 2023. Thirty-three samples of rice grains comprising of two types: seven locally produced rice and four popular imported brands. They were collected thrice in three months from various outlets in the major rice producing regions of Ghana. All the samples coded for laboratory for analysis. The imported rice were from India, China, Thailand and Vietnam.

#### 2.1.2 AAS analysis

The samples were separately milled and labelled, 0.5 grams of each of the milled sample digested and centrifuged. The

clear supernatant used for the arsenic test with AAS (<https://www.sciencedirect.com/journal/journal-of-food-composition-and-analysis>).

## III. RESULTS

Table 1: Average Arsenic Content ( $\mu\text{g}/\text{kg}$ ) of Rice.

Rice type	Arsenic ( $\mu\text{g}/\text{kg}$ )
<i>Local</i>	
R1 Upper East	305 $\pm$ 0.34
R2 North	410 $\pm$ 0.12
R3 Oti	420 $\pm$ 0.25
R4 Ashanti	350 $\pm$ 0.10
R5 Eastern	284 $\pm$ 0.05
R6 Western North	300 $\pm$ 0.10
R7 Volta	256 $\pm$ 0.10
<i>Imported</i>	
R8 India	505 $\pm$ 0.08
R9 China	410 $\pm$ 0.14
R10 Thailand	440 $\pm$ 0.26
R11 Vietnam	500 $\pm$ 0.11
<b>WHO</b>	<b>300</b>
<b>GHANA</b>	<b>100-150</b>
<b>VIETNAM</b>	<b>200</b>
<b>CHINA</b>	<b>200 -250</b>
<b>CODEX</b>	<b>200</b>

Source: Bartels/ Nkuma/ Gadzekpo laboratory results, 2023

R1, R2, R3, R4, R5, R6, R7 -local rice obtained from Ghana  
R8- rice imported from India / R9- rice imported from china  
R10- rice imported from Thailand / R11- rice imported from Vietnam

## IV. DISCUSSION

Rice research in Ghana has mainly been qualitative, there is therefore little published data on the levels of potentially toxic elements (PTEs) in imported or locally produced rice from Ghana (Amisshah et al., 2003, Adu-Kwarteng et al., 2003)<sup>15,16</sup>.

### *Arsenic content in local rice*

As indicated in Table 1, we found out that the respective average arsenic content in the local rice obtained from the regions of Upper East, North, Oti, Ashanti, Eastern,

Western North and Volta in Ghana respectively were  $305 \pm 0.34$ ,  $400 \pm 0.12$ ,  $420 \pm 0.25$ ,  $350 \pm 0.10$ ,  $284 \pm 0.05$ ,  $300 \pm 0.10$  and  $256 \pm 0.10$   $\mu\text{g}/\text{kg}$ . The sample from Oti region had the highest content of  $0.42$   $\text{mg}/\text{kg}$  As, with the least being Volta region having  $0.256$   $\text{mg}/\text{kg}$  As. All the reported concentrations are above the WHO, Codex and Ghana standards of  $0.2$ ,  $0.3$  and  $0.1$ - $0.15$   $\text{mg}/\text{kg}$  respectively confirming the potential risk of As (Adomako et al., 2010)<sup>17</sup>. This finding corroborates earlier study that the arsenic content of raw rice could reach concentrations of about  $1$  ppm (Sun et al., 2008)<sup>19</sup>.

#### *Arsenic content in local and imported rice*

The average concentrations of arsenic obtained for the imported rice on sale from India, China, Thailand and Vietnam respectively were  $505 \pm 0.08$ ,  $410 \pm 0.14$ ,  $440 \pm 0.26$ ,  $500 \pm 0.11$   $\mu\text{g}/\text{kg}$ . The imported rice relatively typically had higher arsenic content than the local rice. These concentrations are also higher than the standards of WHO, CODEX, Vietnam, China and Thailand shown in Table 1.

In similar research in India, the concentration of As in rice grains was in the range of  $0.04 - 0.45$   $\mu\text{g g}^{-1}$  (<https://www.sciencedirect.com/journal/journal-of-food-composition-and-analysis>)<sup>20</sup> of which our reported concentration  $505 \pm 0.08$   $\mu\text{g}/\text{kg}$  As ( $0.505$   $\text{mg}/\text{kg}$  As) obtained in this study is higher for the imported rice from India. Another study in Vietnam reported a mean concentration of As in Vietnamese rice as  $0.115$   $\text{mg}/\text{kg}$  (Dinh Binh Chu et al., 2021)<sup>11</sup>, though below the standard of  $200$   $\text{mg}/\text{kg}$  legislated by Vietnam, the present finding of  $0.5$   $\text{mg}/\text{kg}$  As reported in this study is much higher.

The findings suggest that rice in Ghana contains higher concentrations of As, which could be a recipe for cardiovascular, haematological, renal, endocrine and hepatic diseases (<https://link.springer.com/journal/10653>)<sup>21</sup> since the concentrations are above the legislated thresholds as provided in Table 1.

### CONCLUSION

All the samples analysed contained higher concentrations of As, above both the local and international legislated standards. This implies that Ghana's rice is prone to As contamination, long term exposure could lead to bioaccumulation within the body. Therefore, the presence of arsenic of such a high concentration in the samples is particularly worrying given that the rice is a staple in very high demand in Ghana.

### RECOMMENDATION

The Ministry of Food and Agriculture, the Food and Drugs Authority and other stakeholders must intensify the monitoring of the quality of rice in Ghana.

### ACKNOWLEDGEMENT

We acknowledge the contributions of the Book and Research Allowance of Government of Ghana, the diverse assistance of the University of Cape Coast and authors whose works were cited.

### REFERENCES

- [1] Clemens, S., Aarts, M. G., Thomine, S., & Verbruggen, N. Plant science: the key to preventing slow cadmium poisoning. *Trends in plant science*, 18(2), 92-99. 2013
- [2] Majumder, S., & Banik, P. Geographical variation of arsenic distribution in paddy soil, rice and rice-based products: A meta-analytic approach and implications to human health. *Journal of environmental management*, 233, 184-199. 2019
- [3] González, N., Marquès, M., Nadal, M., & Domingo, J. L. Meat consumption: Which are the current global risks? A review of recent (2010–2020) evidences. *Food Research International*, 137, 109341. 2020
- [4] Zhao, F. J., Ma, J. F., Meharg, A. A., & McGrath, S. P. Arsenic uptake and metabolism in plants. *New Phytologist*, 181(4), 777-794. 2009
- [5] Oberoi, S., Devleeschauwer, B., Gibb, H. J., & Barchowsky, A. Global burden of cancer and coronary heart disease resulting from dietary exposure to arsenic, 2015. *Environmental research*, 171, 185-192. 2019
- [6] [www.fao.org](http://www.fao.org) retrieved on 28/10/23
- [7] <https://www.sciencedirect.com/journal/heliyon>.
- [8] Zavala, Y. J., & Duxbury, J. M. Arsenic in rice: I. Estimating normal levels of total arsenic in rice grain. *Environmental Science & Technology*, 42(10), 3856-3860. 2008
- [9] Rowell, D. L. (2014). *Soil science: Methods & applications*. Routledge.
- [10] Meharg, A. A., Sun, G., Williams, P. N., Adomako, E., Deacon, C., Zhu, Y. G., & Raab, A. Inorganic arsenic levels in baby rice are of concern. *Environmental pollution*, 152(3), 746-749. 2008
- [11] Dinh Binh Chu, Hung Tuan Duong, Minh Thi Nguyet Luu, Hong-An Vu-Thi, Bich-Thuy Ly & Vu Duc Loi, "Arsenic and Heavy Metals in Vietnamese Rice: Assessment of Human Exposure to These Elements through Rice Consumption", *Journal of Analytical Methods in Chemistry*, 2021
- [12] Rice production in Ghana: country profile---AWS retrieved on 28/10/23
- [13] Population Census, GHANA 2010
- [14] USDA/GSS/MOFA 2018-2019
- [15] Amissah, J. G. N., Ellis, W. O., Oduro, I., & Manful, J. T. Nutrient composition of bran from new rice varieties under study in Ghana. *Food control*, 14(1), 21-24. 2003.

- [16] Adu-Kwarteng, E., Ellis, W. O., Oduro, I., & Manful, J. T. Rice grain quality: a comparison of local varieties with new varieties under study in Ghana. *Food control*, 14(7), 507-514. 2003
- [17] Adomako, E. E., Williams, P. N., Deacon, C., & Meharg, A. A.). Inorganic arsenic and trace elements in Ghanaian grain staples. *Environmental pollution*, 159(10), 2435-2442. 2011
- [18] <https://knoema.com/atlas> retrieved on 01/11/23
- [19] **SUN G-X, WILLIAMS P,N, CAREY A-M, ZHU Y-G, DEACON C, RAAB A, FELDMANN J, ISLAM R.M, & ANDREW A. MEHARG A.A INORGANIC ARSENIC IN RICE BRAN AND ITS PRODUCTS ARE AN ORDER OF MAGNITUDE HIGHER THAN IN BULK GRAIN ENVIRON. SCI. TECHNOL. 42, 19, 7542–7546, 2008**
- [20] <https://www.sciencedirect.com/journal/journal-of-food-composition-and-analysis> retrieved on 01/11/23
- [21] <https://link.springer.com/journal/10653> retrieved on 01/11/23



# Adulteration of Honey on the Cape Coast Market in the Central Region of Ghana

Bartels Benjamin<sup>1</sup>, Aggrey Ernestina<sup>2</sup>, Gadzekpo Victor Patrick Yao<sup>3</sup>

<sup>1,2</sup> Department of Laboratory Technology, School of Physical Science, College of Agriculture and Natural Science, University of Cape Coast, Cape Coast, Ghana.

<sup>3</sup> Department of Chemistry, School of Physical Science, College of Agriculture and Natural Science, University of Cape Coast, Cape Coast, Ghana.

Received: 09 Oct 2023; Received in revised form: 18 Nov 2023; Accepted: 29 Nov 2023; Available online: 09 Dec 2023

©2023 The Author(s). Published by Infogain Publication. This is an open access article under the CC BY license

(<https://creativecommons.org/licenses/by/4.0/>).

**Abstract— Background and objectives:** This research is driven by the need to combat the growing concern of honey adulteration, a practice that compromises the quality and authenticity of this natural product. Adulteration of honey is a pressing concern that compromises its quality, authenticity, and nutritional value. This study investigates the presence of adulterants in honey samples collected from the Cape Coast metropolis in the Central Region of Ghana. **Methods:** Seven honey samples were analyzed. They were selected from different outlets in the metropolis. Laser- induced fluorescence (LIF) technique was employed to identify potential adulterants by examining the fluorescence spectra of the samples. The fluorescence patterns were compared to a reference database to determine the authenticity of the honey. **Results:** The LIF analysis revealed distinct fluorescence patterns among the samples, indicating potential adulteration. The control sample exhibited a characteristic fluorescence profile consistent with pure honey, while certain samples exhibited altered fluorescence spectra. This deviation in fluorescence patterns strongly suggests the use of additives or adulterants in the honey samples. **Conclusion:** The findings indicate the presence of adulteration in the samples. The altered fluorescence spectra observed in some samples strongly suggest the use of adulterants, potentially compromising the quality and authenticity of the honey. To combat honey adulteration effectively, stringent regulatory measures, increased consumer awareness, and continuous monitoring are necessary.



**Keywords— adulteration, honey, Laser- Induced Fluorescence, spectra**

## I. INTRODUCTION

Honey's nutritional richness and potential health benefits have been negated by the proliferation of adulteration practices (Guleria et al., 2019)<sup>1</sup>. Adulteration involves the deliberate incorporation of extraneous substances into honey to compromise its quality.

The primary constituents of honey are carbohydrates, specifically sugars. Fructose and glucose are the dominant sugars present, accounting for approximately 85-95% of the total carbohydrate content (Molan, 1999)<sup>2</sup>. These sugars not only impart sweetness but also contribute to honey's unique hygroscopic nature, which helps prevent microbial growth and maintain its stability (Gupta & Kumar, 2017)<sup>3</sup>. The ratio

of fructose to glucose is one of the indicators used to assess the botanical origin and quality of honey (Bogdanov et al., 2017)<sup>4</sup>.

Enzymes play a crucial role in honey's composition and characteristics. Invertase, also known as sucrase, converts sucrose into fructose and glucose, enhancing honey's sweetness (White & Doner, 2018)<sup>5</sup>. Diastase, another enzyme, breaks down complex sugars like starch into simpler sugars, contributing to honey's nutritional value (Codex Alimentarius, 2020)<sup>6</sup>. These enzymatic activities are used as quality indicators and can be affected by factors such as temperature and processing methods.



Honey's natural acidity, reflected by its low pH, inhibits the growth of microorganisms, contributing to its remarkable shelf-life (Molan, 2017)<sup>7</sup>. Organic acids, including gluconic acid and acetic acid, are responsible for honey's acidic pH, which typically ranges from 3.2 to 4.5 (Molan, 2017)<sup>7</sup>. This characteristic pH level also contributes to the release of hydrogen peroxide, a potent antimicrobial compound (Jaganathan & Mandal, 2019)<sup>8</sup>.

Honey is a treasure trove of minor constituents that contribute to its nutritional and therapeutic value. These include proteins, amino acids, vitamins, minerals, and antioxidants. The presence of amino acids such as proline and lysine, which are not found in significant amounts in other sweeteners, enhances honey's nutritional profile (Dramićanin, 2018)<sup>9</sup>. Furthermore, antioxidants like flavonoids and phenolic compounds confer honey's potential health benefits, including its anti-inflammatory and immune-boosting properties (Bertoncelj et al., 2017)<sup>10</sup>.

The color of honey varies widely, ranging from pale yellow to dark amber, depending on its botanical origin (Da Silva et al., 2019)<sup>11</sup>. This variation arises from the different types of nectar and pollen collected by bees. Over time, honey may undergo crystallization, resulting in changes in texture and appearance. Crystallization is influenced by factors such as the ratio of glucose to fructose and storage conditions (Da Silva et al., 2019)<sup>11</sup>.

The physical properties of honey, such as viscosity, density, and refractive index, are influenced by its composition. These properties are essential for various applications, including food processing and quality control (Kumar et al., 2021)<sup>12</sup>. The hygroscopic nature of honey, coupled with its low water content, contributes to its moisture absorbing capacity and makes it effective for preserving products like baked goods (Gupta & Kumar, 2017)<sup>3</sup>.

Honey is used as value as a food and medicine (Sammataro & Avitabile, 2011)<sup>13</sup> for offerings, as sweetener, and in embalming processes (Crane, 1999)<sup>14</sup> and a divine symbol and a source of strength and therapeutic properties (Patel & Patel, 2011; Mazaraki, 2017)<sup>15,16</sup>. Moreover, it has antibacterial properties (Molan, 2017)<sup>7</sup>, wound healing potential (Jull et al., 2015)<sup>17</sup>.

Adulteration can introduce harmful contaminants into honey, including heavy metals, antibiotics, pesticides, and other chemical compounds. Consumption of adulterated honey may lead to acute and chronic health issues, ranging from allergic reactions to gastrointestinal disturbances and even more severe conditions. Contaminants can accumulate in the body over time, triggering allergic responses, organ damage, and adverse long-term health effects. Moreover, the absence or reduction of essential nutrients due to

adulteration may undermine the nutritional benefits that pure honey offers (Bogdanov, 2007; Monakhova, 2014)<sup>18,19</sup>.

The prevalence of adulterated honey not only threatens consumer health but also undermines the ethical and economic principles of fair trade and sustainability. Adulteration practices not only deceive consumers by providing substandard products but also erode the reputation of honest honey producers. This unfair competition compromises the livelihoods of legitimate beekeepers and undermines the integrity of the honey industry as a whole (Codex Alimentarius Commission, 2019; Dutta, 2018)<sup>20,21</sup>.

The global trade of adulterated honey disrupts food safety regulations and standards. Adulterated honey can cross international borders and infiltrate markets, making it challenging for regulatory authorities to ensure that consumers receive safe and genuine products. The lack of comprehensive regulatory frameworks specifically targeting honey adulteration exacerbates these challenges, allowing unscrupulous practices to persist (Perna, 2021; Dutta, 2018)<sup>22,21</sup>.

One of the most significant risks posed by adulterated honey is the erosion of consumer trust in the food supply chain. As consumers become aware of adulteration practices, their confidence in the quality and authenticity of honey may wane. This loss of trust can extend beyond honey consumption, affecting overall consumer confidence in the safety and integrity of food products (Dutta, 2018)<sup>21</sup>.

Adulterated honey undermines the efforts of legitimate beekeepers who adhere to ethical and sustainable practices. The economic viability of genuine beekeeping operations is threatened when the market is flooded with cheaper adulterated alternatives. This can lead to decreased demand for pure honey, pushing beekeepers out of business and disrupting the delicate balance of pollination and environmental conservation that bees facilitate (Perna, 2021; Dutta, 2018)<sup>22,21</sup>.

In addition to individual health risks, the consumption of adulterated honey can have broader public health implications. The presence of contaminants in honey could contribute to the development of antibiotic resistance in humans, as well as the accumulation of harmful substances in the environment. The global nature of the honey trade also means that adulterated honey could potentially spread diseases across borders (Monakhova, 2014)<sup>19</sup>.

Enforcing laws against honey adulteration can be complex due to the diverse range of adulterants and techniques used. Adulteration often involves sophisticated methods that can be challenging to detect without advanced analytical techniques. Developing effective legislation, regulations, and enforcement mechanisms to counteract adulteration

requires collaboration between governments, regulatory agencies, and the industry (Dutta, 2018)<sup>21</sup>.

Several substances are commonly used as adulterants in honey due to their similarities in appearance, taste, and texture. Some of the most frequent adulterants include: Sugar Syrups, High-Fructose Corn Syrup (HFCS), Cane Sugar, Molasses, Starch Syrups, Artificial Flavorings.

In Ghana, honey production has experienced a significant evolution from traditional honey hunting to modern beekeeping practices, contributing to economic growth, livelihood improvement, and agricultural sustainability. Beekeeping has become an important income generating activity, offering both economic and ecological benefits to the people of Ghana.

The history of honey production in Ghana is marked by a transition from traditional honey hunting to more advanced and sustainable beekeeping practices (Darkwa & Boateng, 2004)<sup>23</sup>.

Beekeeping has emerged as a significant economic activity for rural communities in Ghana. Beekeepers can diversify their products, including honey, beeswax, propolis, pollen, venom, and bee brood, thereby increasing their income potential (Darkwa & Opoku, 2016; Abebrese et al., 2019)<sup>24,25</sup>. In 2008, honey production contributed about 23% to a beekeeper's annual income, and by 2009, the overall household income for families involved in the honey sector increased to approximately 37% (Darkwa & Opoku, 2016)<sup>24</sup>.

Ghana's honey production has not only satisfied domestic demand but has also found its place in international markets. The European Union's certification of Ghana as an authorized exporter of honey to the EU market in 2011 opened doors for expanded trade opportunities. This recognition signifies the quality of Ghanaian honey and its potential for export-driven growth (Achiano, 2016)<sup>26</sup>. However, maintaining and improving honey quality remains a challenge. The type of beehives used, harvesting methods, and processing techniques influence the quantity and quality of honey (Darkwa & Opoku, 2013)<sup>27</sup>.

The prevalence of adulteration practices in the honey industry has raised significant concerns about the authenticity and quality of honey. This deceptive practice poses health risks, and unfair trade practices.

Researchers have turned to advanced analytical methods, such as laser-induced fluorescence (LIF), to combat this issue (Li & Yang., 2012)<sup>28</sup>. LIF capitalizes on the principles of spectroscopy and fluorescence to unveil the hidden molecular identity of a sample. Through laser excitation, specific compounds emit distinct fluorescent signals,

allowing for precise identification and differentiation (Lee et al., 2015)<sup>29</sup>.

The Cape Coast market is alleged to experience such adulteration cases. This study shall contribute to industry integrity, consumer protection, and to raise public awareness of the problem. Also, shed light on the prevalence in the Cape Coast metropolis.

With respect to limitations, the study is confined to the Cape Coast metropolis, potentially limiting the generalization of findings to other geographical areas.

## II. MATERIALS AND METHOD

### 2.1 Research Design

#### 2.1.1 Research Approach

A quantitative research approach is adapted to emphasize the collection and analysis of numerical data to derive patterns, relationships, and statistical significance. Thus to provide a clear and objective understanding of the prevalence and characteristics of honey adulteration in the Cape Coast market.

#### 2.1.2 Research Type

The research type chosen for this study is descriptive research. Descriptive research shall focus on providing a comprehensive depiction of the phenomenon of the extent of honey adulteration and its underlying factors within the Cape Coast market. This shall provide insights into the current state of honey quality in the market and identifying potential adulterants.

### 2.2 Data Collection Methods

This shall involve both primary and secondary data collection methods. Respectively provides valuable insights into the physical and chemical attributes of the honey samples and employing a comprehensive review of literature related to honey adulteration, detection methods, and its implications to providing a broader context and facilitating a comparison of findings from various studies.

### 2.3 Study Area

The study area encompasses a selection of key outlets within the Cape Coast Metropolis in the Central Region of Ghana. These outlets are Science, Tantre, Kotokuraba, Ayensu, Pedu and Abura. Each contributing to the metropolis' economic activity. In addition, the Benso Bee Farm was chosen to offer a controlled source serving as a reference point. This controlled source acts as a benchmark against which honey samples can be evaluated for purity and potential adulteration since it conforms to known standards and practices. This approach facilitates the inclusion of diverse vendors, consumers, and regional

variations that may influence the availability and quality of honey.

## 2.4 Sample Collection

### 2.4.1 Sampling Procedure

To ensure a representative and meaningful sample set, a systematic random sampling procedure was employed to capture a cross-section of honey available in the chosen outlets. The sampling was done in three months.

This approach aimed to minimize bias and ensure that various vendors, product types, and honey sources were represented.

### 2.4.2 SAMPLE PREPARATION

Prior to analysis, the samples underwent a series of preparation steps to ensure consistent and accurate measurements:

**Homogenization:** Each sample was thoroughly mixed to ensure uniform distribution of any potential adulterants. This step aimed to eliminate bias arising from variations within the honey product.

**Sample Labeling:** Samples were labeled with unique identifiers to maintain traceability throughout the analysis process. These identifiers linked each sample to the corresponding vendor and market.

**Storage:** Prepared samples were stored in a controlled environment to prevent degradation and maintain the integrity of the collected honey.

### 2.4.3 Laboratory analysis

The Laser Induced Fluorescence transmission data was obtained by incident light on the sample with fiber on one end and collecting with another fiber from the other end at 180°. The procedure was repeated five times for each time transmission. Reference measurement was obtained by measuring the transmitted light as described when there was no sample.

Then, fluorescence spectra of samples measured with the Laser-Induced Fluorescence setup. For each measurement, drops of pure honey were placed on a glass slide. A bi-fabricated fiber probe with one of its ends connected to the laser source (blue LASER of power 100 mW and wavelength 445 nm), and the other end connected to the detector (ocean optics USB 200 spectrometer) that had a high pass filter in front that allowed the longer wavelengths (450 nm) that is fluorescence to enter. The spectrophotometer was connected to a computer that had the Spectra Suite for data acquisition and visualization. The software was set at an integration time of 300 ms, an averaging of 2, and a boxcar width of 10. Five replicates from each sample were taken to minimize measurement error.

### 2.4.4 Data Analysis

Descriptive statistics unveiled honey sample trends, while Principal Component Analysis (PCA) transformed variables into uncorrelated components, exposing patterns and relationships.

The principal components that captured the maximum variance in the data were extracted and ranked based on their eigenvalues. The loadings and scores of the principal components were analyzed to interpret the underlying factors contributing to the variation in the dataset. Scatter plots, biplots, or other graphical representations were generated to visualize the distribution and clustering of the honey samples based on the principal components.

## III. RESULTS

Table 1: Absorbance, Brix (%), And Moisture Content (%) Of Honey Samples

Sample	Absorbance (au)	Brix (%)	Moisture Content (%)
Control (Benso bee farm)	High	78.5	16.2
H1 (Science market)	Medium	75.8	18.4
H2 (Tantre)	High	80.2	15.8
H3 (Kotokuraba)	Low	73.6	19.1
H4 (Ayensu)	Medium	77.9	16.8
H5 (Pedu)	High	79.1	16.5
H6 (Abura)	Medium	76.3	17.9
CODEX	-	80	20

Source: Bartels/Aggrey/Gadzekpo Laboratory analysis 2023

- Brix represents the percentage of total soluble solids in honey, which is an indicator of its sweetness.
- Moisture content refers to the percentage of water present in honey, which affects its quality and stability.

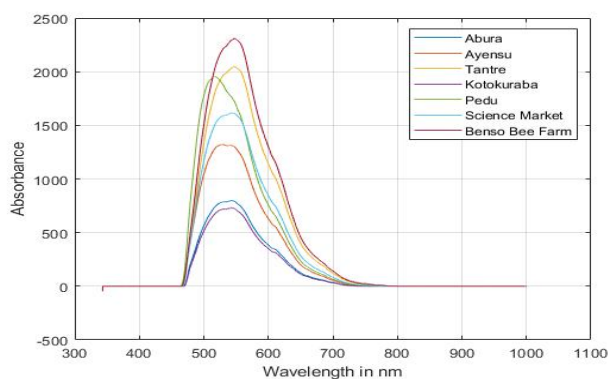


Fig.1: Overall spectra of the samples

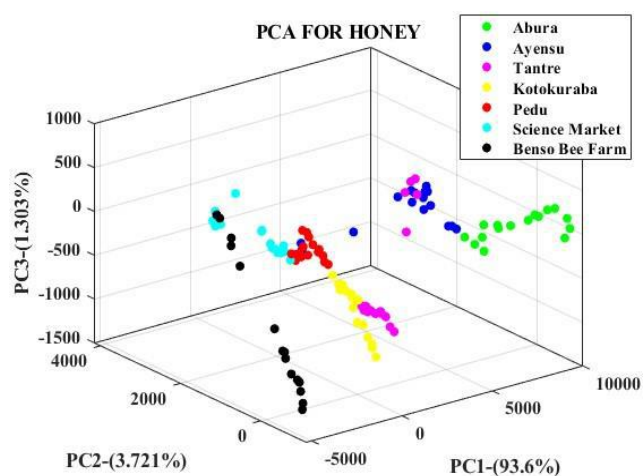


Fig.2: PCA graph

#### IV. DISCUSSION

As shown in **Table 1**, the control sample exhibited a Brix value of 78.5%, indicating a high level of sweetness, and a moisture content of 16.2%, within the acceptable range for quality honey (CODEX, 2019)<sup>20</sup>. Among the market samples, variations in Brix and moisture content were observed. H2 had the highest Brix value of 80.2%, indicating increased sweetness, while H3 had the highest moisture content of 19.1%.

These variations in Brix and moisture content highlight the potential differences in quality and composition among the honey samples obtained from different outlets.

##### 4.1 Control (Benso Bee Farm):

From **Table 1**, Fig 1. The brix content of the control sample (79.5%) is slightly lower than the standard honey from the CODEX standard of 80.0%, indicating a slightly reduced sugar concentration. The moisture content of 19.1% for the control sample is comparable to the CODEX standard. The brix content of most samples is within the range of the standard honey, except the Tantri sample. In relation to the

other samples, the control shows slight differences in both brix and moisture content. These differences might reflect variations in beekeeping practices, environmental conditions, or regional characteristics [Monakhova, 2014]<sup>19</sup>.

##### 4.2 The spectra

The spectra as shown in Fig.1 provides valuable information about the chemical composition and characteristics of the honey samples. The control sample obtained from the Benso farm served as a reference point for the comparison of other samples to establish a baseline for the expected properties of pure, unadulterated honey. Any deviations observed is attributed to potential adulteration or differences in composition.

Again, from **Table 1**, Fig 1, the control sample from the Benso bee farm exhibited a high absorbance, indicating its purity and lack of adulteration. Likewise, H2 and H5 indicating a potential similarity in composition. On the other hand, H1, H4, and H6 displayed a relatively medium absorbance, which suggests a potential level of adulteration or compositional differences (ref), with their Brix and moisture content further supporting the possibility of alterations in composition.

In H3, a significant deviation from the control is observed, suggesting potential adulteration or compositional differences. The Brix value of 73.6% and moisture content of 19.1% also deviate from the expected ranges for unadulterated honey.

##### 4.3 PCA Analysis

From figure 2, the variance explained by each principal component was as follows: PC1, 93.6%; PC2 3.721%; and PC3, 1.303%. These percentages indicate the proportion of total variability in the original data captured by each respective principal component. Key observations are as follows:

4.3 .1. Control Cluster: The black dots representing the control, formed a distinct cluster. This indicates that the control share similar characteristics in terms of their brix and moisture content. The proximity of these dots suggests that they are tightly grouped together in the reduced-dimensional space.

4.3 .2. Inter-Cluster Relationships: Notably, some parts of the black dots formed clusters with parts of the pale blue dots, indicating a certain degree of similarity between the control and H1 (Science Market). This suggests that there might be shared characteristics between these two groups, albeit to a lesser extent compared to the within-group clustering.

4.3 .3. Cluster Separation: The red and blue dots for Pedu(H5) and Ayensu(H6), respectively forming clusters

with the pale blue dots might indicate some level of similarity in brix and moisture content among these groups. However, it is important to note that the rest of the dots were mostly distinct and separate from each other, indicating clear differences in their composition.

## V. CONCLUSION

1. The analysis of Brix and moisture content indicated variations among the honey samples, suggesting the presence of potential adulteration.
2. The investigation utilizing the LIF (Laser-Induced Fluorescence) technique provided valuable insights into adulteration in honey from the Cape Coast market.
3. The analysis involved seven samples, including a control sample obtained from the Benso farm, and each sample was analyzed five times to obtain the mean absorbance spectra using Principal Component Analysis (PCA).
4. The absorbance spectra demonstrated variations among the honey samples, indicating potential adulteration. The control sample from the Benso farm exhibited the highest absorbance, representing the expected properties of pure, unadulterated honey. In contrast, the remaining six samples displayed different absorbance values, suggesting potential adulteration or compositional differences.
5. Among the adulterated samples, Tantre exhibited the highest absorbance, closely resembling the absorbance value of the control sample. This suggests that Tantre honey may have undergone similar adulteration or shared similar compositional characteristics with the control. Following Tantre, Pedu, Science Market, Ayensu, and Abura displayed progressively lower absorbance values, indicating varying degrees of adulteration. Kotokuraba showed the lowest absorbance value among the adulterated samples, signifying a potentially higher level of adulteration or compositional differences compared to the others.
6. These findings highlight the presence of adulteration in the honey samples from the Cape Coast market, as indicated by their deviating absorbance values compared to the control.
7. The variations in absorbance suggest differences in the composition and quality of the adulterated samples compared to the control, emphasizing the need for quality control measures in the honey industry.

## RECOMMENDATIONS

- To address honey adulteration effectively, it is essential to strengthen regulatory measures, enhance consumer education, promote transparency and traceability, and

foster collaboration among beekeepers, regulatory authorities, researchers, and industry associations.

- Additionally, further research and development are required to refine testing and detection methods and establish comprehensive honey quality monitoring programs.
- These findings emphasize the need for strict quality control measures, increased consumer awareness, and continuous monitoring to ensure the availability of pure and authentic honey products.
- By implementing these recommendations and continuing research efforts, we can combat honey adulteration, protect consumer health, support the local honey industry, and ensure the availability of high-quality and authentic honey in the Cape Coast region.

## ACKNOWLEDGEMENT

The Book and Research Allowance of the Government of Ghana, the various contributions of the University of Cape Coast are well appreciated. In addition, authors whose works were cited are well acknowledged.

## REFERENCES

- [1] Guleria, S., Kumar, R., & Bhullar, N. K. Honey adulteration: A comprehensive review. *Journal of Food Science and Technology*, 56(2), 412-426. 2019.
- [2] Molan, P. C. The role of honey in the management of wounds. *Journal of Wound Care*, 8(8), 423-426. 1999
- [3] Gupta, R. S., & Kumar, N. Honey: Its history and religious significance, its nutritional and healing power. *Ayu*, 30(4), 121-127. 2017
- [4] Bogdanov, S. Honey for nutrition and health: a review. *Journal of the American College of Nutrition*, 27(6), 677-689. 2017
- [5] White, J. W., & Doner, L. W. Honey composition and properties. Beekeeping in the United States. *Agricultural Handbook*, 335, 82-91. 2010
- [6] Codex Alimentarius. Codex standard for honey. *CODEX STAN 12-1981 (Rev. 1-2001)*. 2020
- [7] Molan, P. C. The role of hydrogen peroxide in honey. *New Zealand Bee* 2017
- [8] Jaganathan, S. K., & Mandal, M. Antiproliferative effects of honey and of its polyphenols: A review. *Journal of Biomedicine and Biotechnology*, 2016, 1-13. 2019
- [9] Dramićanin, Tanja. Fluorescence spectroscopy in the study of honey flavonoids and polyphenols. *Food Chemistry*, 264, 285-290. 2018
- [10] Bertonec, J., Doberšek, U., & Jamnik, M. Evaluation of the phenolic content, antioxidant activity and colour of Slovenian honey. *Food Chemistry*, 105(2), 822-828. 2017
- [11] Da Silva, Paula M. Analytical methods applied to the study of honey. *Trends in Analytical Chemistry*, 135, 116185. 2021

- [12] Kumar, S. G., Kumar, K. G., & Ravi, R. Physical and chemical characteristics of honey. *Asian Journal of Pharmaceutical and Clinical Research*, 14(4), 15-18. 2021
- [13] [13] Silva, L. R., Videira, R., Monteiro, A. P., Valentão, P., & Andrade, P. B. Honey as a source of nutritional and therapeutic compounds: A review. *Molecules*, 24(22), 1-26. 2019
- [14] [14].Crane, E. The world history of beekeeping and honey hunting. Routledge. 1999
- [15] Patel, R. K., & Patel, S. R. Apiculture and human health: A review. *Research Journal of Pharmaceutical, Biological, and Chemical Sciences*, 2(4), 444-448. 2011
- [16] Mazaraki, D. Honey in the Greco-Roman world and beyond: A status symbolorum. *Apidologie*, 48(4), 553-565. 2017
- [17] Jull, A. B., et al. Honey as a topical treatment for wounds. *Cochrane Database of Systematic Reviews*, 3. 2015
- [18] Bogdanov, S., Lullmann, C., Martin, P., & von der Ohe, W. Harmonized methods of the International Honey Commission. *Apidologie*, 38(1), S1-S61. 2007
- [19] Monakhova, Yulia B. Honey authenticity: A review. *Trends in Food Science & Technology*, 35(1), 41-54. 2014
- [20] Codex Alimentarius Commission. Codex Standard for Honey. *CODEX STAN 12-1981, Rev. 2* (2019). 2019
- [21] Dutta, S. Honey and its medicinal value: A review. *International Journal of Pharmacy & Pharmaceutical Research*, 12(1), 101-107. 2018
- [22] Wei, F., Wu, J., Cui, X., Li, J., & Liang, H. Quantitative determination of fructose/glucose ratios in honey samples using laser-induced breakdown spectroscopy. *Food Analytical Methods*, 8(3), 754-760. 2015
- [23] Darkwa, A. A., & Boateng, B. A. Physico-chemical properties of some Ghanaian honeys. *Food Control*, 15(4), 287-292. 2004
- [24] Darkwa, A. A., & Opoku, D. K. Apicultural practices in Ghana: Their environmental and development implications. *Journal of Sustainable Development in Africa*, 18(6), 95-111. 2016
- [25] Abebrese, E. K. Beekeeping and poverty reduction: Exploring opportunities and constraints in the Volta region of Ghana. *International Journal of Development and Sustainability*, 8(2), 116-129. 2019
- [26] Achiano, K. The European Union's decision to lift the ban on Ghanaian honey: Prospects and challenges for the local apicultural industry. *West African Journal of Industrial and Academic Research*, 12(1), 16-32. 2016
- [27] Darkwa, A. A., & Opoku, D. K. Honey quality in Ghana: A review. *Agricultural Science Research Journal*, 3(7), 173-183. 2013
- [28] Li, Hui. & Yang, Shuqin. Discrimination of Chinese honey using visible and nearinfrared spectroscopy and chemometrics. *Food Research International*, 49(1), 175-182. 2012
- [29] Lee, S. H., Wu, B., & Johnson, M. L. Recent advances in laser-induced fluorescence detection: A review. *Analytica Chimica Acta*, 890, 1-13. 2015



# Research on Soil Erosion Intensity and Spatial Distribution Characteristics in Zhaoyang District of Zhaotong City Based on RS and GIS

Maohua Pan<sup>1</sup>, Ruei-Yuan Wang<sup>2,\*</sup>, Bing-Yuh Lu<sup>3</sup>

<sup>1,2</sup>School of Sciences, Guangdong University of Petrochem Technology(GDUPT), China

<sup>3</sup>Faculty of Automation, Guangdong University of Petrochemical Technology, China

Corresponding author

Received: 13 Oct 2023; Received in revised form: 20 Nov 2023; Accepted: 02 Dec 2023; Available online: 10 Dec 2023

©2023 The Author(s). Published by Infogain Publication. This is an open access article under the CC BY license

(<https://creativecommons.org/licenses/by/4.0/>).

**Abstract**— This article takes Zhaoyang District, Zhaotong City, Yunnan Province, as the study area. By obtaining basic data such as rainfall, soil texture data, digital elevation, land use, and remote sensing images, the RUSLE model is used to estimate the soil erosion modulus in Zhaoyang. Based on this, the soil erosion classification and soil erosion of different land use types in the study area are analyzed. The results have shown that the soil erosion intensity in Zhaoyang, shows a pattern of increasing from southeast to northwest. Most of the land is subject to slight erosion, followed by mild and moderate erosion. The strongly eroded soil is concentrated in the northwest and is greatly affected by altitude and slope factors. The proportion of soil micro erosion is 64.4%, the proportion of mild erosion area is 17.58%, the proportion of moderate erosion area is 11.99%, and the proportion of strong erosion, extremely strong erosion, and severe erosion area are 3.74%, 1.55%, and 0.74%, respectively. The erosion amount of land use types such as construction land and water bodies is very small, and overall it is at a micro erosion level. Shrubs, forests, and grasslands are the main sources of regional erosion, and the soil erosion intensity of cultivated land is high.



**Keywords**— Revised Universal Soil Loss Equation (RUSLE), Land Use-Cover Change (LUCC), Soil Erosion, Remote Sensing (RS), Geographic Information System (GIS)

## I. INTRODUCTION

Soil erosion is the most common form of destruction of soil resources and refers to the processes of destruction, denudation, transportation, and deposition of soil and its parent materials under the action of hydraulic, wind, freeze-thaw, gravity, and other external labor. Soil erosion will not only destroy land resources and reduce land productivity but also aggravate the occurrence of other

disasters such as floods, droughts, and debris flow, threatening the production and development of human society. It will also affect the comprehensive utilization and development of the soil. Therefore, soil erosion and its nutrient loss have become the focus of researchers.

With the continuous development and maturity of RS and GIS technology, researchers at home and abroad have made a lot of achievements in the monitoring and analysis

of regional soil erosion, including the universal soil loss equation (USLE) [1] [2] [3], the general soil loss equation water erosion prediction watershed model (Water Erosion Prediction Project, WEPP) [4] [5] [6], the Chinese soil loss equation (CSLE) [7], the Limburg Soil Erosion Model (LISEM) established in the Loess region of the Netherlands [8], and the European soil erosion model (EUROSEM) proposed by Morgan et al. [9]. Meanwhile, the new soil erosion equation of A=CSLKP proposed by Smith and Whitt [10], the soil erosion model (SWAT) for predicting the long-term impact of land management practices on watershed runoff and sediment yield [11], and the revised universal soil loss equation (RUSLE) [12] [13] [14] include many soil erosion calculation models. Among them, the RUSLE model is the most widely used. The RUSLE model has the characteristics of a simple structure, few parameters, and an accurate prediction of average soil erosion. From the spatial scale of the model, the study of soil erosion based on the RUSLE model includes not only slope scales and watershed scales but also regional scales, so it is suitable for the study of community scales in Zhaoyang District of Zhaotong City.

As an important area of national key management for soil and water loss in the lower reaches of the Jinsha River, Zhaoyang is faced with serious problems of soil and water loss and needs key control and management. As one of the main battlefields of ecological security barrier construction in the upper reaches of the Yangtze River, Zhaoyang, which is located in the lower reaches of the Jinsha River, is not only an important ecological security barrier in the upper reaches of the Yangtze River but also the most frontier pass for Yunnan to build ecological security barriers in the upper reaches of the Yangtze River. Serious soil and water loss not only causes the deterioration of the local ecological environment, people's poverty, and economic backwardness, but also poses a great threat to the safety of downstream flood control, reduces the flood diversion and storage capacity of rivers, and increases flood and waterlogging disasters. It is not conducive to navigation, which shows the urgency and seriousness of the problem of soil and water loss in the Zhaoyang area.

This article takes Zhaoyang District, Zhaotong City,

as the study area and comprehensively uses ArcGIS and ENVI software and the RUSLE model to analyze the changes in land use, vegetation distribution, and soil erosion status in the study area. In order to protect and reasonably develop land resources, effectively prevent and control soil erosion, improve the ecological environment, and promote sustainable economic and social development. Meanwhile, to provide decision-making support for the sustainable development of the region while also strengthening the ecological security barrier in the Jinsha River Basin of Zhaoyang, Yunnan is promoting the construction of ecological security and ecological barriers, which is of great strategic significance for achieving the overall goal of ecological civilization construction in Yunnan and maintaining the overall ecological security of the country.

## II. STUDY AREA AND DATA SOURCES

### 2.1 Study Area

Zhaoyang District is the administrative center of Zhaotong City, the political, economic, cultural, and information center, and the interprovincial central city of Yunnan, Guizhou, and Sichuan provinces, with geographical coordinates of  $27^{\circ}7' \sim 27^{\circ}39' \text{N}$ ,  $103^{\circ}8' \sim 103^{\circ}56' \text{E}$ . Located in the northeast of Yunnan Province (Figure 1), the topography is high in the west and low in the east, which is the northeast end of the concave part of central Yunnan. There is a relatively complete plateau landform in the Wumeng Mountains and Hengduan Mountains. The highest point is Dushi Baobao, Dashanbao Township, with an elevation of 3,364 m, and the lowest is Maopo on the bank of the Jinsha River at an altitude of 494 m, with a large elevation difference and an obvious three-dimensional climate.

It is the monsoon vertical climate of the plateau; the precipitation is concentrated in May–August, mostly in the form of torrential rain, forming a strong surface runoff and serious erosion to the soil. The geological conditions in the area are complex, and the soil types are complex and diverse due to different climates, altitudes, geomorphologies, and topographies. There are 7 types, 9 subclasses, 20 genera, and 80 soil species.



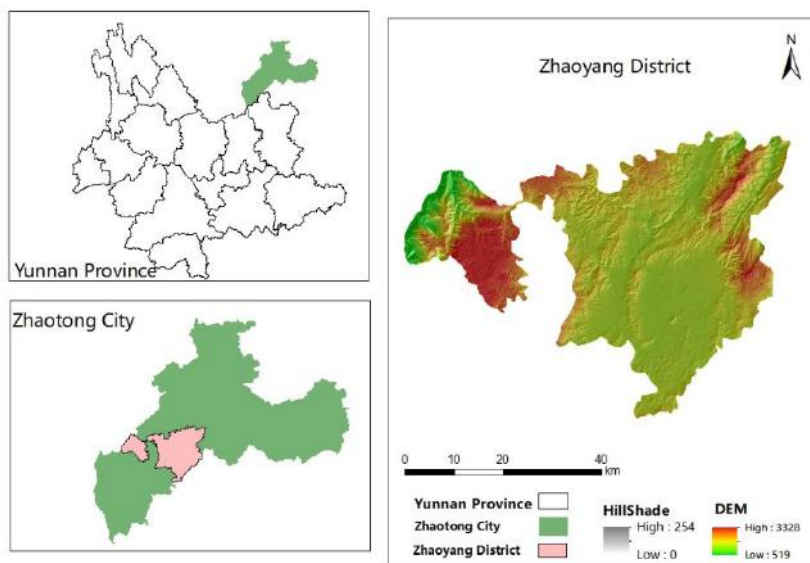


Fig.1 Topographic Map of Zhaoyang

## 2.2 Data Collection

This study mainly uses the following data (Table 1):

Landset-8 OLI\_TIRS image data downloaded from geospatial data cloud (<https://www.gscloud.cn/>), temporal resolution 16 days, spatial resolution 30m × 30m, we download 2019 satellite image map, NDVI map made by ENVI5.3, and land use type map of Zhaoyang District, which are used to calculate vegetation cover factor C value and soil and water conservation P value.

The precipitation data comes from the Resource and Environmental Science and Data Center (RESDC) of the Chinese Academy of Sciences (<https://www.resdc.cn/>), which is used to calculate the rainfall erosivity factor R.

The topographic data comes from the geospatial data cloud (<https://www.gscloud.cn/>). a spatial resolution of 30m × 30m, which is used to extract slope length and calculate the LS value of the slope length factor.

The soil texture type data comes from the Harmonized World Soil Database (HWSD). The soil texture type map of Zhaoyang District, Zhaotong City, is extracted from the HWSD data, and four fields of SAN (sand), SIL (silt), CLA (clay), and C (organic carbon) are added to the layer attributes. Using the field calculator and the soil erodibility K value calculation formula, the soil erodibility K value is calculated.

Table 1 Collection Data Source

Data requirement	Data sources	Application
Landset-8 OLI_TIRS image data	Geospatial Data Cloud ( <a href="https://www.gscloud.cn/home#page1/1">https://www.gscloud.cn/home#page1/1</a> )	Calculate C and P factors
Precipitation data	Resource and Environmental Science and data Center of the Chinese Academy of Sciences ( <a href="https://www.resdc.cn/">https://www.resdc.cn/</a> )	Generate R factor layer
30m DEM	Geospatial Data Cloud ( <a href="https://www.gscloud.cn/home#page1/1">https://www.gscloud.cn/home#page1/1</a> )	Calculate LS factor
Soil texture	National Qinghai Tibet Plateau Scientific Data Center ( <a href="https://data.tpdc.ac.cn/home">https://data.tpdc.ac.cn/home</a> )	Generate K-factor layer

### III. METHODOLOGY

#### 3.1 Method

This study is based on 30m DEM, 2019 precipitation data, HWSD, and 2019 Landset-8 OLI\_TIRS image data in Zhaoyang. The main analysis steps (Figure 2) are as follows:

1. Using the soil texture type data, the soil texture type map of Zhaoyang is extracted, and four fields are added to the attribute of the ArcGIS layer using the formula in the Environmental Policy Integrated Climate (EPIC). Using a field calculator, complete the calculation of soil erodibility factor values (K values) for different soil subclasses in the study area and create a K factor map.
2. The LS factor of slope length is generated on the basis of DEM. The slope length is calculated by filling the depression and calculating the flow direction, and the distance of the flow path is estimated.
3. Using the Landset-8 OLI\_TIRS image of Zhaoyang in 2019, the NDVI and vegetation coverage were calculated, and the land use type map of Zhaoyang was

made by supervised classification. The C value of the study area was calculated according to the relationship between vegetation coverage and the C value, and the C value map of the vegetation cover factor was made.

4. Using ENVI, land use is divided into six types: grassland, farmland, shrub land, water bodies, forests, and artificial land. According to the classification of land use, the soil and water conservation factors are assigned according to the research results of relevant scholars, and then the P value map is calculated.
5. Using the Chinese precipitation data set. csv data and \_PRE annual precipitation data, the precipitation distribution map of Zhaoyang is obtained by mask extraction, and the R factor diagram is obtained by inputting the formula of precipitation erosivity factor into the grid calculator.
6. The soil erosion modulus is obtained by multiplying the layers of the above factors and then classified according to "Standards for classification and gradation of soil erosion (SL 190Mir 2007)".

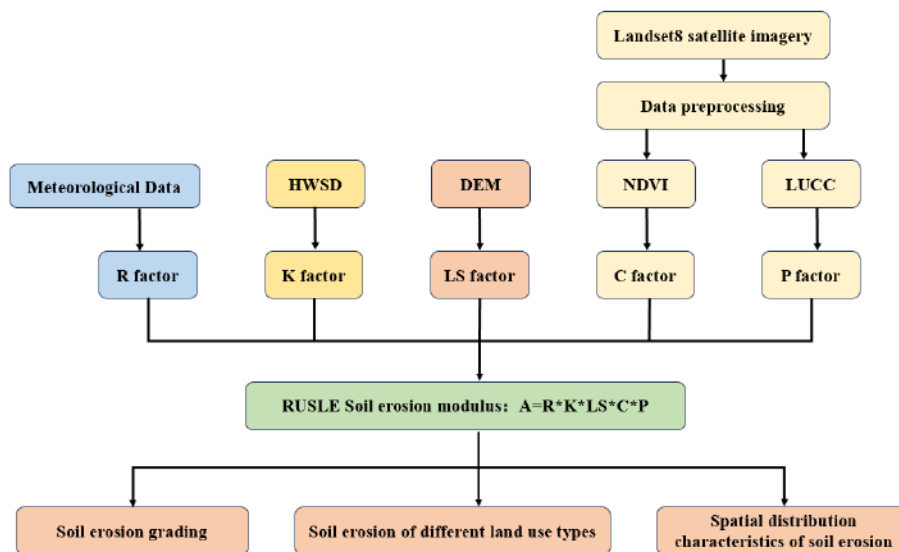


Fig.1 The Scheme of the Study

#### 3.2 RUSLE Model

In this study, the RUSLE based on the USLE was used to calculate the soil erosion status in Zhaoyang. Compared with the USLE and RUSLE models, the structure of the model is simple, the physical meaning of the parameters is clear, the calculation is simple, and it has strong practicability and comprehensiveness. The mathematical expression for RUSLE is as follows:

$$A=R \times LS \times K \times C \times P \dots \dots (1)$$

In formula (1), A is the annual average soil loss (t/(hm<sup>2</sup>·a)); R is the rainfall and runoff erosion factor ((MJ·mm)/(hm<sup>2</sup>·h·a)); K is the soil erodibility factor ((t·hm·h)/(MJ·mm·hm)); LS are the topographic factor, where L is the slope length factor and S is the degree factor; C is the vegetation cover and management factor. P is a factor of soil and water conservation measures, all of

which are dimensionless factors.

### 3.3 Model Parameter Construction

#### ■ LS Factor

Among topographic factors, slope has the greatest impact on soil erosion. The steeper the slope is, the shorter the convergence time, the faster the water flow speed, the greater the runoff energy, and the more severe the erosion on the slope surface. The potential erosion force of the soil is greater. Generally, the erosion amount is directly proportional to the slope. Secondly, the longer the slope length, the larger the surface runoff area and the greater the surface runoff flow, which gradually increases the amount of sediment carried by the water flow and exacerbates soil erosion in the area. The slope length factor is generally generated based on DEM. The calculation of slope length is estimated based on the distance of the water flow path by filling the depression (Figure 3) and calculating the flow direction (Figure 4).

$$L = \left(\frac{\lambda}{22.13}\right)^m$$

$$\lambda = l \times \cos \alpha \quad (2)$$

In equation (2), L is the slope length factor (dimensionless);  $\lambda$  is the horizontal projection slope length (m); L is the length of water flow along the surface flow direction (Figure 5);  $\alpha$  is the slope value of the water flow area (Figure 6); M is a variable slope index; when  $\theta < 0.57^\circ$ ,  $m = 0.2$ ; when  $0.57^\circ \leq \theta < 1.72^\circ$ ,  $m = 0.3$ ; and when  $1.72^\circ \leq \theta < 2.86^\circ$ ,  $m = 0.5$ , from which the slope length factor L value in the Zhaoyang area can be calculated.

The slope calculation is based on grading, with the McCool DK formula used for slopes below  $10^\circ$  and the Liu et al. formula used for slopes above  $10^\circ$ .

$$S = \begin{cases} 10.18 \times \sin \theta + 0.03 & \theta < 5^\circ \\ 16.80 \times \sin \theta - 0.50 & 5^\circ < \theta \leq 10^\circ \\ 21.91 \times \sin \theta - 0.96 & \theta > 10^\circ \end{cases} \quad (3)$$

In the formula, S is the slope factor (dimensionless);  $\theta$  is the slope, and the slope factor S is calculated (Figure 7).

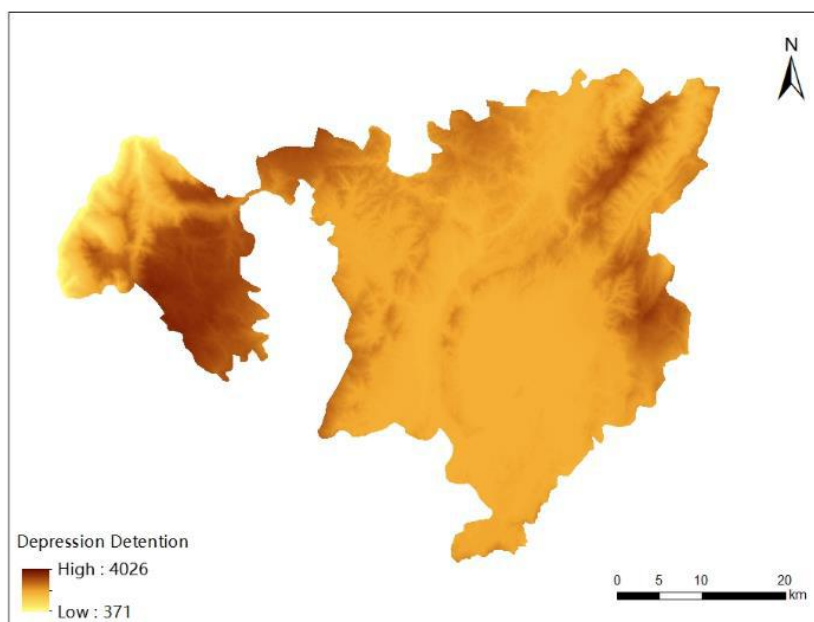


Fig.3 Filling Depression Map

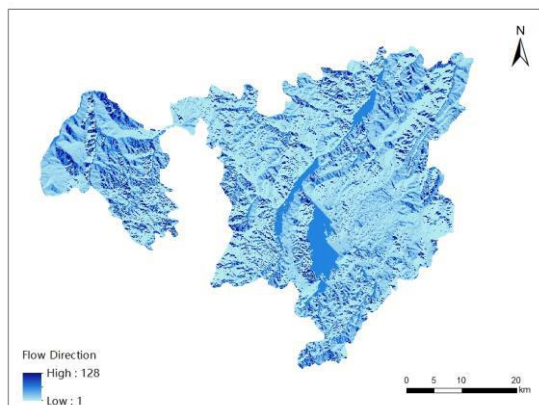


Fig.4 Flow Direction Diagram

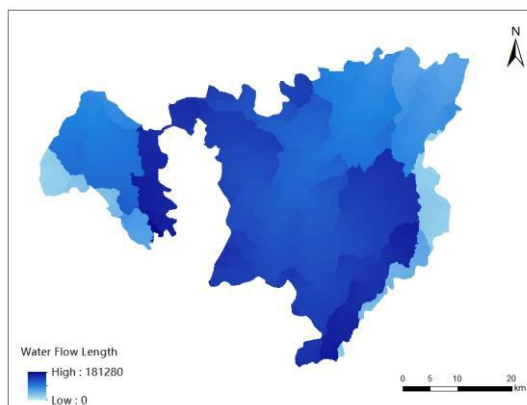


Fig.5 Current Length Map

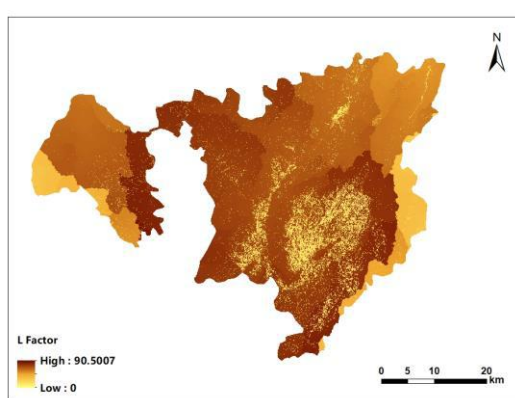


Fig. 6 L-factor

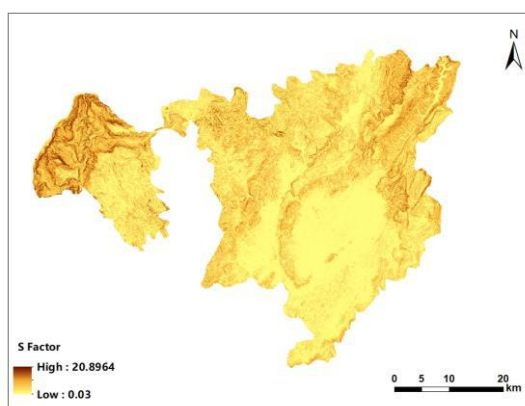


Fig.7 S-factor

### ■ K Factor

At present, there are four main calculation methods to determine the value of the K factor: the direct determination method, the formula method, the look-up table method, and the Nomo diagram method. In the formula method, the EPIC model method proposed by Williams et al. is the most widely used [15]. This method is mainly calculated by measuring soil mechanical composition, soil organic carbon content, and other soil physical and chemical properties. The data is easy to obtain, and the calculation result is reliable. Therefore, this study intends to use the EPIC model method to calculate the soil erodibility factor K value. The calculation formula is as follows:

$$K = 0.1317 \left\{ 0.2 + 0.3 \exp \left[ -0.256 S_a \left( 1 - \frac{S_i}{100} \right) \right] \right\} \times \left( \frac{S_i}{S_i + C_i} \right)^{0.3} \times \left( 1 - \frac{0.25 C_a}{C_a + \exp(3.72 - 2.95 C_a)} \right) \times \left( \frac{0.7 S_n}{S_n + \exp(-0.51 + 22.9 S_n)} \right) \dots (4)$$

In formula (4), K is soil erodibility, and even if the resulting unit is an American unit, the result value needs to be multiplied by a conversion factor of 0.1317 to be converted into an international unit. Sa is sand content, Si is silt content, Ci is clay content, and Ca is organic matter content. The above K-value estimation method is only applicable in the United States and not in China. It is necessary to use the correction formula established by Zhang Jili et al. to correct the soil erodibility factor, KEPIC. The calculation formula is as follows: (K is the modified soil erodibility value, and EPICK is the soil erodibility value estimated by the EPIC formula.)

$$K = -0.01383 + 0.051575 K_{EPIC} \quad (5)$$

### ■ R Factor

Rainfall erosion is one of the key driving factors leading to soil erosion, causing widespread soil erosion worldwide, represented by the capital letter R. The erosive force of rainfall cannot be directly measured, and effective methods need to be used to accurately estimate it. The

main methods include simple algorithms and classical algorithms. However, classical algorithms require extremely high temporal resolution for rainfall data, so this study uses a simple algorithm for calculation. As shown in equation (6),

$$R^n = 0.053 \times P_n^{1.655} \quad (6)$$

In formula (6),  $R^n$  is the annual rainfall erosivity factor,  $P_n$  is the annual rainfall, and the unit is mm.

### ■ C Factor

The type of vegetation will affect the spatial distribution pattern of soil erosion, and the increase or decrease in vegetation coverage will affect soil erosion.

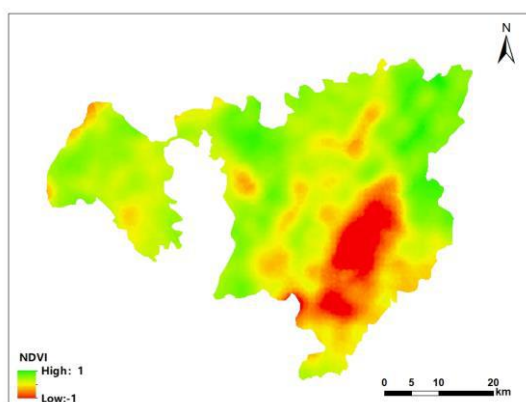


Fig.8 NDVI Value Map

Therefore, it is essential to study the temporal and spatial distribution characteristics of vegetation coverage to effectively control soil erosion and guide the work of soil and water conservation. When calculating the C value, it is necessary to calculate NDVI (Figure 8) and FVC (Figure 9), mainly as formula (7).

$$FVC = \frac{NDVI - NDVI_{min}}{NDVI_{max} - NDVI_{min}} \quad (7)$$

In formula (7), FVC is vegetation coverage, NDVI is pixel value, and  $NDVI_{max}$  and  $NDVI_{min}$  are NDVI values with vegetation cover and NDVI values of bare soil, respectively.

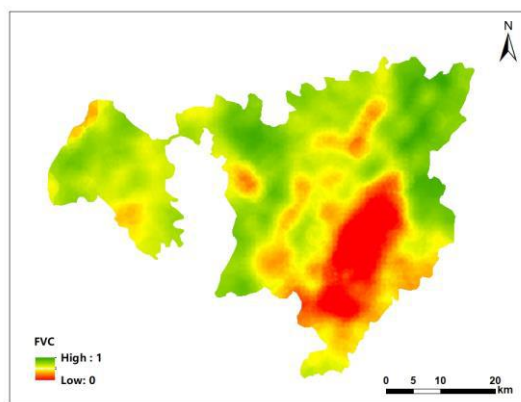


Fig.9 FVC Value Map

### ■ P Factor

The factor of soil and water conservation measures refers to the ratio of soil loss under certain soil and water conservation measures to the soil loss of sloping agricultural plots without implementing soil and water conservation measures. The ratio P is generally between 0-1, where 0 represents areas with good prevention and control measures and minimal erosion, and 1 represents areas where relevant measures have not been implemented. At present, there is no unified standard for assigning

values to soil and water conservation factors in China. After referring to a large amount of literature, this study divides land use into six categories: grassland, farmland, shrubland, water bodies, forests, and artificial land (Figure 10). Based on the classification of land use and referring to the research results of relevant scholars, assign values to soil and water conservation factors, reclassify land use types, assign values of 0.10 to grasslands, forests, and shrublands, 0.35 to cultivated land, 0 to water bodies, and 0 to artificial land (Table 2).

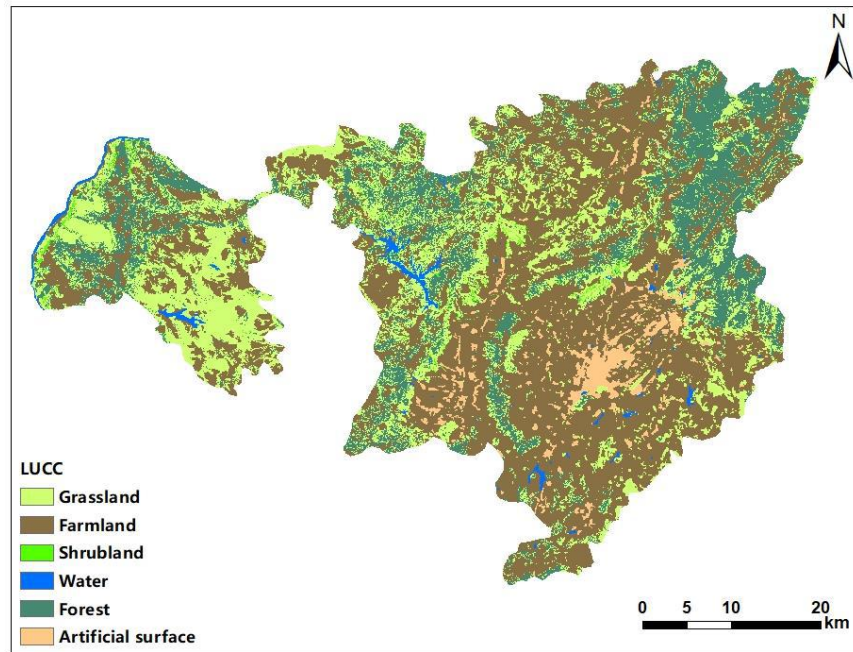


Fig.10 Land Use Map

Table 2 P Value Assignment Table of All Kinds of Land

Land use type	P value	Land use type	P value
Shrub land	0.1	Farmland	0.35
Water bodies	0	Artificial land	0
Grassland	0.1	Forests	0.1

#### IV. ANALYSIS AND RESULTS

##### 4.1 The Spatial Distribution of LS Factor

The results of data analysis show that the high value of the LS factor (Figure 11) in Zhaoyang is mainly distributed in the northern region, especially in the northwest region where the Jinsha River is located, reaching the highest value of 1590.06. Combined with the DEM map (Figure 12) and slope map (Figure 13) of Zhaoyang, the topography of the high-value distribution area is larger, while among the LS factors, the slope has the greatest influence on soil erosion, and the steeper the

slope is, the shorter the confluence time is. The faster the flow speed is, the greater the runoff energy, and the more severe the erosion on the slope, the greater the potential soil erosivity. In general, the amount of erosion is proportional to the slope. Secondly, the longer the slope length is, the larger the surface confluence area and the larger the surface runoff, which makes the sediment carried by the flow gradually increase. However, the low values are mostly distributed in the urban area of Zhaoyang, where the topography is relatively flat.

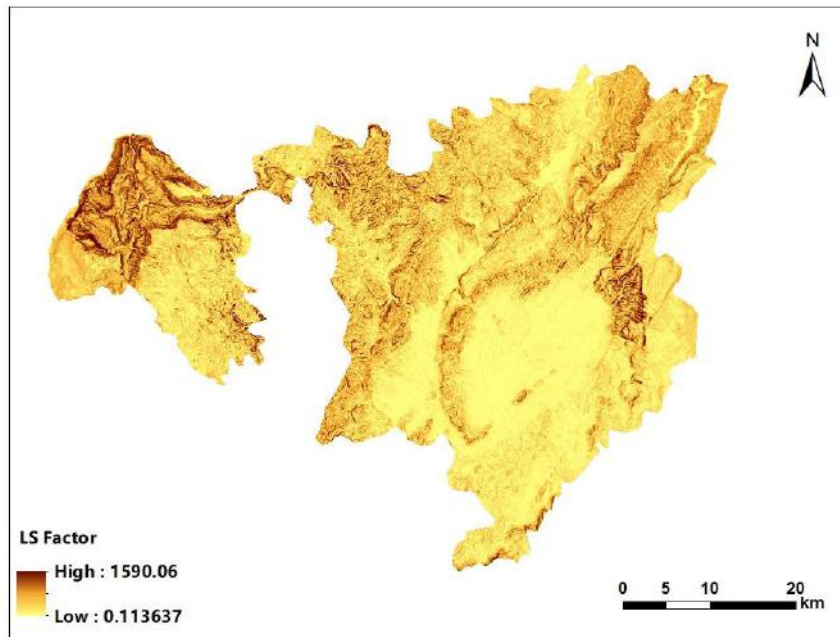


Fig.11 LS factor

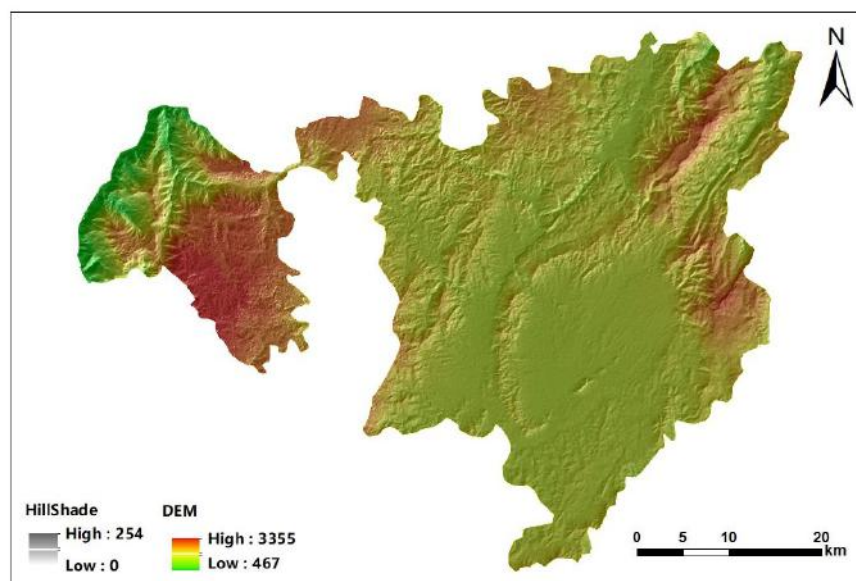


Fig.12 DEM of Zhaoyang District

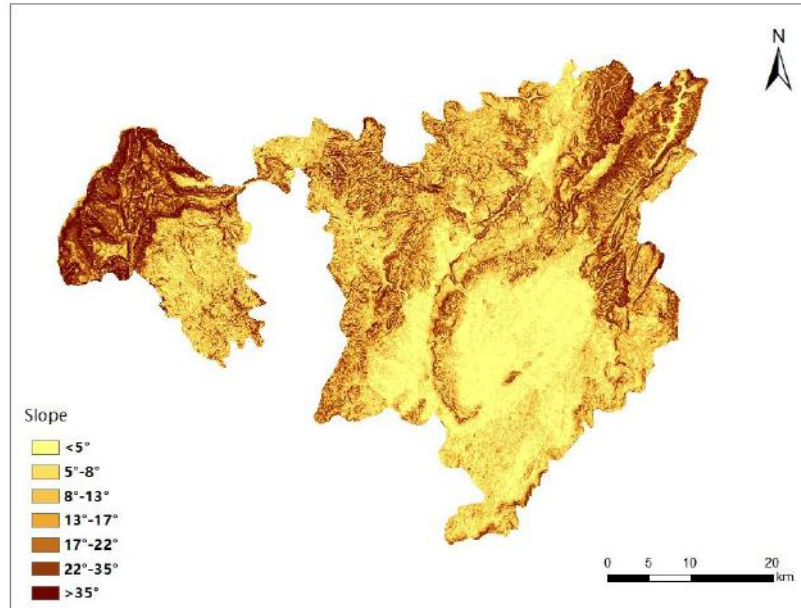


Fig.13 Slope map

#### 4.2 The Spatial Distribution of K Factor

Data analysis shows that the highest soil erodibility K value is distributed in the building area of the urban center of Zhaoyang (Figure 14), and the artificial land is not easy

to seepage, which is an important reason for the high soil erodibility factor. The low value of the K factor is mostly distributed in the covered and luxuriant areas, such as the grassland in the west and the forest in the east.

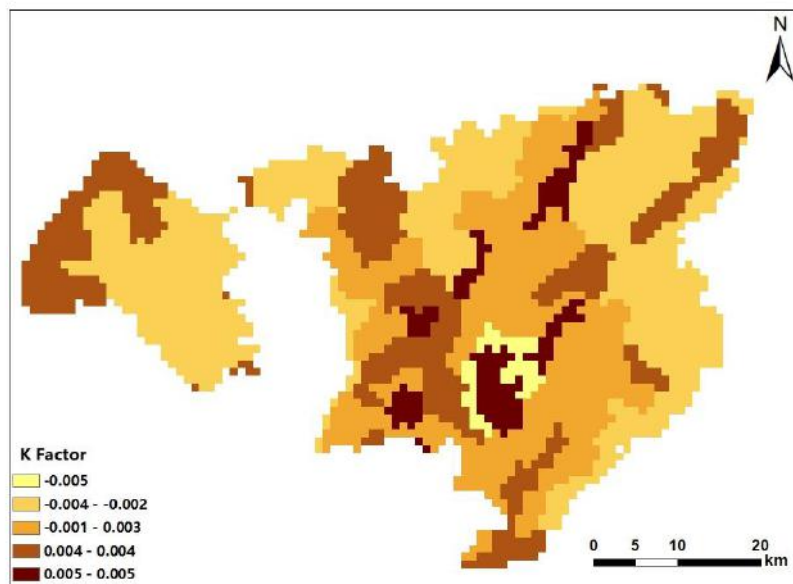


Fig K factor

#### 4.3 The Spatial Distribution of R Factor

From the R factor value distribution map of rainfall erosivity (Figure 15), it can be seen that the rainfall

erosivity intensity is basically caused by the precipitation intensity. In 2019, the rainfall erosivity in Zhaoyang changed to 2336.66-7196.72 (MJ\*mm)/(hm<sup>2</sup>\*h\*a), showing a distribution law decreasing from northwest to



southeast as a whole. The minimum value of the R factor in the study area appears in the southeast, and the maximum value appears in the northwest. According to the climatic characteristics of Zhaoyang, because most of the

precipitation in the area is a short-term concentrated rainstorm, the scouring force on the soil is enhanced, which increases soil erosion.

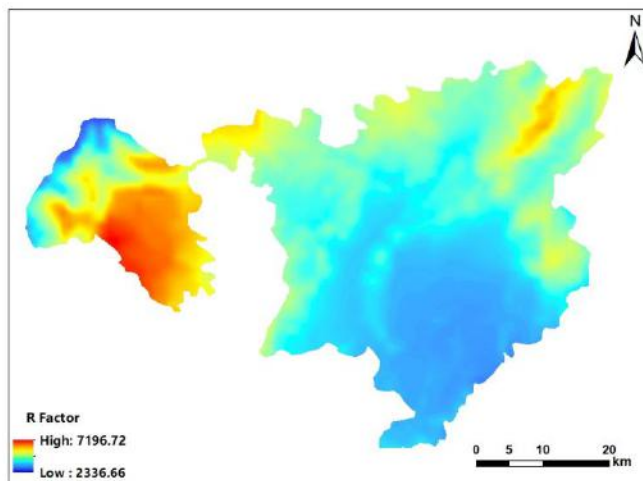


Fig.5 R Factor

#### 4.4 The Spatial Distribution of C Factor

Vegetation is the key factor in controlling the occurrence and development of soil erosion; the type of vegetation will affect the spatial distribution pattern of soil erosion, and the increase or decrease in vegetation coverage will have an impact on soil erosion, as can be seen from the C factor map (Figure 16). The value range is between 0 and 1, and the closer the value is to 1, the higher

the vegetation coverage. The high value of vegetation coverage in the study area is mainly distributed in the areas where the land use type is forests and grassland; the low value is distributed in the area where the land use type is farmland; and the lower value is mainly distributed in the area where the land use type is opaque water surface, less vegetation coverage.

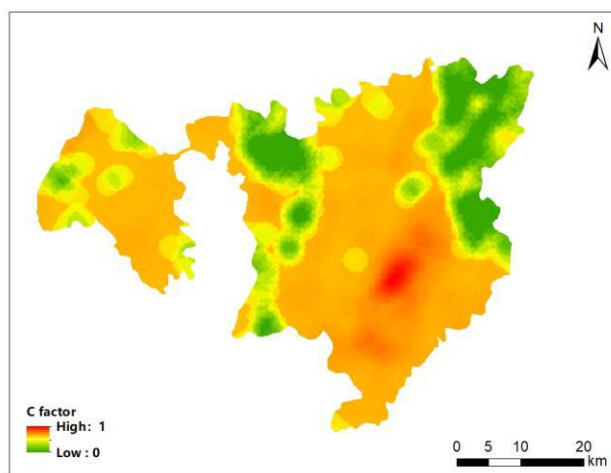


Fig.16 C Factor

#### 4.5 The Spatial Distribution of P Factor

The soil and water conservation measure factor refers

to the ratio of soil loss to the soil loss of the farming land along the slope without soil and water conservation measures under certain soil and water conservation

measures; the ratio P is between 0 and 1, and the prevention and control measures of generation 0 are very good. That is, the area where erosion basically no longer occurs; 1 represents the area where the relevant measures have not been implemented. According to the research results (Figure 17), the high value of the P factor of soil and water conservation measures is distributed in the

southern cultivated area, indicating that the soil and water conservation is poor and the erosion is serious in the Zhaoyang area. The low value of the P factor of soil and water conservation measures is distributed in the artificial land area in the southeast, which makes the surface water unable to seep, and it is also difficult to cause erosion to the surface soil.

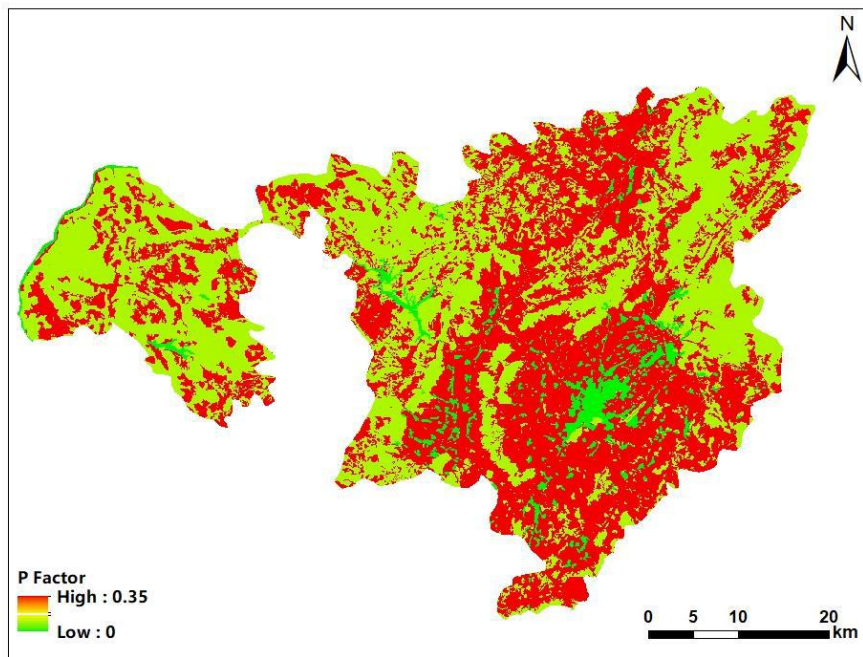


Fig.17 P Factor

#### 4.6 Soil Erosion Characteristics

The soil erosion modulus in Zhaoyang is calculated based on the RULSE model. According to "Standards for classification and gradation of soil erosion (SL 190Mil 2007)," the soil erosion modulus  $([t/(hm^2 \cdot a)])$  in Zhaoyang can be divided into six grades: microscopic erosion, mild erosion, moderate erosion, strong erosion, extremely strong erosion, and severe erosion, and the spatial distribution characteristics of soil erosion are evaluated and analyzed. The results of soil erosion grade classification and spatial analysis are as follows: According to the soil erosion intensity classification map (Figure 18), most of the land in Zhaoyang belongs to microscopic erosion, followed by mild erosion and moderate erosion. The erosion distribution area of the strong grade is small, but it shows the characteristics of concentrated distribution, and the erosion intensity decreases from northwest to southeast, showing certain

regularity. Strong erosion is mainly in the northwest of Zhaoyang, where the topography is undulating, indicating that altitude, slope, and other factors have a special impact on soil erosion.

From the soil erosion area of different intensities (Table 3), microscopic erosion accounts for the largest area, which is 1326 km<sup>2</sup>, accounting for 64.4%. With a mild erosion area of 362 km<sup>2</sup>, next only to microscopic erosion, its erosion area accounts for 17.58%. With a moderate erosion area of 247 km<sup>2</sup>, the proportion is 11.99%. There are small differences in the proportion of areas with strong erosion, extremely strong erosion, and severe erosion, with erosion areas accounting for 3.74%, 1.55%, and 0.74%, respectively. The above analysis indicates that soil erosion in Zhaoyang is characterized by slight and mild erosion, but the proportion of extremely strong and severe erosion is relatively large. Therefore, in the construction of the regional soil and water conservation ecological

environment, attention should be paid to the management of soil and water loss with extremely strong and severe erosion levels.

The erosion environment of different land use types and the intensity affected by human activities are different, which leads to great differences in the soil erosion characteristics of different land uses. Combined with the land use map (Figure 10) and the erosion intensity map (Figure 18) in Zhaoyang, we can see that there are great differences in erosion intensity among different land use types. From the point of view of erosion intensity, the erosion intensity of farmland is large, and the erosion intensity of grassland is in the grade of moderate erosion; the erosion intensity of forests is small, which is in the grade of slight erosion. Which is indicates that the effect of soil and water conservation in forests is good; there is almost no erosion in construction land, water areas, and

other land use types, or the amount of erosion is very small, which is in the range of slight erosion as a whole. In terms of the proportion of erosion of different land use types, shrub land, forests, and grassland are the main sources of regional erosion, while other land use types account for a small proportion of erosion.

Table 3 Area of Soil Erosion at All Levels

Erosion level	Erosion area(km <sup>2</sup> )	Percentage(%)
Microscopic erosion	1326	64.4%
Mild erosion	362	17.58%
Moderate erosion	247	11.99%
Strong erosion	77	3.74%
Extremely strong erosion	32	1.55%
Severe erosion	15	0.74%

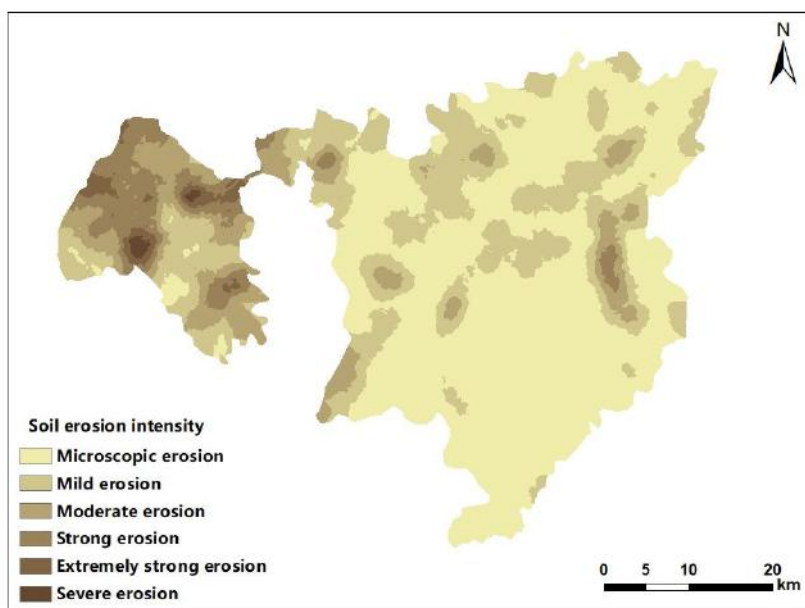


Fig.18 Soil Erosion Intensity Map

## V. CONCLUSION

This study mainly uses the combination of ArcGIS and ENVI, analyzes the spatial distribution characteristics of soil erosion in Zhaoyang based on the RUSLE model, and studies the effects of soil erosion classification and different land use types on soil erosion. The results are as follows:

The intensity of soil erosion in Zhaoyang increases gradually from southeast to northwest, and most of the

land is subject to slight erosion. The second is mild erosion and moderate erosion, and the strongly eroded soil is concentrated in the northwest, which is greatly affected by altitude and slope factors.

In Zhaoyang, the proportion of soil with slight erosion is 64.4%, the proportion of light erosion area is 17.58%, the proportion of moderate erosion area is 11.99%, and the proportion of strong erosion, extremely strong erosion, and severe erosion is 3.74%, 1.55%, and 0.74%,

respectively.

From the perspective of different land uses, the amount of soil erosion in land use types such as construction land and water areas is very small, and it is in the range of slight erosion as a whole. Shrub land, forestland, and grassland are the main sources of regional erosion. Farmland soil and water conservation measures are poor; their P value is larger, so the intensity of soil erosion is high.

### ACKNOWLEDGEMENTS

The author is grateful for the research grants given to Ruei-Yuan Wang from GDUPT Talents Recruitment, Peoples R China under Grant No.2019rc098, and Academic Affairs in GDUPT for Goal Problem-Oriented Teaching Innovation and Practice Project Grant No.701-234660.

### REFERENCES

- [1] Wischmeier, W.H., and Smith, D. Predicting Rainfall-Erosion Losses from Cropland East of the Rocky Mountains. *Agricultural Handbook*, 1965, 282: 1-12.
- [2] Wischmeier, W.H., and Smith, D. Predicting Rainfall Erosion Losses: A Guide to Conservation Planning. *Agricultural Handbook*, 1978, 537: 1-16.
- [3] Xin, J. Soil Erosion Calculation in the Hydro-Fluctuation Belt by Adding Water Erosivity Factor in the USLE Model. *Journal of Mountain Science*, 2020, 17(9): 2123-2135.
- [4] Nearing, M.A., Foster, G.R., Lane, L.J, and Finkner, S. C. A Process-Based Soil Erosion Model for USDA-Water Erosion Prediction Project Technology. *Transactions of the ASAE.*, 1989, 32(5):1587-1593. doi: 10.13031/2013.31195
- [5] Liu, B., and Shi, P. Water Erosion Prediction Project (WEPP) Model for Watershed Scale. *BULLETIN OF SOIL AND WATER CONSERVATION*, 1998, 18(5): 6-12.
- [6] Zheng, F., Yang, K., and Wang, Z. Soil Erodibility for Water Erosion: A Review. *Research of Soil and Water Conservation*, 2013, (01):277-286.
- [7] Liu, B., Zhang, K., and Yun, X. An Empirical Soil Loss Equation, *Proceedings 12th International Soil Conservation Organization Conference*.2002.
- [8] De Roo, A.P.J. THE LISEM Project: An Introduction. *Hydrological Processes*, 1996, 10(8):1021-1025.
- [9] Morgan, R.P.C. and Rickson R J. The European soil erosion model: an update on its structure and research base. *Conserving Soil Resources European Perspectives*, 1994.
- [10] Gogichaishvili, G.P. Kirvalidze, D.R., and Gorjomeladze, O.L. Testing of the hydromechanical prediction model of soil erosion under the conditions of Georgia. *Eurasian Soil Science*, 47(9):917-922
- [11] Arnold, J.G., Srinivasan, R., Muttiah, R.S., and Williams, J. R. Large Area Hydrologic Modeling and Assessment Part I: Model Development. *Journal of the American Water Resources Association (JAWRA)*, 1998, 34(1):1-17.
- [12] Renard, K.G., Foster, G.R., and Weesies, G.A. Predicting Soil Erosion by Water: A Guide to Conservation Planning with the Revised Universal Soil Loss Equation (RUSLE) Washington, DC. *Agricultural Handbook*, 1997, 403: 1-5.
- [13] Gayen, A., Saha, S., and Pourghasemi, H.R. Soil Erosion Assessment Using RUSLE Model and Its Validation by FR Probability Model. *Geocarto International*, 2020, 35(15): 1750-1768.
- [14] Behera, M., Sena, D.R., Mandal, U., Kashyap, P. S. and Dash, S. S. Integrated GIS-Based RUSLE Approach for Quantification of Potential Soil Erosion under Future Climate Change Scenarios. *Environmental Monitoring and Assessment*, 2020, 192, 733. <https://doi.org/10.1007/s10661-020-08688-2>
- [15] Williams, J.R., Jones, C.A., and Dyke, P.T. A modeling approach to determining the relationship between erosion and soil productivity. *Transactions of the American Society of Agricultural Engineers*, 1984,27(1): 129-144



# Proximate Composition, Energy and Nutritional Value of Local Malt (*Asaana*) Prepared from Maize in Ghana

Bartels Benjamin<sup>1</sup>, Atakora, Priscilla Ama<sup>2</sup>, Gadzekpo Victor Patrick Yao<sup>3</sup>

<sup>1,2</sup>Department of Laboratory Technology, School of Physical Sciences, College of Agriculture and Natural Sciences, University of Cape Coast, Cape Coast, Ghana

<sup>3</sup> Department of Chemistry, School of Physical Sciences, College of Agriculture and Natural Sciences, University of Cape Coast, Cape Coast, Ghana

Received: 10 Oct 2023; Received in revised form: 25 Nov 2023; Accepted: 04 Dec 2023; Available online: 11 Dec 2023

©2023 The Author(s). Published by Infogain Publication. This is an open access article under the CC BY license

(<https://creativecommons.org/licenses/by/4.0/>).

**Abstract**— *Background and objectives:* “Asaana” is a local malt consumed by majority of Ghanaians of all ages in all the cultures due to its refreshing and nutritional benefits. Since traditional women and methods prepare it, no nutritional information is available during sale. In addition, research data about it is very scanty. This study therefore aims at determining its nutritional and potential energy value to enrich the existing data. *Method:* The study focused on two types of Asaana preparations. A sample from a local producer prepared by the traditional recipe; and another prepared in the laboratory from two varieties of maize (yellow and white) according to the traditional recipe. Proximate analysis and energy evaluation done to determine nutritional value and energy potential. *Results:* The white variety had higher moisture ( $94.20 \pm 0.01\%$ ), P ( $6324.16 \pm 36.31 \mu\text{g/g}$ ), K ( $6162.76 \pm 128.07 \mu\text{g/g}$ ), Na ( $718.08 \pm 4.51 \mu\text{g/g}$ ), Zn ( $865.65 \pm 9.09 \mu\text{g/g}$ ) contents and fat energy ( $0.44 \text{ kJ/g}$ ). The yellow variety recorded higher dry matter ( $7.39 \pm 0.00\%$ ), and carbohydrate ( $88.33 \pm 0.20\%$ ) contents and carbohydrate energy ( $15.0 \text{ kJ/g}$ ). The traditional preparation had higher protein ( $8.95 \pm 0.11\%$ ), fat ( $1.40 \pm 0.03\%$ ), fibre ( $4.04 \pm 0.08\%$ ), Ca ( $11600 \pm 76.68 \mu\text{g/g}$ ), Mg ( $2000.48 \pm 28.20 \mu\text{g/g}$ ), Fe ( $300.45 \pm 9.86 \mu\text{g/g}$ ) contents and Protein energy ( $1.52 \text{ kJ/g}$ ). *Conclusion:* “Asaana” is potentially nutritious and provides basic energy needed for physiological activities.



**Keywords**— maize, malt, proximate composition, mineral constituents, energy.

## I. INTRODUCTION

Cereal-based beverages account for as much as 77% of total caloric consumption and contribute significantly to the dietary protein intake in Africa. They are processed traditionally through natural fermentation with maize or sorghum as the predominant raw material (Ojokoh & Bello 2014)<sup>1</sup>. “Asaana” is a traditional non - alcoholic beverage prepared and consumed mostly in the Southern part of Ghana. The Gas knows it as “Asaana” (meaning “we taste” or ‘it is tasty’). “Liha” or “Aliha” (corn drink) in the Volta region, and as “Elewonyo” by the Ashantis. It is believed to have originated from the Volta region of Ghana.. “Asaana” is a refreshing drink best consumed fresh with ice cubes and milk (optional). It is a source of essential nutrients, and has medicinal and functional properties (Perez-Armendariz & Cardoso-Ugarte 2020)<sup>2</sup>.

Corn (*Zea mays*) is the main ingredient in “Asaana” and it is grown extensively around the world. *Zea mays* is a great source of minerals such as potassium, which helps regulate the circulatory system. It contains lutein, a vitamin known to reduce the risk of macular degeneration, cataracts and other eye diseases. It is rich in dietary fiber beneficial in regulating bowel movements. It contains the anti-oxidant quercetin, which plays an important role in treating prostatitis protects neuronal cells and reduces neuro inflammation (International Grains Council Market Report, 2013)<sup>3</sup>. Therefore, consuming “Asaana” could provide all these health benefits. The aim of this study is to determine the respective nutritional and energy potential of the samples. The results shall enrich the database on this local beverage.

## II. MATERIALS AND METHODS

### 2.1. Collection of Samples:

A traditionally prepared sample of Asaana from a local producer, and two varieties of maize (yellow and white) from Abura market in Cape Coast, in the Central Region of Ghana were collected.

#### 2.1.1 Laboratory Preparation of Asaana

The maize samples were rid of all foreign materials. They were labelled separately, and the grains soaked in water overnight, strained and allowed to germinate for seven days. They were then sun-dried for four days, ground to coarse flour, mixed with cold water and the mixture boiled with constant stirring for four hours. It, was strained after cooling and allowed to ferment for three days. They were strained, and caramel sugar added to produce the Asaana (Madilo et

al., 2022)<sup>4</sup>. The preparation took place in the Agriculture Research Laboratory of University of Cape Coast, Ghana. Some modifications introduced into the procedure proposed by Madilo et al., 2020 include sorting of foreign materials and insect infected grains; milling by stainless steel industrial blender, and adopting the optimum conditions.

### 2.2. Proximate Analysis of Traditionally and Laboratory Prepared Asaana

The proximate composition and micronutrient analyses were carried out using acceptable protocols (AOAC 2008; Stewart et al., 1974; FAO 2003; IITA 1985; FAO 2008)<sup>5,6,7,8,9</sup>.

### 2.3 Data Analysis

The data analysed by SPSS version 20 at  $p \leq 0.05$ .

## III. RESULTS

Table 1: Mean Proximate Composition (%) of the Asaana.

Test	Traditional method	White variety	Yellow variety
Dry Matter	5.30±0.02	5.80± 0.01	7.39± 0.00
Moisture	93.8±0.01	94.20 ± 0.01	92.61± 0.00
Ash	1.89±0.05	2.06 ± 0.02	1.28± 0.13
Protein	8.95±0.11	7.37± 0.23	6.19± 0.07
Oil / Fat	1.40±0.03	1.20± 0.07	1.11± 0.01
Carbohydrates	76.86±0.10	86.64 ±0.15	88.33 ±0.20
Fibre	4.04±0.08	2.73 ±0.17	3.09 ±0.10

Source: Bartels /Atakora/ Gadzekpo Statistical analysis 2023

Table 2: Mineral Constituents (µg/g) of Samples

Mineral	Traditional	White Variety	Yellow Variety	Codex values (mg)
P	5220± 26.40	6324.16± 36.31	4667.40± 34.88	600-1000mg
Ca	11600.00± 76.68	11581.00± 61.58	11364.67±314.04	800-1000
Mg	2000.48 ± 28.20	1770.33 ± 26.50	1950.33± 53.98	315-365
K	4998.34± 87.79	6162.76± 128.07	5888.42± 45.33	2000
Na	609.98 ± 64.56	718.08 ± 4.51	637.33± 0.72	2000
Zn	800.49 ± 10.12	865.65 ± 9.09	837.05± 6.52	3.6-15
Fe	300.45± 9.86	295.24± 4.57	266.68± 1.43	9.0-43

Source: Bartels/ Atakora/ Gadzekpo Statistical analysis 2023

Table3: Energy Contents for Asaana

Type of Sample	Protein		Fat		Carbohydrate	
	kcal/g	kJ/g	kcal/g	kJ/g	kcal/g	kJ/g
White variety	0.29	1.23	0.11	0.44	3.46	14.71
Yellow variety	0.25	1.06	0.04	0.17	3.53	15.0
Traditional method	0.36	1.52	0.06	0.23	3.07	13.07
Atwater standard (cereals)	3.87	16.2	4.12	17.2	8.37	35.0

Source: Bartels/Atakora/Gadzekpo Statistical results 2023

## IV. DISCUSSION

### 4.1 Proximate composition

As shown in Table 1, for all the preparations, the mean moisture content in the range of 92.61-94.20 %; while ash, protein and fat contents respectively are 1.28-2.06, 6.19-8.95 and 1.1-1.40 %.

The moisture content falls within 93.71– 94.93 %; whereas ash, protein and fat contents respectively are higher than the 0.09 -0.19, 0.33-1.01 and 0.22 - 0.77 % reported in a similar study (Madilo et al., 2022)<sup>4</sup>. Carbohydrate is in the range of 76.86-88.33% and fibre is 2.73-4.04%. Protein is an essential nutrient for the human body (Hermann, 2021)<sup>10</sup>. Fibre lowers cholesterol, which may reduce the risk of cardiovascular diseases (British Nutrition Foundation, 2018)<sup>11</sup>, It also regulates blood sugar and alleviates constipation (Food and Nutrition Board, 2005)<sup>12</sup>. Carbohydrates plays key roles in the immune system as it serves as energy storage.

### 4.2 Energy Contents

Protein, fat and carbohydrates in the body yield energy, which the body needs. As Table 1 indicates, the energy content of the white variety ranges between 0.11-3.46 kcal/g (0.44-14.71 kJ/g); yellow variety ranges between 0.04-3.53 kcal/g (0.17-15.0 kJ/g), while traditional method is in the range of 0.06-3.07 kcal/g (0.23-13.07 kJ/g). These values are within the Atwater standards (www.fao.org)<sup>13</sup> of 4.12-8.37 kcal/g (17.2-35.0 kJ/g).

Basal metabolism requires 1.2-2.4 kcal/24 hours, equivalent to 5.0-10.0 kJ/24 hours for human beings (www.fsps.muni.cz)<sup>14</sup>, this implies that the *Asaana* has the potential to provide the basic energy required for physiological activities by human. In addition, the energy evaluation of the *Asaana* is as follows: fat < protein < carbohydrate.

The energy content from protein in the traditional method (0.36 kcal/g) is relatively higher, the white variety has highest fat energy (0.11 kcal/g), whereas the carbohydrate energy (3.53 kcal/g) is highest in the yellow variety. These

values are within their respective Atwater values for cereals as depicted in Table 1.

### 4.3 Mineral constituents

Table 2, shows phosphorus (P) content for *Asaana* prepared from white variety as 6324.16µg/g, yellow variety as 4667.40µg/g and traditional method as 5220 ± 26.40 µg/g. These concentrations are below the Codex value (FAO/WHO 2019)<sup>15</sup> (600-1000 mg) for Phosphorous. Though very insignificant, the Phosphorus in *Asaana* could be beneficial to the consumer for the formation of bones and teeth and plays an important role in how the body uses carbohydrates and fat.

Calcium content in white corn was 11581.00µg/g and that of yellow corn was 11364.67µg/g, traditional method 11600.00± 76.68. These concentrations are also less than the Codex value of 800-1000 mg, and also less than that reported by Madilo et al., (2022)<sup>4</sup>. Calcium is essential for the development, growth and maintenance of bone, regulate muscle contraction, blood clotting

and lowers the risk of developing high blood pressure (<https://www.medicalnewstoday.com/articles/248958#why-we-need-calcium>)<sup>16</sup>. Magnesium content for *Asaana* prepared from white corn was 1770.33µg/g and that of yellow corn *Asaana* was 1950.33µg/g, traditional method 2000.48 ± 28.20. Consuming *Asaana*, Magnesium promotes healthy blood sugar regulation and nerve function [Kubala J. 2023]<sup>17</sup>.

Potassium and Sodium contents for *Asaana* prepared from white corn were 6162.76 and 718.08µg/g respectively and that of yellow corn were 5888.42 and 637.33µg/g respectively, while traditional method had 4998.34± 87.79 and 609.98 ± 64.56µg/g. Potassium and Sodium help maintain normal level of fluid inside our body. Increasing Potassium intake can help reduce blood pressure, heart disease and stroke. In contrast, high intake of Sodium increases blood pressure, heart disease and stroke (C.D.C 2022)<sup>18</sup>. Therefore, it is best to consume *Asaana* in moderation for people with heart conditions and high blood pressure since there is no provision for appropriate dosage.

Zinc and Iron content for Asaana prepared from white corn was 865.65µg/g and 295.24µg/g respectively and that of yellow corn was 837.05µg/g and 266.68 µg/g respectively, traditional method 800.49± 10.12 and 300.45± 9.86 µg/g. Zinc boost the immune system, accelerates wound healing, treat acne and decreases inflammation

(<http://www.healthline.com/nutrition/zinc#what-it-is>)<sup>19</sup>.

Iron helps in normal oxygen transportation in the body, reduces fatigue increases red cells production and supports the immune system (<http://betteryour.com/blogs/products-guides/iron-benefits>)<sup>20</sup>.

The nutrients in the Asaana as found in the study, are very insignificant to make any meaningful impact on the health of the consumer, but continual intake might provide adequate nutrient for the consumer.

## V. CONCLUSION

1. Asaana, non - alcoholic local malt was found to be nutritious.

2. Asaana has the potential to provide the basic energy required for physiological activities by human, the energy profile is fat < protein < carbohydrate.

## RECOMMENDATION

Stakeholders must provide a framework for its nutritional labelling, and in addition to monitor its preparation and consumption.

## ACKNOWLEDGEMENT

The contributions of Ghana Government's Book and Research Allowance, the University of Cape Coast and authors whose works were cited are well appreciated.

## REFERENCES

- [1] Ojokoh A., Bello B. Effects of fermentation on nutrient and anti-nutrient composition of millet (*Pennisetum glaucum*) and soyabean (*Glycine max*) blend flours. *Journal of Life Sciences* 2014;(8)8. 2014
- [2] Perez-Armendariz B., Cardoso-Ugarte, G.A. Traditional fermented beverages in Mexico: biotechnological, nutritional, and functional approaches. *Food Research International* 2020; 136.
- [3] International Grains Council (International Organization). International Grains Council Market Report 2013.
- [4] Madilo F.K., Kunadu A.P.H., Tano-Debrah K., Mensah G.I., Saalia K.F., Kolanisi, U. Process and Product Characterization of Aliha, A Maize-Based Ghanaian Indigenous Fermented Beverage. *Journal of Food Quality* 2022.

- [5] Association of Official Analytical Chemists AOAC. Official Method of Analysis. Association of Official Analytical Chemists. AOAC International, Maryland; 2008.
- [6] Stewart E.A., Grimshaw H.M., Parkinson J.A., Quarmby C. Chemical analysis of ecological material. Blackwell Scientific Publications, Oxford; 1974.
- [7] Food and Agricultural Organization, FAO. Food Energy- Methods of Analysis and Conversion Factors. Food and Nutrition.2003
- [8] International Institute of Tropical Agriculture, IITA. Laboratory Manual of selected Methods for soil and Plant Analysis. IITA, Ibadan; 1985.
- [9] Food and Agricultural Organization, FAO. Guide for fertilizer and plant nutrient analysis. FAO Communication Division, Rome; 2008.
- [10] Hermann J.R. Protein and the Body. Oklahoma Cooperative Extension Service, Division of Agricultural Sciences and Natural Resources. Oklahoma State University 2021
- [11] British Nutrition Foundation. Dietary Fibre 2018
- [12] Food and Nutrition Board, Institute of Medicine of the National Academics. Dietary Reference Intake for Energy, Carbohydrates, Fibre, Fat, Fatty Acids, Cholesterol, Protein and Amino Acids (Macronutrients). National Academies Press; 2005; 380-382.
- [13] [www.fao.org](http://www.fao.org)
- [14] [www.fsps.muni.cz](http://www.fsps.muni.cz)
- [15] Lewis J Codex nutrient reference values. Rome, FAO/WHO 2019
- [16] <https://www.medicalnewstoday.com/articles/248958#why-we-need-calcium>
- [17] Kubala J. Health Benefits of Magnesium 2023.
- [18] Centers for Disease Control and Prevention C.D.C. Sodium Potassium and Health 2022.
- [19] <http://www.healthline.com/nutrition/zinc#what-it-is>
- [20] <http://betteryour.com/blogs/products-guides/iron-benefits>





# The Influence of Arbuscular Mycorrhizal Fungi (FMA) Dosage and Yomari Liquid Organic Fertilizer on the Growth of Seedlings of Agarwood-Producing Plants (*Aquilaria malacensis* Lamk.) on Former Gold Mining Soil”

Benni Satria, Rachmad Hersi Martinsyah\*, Armansyah, Meisilva Erona, Warnita

Department of Agronomy, Universitas Andalas, Indonesia

\*Email: [Rachmad\\_hm@agr.unand.ac.id](mailto:Rachmad_hm@agr.unand.ac.id)

Received: 13 Oct 2023; Received in revised form: 27 Nov 2023; Accepted: 03 Dec 2023; Available online: 11 Dec 2023

©2023 The Author(s). Published by Infogain Publication. This is an open access article under the CC BY license

(<https://creativecommons.org/licenses/by/4.0/>).

**Abstract**—Former gold mining land exhibits poor soil fertility, both biologically, chemically, and physically due to the damaging effects of the mining process on the land. Marginal land conditions, like former gold mining areas, necessitate high-viability seedlings. Efforts to acquire quality seeds and boost the productivity of this land involve planting adaptable and high-quality plant seeds, such as the agarwood-producing plant (*Aquilaria malaccensis* Lamk.). This plant is among the adaptive non-timber forest products that grow and naturally produce without inoculation (injection) on ex-mining lands—gold, nickel, rocky sand, tin, and coal—supplemented with liquid organic fertilizers like Yomari and Arbuscular Mycorrhizal Fungi (AMF) on *Aquilaria malaccensis* Lamk plants. Yomari liquid organic fertilizer, with its high organic and nutrient content, can enhance soil organisms, improve soil pH, while AMF can promote root growth and expansion, aiding roots in water and nutrient absorption through their external hyphae. Consequently, this facilitates the production of numerous and robust roots. This research aims to determine the optimal interaction between AMF doses and Yomari Liquid Organic Fertilizer for the growth of *Aquilaria malaccensis* Lamk seedlings in former gold mining land. Additionally, it seeks to ascertain the impact of administering the best Yomari organic fertilizer dosage and the best AMF dosage on the growth of *Aquilaria malaccensis* Lamk on ex-gold mining land. This research was conducted from June to November 2022 in the nursery of the Faculty of Agriculture, Andalas University. Employing a factorial experimental method in a Completely Randomized Design (CRD) with two factors—firstly, the AMF dose consisting of four levels: 10 grams (F1), 20 grams (F2), 30 grams (F3), and 40 grams (F4), and secondly, the Yomari organic fertilizer dosage comprising five levels: 0 ml (Y0), 0.75 ml/l (Y1), 1.5 ml/l (Y2), 2.25 ml/l (Y3), and 3.0 ml/l (Y4)—each treatment level comprised four replications. Qualitative and quantitative observation data were analyzed using the F-test at a 5% level of significance. Post-hoc analysis for differences among treatments was conducted using the BNT test at the 5% level. Observations included the percentage of live seeds, seed height increment, leaf number, widest leaf width, root weight, and percentage of roots infected by AMF in ex-gold mining soil media inoculated with *Acaulospora* sp. and *Gigaspora* sp. The administration of 40 grams of FMA with a dose of 3.00 ml/l of liquid organic fertilizer showed an increase in the percentage of survival, an increase in the number of leaves, an increase in the height of the plant seedlings, the widest leaf width, the percentage of root weight, and the seedlings of agarwood-producing plants infected with AMF.



**Keywords—** Gold Mining Land, *Aquilaria malaccensis* Lamk, Liquid Organic Fertilizer, Arbuscular Mycorrhizal Fungi (AMF), Ex-Gold Mining Soil Media

## I. INTRODUCTION

The rehabilitation of former Gold mining areas generally requires high-quality seedlings. However, these seedlings often experience significant mortality after being planted in the field due to insufficient availability of nutrients and water for growth and development. This is a result of plants having few, shallow, weak, and damaged roots (Sari, 2018; Intan, Sutoyo, and Satria, 2019, and Kimi, Sutoyo, and Satria, 2021). The root issues can be addressed by using liquid organic fertilizers such as Yomari fertilizer and Arbuscular Mycorrhizal Fungi (AMF) at specific doses. Yomari organic liquid fertilizer functions to enhance the development of soil organisms, increase soil pH, stimulate vegetative plant growth, play a role in the formation of green leaf substances, and promote stronger and more numerous plant roots. Soaking coffee cuttings in 1 ml/l Yomari organic liquid fertilizer and spraying the cuttings three times at a dose of 1 ml/l within 10 days will result in numerous shoot cuttings with many strong roots (Satria et al., 2021). The presence of AMF can improve the availability of nutrients, especially phosphorus (P), which is usually low in former Gold mining soil. This improves soil structure, enhances water absorption, and protects plants from root pathogens and toxic elements. Inoculating 40 grams of AMF in ultisol and in planting media from former Gold mining soil can enhance the growth of seedlings of *Aquilaria malaccensis* Lamk., especially those with high AMF infection and more extensive roots (Satria and Raesi, 2021; Kimi et al., 2021, and Satria, Fadli, Herawati, and Aprisal, 2021).

This plant has great potential for development in former mining areas, considering it is an adaptive non-wood forest product that naturally grows and produces on former mining lands such as nickel, sandy gravel, tin, and coal (Sari, 2018; Intan et al., 2019, and Kimi et al., 2021). In connection with the above explanation, the researcher is interested in conducting a study with the title "The Influence of Yomari Liquid Organic Fertilizer and AMF (Arbuscular Mycorrhizal Fungi) Doses on the Growth of Agarwood-Producing Plant Seedlings (*Aquilaria malaccensis* Lamk.) in Former Gold Mining Soil." This research is conducted to address several formulated problems in the following questions: 1. Is there an interaction between AMF dose and Yomari organic fertilizer on the growth of agarwood-producing plant seedlings (*Aquilaria malaccensis* Lamk.) in former Gold mining soil? 2. What is the effect of Yomari organic fertilizer dose on the growth of these seedlings in former

Gold mining soil? 3. What is the effect of AMF dose on the growth of these seedlings in former Gold mining soil?

The long-term goal of this research is to obtain naturally produced *Aquilaria malaccensis* Lamk. (without inoculation) and improve the productivity of former Gold mining soil. The specific objectives of this research are: 1. To determine the best interaction between Yomari organic fertilizer dose and AMF dose for the growth of agarwood-producing plant seedlings (*Aquilaria malaccensis* Lamk.) in former Gold mining soil. 2. To determine the effect of the best Yomari organic fertilizer dose on the growth of these seedlings in former Gold mining soil. 3. To determine the effect of the best AMF dose on the growth of these seedlings in former Gold mining soil.

This research is expected to provide information about agarwood-producing plant seedlings (*Aquilaria malaccensis* Lamk.) that can associate well with Yomari organic fertilizer and AMF doses and are compatible for planting in former Gold mining areas. The results of this research are expected to contribute to the development of plant science, especially plant breeding. Contributions include: 1. Providing information on the standard method of AMF Doses and Yomari Liquid Organic Fertilizer on the Growth of Agarwood-Producing Plant Seedlings (*Aquilaria malaccensis* Lamk.) in Former Gold Mining Soil. 2. Making a positive contribution to the development of science and technology in agarwood cultivation (*Aquilaria malaccensis*) and serving as a reference for adaptation and preservation of its germplasm.

## II. METHODS

The research will be conducted in the experimental farm of the Faculty of Agriculture, Andalas University. The planned duration of the study is 6 months, starting from May 2023 to November 2023.

The tools utilized in this research include a hoe, bucket, polybags, scissors, hotplate, ruler, digital scale, meter, writing tools, tweezers, scissors, cover glass, hose, tea strainer, object glass, camera, and microscope. The materials employed consist of seedlings of agarwood-producing plants, *Aquilaria malaccensis* Lamk species, former Gold mining soil, ultisol, compost, Yomari liquid organic fertilizer, Arbuscular Mycorrhizal Fungi (including *Acaulospora* sp., *Gigaspora* sp., and a combination of *Acaulospora* sp. with *Gigaspora* sp.), NPK fertilizer, Curater 3 G, Aquadest, KOH 10%, HCl 2%, Trypan blue for root staining, and clean water.

This study adopts a factorial experiment method within a Completely Randomized Design (CRD) with two factors. The first factor involves the dosage of AMF with 4 levels: 10 grams (F1), 20 grams (F2), 30 grams (F3), and 40 grams (F4). The second factor includes the dosage of Yomari organic fertilizer with 5 levels: 0 ml (Y0), 0.75 ml/l (Y1), 1.5 ml/l (Y2), 2.25 ml/l (Y3), and 3.0 ml/l (Y4).

Each treatment level consists of 4 replications. The observational data, both qualitative and quantitative, will be analyzed using an F-test at a significance level of 5%. Differential effects on treatments will be further analyzed using the Tukey's Honestly Significant Difference (HSD) test at a 5% significance level

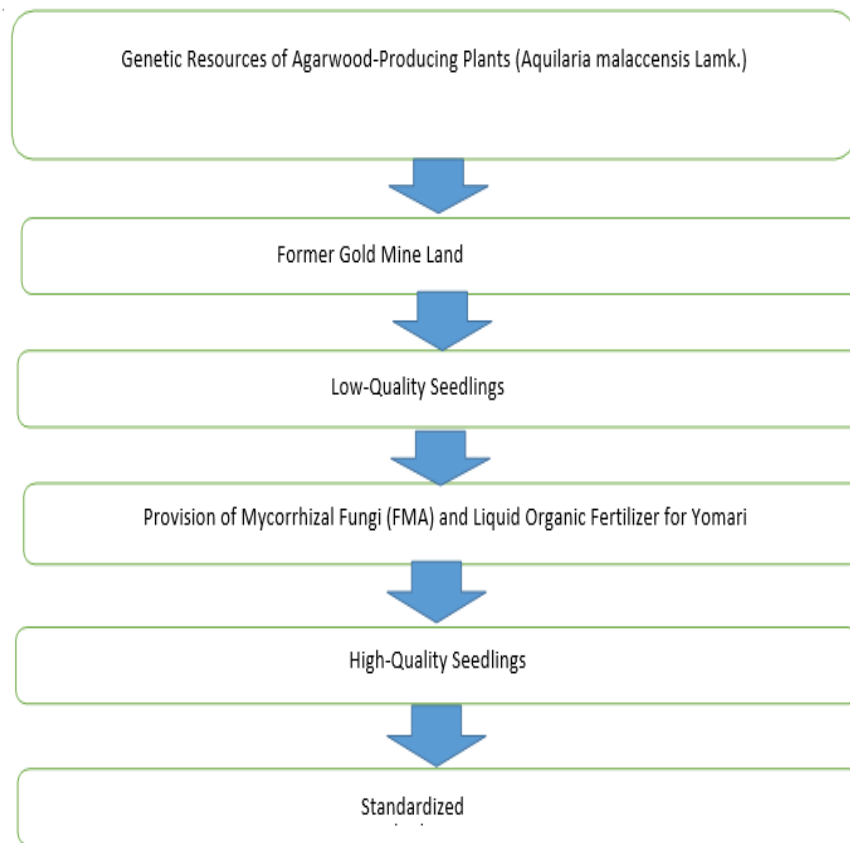


Fig.2. Flowchart of the Study: The Effect of the Application of FMA Doses and Yomari Liquid Organic Fertilizer on the Growth of Gaharu-Producing Plant Seedlings (*Aquilaria malaccensis Lamk.*) on Former Gold Mining Soil

Seedlings of *Aquilaria malaccensis Lamk*, the agarwood-producing plant species, are sourced from the Gaharu farmer group in Kanagarian Muaro Linggae, Sijunjung Regency. These seedlings are initially prepared in polybags measuring 8 cm x 9 cm. When the research is set to begin, the plants are transplanted into larger polybags, sized 12 cm x 17 cm. The seedlings meet specific criteria, including being free from pests and diseases, having a height ranging from 5-15 cm, and possessing 2-5 leaves.

The soil used is a mixture of former Gold mining soil from Dharmasraya Regency and Ultisol obtained from the experimental farm of the Faculty of Agriculture, Andalas University. The soil is evenly processed, and the planting medium is filled into polybags measuring 12 cm x 17 cm.

Seedlings are then transferred from the previously mentioned polybags, which already contain the planting medium (a mixture of former Gold mining soil and Ultisol). Before planting, the seedlings, which have been immersed for 15 minutes in Yomari liquid organic fertilizer solution (according to the treatment), are inserted into the planting hole where their roots come into contact with FMA (according to the treatment) in the planting medium. The hole is then covered with the soil within the polybag.

The FMA used is a combination of *Acaulospora sp.* and *Gigaspora sp.* The FMA is weighed according to the treatment doses (10, 20, 30, and 40 grams per polybag) using a digital scale, following the research by

Nurmasyitah *et al.*, (2013), and Satria et al., (2021), which states that the application of 40 grams of FMA is the optimal dose. FMA treatment is applied by sprinkling it into the planting hole, then placing the pre-soaked seedlings into the hole and covering it again with the soil in the polybag. Starting two weeks after planting, the seedlings are sprayed with POC fertilizer according to the treatment doses (0, 0.75, 1.5, 2.25, and 3 ml/liter), with additional spraying at 8 weeks after planting.

Gaharu seedlings are watered in the morning and evening to maintain soil moisture in the polybag, using a hose for watering. After the study, it was found that the percentage of surviving seedlings was 100%, indicating that replanting was unnecessary.

Weeding is done when weeds appear inside or around the polybag, with weeding performed every 2 weeks. Weeding involves manually pulling out the weeds. Root pruning is done to trim roots growing outside the polybag, preventing the roots from spreading beyond the polybag. Pruning is carried out using cutting tools such as scissors. According to Rusmana (2014), root pruning encourages lateral root growth within the polybag and reduces stress during transportation. The illustration of seedling root pruning can be seen in Figure 2. After the study, no weeds were found growing outside the polybag.

Observations on the survival of seedlings during the study can be calculated at the end of the observation period (16 weeks after FMA inoculation). The percentage of surviving seedlings is calculated as follows: Measurements of plant height increment were conducted starting from the inoculation of FMA to the seedlings. These measurements were performed once a week until the end of the observation period (16 weeks after FMA inoculation). Plant height was measured from the base of the lower stem to the tip of the upper stem using a measuring tape.

Observations on the number of leaves were initiated after FMA inoculation to the seedlings. These observations were conducted once a week until the end of the observation period (16 weeks after FMA inoculation). The observed leaves were those that had fully opened and remained on the plant during the observation. Measurements of the widest leaf width were conducted weekly starting from FMA inoculation to the seedlings until the end of the observation period (16 weeks after FMA inoculation). The leaves measured were those that had fully opened. The measurement of the widest leaf width was carried out by measuring all the leaves on the agarwood seedlings using a measuring tape, then marking the leaves with the widest width for further observation.

Observations on roots emerging from the polybag during the implementation of the agarwood seedling study were conducted from week 1 to week 16, and no roots were found outside the polybag. After the observations, it was confirmed that there were no roots emerging from the polybag. Observations on the weight of the roots of agarwood-producing plant seedlings in each treatment were conducted at the end of the experiment (16 weeks after FMA inoculation),

Using a scale, observations of root weight were conducted by tearing the polybag, then loosening the planting medium in a bucket containing water while rinsing until the roots were clean. After cleaning the root samples, the roots were dried, and then the weighing of the roots was carried out.

Observations of FMA infection on the roots of agarwood-producing plants were conducted at the end of the observation period (16 weeks after FMA inoculation) by taking root samples. The observation of the percentage of FMA-infected roots was conducted at the Plant Physiology Laboratory, Andalas University, after field observations were completed. The percentage of FMA-infected roots can be calculated as follows:

The roots were thoroughly cleaned using distilled water (aquadest). After cleaning, the roots were immersed in a 10% KOH solution. The KOH immersion aims to release oxygen from the cell walls for 2 days (48 hours). Once the immersion is complete, the roots were rinsed again using distilled water 3-5 times, with the assistance of a tea strainer as a container. Subsequently, the roots were soaked in a 2% HCl solution to soften the cell walls for 2 days (48 hours), followed by immersion in a trypan blue solution for another 2 days (48 hours). Trypan blue is utilized for root staining.

Next, the plant roots were cut using a knife to a length of 1 cm, with 5 pieces taken from each treatment and 3 replications. The glass slides were cleaned using 95% alcohol, and the cut roots were placed on the glass slides and covered with a cover glass. Each sample was labeled on the glass slide. Each prepared sample was observed under a microscope at a magnification of 400X. Root infection could be determined by the presence of hyphae, vesicles, and arbuscules

### III. RESULT AND DISCUSSIONS

#### 1. Percentage of Life of Agarwood-Producing Plant Seeds

Based on the analysis of variance, it is indicated that there is an interaction between the dosage of FMA and the dosage of POC concerning the percentage of live

agarwood-producing plant seedlings. The average percentage of live agarwood-producing plant seedlings can be observed in Table 1.

Table 1. Percentage of Life of Agarwood-Producing Plant Seeds due to AMF and LOF treatment at 16 weeks of age

Dosis FMA (g)	Dosis POC (ml/l)				
	0,00	0,75	1,50	2,25	3,00
10	32,50 B c	37,50 C c	55,00 B b	62,50 B b	80,00 B b
20	37,50 AB d	42,00 BC cd	50,00 B c	62,50 B b	75,50 B a
30	37,50 AB d	52,50 B c	55,00 B c	67,50 B b	85,00 B a
40	42,50 A d	62,00 A c	75,00 A b	90,00 A a	97,50 A a

KK = 9,13%

Note: The numbers followed by the same uppercase letter in the same row and the numbers followed by the same lowercase letter in the same column are not significantly different according to the LSD 5%.

Based on Table 1, it can be observed that there is a significant interaction between the dosage of FMA and the dosage of POC regarding the percentage of live agarwood-producing plant seedlings. The application of 10 g of FMA has a similar effect on the percentage of live seedlings when combined with POC dosages of 0 ml, 1.50 ml, 2.25 ml, and 3 ml. Similarly, the application of 20 g of FMA has a consistent effect on the percentage of live seedlings with POC dosages of 1.50 ml, 2.25 ml, and 3 ml. The application of 30 g of FMA shows a similar effect on the percentage of live seedlings with POC dosages of 0.75 ml, 1.50 ml, 2.25 ml, and 3 ml. Lastly, the application of 40 g of FMA exhibits a uniform impact on the percentage of live seedlings across all POC dosage applications.

The results of the research depict the complexity of the interaction between FMA and POC in influencing the growth of agarwood plants in former gold mining areas. The use of liquid organic fertilizer and mycorrhiza can have a positive impact on the growth of agarwood plants in former gold mining areas. Liquid organic fertilizer provides the necessary nutrients for plants, while mycorrhiza helps enhance nutrient absorption and improve soil structure. The combination of both can increase plant resilience to less fertile conditions, such as former gold mining areas, and enhance agarwood plant productivity. Perez and Urcelay (2009) stated that FMA can improve the height growth of specific host plants that are compatible with FMA. Different FMA types can have different effects on different host plants. FMA is a

biological fertilizer that only needs to be infected into its host plants once because it is a living organism that can continue to grow and develop (Setiadi and Setiawan, 2011).

Table 1 also indicates that the application of 0 ml POC has a similar effect on the percentage of live seedlings with the application of 20 g, 30 g, and 40 g FMA. The application of 0.75 ml POC has a consistent effect on the percentage of live seedlings with the application of 10 g, 30 g, and 40 g FMA. The application of 1.5 ml POC has a similar effect on the percentage of live seedlings with the application of 10 g and 40 g FMA. The application of 2.25 ml POC yields the highest percentage of live seedlings with the application of 40 g FMA. Lastly, the application of 3 ml POC has a similar effect on the percentage of live seedlings with the application of 20 g, 30 g, and 40 g FMA.

POC can help improve soil structure in former gold mining areas, which may have less than ideal soil textures. Well-structured soil can facilitate the movement of water and air, as well as improve plant access to nutrients. Liquid organic fertilizer can also help increase the soil's capacity to retain water, which is crucial, especially in former gold mining areas that may have water retention issues. Soil that can retain water effectively can help agarwood plants thrive in unstable environmental conditions.

POC can provide essential nutrients for agarwood plants in former gold mining areas through organic substances. POC contains organic substances such as humic acid and fulvic acid. These substances can help increase the availability of nutrients in the soil by enhancing ion exchange and binding available nutrients. Additionally, liquid organic fertilizer also contains microorganisms such as bacteria and fungi that are beneficial to plants. These microorganisms help break down organic matter in the soil into forms that are more easily absorbed by plant roots. Liquid organic fertilizer can also stimulate the growth of soil microbes, which play a role in breaking down organic

matter and releasing trapped nutrients. This can enhance nutrient availability for plants.

## 2. Increase in the number of leaves of agarwood producing plant seeds

Based on the analysis of variance, there is an interaction between the application of FMA dosage and POC dosage concerning the increase in the number of leaves on agarwood plant seedlings. The increase in the number of leaves on agarwood plant seedlings can be observed in Table 2.

Table 2. Increase in the number of leaves of agarwood-producing plant seeds Due to AMF and LOF treatment at the age of after 16 weeks of seedlings

Dosis FMA (g)	Dosis POC (ml/l)				
	0,00	0,75	1,50	2,25	3,00
10	3,25 A d	4,00 B cd	4,75 B c	6,00 B b	7,00 C a
20	3,50 A d	4,25 AB cd	5,00 AB c	6,50 BC b	7,50 B a
30	3,75 A c	4,75 AB b	5,25 AB c	7,25 AB a	7,75 B a
40	3,75 A c	5,00 A c	5,75 A b	8,00 A a	10,25 A a

KK = 10,99%

Note: The numbers followed by the same uppercase letter in the same row and the numbers followed by the same lowercase letter in the same column are not significantly different according to the LSD 5%.

Based on Table 2, it can be observed that there is a significant interaction between the dosage of FMA (Arbuscular Mycorrhizal Fungi) and the dosage of POC (Liquid Organic Fertilizer) regarding the increase in the number of leaves on agarwood-producing plants. The application of 10 g, 20 g, and 30 g of FMA results in the highest increase in the number of leaves when combined with a POC dosage of 3 ml. The application of 40 g of FMA has a similar effect on the increase in the number of leaves across all POC dosage applications. Table 2 also shows that the application of 0 ml POC has a similar effect on the increase in the number of leaves with the application of 30 g and 40 g of FMA. The application of 0.75 ml and 1.50 ml POC results in the highest increase in the number of leaves with the application of 40 g of FMA. The application of 2.25 ml POC has a similar effect on the highest increase in the number of leaves with the application of 30 g and 40 g of FMA. The application of 3

ml POC has a similar effect on the increase in the number of leaves across applications 40 g of FMA dosage.

The significant interaction between the application of FMA (Arbuscular Mycorrhizal Fungi) dosage and POC (Liquid Organic Fertilizer) dosage regarding the increase in the number of leaves on agarwood-producing plants is due to the mechanisms involving both in enhancing the health and growth of plants. This includes a symbiotic mutualistic interaction between FMA and plant roots. FMA forms a symbiotic mutualistic relationship with plant roots. The mycorrhiza (fungus) on FMA forms structures such as mycelium that reach into the soil and create root-like structures, enhancing nutrient absorption by plants.

In this relationship, plant roots provide carbohydrates from photosynthesis to FMA, while FMA assists plants in nutrient absorption, especially phosphorus. Liquid Organic Fertilizer (POC) as an Additional Nutrient Source. POC contains organic substances, nutrients, and

microorganisms that can increase nutrient availability in the soil. Additional nutrients from POC can strengthen the symbiotic relationship between FMA and plants by providing the resources needed for the growth of mycorrhiza and plants. Optimization of Phosphorus Availability.

FMA plays a critical role in increasing phosphorus uptake by plants. Phosphorus is crucial for leaf formation and overall plant growth. The application of FMA dosage can improve phosphorus uptake efficiency, especially at specific dosages. Specific Dose Interaction. The research results show that FMA dosages of 10 g, 20 g, and 30 g result in the highest increase in the number of leaves at a POC dosage of 3 ml. This may reflect an optimal point where the interaction between FMA and POC achieves maximum results.

The interaction between FMA and POC creates a synergistic effect, where the combination of both provides better results than the application of each separately. Thus, through the synergy of increased nutrient absorption through FMA and the provision of additional nutrients from POC, this interaction can significantly enhance the growth of agarwood plants, especially in terms of the increase in the number of leaves (Satria et al., 2022). The specific dose factors of each component also provide an additional dimension that needs to be considered in

Table 3. Plant Seed Height Increase due to AMF and LOF treatment at seedling age of after 16 weeks

Dosis FMA (g)	Dosis POC (ml/l)					Rata-Rata
	0,00	0,75	1,50	2,25	3,00	
10	15,0	22,5	27,5	30,0	35,0	26,00 c
20	17,5	25,0	30,0	35,0	45,0	30,50 b
30	17,5	27,5	30,0	35,0	45,0	31,00 b
40	20,0	30,0	35,0	40,0	57,5	36,50 a
<b>Rata-Rata</b>	17,50 E	26,25 D	30,62 C	35,00 B	45,62 A	

KK = 18,86%

Note: The numbers followed by the same uppercase letter in the same row and the numbers followed by the same lowercase letter in the same column are not significantly different according to the LSD 5%.

Based on Table 3, FMA with a dosage of 40 g provides an average seedling height for agarwood-producing plants that is higher than other dosages, reaching 36.50 cm. POC dosage also has a significant effect on the seedling height of agarwood-producing plants. The average results show that a POC dosage of 3 ml reaches 45.62 cm. The occurrence of separate mechanisms between FMA and

managing agarwood cultivation in former gold mining areas. The percentage of live seeds is influenced by various biotic and abiotic factors. Biotic factors such as seed quality, plant seeds used from both species came from healthy seeds. The characteristics of healthy plants are that they have green leaves and stems, the seeds are not diseased, the stems are straight, which is in accordance with the Indonesian national standard (SNI) 01-5006.1-2006 regarding seed quality which states that healthy seeds are fresh seeds. that are not attacked by pests and diseases, and do not show symptoms of nutrient deficiency (stems are not straight and pale yellow in color). The high percentage value of live seedlings *Aquilaria malacensis* seedlings had the best growth response to the AMF dose treatment with the highest LOF concentration.

### 3. Agarwood-producing Plant Seed Height Increase

Based on the analysis of variance, the seedling height of agarwood-producing plants indicates that there is no interaction between the dosage of FMA (Arbuscular Mycorrhizal Fungi) and the dosage of POC (Liquid Organic Fertilizer). Individually, both types of FMA and POC dosage have a significant effect. The data can be seen in Table 3.

POC, where both contribute independently to plant growth.

FMA can influence nutrient absorption through a symbiotic relationship with plant roots, while POC can directly provide additional nutrients to the soil (Satria et al., 2022). The absence of interaction between the application of POC (Liquid Organic Fertilizer) and FMA (Arbuscular Mycorrhizal Fungi) on the height of agarwood

seedlings can be influenced by several factors, including the existence of Separate Mechanisms (Independent Actions) between the application of POC and FMA. FMA enhances nutrient absorption and improves the condition of plant roots, while POC provides additional nutrients and improves soil structure.

The same impact on seedling height. Factors such as nutrient availability, water absorption, and improved plant health may have a similar impact on the height of agarwood seedlings without depending on each other. Both factors may have a positive additive contribution, but they do not modify or enhance each other's effects. Optimal Conditions Without Dependency. In situations where the dosage of POC and FMA has reached its optimal conditions, no additional improvement can be achieved through the interaction between the two. POC and FMA dosages have already provided an optimal level of nutrition and soil support for the growth of agarwood

plants. Linear or Saturated Response. The addition of POC or FMA dosages has reached a level where plants respond linearly or even reach a saturation point, where further addition does not provide additional increases in seedling height. This is because this is because the higher the dose of LOF given and the higher the dose of AMF given to agarwood-producing plants, the higher the growth of agarwood-producing plant seeds. In addition, this plant is able to utilize N<sub>2</sub> in the air, and the organic matter produced by this plant is rich in N nutrients (Kimi *et al.*,2020 and Satria *et al.*, 2022)).

#### 4. Widest Leaf Width of Agarwood Seedlings

Based on the analysis of variance, it is evident that there is an interaction between the treatment doses of FMA and POC on the longest leaf length of seedlings from agarwood-producing plants. The longest leaf length of seedlings from agarwood-producing plants can be observed in Table 4.

Table 4. Widest Leaf Width of Agarwood-Producing Plant Seeds due to AMF and LOF treatment at 16 weeks of seedling

Dosis FMA (g)	Dosis POC (ml/l)				
	0,00	0,75	1,50	2,25	3,00
10	4,7500 B d	5,6250 B c	6,1250 C bc	6,5000 B b	7,4750 C a
20	5,0250 AB c	6,2500 AB b	6,5500 BC b	6,7500 B b	8,0000 C a
30	5,2500 AB c	6,4750 A b	6,9500 AB b	6,9750 B b	9,1250 B a
40	5,5750 A d	6,7250 A c	7,3700 A bc	7,7500 A b	10,3750 A a

KK = 6,99%

Note: The numbers followed by the same uppercase letter in the same row and the numbers followed by the same lowercase letter in the same column are not significantly different according to the LSD 5%.

Table 4 also indicates that the application of POC dosages 0 ml, 0.75 ml, and 1.5 ml has the same effect on the percentage of live seedlings with the application of FMA dosages of 10 g and 40 g. The application of POC dosages 2.25 ml and 3 ml has the same effect on the longest leaf length in all FMA dosage applications. The research results indicate a significant interaction between FMA and POC dosages on the longest leaf length of agarwood-producing plants. A dosage of FMA 10 g may have reached its optimal limit for the application of POC dosages of 1.50 ml and 3 ml, while higher FMA dosages of 40 g are needed to see an improvement with POC dosage of 3 ml.

The simultaneous application of FMA and POC can support the growth of agarwood leaf length by increasing nutrient availability, activating plant hormones, and improving soil quality. In this context, the interaction between FMA and POC dosages plays a crucial role in optimizing the plant's response to the given treatments (Satria *et al.*,2022). The higher the dose of AMF given to the producing plant, the wider the width of the widest leaf of agarwood-producing plant seeds. In addition, this plant is able to utilize N<sub>2</sub> in the air, and the organic matter produced by this plant is rich in N nutrients (Kimi *et al.*,2020)



#### 4. Longest Leaf Length

Based on the analysis of variance, it is indicated that there is an interaction between the treatment of FMA dosage and POC dosage on the widest leaf width of

agarwood-producing plant seedlings. The average widest leaf width of agarwood-producing plant seedlings can be seen in Table 5.

Table 5. Longest Leaf Length of Agarwood-Producing Plant Seeds due to AMF and LOF treatment at 16 weeks of seedling

Dosis FMA (g)	Dosis POC (ml/l)				
	0,00	0,75	1,50	2,25	3,00
10	1,9250 A d	2,2250 A c	2,3500 B bc	2,5500 A b	2,8500 C a
20	1,9000 A d	2,3250 A c	2,7500 A b	2,6500 A b	3,0500 BC a
30	2,0000 A d	2,3000 A c	2,5500 AB b	2,6250 A b	3,0750 B a
40	2,0750 A d	2,4000 A c	2,5750 A bc	2,7250 A b	3,4250 A a

KK = 5,84

Note: The numbers followed by the same uppercase letter in the same row and the numbers followed by the same lowercase letter in the same column are not significantly different according to the LSD 5%.

Based on Table 5, it can be observed that there is a significant interaction between the dosage of FMA and POC on the widest leaf width of agarwood-producing plants. The application of FMA dosages of 10 g, 20 g, 30 and 40 g resulted in an increase in the widest leaf width when combined with a POC dosage of 3 ml. The application of FMA dosage of 40 g had the same effect on the widest leaf width for all POC dosages. Table 5 also indicates that the application of POC dosages of 0 ml, 0.75 ml, 2.25 ml, and 3 ml had the same effect on the widest leaf width for all FMA dosages. Meanwhile, the application of POC dosage of 1.50 ml had the same effect on the widest leaf width for the application of FMA dosages of 20 g and 30 g.

The positive interaction between the application of Arbuscular Mycorrhizal Fungi (FMA) and Liquid Organic Fertilizer (POC) affecting the growth of agarwood leaf width can be explained through several mechanisms related to increased nutrient availability, increased soil microbial activity, and soil condition improvement. FMA forms a symbiotic relationship with plant roots, creating arbuscular mycorrhizal mycelium structures that can enhance the absorption of nutrients, especially nutrients that are less soluble in water, such as phosphorus and other minerals. POC, as a liquid organic fertilizer, can provide organic nutrients that are more easily accessible to plants.

The combination of increased mineral absorption by FMA and the provision of organic nutrients by POC provides better nutritional support for the growth of agarwood leaves (Satria et al., 2021 and Satria et al., 2022). POC provides sources of organic nutrients that support the growth and activity of soil microbes. This microbial activity plays a crucial role in breaking down organic matter into forms that can be used by plants. Increased microbial activity can enhance the circulation of nutrients in the soil, which in turn supports plant growth, including leaf width. Hormone stimulation can also influence leaf width growth. FMA can stimulate the production of plant hormones, which can affect the growth and development of leaves (Intan et al., 2019). The combination with POC may provide additional support in triggering plant hormone responses leading to broader leaf growth.

#### 6. Root Weight of Agarwood-Producing Plant Seedlings

The analysis of variance results indicates that there is an interaction between the AMF treatment and the POC treatment on the root weight of agarwood-producing plant seedlings (Appendix 4 and Table 3). The best response is shown in the treatment of 40 grams of AMF with a POC treatment of 3.00 ml, which is significantly different from other treatments at 3 months after planting (MAP).

Table 6. Root Weight of Agarwood-Producing Plant Seedlings due to AMF and POC Treatment at 16 Weeks After Planting (WAP).

Dosis FMA (g)	Dosis POC (ml)				
	0	0,75	1,50	2,25	3,00
	-----g-----				
10	11.3000 c C	12.3175 b B	12.9925 c B	13.1600 c AB	13.8675 c A
20	12.2325 b C	13.0750 b BC	13.5550 c AB	13.7150 c AB	13.9900 c A
30	13.0275 b D	14.1000 a C	15.1225 b B	15.8875 b B	19.2300 b A
40	14.3925 a C	15.8600 a C	16.8500 a B	17.5800 a B	24.6975 a A
<b>KK = 4.12%</b>					

The higher the dose of AMF (Arbuscular Mycorrhizal Fungi) and the higher the concentration of POC (Yomari Liquid Organic Fertilizer) given to agarwood-producing plants, the higher the root weight of agarwood-producing plant seedlings. Nitrogen is crucial for the formation and growth of vegetative parts of plants such as leaves, stems and roots. Meanwhile, phosphorus can help enhance plant growth, produce chlorophyll, increase protein levels, and accelerate leaf growth (Satria *et al.*, 2021 and Satria *et al.*, 2022).

### 7. Percentage of Roots of Agarwood-Producing Plant Seedlings Infected with AMF

The analysis of variance results show that there is an interaction between the AMF (Arbuscular Mycorrhizal Fungi) treatment and the POC (Yomari Liquid Organic

Fertilizer) treatment on the widest leaf width of agarwood-producing plant seedlings (Appendix 4 and Table 3). The best response is shown in the treatment of 40 g AMF dosage with 3.00 ml POC treatment, which significantly differs from other treatments at 16 weeks after planting (MAP). This may be due to the mycorrhizal fungi with the AMF dosage and POC concentration being able to thrive in a planting medium dominated by sandy soil with larger soil pores compared to clayey soil. This condition is believed to be suitable for the development of larger AMF spores, capable of infecting plant roots (Kimi *et al.*, 2020; and Asmaraman *et al.*, 2018).

Table 7. Percentage of Roots of Agarwood-Producing Plant Seedlings Infected with AMF due to AMF and POC treatments at 16 Weeks After Planting (WAP).

Dosis FMA (g)	Dosis POC (ml)				
	0	0,75	1,50	2,25	3,00
	----- % -----				
10	17.5000 a D	19.0000 a C	20.0000 a C	23.0000 a B	25.0000 a A
20	32.7500 b E	34.5000 b D	36.2500 b C	38.2500 b B	44.2500 b A
30	36.0000 b E	43.5000 c D	46.5000 c C	51.5000 c B	58.0000 c A
40	57.5000 c E	62.5000 d D	65.7500 d C	85.7500 d B	95.5000 d A
<b>KK = 1.85%</b>					

Note: Numbers followed by the same uppercase letter in the same row and numbers followed by the same lowercase letter in the same column are not significantly different according to the LSD.

According to Brundrett (1996), mycorrhiza is a form of mutualistic symbiotic relationship between fungi and plant roots, where both symbionts benefit from each other. Arbuscular mycorrhizae (CMA) are considered obligate symbionts, meaning that CMA can function only after infecting the host plant. CMA can infect the root system of the host plant, as depicted in Figure 1, and subsequently produce an extensive network of hyphae. This mycorrhizal association enables the plant to enhance its capacity for nutrient absorption from both organic liquid fertilizer (POC) and water (Satria *et al.*, 2022).

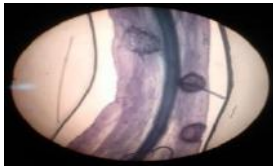


Fig.1. Form of roots infected by Arbuscular Mycorrhizae (CMA) as viewed under a microscope at 400X magnification.

The colonization increase by Arbuscular Mycorrhizae (CMA) begins with the formation of an appressorium. The appressorium is a crucial structure in the life cycle of CMA, representing a key event for a successful interaction with the potential host plant. Subsequently, the contact phase is followed by the symbiotic phase. From that phase onward, the fungus perfects the complex morphogenetic process by producing intercellular and intracellular hyphae, vesicles, and arbuscules. The main structures of CMA are arbuscules, vesicles, external hyphae, and spores (Dewi, 2007). According to Sufaati *et al.*, (2011), arbuscules are hyphal structures originating from branching hyphae inside the cortex cells of the host plant's roots. Arbuscules have a small tree-like appearance and function as sites for the exchange of primary metabolites (especially glucose and phosphorus) between the fungus and plant roots. The distribution of external hyphae is influenced by biotic and abiotic factors such as soil chemical and physical properties, organic matter, and microflora and microfauna present in the soil as the growing medium (Trisilawati *et al.*, 2012).

#### IV. CONCLUSION

Based on the results of the above research, it can be concluded that: 1. there is an interaction between the administration of AMF doses and the concentration of liquid organic fertilizer on the growth of seedlings of agarwood-producing plants (*Aquilaria malacensis* Lamk.) on former gold mining soil, and 2. Administration of 40 grams of AMF with a concentration of 3.00 ml/l of liquid organic fertilizer is the most effective in increasing the

percentage of survival, the number of leaves, the height of seedlings, the widest leaf width, and the percentage of agarwood-producing plant seedlings infected with CMA.

#### ACKNOWLEDGEMENTS

Special thanks to the Dean of the Faculty of Agriculture for funding our research through fund basic research FAPERTA UNAND with contract number: 06/PL/SPK/PNP/ FAPERTA-Unand/2023, dated March 1, 2023.

#### REFERENCES

- [1] Asmarahman, C., S.W. Budi., I. Wahyudi., E. Santoso. 2018. *Identifikasi Mikroba Potensi Fungi Mikoriza Arbuskula (FMA) Pada Lahan Pasca Tambang PT. Holcim Indonesia Tbk. Cibinong, Jawa Barat.* Jurnal Pengelolaan Sumber Daya Alam dan Lingkungan Vol.8(3):279-285.
- [2] Brundrett M, N Bougher, B Dell, T Grove and N Majalaczuk. 1996. Working with mycorrhizas in forestry and agriculture, 174-208. Australian Centre for International Agriculture Research, Canberra.
- [3] Dewi, I.R. 2007. Peranan dan Fungsi Fitohormon Bagi Pertumbuhan Tanaman. [Skripsi]. Bandung. Fakultas Pertanian. Universitas Padjajaran. 43 Hal.
- [4] Mosse, S. 1981. Vesicular Arbuscular Mycoriza Research For Tropical Agriculture. Research Bulletin. Vol 88(2): 207-212.
- [5] Rusmana. 2014. Penentuan Indeks Kualitas Tanah Berdasarkan Sifat Fisik Tanah Pada Berbagai Penggunaan Lahan di DAS Arau Bagian Hulu. [Skripsi]. Padang. Fakultas Pertanian. Universitas Andalas. 86 Hal.
- [6] Sari, N.I. 2018. Respon Dua Jenis Bibit Tanaman Gaharu Yang Diinokulasi Fungi Mikoriza Arbuskular Pada Media Tanah Bekas Tambang Batubara. Fakultas Pertanian. Universitas Andalas. Padang. 67 hal
- [7] Satria B dan Raesi S. 2021. Pengaruh Pemberian Pupuk Organik Cair Yomari terhadap Pertumbuhan dan Perkembangan Bibit Kopi (*Coffea sp.*). Penelitian Mandiri Fakultas Pertanian Universitas Andalas. 40 hal.
- [8] Satria B, M.Fadli, N.Herawati and Aprisal. 2021. Utilization of Arbuskular Mikoriza Fungi (AMF) for growth and ready to release of three genotype gaharu (*Aquilaria spp.*(Lamk.). dipresentasi di seminar ICBEAU dan dimuat di IOP Conference Series: Earth and Environment Science. Vol.741. No.1.2021.
- [9] Satria B, R.Hersi.M, Armasyah, D.Hervani and Warnita. 2022. The Effect of Addition of AMF (Arbuscular Mycorrhizal Fungi) and Yomari Liquid Organic Fertilizer Concentration on the Growth of Agarwood Production Plants (*Aquilaria malacensis* Lamk.) on Ex-Lime Mining Soil.
- [10] Setiadi, 2001. Karakterisasi Fungi Mikoriza Arbuskula Pada Rhizosfer *Aren Arenga pinnata* (WrmB)Merr.) dari Jawa Barat dan Banten. Jurnal Silvikultur Tropika. Vol. 7(1): 18-23.
- [11] Sufaati S, Suharno, Bone I. 2011. Endomikoriza yang

Berasosiasi Dengan Tanaman Pertanian Non-Legum di lahan Pertanian Daerah Transmigrasi, Kota Jayapura. *Jurnal Biologi Papua*. Vol. 3(1): 8 Hal.

- [12] Trisilawati O, Towaha J, Daras U. 2012. Pengaruh Mikoriza dan Pupuk NPK Terhadap Pertumbuhan dan Produksi Jambu Mete Muda. *Buletin RISTRI*. Vol. 3(1) : 263-273.



# **The economic and environmental effects of gold panning in a zone of armed conflict in the circle of Gao**

## **Les effets économiques et environnementaux de l'orpaillage en zone de conflit armé dans le cercle de Gao**

Abdoulkadri Oumarou Toure<sup>1</sup>, Fatoumata Maiga<sup>1</sup>, Baba Faradji N'diaye<sup>1</sup>, Issa Ouattara<sup>2</sup>, Bamoussa Yalcouye<sup>3</sup>

<sup>1</sup>Département de Géographie, Faculté d'Histoire et de Géographie (FHG), Bamako, Mali

<sup>2</sup>Institut National de Formation des Travailleurs Sociaux (INFTS), Bamako, Mali.

<sup>3</sup>Institut National de la Statistique (INSAT)

\*Auteur correspondant : [toureabdoulkadri@gmail.com](mailto:toureabdoulkadri@gmail.com)

Received: 15 Oct 2023; Received in revised form: 25 Nov 2023; Accepted: 05 Dec 2023; Available online: 12 Dec 2023

©2023 The Author(s). Published by Infogain Publication. This is an open access article under the CC BY license

(<https://creativecommons.org/licenses/by/4.0/>).

**Abstract**— Since 2018, the Gao region has been the focus of a massive influx of people from all walks of life in search of the gold nugget that would make them rich. Indeed, gold has been discovered at various sites in the region, successively up to the present day. In a context of insecurity and occupation of the sites by armed groups, gold mining is carried out in an anarchic fashion with little regard for the environmental regulations in force. The aim of the study was to analyze the economic and environmental effects of gold panning in a context of armed conflict in the Gao circle, Mali. The methodology adopted consisted in conducting surveys among gold miners and local authorities in the region. Analysis of the survey results revealed that the positive impact was a drop in the unemployment rate among young people and an increase in their income above the minimum wage, according to 86% of respondents. However, the uncontrolled exploitation of sites using inappropriate machinery and techniques poses serious environmental problems, particularly for water, soil, flora and fauna resources. What's more, the waste generated is very poorly managed (59% of respondents dump it in the open air and 35.24% burn it). This has serious consequences for renewable natural resources. One of the main factors encouraging uncontrolled mining on gold panning sites is the failure of operators to comply with, or even ignore, current legislation in areas of insecurity. The Malian government must seek to secure these areas so as to ensure compliance with appropriate operating measures and better organize the industry. This will have the dual advantage of bolstering the coffers of the state and local authorities, as well as ensuring the safety of gold miners on the sites.



**Keywords**— *Effects economy, effects environment, gold panning, armed conflict, Gao.*

**Résumé**— Depuis 2018, la région de Gao fait l'objet d'un flux massif de personnes venues de tous les horizons à la recherche de pépite d'or qui ferait leur richesse. En effet, l'or a été découvert sur divers sites de la région et de façon successive jusqu'à nos jours. Dans un contexte d'insécurité et d'occupation des sites par les groupes armés, l'exploitation aurifère se fait de façon anarchique avec peu d'égard pour la réglementation environnementale en vigueur. L'objectif de l'étude est d'analyser les effets économiques et environnementaux de l'orpaillage dans un contexte de conflit armé dans le cercle de Gao au Mali. La méthodologie adoptée a consisté à mener des enquêtes auprès des orpailleurs et des autorités locales de la région. De l'analyse des résultats des enquêtes, il ressort que la conséquence positive a été la baisse du

taux de chômage auprès de la couche jeune et une augmentation de leur revenu supérieur au SMIG selon 86% des enquêtés. Cependant, l'exploitation anarchique des sites avec des engins et techniques inappropriés pose de graves problèmes environnementaux notamment sur les ressources hydriques, pédologiques, floristiques et fauniques. En outre, les déchets générés sont très mal gérés (59% des enquêtés jettent à l'air libre et 35,24% les brûlent). Il en résulte de graves conséquences sur les ressources naturelles renouvelables. Le non-respect des textes en vigueur, voire leur ignorance par les exploitants sur une zone d'insécurité constitue l'un des principaux facteurs favorisant l'exploitation anarchique sur les sites d'orpaillage. L'Etat malien doit chercher à sécuriser ces zones afin d'y faire respecter les mesures appropriées d'exploitation et mieux organiser la filière. Ceci aura le double avantage de faire renflouer les caisses de l'Etat et des collectivités, mais aussi d'assurer la sécurité des orpailleurs sur les sites.

**Mots clés**— Effets économiques, effets environnementaux, orpaillage, conflit armé, Gao.

## I. INTRODUCTION

Au Mali, l'exploitation artisanale de l'or aussi appelée orpaillage est une pratique séculaire, en témoigne les récits datant des empires du Ghana et du Mali. De cette époque des grands empires (du Ghana, du Mali et du Songhay), où elle était essentiellement traditionnelle, à nos jours, cette activité a connu plusieurs types de pratiques (Maiga et al, 2022, p.39). Aujourd'hui, l'exploitation aurifère artisanale contribue au Mali à la survie de nombreuses populations (emploi plus de 250.000 personnes) sur 350 sites différents (Camara, 2017, p.1). Selon l'étude de l'OCDE/ALG (2018, p. 6), environ 300 à 350 sites d'exploitation ont été répertoriés avec une production d'or artisanale et à petite-échelle d'environ 04 tonnes par an.

Ces dernières années, l'orpaillage connaît une mutation très spectaculaire matérialisée par l'introduction des méthodes et techniques modernes (broyeurs, engins miniers, détecteurs de métaux, etc.) ainsi que des produits chimiques dangereux (cyanure et mercure) dont l'utilisation ne respecte aucune norme environnementale, d'hygiène et de sécurité. Avec l'utilisation de plus en plus courante des détecteurs de métaux par les orpailleurs, les sites d'orpaillage peuvent être ouverts n'importe où dès l'instant que la présence d'indices est signalée. D'autres variantes d'orpaillage verront le jour comme l'orpaillage par dragage des cours d'eau avec utilisation de dragues industrielles et artisanales et de « cracheurs ». En pleine crise sécuritaire, l'orpaillage constitue de nos jours, une source de revenus et d'emplois malgré les menaces qu'elle fait peser sur l'environnement.

L'exploitation artisanale de l'or, bien qu'étant une tradition au Mali, s'est étendue au Nord du pays cette dernière décennie notamment dans les régions de Kidal et de Gao qui sont aussi en proie à des conflits armés qui durent depuis 2012. Dans le nord du pays, la prospection artisanale de l'or représenterait plus de 15% de la production nationale, mais elle échappe au contrôle du pouvoir malien (ouest-france.fr). Les gisements de mines d'or ainsi découverts font l'objet de convoitise et attirent

beaucoup de jeunes de toutes les nationalités surtout de la sous-région. Ce qui a accentué la pression humaine sur les sites miniers avec son corollaire de dégradation de l'environnement. L'insécurité persistante, réduisant de façon considérable le contrôle de l'Etat dans cette partie du pays fait que les normes d'exploitation sont peu, voire pas respectées. Par ailleurs, les sites sont contrôlés par les groupes armés pour renforcer leur capacité d'autofinancement afin de mieux s'armer. Dans la région de Gao, de la découverte des premiers filons d'or en 2018, le passage des matériaux simples aux cracheurs s'est fait avec grande célérité. Cette situation nonobstant le fait qu'elle contribue à créer des emplois et occuper les jeunes, compromet sérieusement la régénération des maigres ressources naturelles de la zone comme les sols, les eaux de surface, les zones de pâturage, les rares forêts.

Le cercle de Gao connaît un afflux important du fait de la découverte de sites qui regorgent du précieux minerai. En quelques années, l'orpaillage a connu une mutation rapide avec l'introduction des méthodes et techniques modernes et aussi l'utilisation des produits chimiques dangereux. Au-delà des aspects économiques rentables, l'orpaillage pratiqué avec des méthodes d'extraction ainsi que les procédés ne respectant pas les normes environnementales est à la base des problèmes de santé et environnementaux auxquels les travailleurs ainsi que les riverains sont confrontés.

Beaucoup de travaux ont été réalisés sur l'orpaillage dans les régions Sud du pays en raison de l'existence de sites miniers depuis le temps des empires et très peu sur la partie Nord. La découverte de sites miniers dans cette partie nous donne ainsi l'opportunité d'étudier les implications de cette activité surtout dans un contexte de conflit armé. L'objectif de la présente étude est d'analyser les effets économiques et environnementaux de l'orpaillage dans un contexte de conflit armé dans le cercle de Gao au Mali.

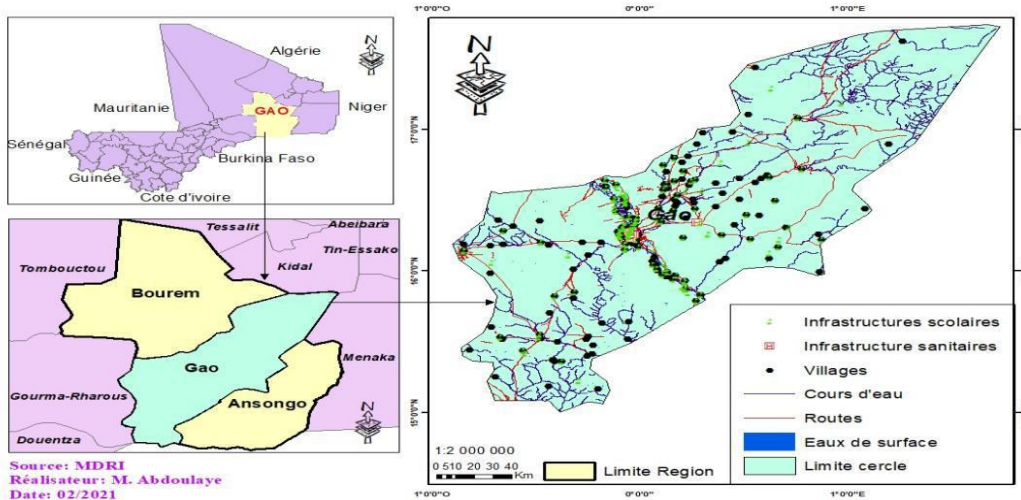
**II. METHODES ET MATERIELS**

**2.1 Méthodes**

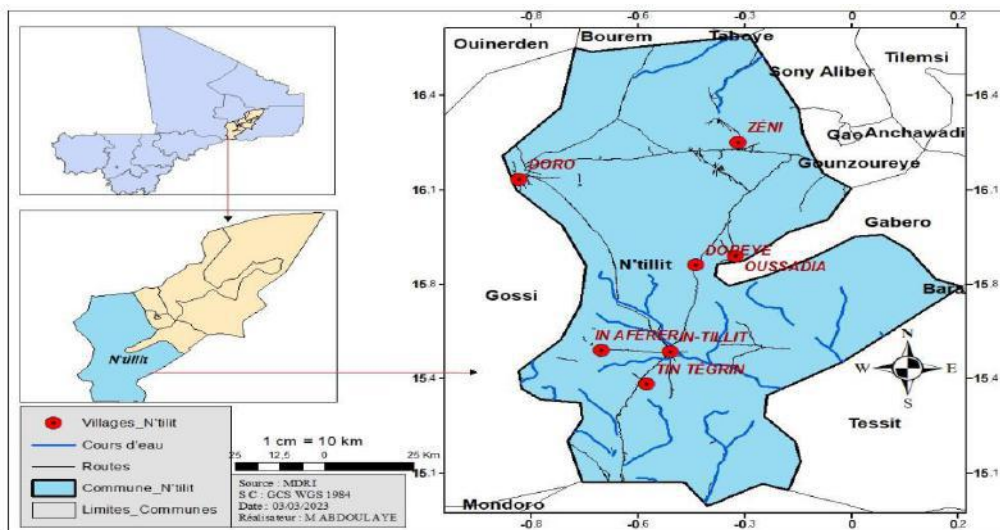
**2.1.1 Zone d'étude**

Le cercle de Gao est situé entre 15 et 17° latitude Nord et de 1° Ouest à 1° Est sur une superficie de 31 288 km<sup>2</sup> soit 35% de la superficie totale de la région de Gao (carte 1).

Sa population estimée à 338 595 habitants en 2020 (DRSIAPS). Le cercle de Gao est composé de 07 communes (Gao, Gounzourèye, Gabéro, Soni Aliber, N'tillit, Anchawaji, Tilemsi). Notre commune d'étude est celle de N'tillit où l'activité d'orpaillage est beaucoup plus développée depuis quelques années (carte 2).



Carte 1 : Présentation du cercle de Gao.



Carte 2 : Présentation de la commune rurale de N'Tillit dans le cercle de Gao.

**2.1.2 Démarche méthodologique**

Le cercle de Gao compte sept communes. Notre choix a porté sur la commune de N'Tillit au niveau de laquelle l'activité d'orpaillage est très développée. Le travail de terrain a consisté à mener des enquêtes quantitatives auprès de 105 orpailleurs et des enquêtes qualitatives auprès de 05 responsables du domaine des mines et de services techniques. Le choix des orpailleurs (concasseurs, puisatiers, laveurs, transporteurs de minerai) s'est fait de

façon aléatoire et a concerné ceux sur le site et ceux de passage à Gao en fonction de leur disponibilité. Pour des raisons de sécurité, une grande partie des enquêtes a eu lieu à Gao. Cependant, le terrain a aussi été exploré, ce qui nous a permis de prendre les coordonnées des zones d'étude, des photos qui témoignent de la réalité et de collecter aussi des données.

**2.2 Matériels**

Les données collectées sont des données climatiques, sociodémographiques et des relevés de points de coordonnées du site. Les données socioéconomiques ont été collectées à l'aide de l'application mobile KoboCollect et les relevés de points de coordonnées sur le site d'orpaillage pris à l'aide de GPS. Les matériels utilisés sont le Smartphone, le GPS, l'appareil photographique, le questionnaire et le guide d'entretien. Les données climatiques et socioéconomiques ont été traitées sur le logiciel Excel et celles cartographiques sur le logiciel Arc GIS 10.8. Les résultats obtenus sont présentés sous diverses formes de figures et de tableaux.

### III. RESULTATS ET DISCUSSION

#### 3.1 Résultats

##### 3.1.1 Site d'exploitation aurifère et sa réglementation

Sur les sites d'exploitation, le paysage fait ressortir les habitations de fortune implantées çà et là et les excavations qui s'éparpillent à perte de vue. Les habitations (sous forme de baraque) sont faites, selon les moyens des orpailleurs, en bois ou métal et couvertes de bâches ou de palissades. Elles constituent le foyer d'accueil des travailleurs. Il y a peu de toilettes qui sont très souvent réalisées non loin des baraques. Il est à noter que la majorité des personnes sur les sites d'orpaillage ne dispose pas de toilette. La défécation à l'air libre est fréquente avec son corollaire de risque de maladies diarrhéiques. Quant aux espaces d'excavation d'or, ils sont disséminés un peu partout sur le site. Avec des formes variées (rectangulaire, carré ou ronde), leur profondeur varie de 1 à 100 m voire 130m selon la structure du sol ou la volonté des orpailleurs de creuser en profondeur en suivant le filon d'or.

##### 3.1.2 Provenance, expérience, niveau d'instruction des orpailleurs

La région de Gao est la principale provenance des orpailleurs. En effet, 90% des orpailleurs proviennent de la région. Dans des proportions plus faibles, le reste des orpailleurs provient des régions de Sikasso suivis de Mopti, Ségou (6%) et d'autres pays d'Afrique (4%) comme le Soudan, le Tchad, le Burkina Faso, l'Algérie. La majorité des orpailleurs enquêtés soit 63% ont moins d'une année d'expérience dans la pratique de l'orpaillage, contre 32% ont entre 1 et 2 années d'expérience. Seulement 5% ont plus de 2 années d'expérience. Ce qui veut dire qu'il y a beaucoup plus de nouvelles personnes qui viennent à l'activité sur le site sans expérience. Ce qui peut avoir des conséquences néfastes quant à la manière et aux procédés de travail qui peuvent s'avérer néfastes pour l'environnement. La majorité des orpailleurs soit 72% a un

niveau minimum du 1<sup>er</sup> cycle. Seulement 28% ne sont pas instruits. Ce qui traduit de plus en plus qu'il n'est plus une activité réservée aux seuls illettrés. On y trouve beaucoup de jeunes diplômés qui viennent chercher fortune.

##### 3.1.3 Etapes de l'extraction de l'or sur le site

Dans la région de Gao, de la découverte des premiers filons d'or en 2018, le passage des matériaux simples aux cracheurs s'est fait avec grande célérité. Malgré sa contribution dans la création d'emplois, la pratique actuelle de l'orpaillage compromet sérieusement la régénération des maigres ressources naturelles de la zone comme les sols, les eaux de surface, les zones de pâturage, les rares forêts.

Sur le site, les étapes de l'extraction de l'or sont les suivantes :

- **Le fonçage** : consiste à creuser des trous (photo 1) afin d'atteindre le minerai

qui se trouve dans une roche. Il se fait manuellement et constitue la phase la plus difficile et pénible du circuit d'extraction. L'orientation du trou suit le lit du minerai et peut être verticale ou horizontale.

- **Le test du minerai** : Afin de vérifier si le minerai extrait contient de l'or, un

test est fait au niveau du site. Si le test est positif, on récupère le minerai pour la suite de la chaîne ; dans le cas contraire, il est mis en dépôt. Ce test consiste à broyer la roche avec un mortier et un pilon en métal, ensuite une assiette et une cuvette permettent de laver le minerai et évaluer sa teneur en or.

- **Le concassage** : Cette phase consiste à rendre la taille du minerai extrait en

petite taille. Il se fait sur l'aire de concassages. Le concassage est manuel et se fait à l'aide d'un marteau, d'une enclume (pierre de granite), d'un nœud de sac pour éviter les projections de particules et protéger les doigts (photo 2).

- **Le broyage** :

Durant cette phase le minerai est réduit en poudre, appelé farine. Le minerai est broyé dans les moulins à énergie gazole deux fois de suite et est séché entre chaque broyage quand le taux d'humidité est élevé (photo 3). Le broyage est fait par deux à trois personnes dans un moulin. Le dispositif de broyage est constitué d'un moulin, d'un moteur relié au moulin par une courroie pour le faire fonctionner, deux fûts de gasoil pour alimenter le moteur, deux fûts d'eau pour refroidir le moteur, d'un « dynamo à meule » qui sert à aiguiser les meules, des cuvettes pour recueillir la farine, les bâches pour sécher la farine.





Photo 1 : Fonçage



Photo 2 : Concassage



Photo 3 : Broyage

- **Le lavage :** La farine issue du broyage (sac de 50 kg) est mélangée avec de

l'eau. Ce mélange est ensuite lavé sur une rampe. Une petite quantité du mélange est placée dans une passoire, ensuite de l'eau y est versée pour être liquéfié. La rampe est couverte d'un tapis (moquette) qui, par gravimétrie, piège l'or et la matière légère est entraînée vers le bas dans un trou peu profond. Le tapis est rincé dans une cuvette d'eau pour être débarrassé de l'or. Cette opération se fait après une certaine quantité de mélange lavé. Après cette étape, la boue restée dans la cuvette où est rincé le tapis est nettoyée jusqu'à obtention de la « poudre noire ».

- **La récupération de l'or :** C'est la dernière phase d'extraction de l'or. Les

orpailleurs de cette zone utilisent un moyen, à savoir l'amalgamation au mercure (Hg). La poudre noire obtenue après le lavage est mélangée à mains nues au mercure pour amalgamation. L'ensemble or-mercure sera ensuite brûlé au chalumeau pour avoir l'or. L'or est pesé sur place par un acheteur qui est un employé du propriétaire du site. Il se vend aussi à Gao.

### 3.1.4 Conditions de travail et revenus tirés de l'activité d'orpaillage

Les conditions de travail sur le site sont très difficiles (53%), pénibles (34%) et moins pénibles (13%). Cependant, une grande majorité (86%) affirme gagner par mois plus de l'équivalent du Salaire Minimum

Interprofessionnel Garanti (SMIG) au Mali fixé à 40 000 F CFA, tandis que 14% affirment gagner moins. Les conditions sécuritaires sur le site sont mauvaises en ce sens que 88% des orpailleurs ne se sentent pas en sécurité sur le site. En effet, 46% des orpailleurs affirment avoir été agressés au moins une fois. Les cas d'accident sont fréquents soit 88% des enquêtés. Ces accidents peuvent aller de blessures légères à graves (cas piqûre avec objet, de fracture, lésions, luxation, etc.).

### 3.1.5 Impacts environnementaux de l'orpaillage

Les sites d'orpaillage constituent des dépotoirs à ciel ouvert de déchets solides en raison du nombre important de déchets générés sur le site. Ces déchets sont des plastiques, de la ferraille, des verres, de biomasse (résidus de bois et de tiges). Les résultats des enquêtes font état de 59% des enquêtés qui rejettent les ordures à l'air libre, 35,24% les brûlent et 5,71% ramassent et enfouissent les déchets dans le sol dans des trous ou fosses qui affleurent le sol (figure 1). Quant à ceux liquides, 64,76% affirment mettre en place un système d'évacuation des eaux usées bien que sommaire, 9,52% enfouissent les eaux dans le sol, 25,71% rejettent les eaux usées à l'air libre (figure 2). Les produits chimiques, carburants et lubrifiants sont déposés à même le sol (photo 4). 26% des enquêtes affirment utiliser des produits chimiques. La gestion des déchets solides et liquides ne répond dans la plupart des cas aux normes environnementales.

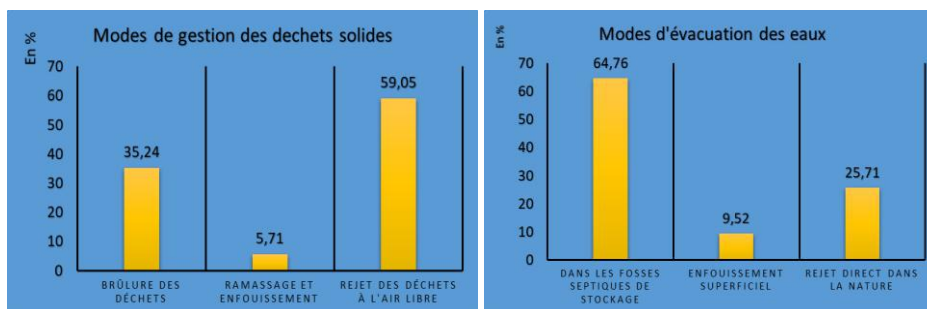


Fig.1 : Mode de gestion des déchets solides Figure 2 : Modes d'évacuation des eaux usées

La coupe du bois constitue une réelle menace dans une zone presque dépourvue d'arbre. Le bois coupé sur le site (ou transporté depuis Gao ou Gossi) sert dans la construction des hangars, des soutènements dans les fosses, de chauffage (photo 5).



Photo 4 : Dépôt de fût de carburant à même le sol



Photo 5 : Coupe et vente de bois.

La qualité de l'air est très mauvaise. La zone étant aride avec une vitesse de vent allant jusqu'à 3,5m/s en saison sèche, la zone d'orpillage vue à distance donne l'impression d'une tempête de sable avec le dégagement de tonnes d'argiles ventilés par le vent. Les orpailleurs à 57% trouvent que la qualité de l'air est mauvaise (niveau de pollution élevé), 41% trouvent qu'elle est moyenne

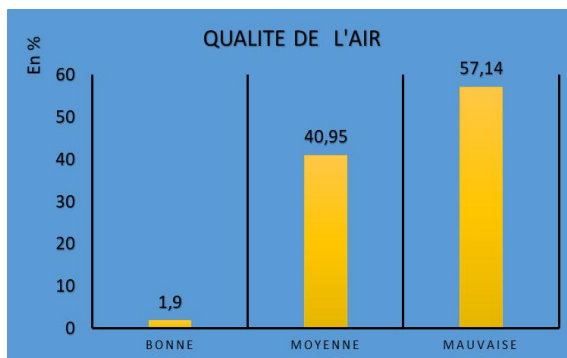


Fig.3 : Avis des orpailleurs sur la qualité de l'air.

(niveau de pollution moyenne) et 2% trouvent qu'elle est bonne (niveau de pollution acceptable) (figure 3).

L'insalubrité du site d'orpillage en raison du non-respect des règles d'hygiène et d'assainissement, fait que les orpailleurs contractent des maladies (figure 4) telles que le paludisme, la diarrhée, les maladies dermiques et oculaires.

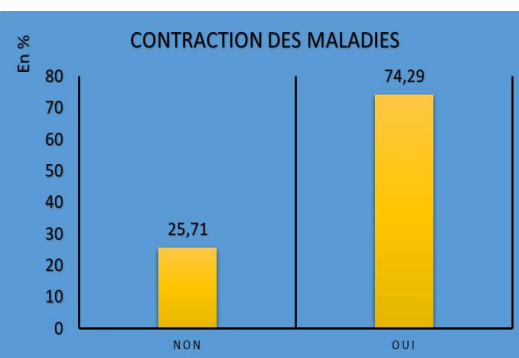


Fig.4 Situation de contraction des maladies.

Sur notre site d'étude, les ordures sont jetées de façon anarchique dans la nature et très souvent non loin des habitations (photo 6). Ce qui donne libre cours au vent de faire trainer les plastiques dans tous les sens et qui sont accrochés par les épineux (photo 7). 74,29% des personnes

enquêtées disent avoir contracté au moins une maladie sur le site depuis leur arrivée contre 25,71% qui ont affirmé n'avoir contracté aucune maladie. Ce taux élevé s'explique aussi par le fait que certains orpailleurs (18%) n'utilisent pas de moyens individuels de protection.



Photo 6 : Dépôt anarchique d'ordures près des habitations (en bleu).



Photo 7 : Des plastiques accrochés aux épineux.

### 3.1.6 Sécurité sur le site

La sécurité dans les conditions de travail sur le site est pénible et 88,57% des personnes affirment avoir été victime au moins d'un accident. Le niveau d'insécurité est assez élevé dans la mesure où 54,59% affirment avoir été agressés sur le site contre 45,71% qui n'ont subi aucune agression. Les agressions sur le site vont de l'intimidation (24,76%), à la menace avec arme à feu (20%), avec arme blanche (1%) en passant par d'autres formes d'agression verbales (54,29%). En un mot, 87,62% des orpailleurs ne se sentent pas en sécurité (86,67%). Cependant, ce qui les motive à rester est le gain car 85,66% affirment avoir un revenu supérieur au SMIG malien.

L'état de sécurité sur le site et les axes routiers menant au site est mauvais selon 86,67% des enquêtés dont certains ont affirmé avoir été victimes de braquage lors duquel ils ont été dépossédés de leur gain (or ou argent).

### 3.2 Discussion des résultats

Les résultats de l'étude montrent que malgré la situation d'insécurité qui prévaut au Nord du Mali depuis 2012, la découverte de sites aurifères a occasionné un afflux massif de personnes vers le cercle de Gao à la recherche du précieux métal.

Les résultats de l'étude ont montré que la majorité des orpailleurs enquêtés ont un niveau minimum du 1er cycle, contre seulement 28% de non scolarisés. La présence de personnes de niveau primaire dans l'orpaillage s'expliquerait par l'abandon scolaire au profit de l'orpaillage. Bien que peu nombreux sur les sites d'orpaillage enquêtés, la présence de personnes de niveaux secondaire et supérieur serait liée au chômage. Ces résultats divergent de ceux de Camara (2017) qui a trouvé dans son étude que plus de 61% des orpailleurs enquêtés sont non scolarisés. Toute chose qui prouve que l'orpaillage est un secteur informel. L'auteur explique que les non scolarisés sont beaucoup plus représentés sur les

sites d'orpaillage, par ce que le processus d'extraction de l'or ne nécessite pas forcément un niveau d'instruction conséquent. Les résultats obtenus par Diarra (2020) abondent dans le même sens. Cet auteur a trouvé que la majorité des orpailleurs enquêtés sont non scolarisés, soit 57%. Certains considèrent même l'orpaillage comme une opportunité exclusive pour les non scolarisés.

Il ressort des résultats que dans un contexte marqué par l'insécurité dans la zone ayant impacté de nombreuses activités, l'orpaillage contribue à l'économie locale. En effet, de l'analyse des retombées économiques de l'activité, il ressort que les gains mensuels de la plupart des orpailleurs dépassent le SMIG malien dont le montant se chiffre à 40 000 francs CFA. Ainsi, de nombreuses personnes, notamment les jeunes au chômage trouvent dans cette activité leur moyen de survie, voire une source d'enrichissement. Ces résultats sont corroborés par Camara (2017) qui affirme que l'orpaillage dans la commune rurale de Séléfougou dans le cercle de Kangaba au Mali, offre des opportunités d'emploi aux populations résidentes et environnantes et ralentit l'exode rural vers les grandes villes. L'auteur ajoute que l'impact économique de l'orpaillage se traduit par une activité commerciale plus intense dans les villages/fraction abritant les sites. Les revenus générés par cette activité contribuent de façon significative à la réduction de la pauvreté dans la commune. Les services et les activités annexes et connexes apportent aussi une part non négligeable dans les recettes des populations du cercle voire de la région, ce qui peut contribuer à diminuer la pauvreté et le taux de chômage ; Cette réduction de la pauvreté passe par l'augmentation au niveau du panier des ménagères, par la création des activités qui se développent autour des sites (commerce, restauration) ; par un afflux massif de véhicules de transport en commun assurant la liaison entre la commune et les communes voisines, voire les villes les plus proches. Nos résultats convergent également vers

ceux de Diarra (2020), qui a montré que l'orpaillage contribue à augmenter les revenus des orpailleurs par la vente directe de l'or et la création des activités annexes qui se développent autour des sites (restauration, bars, boutiques, forges, vente d'habits, jeux vidéo, etc.). Cependant, il est à noter que les recettes engendrées par l'orpaillage ne profitent pas directement ni à l'Etat, ni à la commune car la filière n'est pas encadrée par ces derniers du fait de l'insécurité qui sévit dans la zone. L'Etat doit fournir des efforts dans ce sens pour que la filière soit mieux organisée afin qu'elle lui profite ainsi qu'à la commune. Malgré ses impacts positifs au plan économique, la pratique de l'orpaillage dans le cercle de Gao représente une véritable menace pour l'environnement. Ainsi, dans la zone d'étude, la pratique de l'orpaillage se traduit entre autres par la production de déchets solides et liquides dont la gestion reste précaire, la pollution de l'eau et du sol suite à l'utilisation des produits dangereux comme le mercure et le cyanure, la mauvaise qualité de l'air, l'insalubrité. Ces résultats sont confirmés par ceux de Camara (2017) qui a montré que l'orpaillage se traduit par des déboisements, la destruction du couvert végétal et les sols, la pollution des eaux qui résulte de l'usage des produits chimiques (mercure, cyanure) dans le traitement de l'or.

Nos résultats sont également corroborés par ceux de l'étude de Diallo et al (2003). Ces auteurs confirment que les incidences provoquées par l'exploitation aurifère se manifestent sur la flore et sur le sol, par conséquent sur les eaux (souterraine et de surface) et sur la faune, à savoir : les bruits des orpailleurs, la perturbation et la destruction des habitats, etc. Cet auteur souligne aussi que ces incidences entraînent la raréfaction et/ou la disparition de certaines espèces, la destruction de l'aire de nidification et des ressources alimentaires des oiseaux. Ce qui occasionne le déplacement de ces populations. Les études de l'ONUDI/DNACPN (2009) et de l'OCDE/ALG (2018) confirment nos résultats. La première mentionne que les produits chimiques utilisés pour le traitement de l'or (mercure et cyanure) vont polluer les cours d'eau et les aquifères. En cas de présence de sulfures, le contact avec l'eau et l'air peut entraîner la formation des acides qui pourraient polluer également les nappes aquifères et les cours d'eau. La seconde souligne que le lessivage par les eaux de ruissellement favorise la mobilisation et la dispersion des métaux lourds dans l'environnement, notamment dans les eaux de surface (fleuves, rivières, lacs, barrages et retenues d'eau) et dans les eaux souterraines par infiltration.

Dans la région de Gao, l'exploitation artisanale de l'or s'est produite dans un contexte de conflit armé avec la présence de plusieurs groupes armés. Le contrôle de

certains sites miniers artisanaux par les groupes armés et les organisations criminelles est une réelle menace. Des braquages et attaques surviennent surtout à l'approche des fêtes. Cet état de fait est confirmé par le journal l'indépendant. Dans sa parution du 24 Juin 2023, il a fait état d'un braquage contre un bus en provenance du site d'extraction d'or de Intahaka qui a fait 02 morts et 11 autres brutalisées et dépouillées de tous leurs biens. Les études menées par ICG (2019) et par Munshi (2021) montrent qu'en l'absence de l'Etat, les groupes armés ciblent les exploitants miniers artisanaux pour extraire de l'or et soutirer des taxes. Dans une étude récente, IISD (2022) en vient à la conclusion que l'orpaillage en zone de conflit armé constitue un cercle vicieux se basant sur le fait qu'un financement plus important provenant de l'orpaillage augmente la capacité et l'incitation des groupes armés non étatiques à s'emparer de plus de territoires et de sites miniers artisanaux, tout en augmentant leurs effectifs et les quantités d'or collectées.

#### IV. CONCLUSION

Les résultats de l'étude montrent que l'orpaillage attire un nombre important de personnes aussi bien au Mali que dans la sous-région et même au-delà. La majorité des personnes sur le site affirment qu'elles tirent profit de l'orpaillage qui draine de plus en plus des personnes qui ont un niveau d'instruction plus ou moins élevé. Ce qui a contribué à tirer beaucoup de jeunes du tréfonds du chômage et atténué quelque part le niveau d'insécurité par la réduction des attaques et braquages de façon globale. Cependant, force est de constater que la hausse des revenus est accompagnée d'une cherté de la vie avec une hausse de prix des denrées de première nécessité. La filière reste mal organisée et la traçabilité inexistante, l'insécurité dans la zone aidant. En effet, l'Etat et ses représentants (services techniques et organisations faitières) ne sont pas présents sur le terrain qui demeure sous le contrôle des groupes armés qui font la loi très souvent au détriment de celle de la république. Et donc ni l'Etat, ni la collectivité ne profite des retombés de l'orpaillage. Par ailleurs, leur absence laisse libre cours aux orpailleurs à procéder à des pratiques d'orpaillage peu respectueuses de l'environnement. Les effets environnementaux s'avèrent déjà graves sur les hommes, leurs activités et la durabilité de la biodiversité locale.

Définit comme une « *activité à petite échelle consistant à récupérer l'or contenu dans les gîtes primaires, alluvionnaires et éluvionnaires à l'intérieur d'un couloir d'exploitation artisanale par les procédés manuels associant des équipements rudimentaires, sans utilisation de produits chimiques* » (Code minier, 2019), l'orpaillage,

depuis son transfert aux collectivités territoriales, connaît une autre pratique totalement différente qui fait que dans la pratique le Code Minier actuel apparaît comme un outil complètement inadapté à gérer efficacement la problématique de l'orpaillage au Mali. Aucune de ses dispositions<sup>1</sup> n'est observée. Ce qui donne l'impression d'un vide juridique inexplicable. Profitant de ce vide, de nombreux acteurs sont apparus dans ce domaine et se réclament de ce fait comme étant les véritables organisateurs de la filière. En d'autres termes, le cadre juridique actuel de l'orpaillage présente des insuffisances structurelles et rencontre des difficultés pratiques dans son application sur le terrain. Il constitue des handicaps majeurs pour l'ouverture de ce secteur vers les investissements privés d'une certaine envergure. L'orpaillage reste ainsi un secteur toujours informel non imposé qui mobilise une grande diversité d'acteurs de plusieurs nationalités. Des mesures devront être prises pour mieux sécuriser la zone, y étendre l'influence de l'Etat, règlementer la filière afin que l'orpaillage profite mieux aux orpailleurs et à la collectivité et à l'Etat malien.

### REFERENCES

- [1] Camara, S. (2017) : *Impacts de l'exploitation aurifère artisanale dans la Commune Rurale de Séléfougou, Cercle de Kangaba*, Mémoire de Master en Histoire-Géographie, Ecole Normale Supérieure (ENSup) de Bamako.
- [2] Diallo, A.I.P ; Wade, F ; et Kourouma, S. (2003). Effets de l'exploitation artisanale de l'or sur les ressources forestières à Siguiri, République de Guinée.
- [3] Diarra, M. (2020) : Analyse des impacts environnementaux et sociaux de l'exploitation artisanale de l'or sur les sites de Galamakourou et Dadjian dans la Commune rurale de Fourou, Mémoire de Master en Gestion de l'Environnement, Institut de Développement Economique et Social (IDES) de Bamako.
- [4] Journal l'indépendant : Braquage contre un bus en provenance du site d'extraction d'or de Intahaka (Gao). Parution du Mardi 27 Juin 2023.
- [5] Maïga, F., Touré, A.O, Diya, A., Ouattara, I., Doumbia, S. (2022) : Les effets de l'orpaillage par drague sur la biodiversité aquatique de la rivière Baoulé dans la commune rurale de Kémékafo, région de Dioila, Revue Africaine des Sciences Sociales et de la Santé Publique (RASP), Vol.4, N°1, Janvier-Juin 2022, pp.39-47.
- [6] Organisation pour la Coopération et le Développement Economique et Autorité de Développement Intégré de la Région du Liptako-Gourma. (2018) : L'or à la croisée des chemins, Étude d'évaluation des chaînes d'approvisionnement en or produit au Burkina Faso, Mali et Niger, UE/ALG, France.
- [7] Organisation des Nations-Unies pour le Développement Industriel/Direction Nationale de l'Assainissement et du Contrôle des Pollutions et des Nuisances. (2009). Atelier Sous régional d'information des pays de l'Afrique de l'Ouest Francophone sur les problèmes liés à l'orpaillage, Bamako, rapport de synthèse.
- [8] Fané, S et Dembelé, A. (2020) : Orpaillage, un mal rongeur de l'agriculture dans la commune rurale de Nougua, Mali, Revue HoPE, Vol 1, N°1, Juin 2020, PP1-11.
- [9] <https://www.ouest-france.fr/monde/mali/au-mali-la-ruee-risque-vers-l-or-d-intahaka>
- [10] <https://maliactu.net/region-de-gao-pour-les-predateurs-miniers/consulte> 07/07/2022

<sup>1</sup> Article 47 : L'exploitation artisanale à l'intérieur des couloirs d'exploitation artisanale est gérée par les Collectivités territoriales. Le permis d'exploitation artisanale est accordé par les autorités des Collectivités territoriales sur un périmètre à l'intérieur d'un couloir d'exploitation artisanale de leur ressort. La forme, le contenu et les procédures d'attribution et de renouvellement du permis d'exploitation artisanale à l'intérieur d'un couloir d'exploitation artisanale sont fixés par les autorités des Collectivités territoriales suivant l'avis technique de l'administration chargée des Mines.



# Lipases: Sources, immobilization techniques, and applications

Mudassar Hussain<sup>1</sup>, Imad Khan<sup>1</sup>, Bangzhi Jiang<sup>1</sup>, Lei Zheng<sup>1</sup>, Yuechao Pan<sup>1</sup>, Jijie Hu<sup>1</sup>, Azqa Ashraf<sup>2</sup>, Aiman Salah Ud Din<sup>2</sup>, Waleed AL-Ansi<sup>1</sup>, Adil Khan<sup>3</sup>, Xiaoqiang Zou\*

<sup>1</sup>State Key Laboratory of Food Science and Resources, National Engineering Research Center for Functional Food, National Engineering Research Center of Cereal Fermentation and Food Biomanufacturing, Collaborative Innovation Center of Food Safety and Quality Control in Jiangsu Province, School of Food Science and Technology, Jiangnan University, 1800 Lihu Road, Wuxi 214122, Jiangsu, China.

<sup>2</sup>School of Food Science and Engineering, Ocean University of China, Qingdao 2666100, China.

<sup>3</sup>Lab of Biocatalysis and Fermentation Engineering, Key Laboratory of Industrial Biotechnology of Ministry of Education, College of Biotechnology, Jiangnan University, 1800 Lihu Road, Wuxi 214122, Jiangsu, China.

\*Corresponding author: Xiaoqiang Zou

Received: 30 Oct 2023; Received in revised form: 01 Dec 2023; Accepted: 08 Dec 2023; Available online: 16 Dec 2023

©2023 The Author(s). Published by Infogain Publication. This is an open access article under the CC BY license

(<https://creativecommons.org/licenses/by/4.0/>).

**Abstract**— *Enzymes serve as natural catalysts that exhibit high specificity to their respective substrates and function effectively under mild temperature, pressure, and pH conditions, resulting in superior conversion rates compared to traditional chemical catalysts. These catalysts, sourced from animals, plants, and microorganisms, offer versatility, with lipases standing out for their broad applicability, capturing the interest of various industries. However, the widespread adoption of soluble lipases is hindered by challenges such as high acquisition costs, limited operational stability, and difficulties in recovery and reuse. To address these limitations, enzymatic immobilization has emerged as a viable alternative, aiming to enhance the stability of soluble enzymes while simplifying their recovery and reuse processes. This approach significantly mitigates the overall cost associated with enzyme-dependent processes. This review examines the diverse sources of enzymes, explores various immobilization methods for lipases, and discusses their wide-ranging applications.*



**Keywords**— *Lipase, Classification, Sources, Immobilization, Application.*

## I. INTRODUCTION

Enzymes stand out as efficient biocatalysts with significant potential, particularly in the food industry, where they offer a range of benefits such as safety, efficiency, specificity, controlled reactions, and minimal energy and chemical consumption. Their widespread application in the manufacturing of fats and oils, guiding the transformation of raw materials into final products, has become increasingly prevalent (Cieh et al., 2023; Dijkstra, 2009). The use of various enzymes in lipid processing and modification, though met with varied success within the inherent limitations of bio-catalytic reactions, has gained considerable attention in the field of enzymology over the past few decades (Pliego et al., 2015). Enzyme catalysis represents a notable initiative facilitating reaction

processes under near-ambient conditions, showcasing enhanced specificity and velocity. This approach has played a key role in numerous industrial scenarios, contributing significantly to process intensification (Wohlgemuth et al., 2015).

Lipases (E.C.3.1.1.3) are enzymes that possess specific properties concerning their substrates. These properties include chemo-, region-, and stereo-specificity. They can facilitate heterogeneous reactions in systems that are both water-soluble and water-insoluble. Due to their broad catalytic properties, lipases are widely utilized as biocatalysts in numerous industries, including agrochemicals, pharmaceuticals, detergents, tanning, food, and surfactant production (Ananthi et al., 2014; Iftikhar et al., 2012; Kumar et al., 2012; Thakur et al., 2014).

Additionally, lipases are positioned as the third most prevalent enzymes in terms of usage, after amylases (carbohydrases) and proteases, owing to their diverse utility (Ülker et al., 2011). Lipases, also known as fat-splitting enzymes, triacylglycerol acylhydrolases, or glycerol ester hydrolases, are a class of enzymes that catalyze hydrolysis processes. They catalyze the hydrolysis of triglycerides in these processes, transforming them into fatty acids and glycerol at the oil-water interface. Notably, lipases can also reverse this reaction in aqueous and non-aqueous conditions. (Laachari, El Bergad, et al., 2015; Lee et al., 2015; Nadeem et al., 2015; Priji et al., 2015; Ramos-Sánchez et al., 2015). Parts of the  $\alpha/\beta$ -hydrolase fold family, lipases, possess an active site containing a catalytic triad of Ser-His-Asp/Glu located beneath a brief amphiphilic helical segment that obstructs substrate access. Interacting with hydrophobic substrates prompts a structural rearrangement, leading the enzyme to shift from a closed to an open conformation, allowing accessibility to the active site (Miled et al., 2003; Verger, 1997). Specific lipases exhibit enantioselective properties and catalyze processes such as esterification, interesterification, transesterification, acidolysis, and aminolysis (Hasan et al., 2009). The substrates of lipases, which consist of triacylglycerols with lengthy chain lengths, are water-insoluble. A two-phase system is produced by dissolving these substrates in organic solvents before combining them with a buffer. Lipases, which can catalyze reactions in both aqueous and organic media, are water-soluble. However, applying organic solvents presents difficulties due to the potential for denatured and conformationally altered lipases, which could impact their functional and catalytic capabilities (Guo et al., 2015). In particular, several lipases have a movable lid structure that, depending on displacement, either permits or prohibits access to their active site. The lipase lid usually remains closed in an aqueous media, hiding the active site. But the lid can open at a contact between water and an organic solvent. Based on molecular dynamics simulations, the lipase lid can move in nonpolar conditions, providing access to the active site and making the lipase active while the lid is open. In contrast, the lipase is inactive when the lid is closed (Barbe et al., 2009). The benefits of using lipases as biocatalysts include excellent specificity and selectivity and the capacity to sustain catalytic activity in both aqueous and non-aqueous conditions (Sánchez et al., 2018; Vanleeuw et al., 2019; Zou et al., 2023). As the manufacturing industry increasingly focuses on climate change and environmental concerns, there is a gradual shift towards developing alternative, greener, safer, and sustainable processes (Wohlgemuth et al., 2015).

"Immobilized enzymes" are enzymes that are restricted or localized physically; however, they still can catalyze reactions and be recycled (Brena et al., 2013). Enzyme immobilization technology is acknowledged as a potent tool for adjusting and customizing a range of catalytic characteristics, such as enzyme activity, selectivity, specificity, stability at varying pH and temperature ranges, inhibitor resistance, and recyclability over multiple catalytic cycles (Bilal, Asgher, et al., 2019; Bilal, Zhao, et al., 2019). Additionally, the products produced have a higher purity because the biocatalyst may be easily removed from the reaction medium when enzymes are attached to solid supports (Homaei et al., 2013; Singh et al., 2013; Zdarta et al., 2018; Zhang et al., 2015). Choosing the suitable support materials and the immobilization techniques used is an important challenge to obtaining the desired immobilization results. This is important because it significantly affects the catalytic system's and the enzyme's characteristics. Several parameters define suitable immobilization support, including pore width, specific surface area, mechanical resistance, internal geometry, and support activation degree (Bilal, Asgher, et al., 2019). This contribution offers a thorough overview and discussion of the most recent advancements in the application of immobilized enzymes in the food industry, taking into account the body of knowledge currently available on enzyme immobilization, which includes a variety of strategies, supports, and applications (Bilal, Asgher, et al., 2019; Datta et al., 2013; Jesionowski et al., 2014; Mohamad et al., 2015; Zdarta et al., 2018). They are used in the fruit juice, dairy, baking, and brewing industries and provide fresh perspectives, especially when considering the food industry.

This review aims to provide a comprehensive and up-to-date overview of lipase research by combining recent studies and developments in classification, sources, immobilization techniques, and various industrial applications.

## II. CLASSIFICATION OF LIPASES

This section discusses the categorization of lipases based on their specificity, while the subsequent part is focused on exploring the sources of lipases. Basically, lipases can be categorized according to specificity and origin, as depicted in **Fig. 1**. **Table 1** summarizes the functional characteristics of distinct lipase classes, highlighting examples from previous year's research developments.

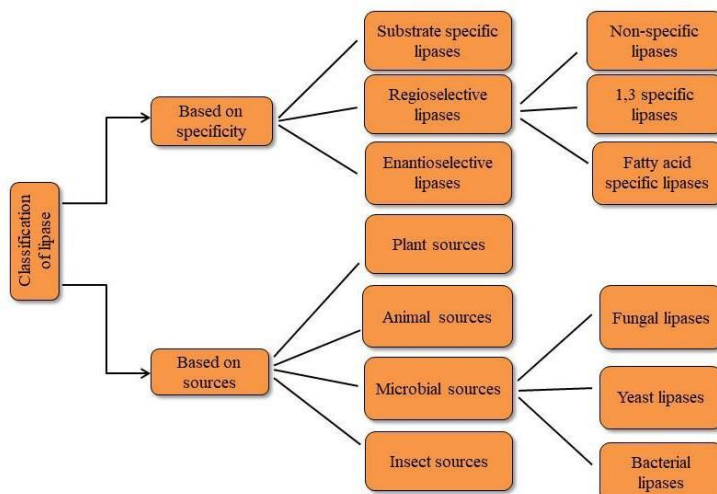


Fig.1: Classification of lipases

## 2.1. Based on specificity

This section provides an overview of the classification of lipases according to their specificity. The subsequent section focuses on the sources of lipases. Their specificity significantly influences the characterization of the industrial applications of lipases; thus, these uses can be classified into three broad categories: (i) substrate-specific, (ii) regioselective, and (iii) enantioselective.

### 2.1.1. Substrate specific lipases

Lipases exhibiting substrate specificity play an important role in reactions that precisely target particular substrates within a mixture of raw materials. This precision is instrumental in achieving desired outcomes, as exemplified by the effective utilization of lipases in processes such as biodiesel production (Ribeiro et al., 2011) and the production of high-purity diacylglycerols (Borza et al., 2015). Typically, these specialized lipases demonstrate proficiency with substrates like fatty acids and alcohols (Kapoor & Gupta, 2012). Recent research underscores the paramount importance of considering both substrate specificity and enzyme stability, highlighting their fundamental roles in optimizing the application of lipases across various industrially significant processes (Brígida et al., 2014).

### 2.1.2. Regioselective lipases

Regioselective lipases are essential for maximizing desirable side effects and guiding reactions in the right direction. This characteristic is very important, especially in the chemical and pharmaceutical industries, where it is crucial to produce isomeric molecules that perform best in specific configurations. The acylation of quercetin with ferulic acid, using *Rhizopus oryzae* lipase to synthesize

flavonoid derivatives (Kumar et al., 2016), the deprotection of per-O-acetylated thymidine, producing 3'-OH-5'-OAc-thymidine using lipase from *Candida rugosa* (Rivero & Palomo, 2016), and the synthesis of acacetin and resveratrol 3,5-di-O-beta-glucopyranoside using *Candida antarctica* lipase B (Novozym 435) and *Burkholderia cepacia* lipase (Amano PS-IM) are examples of recent discoveries in the field of regioselective lipase (Hanamura et al., 2016). Lipases are classified into three classes based on positional specificity or regiospecificity.

#### 2.1.2.1. Non-specific lipases

These particular types of lipases are exceptionally versatile, acting on a wide range of substrates. *Mucor meihei* lipases are a prime example of this, as they are versatile enough to catalyze a wide range of reactions, from the manufacture of biodiesel to uses in the cosmetics sector. These lipases generally catalyze the hydrolysis of triacylglycerols into glycerol and free fatty acids, using mono- and diacylglycerols as intermediates. The method's ability to function under ambient circumstances with little thermo-degradation makes it very beneficial (Kapoor & Gupta, 2012; Ribeiro et al., 2011). High-purity structured lipids have been produced through the acidolysis of canola oil with caprylic acid using the non-specific *Candida Antarctica* lipase, according to a study by Savaghebi et al. (2012).

#### 2.1.2.2. 1,3 specific lipases

These lipases help hydrolyze triacylglycerols at the C<sub>1</sub> and C<sub>3</sub> locations, which produces fatty acids 1, 3 or 2, 3 diacylglycerols and 2-monoacylglycerols. The latter two molecules become unstable, which causes acyl migration and the synthesis of 1- or 3-monoacylglycerols and 1,3-



diacylglycerol (Barros et al., 2010). It is noted that the synthesis of diacylglycerols happens considerably more quickly than the conversion of triacylglycerols into monoacylglycerols (Ribeiro et al., 2011). A specific conformation is produced by the 1,3 specificity, as demonstrated in the example of *Carica papaya* latex lipase (Rivera et al., 2017). Recently, long-chain fatty acids have been synthesized by acidolyzing walnut oil with caprylic acid using 1,3-specific immobilized lipases from *Rhizomucor miehei* (Lipozyme) and *Rhizopus delemar* (PP-RhDL) (Todorova et al., 2015). Moreover, biodiesel production has used 1,3-specific immobilized *Rhizopus oryzae* lipase produced in *Pichia pastoris* (Clementz et al., 2016).

### 2.1.2.3. Fatty acid-specific lipases

These lipases work well to degrade esters that contain double bonds on C-9 of long-chain fatty acids (Ribeiro et al., 2011). A detailed study into lipases with fatty acid selectivity showed several enzymes that target various substrates with various carbon chain lengths, saturation levels, and unique side chains. Some lipases showed

strong selectivity for medium- or long-chain and branched esters. In contrast, lipases sourced from S9 *Geotrichum candidum*, S11 *Candida lipolytica*, YM *Bacillus coughing*, MJ1 *Aspergillus niger*, MJ2 *Aspergillus oryzae*, and S3 *Penicillium citrinum* showed unique specificity for short-chain esters (Song et al., 2008). Selected microbial strains that could produce lipases suited for medium- and long-chain saturated fatty acids were found through screening in another study (Miettinen et al., 2013).

### 2.1.3. Enantioselective lipases

In a racemate, enantioselective lipases hydrolyze one isomer more than the other, especially when starting with prochiral precursors. These lipases are very good at separating enantiomers from a racemic mixture (Barros et al., 2010). Enantiospecific lipases catalyze various processes, such as the transesterification of secondary alcohols into drugs (Borza et al., 2015), the hydrolysis of menthol benzoate for the production of cosmetic and food items (Dhake et al., 2013), and the hydrolysis of glycidic acid methyl ester for the synthesis of medical and health care products (Su et al., 2014).

Table 1: Classification of lipases based on specificities.

Classification basis	Reaction details			Application	References
	Substrate-enzyme system	Type	Mode		
Substrate specific	Camellia oil + <i>Penicillium camembertii</i> lipase	Esterification	Batch	Production of high purity di-acylglycerols	(P. Zheng et al., 2014)
Regio-selective	Novozym 435, nonspecific <i>Candida antarctica</i> lipase + refined, bleached and deodorized (RBD) canola oil	Acidolysis (nonspecific)	Batch-shaker flask systems	Production of structured lipids (SLs)	(Savaghebi et al., 2012)
	1,3-specific immobilized lipases from <i>Rhizomucor miehei</i> +Walnut oil + caprylic acid	Acidolysis (1,3 specific)	Batch-immobilized enzyme system	Production of MLM-type structured lipids	(Todorova et al., 2015)
	1,3 specific immobilized lipase from <i>Rhizopus oryzae</i>	Transesterification (1,3 specific)	Fed-batch shake flask system	Biodiesel	(Clementz et al., 2016)

+ olive oil + methanol + hexane					
	MJ2 <i>Aspergillus oryzae</i> lipase is highly specific to methyl butyrate	Hydrolysis (fatty acid specific)	Batch-silica gel GF <sub>254</sub> plates	Transportation fuel, wastewater denitrification, fuel cell hydrogen carrier production, biodiesel transesterification, electricity generation	(Song et al., 2008)
Enantio-specific	<i>C. antarctica</i> lipase A entrapped in sol-gel + Secondary alcohols	Transesterification	Batch-shaker flask systems	Large-scale processes in pharmaceutical industry	(Borza et al., 2015)

**2.2. Based on sources**

Lipases are found extensively in plants, animals, insects, and microbial organisms (Maldonado et al., 2014; Patil et al., 2011; Ray, 2012). Microbes are particularly important among the various sources of lipase due to their substantial industrial potential, easy culture handling, wide availability, and potential for scalable production (Patil et al., 2011).

**2.2.1. Plant sources**

Plant materials that include lipases include latex, leaves, bran, seeds, beans, and fruits. Plant lipases are particularly abundant in seed sources such as castor bean, African bean, elm, sunflower, physic nut, lupin, linseed, coconut, almond, black cumin, wheat grain, rice, corn, oat, barley, sesame, sorghum, etc. Since seeds are the primary energy source for plant growth and contain a high concentration of triacylglycerols, they have higher lipase activity than other plant components. Due to increased lipase activity, triacylglycerols in plant seeds are converted into soluble sugars during germination (Patil et al., 2011). As detailed in the provided **Table 2**, these lipases find diverse applications, including the hydrolysis of vegetable

oils (Salaberría et al., 2017), processing of seeds and oils (Lampi et al., 2015; Mohd Zin et al., 2017), production of structured lipids (da Silva Serres et al., 2017), beverage production (Moreau et al., 2016), and synthesis of pharmaceutical and therapeutically significant compounds (Hamden et al., 2017). Lipases derived from palm fruit mesocarp have proven effective in manufacturing pharmaceuticals, detergents, and cosmetic products (Suwanno et al., 2017). Recent studies highlight the efficiency of lipases from the drumstick tree in treating obesity (Kadouf et al., 2015).

Plant lipases are attractive because of their direct use as biocatalysts, accessible acceptability, particular uses, and inexpensive cost. However, their investigation has been restricted due to poor abundance, instability, and activity loss during conventional purifying procedures (Seth et al., 2014). Addressing these challenges, a novel technique based on immuno-purification has been developed for rapeseed lipase preparation (Belguith et al., 2013). Research is ongoing to get lipases from inedible plant sources so that different fatty acids can be hydrolyzed to produce biodiesel (Banković-Ilić et al., 2012).

Table 2: Lipases from plant sources.

Lipase source	Applications	References
Castor bean	Hydrolysis of vegetable oils.	(Salaberría et al., 2017)
Barley	Hydrolysis of lower molecular weight water-soluble substrates and long-chain insoluble triglycerides.	(Schneider et al., 2016)
Rice/rice bran	Preferential hydrolysis of <i>sn</i> -2 position of phosphatidylcholine.	(Qi et al., 2015)
Almond	Hydrolysis of oil.	(Huang et al., 2017)

Carica papaya latex	In reactions involving fats and oils demanding <i>sn</i> -3 selectivity, interesterification, transesterification and acidolysis using homogenous triacylglycerol and various other acyl donors industrially and also a crucial component in cure for dengue.	(Rivera et al., 2017)
Elm	Synthesis of emulsifiers or oiling agents for foods, spin finishes and textiles, antifoaming and antistatic agents for plastics and lubricants, water treatment, metal working fluids, personal care products and dispersing agents from tricaprin.	(Barros et al., 2010)
Fenugreek	Synthesis of pharmaceutical and therapeutically significant products.	(Hamden et al., 2017)
African bean	Production of fermented condiments such as Iru, Soumbala, daddawa, sonsu, afitin, ugba	(Seth et al., 2014)
Sunflower seed	Production of structured lipids by action on other oils.	(da Silva Serres et al., 2017)
Physic nut	Production of biodiesel within a hybrid system of chemical and enzymatic process.	(Sousa et al., 2015)
Sorghum	Production of alcoholic beverages.	(Moreau et al., 2016)
Palm fruit mesocarp	Pharmaceuticals, industrial detergent, food and cosmetics.	(Suwanno et al., 2017)
Coconut	Processing coconut oil.	(Mohd Zin et al., 2017)
Oat	Processing oats.	(Lampi et al., 2015)
Vermonia sp	Specific towards trivernolei.	(Barros et al., 2010)
Lupin	Specific towards lupin oil to release fatty acids from them.	(Stephany et al., 2016)
Sesame	Non-specific lipases.	(Oliveira et al., 2017)
Linseed	Treatment of triacylglycerols in acidic environment.	(Qiu et al., 2017)
<i>Moringa olifera</i> (Drum stick tree)	Treatment of obesity.	(Kadouf et al., 2015)
Black cumin	For enrichment of $\Gamma$ - Linolenic acid in the unhydrolyzed acylglycerol fractions of $\Gamma$ -Linolenic acid containing oils.	(Siow et al., 2016)
Wheat grain	Determination of the storage quality of wheat and wheat bran.	(Ahmad et al., 2015)
Corn	To act on oleyl ester than stearyl ester to release fatty acids.	(Eze et al., 2007)

### 2.2.2. Animal and insect sources

Lipases are produced by animal cells and are necessary for digesting fats and lipids (Patil et al., 2011). However, because of the difficulties in managing cultures and separating products, these animal lipases are used

more frequently in clinical diagnosis than in commercial production. Animal lipases have not been explored as much as plant and microbial lipases. **Table 3** below lists several animal tissue-derived lipases used in different research projects. Among the variety of animal lipases, pancreatic lipase has been widely used as a tool for lipid

chemistry and biochemistry research, exhibiting efficient catalysis in the hydrolysis of primary alcohol esters (Pahoja & Sethar, 2002).

Lipases derived from the porcine pancreas play a significant role in preparing Monoacylates of 2-Substituted (Z)-But-2-ene-1,4-diols (Kawashima et al., 2016), asymmetric aldol reactions (J. Zheng et al., 2014), and the synthesis of bis (indolyl) alkanes (Xiang et al., 2013). Furthermore, starfish lipases are a viable substitute for porcine pancreatic lipases and have significant uses in the food processing sector, as shown in **Table 3**. It is

*Table 3: Lipases from animal and insect sources.*

Lipase sources	References
Human pancreas	(Borrelli & Trono, 2015)
Human gastric cells	(Patil et al., 2011)
Porcine pancreas	(Borrelli & Trono, 2015)
Guinea pig pancreas	(Borrelli & Trono, 2015)
<i>Cyprinion macrostomus</i>	(Patil et al., 2011)
Chicken adipose cells	(Patil et al., 2011)
Scorpion	(Patil et al., 2011)
Rainbow trout	(Kittilson et al., 2011)
<i>Dasyatis pastinaca</i>	(Borrelli & Trono, 2015)
Seabass liver	(Sae-Leaw & Benjakul, 2018)

### 2.2.3. Microbial sources

Microbial lipases, derived from bacteria, yeast, and fungi, are desirable for industrial use because of their ease of production and adaptability (Ray, 2012). The following lists the several biotechnological uses for which microbial lipases are helpful because of their remarkable selectivity. These lipases are predominantly extracellular and mainly produced from bacterial and fungal species. Physical and chemical parameters like temperature, pH, and dissolved oxygen significantly impact their creation, as does the makeup of the medium (Thakur, 2012). Further insights into microbial lipases can be gained from recent review papers covering topics like the general overview of microbial lipases (P Kanmani et al., 2015), microbial alkaline lipases (Niyonzima & More, 2015), and the purification of microbial lipases (Show et al., 2015). Recent findings indicate that microbial lipases can be obtained through the fermentation of agricultural waste (Zubiolo et al., 2015) and dairy waste (Marques et al., 2014), contributing to environmental protection. This opens up possibilities for potential future bio-catalytic applications.

important that insect tissues also yield lipases, primarily contributing to the development of the insect's larval stage (Sakate & Salunkhe, 2013) or residing in their gut (Delkash-Roudsari et al., 2014; Rong et al., 2014). Research shows that lipases active against diacylglycerols are found in various insect flight muscles and bodily tissues, except for the alimentary canal (Pahoja & Sethar, 2002). Research on gut lipase activity to create bio-control agents is becoming increasingly popular (Khan et al., 2012; Sandhu et al., 2012).

#### 2.2.3.1. Fungal lipases

Among the several types of microbial lipases, fungal lipases are widely used due to their unique characteristics, which include substrate specificity, stability at both pH and temperature, affordability during extraction, and effective activity in organic solvents (Patil et al., 2011). Because of the carbon and nitrogen content of the medium, these lipases can be found either intracellularly or extracellularly (Sharma et al., 2010). Fungal lipases are interesting for their exceptional adaptability, as they may catalyze a variety of processes such as alcoholysis, acidolysis, saponification, ethanolsis, hydrolysis, esterification, transesterification, deacetylation, and hydrolytic kinetic resolution.

Solid-state fermentation technology holds great potential for producing fungal lipases, as evidenced by the latest developments in this field (Ramos-Sánchez et al., 2015). A further review focuses on the molecular and functional variety of fungal lipases, examining transdisciplinary strategies that lead to enhanced substrate selectivity and thermostability (Gupta et al., 2015). A special review also covers the use of fungal lipases to produce biodiesel, outlining developments and important

variables that impact lipase stability and activity, like the type of biocatalyst used, the water content, solvent usage, and raw material selection (Aguieiras et al., 2015).

Recent research on fungal lipases includes isolating several fungal strains from Divle Cave cheese, which identified *Mucor racemosus* as a strong lipase producer with possible uses in the cheese industry (Ozturkoglu-Budak et al., 2016). Several fungal strains were screened to assess their lipase-producing capabilities using various substrates, such as sugar cane bagasse, soybean bran, and wheat bran (Fleuri et al., 2014). *Aspergillus niger*, *Nectria haematococca*, and *Trichoderma reesei* are a few examples of fungal sources whose lipases were cloned, expressed, and characterized, and their catalytic activity was compared by Vaquero et al. (2015). A study by Khasanov et al. (2015) examined the catalytic activity of fungal lipases isolated from *Rhizopus microsporus*, *Penicillium sp.*, and *Oospora lactis*. In addition, the immobilization of fungal lipases from *Rhizomucor miehei* and *Thermomyces lanuginosus* on nanozeolite supports was studied by de Vasconcellos et al. (2015).

### 2.2.3.2. Yeast lipases

Because of their unique properties and ease of cultivation, yeast lipases are an essential source of enzymes in great demand across various industries, including biodiesel, chemicals, and pharmaceuticals. The primary yeast producers of lipases are *Candida antarctica*, *Candida rugosa*, *Candida utilis*, and *Saccharomyces* species. These enzymes catalyze a wide range of processes and find applications in various industrial sectors. A literature review indicates that lipases derived from *Candida rugosa* are important examples of biocatalysts that are effective in various reactions. These reactions include the hydrolysis of conjugated linoleic acid methyl ester by adding an organic solvent (Kobayashi et al., 2012), transesterification of palm oil with methanol and ethanol (Moreno-Pirajan & Giraldo, 2011), and enantioselective hydrolysis of menthol benzoate (Dhake et al., 2013), etc. Another significant yeast source is *Candida antarctica*, effectively employed in the synthesis of valuable fatty acids (L. D. Santos et al., 2015), biodiesel production through the transesterification of *Simarouba glauca* oil (Garlapati et al., 2013), and the production of pharmaceutical products through acylation and alcoholysis (Baldessari & Iglesias, 2012). Additionally, *Candida antarctica* lipases are utilized in the synthesis of cosmetic and detergent products by acidolysis of butter oil with conjugated linoleic acid (Garcia et al., 2001) and acidolysis of acyl glycerols (Senanayake & Shahidi, 2002).

Yeast lipases, enzymes from different yeast species involved in diverse processes, are essential to biodiesel synthesis. *Thermomyces lanuginosus* lipases, for example, are used in the hydro esterification of soybean oil (Cavalcanti-Oliveira et al., 2011), *Rhodotorula mucilaginosa* in the esterification of palm oil (Nuylert & Hongpattarakere, 2013), *Thermomyces lanuginosus* in the hydrolysis of soybean oil (Cavalcanti-Oliveira et al., 2011), and *Thermomyces lanuginosus* in the transesterification of rapeseed oil (Price et al., 2014). An overview of the production and use of *Candida lipolytica*/*Yarrowia lipolytica* lipases in the bio-surfactant manufacturing process is given in a recent review by Brígida et al. (2014).

### 2.2.3.3. Bacterial lipases

Bacterial lipases can be found in several parts of cells, such as extracellular, intracellular, or membrane-bound. Some extracellular bacterial lipases are lipoproteins, while the majorities are glycoproteins. Bacterial lipases are remarkably numerous and frequently described as thermo-stable and substrate non-specific (Dhake et al., 2013; Vaquero et al., 2016). Recent studies highlight the thermal stability and industrial potential of bacterial lipases, such as those from *Thermophilic Bacterium*, *Bacillus licheniformis* lipases (Rashid et al., 2013), *Bacillus pumilus* lipase isolated from tannery waters (Laachari, El Bergadi, et al., 2015), and extracellular lipase of *Bacillus licheniformis* (Rashid et al., 2013). For instance, the lipase *Serratia marcescens* N3 is used to hydrolyze several types of edible oils, and it is most active when applied to Gingily oil (Zaki & Saeed, 2012). *Serratia* effectively carries out the kinetic resolution of racemic alcohols in organic solvents *marcescens* H30 lipase (Su et al., 2014). *Staphylococcal* lipases isolated from facial sebaceous skin are used as biocatalysts in the food, cosmetic, pharmaceutical, and detergent sectors (Xie et al., 2012).

Several bacterial lipases exhibit promising applications in biodiesel production, such as *Geobacillus thermodenitrificans* AV-5 (Christopher et al., 2015), cross-linked *Staphylococcus haemolyticus* lipase immobilized on solid polymeric carriers (Kim et al., 2013), *Pseudomonas fluorescens* lipase (Salis et al., 2009), *Staphylococcus haemolyticus* L62 lipase expressed in *Escherichia coli* cells (Kim et al., 2013), and *Staphylococcus haemolyticus* L62 lipase (Jo et al., 2014). Furthermore, the use of elite-immobilized crude lipase produced from *Staphylococcus pasteurii* for the pretreatment of coconut mill effluent shows the effectiveness of bacterial lipases in waste management and treatment (Palanisamy Kanmani et al., 2015) and by the lipase from *Pseudomonas aeruginosa*

AAU2 in treating lipid-rich industrial effluents (Bose & Keharia, 2013).

### III. IMMOBILIZATION TECHNIQUES

Enzymes function as biological catalysts in enzymatic reactions, enhancing reaction rates without undergoing

depletion. This property allows for the repeated utilization of enzymes as long as they remain active. Various methods for immobilizing enzymes on solid surfaces have been developed, and these methods are classified as follows and shown in Fig. 2.

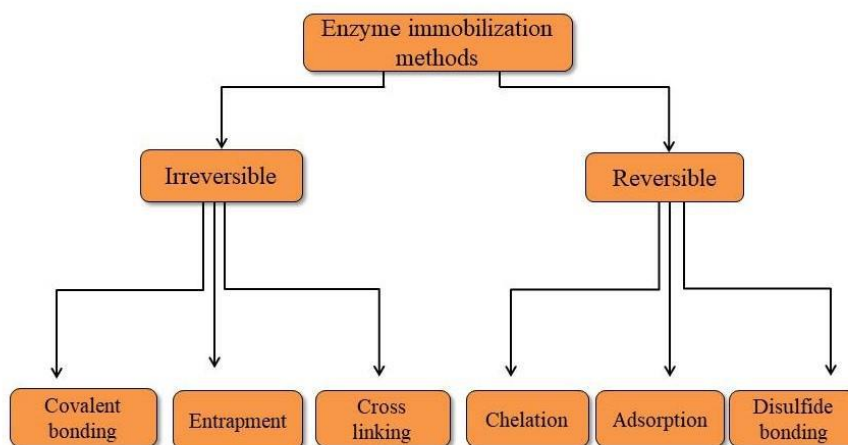


Fig.2: Schemes for major enzyme immobilization methods

#### 3.1. Irreversible mechanism

In irreversible immobilization, the only way to separate a biocatalyst from a support is to undermine its biological activity. The most popular approaches for permanently immobilizing enzymes include coupling and cross-linking procedures and covalent trapping like microencapsulation.

##### 3.1.1. Covalent bonding

Making covalent connections between proteins and a support matrix is often used for permanently immobilizing enzymes. Because of the stronger interactions created between the matrix and the enzyme, this method has the benefit of keeping the enzyme from escaping into the solution while it is being used. In some cases, keeping amino acid residues essential for catalytic action from being involved in the covalent attachment to the support can be challenging, which makes achieving high binding activity difficult. During the coupling reaction, substrate analogues can be added to the reaction media as a simple way to improve this activity (Brena et al., 2013). Covalent techniques are usually used for immobilization when the enzyme does not need to remain in the finished product. Researchers have developed various reactions, considering the functional groups present in the matrix (Jasti et al., 2014). In a broad classification, coupling methods are divided into two main groups: (1)

activating the matrix by adding a reactive function to a polymer and (2) modifying the polymer backbone to generate an activated group. Activation approaches are typically recommended to provide electrophilic groups on a set of supports that react with potent nucleophiles on proteins during the coupling step. The covalent binding of covalents to matrices is governed by parameters comparable to those used in protein chemical modification. Various commercially available supports are available for immobilization; the best one to employ will rely on the properties of the catalyst and its intended usage. To find the best method depending on specific circumstances, it is often essential to experiment with a number of different approaches (J. C. S. d. Santos et al., 2015). When covalent processes are used, ether, amide, carbamate, and thioether bonding are frequently used by enzymes to attach to the support. As a result, a strong link known for its high stability is established between the matrix and the enzyme. Because the linkage is covalent, throwing out the matrix and the enzyme becomes important when the enzymatic activity decreases.

A leak-proof link between the enzyme and the matrix can be formed using the covalent immobilization technique, but there are also disadvantages, including high cost, limited immobilization activity yield, and irreversibility. However, modifications to the immobilization method can alleviate these constraints to

differing degrees. A number of variables, including the carrier material's size, shape, and composition, as well as the particulars of the coupling reactions, affect the activity of covalently immobilized enzymes (Bilal, Asgher, et al., 2019). For covalent bond-based immobilization, hydrophobic or hydrophilic supports can be used; silica/chitosan-based supports have also been shown to be effective carriers for covalent immobilization in recent research (Cazaban et al., 2018; Manzo et al., 2018; Singh et al., 2017; Van Den Biggelaar et al., 2017). Due to its high surface area, low diffusional limitations, good mechanical properties, chemical resistance, and abundance of hydroxyl groups, silica is well-suited for surface functionalization with agents such as glutaraldehyde and 3-aminopropyltriethoxysilane (APTES) and enzyme attachment. Because of its advantageous structural characteristics, chitosan, a common natural biopolymer, is a hydrophilic, biodegradable, and biocompatible polysaccharide frequently employed for enzyme immobilization. Many covalent attachments of the amino groups on the enzyme's surface onto cross-linked agarose beads are an effective covalent technique for immobilizing enzymes. This procedure increases the enzyme structure's stiffness, giving it more stability against conformational changes by denaturing chemicals (Romero-Fernández & Paradisi, 2020). Covalent immobilization can also be site-directed to obtain immobilized enzymes with enhanced stability and reactivity. Using the Huisgen 1,3-dipolar cycloaddition "click" reaction and non-canonical amino acid incorporation, Wu et al. (2015) developed the PRECISE (protein residue-explicit covalent immobilization for stability enhancement) system, which allows for directed enzyme immobilization at specifically selected residues throughout an enzyme. This system facilitates the evaluation of the impact on activity and stability under severe conditions by enabling immobilization at both close and remote locations from the active site.

### 3.1.2. Entrapment and cross-linking

The entrapment approach works by encasing enzymes in a network of polymers, which allows products and substrates to pass through while keeping the enzyme in place. In contrast, this strategy does not limit the enzyme to a matrix or membrane-like coupling system. Numerous methods for entangling enzymes, including fiber entrapment, gel and microencapsulation, have been suggested by Livage and Coradin (2018). These approaches change the encapsulating material for ideal pH, polarity, or amphiphilicity to improve enzyme stability, minimize leaching and denaturation, and optimize the microenvironment (Nguyen & Kim, 2017). However, mass transfer limits through gels or membranes limit the

practical applicability of these techniques. It's important to remember that more recent approaches, including cross-linked enzyme aggregates (CLEAs) and crystals (CLECs), have been proposed to immobilize enzymes (Galliani et al., 2018; Tran & Balkus Jr, 2011) and differ from conventional immobilization approaches. Though these techniques developed at the turn of the century, they are still the go-to option for enzymatic applications in biorefineries and the food sector. With their highly active immobilized enzymes and adjustable particle sizes, high catalytic and volumetric productivities, ease of recycling, and operational stability, CLECs are perfect for industrial biotransformations. However, a major drawback of this technique is the thorough protein purification needed to generate CLECs. With the addition of salts or nonionic polymers, enzymes from an aqueous solution precipitate to form physical aggregates of protein molecules, which is how the more recently produced CLEAs are an upgraded version of CLECs (Homaei et al., 2013; Nguyen & Kim, 2017). Because of their increased catalytic activity, improved operational and storage stabilities, ease of use, superior reusability, and multi-point attachment through intermolecular cross-linking between enzyme molecules, cleavage-free amnesias CLEAs have become a promising carrier-free immobilization system. Enzyme preparation from lipases, horseradish peroxidase, penicillin acylases, and laccases is the subject of many ongoing investigations to produce CLEAs of high yield (Šulek et al., 2011).

The development of multipurpose cross-linked enzyme aggregates (multi-CLEAs) and combined cross-linked enzyme aggregates (combi-CLEAs), which cross-link multiple enzymes together, is a development in the immobilization process. As a result, CLEAs have an increased ability to catalyze a range of biotransformation reactions, either one at a time or in succession as catalytic cascade processes (Bilal, Zhao, et al., 2019). Recent examples have been reported for these cross-linked immobilization approaches. Periyasamy et al. (2016) successfully combined b-1, 3-glucanase, cellulase, and xylanase for one-pot cascade saccharification of sugarcane bagasse (SCB). After six consecutive applications, the combi-CLEAs produced improved temperature and storage qualities, maintaining 90% of their activity (Periyasamy et al., 2016). Another example is the production of three distinct, independent catalytic reactions using multi-CLEAs of pectinase, xylanase, and cellulase. The produced multi-CLEAs showed excellent recyclability and thermostability (Dalal et al., 2007). Combining CLEAs with magnetic nanoparticles (M-CLEAs) has also increased their stability and reusability in the food industry. The benefit of this integration is that it is simple to separate from the reaction mixture, making it

easier to use again and increasing the possibility of developing continuous biocatalytic processes (Martins et al., 2018; Nadar & Rathod, 2016). In a recent advancement, magnetic combi-CLEAs based on glucose dehydrogenase and ketoreductase have been developed. Compared to the original CLEAs, they demonstrated better catalytic activity and stability in both aqueous and biphasic media (Su et al., 2018).

Furthermore, using CLEAs combined with the bio-imprinting process has been extensively investigated over the past years to improve the stability and catalytic efficacy of various enzymes. Imprinted CLEAs are a revolutionary combinatorial cross-linked imprinting technique (iCLEAs). Bio-imprinting technology is valuable for adjusting enzymes' stability, enantioselectivity, reusability, and catalytic characteristics. (Bilal, Asgher, et al., 2019; Cui & Jia, 2015; De Winter et al., 2012).

### 3.2. Reversible mechanism

Regarding the binding between the support and the enzyme, reversibly immobilized enzymes can separate from the support in mild circumstances. In response to this issue, reversible techniques have attracted much interest in enzyme immobilization, primarily because of their sound financial basis. The principal factor contributing to these enzymes' cost-effectiveness is their declining activity, which triggers regeneration and reloading of the support with new enzymes. The support cost primarily determines the catalyst's total immobilization cost. Reversible enzyme immobilization is very important for bioanalytical systems and the immobilization of labile enzymes (Bilal, Zhao, et al., 2019).

#### 3.2.1. Adsorption (Non-covalent interactions)

**Nonspecific adsorption:** Nonspecific adsorption is a relatively simple technique for immobilization that operates predominantly through physical or ionic means of binding (Mohamad et al., 2015). Enzymes bind to the matrix through salt bonds in ionic bonding. On the other hand, in physical adsorption, the enzymes use hydrophobic interactions, hydrogen bonds, and van der Waals forces to bind to the matrix. Changes in ionic strength, pH, solvent polarity, and temperature, among other factors that regulate interaction strength, can reverse the process caused by the forces involved in non-covalent immobilization. The procedure of adsorption immobilization is mild and straightforward, usually maintaining the enzyme's catalytic activity. Despite their economic appeal, these methods have certain disadvantages, such as the possibility of enzyme leakage from the matrix in the event of weak connections.

**Ionic binding:** Utilizing protein-ligand interactions via chromatography is commonly used for reversibly immobilizing enzymes. The use of ion exchangers for enzyme reversible immobilization is an example of an early application of this method (Vaz & Filho, 2019). This method is reversible and convenient, but it can be challenging to identify the exact circumstances that ensure strong bonding and high enzyme activity. Lately, immobilized polymeric ionic ligands have been used to manipulate the protein-matrix interaction, allowing for the optimization of derivative characteristics. Despite the advantages, problems could occur, especially if highly charged supports are used, especially if the goods or substrates are charged. Diffusion and partition, for example, might upset kinetics in certain situations and change the enzyme's ideal pH and pH stability range (Ward et al., 2016). However, recent research over the last few years has shown that pH values can be adjusted to achieve ideal circumstances for a particular enzyme. (Benítez-Mateos et al., 2017; Furuya et al., 2017; Wang et al., 2017).

**Hydrophobic adsorption:** Hydrophobic interactions driven by entropy instead of chemical bond formation can also be achieved by the reversible immobilization of enzymes. This technique has been a chromatographic concept for over thirty years, relying on conventional experimental parameters; including temperature, pH, and salt content (Mohamad et al., 2015). Both the hydrophobicity of the protein and the adsorbent influence the intensity of the interaction. The size of hydrophobic ligand molecules and the support substitution level can be changed to modify the adsorbent's hydrophobicity. It has been possible to immobilize reversible  $\beta$ -amylase and amyloglucosidase to hexylagarose carriers (Das & Kayastha, 2019). The use of different supports, such as silica, magnetic nanoparticles, and synthetic beads made of polymethacrylate matrices, as support materials for the hydrophobic adsorption method has been reported in research in recent years (Abreu Silveira et al., 2017; Gao et al., 2019; Hüttner et al., 2017; Koutinas et al., 2018; Srivastava et al., 2012; Vescovi et al., 2017).

**Affinity binding:** Determining the immobilization of enzymes has been attributed to the fundamental principle of utilizing the attraction between complementary biomolecules. The approach shows a significant benefit through a highly selective interaction. The requirement for covalent attachment of a costly affinity ligand to the matrix, such as an antibody or lectin, is a drawback (Brena et al., 2013). Strong connections between the protein structure and a surface functionalized with a complementary affinity ligand can be established using affinity tags, which can be intrinsic or injected at a



specified place away from the active site in the original enzyme structure. In contrast to random immobilization, which can result in the immobilized enzyme in numerous orientations, directed immobilization results from greater specificity in enzyme adsorption to support materials (Bolivar & Nidetzky, 2013).

One of the two methods for achieving enzyme immobilization based on affinity binding between enzymes and support materials is the ionic exchange or covalent bonding. A recent advancement in ionic immobilization is affinity binding, in which enzymes are fixed to substrates containing metal ions such as  $\text{Ni}^{2+}$ ,  $\text{Cu}^{2+}$ ,  $\text{Co}^{2+}$ ,  $\text{Fe}^{3+}$ , and  $\text{Zn}^{2+}$  by use of a fused peptide tag containing a polyhistidine chain (His-tag) (Böhmer et al., 2018; Liu et al., 2017; Vahidi et al., 2018). (Böhmer et al., 2018) showed how ionic affinity binding allowed co-immobilizing chimeric amine dehydrogenase (AmDH) and alcohol dehydrogenase (ADH) on regulated porosity glass  $\text{Fe}^{3+}$  ion-affinity beads. Over five cycles, the immobilized dual-enzyme system demonstrated recyclability, with total turnover numbers for ADH and AmDH surpassing 4000 and 1000, respectively. Immobilization of enzymes with a fused discrete protein domain is a further form. Enzymes, for instance, fused to the modified  $Z_{\text{basic2}}$  binding domain are bonded to immobilization matrices with anionic surface groups by ionic interactions. Compared with smaller tags like the His-tag, this method provides a substantial benefit for oriented immobilization. Oriented immobilization is highly preferred because it uses the  $Z_{\text{basic2}}$  module more efficiently to achieve spatial separation between the immobilization matrix and the enzyme catalytic activity. This method reduces the possibility that surface binding will negatively affect the enzyme's activity (Bolivar et al., 2017; Romero-Fernández & Paradisi, 2020). The formation of covalent bonds between the enzyme and the immobilization support is another method for achieving affinity-based enzyme immobilization. This approach integrates a tiny peptide tag, a distinct protein domain, or a genetically fused protein into the target enzyme. It is comparable to affinity binding via ionic exchange. Attaching horse liver alcohol dehydrogenase, fused to a polyhistidine tag, onto metal-activated polymethacrylate support using epoxy groups is a recent development in covalent affinity binding (Contente & Paradisi, 2018). Using a second protein as a spacer to block the direct covalent connection between the enzyme and the immobilization matrix, this novel method of covalent immobilization via affinity binding increases the catalytic activity of the target enzyme. His-tag and different target enzymes are fused to form T4L lysozyme, the second protein rich in lysine amino acid, increasing immobilized enzymes' recovered activity

(Planchestainer et al., 2017). A recent development is affinity binding to immobilize enzymes on magnetic beads, which improves the functionality of immobilized enzymes in analytical tests. Faster assay kinetics are achieved by the abundance of binding sites that magnetic beads provide for biological reactions (Sassolas et al., 2020).

### 3.2.2. Chelation or metal binding

Salts of transition metals or metal hydroxides, such as zirconium or titanium, applied to the surface of an organic carrier can create bonds by coordinating with nucleophilic groups on the matrix. The term "metal link immobilization" describes this method well (Singh et al., 2013). Usually, heating or neutralization causes the hydroxide or metal salt (such as chitin, cellulose, alginic acid, and silica-based carriers) to precipitate onto the support. Some coordination places in the metal still need to be occupied for coordination with groups in enzymes because steric constraints prevent the matrix from occupying all the coordination positions in the metal. Even though the process is relatively simple, the immobilized specific activity of enzymes ranges from 30% to 80%. However, the operational stabilities that are attained are frequently irregular and difficult to replicate, potentially because of irregular adsorption sites and metal ion leakage from the support. A way to overcome these difficulties is to use stable covalent bonds to immobilize chelator ligands on solid supports, enabling metal ions to be bound via coordination. As a result, stable complexes are formed, which can be used to retain proteins. Elution of the bound proteins can be accomplished by lowering the pH of the process or by competing with soluble ligands. The support is renewed by rewashing it with a potent chelator (such as ethylenediaminetetraacetic acid or EDTA). Immobilized Metal-Ion Affinity (IMA) adsorbents, which are these supports, are widely used in protein chromatography (Kagedal, 2011).

### 3.2.3. Disulfide bonds

This study's unique approach to irreversible enzyme immobilization is its capacity to create a stable covalent link between the enzyme and matrix that can be selectively broken down under mild conditions with the help of a suitable chemical such as dithiothreitol (DTT). Furthermore, thiol groups' reactivity can be managed by varying the pH, which produces high activity yields when disulfide bonds are created with the help of an appropriate thiol-reactive adsorbent (Batista-Viera et al., 2011). Under mild circumstances, enzymes with exposed nonessential thiol (SH) groups can be immobilized onto thiol-reactive substrates, producing reactive disulfides or disulfide oxides. One important benefit of this strategy is that the

bonds created between the thiol enzyme and the activated solid phases are reversible and can be removed with an excess of a low molecular weight thiol. This characteristic becomes essential when the enzyme breaks down more quickly than the absorbent, enabling subsequent reloading (Ovsejevi et al., 2013).

In conclusion, covalent interactions usually help maintain enzymes' structural stability. Some cost-related issues arise from the irreversible attachment of enzymes to the matrix, which necessitates discarding both the matrix and the enzyme once enzymatic activity falls. However, adopting reversible techniques is quite interesting, mainly due to financial considerations; the support can be renewed and reloaded with new enzymes when enzymatic activity declines. The price of support materials frequently significantly impacts the total cost of an immobilized catalyst. In bioanalytical systems, reversible enzyme immobilization is particularly useful for labile enzymes.

#### IV. MATERIALS USED FOR THE FABRICATION OF IMMOBILIZATION SUPPORT

Enhancing the immobilization of lipase involves the development of novel support materials characterized by optimal porosity, surface area, and a balanced hydrophobic/hydrophilic profile. These materials should possess specific attributes, as illustrated in **Fig.3**, such as thermal and chemical stability, inertness, renewability, heterogeneity, a strong affinity for lipase, interactive functional groups, physical robustness, availability, and cost-effectiveness (Rodríguez-Restrepo & Orrego, 2020; Zdarta et al., 2018). Moreover, an ideal support material would facilitate the binding of active lipase sites to substrate molecules and exhibit a distinct morphology to minimize diffusional limitations (Wong et al., 2009).

It is important to note that lipase, being an essential enzyme widely applied in biotechnology and various industrial processes, has garnered significant attention from researchers. Consequently, the development of new support materials for lipase can be categorized into three fundamental groups based on their properties.



Fig.3: Properties of support materials used for lipase immobilization

#### 4.1. Natural polymers as supports

**Alginate:** Alginate, extracted from the cell walls of brown algae, constitutes the calcium, magnesium, and sodium salts of alginic acid. Its utilization in immobilization is widespread, such as in the formation of xanthan–alginate beads, alginate–polyacrylamide gels, and calcium alginate beads. These configurations result in heightened enzyme activity and reusability. The stability of enzymes is further enhanced through cross-linking alginate with divalent ions, such as  $\text{Ca}^{2+}$  and glutaraldehyde. This cross-linking process, as documented by Flores-Maltos et al. (2011), contributes to the improved durability of the immobilized enzymes.

**Chitosan and chitin:** Natural polymers such as chitin and chitosan serve as effective supports for immobilization, as documented by Kapoor and Kuhad (2007). The binding of enzymes to chitosan involves the utilization of protein or carbohydrate moieties, as outlined by Hsieh et al. (2000). Notably, the combination of chitosan with alginate has demonstrated reduced leaching effects, attributed to physical and ionic interactions between the enzyme and the support, as observed by Betigeri and Neau (2002). Additionally, a wet composite comprising chitosan and clay has proven to be a reliable method for enzyme trapping due to its hydroxyl and amino groups, facilitating easy enzyme linkage, favorable hydrophilicity and high porosity. In bead form, chitosan exhibits superior enzyme entrapment, capturing twice the amount of enzymes, as highlighted by Chang and Juang (2007), emphasizing the high affinity of the chitin-binding domain of chitinase A1 from *Bacillus circulans* to chitin, which has been strategically employed for the retention of D-hydantoinase.

**Collagen:** Given its natural polymer composition, collagen has found application in immobilizing tannase, utilizing glutaraldehyde as a cross-linking agent, as detailed by Katwa et al. (1981). The utilization of Fe<sup>+3</sup>-collagen fibers has demonstrated remarkable efficacy as a supporting matrix for catalase immobilization. Even after 26 consecutive reuses, significant catalase activity was retained, according to findings by Chen et al. (2011).

**Carrageenan:** Carrageenan, characterized as a linear sulfated polysaccharide, has consistently been employed in the immobilization of various enzymes, such as lipase, to enhance stability, as discussed by Tümtürk et al. (2007). Notably, this support exhibits pseudoplastic behavior, thinning under shear stress and promptly recovering viscosity once the stress is alleviated. (Jegannathan et al., 2010) achieved an encapsulation efficiency of 42.6% through the co-extrusion method, utilizing Carrageenan to support biodiesel production. Carrageenan has been recognized for its cost-effectiveness and durability as a support, demonstrating superior entrapment capabilities for lactic acid and agalactosidase enzymes, according to reports by Rao et al. (2008).

**Gelatin:** Gelatin, characterized as a hydrocolloid material abundant in amino acids, can adsorb up to ten times its weight in water, making it a noteworthy candidate for enzyme immobilization due to its extended shelf life. In a mixed carrier system with polyacrylamide, Emregul et al. (2006) found that cross-linking with chromium (III) acetate yielded superior results compared to chromium (III) sulfate and potassium chromium (III) sulfate. Additionally, combining calcium alginate with gelatin is an effective template for calcium phosphate deposition in enzyme immobilization. Moreover, when gelatin is paired with polyester films, it promotes a loading efficiency of 75%, a notable improvement compared to previous studies with 50% loading efficiency (Ates & Dogan, 2010; Shen et al., 2011).

**Cellulose:** Cellulose, the most abundant natural polymer, has found extensive applications in the immobilization of various enzymes, including fungi laccase, penicillin G acylase, glucoamylase,  $\alpha$ -amylase, tyrosinase, lipase, and  $\beta$ -galactosidase (Huang et al., 2011; Klein et al., 2011; Namdeo & Bajpai, 2009). Notably, the storage capacity of Diethylaminoethyl (DEAE)-modified cellulosic supports has been demonstrated to be prolonged (Al-Adhami et al., 2002). Cellulose-coated magnetite nanoparticles, employed for starch degradation, showcased the development of a novel starch-degrading system when  $\alpha$ -amylase was attached to cellulose dialdehyde-coated magnetite nanoparticles, as observed in the work by Namdeo and Bajpai (2009). Furthermore, the

immobilization process using ionic liquid-cellulose film activated by glutaraldehyde exhibited enhanced formability and flexibility, as detailed by Klein et al. (2011).

**Starch:** Comprising linear amylase and branched amylopectin units, starch is an effective enzyme immobilizer. Hybrid supports, specifically those combining calcium alginate and starch, were utilized for the surface immobilization and entrapment of bitter melon peroxidase in a study by Matto and Husain (2009). The entrapped enzyme exhibited enhanced stability in the presence of denaturants such as urea, attributed to internal carbohydrate moieties. Conversely, the surface-immobilized enzyme demonstrated superior activity. Industrial techniques widely adopted for a high product yield include radiation grafting of substances like acrylamide and dimethylaminoethyl methacrylate onto starch (anh Dung et al., 1995; Raafat et al., 2012).

**Pectin:** This heteropolysaccharide, combined with 0.2–0.7% glycerol acting as a plasticizer, mitigates the support's brittleness. It has been employed in immobilizing papain and developing novel materials for treating skin injuries, as discussed by Ceniceros et al. (2003). Pectin–chitin and pectin–calcium alginate supports have demonstrated improved thermal and denaturant resistance and enhanced entrapped enzyme catalytic properties. This enhancement is attributed to the formation of highly stable polyelectrolyte complexes between the enzyme and the pectin-coated support (Gomez et al., 2006; Satar et al., 2008).

**Sepharose:** The immobilization of amylase and glucoamylase has been achieved using CNBr-activated Sepharose-4B due to its porous nature and facile adsorption of macromolecules. Matrix modifications, such as the use of alkyl-substituted Sepharose with multipoint attachment between hydrophobic clusters of the enzyme and alkyl residues of the support, play a crucial role in preserving catalytic properties under extreme conditions such as pH extremes, high salt concentrations, and elevated temperatures (Hosseinkhani et al., 2003). An additional illustration of a modified Sepharose matrix involves Concanavalin A (Con A)–Sepharose 4B. In this case, the biospecific interaction between the glycosyl chains of the enzyme and Con A is pivotal in fabricating various biosensors (Mirouliaei et al., 2007).

#### 4.2. Synthetic polymers as supports

Insoluble supports with porous surfaces, such as ion exchange resins/polymers, serve as effective platforms for enzyme entrapment. Renewable matrices like Amberlite and DEAE cellulose, known for their substantial surface areas, have been utilized for immobilizing  $\alpha$ -amylase

(Kumari & Kayastha, 2011). In immobilizing white radish peroxidase, introducing glutaraldehyde and polyethylene glycol serves a dual purpose by acting as both an additive and a protective layer around the enzyme's active center. This protective layer prevents free radical attacks (Ashraf & Husain, 2010).

Various synthetic polymers have also found application as enzyme supports. Polyvinyl chloride, for instance, hinders thermal inactivation of cyclodextrin glucosyltransferase. Polyurethane microparticles, derived from polyvinyl alcohol and hexamethyl diisocyanate in a specific ratio, exhibit high enzyme loading and efficiency. UV-curable methacrylated/fumaric acid-modified epoxy is proposed for industrial applications, while polyaniline in emeraldine salt and emeraldine base powder forms facilitates the covalent binding of  $\alpha$ -amylase. Other examples include glutaraldehyde-activated nylon for lipase immobilization and UV-activated polyethylene glycol with high porosity for wastewater treatment (Ashly et al., 2011; Pahujani et al., 2008; Romaskevicius et al., 2010; Xiangli et al., 2010).

#### 4.3. Inorganic materials as supports

**Zeolites:** Zeolites, also known as 'molecular sieves,' are crystalline solids with well-defined structures and shape-selective properties, extensively employed in molecular adsorption. Compared to microporous de-aluminized counterparts, microporous zeolites are more effective supports for  $\alpha$ -chymotrypsin immobilization. This superiority stems from the increased presence of hydroxyl groups, fostering robust hydrogen bonds with the enzyme (Xing et al., 2000). Similarly, Na Y zeolite emerges as a preferred choice for lysozyme immobilization due to its heightened activity compared to alternative supports, as documented by Chang and Chu (2007). The heterogeneous surface of zeolites, characterized by multiple adsorption sites, is conducive to regulating interactions between enzymes and supports (Serralha et al., 1998).

**Ceramics:** The utilization of ceramic membrane for *Candida antarctica* lipase immobilization demonstrated the potential of this inert support for conducting hydrolytic and synthetic reactions while mitigating feedback inhibition, as elucidated by Magnan et al. (2004). Ceramic foams, incorporating both macro (77 nm) and micropores (45  $\mu$ m), proved effective in reducing diffusion rates and enhancing specific surface area, as evidenced by the research of Huang and Cheng (2008). Another illustration involves toyonite ceramics, whose variable pore structure can be adjusted through diverse organic coatings, as explored by Kamori et al. (2000).

**Celite:** Celite, characterized as a highly porous diatomaceous material with bio-affinity properties, has

found application in immobilizing enzymes such as lipase, polyphenol oxidases, and  $\beta$ -galactosidase. This preference arises from its cost-effectiveness, low polarity, and extensive adhesion area (Ansari & Husain, 2012; Khan et al., 2006; Liu et al., 2009). Notably, Celite exhibits resilience against elevated pH or temperature, urea, detergents, and organic solvents, as outlined by Khan et al. (2006). In the realm of x-transaminases immobilization within sol-gel matrices, Celite is an additive of choice due to its chemical inertness and interconnected pore structure, as highlighted by Koszelewski et al. (2010).

**Silica:** The effective removal of chlorolignins from eucalyptus kraft effluent has been achieved using enzymes such as lignin peroxidase and horseradish peroxidase (HRP) when immobilized on activated silica, as demonstrated by Dezott et al. (1995). Additionally, the enhancement of detergent cleaning performance is observed with  $\alpha$ -amylase immobilized on silica nanoparticles. The utilization of these enzymes is attributed to their nano-sized structures, featuring a high surface area, ordered arrangement, and remarkable stability against chemical and mechanical forces, as explored by Soleimani et al. (2012). The reinforcement of enzyme and support bonds is achieved through surface modifications of silica, involving the amination of hydroxyl and reactive siloxane groups, as well as the addition of methyl or polyvinyl alcohol groups (Narsimha Rao et al., 2000; Pogorilyi et al., 2007; Shioji et al., 2003).

**Glass:** Glass, characterized as a highly viscous liquid, has been utilized to immobilize  $\alpha$ -amylase. In this process, phthaloyl chloride-containing amino group functionalized glass beads demonstrated robustness and renewability, as evidenced by Kahraman et al. (2007). Another enzyme, nitrite reductase, found immobilization on controlled pore glass beads, which served as a biosensing device for continuous monitoring, as reported by Rosa et al. (2002). Furthermore, urease immobilized on glass pH-electrodes has proven to be an effective and stable biosensor, enabling the monitoring of urea levels as low as 52  $\mu$ g/ml in blood samples, as highlighted by Sahney et al. (2005).

**Activated carbon:** Both natural and hydrochloric acid-modified activated carbon are valuable supports for enzyme adsorption, as discussed by Alkan et al. (2009). Recently, mesoporous-activated carbon particles have been employed in immobilizing acid protease and acidic lipases, featuring ample contact sites for enzyme immobilization. Notably, catalytic efficiency has been well-maintained even after 21 cycles of reuse, as indicated in the work of Ramani et al. (2012). Additionally, it has been observed that activated carbon with a high surface area (600-1,000  $\text{m}^2 \text{g}^{-1}$ ) and a significant fraction of its pore volume in the

300-1,000 Å range is well-suited for enzyme immobilization, as reported by Daoud et al. (2010).

**Charcoal:** The chemical modification of charcoal through the adsorption of papain with sulfhydryl groups has resulted in an increased number of active sites. This modified charcoal has been effectively applied to recover mercury from aqueous solutions and has proven efficient in industrial wastewater treatment, as documented by Dutta et al. (2009). Furthermore, charcoal supports have found application in the food industry, particularly for immobilizing amyloglucosidase in starch hydrolysis without the need for any crosslinking agent, achieving a remarkable 90% catalytic activity, as reported by Rani et al. (2000). The excellent adsorptive capacity of charcoal with minimal release of fine particulate matter has been underscored in earlier findings by Kibarer and Akovali (1996).

## V. APPLICATIONS OF IMMOBILIZED LIPASES

Microbial lipases stand out as the primary choice for various biotechnological applications in today's industries, and it is anticipated that this market will experience further growth in the upcoming years. Substantial efforts are directed towards the advancement of new technologies to enhance the production and preservation (reuse) of microbial lipases. These enzymes find widespread use in diverse industrial sectors such as food, oil and fat, soap and detergent, paper and cellulose, leather, textiles, cosmetics, and biodiesel, showcasing their versatility. Immobilized lipases offer specific applications in industries. The various factors that impact enzyme immobilization and potential modifications to enhance their activity have been outlined in **Fig.4**.

As of 2016, most of the global market for technical enzymes is reported in Europe, the Middle East, and Africa (EMEA). Projections for 2021 indicate an expansion of this market into North America and the Asia-Pacific region, with annual growth rates of 6.8% and 7.9%, respectively. Furthermore, the technical enzyme market is anticipated to surpass the EMEA market to become the largest global market in the following years. This suggests that significant progress in process development within the enzyme industry will predominantly occur in the Asia-Pacific and North America regions by the specified year.

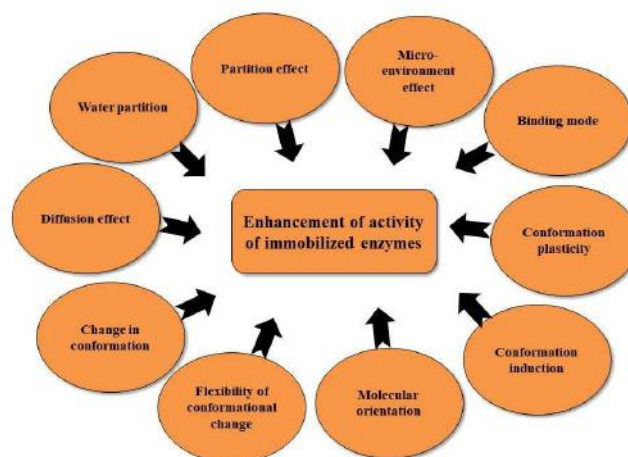


Fig.4: Determinants of enzyme immobilization and activity

### 5.1. Biosensors

An electrochemical biosensor is designed to offer analytical, quantitative, or semi-quantitative information by utilizing a biological recognition device in direct contact with an electrochemical signal transduction system. Today's prevalence of biosensors is attributed to their cost-effectiveness, rapid analysis, efficiency, sensitivity, and selectivity of enzymes for specific analytes, as highlighted by the International Union of Pure and Applied Chemistry in 2014.

Lipase-based biosensors have proven utility in detecting environmental pollutants, such as pesticides, as noted by Ma et al. (2018). In the food industry, biosensors play a crucial role in monitoring food quality, particularly the presence of triacylglycerol. Meanwhile, in the medical field, lipase and phospholipase sensors serve as diagnostic tools for detecting levels of triglycerides, cholesterol, and phospholipids in blood samples, according to Herrera-López (2012).

In a notable example by Zhang et al. (2014), an electrochemical biosensor was developed for monitoring tributyrin in human serum. Tributyrin, a triacylglycerol naturally present in butter, was detected using a biosensor constructed from polydopamine (PDA) and gold nanoparticles (GNPs), forming a hybrid material (GNPs@PDA) deposited on pretreated indium oxide and tin (ITO) electrodes. Lipase was then immobilized onto the GNPs@PDA. The cyclic voltammetry technique was employed for tributyrin determination in conjunction with the electrochemistry of lipase/GNPs/PDA/ITO electrodes. The optimized methodology utilized a scan rate of 50 mV s<sup>-1</sup> in phosphate buffer (50 mM, pH 7.5, 0.9% NaCl), achieving a detection limit of 0.84 mg/dL. This biosensor exhibited excellent performance for determining tributyrin in human serum, showcasing potential applications in

clinical settings and related research for triglyceride determination in biological samples, offering fast, safe, and cost-effective results.

## 5.2. Structured lipids

Immobilized lipases serve as efficient and selective catalysts in synthesizing structured lipids. Their role in esterification and interesterification allows for the customization of lipid structures, leading to the production of fats and oil with improved nutritional, functional, and sensory properties. Structured lipids are effectively synthesized through lipase-mediated esterification and interesterification reactions (Kim & Akoh, 2015). Additionally, lipases play a vital role in enhancing the quality of food products within the food processing industry, primarily by modifying fats and oils. This enzymatic activity is applied to a diverse range of vegetable oils, including sunflower, coconut, olive, corn, and rice bran oil, all rich in omega-6 fatty acids. Similarly, lipases are utilized to modify oils from fish, linseed, walnuts, and milk, which are abundant in omega-3 fatty acids. Both omega-6 and omega-3 fatty acids are crucial for maintaining optimal health by regulating essential fatty acid levels within acceptable limits (Khan et al., 2023; Sangeetha et al., 2011). Additionally, phospholipases find industrial applications in processes such as egg yolk treatment for mayonnaise production, lecithin modification, and the oil-degumming step in refining vegetable oils. Novozymes 435 is an example of a lipase that demonstrates effectiveness in esterifying free fatty acids with octanol to produce octyl esters. Lipase-catalyzed transesterification, esterification, and epoxidation processes successfully modify vegetable oils, forming bio-lubricant components.

To enhance the industrial viability of lipases, immobilization techniques are employed, leveraging their inherent "interfacial" hydrophobicity. Various immobilization methods include adsorption on hydrophobic adsorbents like glass beads coated with hydrophobic materials, methylated silica, phenyl-Sepharose, poly-(ethylene glycol)-Sepharose, polypropylene particles, polypropylene hollow-fibers, nonwoven fabric, and nitrocellulose membranes (Sharma & Kanwar, 2014). Silica and solgels are also utilized, offering high compositional and morphological flexibility (Borza et al., 2015). For a more in-depth understanding of the diverse applications of lipases in oil and fat modifications, additional insights can be gained from the following literature (Ramani et al., 2010; Rodrigues & Fernandez-Lafuente, 2010).

## 5.3. Flavor production

The sensory experience of flavor and fragrance is pivotal in determining consumer preferences for various products. Consequently, synthesizing and utilizing these compounds are crucial for providing a distinct identity to a product. Flavor and fragrance are intentionally incorporated into formulations for food, beverages, pharmaceuticals, and personal care items. Ethers serve as primary contributors to flavor, but their high cost renders the production process impractical. Chemical methods, while an option, often result in the formation of undesirable compounds, limiting their application in the food and beverage industries (Aravindan et al., 2007; Dhake et al., 2013; Ray, 2012). An alternative approach involves enzymatic catalysis for flavor and fragrance synthesis, eliminating the need for toxic solvents and intricate product recovery procedures. Notably, lipase stands out among enzymes, capable of producing diverse flavors depending on the reaction medium. In the food industry, lipases find applications to enhance the organoleptic characteristics of products. They are employed in flavored dairy items to improve the taste of cheese, milk, and butter, contribute to aroma development in beverages, extend shelf life in baking, enhance quality in mayonnaise, facilitate cocoa butter processing, and serve various other purposes (Aravindan et al., 2007; Dhake et al., 2013; Ray, 2012).

To demonstrate the effectiveness of enzymatic synthesis in flavor production, (Sadighi et al., 2017; Silva et al., 2014) devised methods for immobilizing lipases from various sources, such as porcine pancreatic lipase (PPL) and *Thermomyces lanuginosa* lipase (TLL), respectively. Silva et al. (2014) employed polyhydroxybutyrate (PHB) particles to immobilize porcine pancreatic lipase (PPL) for synthesizing pineapple flavor through the esterification of butanol and butyric acid in a heptane medium. The optimized pH and temperature for hydrolysis reaction with immobilized PPL were at 8.5 and 50°C. In the esterification reaction, the optimum conversion reached approximately 93% after 2 hours. Operational stability tests suggested that this methodology could be a valuable tool for lipase immobilization for ester synthesis, with the biocatalyst retaining 63% of its initial activity after six cycles of esterification. In a separate study, Sadighi et al. (2017) utilized mesoporous silica nanoparticles (MCM-41) coated with polyethyleneimine (MCM-41 @ PEI) and modified with divalent metal ions ( $M = \text{Co}^{2+}$ ,  $\text{Cu}^{2+}$ , or  $\text{Pd}^{2+}$ ) to produce chelated silica nanoparticles (MCM 41 & M) for lipase immobilization. The MCM-41 @ PEI Co carrier demonstrated higher catalytic activity at 75°C, retaining 70% of its initial activity after 14 days of storage at room temperature. When applied to the synthesis of ethyl valerate (green

apple flavor) in the presence of valeric acid and ethanol, a reduction of 60% and 53%, respectively, was observed after 24 hours of incubation in n-hexane and dimethylsulfoxide medium.

These studies underscore the versatility of lipases in the food and pharmaceutical industries, showcasing their high yield in esterifying lipids for flavor production. Using non-polar substrates in organic chemical synthesis further highlights their broad applicability. Immobilization of enzymes proves crucial, enhancing storage stability and maintaining enzymatic activity across a wide range of temperatures and pH. Moreover, this approach reduces operational costs by facilitating the easy recovery of lipases for subsequent reuse, with minimal activity loss over multiple cycles.

#### 5.4. Biodiesel production

Biofuels have emerged as a sustainable and renewable alternative to conventional fossil fuels, with biodiesel being a notable example. Biodiesel production involves the use of biomass, often comprising fats and vegetable oils, positioning it as a cleaner energy source compared to petroleum-based diesel fuels. The transformation of triacylglycerols found in oils and fats into esters through a process called transesterification is the key method for biodiesel synthesis. This reaction can be influenced by various factors, including the molar ratio of alcohol, catalyst type, presence of water and free fatty acid, temperature, time, and stirring speed (Vargas et al., 2018; Yücel et al., 2012). Enzymatic immobilization has proven to be a highly advantageous approach. Comparative studies reveal that the catalytic activities of the same lipase molecule can differ significantly based on the immobilization support used (Sankaran et al., 2016; Vargas et al., 2018; Yücel et al., 2012). Khosla et al. (2017) explored the potential of an extracellular lipase from *Pseudomonas* sp. ISTPL3 was isolated from Pangong Lake for the transesterification of lipids produced by the oleaginous chemolithotrophic bacterium *Serratia* sp. ISTD04, contributing to biodiesel production. Immobilizing the lipase on activated biochar resulted in a higher yield of fatty acid methyl esters (FAMEs) at 92.23%, compared to 87.81% for the non-immobilized lipase. The authors attribute this increase to the enhanced stability and catalytic activity achieved through lipase immobilization. Furthermore, the immobilized lipase retained 75.11% of its activity after three cycles of biodiesel production, highlighting the potential for cost reduction through lipase reuse and improved production efficiency.

Numerous other studies have also demonstrated favorable outcomes in immobilizing lipases from various

microorganisms on different supports (Cruz-Izquierdo et al., 2014; Kalantari et al., 2013; Miao et al., 2018; Picó et al., 2018; Sankaran et al., 2016; Vargas et al., 2018; Xie & Huang, 2018; Yücel et al., 2012). These studies underscore the potential of immobilized enzymatic catalysts to enhance biodiesel production processes, offering advantages such as increased yield, improved lipase stability in reaction media, and cost reduction through the repeated use of lipases.

#### 5.5. Treatment of wastewater

Industrial waste comprises organic and inorganic substances found in solvents or suspensions, varying in levels of harmfulness. Various effluent treatment processes aim to eliminate these characteristic residues from different industrial processes (Meng et al., 2015; Sarmah et al., 2018). Typically, these treatments involve physical, biological, and chemical stages, with the effectiveness directly impacted by the combination of treatments suitable for the specific waste type. Biological treatment, often following physical or chemical-physical treatment, employs microorganisms that produce enzymes capable of breaking down organic matter. In this process, microorganisms hydrolyze triacylglycerols in the extracellular medium through the action of lipases, resulting in the production of fatty acids and glycerol. Lipases can be utilized in various forms, such as in the crude form of a fermented broth or isolated, for pretreating effluents before anaerobic digestion. Alternatively, they can be used as an enzyme complex containing lipase and other enzymes to enhance treatment efficiency. These enzymes find extensive application in removing fats from treatment plant aerators utilizing activated sludge and are commonly employed in treating industrial effluents from sectors like food processing, textiles, paper and cellulose, tanneries, and automotive industries (Mendes et al., 2005; Meng et al., 2015; Ramani et al., 2013; Sarmah et al., 2018; Shen et al., 2013).

Recent trends indicate a growing interest in the study and application of marine lipases, driven by their ability to function in more extreme environments than other lipases. In this context, microorganisms are introduced into the reaction medium, and liquid fermentation is performed. The microorganisms utilize the lipids catalyzed by the lipases to obtain energy for maintenance and replication. Hassan et al. (2018) conducted studies involving isolating marine bacteria from the Mediterranean Sea for lipase production. They optimized cell production, immobilized the bacteria, and applied them in effluent treatment. *Bacillus cereus* HSS emerged as the most promising microorganism, exhibiting the highest lipolytic capacity. Immobilization through the adsorption of sponge cells and

recycling significantly increased lipase activity by 2.8-fold compared to free cells. The repeated reuse of immobilized *B. cereus* HSS maintained reasonable lipase activity. An economic study focusing on oily wastewater treatment demonstrated 87.63% efficiency in removing biological oxygen demand, a 90% removal of total suspended solids, and a 94.7% removal of oil and grease. This highlights the potential of immobilized microorganisms as a cost-effective method for wastewater treatment. The positive results suggest promising applications for the large-scale implementation of immobilized microorganisms, encouraging further research in this direction.

## VI. CONCLUSION AND FUTURE PERSPECTIVES

Lipases are versatile tools and established biocatalysts in diverse industrial sectors due to their remarkable ability to catalyze reactions in aqueous and non-aqueous environments. The comprehensive overview presented in this review underscores the ongoing imperative for continuous development in the lipase immobilization process. Researchers are particularly concerned about its advancement, given its widespread application in numerous industrial-scale chemical reactions, spanning areas such as food, pharmaceuticals, cosmetics, and fuel production. The review further delves into lipase sources, categorization based on specificity, and various applications. Moreover, the lipase immobilization process brings significant advantages, including heightened chemical and thermal stability compared to the free form of lipase and ease of recovery and reuse. The diverse range of materials serving as supports for lipase immobilization, along with the methods employed in the immobilization process, not only confer crucial advantages but also provide ample scope for tailoring biocatalytic systems to specific chemical reactions and applications. The review discusses different support materials and immobilization techniques, highlighting the critical challenge of judiciously selecting the appropriate support material and immobilization method in this evolving field.

However, improving the lipase immobilization process comes with challenges, like the high cost of making lipases. So, future research should focus on using molecular biology and genetic engineering to make more microbial lipases and make the whole process cheaper. Also, from an economic standpoint, creating new supports from cheap waste biomass or natural materials that are easy to find can be a big advantage in using lipases in industries. Another way to cut costs is by using co-immobilization, where different enzymes, including lipase, are put together on the same material to do different jobs.

In the future, we expect to see more reports about new materials with different properties and ways to use them in the lipase immobilization process.

## ACKNOWLEDGMENTS

This work was supported by the National Natural Science Foundation of China (31601433).

## REFERENCES

- [1] Abreu Silveira, E., Moreno-Perez, S., Basso, A., Serban, S., Pestana Mamede, R., Tardioli, P. W., Sanchez Farinas, C., Rocha-Martin, J., Fernandez-Lorente, G., & Guisan, J. M. (2017). Modulation of the regioselectivity of *Thermomyces lanuginosus* lipase via biocatalyst engineering for the Ethanolysis of oil in fully anhydrous medium. *BMC biotechnology*, 17(1), 1-13.
- [2] Agueiras, E. C., Cavalcanti-Oliveira, E. D., & Freire, D. M. (2015). Current status and new developments of biodiesel production using fungal lipases. *Fuel*, 159, 52-67.
- [3] Ahmad, F. T., Mather, D. E., Law, H.-Y., Li, M., Yousif, S. A.-J., Chalmers, K. J., Asenstorfer, R. E., & Mares, D. J. (2015). Genetic control of lutein esterification in wheat (*Triticum aestivum* L.) grain. *Journal of Cereal Science*, 64, 109-115.
- [4] Al-Adhami, A. J., Bryjak, J., Greb-Markiewicz, B., & Peczyńska-Czoch, W. (2002). Immobilization of wood-rotting fungi laccases on modified cellulose and acrylic carriers. *Process Biochemistry*, 37(12), 1387-1394.
- [5] Alkan, S., Gür, A., Ertan, M., Savran, A., Gür, T., & Genel, Y. (2009). Immobilization of catalase via adsorption into natural and modified active carbon obtained from walnut in various methods. *African Journal of Biotechnology*, 8(11).
- [6] Ananthi, S., Ramasubburayan, R., Palavesam, A., & Immanuel, G. (2014). Optimization and purification of lipase through solid state fermentation by *Bacillus cereus* MSU as isolated from the gut of a marine fish *Sardinella longiceps*. *Int. J. Pharm. Pharm. Sci*, 6(5), 291-298.
- [7] Anh Dung, N., Dinh Huyen, N., Duy Hang, N., & Tich Canh, T. (1995). Immobilization of urease on grafted starch by radiation method. *Radiation Physics and Chemistry*, 46(4-6), 1037-1042.
- [8] Ansari, S. A., & Husain, Q. (2012). Lactose hydrolysis from milk/whey in batch and continuous processes by concanavalin A-Celite 545 immobilized *Aspergillus oryzae*  $\beta$  galactosidase. *Food and Bioproducts Processing*, 90(2), 351-359.
- [9] Aravindan, R., Anbumathi, P., & Viruthagiri, T. (2007). Lipase applications in food industry.
- [10] Ashly, P., Joseph, M., & Mohanan, P. (2011). Activity of diastase  $\alpha$ -amylase immobilized on polyanilines (PANIs). *Food chemistry*, 127(4), 1808-1813.
- [11] Ashraf, H., & Husain, Q. (2010). Use of DEAE cellulose adsorbed and crosslinked white radish (*Raphanus sativus*) peroxidase for the removal of  $\alpha$ -naphthol in batch and



- continuous process. *International Biodeterioration & Biodegradation*, 64(1), 27-31.
- [12] Ates, S., & Dogan, N. (2010). Properties of immobilized phenylalanine ammonia lyase and investigation of its use for the prediagnosis of phenylketonuria. *TURKISH JOURNAL OF BIOCHEMISTRY-TURK BIYOKIMYA DERGISI*, 35(1).
- [13] Baldessari, A., & Iglesias, L. E. (2012). Lipases in green chemistry: acylation and alcoholysis on steroids and nucleosides. *Lipases and phospholipases: Methods and Protocols*, 457-469.
- [14] Banković-Ilić, I. B., Stamenković, O. S., & Veljković, V. B. (2012). Biodiesel production from non-edible plant oils. *Renewable and sustainable energy reviews*, 16(6), 3621-3647.
- [15] Barbe, S., Lafaquiere, V., Guieysse, D., Monsan, P., Remaud-Siméon, M., & Andre, I. (2009). Insights into lid movements of Burkholderia cepacia lipase inferred from molecular dynamics simulations. *Proteins: structure, function, and bioinformatics*, 77(3), 509-523.
- [16] Barros, M., Fleuri, L., & Macedo, G. (2010). Seed lipases: sources, applications and properties-a review. *Brazilian Journal of Chemical Engineering*, 27, 15-29.
- [17] Batista-Viera, F., Rydén, L., & Carlsson, J. (2011). Covalent chromatography. *Protein Purification: Principles, High Resolution Methods, and Applications*, 203-219.
- [18] Belguith, H., Fattouch, S., Jridi, T., & Ben, H. J. (2013). Immunopurification and characterization of a rape (Brassica napus L.) seedling lipase. *African Journal of Biotechnology*, 12(21).
- [19] Benítez-Mateos, A. I., San Sebastian, E., Ríos-Lombardía, N., Morís, F., González-Sabín, J., & López-Gallego, F. (2017). Asymmetric reduction of prochiral ketones by using self-sufficient heterogeneous biocatalysts based on NADPH-dependent ketoreductases. *Chemistry—A European Journal*, 23(66), 16843-16852.
- [20] Betigeri, S. S., & Neau, S. H. (2002). Immobilization of lipase using hydrophilic polymers in the form of hydrogel beads. *Biomaterials*, 23(17), 3627-3636.
- [21] Bilal, M., Asgher, M., Cheng, H., Yan, Y., & Iqbal, H. M. (2019). Multi-point enzyme immobilization, surface chemistry, and novel platforms: a paradigm shift in biocatalyst design. *Critical reviews in biotechnology*, 39(2), 202-219.
- [22] Bilal, M., Zhao, Y., Noreen, S., Shah, S. Z. H., Bharagava, R. N., & Iqbal, H. M. (2019). Modifying bio-catalytic properties of enzymes for efficient biocatalysis: A review from immobilization strategies viewpoint. *Biocatalysis and Biotransformation*, 37(3), 159-182.
- [23] Böhmer, W., Knaus, T., & Mutti, F. G. (2018). Hydrogen-borrowing alcohol bioamination with coimmobilized dehydrogenases. *ChemCatChem*, 10(4), 731-735.
- [24] Bolivar, J. M., Gascon, V., Marquez-Alvarez, C., Blanco, R. M., & Nidetzky, B. (2017). Oriented coimmobilization of oxidase and catalase on tailor-made ordered mesoporous silica. *Langmuir*, 33(20), 5065-5076.
- [25] Bolivar, J. M., & Nidetzky, B. (2013). Smart enzyme immobilization in microstructured reactors. *Chimica Oggi*, 31(3), 50-54.
- [26] Borrelli, G. M., & Trono, D. (2015). Recombinant lipases and phospholipases and their use as biocatalysts for industrial applications. *International Journal of Molecular Sciences*, 16(9), 20774-20840.
- [27] Borza, P., Peter, F., & Paul, C. (2015). Improved enantioselectivity of Candida antarctica a lipase through sol-gel entrapment. *Chem Bull, "POLYTECHNICA" Univ.(Timisoara)*, 60, 49-54.
- [28] Bose, A., & Keharia, H. (2013). Production, characterization and applications of organic solvent tolerant lipase by Pseudomonas aeruginosa AAU2. *Biocatalysis and Agricultural Biotechnology*, 2(3), 255-266.
- [29] Brena, B., González-Pombo, P., & Batista-Viera, F. (2013). Immobilization of enzymes: a literature survey. *Immobilization of Enzymes and Cells: Third Edition*, 15-31.
- [30] Brígida, A. I., Amaral, P. F., Coelho, M. A., & Goncalves, L. R. (2014). Lipase from Yarrowia lipolytica: Production, characterization and application as an industrial biocatalyst. *Journal of Molecular Catalysis B: Enzymatic*, 101, 148-158.
- [31] Cavalcanti-Oliveira, E. d. A., Silva, P. R. d., Ramos, A. P., Aranda, D. A. G., & Freire, D. M. G. (2011). Study of soybean oil hydrolysis catalyzed by Thermomyces lanuginosus lipase and its application to biodiesel production via hydroesterification. *Enzyme research*, 2011.
- [32] Cazaban, D., Illanes, A., Wilson, L., & Betancor, L. (2018). Bio-inspired silica lipase nanobiocatalysts for the synthesis of fatty acid methyl esters. *Process Biochemistry*, 74, 86-93.
- [33] Cenicerós, E. S., Ilyina, A., Esquivel, J. C., Menchaca, D. R., Espinoza, J. F., & Rodríguez, O. M. (2003). Entrapment of enzymes in natural polymer extracted from residue of food industry: preparation methods, partial characterisation and possible application. *Becth Mock*, 44, 84-87.
- [34] Chang, M.-Y., & Juang, R.-S. (2007). Use of chitosan-clay composite as immobilization support for improved activity and stability of  $\beta$ -glucosidase. *Biochemical Engineering Journal*, 35(1), 93-98.
- [35] Chang, Y., & Chu, L. (2007). A simple method for cell disruption by immobilization of lysozyme on the extrudate-shaped NaY zeolite. *Biochemical Engineering Journal*, 35(1), 37-47.
- [36] Chen, S., Song, N., Liao, X., & Shi, B. (2011). Immobilization of catalase on Fe (III) modified collagen fiber. *Sheng wu gong cheng xue bao= Chinese journal of biotechnology*, 27(7), 1076-1081.
- [37] Christopher, L. P., Zambare, V. P., Zambare, A., Kumar, H., & Malek, L. (2015). A thermo-alkaline lipase from a new thermophile Geobacillus thermodenitrificans AV-5 with potential application in biodiesel production. *Journal of Chemical Technology & Biotechnology*, 90(11), 2007-2016.

- [38] Cieh, N. L., Mokhtar, M. N., Baharuddin, A. S., Mohammed, M. A. P., & Wakisaka, M. (2023). Progress on lipase immobilization technology in edible oil and fat modifications. *Food Reviews International*, 1-47.
- [39] Clementz, A. L., Del Peso, G., Canet, A., Yori, J. C., & Valero, F. (2016). Utilization of discard bovine bone as a support for immobilization of recombinant *Rhizopus oryzae* lipase expressed in *Pichia pastoris*. *Biotechnology progress*, 32(5), 1246-1253.
- [40] Contente, M. L., & Paradisi, F. (2018). Self-sustaining closed-loop multienzyme-mediated conversion of amines into alcohols in continuous reactions. *Nature Catalysis*, 1(6), 452-459.
- [41] Cruz-Izquierdo, A., Picó, E. A., López, C., Serra, J. L., & Llama, M. J. (2014). Magnetic cross-linked enzyme aggregates (mCLEAs) of *Candida antarctica* lipase: an efficient and stable biocatalyst for biodiesel synthesis. *PLoS One*, 9(12), e115202.
- [42] Cui, J. D., & Jia, S. R. (2015). Optimization protocols and improved strategies of cross-linked enzyme aggregates technology: current development and future challenges. *Critical reviews in biotechnology*, 35(1), 15-28.
- [43] da Silva Serres, J. D., Balmant, W., Soares, D., Corazza, M. L., Krieger, N., & Mitchell, D. A. (2017). A combined sorption and kinetic model for multiphasic ethyl esterification of fatty acids from soybean soapstock acid oil catalyzed by a fermented solid with lipase activity in a solvent-free system. *Biochemical Engineering Journal*, 120, 84-92.
- [44] Dalal, S., Sharma, A., & Gupta, M. N. (2007). A multipurpose immobilized biocatalyst with pectinase, xylanase and cellulase activities. *Chemistry Central Journal*, 1, 1-5.
- [45] Daoud, F. B.-O., Kaddour, S., & Sadoun, T. (2010). Adsorption of cellulase *Aspergillus niger* on a commercial activated carbon: kinetics and equilibrium studies. *Colloids and Surfaces B: Biointerfaces*, 75(1), 93-99.
- [46] Das, R., & Kayastha, A. M. (2019). Enzymatic hydrolysis of native granular starches by a new  $\beta$ -amylase from peanut (*Arachis hypogaea*). *Food chemistry*, 276, 583-590.
- [47] Datta, S., Christena, L. R., & Rajaram, Y. R. S. (2013). Enzyme immobilization: an overview on techniques and support materials. *3 Biotech*, 3, 1-9.
- [48] de Vasconcellos, A., Laurenti, J. B., Miller, A. H., da Silva, D. A., de Moraes, F. R., Aranda, D. A., & Nery, J. G. (2015). Potential new biocatalysts for biofuel production: The fungal lipases of *Thermomyces lanuginosus* and *Rhizomucor miehei* immobilized on zeolitic supports ion exchanged with transition metals. *Microporous and Mesoporous Materials*, 214, 166-180.
- [49] De Winter, K., Soetaert, W., & Desmet, T. (2012). An imprinted cross-linked enzyme aggregate (iCLEA) of sucrose phosphorylase: Combining improved stability with altered specificity. *International Journal of Molecular Sciences*, 13(9), 11333-11342.
- [50] Delkash-Roudsari, S., Zibae, A., & AbbaciMozhdehi, M. (2014). Determination of lipase activity in the larval midgut of *Bacterocera oleae* Gmelin (Diptera: Tephritidae). *Invertebrate Survival Journal*, 11(1), 66-72.
- [51] Dezott, M., Innocentini-Mei, L. H., & Durán, N. (1995). Silica immobilized enzyme catalyzed removal of chlorolignins from eucalyptus kraft effluent. *Journal of Biotechnology*, 43(3), 161-167.
- [52] Dhake, K. P., Thakare, D. D., & Bhanage, B. M. (2013). Lipase: A potential biocatalyst for the synthesis of valuable flavour and fragrance ester compounds. *Flavour and Fragrance Journal*, 28(2), 71-83.
- [53] Dijkstra, A. J. (2009). Recent developments in edible oil processing. *European journal of lipid science and technology*, 111(9), 857-864.
- [54] Dutta, S., Bhattacharyya, A., De, P., Ray, P., & Basu, S. (2009). Removal of mercury from its aqueous solution using charcoal-immobilized papain (CIP). *Journal of Hazardous Materials*, 172(2-3), 888-896.
- [55] Emregul, E., Sungur, S., & Akbulut, U. (2006). Polyacrylamide-gelatine carrier system used for invertase immobilization. *Food chemistry*, 97(4), 591-597.
- [56] Eze, S. O., Chilaka, F. C., & Akunwata, C. U. (2007). Properties of lipase (EC 3.1. 1.3) from different varieties of maize. *Animal Research International*, 4(2), 650-652.
- [57] Fleuri, L. F., de Oliveira, M. C., de Lara Campos Arcuri, M., Capoville, B. L., Pereira, M. S., Delgado, C. H. O., & Novelli, P. K. (2014). Production of fungal lipases using wheat bran and soybean bran and incorporation of sugarcane bagasse as a co-substrate in solid-state fermentation. *Food science and biotechnology*, 23, 1199-1205.
- [58] Flores-Maltos, A., Rodríguez-Durán, L. V., Renovato, J., Contreras, J. C., Rodríguez, R., & Aguilar, C. N. (2011). Catalytic properties of free and immobilized *Aspergillus niger* tannase. *Enzyme research*, 2011.
- [59] Furuya, T., Kuroiwa, M., & Kino, K. (2017). Biotechnological production of vanillin using immobilized enzymes. *Journal of Biotechnology*, 243, 25-28.
- [60] Galliani, M., Santi, M., Del Grosso, A., Cecchettini, A., Santorelli, F. M., Hofmann, S. L., Lu, J.-Y., Angella, L., Cecchini, M., & Signore, G. (2018). Cross-Linked enzyme aggregates as versatile tool for enzyme delivery: Application to polymeric nanoparticles. *Bioconjugate chemistry*, 29(7), 2225-2231.
- [61] Gao, F., Guo, Y., Fan, X., Hu, M., Li, S., Zhai, Q., Jiang, Y., & Wang, X. (2019). Enhancing the catalytic performance of chloroperoxidase by co-immobilization with glucose oxidase on magnetic graphene oxide. *Biochemical Engineering Journal*, 143, 101-109.
- [62] Garcia, H. S., Arcos, J. A., Keough, K. J., & Hill Jr, C. G. (2001). Immobilized lipase-mediated acidolysis of butteroil with conjugated linoleic acid: batch reactor and packed bed reactor studies. *Journal of Molecular Catalysis B: Enzymatic*, 11(4-6), 623-632.
- [63] Garlapati, V. K., Kant, R., Kumari, A., Mahapatra, P., Das, P., & Banerjee, R. (2013). Lipase mediated transesterification of *Simarouba glauca* oil: a new feedstock for biodiesel production. *Sustainable chemical processes*, 1, 1-6.

- [64] Gomez, L., Ramírez, H. L., Neira-Carrillo, A., & Villalonga, R. (2006). Polyelectrolyte complex formation mediated immobilization of chitosan-invertase neoglycoconjugate on pectin-coated chitin. *Bioprocess and Biosystems Engineering*, 28, 387-395.
- [65] Guo, J., Chen, C.-P., Wang, S.-G., & Huang, X.-J. (2015). A convenient test for lipase activity in aqueous-based solutions. *Enzyme and Microbial Technology*, 71, 8-12.
- [66] Gupta, R., Kumari, A., Syal, P., & Singh, Y. (2015). Molecular and functional diversity of yeast and fungal lipases: Their role in biotechnology and cellular physiology. *Progress in lipid research*, 57, 40-54.
- [67] Hamden, K., Keskes, H., Elgomdi, O., Feki, A., & Alouche, N. (2017). Modulatory effect of an isolated triglyceride from fenugreek seed oil on of  $\alpha$ -amylase, lipase and ACE activities, liver-kidney functions and metabolic disorders of diabetic rats. *Journal of oleo science*, 66(6), 633-645.
- [68] Hanamura, S., Hanaya, K., Shoji, M., & Sugai, T. (2016). Synthesis of acacetin and resveratrol 3, 5-di-O- $\beta$ -glucopyranoside using lipase-catalyzed regioselective deacetylation of polyphenol glycoside peracetates as the key step. *Journal of Molecular Catalysis B: Enzymatic*, 128, 19-26.
- [69] Hasan, F., Shah, A. A., & Hameed, A. (2009). Methods for detection and characterization of lipases: a comprehensive review. *Biotechnology advances*, 27(6), 782-798.
- [70] Hassan, S. W., Abd El Latif, H. H., & Ali, S. M. (2018). Production of cold-active lipase by free and immobilized marine *Bacillus cereus* HSS: application in wastewater treatment. *Frontiers in microbiology*, 9, 2377.
- [71] Herrera-López, E. J. (2012). Lipase and phospholipase biosensors: a review. *Lipases and phospholipases: Methods and Protocols*, 525-543.
- [72] Homaei, A. A., Sariri, R., Vianello, F., & Stevanato, R. (2013). Enzyme immobilization: an update. *Journal of chemical biology*, 6, 185-205.
- [73] Hosseinkhani, S., Szittner, R., Nemat-Gorgani, M., & Meighen, E. A. (2003). Adsorptive immobilization of bacterial luciferases on alkyl-substituted Sepharose 4B. *Enzyme and Microbial Technology*, 32(1), 186-193.
- [74] Hsieh, H.-J., Liu, P.-C., & Liao, W.-J. (2000). Immobilization of invertase via carbohydrate moiety on chitosan to enhance its thermal stability. *Biotechnology letters*, 22, 1459-1464.
- [75] Huang, L., & Cheng, Z.-M. (2008). Immobilization of lipase on chemically modified bimodal ceramic foams for olive oil hydrolysis. *Chemical Engineering Journal*, 144(1), 103-109.
- [76] Huang, W.-C., Chen, C.-Y., & Wu, S.-J. (2017). Almond skin polyphenol extract inhibits inflammation and promotes lipolysis in differentiated 3T3-L1 adipocytes. *Journal of medicinal food*, 20(2), 103-109.
- [77] Huang, X.-J., Chen, P.-C., Huang, F., Ou, Y., Chen, M.-R., & Xu, Z.-K. (2011). Immobilization of *Candida rugosa* lipase on electrospun cellulose nanofiber membrane. *Journal of Molecular Catalysis B: Enzymatic*, 70(3-4), 95-100.
- [78] Hüttner, S., Gomes, M. Z. D. V., Iancu, L., Palmqvist, A., & Olsson, L. (2017). Immobilisation on mesoporous silica and solvent rinsing improve the transesterification abilities of feruloyl esterases from *Myceliophthora thermophila*. *Bioresource technology*, 239, 57-65.
- [79] Iftikhar, T., Niaz, M., Ali, E. A., Jabeen, R., & Abdullah, R. (2012). Production process of extracellular lipases by *Fusarium* sp. using agricultural by products. *Pak J Bot*, 44, 335-339.
- [80] Jasti, L. S., Dola, S. R., Kumaraguru, T., Bajja, S., Fadnavis, N. W., Addepally, U., Rajdeo, K., Ponrathnam, S., & Deokar, S. (2014). Protein-coated polymer as a matrix for enzyme immobilization: Immobilization of trypsin on bovine serum albumin-coated allyl glycidyl ether-ethylene glycol dimethacrylate copolymer. *Biotechnology progress*, 30(2), 317-323.
- [81] Jegannathan, K. R., Jun-Yee, L., Chan, E.-S., & Ravindra, P. (2010). Production of biodiesel from palm oil using liquid core lipase encapsulated in  $\kappa$ -carrageenan. *Fuel*, 89(9), 2272-2277.
- [82] Jesionowski, T., Zdarta, J., & Krajewska, B. (2014). Enzyme immobilization by adsorption: a review. *Adsorption*, 20, 801-821.
- [83] Jo, J. C., Kim, S.-j., & Kim, H. K. (2014). Transesterification of plant oils using *Staphylococcus haemolyticus* L62 lipase displayed on *Escherichia coli* cell surface using the OmpA signal peptide and EstA $\beta$ 8 anchoring motif. *Enzyme and Microbial Technology*, 67, 32-39.
- [84] Kadouf, Y. H. A., Kabbashi, N. A., Alam, M. Z., & Mirghani12, M. E. S. (2015). Enzymatic synthesis of biodiesel from moringa oleifera oil via transesterification. *Juarnl, Teknologi*.
- [85] Kagedal, L. (2011). Immobilized metal ion affinity chromatography. *Protein Purification, Principles, High Resolution Methods, and Applications*, 183-201.
- [86] Kahraman, M. V., Bayramoğlu, G., Kayaman-Apohan, N., & Güngör, A. (2007). UV-curable methacrylated/fumaric acid modified epoxy as a potential support for enzyme immobilization. *Reactive and Functional Polymers*, 67(2), 97-103.
- [87] Kalantari, M., Kazemeini, M., & Arpanaei, A. (2013). Evaluation of biodiesel production using lipase immobilized on magnetic silica nanocomposite particles of various structures. *Biochemical Engineering Journal*, 79, 267-273.
- [88] Kamori, M., Hori, T., Yamashita, Y., Hirose, Y., & Naoshima, Y. (2000). Immobilization of lipase on a new inorganic ceramics support, toyonite, and the reactivity and enantioselectivity of the immobilized lipase. *Journal of Molecular Catalysis B: Enzymatic*, 9(4-6), 269-274.
- [89] Kanmani, P., Aravind, J., & Kumaresan, K. (2015). An insight into microbial lipases and their environmental facet. *International journal of environmental science and technology*, 12, 1147-1162.
- [90] Kanmani, P., Kumaresan, K., & Aravind, J. (2015). Pretreatment of coconut mill effluent using celite-immobilized hydrolytic enzyme preparation from

- Staphylococcus pasteurii and its impact on anaerobic digestion. *Biotechnology progress*, 31(5), 1249-1258.
- [91] Kapoor, M., & Gupta, M. N. (2012). Lipase promiscuity and its biochemical applications. *Process Biochemistry*, 47(4), 555-569.
- [92] Kapoor, M., & Kuhad, R. C. (2007). Immobilization of xylanase from *Bacillus pumilus* strain MK001 and its application in production of xylo-oligosaccharides. *Applied biochemistry and biotechnology*, 142, 125-138.
- [93] Katwa, L., Ramakrishna, M., & Rao, M. R. (1981). Spectrophotometric assay of immobilized tannase. *Journal of Biosciences*, 3, 135-142.
- [94] Kawashima, Y., Ezawa, T., Harada, T., Noguchi, T., Kawasaki, M., Kirihara, M., & Imai, N. (2016). Preparation of the monoacylates of 2-substituted (Z)-but-2-ene-1, 4-diols using porcine pancreas lipase. *Bulletin of the Chemical Society of Japan*, 89(2), 257-267.
- [95] Khan, A. A., Akhtar, S., & Husain, Q. (2006). Direct immobilization of polyphenol oxidases on Celite 545 from ammonium sulphate fractionated proteins of potato (*Solanum tuberosum*). *Journal of Molecular Catalysis B: Enzymatic*, 40(1-2), 58-63.
- [96] Khan, I., Hussain, M., Jiang, B., Zheng, L., Pan, Y., Hu, J., Khan, A., Ashraf, A., & Zou, X. (2023). Omega-3 long-chain polyunsaturated fatty acids: Metabolism and health implications. *Progress in lipid research*, 101255.
- [97] Khan, S., Guo, L., Maimaiti, Y., Mijit, M., & Qiu, D. (2012). Entomopathogenic fungi as microbial biocontrol agent. *Molecular Plant Breeding*, 3(7).
- [98] Khasanov, K. T., Davranov, K., & Rakhimov, M. (2015). State of fungal lipases of *Rhizopus microsporus*, *Penicillium* sp. and *Oospora lactis* in border layers water—solid phase and factors affecting catalytic properties of Enzymes. *Applied biochemistry and microbiology*, 51, 600-607.
- [99] Khosla, K., Rathour, R., Maurya, R., Maheshwari, N., Gnansounou, E., Larroche, C., & Thakur, I. S. (2017). Biodiesel production from lipid of carbon dioxide sequestering bacterium and lipase of psychrotolerant *Pseudomonas* sp. ISTPL3 immobilized on biochar. *Bioresource technology*, 245, 743-750.
- [100] Kibarer, G. D., & Akovali, G. (1996). Optimization studies on the features of an activated charcoal-supported urease system. *Biomaterials*, 17(15), 1473-1479.
- [101] Kim, B. H., & Akoh, C. C. (2015). Recent research trends on the enzymatic synthesis of structured lipids. *Journal of food science*, 80(8), C1713-C1724.
- [102] Kim, S. H., Kim, S.-j., Park, S., & Kim, H. K. (2013). Biodiesel production using cross-linked *Staphylococcus haemolyticus* lipase immobilized on solid polymeric carriers. *Journal of Molecular Catalysis B: Enzymatic*, 85, 10-16.
- [103] Kittilson, J. D., Reindl, K. M., & Sheridan, M. A. (2011). Rainbow trout (*Oncorhynchus mykiss*) possess two hormone-sensitive lipase-encoding mRNAs that are differentially expressed and independently regulated by nutritional state. *Comparative Biochemistry and Physiology Part A: Molecular & Integrative Physiology*, 158(1), 52-60.
- [104] Klein, M. P., Scheeren, C. W., Lorenzoni, A. S. G., Dupont, J., Frazzon, J., & Hertz, P. F. (2011). Ionic liquid-cellulose film for enzyme immobilization. *Process Biochemistry*, 46(6), 1375-1379.
- [105] Kobayashi, T., Nagao, T., Watanabe, Y., & Shimada, Y. (2012). Promotion of the lipase-catalyzed hydrolysis of conjugated linoleic acid 1-menthyl ester by addition of an organic solvent. *SpringerPlus*, 1, 1-5.
- [106] Koszelewski, D., Müller, N., Schrittwieser, J. H., Faber, K., & Kroutil, W. (2010). Immobilization of  $\omega$ -transaminases by encapsulation in a sol-gel/celite matrix. *Journal of Molecular Catalysis B: Enzymatic*, 63(1-2), 39-44.
- [107] Koutinas, M., Yiangou, C., Osório, N. M., Ioannou, K., Canet, A., Valero, F., & Ferreira-Dias, S. (2018). Application of commercial and non-commercial immobilized lipases for biocatalytic production of ethyl lactate in organic solvents. *Bioresource technology*, 247, 496-503.
- [108] Kumar, A., Parihar, S. S., & Batra, N. (2012). Enrichment, isolation and optimization of lipase-producing *Staphylococcus* sp. from oil mill waste (Oil cake). *Journal of Experimental Sciences*, 3(8), 26-30.
- [109] Kumar, V., Jahan, F., Mahajan, R. V., & Saxena, R. K. (2016). Efficient regioselective acylation of quercetin using *Rhizopus oryzae* lipase and its potential as antioxidant. *Bioresource technology*, 218, 1246-1248.
- [110] Kumari, A., & Kayastha, A. M. (2011). Immobilization of soybean (*Glycine max*)  $\alpha$ -amylase onto Chitosan and Amberlite MB-150 beads: Optimization and characterization. *Journal of Molecular Catalysis B: Enzymatic*, 69(1-2), 8-14.
- [111] Laachari, F., El Bergad, F., Sadiki, M., Sayari, A., Bahafid, W., Elabed, S., Mohammed, I., & Ibsouda, S. K. (2015). Higher tolerance of a novel lipase from *Aspergillus flavus* to the presence of free fatty acids at lipid/water interface. *African Journal of Biochemistry Research*, 9(1), 9-17.
- [112] Laachari, F., El Bergadi, F., Sayari, A., Elabed, S., Mohammed, I., Harchali, E. H., & Ibsouda, S. K. (2015). Biochemical characterization of a new thermostable lipase from *Bacillus pumilus* strain/[*Bacillus pumilus* suşundan elde edilen yeni termotabil lipazın biyokimyasal karakterizasyonu]. *Turkish Journal of Biochemistry*, 40(1), 8-14.
- [113] Lampi, A.-M., Damerou, A., Li, J., Moisio, T., Partanen, R., Forsell, P., & Piironen, V. (2015). Changes in lipids and volatile compounds of oat flours and extrudates during processing and storage. *Journal of Cereal Science*, 62, 102-109.
- [114] Lee, L. P., Karbul, H. M., Citartan, M., Gopinath, S. C., LakshmiPriya, T., & Tang, T.-H. (2015). Lipase-secreting *Bacillus* species in an oil-contaminated habitat: promising strains to alleviate oil pollution. *BioMed research international*, 2015.
- [115] Liu, C.-H., Lin, Y.-H., Chen, C.-Y., & Chang, J.-S. (2009). Characterization of *Burkholderia* lipase immobilized on

- celite carriers. *Journal of the Taiwan Institute of Chemical Engineers*, 40(4), 359-363.
- [116] Liu, J., Pang, B. Q., Adams, J. P., Snajdrova, R., & Li, Z. (2017). Coupled immobilized amine dehydrogenase and glucose dehydrogenase for asymmetric synthesis of amines by reductive amination with cofactor recycling. *ChemCatChem*, 9(3), 425-431.
- [117] Livage, J., & Coradin, T. (2018). Encapsulation of enzymes, antibodies, and bacteria. *Handbook of Sol-Gel Science and Technology; Springer International Publishing: Cham, Switzerland*, 2909-2931.
- [118] Ma, B., Cheong, L.-Z., Weng, X., Tan, C.-P., & Shen, C. (2018). Lipase@ ZIF-8 nanoparticles-based biosensor for direct and sensitive detection of methyl parathion. *Electrochimica Acta*, 283, 509-516.
- [119] Magnan, E., Catarino, I., Paolucci-Jeanjean, D., Preziosi-Belloy, L., & Belleville, M. (2004). Immobilization of lipase on a ceramic membrane: activity and stability. *Journal of Membrane Science*, 241(1), 161-166.
- [120] Maldonado, R. R., Macedo, G. A., & Rodrigues, M. I. (2014). Lipase production using microorganisms from different agro-industrial by-products. *International journal of applied science and technology*.
- [121] Manzo, R. M., Ceruti, R. J., Bonazza, H. L., Adriano, W. S., Sihufe, G. A., & Mammarella, E. J. (2018). Immobilization of carboxypeptidase A into modified chitosan matrixes by covalent attachment. *Applied biochemistry and biotechnology*, 185, 1029-1043.
- [122] Marques, T. A., Baldo, C., Borsato, D., Buzato, J. B., & Celligoi, M. (2014). Utilization of dairy effluent as alternative fermentation medium for microbial lipase production. *Romanian Biotechnological Letters*, 19(1), 9042-9050.
- [123] Martins, S. L., Albuquerque, B. F., Nunes, M. A., & Ribeiro, M. H. (2018). Exploring magnetic and imprinted cross-linked enzyme aggregates of rhamnopyranosidase in microbioreactors. *Bioresource technology*, 249, 704-712.
- [124] Matto, M., & Husain, Q. (2009). Calcium alginate–starch hybrid support for both surface immobilization and entrapment of bitter melon (Momordica charantia) peroxidase. *Journal of Molecular Catalysis B: Enzymatic*, 57(1-4), 164-170.
- [125] Mendes, A. A., Castro, H. F. d., Pereira, E. B., & Furigo Júnior, A. (2005). Aplicação de lipases no tratamento de águas residuárias com elevados teores de lipídeos. *Química Nova*, 28, 296-305.
- [126] Meng, Y., Li, S., Yuan, H., Zou, D., Liu, Y., Zhu, B., & Li, X. (2015). Effect of lipase addition on hydrolysis and biomethane production of Chinese food waste. *Bioresource technology*, 179, 452-459.
- [127] Miao, C., Yang, L., Wang, Z., Luo, W., Li, H., Lv, P., & Yuan, Z. (2018). Lipase immobilization on amino-silane modified superparamagnetic Fe<sub>3</sub>O<sub>4</sub> nanoparticles as biocatalyst for biodiesel production. *Fuel*, 224, 774-782.
- [128] Miettinen, H., Nyssölä, A., Rokka, S., Kontkanen, H., & Kruus, K. (2013). Screening of microbes for lipases specific for saturated medium and long-chain fatty acids of milk fat. *International Dairy Journal*, 32(2), 61-67.
- [129] Miled, N., Bussetta, C., Rivière, M., Berti, L., & Canaan, S. (2003). Importance of the lid and cap domains for the catalytic activity of gastric lipases. *Comparative Biochemistry and Physiology Part B: Biochemistry and Molecular Biology*, 136(1), 131-138.
- [130] Mirouliaei, M., Nayyeri, H., SAMSAM, S. S., & MOVAHEDIAN, A. A. (2007). Biospecific immobilization of lactoperoxidase on Con A-Sepharose 4B.
- [131] Mohamad, N. R., Marzuki, N. H. C., Buang, N. A., Huyop, F., & Wahab, R. A. (2015). An overview of technologies for immobilization of enzymes and surface analysis techniques for immobilized enzymes. *Biotechnology & Biotechnological Equipment*, 29(2), 205-220.
- [132] Mohd Zin, N. B., Mohamad Yusof, B., Oslan, S. N., Wasoh, H., Tan, J. S., Ariff, A. B., & Halim, M. (2017). Utilization of acid pre-treated coconut dregs as a substrate for production of detergent compatible lipase by *Bacillus stratosphericus*. *AMB Express*, 7, 1-13.
- [133] Moreau, R. A., Harron, A. F., Powell, M. J., & Hoyt, J. L. (2016). A comparison of the levels of oil, carotenoids, and lipolytic enzyme activities in modern lines and hybrids of grain sorghum. *Journal of the American Oil Chemists' Society*, 93(4), 569-573.
- [134] Moreno-Pirajan, J., & Giraldo, L. (2011). Study of immobilized candida rugosa lipase for biodiesel fuel production from palm oil by flow microcalorimetry. *Arabian Journal of Chemistry*, 4(1), 55-62.
- [135] Nadar, S. S., & Rathod, V. K. (2016). Magnetic macromolecular cross linked enzyme aggregates (CLEAs) of glucoamylase. *Enzyme and Microbial Technology*, 83, 78-87.
- [136] Nadeem, U., Muhammad, D., Muhammad, S., Özkan, A., Sami, U., & Muhammad, Q. (2015). Screening identification and characterization of lipase producing soil bacteria from Upper Dir and Mardan Khyber Pakhtunkhwa, Pakistan. *International Journal of Biosciences (IJB)*, 6(2), 49-55.
- [137] Namdeo, M., & Bajpai, S. (2009). Immobilization of  $\alpha$ -amylase onto cellulose-coated magnetite (CCM) nanoparticles and preliminary starch degradation study. *Journal of Molecular Catalysis B: Enzymatic*, 59(1-3), 134-139.
- [138] Narsimha Rao, M., Kembhavi, A., & Pant, A. (2000). Immobilization of endo-polygalacturonase from *Aspergillus ustus* on silica gel. *Biotechnology letters*, 22, 1557-1559.
- [139] Nguyen, H. H., & Kim, M. (2017). An overview of techniques in enzyme immobilization. *Applied Science and Convergence Technology*, 26(6), 157-163.
- [140] Niyonzima, F., & More, S. (2015). Microbial detergent compatible lipases.
- [141] Nuyler, A., & Hongpattarakere, T. (2013). Improvement of cell-bound lipase from *Rhodotorula mucilaginosa* P11189 for use as a methanol-tolerant, whole-cell biocatalyst for production of palm-oil biodiesel. *Annals of Microbiology*, 63, 929-939.

- [142] Oliveira, F., Souza, C. E., Peclat, V. R., Salgado, J. M., Ribeiro, B. D., Coelho, M. A., Venâncio, A., & Belo, I. (2017). Optimization of lipase production by *Aspergillus ibericus* from oil cakes and its application in esterification reactions. *Food and Bioproducts Processing*, 102, 268-277.
- [143] Ovsejevi, K., Manta, C., & Batista-Viera, F. (2013). Reversible covalent immobilization of enzymes via disulfide bonds. *Immobilization of Enzymes and Cells: Third Edition*, 89-116.
- [144] Ozturkoglu-Budak, S., Wiebenga, A., Bron, P. A., & de Vries, R. P. (2016). Protease and lipase activities of fungal and bacterial strains derived from an artisanal raw ewe's milk cheese. *International Journal of Food Microbiology*, 237, 17-27.
- [145] Pahoja, V. M., & Sethar, M. A. (2002). A review of enzymatic properties of lipase in plants, animals and microorganisms. *Journal of Applied Sciences*, 2(4), 474-484.
- [146] Pahujani, S., Kanwar, S. S., Chauhan, G., & Gupta, R. (2008). Glutaraldehyde activation of polymer Nylon-6 for lipase immobilization: enzyme characteristics and stability. *Bioresource technology*, 99(7), 2566-2570.
- [147] Patil, K. J., Chopda, M. Z., & Mahajan, R. T. (2011). Lipase biodiversity. *Indian Journal of Science and Technology*, 4(8), 971-982.
- [148] Periyasamy, K., Santhalembi, L., Mortha, G., Aourousseau, M., & Subramanian, S. (2016). Carrier-free co-immobilization of xylanase, cellulase and  $\beta$ -1, 3-glucanase as combined cross-linked enzyme aggregates (combi-CLEAs) for one-pot saccharification of sugarcane bagasse. *RSC advances*, 6(39), 32849-32857.
- [149] Picó, E. A., López, C., Cruz-Izquierdo, A., Munarriz, M., Iruretagoyena, F. J., Serra, J. L., & Llama, M. J. (2018). Easy reuse of magnetic cross-linked enzyme aggregates of lipase B from *Candida antarctica* to obtain biodiesel from *Chlorella vulgaris* lipids. *Journal of bioscience and bioengineering*, 126(4), 451-457.
- [150] Planchestainer, M., Contente, M. L., Cassidy, J., Molinari, F., Tamborini, L., & Paradisi, F. (2017). Continuous flow biocatalysis: production and in-line purification of amines by immobilised transaminase from *Halomonas elongata*. *Green Chemistry*, 19(2), 372-375.
- [151] Pliego, J., Mateos, J. C., Rodriguez, J., Valero, F., Baeza, M., Femat, R., Camacho, R., Sandoval, G., & Herrera-López, E. J. (2015). Monitoring lipase/esterase activity by stopped flow in a sequential injection analysis system using p-nitrophenyl butyrate. *Sensors*, 15(2), 2798-2811.
- [152] Pogorilyi, R., Siletskaya, E. Y., Goncharik, V., Kozhara, L., & Zub, Y. L. (2007). Immobilization of urease on the silica gel surface by sol-gel method. *Russian Journal of Applied Chemistry*, 80, 330-334.
- [153] Price, J., Hofmann, B., Silva, V. T., Nordblad, M., Woodley, J. M., & Huusom, J. K. (2014). Mechanistic modeling of biodiesel production using a liquid lipase formulation. *Biotechnology progress*, 30(6), 1277-1290.
- [154] Priji, P., Unni, K. N., Sajith, S., Binod, P., & Benjamin, S. (2015). Production, optimization, and partial purification of lipase from *Pseudomonas* sp. strain BUP 6, a novel rumen bacterium characterized from M alabari goat. *Biotechnology and Applied Biochemistry*, 62(1), 71-78.
- [155] Qi, J., Li, Y., Yokoyama, W., Majeed, H., Masamba, K. G., Zhong, F., & Ma, J. (2015). Cellulosic fraction of rice bran fibre alters the conformation and inhibits the activity of porcine pancreatic lipase. *Journal of Functional Foods*, 19, 39-48.
- [156] Qiu, H., Jin, M., Li, Y., Lu, Y., Hou, Y., & Zhou, Q. (2017). Dietary lipid sources influence fatty acid composition in tissue of large yellow croaker (*Larimichthys crocea*) by regulating triacylglycerol synthesis and catabolism at the transcriptional level. *PLoS One*, 12(1), e0169985.
- [157] Raafat, A. I., Araby, E., & Lotfy, S. (2012). Enhancement of fibrinolytic enzyme production from *Bacillus subtilis* via immobilization process onto radiation synthesized starch/dimethylaminoethyl methacrylate hydrogel. *Carbohydrate polymers*, 87(2), 1369-1374.
- [158] Ramani, K., Karthikeyan, S., Boopathy, R., Kennedy, L. J., Mandal, A., & Sekaran, G. (2012). Surface functionalized mesoporous activated carbon for the immobilization of acidic lipase and their application to hydrolysis of waste cooked oil: isotherm and kinetic studies. *Process Biochemistry*, 47(3), 435-445.
- [159] Ramani, K., Kennedy, L. J., Ramakrishnan, M., & Sekaran, G. (2010). Purification, characterization and application of acidic lipase from *Pseudomonas gessardii* using beef tallow as a substrate for fats and oil hydrolysis. *Process Biochemistry*, 45(10), 1683-1691.
- [160] Ramani, K., Saranya, P., Jain, S. C., & Sekaran, G. (2013). Lipase from marine strain using cooked sunflower oil waste: production optimization and application for hydrolysis and thermodynamic studies. *Bioprocess and Biosystems Engineering*, 36, 301-315.
- [161] Ramos-Sánchez, L. B., Cujilema-Quitio, M. C., Julian-Ricardo, M. C., Cordova, J., & Fickers, P. (2015). Fungal lipase production by solid-state fermentation. *J Bioprocess Biotech*, 5(2), 1-9.
- [162] Rani, A., Das, M., & Satyanarayana, S. (2000). Preparation and characterization of amyloglucosidase adsorbed on activated charcoal. *Journal of Molecular Catalysis B: Enzymatic*, 10(5), 471-476.
- [163] Rao, C. S., Prakasham, R., Rao, A. B., & Yadav, J. (2008). Functionalized alginate as immobilization matrix in enantioselective L (+) lactic acid production by *Lactobacillus delbrueckii*. *Applied biochemistry and biotechnology*, 149, 219-228.
- [164] Rashid, F. A. A., Rahim, R. A., Ibrahim, D., Balan, A., & Bakar, N. M. A. (2013). Purification and properties of thermostable lipase from a thermophilic bacterium, *Bacillus licheniformis* IBRL-CHS2. *J Pure Appl Microbiol*, 7, 1635-1645.
- [165] Ray, A. (2012). Application of lipase in industry. *Asian Journal of Pharmacy and technology*, 2(2), 33-37.
- [166] Ribeiro, B. D., Castro, A. M. d., Coelho, M. A. Z., & Freire, D. M. G. (2011). Production and use of lipases in

- bioenergy: a review from the feedstocks to biodiesel production. *Enzyme research*, 2011.
- [167] Rivera, I., Robles, M., Mateos-Díaz, J. C., Gutierrez-Ortega, A., & Sandoval, G. (2017). Functional expression, extracellular production, purification, structure modeling and biochemical characterization of *Carica papaya* lipase 1. *Process Biochemistry*, 56, 109-116.
- [168] Rivero, C. W., & Palomo, J. M. (2016). Covalent immobilization of *Candida rugosa* lipase at alkaline pH and their application in the regioselective deprotection of per-O-acetylated thymidine. *Catalysts*, 6(8), 115.
- [169] Rodrigues, R. C., & Fernandez-Lafuente, R. (2010). Lipase from *Rhizomucor miehei* as a biocatalyst in fats and oils modification. *Journal of Molecular Catalysis B: Enzymatic*, 66(1-2), 15-32.
- [170] Rodríguez-Restrepo, Y. A., & Orrego, C. E. (2020). Immobilization of enzymes and cells on lignocellulosic materials. *Environmental Chemistry Letters*, 18, 787-806.
- [171] Romaskevicius, T., Viskantienė, E., Budriene, S., Ramanaviciene, A., & Dienys, G. (2010). Immobilization of maltogenase onto polyurethane microparticles from poly(vinyl alcohol) and hexamethylene diisocyanate. *Journal of Molecular Catalysis B: Enzymatic*, 64(3-4), 172-176.
- [172] Romero-Fernández, M., & Paradisi, F. (2020). General overview on immobilization techniques of enzymes for biocatalysis. *Catalyst Immobilization: Methods and Applications*, 409-435.
- [173] Rong, H., ChengQun, L., BaoLing, H., LiJuan, G., JiangMing, Y., RuiLong, L., JinHua, H., Yu, H., & Qiang, L. (2014). Relationships between virulence and activities of protease, chitinase and lipase produced by entomogenous *Pestalotiopsis disseminata*. *J South Agric*, 45, 1172-1177.
- [174] Rosa, C. C., Cruz, H. J., Vidal, M., & Oliva, A. G. (2002). Optical biosensor based on nitrite reductase immobilised in controlled pore glass. *Biosensors and Bioelectronics*, 17(1-2), 45-52.
- [175] Sadighi, A., Motevalizadeh, S. F., Hosseini, M., Ramazani, A., Gorgannezhad, L., Nadri, H., Deiham, B., Ganjali, M. R., Shafiee, A., & Faramarzi, M. A. (2017). Metal-chelate immobilization of lipase onto polyethylenimine coated MCM-41 for apple flavor synthesis. *Applied biochemistry and biotechnology*, 182, 1371-1389.
- [176] Sae-Leaw, T., & Benjakul, S. (2018). Lipase from liver of seabass (*Lates calcarifer*): Characteristics and the use for defatting of fish skin. *Food chemistry*, 240, 9-15.
- [177] Sahney, R., Puri, B., & Anand, S. (2005). Enzyme coated glass pH-electrode: Its fabrication and applications in the determination of urea in blood samples. *Analytica chimica acta*, 542(2), 157-161.
- [178] Sakate, P., & Salunkhe, P. (2013). Study of lipase activity during development of *Chilo partellus* (Swinhoe). *Uttar Pradesh Journal of Zoology*, 33(1), 61-68.
- [179] Salaberría, F., Palla, C., & Carrín, M. E. (2017). Hydrolytic activity of castor bean powder: effect of gum arabic, lipase and oil concentrations. *Journal of the American Oil Chemists' Society*, 94(5), 741-745.
- [180] Salis, A., Bhattacharyya, M. S., Monduzzi, M., & Solinas, V. (2009). Role of the support surface on the loading and the activity of *Pseudomonas fluorescens* lipase used for biodiesel synthesis. *Journal of Molecular Catalysis B: Enzymatic*, 57(1-4), 262-269.
- [181] Sánchez, D. A., Tonetto, G. M., & Ferreira, M. L. (2018). Burkholderia cepacia lipase: A versatile catalyst in synthesis reactions. *Biotechnology and bioengineering*, 115(1), 6-24.
- [182] Sandhu, S. S., Sharma, A. K., Beniwal, V., Goel, G., Batra, P., Kumar, A., Jaglan, S., Sharma, A., & Malhotra, S. (2012). Myco-biocontrol of insect pests: factors involved, mechanism, and regulation. *Journal of pathogens*, 2012.
- [183] Sangeetha, R., Arulpandi, I., & Geetha, A. (2011). Bacterial lipases as potential industrial biocatalysts: An overview. *Research journal of microbiology*, 6(1), 1.
- [184] Sankaran, R., Show, P. L., & Chang, J. S. (2016). Biodiesel production using immobilized lipase: feasibility and challenges. *Biofuels, Bioproducts and Biorefining*, 10(6), 896-916.
- [185] Santos, J. C. S. d., Barbosa, O., Ortiz, C., Berenguer-Murcia, A., Rodrigues, R. C., & Fernandez-Lafuente, R. (2015). Importance of the support properties for immobilization or purification of enzymes. *ChemCatChem*, 7(16), 2413-2432.
- [186] Santos, L. D., Coutinho, J. A., & Ventura, S. P. (2015). From water-in-oil to oil-in-water emulsions to optimize the production of fatty acids using ionic liquids in micellar systems. *Biotechnology progress*, 31(6), 1473-1480.
- [187] Sarmah, N., Revathi, D., Sheelu, G., Yamuna Rani, K., Sridhar, S., Mehtab, V., & Sumana, C. (2018). Recent advances on sources and industrial applications of lipases. *Biotechnology progress*, 34(1), 5-28.
- [188] Sassolas, A., Hayat, A., & Marty, J.-L. (2020). Immobilization of Enzymes on Magnetic Beads Through Affinity Interactions. *Immobilization of Enzymes and Cells: Methods and Protocols*, 189-198.
- [189] Satar, R., Matto, M., & Husain, Q. (2008). Studies on calcium alginate-pectin gel entrapped concanavalin A-bitter melon (*Momordica charantia*) peroxidase complex.
- [190] Savaghebi, D., Safari, M., Rezaei, K., Ashtari, P., & Farmani, J. (2012). Structured lipids produced through lipase-catalyzed acidolysis of canola oil.
- [191] Schneider, L. M., Adamski, N. M., Christensen, C. E., Stuart, D. B., Vautrin, S., Hansson, M., Uauy, C., & von Wettstein-Knowles, P. (2016). The Cer-cqu gene cluster determines three key players in a  $\beta$ -diketone synthase polyketide pathway synthesizing aliphatics in epicuticular waxes. *Journal of Experimental Botany*, 67(9), 2715-2730.
- [192] Senanayake, S. N., & Shahidi, F. (2002). Lipase-catalyzed incorporation of docosahexaenoic acid (DHA) into borage oil: optimization using response surface methodology. *Food chemistry*, 77(1), 115-123.
- [193] Serralha, F., Lopes, J., Lemos, F., Prazeres, D., Aires-Barros, M., Cabral, J., & Ribeiro, F. R. (1998). Zeolites as supports for an enzymatic alcoholysis reaction. *Journal of Molecular Catalysis B: Enzymatic*, 4(5-6), 303-311.

- [194] Seth, S., Chakravorty, D., Dubey, V. K., & Patra, S. (2014). An insight into plant lipase research—challenges encountered. *Protein Expression and Purification*, 95, 13-21.
- [195] Sharma, D., Sharma, B., & Shukla, A. (2010). Biotechnological approach of microbial lipase: a review. *Biotechnology (Faisalabad)*, 10(1), 23-40.
- [196] Sharma, S., & Kanwar, S. S. (2014). Organic solvent tolerant lipases and applications. *The Scientific World Journal*, 2014.
- [197] Shen, F., Yuan, H., Pang, Y., Chen, S., Zhu, B., Zou, D., Liu, Y., Ma, J., Yu, L., & Li, X. (2013). Performances of anaerobic co-digestion of fruit & vegetable waste (FVW) and food waste (FW): single-phase vs. two-phase. *Bioresource technology*, 144, 80-85.
- [198] Shen, Q., Yang, R., Hua, X., Ye, F., Zhang, W., & Zhao, W. (2011). Gelatin-templated biomimetic calcification for  $\beta$ -galactosidase immobilization. *Process Biochemistry*, 46(8), 1565-1571.
- [199] Shioji, S., Hanada, M., Hayashi, Y., Tokami, K., & Yamamoto, H. (2003). Continuous surface modification of silica particles for enzyme immobilization. *Advanced Powder Technology*, 14(2), 231-245.
- [200] Show, P.-L., Ling, T.-C., C-W Lan, J., Tey, B.-T., N Ramanan, R., Yong, S.-T., & Ooi, C.-W. (2015). Review of microbial lipase purification using aqueous two-phase systems. *Current Organic Chemistry*, 19(1), 19-29.
- [201] Silva, N. C., Miranda, J. S., Bolina, I. C., Silva, W. C., Hirata, D. B., de Castro, H. F., & Mendes, A. A. (2014). Immobilization of porcine pancreatic lipase on poly-hydroxybutyrate particles for the production of ethyl esters from macaw palm oils and pineapple flavor. *Biochemical Engineering Journal*, 82, 139-149.
- [202] Singh, R., Singh, R., & Kennedy, J. (2017). Immobilization of yeast inulinase on chitosan beads for the hydrolysis of inulin in a batch system. *International journal of biological macromolecules*, 95, 87-93.
- [203] Singh, R. K., Tiwari, M. K., Singh, R., & Lee, J.-K. (2013). From protein engineering to immobilization: promising strategies for the upgrade of industrial enzymes. *International Journal of Molecular Sciences*, 14(1), 1232-1277.
- [204] Siow, H.-L., Choi, S.-B., & Gan, C.-Y. (2016). Structure–activity studies of protease activating, lipase inhibiting, bile acid binding and cholesterol-lowering effects of pre-screened cumin seed bioactive peptides. *Journal of Functional Foods*, 27, 600-611.
- [205] Soleimani, M., Khani, A., & Najafzadeh, K. (2012).  $\alpha$ -Amylase immobilization on the silica nanoparticles for cleaning performance towards starch soils in laundry detergents. *Journal of Molecular Catalysis B: Enzymatic*, 74(1-2), 1-5.
- [206] Song, X., Qi, X., Hao, B., & Qu, Y. (2008). Studies of substrate specificities of lipases from different sources. *European journal of lipid science and technology*, 110(12), 1095-1101.
- [207] Sousa, J., Torres, A., & Freire, D. M. (2015). Nutritional enrichment of vegetable oils with long-chain n-3 fatty acids through enzymatic interesterification with a new vegetable lipase. *Grasas y Aceites*, 66(2), e071-e071.
- [208] Srivastava, A., Rao, L. J. M., & Shivanandappa, T. (2012). A novel cytoprotective antioxidant: 4-Hydroxyisophthalic acid. *Food chemistry*, 132(4), 1959-1965.
- [209] Stephany, M., Eckert, P., Bader-Mittermaier, S., Schweiggert-Weisz, U., & Carle, R. (2016). Lipoxigenase inactivation kinetics and quality-related enzyme activities of narrow-leafed lupin seeds and flakes. *LWT-Food Science and Technology*, 68, 36-43.
- [210] Su, E., Meng, Y., Ning, C., Ma, X., & Deng, S. (2018). Magnetic combined cross-linked enzyme aggregates (Combi-CLEAs) for cofactor regeneration in the synthesis of chiral alcohol. *Journal of Biotechnology*, 271, 1-7.
- [211] Su, E., Xu, J., & You, P. (2014). Functional expression of *Serratia marcescens* H30 lipase in *Escherichia coli* for efficient kinetic resolution of racemic alcohols in organic solvents. *Journal of Molecular Catalysis B: Enzymatic*, 106, 11-16.
- [212] Šulek, F., Fernández, D. P., Knez, Ž., Habulin, M., & Sheldon, R. A. (2011). Immobilization of horseradish peroxidase as crosslinked enzyme aggregates (CLEAs). *Process Biochemistry*, 46(3), 765-769.
- [213] Suwanno, S., Rakkan, T., Yunu, T., Paichid, N., Kimtun, P., Prasertsan, P., & Sangkharak, K. (2017). The production of biodiesel using residual oil from palm oil mill effluent and crude lipase from oil palm fruit as an alternative substrate and catalyst. *Fuel*, 195, 82-87.
- [214] Thakur, S. (2012). Lipases, its sources, properties and applications: a review. *Int J Sci Eng Res*, 3(7), 1-29.
- [215] Thakur, V., Tewari, R., & Sharma, R. (2014). Evaluation of production parameters for maximum lipase production by *P. stutzeri* MTCC 5618 and scale-up in bioreactor. *Chinese Journal of Biology*, 2014.
- [216] Todorova, T., Guncheva, M., Dimitrova, R., & Momchilova, S. (2015). Walnut oil—unexplored raw material for lipase-catalyzed synthesis of low-calorie structured lipids for clinical nutrition. *Journal of Food Biochemistry*, 39(5), 603-611.
- [217] Tran, D. N., & Balkus Jr, K. J. (2011). Perspective of recent progress in immobilization of enzymes. *AcS catalysis*, 1(8), 956-968.
- [218] Tümtürk, H., Karaca, N., Demirel, G., & Şahin, F. (2007). Preparation and application of poly (N, N-dimethylacrylamide-co-acrylamide) and poly (N-isopropylacrylamide-co-acrylamide)/ $\kappa$ -Carrageenan hydrogels for immobilization of lipase. *International journal of biological macromolecules*, 40(3), 281-285.
- [219] Ülker, S., Özel, A., Colak, A., & Karaoğlu, Ş. A. (2011). Isolation, production, and characterization of an extracellular lipase from *Trichoderma harzianum* isolated from soil. *Turkish Journal of Biology*, 35(5), 543-550.
- [220] Vahidi, A. K., Wang, Z., & Li, Z. (2018). Facile synthesis of s-substituted l-cysteines with nano-sized immobilized o-acetylserine sulfhydrylase. *ChemCatChem*, 10(17), 3671-3674.
- [221] Van Den Biggelaar, L., Soumillion, P., & Debecker, D. P. (2017). Enantioselective transamination in continuous flow



- mode with transaminase immobilized in a macrocellular silica monolith. *Catalysts*, 7(2), 54.
- [222] Vanleeuw, E., Winderickx, S., Thevissen, K., Lagrain, B., Dusselier, M., Cammue, B. P., & Sels, B. F. (2019). Substrate-specificity of *Candida rugosa* lipase and its industrial application. *ACS Sustainable Chemistry & Engineering*, 7(19), 15828-15844.
- [223] Vaquero, M. E., Barriuso, J., Martínez, M. J., & Prieto, A. (2016). Properties, structure, and applications of microbial sterol esterases. *Applied microbiology and biotechnology*, 100, 2047-2061.
- [224] Vaquero, M. E., Prieto, A., Barriuso, J., & Martínez, M. J. (2015). Expression and properties of three novel fungal lipases/sterol esterases predicted in silico: comparison with other enzymes of the *Candida rugosa*-like family. *Applied microbiology and biotechnology*, 99, 10057-10067.
- [225] Vargas, M., Niehus, X., Casas-Godoy, L., & Sandoval, G. (2018). Lipases as biocatalyst for biodiesel production. *Lipases and phospholipases: Methods and Protocols*, 377-390.
- [226] Vaz, R. P., & Filho, E. X. F. (2019). Ion exchange chromatography for enzyme immobilization. *Applications of ion exchange materials in biomedical industries*, 13-27.
- [227] Verger, R. (1997). 'Interfacial activation' of lipases: facts and artifacts. *Trends in biotechnology*, 15(1), 32-38.
- [228] Vescovi, V., Giordano, R. L., Mendes, A. A., & Tardioli, P. W. (2017). Immobilized lipases on functionalized silica particles as potential biocatalysts for the synthesis of fructose oleate in an organic solvent/water system. *Molecules*, 22(2), 212.
- [229] Wang, J., Liu, Z., & Zhou, Z. (2017). Improving pullulanase catalysis via reversible immobilization on modified Fe<sub>3</sub>O<sub>4</sub>@ polydopamine nanoparticles. *Applied biochemistry and biotechnology*, 182, 1467-1477.
- [230] Ward, K., Xi, J., & Stuckey, D. C. (2016). Immobilization of enzymes using non-ionic colloidal liquid aphrons (CLAs): Activity kinetics, conformation, and energetics. *Biotechnology and bioengineering*, 113(5), 970-978.
- [231] Wohlgemuth, R., Plazl, I., Žnidaršič-Plazl, P., Germaey, K. V., & Woodley, J. M. (2015). Microscale technology and biocatalytic processes: opportunities and challenges for synthesis. *Trends in biotechnology*, 33(5), 302-314.
- [232] Wong, L. S., Khan, F., & Micklefield, J. (2009). Selective covalent protein immobilization: strategies and applications. *Chemical reviews*, 109(9), 4025-4053.
- [233] Wu, J. C. Y., Hutchings, C. H., Lindsay, M. J., Werner, C. J., & Bundy, B. C. (2015). Enhanced enzyme stability through site-directed covalent immobilization. *Journal of Biotechnology*, 193, 83-90.
- [234] Xiang, Z., Liu, Z., Chen, X., Wu, Q., & Lin, X. (2013). Biocatalysts for cascade reaction: porcine pancreas lipase (PPL)-catalyzed synthesis of bis (indolyl) alkanes. *Amino Acids*, 45, 937-945.
- [235] Xiangli, Q., Zhe, L., Zhiwei, L., Yinglin, Z., & Zhengjia, Z. (2010). Immobilization of activated sludge in poly (ethylene glycol) by UV technology and its application in micro-polluted wastewater. *Biochemical Engineering Journal*, 50(1-2), 71-76.
- [236] Xie, W., & Huang, M. (2018). Immobilization of *Candida rugosa* lipase onto graphene oxide Fe<sub>3</sub>O<sub>4</sub> nanocomposite: Characterization and application for biodiesel production. *Energy Conversion and Management*, 159, 42-53.
- [237] Xie, W., Khosasih, V., Suwanto, A., & Kim, H.-K. (2012). Characterization of lipases from *Staphylococcus aureus* and *Staphylococcus epidermidis* isolated from human facial sebaceous skin. *Journal of microbiology and biotechnology*, 22(1), 84-91.
- [238] Xing, G.-W., Li, X.-W., Tian, G.-L., & Ye, Y.-H. (2000). Enzymatic peptide synthesis in organic solvent with different zeolites as immobilization matrixes. *Tetrahedron*, 56(22), 3517-3522.
- [239] Yücel, S., Terzioğlu, P., & Özçimen, D. (2012). Lipase applications in biodiesel production. *Biodiesel-Feedstocks, Production and Applications. InTech, Croatia*, 209-250.
- [240] Zaki, N. H., & Saeed, S. E. (2012). Production, purification and characterization of extra cellular lipase from *Serratia marcescens* and its potential activity for hydrolysis of edible oils. *Al-Nahrain Journal of Science*, 15(1), 94-102.
- [241] Zdarta, J., Meyer, A. S., Jesionowski, T., & Pinelo, M. (2018). A general overview of support materials for enzyme immobilization: characteristics, properties, practical utility. *Catalysts*, 8(2), 92.
- [242] Zhang, W., Tang, Y., Liu, J., Ma, Y., Jiang, L., Huang, W., Huo, F.-w., & Tian, D. (2014). An electrochemical sensor for detecting triglyceride based on biomimetic polydopamine and gold nanocomposite. *Journal of Materials Chemistry B*, 2(48), 8490-8495.
- [243] Zhang, Y., Ge, J., & Liu, Z. (2015). Enhanced activity of immobilized or chemically modified enzymes. *ACS catalysis*, 5(8), 4503-4513.
- [244] Zheng, J., Xie, B.-H., Chen, Y.-L., Cao, J.-F., Yang, Y., Guan, Z., & He, Y.-H. (2014). Direct asymmetric aldol reactions catalyzed by lipase from porcine pancreas. *Zeitschrift für Naturforschung C*, 69(3-4), 170-180.
- [245] Zheng, P., Xu, Y., Wang, W., Qin, X., Ning, Z., Wang, Y., & Yang, B. (2014). Production of diacylglycerol-mixture of regioisomers with high purity by two-step enzymatic reactions combined with molecular distillation. *Journal of the American Oil Chemists' Society*, 91(2), 251-259.
- [246] Zou, X., Su, H., Zhang, F., Zhang, H., Yeerbolati, Y., Xu, X., Chao, Z., Zheng, L., & Jiang, B. (2023). Bioimprinted lipase-catalyzed synthesis of medium-and long-chain structured lipids rich in docosahexaenoic acid for infant formula. *Food chemistry*, 424, 136450.
- [247] Zubiolo, C., Santos, R. C. A., Figueiredo, R. T., Soares, C. M. F., & de Aquino Santana, L. C. L. (2015). Morphological and physicochemical aspects of microbial lipase obtained from novel agroindustrial waste encapsulated in a sol-gel matrix. *Journal of Thermal Analysis and Calorimetry*, 120, 1503-1509.



## Laying and growth performance of local chicken (*Gallus gallus domesticus*) ecotype Konde in Burkina Faso

ZARE Yacouba<sup>1,2\*</sup>, GNANDA B. Isidore<sup>1</sup>, KERE Michel<sup>2</sup>, TRAORE Boureima<sup>3</sup>, HOUAGA Isidore<sup>4</sup>, SANON F. Boris<sup>1,2</sup>, ILBOUDO W. Fernand 1<sup>er</sup> jumeau<sup>1,2</sup>, BOUGOUMA-YAMEOGO M. C. Valérie<sup>2</sup>, REKAYA Romdhane<sup>5</sup>, NIANOGO A. Joseph<sup>2</sup>

<sup>1</sup>Institut de l'Environnement et de Recherches Agricoles (INERA), Département Productions Animales, Ouagadougou, Burkina Faso

<sup>2</sup>Université Nazi BONI, Institut du Développement Rural, Bobo-Dioulasso, Burkina Faso

<sup>3</sup>Université Joseph KI-ZERBO, Unité de Formation en Sciences de la vie et de la Terre (UFR/SVT), Laboratoire de Physiologie Animale, Burkina Faso

<sup>4</sup>University of Edinburgh, Centre for Tropical Livestock Genetics and Health (CTLGH), Roslin Institute, Midlothian, EH25 9RG, United Kingdom

<sup>5</sup> University of Georgia, Athens, Department of Animal and Dairy Science, Department of Statistics, Institute of Bioinformatics, 106 Animal and Dairy Science Complex, GA 30602, USA

\* Adresse de l'auteur correspondant : ZARE Yacouba, [yacoubzar@yahoo.fr](mailto:yacoubzar@yahoo.fr)

Received: 17 Oct 2023; Received in revised form: 25 Nov 2023; Accepted: 02 Dec 2023; Available online: 16 Dec 2023

©2023 The Author(s). Published by Infogain Publication. This is an open access article under the CC BY license

(<https://creativecommons.org/licenses/by/4.0/>).

**Abstract**— Limited information exists regarding the zootechnical performance of the local chicken ecotype Konde. The objective of this study was to evaluate the laying and growth performance of local hens *Gallus gallus domesticus* ecotype Konde in a semi-intensive production system. A founder group of breeders (30 hens and 6 roosters) from the Boulgou Province (Garango, Zabré and Tenkodogo) was set up at a ratio of one (1) rooster for five (5) hens. Eggs were collected and identified daily. After five days of collection, eggs were naturally incubated under large brood hens (15 to 20 eggs) and then transferred to a compartmentalized and numbered hatcher. These incubations resulted in 306 identifiable one-day-old chicks (106 in the wet season, 103 in the cold dry season and 100 in the hot dry season). The individual weight (IW) of the chicks was recorded every week from hatching to three (3) months of age. Carcass characteristics were assessed on 10 birds per rearing period at 3 months of age. The laying rate was 33.60% during a 180-day laying period. Observed fertility and hatching rates were 60.33 and 80.31%, respectively. The average weight, length and large diameter of the eggs were 41.33 g, 48.75±2.07mm and 36.42±1.6mm, respectively. The results showed that chicks with an average hatching weight of around 28g reached, at three months of age, 926.64 ± 153 g, 884.06 ± 133 g, and 857.44 ± 105 g during the rainy, cold-dry, and hot-dry seasons, respectively. Carcass yield was 62.19, 66.46, and 65.91% in the rainy, hot, and dry seasons, respectively. A detailed economic evaluation showed a gross profit of 922 FCFA per bird at 3 months of age. Based on the growth performance, the local chicken ecotype Konde could be used for meat production. However, further improvement of performance and sustainability of the chicken's ecotype Konde through genetic selection and management tools is still needed.



**Keywords**— local chicken ecotype Konde, laying, growth, carcass yield, Burkina Faso

## I. INTRODUCTION

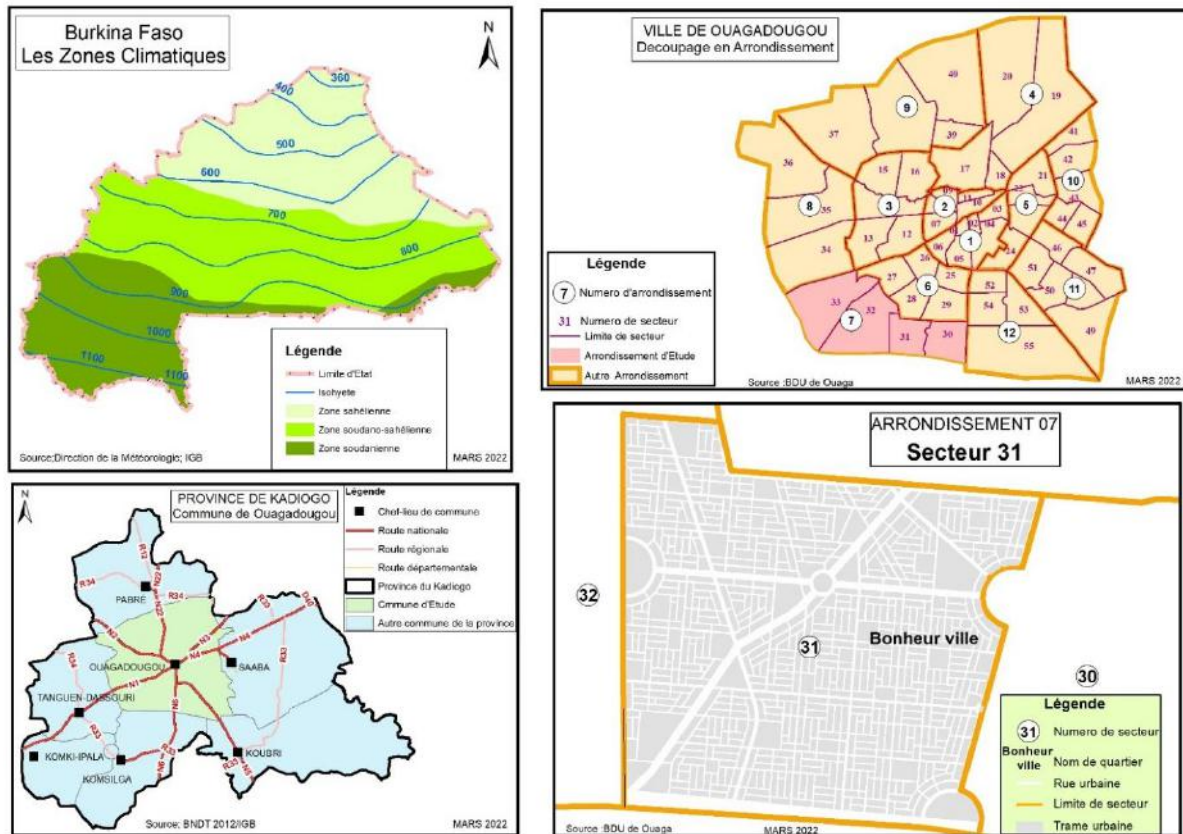
Poultry farming is practiced in all countries of the world and conducted by all social strata of the population (Lara and Rostagno, 2013; FAO, 2019a; Ngongolo *et al.*, 2021). It is therefore an important lever for economic growth and a powerful tool to tackle poverty and food insecurity in several areas of the world including Burkina Faso (Ouattara *et al.*, 2014a; Ouedraogo *et al.*, 2015). In Burkina Faso, the poultry population is estimated at around 45 million birds and is composed of chickens (76.3%), guinea fowl (19.2%), pigeons (3.7%), ducks (0.7%), and turkeys (0.1%) (FAO, 2019b). The poultry sector plays a prominent role in the Burkinabe livestock sub-sector. It accounts for 6% of agricultural value added (\$0.14 billion) and contributes more than 140,000 and 6,000 tons of meat and eggs per year, respectively (FAO, 2019b). The per capita consumption of poultry meat and eggs in Africa is estimated at 8kg and between 45 and 50 eggs (about 1kg) per person and year (FAO, 2019b). Local chicken and other local poultry products are better appreciated by the consumers compared to products of exotic breeds (Rajkumar *et al.*, 2017) largely due to hardness and organoleptic properties of the meat. Local poultry breeds accounts for over 98% of the national poultry population (FAO, 2019b). Despite its socio-economic impact and its important contribution to the population food security, the productivity of the local poultry population remains low compared to exotic breeds (FAO, 2019b). Thus, local poultry production is well below the needs of the population. The unbalance between the demand and the supply produced by local poultry breeds has forced Burkina Faso to turn to imports of exotic chickens to meet national consumption needs, estimated at about 37,000 tons of chicken meat annually (FAO, 2019b). The poor performance of traditional poultry farming is due

to several factors; chief among them is the low genetic potential of the breeding stock and the artisanal husbandry system characterized by low scientific and economic investments (Ouattara *et al.*, 2014a; Ouedraogo *et al.*, 2015). However, the promotion of local poultry farming and the gradual improvement of farming technique are proving to be the determining factors for economic development (Yapi-Gnaore *et al.* 2011) and the safeguarding of genetic resources and biodiversity (Yapi-Gnaore *et al.*, 2011; Tadano *et al.*, 2013). Several studies (Akouango *et al.*, 2010; Yapi-Gnaore *et al.*, 2011; Rajkumar *et al.*, 2017) have been carried out to investigate the laying and growth potentials of local chicken. However, information about the zootechnical performance of the ecotype Konde is scant at best. In spite of the good potential of the ecotype Konde to be used as a broiler breed (Zare *et al.*, 2021), there is a persistent danger for its disappearance (Ouandaogo, 1975; Zare *et al.*, 2021). The general aim of the present study is to dissect the performance of the local hen (*Gallus gallus domesticus*), particularly that of the ecotype Konde in improved breeding systems with the specific objective of evaluating the laying and growth performance of the local chicken ecotype Konde in a semi-intensive rearing system.

## II. MATERIAL AND METHODS

### 2.1. Presentation of the study area

The present study was carried out at a poultry farm belonging to the station of the Institut de l'Environnement et de Recherches Agricoles (INERA) in Ouagadougou, Burkina Faso. This poultry farm is located in the peri-urban area of the town of Ouagadougou in sector 31 of the seventh district, capital of the province of Kadiogo and it is located in the center of Burkina Faso (Map 1).



Map 1: Map location of the study area in the commune of Ouagadougou (IGB, 2014).

## 2.2 Materials

### 2.2.1. Biological material

In concordance with the sample size requirements per breed or population for the study of domestic animal biodiversity, the FAO guidelines recommend at least 25 individuals per breed/population (FAO, 1998). The current study involved 36 ecotype Konde chicken birds aged between 5 and 6 months. Hens (n=30) and roosters (n=6) of the breeding nucleus came from different villages in the Boulgou province. These chickens were selected based on their morpho-biometric characteristics, notably plumage, crest, height on legs, and leg color as suggested by Zare *et al.* (2021). They were randomly distributed into 6 pens according to their area of origin. Several incubations were carried out and resulted in 306 identifiable day-old chicks distributed across three time periods: 106 birds in the rainy season, 103 birds in the cold dry season, and 100 birds in the hot dry season.

### 2.2.2. Rearing building

The trial building was subdivided into eleven pens (3 m high, 2.25 m long and 1.15 m wide). Each pen housed one rooster and 5 hens. The building model used was an open structure where the environmental conditions were not controlled. A hygrometer was used to measure relative

humidity and temperature. Wood shavings were used as bedding for the welfare of the chickens.

## 2.3 Method

### 2.3.1. Monitoring of laying and incubation

Eggs were removed as soon as they were laid and coded based on the pen location "C", the hen's y-number "P" and the egg's rank n (CxPyn). Each egg was recorded according to the breeding cock and the hen on individual identification cards. Eggs that could not be properly identified were coded as non-identifiable (NI). Properly identified eggs were placed in natural brooding on the basis of 15 to 20 eggs per broody hen. Two candling sessions were carried out at day 7 and 18 respectively. Immediately after the second candling, the eggs in the beginning of hatching were taken from under the broody hens and put in an electronic incubator transformed into a hatcher containing a labeled (1 to 35) box. Replication (R) involved the egg-laying cycle (duration of egg-laying until brooding instinct or pause period) of the parents and the first generation. The egg collection was extended over a period of 6 months in order to generate five replicates.

The collected data was used to evaluate the following zootechnical parameters: General laying rate (GLR) and individual laying rate (ILR);

$$GLR = \frac{\text{number of eggs laid}}{\text{laying duration} * \text{hens}} \times 100$$

$$ILR = \frac{\text{number of eggs laid by a hen}}{\text{laying duration}} \times 100$$

The actual fertility (FR) and hatching (HR) rates were calculated according to the formulas of Sauveur (1988):

$$FR = \frac{\text{number of fertile eggs}}{\text{number of eggs laid}} \times 100$$

$$HR = \frac{\text{number of hatched eggs}}{\text{number of fertile eggs}} \times 100$$

Embryonic mortality rates were calculated using the following formulas: early embryonic mortality rate (EEMR), late embryonic mortality rate (LEMUR) and chick mortality rate (CMR),

$$EEMR = \frac{\text{number of eggs with dead embryo at day 15}}{\text{number of fertile eggs}} \times 100$$

$$LEMUR = \frac{\text{number of eggs with dead embryo at day 24}}{\text{number of fertile eggs}} \times 100$$

$$CMR = \frac{\text{number of deaths in a period}}{\text{number of birds during the same period}} \times 100$$

The average egg Shape index (ESI) used to measure the mechanical strength of the shell was calculated according to the formulas presented by Sanfo *et al.*, (2012)

$$ESI = \frac{\text{length}}{\text{width}}$$

Egg characteristics were calculated using the following formulas: clear egg rate (CER), average egg weight (AEW) and average number of eggs per hen and per year (ANEHY).

$$CER = \frac{\text{number of clear eggs}}{\text{number of incubated eggs}} \times 100$$

$$AEW = \frac{\text{sum of egg weights}}{\text{number of eggs}}$$

$$ANEHY = \frac{\text{sum of eggs laid by all hens per year}}{\text{number of hens}}$$

### 2.3.2. Production and rearing of chicks

Eggs were collected and identified daily and kept in incubators then put in natural incubation from the 5th and 7th day of collection in the dry and rainy seasons, respectively. The chicks were weighed and identified as soon as they hatched. They were reared in the brooder from the first week to the third week at a density of 25 chicks/m<sup>2</sup> and then from the fourth week at a density of 10 chicks/m<sup>2</sup> in screened pens (4.5m x 1.15m). Each chick was identified with a numbered plastic ring placed on its leg. These bands were replaced at five (5) weeks of age with numbered metal bands attached to the right-wing membrane.

### 2.3.3. Feeding of hens and chicks

Each laying hen received 80 g of feed per day. A summary of the feed characteristics is presented in Table 1. The chicks received the same ration consisting of the starter feed (galdus) up to 2 weeks of age followed by the feed presented in Table 1. The chicks received 7 g of galdus feed per day for 3 days and 10 g of galdus feed per day for 4 days for the first week of age (galdus is a high nutritional value starter feed). Starting at day 14, they received the growth feed. Birds were weighed weekly at which time the ration was increased by 5 g for each bird during the three months of the study. The feed was distributed in the mornings. Water was provided ad libitum using the national water distribution network. The individual weights (IW) of chicks were recorded weekly from hatching to three (3) months of age. Weighs were collected before feed distribution. After hatching, the chicks were placed in a brooder equipped with a heating bulb (60 W) for one month.

The following intake related parameters were calculated: feed intake index (FII) and average consumption per bird (ACB).

$$FII = \frac{\text{feed consumption during a period (g)}}{\text{Egg mass during the period (g)}}$$

$$ACB = \frac{\text{amount of feed served} - \text{refusals}}{\text{number of birds}}$$

Table 1. Bromatological composition of feed rations

Ingredients (%)	Starter feed (galdus)	Growth feed	Laying feed
	1 to 14 days	15 to 84 days	≥85 days
Corn (Maize)	-	60	66.5
Wheat bran	-	0	9.35
Soybean	-	10.85	0
Soybean meal	-	14	9
Cottonseed cake	-	3	2
Fish meal	-	6	5.3
Oyster shells	-	2	4.5
Salt	-	0.15	0.15
Broiler premix	-	2.5	2.5
Methionine	-	0.1	0.25
Lysine	-	0.3	0.21
Iron Sulfate	-	0.1	0.14
Bicalcium phosphate	-	1	0.1
<b>Total</b>	-	<b>100</b>	100
Nutritional composition			
<b>Metabolizable energy (kcal/kg)</b>	<b>3150</b>	<b>3016.24</b>	<b>2855.8</b>
<b>Fat (%)</b>	-	<b>5.15</b>	<b>3.59</b>
<b>Crude protein (%)</b>	<b>22</b>	<b>21.19</b>	<b>16</b>
<b>Crude fiber (%)</b>	-	<b>3.15</b>	<b>3.16</b>
<b>Lysine (%)</b>	<b>1.3</b>	<b>0.48</b>	<b>0.92</b>
<b>Methionine (%)</b>	<b>0.6</b>	<b>0.82</b>	<b>0.56</b>
<b>Methionine + Cys (%)</b>	<b>0.95</b>	<b>1.38</b>	<b>0.82</b>
<b>Calcium (%)</b>	<b>0.95</b>	<b>0.46</b>	<b>2.05</b>
<b>Phosphorus (%)</b>	<b>0.60</b>	<b>0.13</b>	<b>0.28</b>
<b>Sodium (%)</b>	-	<b>0.25</b>	<b>0.13</b>
<b>Chloride (%)</b>			<b>0.23</b>

#### 2.3.4. Growth rate and carcass characteristics

Carcass characteristics were assessed by sacrificing ten (10) animals at the age of twelve (12) weeks per rearing period. Birds were slaughtered in the morning on an empty stomach. The birds were first weighed to determine their live weight. After bleeding, they were plucked to determine the weight of feathers, carcass, liver, gizzard, intestines, legs, and head. The data collected allowed us to calculate the following zootechnical parameters: average daily gain (ADG), feed conversion (FC) and carcass yield (CY).

$$ADG = \frac{\text{weight gain during a week}}{7}$$

$$FC = \frac{\text{feed consumed during a period}}{\text{weight gain during the same period}}$$

$$CY = \frac{\text{carcass weight}}{\text{live weight at slaughter}} \times 100$$

#### 2.3.5. Economic studies

In order to evaluate the economic performance, a financial analysis in the form of a profit and loss account was carried out during all the breeding seasons. The results

obtained were divided into variable expenses, fixed expenses, and products.

To assess the economic profitability, the following formulas were used:

Feed cost/phase = FC \* price per kg of feed (FCFA)

where FC is the total feed consumed (in kg) per phase (Start-up and growth)

Feed cost =  $\sum$  Feed cost/phase (FCFA)

Sale of chickens = Number of chickens \* sale price of a chicken (FCFA)

Cost of production =  $\sum$  expenses (FCFA)

Profit = Income - expenses (FCFA)

### 2.3.6. Sanitary protocol

Basic hygiene measures were applied at the level of the rearing equipment by regular washing and disinfection and sometimes the application of sanitary voids in the pens. In general, the animals were maintained in accordance with the vaccination schedule for local chickens. As biosecurity measure, a foot bath was installed. The health monitoring adopted in the trial was that established by the Centre de Promotion de l'Aviculture Villageoise (CPAVI).

### 2.3.7. Statistical analyses

Table 2. Production and reproductive performance of Konde ecotype hens during a 24-week period.

Production performance					
	AL (Weeks)	ANE/ Laying Cycle	ALI/ Cycle	AEH / P	ALR (%)
<b>Mean</b>	20 ± 1.16	11 ± 3	16 ± 2	61 ± 3	33.60
<b>Maximum</b>	24	17	18	81	44.94
<b>Minimum</b>	20	10	11	48	26.20
Reproduction performance					
	FR (%)	CER (%)	EEMR (%)	LEMR (%)	HR (%)
<b>Mean</b>	60.33	39.67	7.80	18.44	81.56
<b>Maximum</b>	68.26	45.85	10.17	25.18	84.60
<b>Minimum</b>	54.15	31.74	6.19	15.40	74.82

AL: Age at laying; ANE: Average number of eggs; ALI: Average laying interval; ALR: Average laying rate; AEH/P: Average eggs per hen; EEMR: Early embryonic mortality rate; LEMR: Late embryonic mortality rate; HR: Hatching rate; FR: Fertility rate; CER: Clear egg rate

### 3.2. External egg quality characteristics of local ecotype Konde

The average egg weight (AEW) was 41.33 g and varied between 38.37 (first month of laying) and 42.54 g (six month of laying) as indicated in Table 2. The AEW increased, as expected, with the age of the hen. The average egg length (EL) and large diameter of the eggs

The collected data was stored as an Excel spreadsheet (Microsoft Excel 2016). Data processing and analysis were implemented using "R" software (version 4.1.1). Charts and tables were produced using Microsoft Excel 2016 software. Analysis of variance using Turkey's test for mean separation was performed on the parametric quantitative data. Nonparametric analyses were performed by the Kruskal Wallys test using the Pairwise Test for median separation.

## III. RESULTS

### 3.1. Laying performance

The laying rate average was 33.60% and ranged between 26.20 and 44.94%. This translates to an average of around 61 ± 3 eggs per hen during a six-month period (Table 2). In average, hens start laying at about 20 weeks of age. However, there is substantial variation as some hens start laying at 2 years of age. Fertility rate ranged between 54 and 68.26% with an average of 60.33%. The early and late embryonic mortality rates were 7.80% and 18.44%, respectively. The average hatching rate was around 82% with a maximum and minimum of 84.60% and 74.82%, respectively.

(LD) were 48.75±2.07mm and 36.42±1.6mm, respectively (Table 3). Mean egg shape index (ESI) ranged between 0.74±1.31 to 0.75±1.58 with a mean of 0.75±0.01. Out of a total of 1815 eggs collected, hens laid more eggs with white shells (79.12%) than with dirty white shells (20.88%) (Table 3). All eggs were oval in shape (100%).

Table 3. Local chicken ecotype Konde egg characteristics

Quantitative external egg characteristics								
	M1	M2	M3	M4	M5	M6	Mean	
<b>AEW</b> (g)	38.37±3.06	39.72±3.10	41.6±3.37	42.52±4.15	44.44±7.11	42.54±3.84	41.33±2.37	
<b>EL</b> (mm)	46.27±1.45	47.14±1.50	47.85±1.93	48.89±1.79	51.23±3.60	51.12±1.38	48.75±2.07	
<b>LD</b> (mm)	34.56±1.25	34.93±1.12	35.67±1.24	36.94±1.17	38.06±2.03	38.33±0.95	36.42±1.6	
<b>ESI</b>	0.75±1.35	0.74±1.31	0.75±1.58	0.76±1.48	0.74±2.81	0.75±1.16	0.75±0.01	
External egg qualitative characteristics								
Egg characteristics				N				%
<b>Color</b>	white shells			1436				79.12
	dirty white shells			379				20.88
<b>Total</b>				1815				100
<b>Egg shape</b>	<b>Round</b>			0				0
	Oval			1815				100
<b>Total</b>				1815				100

M<sub>i</sub>: Month i (i=1, 2, ..., 6); N: number of eggs; %: total percentage

### 3.3. Quantity of feed served and consumed

Feed intake index for egg production (FIIE) ranged from 6.23 to 7.33 with an average of 6.62±0.5 (Table 4). The average daily feed consumption per hen (ADFCB) was 53.91±4.10 g and ranged between 49.72 and 59.38 g (Table 4).

Table 4. Feed consumption parameters of local Konde ecotype chickens

	N	AFSB(g)	RB	ADFCB	FIIE
<b>Mean</b>	30	80	26.09±4,10	53.91±4,10	6.62±0.5
<b>Maximum</b>		80	30.28	59.38	7.33
<b>Minimum</b>		80	20.62	49.72	6.23

N: Number of birds; AFSB B: **amount of feed served** per bird; RB: Refusals per bird ; AFB: Average daily feed consumption per bird; FII / B: Feed intake Index per bird for eggs production.

### 3.4. Average daily gain, feed intake, and mortality rate at 12 weeks of age

The average daily gain (ADG) varied with the age of the chicks (Table 5). The mean ADG was 10.69, 10.17, and 9.88 g in the wet, cold dry, and hot dry seasons, respectively. Across all rearing seasons, the ADG was 10.25 g. There was no significant difference in ADG between seasons. The feed intake index per bird for meat production (FIIM) showed significant changes across the different rearing seasons (Table 5). The farm recorded cumulative FIIM was 3.41, 3.58 and 3.55 for the rainy, cold dry and hot dry seasons respectively. The highest

FIIM was 4.48 and was observed in the seventh week during the hot dry season and the lowest (1.88) was recorded during the second week of the rainy season. The overall FIIM was 3.51 over the entire rearing period. However, there was no significant difference between the overall FIIM across seasons, although there were significant differences across some weeks.

Twenty-one birds died resulting in a general mortality rate of 6.80% (Table 5). The highest mortality rate (9.43%) was observed during the rainy season (10 birds died), followed by the warm season with a total of seven deaths (mortality rate of 6.80%). The lowest mortality rate (4%)



was observed during the cold dry season with only four deaths. For the rainy season, the highest mortality rate was observed during the 4th week with four (4) losses or 3.81%. During the cold dry season, the highest mortality

rate was observed during the 6th week with two (2) deaths or 2.02%. For the hot dry season, the highest mortality rate was observed during the 2nd week with two (2) deaths or 1.98%.

Table 5. Evolution of average daily gain (ADG), feed intake index for muscle (FIIM), and mortality rate during 3 seasons for Konde ecotype hens

	ADG RS (g)	FIIM RS	Mortality RS	ADG CDS (g)	FIIM CDS	Mortality CDS	ADG HDS (g)	FIIM HDS	Mortality HDS
<b>S1</b>	4.23 <sup>a</sup>	1.89 <sup>a</sup>	0.94	2.20 <sup>b</sup>	3.80 <sup>b</sup>	0	2.01 <sup>b</sup>	4.08 <sup>b</sup>	1.94
<b>S2</b>	7.15 <sup>a</sup>	1.88 <sup>a</sup>	0	3.71 <sup>b</sup>	3.85 <sup>b</sup>	0	4.89 <sup>c</sup>	2.87 <sup>a</sup>	1.98
<b>S3</b>	6.50 <sup>a</sup>	2.67 <sup>a</sup>	0	5.83 <sup>b</sup>	3.35 <sup>b</sup>	0	6.50 <sup>a</sup>	2.11 <sup>a</sup>	0
<b>S4</b>	6.39 <sup>a</sup>	3.53 <sup>a</sup>	3.81	7.99 <sup>b</sup>	2.95 <sup>b</sup>	0	7.00 <sup>a</sup>	3.19 <sup>ab</sup>	0
<b>S5</b>	8.45 <sup>a</sup>	3.21 <sup>a</sup>	1.98	7.59 <sup>a</sup>	3.73 <sup>a</sup>	1	8.38 <sup>a</sup>	3.09 <sup>a</sup>	0
<b>S6</b>	10.13 <sup>a</sup>	3.42 <sup>a</sup>	0	9.27 <sup>a</sup>	3.62 <sup>a</sup>	2.02	9.01 <sup>a</sup>	3.45 <sup>a</sup>	0
<b>S7</b>	13.20 <sup>a</sup>	3.03 <sup>a</sup>	2.02	9.81 <sup>b</sup>	3.99 <sup>b</sup>	0	8.58 <sup>b</sup>	4.48 <sup>b</sup>	1.01
<b>S8</b>	12.70 <sup>a</sup>	3.54 <sup>a</sup>	1.03	13.20 <sup>a</sup>	3.36 <sup>a</sup>	0	10.19 <sup>b</sup>	4.02 <sup>a</sup>	0
<b>S9</b>	14.47 <sup>a</sup>	3.43 <sup>a</sup>	0	13.67 <sup>a</sup>	3.64 <sup>a</sup>	0	12.65 <sup>a</sup>	3.92 <sup>a</sup>	1.02
<b>S10</b>	15.24 <sup>a</sup>	3.61 <sup>a</sup>	0	14.80 <sup>a</sup>	3.72 <sup>a</sup>	1.03	16.55 <sup>a</sup>	3.29 <sup>a</sup>	0
<b>S11</b>	15.35 <sup>a</sup>	3.90 <sup>a</sup>	0	16.56 <sup>b</sup>	3.62 <sup>a</sup>	0	14.81 <sup>a</sup>	3.93 <sup>a</sup>	1.03
<b>S12</b>	14.44 <sup>a</sup>	4.49 <sup>a</sup>	0	17.45 <sup>b</sup>	3.71 <sup>b</sup>	0	18.05 <sup>b</sup>	3.56 <sup>b</sup>	0
<b>Mean</b>	10.69 <sup>a</sup>	<b>3.41<sup>a</sup></b>	9.43	10.17 <sup>a</sup>	<b>3.58<sup>a</sup></b>	4	9.88 <sup>a</sup>	<b>3.55<sup>a</sup></b>	6.8

Means marked with the same letter in the same row are not significantly different ( $p > 0.05$ ) at the Kruskal Wallis pairwise test; RS: Rainy Season; CDS: Cold Dry Season; HDS: Hot Dry Season; S: week; each number indicates week number or age of birds;

### 3.5. Growth curve of chicks

The average hatch weight was 29.61 ( $\pm 3.16$ ), 28.85 ( $\pm 3.32$ ), and 27.19 g ( $\pm 3.10$  g) during the cold dry (CDS), the rainy (RS), the hot dry (HDS) seasons, respectively. The average hatch weight for all rearing seasons was 28.55 g (Fig 1). Difference in hatch weight was not significant between RS and CDS. However, hatching weights were significantly different between the latter seasons and HDS. The mean body weight (BW) of chickens at twelve (12) weeks of age was 926.64 g  $\pm$  153.18 g (877.27 g  $\pm$  120.06

g and 976 g  $\pm$  167.43 g for females and males, respectively) during RS, 884.06 g  $\pm$  132.92 g (839, 69 g  $\pm$  101.85 g and 923.22 g  $\pm$  145.85 g for females and males, respectively) during SSF, and 857.44 g  $\pm$  105.43g (837g  $\pm$  96.68 g and 884.85 g  $\pm$  111.51 g for females and males, respectively) during HDS as presented in Fig 1. The highest (1,400g  $\pm$  132.92g) and lowest (644g  $\pm$  132.92g) live weights at twelve (12) weeks of age were observed in CDS.

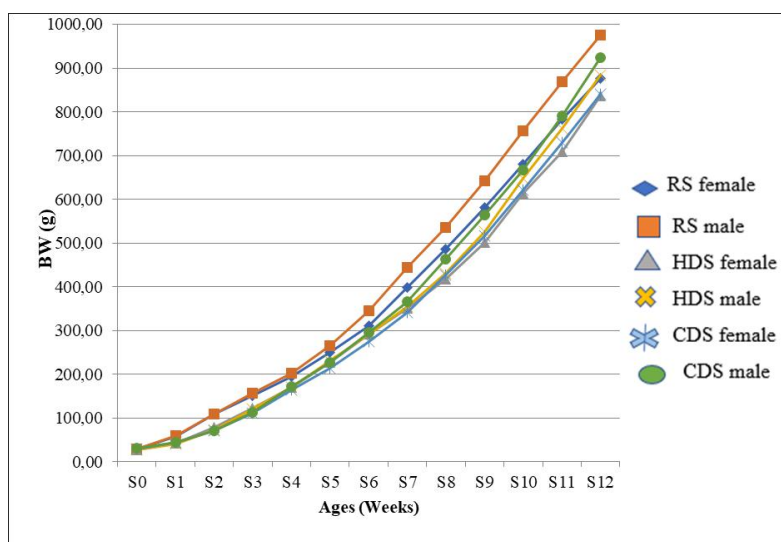


Fig 1. Evolution of body weight of local chicken ecotype Konde during the Rainy (RS), Cold and Dry (CDS), and Hot and Dry (HDS) seasons

### 3.6. Carcass yield

The carcass characteristics at 12 weeks of age are presented in Table 6. Across all rearing seasons, the average body weight of birds used for carcass characteristics was 998.73 g. The Average carcass weight was 648.50 g and the overall carcass yield was 64.93% (Table 6). The highest carcass yield (65.91%) was

observed during the HDS season followed by the cold dry season with a carcass yield of 65.37%. The rainy season had the lowest carcass yield (62.19%). Carcass yield was significantly difference between the RS and both CDS and HDS. A significant difference in carcass yield was observed between males and females (males had higher carcass yield).

Table 6. Organ weights and carcass yield at 12 weeks of age

Season	Sex	Body Weight(g)	Carcass Weight (g)	Feathers (g)	Head+tarsus (g)	Intestines (g)	Liver (g)	Gizzard (g)	carcass yield (%)
RS	F(n=5)	862.40	516.60	44.80	79.40	74.20	20.40	27.60	59.90 <sup>a</sup>
	M(n=5)	1033.40	662.40	44.20	136.80	77.60	26.80	34.20	64.10 <sup>b</sup>
	<b>Total (n=10)</b>	<b>947.90</b>	<b>589.50</b>	<b>44.50</b>	<b>108.10</b>	<b>75.90</b>	<b>23.60</b>	<b>30.90</b>	<b>62.19<sup>a</sup></b>
CDS	F(n=6)	1059	688.00	46.67	81.00	43.00	25.00	25.33	64.96 <sup>b</sup>
	M(n=5)	1131.00	744.00	85.00	90.14	79.43	27.00	42.00	65.78 <sup>c</sup>
	<b>Total (n=11)</b>	<b>1094.20</b>	<b>727.20</b>	<b>73.50</b>	<b>87.40</b>	<b>68.50</b>	<b>26.40</b>	<b>37.00</b>	<b>65.37<sup>b</sup></b>
HDS	F(n=5)	826.50	532.50	45.00	78.00	35.50	22.50	29.00	64.43 <sup>b</sup>
	M(n=5)	986.00	652.88	74.75	84.13	59.88	21.63	35.00	66.21 <sup>c</sup>
	<b>Total (n=10)</b>	<b>954.10</b>	<b>628.80</b>	<b>68.80</b>	<b>82.90</b>	<b>55.00</b>	<b>21.80</b>	<b>33.80</b>	<b>65.91<sup>b</sup></b>
<b>Mean</b>	<b>Total (n= 31)</b>	<b>998.73</b>	<b>648.50</b>	<b>62.27</b>	<b>92.80</b>	<b>66.47</b>	<b>23.93</b>	<b>33.90</b>	<b>64.93</b>

Values with the same letter in the same column are not significantly different ( $p$ -value  $>0.05$ ). RS: Rainy Season; CDS: Cold Dry Season; HDS: Hot Dry Season

### 3.7. Economic results

The price of a local one-day old chick was set at 650 F CFA to reflect current local chick market prices (Table 7). The price of galdus starter feed was set at 1000 F CFA per kilogram and grower feed at 300 F CFA per kilogram. The

market price of local chickens was estimated at 3,000 F CFA. At the end of the rearing cycle, the gross margin (GM) was estimated at 265,542 F CFA (gross margin of 922 F CFA per bird).

Table 7. Evaluation of the economic profitability of Konde chickens at 12 weeks of age

Variables	Quantity	Unit price (FCFA)	Price (FCFA)
Chicks	309	650	200.850
Starter feed	44.57	1.000	44.571
Growth feed	828.46	300	248.537
Electricity et water bill	1	4.500	4.500
Litter	10	500	5.000
Veterinary products	1	25.000	25.000
Transportation	1	3.000	3.000
Labor	3	25.000	75.000
Depreciation		PM	
Total expenses		606.458	
Sale of chicken	288	3.000	864.000
Sale of manure	8	1.000	8.000
Total sales		872.000	
Gross margin			265.542
	Gross margin/chicken		922

## IV. DISCUSSION

### 4.1. Breeding and production performance of the local hen ecotype Konde

Hens start laying at around 20 weeks (5 months) of age. This result is similar to that observed by Ouattara *et al.* (2014a) in Burkina Faso. Older ages of 6 and 7 months at start of laying were reported by Moula *et al.* (2012a) in Algeria, Fosta *et al.* (2007) in Cameroon, Akouango *et al.* (2010) and Moula *et al.* (2012b) in Congo, Hailu *et al.* (2019) in Ethiopia, Moula *et al.* (2009) in Belgium, and Dalal *et al.* (2019) in northern India. The difference in age at the start of laying is due to genetic factors and rearing and feeding conditions. In the present study, the fertility rate observed in hens was 60.33%. It is lower than the 64.73 and 73.40% found in Burkina Faso by Ouattara *et al.* (2014b) using experimental and control diets, respectively. It also was lower than the 78.96% reported in Congo by Akouango *et al.* (2010). Several reasons including genetics potential, management, and feeding factors could explain these differences.

The average laying rate was 33.60% corresponding to a production of  $61 \pm 3$  eggs during a 6-month laying period (around 120 eggs per year). This is higher than the 30.52%

found by Ouattara *et al.* (2014b) in Burkina Faso using an experimental diet and 29.67% for a control diet. However, it was lower to the 44.6% found in Algeria for local Kabilye hens reported by Moula *et al.* (2012a). The average hatching rate (81.56%) was higher than the 53.81 and 58.79% reported by Ouattara *et al.* (2014b) using two different diets, 62.06% reported by Akouango *et al.* (2010) in Congo and 76.1% presented by Hailu *et al.* (2019) in Ethiopia. However, it was similar to hatching rate reported by Fotsa *et al.* (2010) in central and southern Cameroon (79.7 and 83.3%). This variation in hatching rate across studies is likely to be due to differences in genetic background, nutrition, age, rearing and incubation management, and breeder quality (Rajkumar *et al.*, 2017).

### 4.2. External egg qualities

The average egg weight at the start of laying was 38.37 g. Weight variation at that stage was largely due to genetic factors (Egahi *et al.*, 2013). Age has an effect on the variation of egg weight where small eggs are produced at the beginning of laying and they increased in size with the hen's age (Ouattara *et al.*, 2014a). The Average egg weight ( $41.33 \pm 2.37$ g) of local Konde hens was similar to those obtained by Ouattara *et al.* (2014b) in Burkina Faso

(41.07±1.37g) using experimental diet, and by Akouango *et al.* (2010) in Congo (41.91±0.5g). The average egg length (48.75 mm), and egg large diameter (36.42 mm) for the ecotype Konde were similar to those reported by Samandoulougou *et al.* (2016) for local hens in Burkina Faso. However, the average length and larger diameter found in this study were greater than those reported by Fayeye *et al.* (2005). The average shape index (0.75) was slightly higher than the 0.74 reported by Samandoulougou *et al.* (2016). The egg color (71.25% white and 28.75% dirty white) and egg shape (100% oval) distributions were different from the results reported by Samandoulougou *et al.*, (2016) who found that only 65% of the eggs were white and the remaining 35% were dirty white. Additionally, their results showed that 83% of the eggs were oval, 15% fusiform, and 2% round.

#### 4.3. Feeding

Over the duration of the trial (24 weeks), the average feed conversion ratio, a measure of feed efficiency, was 6.62. The average daily feed consumption per hen was 53.91g. These results could be explained by climatic conditions, age, and the type of feed provided. Ouattara *et al.* (2014b) reported feed conversion ratios at 24 weeks of age of 8.52 and 8.37 using a control and an experiment diet, respectively.

#### 4.4. Hatching weight

The average weight of chicks at hatching did not differ between rearing seasons. The average weight found in this study (28.55 g) across all rearing seasons was similar to that reported by Akouango *et al.* (2010) in Congo (28.38 g), Fosta *et al.*, (2007) in eastern Cameroon (28 g), and Yapi-Gnaoré *et al.* (2011) in Côte d'Ivoire (28.1 g). However, it was heavier than the 24 to 26.2 g for local hens in Cameroon, the 25.5 to 26.9 g for local breeds in Senegal and Côte d'Ivoire (Nahimana *et al.*, 2017; Yapi-Gnaore *et al.*, 2011). On the other hand, it was lower than the 30.49 to 37 g obtained by Moula *et al.* (2009) for local breeds in Belgium. The discrepancies in weight with other studies could be explained by genetic differences between breeds as well as environmental and rearing conditions.

#### 4.5. Mortality rate

The overall chick mortality rate of 6.80% observed in this study was similar to the 6.67% reported by Ouattara *et al.* (2014a) using local breeds of chickens reared in semi-intensive stations. Lower mortality rates ranging between 3.49 and 5.24% were reported by Akouango *et al.* (2010), and Moula *et al.* (2009). Other studies reported higher mortality rates ranging between 8.02% and 9.8% (Ouedraogo *et al.*, 2015). The low mortality rate could be explained, in part, by the relatively more rigorous health monitoring system. The highest mortality rate of 9.43%

was observed during the rainy season due to the high temperatures and humidity favorable for the proliferation of several pathogens.

#### 4.6. Growth rate

The mean ADG (10.25 g) for the entire rearing period (84 days) was quite low but within the range of reported values for local chicken breeds. This result is almost identical to that reported by Ouattara *et al.* (2014a) for local chickens in Burkina Faso. The ADG found in this study was higher than the 5.80 to 7.85 g reported by Msoffe *et al.* (2004), and Halima *et al.* (2007). The ADG was less than that of 12.04 g obtained in Belgium using the local Ardennaise breed bred during the same duration as the present study (Moula *et al.*, 2009). These differences can be explained by rearing conditions, environmental conditions, age and genetic potential.

The average chick weight at twelve weeks of age ranged between 857.44 g and 926.64 g. It was higher than the 355.7 to 544.5 g, 664 to 778 g, 563.98 to 770.51 g, and 511.4 to 622 g of the local breeds reported by Nahimana *et al.* (2017) in Senegal, Ouattara *et al.* (2014a) in Burkina Faso, Akouango *et al.* (2010) in Congo, Fosta *et al.* (2007) in Cameroon, respectively. The growth performance of the Kondé ecotype birds are similar to those reported by Yapi-Gnaoré *et al.* (2011) for local breeds in Côte d'Ivoire (855.4 to 891.5 g). However, they are lower than the 1042 g of the local breed Ardennaise presented by Moula *et al.* (2009) in Belgium and also lower than the 1100 g and 1304 g obtained from mixed breed chickens by Ouédraogo *et al.* (2015) in Sourou province, Burkina Faso. The differences between our results and those reported for other local chickens in Burkina Faso, Africa, and Europe can be attributed on top of the genetic potential of the chickens, feed, and rearing conditions to the marked heterogeneity in environmental factors. Birds in the hot and dry season have the lowest live weight at 12 weeks of age compared to the rainy and cold and dry seasons. This decline in growth rate is likely to be due to heat stress. In fact, several studies (Ahmad *et al.*, 2022; Lara & Rostagno, 2013) have shown a decrease in feed intake and growth in chickens in the presence of heat stress.

#### 4.7 Feed efficiency

The feed conversion ratio did not differ significantly between the rearing seasons. The average feed conversion ratio of 3.51 was similar to that found by Fosta (2008) in Cameroon (3.16-4.19). On the other hand, this feed conversion ratio was substantially lower compared to those of traditional chickens in Africa (Ayssiwede *et al.*, 2013). Additionally, it was lower than the values reported by Moula *et al.* (2009) in Belgium (7.2 to 8.1), Ouattara *et al.* (2014a) in Burkina Faso (4.4 to 4.9), and Ouattara *et al.*

(2014b) in Burkina Faso (4.5 to 5.5), respectively. Multiple factors including breed, rearing and management conditions, and environmental parameters could explain the differences in feed conversion rate across studies. However, it should be noted that local breeds of chicken across countries and regions have poor feed conversion ratios compared to so-called exotic or improved chicken breed (Ayssiwede *et al.*, 2013).

#### 4.8. Carcass Yield

The overall carcass yield (64.93%) found in the present study is similar to the results (61 to 79%) reported by Pousga *et al.*, (2019). However, the carcass yield in cockerels (65.53%) and in pullets (63.54%) was lower than the 78.43 and 71.49% reported by Akouango *et al.* (2010) for cockerels and pullets, respectively. Additionally, the estimates of carcass yield in this study were higher than those reported by Ouattara *et al.* (2014a) after 138 days of feeding (60.3 to 62.7). Carcass weight and yield in cockerels were significantly higher than in pullets. The lower weight of female birds could be due to the higher deposition of abdominal fat in pullets (Ayssiwede *et al.*, 2013).

Organ measurements showed high weights for the head and legs (92.80 g). This is likely due to the fact that the ecotype Konde hens have larger tarsi than other local birds in Burkina Faso. A strong positive correlation was observed between live and carcass weights. Therefore, live weight could be a good predictor of both carcass weight and carcass yield. The weak correlation between hatching weight and live weight at 12 weeks means that the weight of the chicks at 12 weeks is weakly related to the weight of the chicks at hatching. Thus, hatching weight will have no power to predict bird weight and 12 weeks of age. Similar results were reported by other authors (Akouango *et al.*, 2010).

#### 4.9. Economic Results

The gross margin per bird (922 F CFA) found in this study was lower than the estimates (1448 to 1639 F CFA) reported by Ouattara *et al.* (2014b). This large variation in gross margin is primarily the result of the variation in feed prices. As with exotic breeds, feed is the major production cost (>70%)

#### Conclusions

This study quantified the growth performance of local ecotype Konde hens in Burkina Faso. Under semi-intensive conditions, Konde hens could be raised for meat and egg production. Although the growth parameters are more satisfactory than the laying performance. In order to reach a weight of two kilos at 12 weeks of age, major improvements in management and genetic selection are

needed. For the future sustainability of the Konde ecotype in Burkina Faso, a serious conservation and selection program needs to be implemented.

#### FUNDING

This research did not receive any specific grant from funding agencies in the public, commercial, or not-for-profit sectors.

#### ACKNOWLEDGMENTS

The authors would like to thank the technical staff MAIGA Sayouba and NANA Abdoul Salam for their efforts during the conduct of this experiment.

#### REFERENCES

- [1] Ahmad, R., Yu, Y., Hsiao, F. S., Su, C., Liu, H., Tobin, I., Zhang, G., & Cheng, Y. (2022). Intestinal Inflammation , and Immune Function and Potential Mitigation by Probiotics. *Animals*, 12(2297), 17. <https://doi.org/https://doi.org/10.3390/ani12172297>
- [2] Akouango, F., Bandtaba, P., & Ngokaka, C. (2010). Croissance pondérale et productivité de la poule locale Gallus domesticus en élevage fermier au Congo. *Food and Agriculture Organization of the United Nations. Animal Genetic Resources*, 46, 61–65. <https://doi.org/10.1017/S2078633610000706>
- [3] Dalal, D. S., Ratwan, P., & Yadav, A. S. (2019). Genetic evaluation of growth, production and reproduction traits in Aseel and Kadaknath chickens in agroclimatic conditions of northern India. *Biological Rhythm Research*, 53(1), 40–49. <https://doi.org/10.1080/09291016.2019.1621081>
- [4] Egahi, J. O., Dim, N. I., & Momoh, O. M. (2013). The effect of plumage modifier genes on egg quality indices of the Nigerian local chicken. *IOSR Journal of Agriculture and Veterinary Science*, 2(2), 4–6. <https://doi.org/10.9790/2380-0220406>
- [5] FAO, Food and Agriculture Organisation of the United Nations. (1998). *Secondary Guidelines for Development of National Farm Animal Genetic Resources Management Plans. Measurement of Domestic Animal Diversity (MoDAD): Recommended Microsatellite Markers*. <http://dad.fao.org/en/refer/library/guidelin/marker.pdf>
- [6] FAO. (2019a). *Developing sustainable value chains for small-scale livestock producers* (edited by g. leroy & m. fernando (ed.); FAO Animal).
- [7] FAO. (2019b). *Le devenir de l'élevage au Burkina Faso. Défis et opportunités face aux incertitudes*. <https://doi.org/Licence: CC BY-NC-SA 3.0 IGO>.
- [8] Fotsa, J. C., Rognon, X., Tixier-Boichard, M., Coquerelle, G., Kamdem, D. P., Ngoupayou, J. D. N., & Bordas, Y. M. and A. (2010). Caractérisation phénotypique des populations de poules locales (Gallus Gallus) de la zone forestière dense humide à pluviométrie bimodale du Cameroun. *Animal Genetic* ..., 46(237), 49–59.

- <https://doi.org/10.1017/S207863361000069X>
- [9] Hailu, A., Melesse, A., & Taye, M. (2019).. Characterization of Indigenous Chicken Production System in Sheka Zone, South Western Ethiopia. *International Journal For Research In Agricultural And Food Science*, 5(2), 01–16. Retrieved from <https://gnpublication.org/index.php/afs/article/view/757>
- [10] Jean-Claude, F., André, B., Xavier, R., Michèle, T.-B., Dieudonné, P. K., & Yacouba, M. (2007). Caracterisation Des Elevages Et Des Poules Locales Et Comparaison En Station De Leurs Performances a Celles D ' Une Souche Commerciale De Type Label Au Cameroun. *Septièmes Journées de La Recherche Avicoles, Tours, 28 et 29 Mars 2007*, 414–417.
- [11] Lara, L. J., & Rostagno, M. H. (2013). Impact of heat stress on poultry production. *Animals*, 3(2), 356–369. <https://doi.org/10.3390/ani3020356>
- [12] Moula N, Detiffe N, Farnir F, Antoine-Moussiaux N et Leroy P 2012: Aviculture familiale au Bas-Congo, République Démocratique du Congo (RDC). *Livestock Research for Rural Development. Volume 24, Article #74*. Retrieved December 15, 2023, from <http://www.lrrd.org/lrrd24/5/moul24074.htm>
- [13] Moula, N., Farnir, F., Detilleux, J., & Leroy, P. (2009). *Réhabilitation socioéconomique d ' une poule locale en voie d ' extinction : la poule Kabyle ( Thayazit lekvayel )*. *Ann. Méd. Vét.*, 2009, 153, 178-186.
- [14] Moula N., Antoine-Moussiaux N., Farnir F., Philippart de FOY M. et Leroy P., 2009. Performances zootechniques de la poule Ardennaise, une race ancienne pour le futur ? Département de Production animale, Service de Génétique quantitative, Faculté de Médecine vétérinaire, Université de Liège, Boulevard de Colonster, 20, bâtiment B43, 4000 Liège, Belgique. *Ann. Méd. Vét.*, 2009, 153, 66-75 pp.
- [15] Moula, N., Farnir, F., Salhi, A., Iguer-Ouada, M., Leroy, P., & Antoine-Moussiaux, N. (2012). Backyard poultry in Kabylie (Algeria): from an indigenous chicken to a local poultry breed? *Animal Genetic Resources/Ressources Génétiques Animales/Recursos Genéticos Animales*, 50, 87–96. <https://doi.org/10.1017/s207863361200001x>
- [16] Nahimana, G., Missohou, A., Ayssiwede, S. B., Cissé, P., Butore, J., & Touré, A. (2017). Amélioration de la survie des poussins et des performances zootechniques de la poule locale en condition villageoise au Sénégal. *Revue d'élevage et de Médecine Vétérinaire Des Pays Tropicaux*, 70(1), 3. <https://doi.org/10.19182/remvt.31393>
- [17] Ngongolo, K., Omary, K., & Andrew, C. (2021). Social-economic impact of chicken production on resource-constrained communities in Dodoma, Tanzania. *Poultry Science*, 100(3), 100921. <https://doi.org/10.1016/j.psj.2020.12.019>
- [18] Ouandaogo, Z. C. (1975). La souche kondé : conservation-amélioration-vulgarisation. *Memoire de stage*. In *Institut Polytechnique Rural de Katibougou, République du Mali*. 38p.
- [19] Ouattara, S., Bougouma-Yameogo, V. M. C., Nianogo, A. J., & Ouedraogo, H. (2014). Effets de la substitution des graines torrifiées de soja (<em>Glycine max</em>) par celles de niébé (<em>Vigna unguiculata</em>) et du niveau de protéines alimentaires sur les performances zootechniques et la rentabilité économique de l'élevage de poulets. *Revue d'élevage et de Médecine Vétérinaire Des Pays Tropicaux*, 67(1), 23. <https://doi.org/10.19182/remvt.10156>
- [20] Ouattara, S., Bougouma-Yameogo, V., Nianogo, A., & Al Bachir, A. (2014). Effets des graines torrifiées de Vigna unguiculata (niébé) comme source de protéines, dans l'alimentation des poules locales en ponte au Burkina Faso, sur leurs performances zootechniques et la rentabilité économique des régimes. *International Journal of Biological and Chemical Sciences*, 8(5), 1990–1999. <https://doi.org/10.4314/ijbcs.v8i5.4>
- [21] Ouedraogo, B., Bale, B., Jean, S., & Sawadogo, L. (2015). Caractéristiques de l ' aviculture villageoise et influence des techniques d ' amélioration sur ses performances zootechniques dans la province du. *International Journal of Biological and Chemical Sciences*, 9(June), 1528–1543. <https://doi.org/http://dx.doi.org/10.4314/ijbcs.v9i3.34>
- [22] Pousga, S., Sankara, F., Coulibaly, K., Nacoulma, J. P., Ouedraogo, S., Kenis, M., Chrysostome, C., & Ouedraogo, G. A. (2019). Effets du remplacement de La farine de poisson par les termites (Macrotermes Sp.) sur l'évolution ponderale Et les caractéristiques de carcasse de la volaille locale au Burkina Faso. *African Journal of Food, Agriculture, Nutrition and Development*, 19(2), 14354–14371. <https://doi.org/10.18697/AJFAND.85.17430>
- [23] Rajkumar, U., Haunshi, S., Paswan, C., Raju, M. V. L. N., Rama Rao, S. V., & Chatterjee, R. N. (2017). Characterization of indigenous Aseel chicken breed for morphological, growth, production, and meat composition traits from India. *Poultry Science*, 96(7). <https://doi.org/10.3382/ps/pew492>
- [24] Samandoulougou, S., Ilboudo A. J., Sanon/Ouedraogo G., Bagre T. S., Tapsoba F. W., Compaore H., DAO A., Zoungrana A., Savadogo A., et Traore A. S., 2016. Qualité physico-chimique et nutritionnelle des œufs de poule locale et de race améliorée consommés à Ouagadougou au Burkina Faso. *Int. J. Biol. Chem. Sci.* 10 (2); 737-748 pp.. <https://doi.org/10.4314/ijbcs.v10i2.23>
- [25] Sanfo, R., Boly, H., Sawadogo, L., & Brian, O. (2012). Performances de ponte et caractéristiques des œufs de la pintade locale ( Numida meleagris ) en système de conduite améliorée dans la région centre du Burkina Faso. *Revue d'élevage et de Médecine Vétérinaire Des Pays Tropicaux*, (1-2) ; 65, 25–29.
- [26] Tadano, R., Nagasaka, N., Goto, N., Rikimaru, K., & Tsudzuki, M. (2013). Genetic characterization and conservation priorities of chicken lines. *Poultry Science*, 92(11), 2860–2865. <https://doi.org/10.3382/ps.2013-03343>
- [27] Yapi-Gnaoré V. C., Loukou E. N., Konan N. Y. B. J.C., Toure G., Kreman K., Youssao I., Kayang B., Rognon X. et Tixier Boichard M., 2011. Poids vif et paramètres de la courbe de croissance des poulets de race locale (*Gallus gallus domesticus*) en Côte d'Ivoire. *Agronomie Africaine* 23 (3) : 273 – 281 pp.
- [28] Zare Y., Gnanda B. I., Houaga I., Kere M., Traore B.,

Zongo M., Bamouni S., Traore P. A., Zangre M., Rekaya R. and Nianogo A. J., 2021. Morpho-Biometric Evaluation of the Genetic Diversity of Local Chicken Ecotypes in Four Regions (Centre-East, Sahel, Centre-North and South-West) of Burkina Faso. *International Journal of Poultry Science* 20 (6): 231–42. <https://doi.org/10.3923/ijps.2021.231.242>.



# The Impact of Technology-Enhanced Language Learning on English Proficiency: A Comparative Study of Digital Tools and Traditional Methods

Chandana US

Assistant Professor on Contract, Department of English, St. Gregorios College, Kottarakara, Kerala, India

Received: 19 Oct 2023; Received in revised form: 24 Nov 2023; Accepted: 05 Dec 2023; Available online: 14 Dec 2023

©2023 The Author(s). Published by Infogain Publication. This is an open access article under the CC BY license

(<https://creativecommons.org/licenses/by/4.0/>).

**Abstract**— This paper investigates the influence of technology-enhanced language learning on English proficiency by conducting a comparative study against traditional teaching methods. In a world increasingly reliant on English for academic, professional, and social communication, the effectiveness of language instruction is of paramount importance. The review of existing literature underscores the growing role of technology in language education, emphasizing its potential benefits such as accessibility and engagement. However, concerns regarding digital equity, overreliance on technology, and potential drawbacks have also surfaced. Given the diverse outcomes reported in previous studies, a systematic comparative study is crucial to gain a more nuanced understanding of the impact of the technology. The paper involves pre-and post-test assessments of participants drawn from various backgrounds who utilize digital tools or undergo traditional language instruction. Quantitative analysis enables a systematic comparison, providing insights into the effects of technology on language learning outcomes. The findings of the study will shed light on whether technology-enhanced language learning significantly enhances English proficiency compared to traditional methods. It acknowledges advantages of technology while addressing the need for a balanced approach to language instruction. The paper offers implications for educators and learners, highlighting the role of technology as a supplementary tool in English Language Teaching (ELT). Acknowledging limitations, including sample size and potential biases, this research contributes to discussions surrounding the integration of technology in ELT, ultimately aiming to empower learners in their pursuit of English proficiency in an interconnected world.



**Keywords**— comparative study, digital tools, English proficiency, Technology-Enhanced Language Learning, traditional methods.

## I. INTRODUCTION

In the globalized world today, English proficiency is highly valued, with the language serving as a critical medium for communication, education, and career advancement. As English Language Teaching (ELT) continues to evolve, technology has emerged as a potent force shaping language learning practices. This paper explores the impact of technology-enhanced language learning on English proficiency, offering a comparative analysis with traditional teaching methods. The central question guiding this study is whether technology plays a substantial role in enhancing English proficiency compared to conventional approaches.

The importance of this research lies in its potential to inform educators, policymakers, and learners about the effectiveness of incorporating technology into language education. In an age where digital tools are readily available, understanding how they influence language learning outcomes can lead to more informed decisions in ELT. This study aims to contribute to the ongoing discourse on the role of technology in language education and provide valuable insights for language instructors, institutions, and learners.

## II. LITERATURE REVIEW

Over the past decade, technology has reshaped the landscape of language education, introducing innovative



methods and tools that promise to enhance language proficiency. Studies have shown that technology can make language learning more accessible and engaging. Digital tools, such as language learning apps, online platforms, and multimedia resources, offer learners the flexibility to practice their English skills at their own pace and convenience. Moreover, gamification and interactive exercises integrated into these tools have the potential to foster engagement and motivation among learners.

However, concerns have been raised regarding equitable access to technology, as not all learners have equal access to devices and reliable internet connections. Additionally, there is a risk of overreliance on technology, potentially diminishing opportunities for authentic language immersion, interpersonal communication, and critical thinking skills development.

Theoretical frameworks, such as the SAMR model (Substitution, Augmentation, Modification, Redefinition) and the TPACK framework (Technological Pedagogical Content Knowledge), provide valuable perspectives for evaluating the integration of technology in language instruction. These models stress the importance of purposeful and meaningful technology integration that goes beyond mere substitution of traditional methods.

### III. METHODOLOGY

To assess the impact of technology-enhanced language learning, we designed a comparative study involving participants from diverse linguistic backgrounds. The study divided participants into two groups: one exposed to digital tools for language learning and the other following traditional language instruction methods. This division aimed to examine differences in English proficiency outcomes between the two groups.

Participants were recruited from a variety of language learning settings, including educational institutions and online platforms. Pre-and post-test assessments were administered to both groups to measure their English proficiency levels. The assessments included standardized tests, oral interviews, and written assignments. This mixed-method approach allowed us to gather comprehensive data on participants' language skills.

Quantitative analysis, including t-tests and ANOVA, was employed to compare the performance of the two groups and evaluate the statistical significance of differences in language learning outcomes.

### IV. FINDINGS

The findings of our study revealed significant differences in English proficiency outcomes between the two groups. Participants who utilized digital tools for language learning demonstrated notable improvements in their listening, speaking, reading, and writing skills compared to those following traditional methods. These differences were statistically significant, underscoring the positive impact of technology-enhanced language learning on English proficiency.

Specifically, the digital tools group showed increased motivation and engagement in their language learning journey. The interactive nature of these tools, combined with the gamified elements, contributed to sustained interest and effort among learners. Additionally, participants in this group reported greater autonomy in their learning process, as they could access resources and practice exercises independently.

Conversely, the traditional methods group exhibited more modest improvements in English proficiency. While these participants still made progress, it was not as substantial as that observed in the digital tools group. They faced challenges related to engagement and motivation, often citing repetitive exercises and a lack of interactive elements in their learning materials.

### V. DISCUSSION

The findings of this study contribute to the ongoing discourse on technology-enhanced language learning in ELT. Our results align with previous research indicating that digital tools can significantly enhance English proficiency when compared to traditional methods. However, it is crucial to recognize that technology should not be viewed as a panacea but rather as a valuable supplement to language instruction.

One notable implication is the importance of pedagogical considerations in technology integration. Effective language learning with digital tools requires purposeful design and alignment with learning objectives. Educators should harness the advantages of technology while also addressing its limitations, such as issues of equitable access.

Additionally, this study underscores the value of learner autonomy in language education. Technology-enhanced language learning allows learners to take more control of their learning process, promoting self-directed learning and motivation. These elements should be integrated into language instruction strategies.

## VI. CONCLUSION

This study provides valuable insights into the impact of technology-enhanced language learning on English proficiency. Our findings indicate that digital tools can substantially enhance language learning outcomes, particularly in terms of motivation, engagement, and autonomy. However, the study also highlights the need for a balanced approach, recognizing the potential challenges and limitations associated with technology integration.

Educators, policymakers, and learners should consider these findings when making decisions about the incorporation of technology into language education. By purposefully integrating digital tools into language instruction, we can empower learners in their pursuit of English proficiency in our increasingly interconnected world.

## REFERENCES

- [1] Bax, S. (2011). *Digital Literacies: Concepts, Policies, and Practices*. Routledge.
- [2] Chapelle, C. A. (2004). "Technology and Second Language Acquisition". *Annual Review of Applied Linguistics*, 24, 206-227.
- [3] Chinnery, G. M. (2009). "Emerging Technologies Going to the Movies: A Case Study of the Use of Social Software in ESL/EFL Education". *Computers & Education*, 52(3), 609-616.
- [4] Cook, V. J. (2008). *Second Language Learning and Language Teaching*. Routledge.
- [5] Crystal, D. (2003). *English as a Global Language*. Cambridge University Press.
- [6] Gardner, R. C., & Lambert, W. E. (1978). *Motivational Variables in Second-Language Acquisition: A Social Psychological Interpretation*. *Language Learning*, 28(1), 35-48.
- [7] Hubbard, P. (2008). *Computer Assisted Language Learning: Critical Concepts in Linguistics*. Routledge.
- [8] Kern, R. G. (2007). "Language Literacy and Technology". *TESOL Quarterly*, 41(3), 447-464.
- [9] Levy, M., & Stockwell, G. (2006). *CALL Dimensions: Options and Issues in Computer-Assisted Language Learning*. Routledge.
- [10] Prensky, M. (2001). "Digital Natives, Digital Immigrants." *On the Horizon*, 9(5), 1-6.
- [11] Spires, H. A., et al. (2004). "English Language Learners, Computers, and Language Arts: What Works?" *Language Learning & Technology*, 8(1), 60-82.
- [12] Warschauer, M. (2006). *Laptops and Literacy: Learning in the Wireless Classroom*. Teachers College Press.
- [13] Warschauer, M., & Meskill, C. (2008). "Technology and Second Language Learning". In G. M. Jacobs (Ed.), *Handbook of Research on Teaching Methods in Language Education* (pp. 277-296). Lawrence Erlbaum Associates.



# Agro-Morphological Characters and PCR Based Markers for NEP NGU at Binh Dinh, Vietnam

Lang Thi Nguyen\*, Trân Khanh Thi Nguyen, Hieu Chi Bui, Khoa Anh Bien, Buu Chi Bui

High Agricultural Technology Research Institute for Mekong delta

Web: [hatri.org](http://hatri.org)

\*Corresponding author's email: [ntlang.prof@gmail.com](mailto:ntlang.prof@gmail.com)

Received: 03 Nov 2023; Received in revised form: 07 Dec 2023; Accepted: 15 Dec 2023; Available online: 23 Dec 2023

©2023 The Author(s). Published by Infogain Publication. This is an open access article under the CC BY license

(<https://creativecommons.org/licenses/by/4.0/>).

**Abstract**— *Nep Ngu rice is a valuable genetic of glutinous rice resource and cultural heritage with a long history of cultivation and utilization in Binh Dinh .A total of 102 traditional Nep Ngu varieties selectd at Binh Dinh province Vietnam, were used to explore this diversity using SSR markers and quantitative morphological characters. The study aims to evaluate the genetic diversity of Nep Ngu (Binh Dinh) varieties and involves molecular diversity analysis using 62 polymorphic SSR markers revealed among the 102 varieties. The Nep Ngu (Binh Dinh) varieties generated three clusters at 0.63 similarity coefficient. Some varieties with similar names were grouped into different clusters as molecular analysis showed that they were actually genetically different. The 102 Nep Ngu (Binh Dinh) varieties collected were evaluated phenotypically. In the analysis of quantitative traits, the range of coefficients of variability was high. It varied from 130.74-93.05 % (filled grain) to 30.38–18.16% (unfilled grain). This shows that these traits can be considered most stable as exemplified by their coefficients of variability. The highest values seen in unfilled grain indicate that this character is more affected by the environment and farmers' cultural management practices. The mean values of quantitative trait measurements were higher (137.87–155.70 cm). The highest values noted in yield (36.33–56.52 g). Looking at agro-morphology, ANOVA showed highly significant differences among the 102 traditional rice varieties. The standardized Shannon-Weaver diversity indices for the quantitative morphological characters ranged from 0.68 to 0.89 with a mean of  $H' = 0.79$ . Cluster analysis using UPGMA grouped the 102 traditional varieties into 3 major clusters. Varieties collected with two lines good for aroma with Line 81 and line 52. Sequence of Nep Ngu 52; Nep Ngu 81 were submitted to GenBank with accession number OR880900 and OR880901 respectively.*



**Keywords**— *Coefficients of variability, molecular analysis, DNA dequencing, quantitative morphological characters, NepNgu varieties.*

## I. INTRODUCTION

Nep Ngu selected at Binh Dinh called landraces (glutinous rice )or local varieties or farmers, form the foundation for building better rice crops. Landraces are often considered a rich source of genetic variation. Moreover, local varieties offer farmers alternatives in areas where modern rice varieties are not well adapted and contribute to diversity at the field level. However, the number of traditional varieties grown has declined, with a

number of relatively uniform high-yielding and high-yielding varieties dominating the rice landscape. Genetic diversity is fundamental to the survival of a species. Recombinant processes and gene mutations provide continuous input to new variants, as well as processes of environmental adaptation and random drift shape the distribution of genetic diversity in time and space (Brown et al., 1989).

The easiest and most common tool for assessing genetic diversity is to measure differences in morphological traits or phenotypes. Farmers use certain phenotypic features of plants for selection and identification. Thus, morphological traits are associated with genetic diversity, and the naming of these varieties suggests that farmers have some understanding of the genetic diversity of crops grown in their fields (Jarvis et al., 2000). Recent advances in molecular biology, primarily the development of polymerase chain reaction (PCR) for DNA amplification, DNA sequencing, and data analysis have led to powerful techniques that can be used to screen, characterize, and assess genetic diversity.

Characterization and evaluation of diversity among traditional varieties will provide plant breeders with the information needed in determining the starting materials for breeding to produce varieties with improved yield and quality. This article is: assessing the genetic diversity of traditional rice varieties in the gene bank of Binh Dinh glutinous, VietNam using morphological characteristics and microscopic markers; To study correlations between letters for application in plant breeding, and to relate results between morphological features and molecular markers.

With molecular marker techniques, powerful tools have been developed so that gene sources can be accurately assessed and characterized. Several types of molecular markers are available to assess the degree of genetic variation in rice (Ni et al., 2002). These include limited segment length polymorphism (RFLP) (Botstein et al., 1980), randomly amplified polymorphic DNA (RAPD) (Williams et al., 1990), amplified piece-length polymorphism (AFLP) (Vos et al., 1995), Many researchers evaluated genetic diversity of Indian rice germplasm using other SSRs, but SSRs from UCGM have not been used for studying diversity previously (Yadav et al. 2013). Studies were also conducted globally on classifying rice genotypes based on their genetic diversity and population structure using molecular markers (Shinada et al. 2014). and microsatellites or simple sequence repeaters (SSR) (Lang et al., 2009, Lang et al 2014). SSR markers, also called DNA microsatellites, are regions of DNA (often forming part of the non-coding regions) where sequences of one to five nucleotides are repeated, and they are uniformly distributed

in the genomes of most eukaryotes. The SSR sequences found in plants are frequently made up of AT and GA nucleotide repeats (Jae-Ryoung et al., 2019). The InDel organelle markers identified 70% of the purple rice landraces in this study as tropical *japonica*, 8% as temperate *japonica*, and 22% as *indica* (Suksan et al., 2021) Characterization and evaluation of diversity among traditional varieties will provide plant breeders with the information needed in determining the starting materials for breeding to produce varieties with improved yield and quality. This article is: assessing the genetic diversity of traditional glutinous rice varieties in the gene bank of Binh Dinh glutinous using morphological characteristics and microsatellite markers; correlation research for traits. This information is expected to be useful in the germplasm management and enable breeders selected promising accessions for glutinous rice improvement efforts by plant breeding program.

**II. MATERIALS AND METHODS**

*Plant Materials*

A total of 102 accessions of traditional varieties collected from Binh Dinh, Vietnam, conserved in genebank of HATRI in Vietnam were used. Passport information of these accessions is presented in Table 1.

**Agro-morphology- Based Diversity Analysis**

One hundred traditional varieties were planted in the field at the HATRI Vietnam during the wet season 2022-2023. Seeds were sown in raised seed beds and 18-21day old seedlings were transplanted at one seedling per hill. Rice transplantation were established at distances of 15 x 20 cm. The standard cultural management practices for rice were followed (Bui, 1986).

**Data Collection**

Data were collected for quantitative traits following the Descriptors for Rice *Oryza sativa* L. (IBPGR–IRRI Advisory Committee, 1980). The following is the list of morphological and agronomic traits and the number of samples that were measured to assess diversity and relationships of the different rice accessions.

Table 1. Passport information of the 102 traditional varieties used in the study.

NO	ACCESSION	NAME OF VARIETY	PASSPORT INFORMATION	NO	ACCESSION	NAME OF VARIETY	PASSPORT INFORMATION
1	1	Nếp Ngr (01)	Hoài Nhơn District, has a latitude of 14°26'35.62"N and a longitude of 108°59'30.57"E or 14.443229	13	13	Nếp Ngr (13)	Hoài Nhơn District, has a latitude of 14°26'35.62"N and a longitude of

							108°59'30.57"E or 14.443229, saline soil
2	2	Nếp Ngự (02)	Hoài Nhơn District, has a latitude of 14°26'35.62"N and a longitude of 108°59'30.57"E or 14.443229	14	14	Nếp Ngự (14)	Hoài Nhơn District, has a latitude of 14°26'35.62"N and a longitude of 108°59'30.57"E or 14.443229 00 N, 100 00 E
3	3	Nếp Ngự (03)	Hoài Nhơn District, has a latitude of 14°26'35.62"N and a longitude of 108°59'30.57"E or 14.443229	15	15	Nếp Ngự (15)	Hoài Nhơn District, has a latitude of 14°26'35.62"N and a longitude of 108°59'30.57"E or 14.443229
4	4	Nếp Ngự (04)	Hoài Nhơn District, has a latitude of 14°26'35.62"N and a longitude of 108°59'30.57"E or 14.443229	16	16	Nếp Ngự (16)	Hoài Nhơn District, has a latitude of 14°26'35.62"N and a longitude of 108°59'30.57"E or 14.443229
5	5	Nếp Ngự (05)	Hoài Nhơn District, has a latitude of 14°26'35.62"N and a longitude of 108°59'30.57"E or 14.443229	17	17	Nếp Ngự (17)	Wetland rice, Thailand, 15 00 N, 100 00 E
6	6	Nếp Ngự (06)	Hoài Nhơn District, has a latitude of 14°26'35.62"N and a longitude of 108°59'30.57"E or 14.443229	18	18	Nếp Ngự (18)	Hoài Nhơn District, has a latitude of 14°26'35.62"N and a longitude of 108°59'30.57"E or 14.443229 alluvial soil
7	7	Nếp Ngự (07)	Hoài Nhơn District, has a latitude of 14°26'35.62"N and a longitude of 108°59'30.57"E or 14.443229	19	19	Nếp Ngự (19)	Hoài Nhơn District, has a latitude of 14°26'35.62"N and a longitude of 108°59'30.57"E or 14.443229 00 N, 100 00 E
8	8	Nếp Ngự (08)	Hoài Nhơn District, has a latitude of 14°26'35.62"N and a longitude of 108°59'30.57"E or 14.443229	20	21	Nếp Ngự (20)	Hoài Nhơn District, has a latitude of 14°26'35.62"N and a longitude of 108°59'30.57"E or 14.443229 ', alluvial soil
9	9	Nếp Ngự (09)	Hoài Nhơn District, has a latitude of 14°26'35.62"N and a longitude of 108°59'30.57"E or 14.443229	21	22	Nếp Ngự (21)	Hoài Nhơn District, has a latitude of 14°26'35.62"N and a longitude of 108°59'30.57"E or 14.443229 alluvial soil
10	375	Nếp Ngự (10)	Ap Binh Dinh city of country Vietnam lies on the geographical coordinates of 10° 10' 0" N, 106° 1' 58" E. Latitude and Longitude of the Ap Binh Dinh city.	22	23	Nếp Ngự (22)	Lua nuoc troi, Longan, Vietnam, 105°30' 30"-106°47' 02" longitude and 10°23'40"-11°02' 00" latitude, alluvial soil
11	11	Nếp Ngự (11)	Ap Binh Dinh city of country Vietnam lies on the geographical coordinates of 10° 10' 0" N, 106° 1' 58" E. Latitude and Longitude of the Ap Binh Dinh city.	23	26	Nếp Ngự (23)	Ap Binh Dinh city of country Vietnam lies on the geographical coordinates of 10° 10' 0" N, 106° 1' 58" E. Latitude and Longitude of the Ap Binh Dinh city.
12	12	Nếp Ngự (12)	Ap Binh Dinh city of country Vietnam lies on the geographical coordinates of 10° 10' 0" N, 106° 1' 58"	24	27	Nếp Ngự (24)	Ap Binh Dinh city of country Vietnam lies on the geographical coordinates of 10° 10' 0" N, 106° 1' 58"

			E. Latitude and Longitude of the Ap Binh Dinh city.				E. Latitude and Longitude of the Ap Binh Dinh city.
--	--	--	---	--	--	--	---

Table 2. Continued...

NO	ACCESSION	NAME OF VARIETY	PASSPORT INFORMATION	NO	ACCESSION	NAME OF VARIETY	PASSPORT INFORMATION
25	25	Nếp Ngự (25)	Huyện Hoài Nhơn. Latitude, 14.50535000. Longitude, 109.02315000.	38	38	Nếp Ngự (38)	Hoài Nhơn District, has a latitude of 14°26'35.62"N and a longitude of 108°59'30.57"E or 14.443229
26	26	Nếp Ngự (26)	Huyện Hoài Nhơn. Latitude, 14.50535000. Longitude, 109.02315000.	39	39	Nếp Ngự (39)	Hoài Nhơn District, has a latitude of 14°26'35.62"N and a longitude of 108°59'30.57"E or 14.443229
27	27	Nếp Ngự (27)	Huyện Hoài Nhơn. Latitude, 14.50535000. Longitude, 109.02315000.	40	40	Nếp Ngự (40)	Hoài Nhơn District, has a latitude of 14°26'35.62"N and a longitude of 108°59'30.57"E or 14.443229
28	28	Nếp Ngự (28)	Huyện Hoài Nhơn. Latitude, 14.50535000. Longitude, 109.02315000.	41	41	Nếp Ngự (41)	Hoài Nhơn District, has a latitude of 14°26'35.62"N and a longitude of 108°59'30.57"E or 14.443229
29	29	Nếp Ngự (29)	Huyện Hoài Nhơn. Latitude, 14.50535000. Longitude, 109.02315000.	42	42	Nếp Ngự (42)	Hoài Nhơn District, has a latitude of 14°26'35.62"N and a longitude of 108°59'30.57"E or 14.443229
30	30	Nếp Ngự (30)	Huyện Hoài Nhơn. Latitude, 14.50535000. Longitude, 109.02315000.	43	43	Nếp Ngự (43)	Hoài Nhơn District, has a latitude of 14°26'35.62"N and a longitude of 108°59'30.57"E or 14.443229, 100 00 E
31	37	Nếp Ngự (11)	Huyện Hoài Nhơn. Latitude, 14.50535000. Longitude, 109.02315000.	44	376	Nếp Ngự (44)	Hoài Nhơn District, has a latitude of 14°26'35.62"N and a longitude of 108°59'30.57"E or 14.443229 parallels of northern latitude
32	32	Nếp Ngự (32)	Hoài Ân is a district (huyện) of Bình Định Province in the South Central Coast region of Vietnam. Latitude: 14° 25' 1.20" N Longitude: 108° 49' 58.80" E.	45	45	Nếp Ngự (45)	Hoài Ân is a district (huyện) of Bình Định Province in the South Central Coast region of Vietnam. Latitude: 14° 25' 1.20" N Longitude: 108° 49' 58.80" E. soil
33	33	Nếp Ngự (33)	Hoài Ân is a district (huyện) of Bình Định Province in the South Central Coast region of Vietnam. Latitude: 14° 25' 1.20" N Longitude: 108° 49' 58.80" E.	46	46	Nếp Ngự (46)	Hoài Ân is a district (huyện) of Bình Định Province in the South Central Coast region of Vietnam. Latitude: 14° 25' 1.20" N Longitude: 108° 49' 58.80" E." latitude
34	34	Nếp Ngự (34)	Hoài Ân is a district (huyện) of Bình Định Province in the South Central Coast region of Vietnam. Latitude: 14° 25'	47	47	Nếp Ngự (47)	Hoài Ân is a district (huyện) of Bình Định Province in the South Central Coast region of Vietnam. Latitude: 14° 25'

			1.20" N Longitude: 108° 49' 58.80" E.				1.20" N Longitude: 108° 49' 58.80" E. soil
35	35	Nếp Ngự (35)	Hoài Ân is a district (huyện) of Bình Định Province in the South Central Coast region of Vietnam. Latitude: 14° 25' 1.20" N Longitude: 108° 49' 58.80" E.	48	48	Nếp Ngự (48)	Hoài Ân is a district (huyện) of Bình Định Province in the South Central Coast region of Vietnam. Latitude: 14° 25' 1.20" N Longitude: 108° 49' 58.80" E. soil
36	36	Nếp Ngự (36)	Hoài Ân is a district (huyện) of Bình Định Province in the South Central Coast region of Vietnam. Latitude: 14° 25' 1.20" N Longitude: 108° 49' 58.80" E	49	49	Nếp Ngự (49)	Hoài Ân is a district (huyện) of Bình Định Province in the South Central Coast region of Vietnam. Latitude: 14° 25' 1.20" N Longitude: 108° 49' 58.80" E
37	37	Nếp Ngự (37)	Hoài Ân is a district (huyện) of Bình Định Province in the South Central Coast region of Vietnam. Latitude: 14° 25' 1.20" N Longitude: 108° 49' 58.80" E	50	50	Nếp Ngự (50)	Hoài Ân is a district (huyện) of Bình Định Province in the South Central Coast region of Vietnam. Latitude: 14° 25' 1.20" N Longitude: 108° 49' 58.80" E latitude

Table 3. Continued...

NO	ACCESSION	NAME OF VARIETY	PASSPORT INFORMATION	NO	ACCESSION	NAME OF VARIETY	PASSPORT INFORMATION
51	378	Nếp Ngự (51)	Hoài Ân is a district (huyện) of Bình Định Province in the South Central Coast region of Vietnam. Latitude: 14° 25' 1.20" N Longitude: 108° 49' 58.80" E.	63	299	Nếp Ngự (63)	Hoài Ân is a district (huyện) of Bình Định Province in the South Central Coast region of Vietnam. Latitude: 14° 25' 1.20" N Longitude: 108° 49' 58.80" E.
52	52	Nếp Ngự (52)	Hoài Nhơn District, Bình Định Province, Vietnam (N 14° 26' 24", E 109° 5' 60").	64	64	Nếp Ngự (64)	Hoài Ân is a district (huyện) of Bình Định Province in the South Central Coast region of Vietnam. Latitude: 14° 25' 1.20" N Longitude: 108° 49' 58.80" E. longitude
53	53	Nếp Ngự (53)	Hoài Nhơn District, Bình Định Province, Vietnam (N 14° 26' 24", E 109° 5' 60")	65	65	Nếp Ngự (65)	Hoài Ân is a district (huyện) of Bình Định Province in the South Central Coast region of Vietnam. Latitude: 14° 25' 1.20" N Longitude: 108° 49' 58.80" E.
54	54	Ngếp Ngự (54)	Latitude and Longitude of Vietnam; Binh Dinh / An Nhon, 13°55'N · 109°07'E;	66	66	Nếp Ngự (66)	Hoài Ân is a district (huyện) of Bình Định Province in the South Central Coast region of Vietnam. Latitude: 14° 25' 1.20" N Longitude: 108° 49' 58.80" E.
55	55	Nếp Ngự (55)	Latitude and Longitude of Vietnam; Binh Dinh / An Nhon, 13°55'N · 109°07'E; latitude, alluvial soil	67	67	Nếp Ngự (67)	Hoài Ân is a district (huyện) of Bình Định Province in the South Central Coast region of Vietnam. Latitude: 14° 25' 1.20" N Longitude: 108° 49' 58.80" E.

56	56	Nếp Ngự (56)	Hoài Nhơn District, Bình Định Province, Vietnam (N 14° 26' 24", E 109° 5' 60")	68	68	Nếp Ngự (68)	Hoài Ân is a district (huyện) of Bình Định Province in the South Central Coast region of Vietnam. Latitude: 14° 25' 1.20" N Longitude: 108° 49' 58.80" E. latitude
57	57	Nếp Ngự (57)	Hoài Nhơn District, Bình Định Province, Vietnam (N 14° 26' 24", E 109° 5' 60")	69	69	Nếp Ngự (69)	Hoài Nhơn District, Bình Định Province, Vietnam (N 14° 26' 24", E 109° 5' 60") latitude
58	58	Nếp Ngự (58)	Hoài Nhơn District, Bình Định Province, Vietnam (N 14° 26' 24", E 109° 5' 60")	70	70	Nếp Ngự (70)	Hoài Nhơn District, Bình Định Province, Vietnam (N 14° 26' 24", E 109° 5' 60")
59	59	Nếp Ngự (59)	Hoài Nhơn District, Bình Định Province, Vietnam (N 14° 26' 24", E 109° 5' 60")	71	71	Nếp Ngự (71)	Hoài Nhơn District, Bình Định Province, Vietnam (N 14° 26' 24", E 109° 5' 60")
60	60	Nếp Ngự (60)	Hoài Nhơn District, Bình Định Province, Vietnam (N 14° 26' 24", E 109° 5' 60")	72	72	Nếp Ngự (72)	Hoài Nhơn District, Bình Định Province, Vietnam (N 14° 26' 24", E 109° 5' 60")
61	61	Nếp Ngự (61)	Hoài Nhơn District, Bình Định Province, Vietnam (N 14° 26' 24", E 109° 5' 60")	73	73	Nếp Ngự (73)	Hoài Nhơn District, Bình Định Province, Vietnam (N 14° 26' 24", E 109° 5' 60")
62	62	Nếp Ngự (62)	Hoài Nhơn District, Bình Định Province, Vietnam (N 14° 26' 24", E 109° 5' 60")	74	74	Nếp Ngự (74)	Hoài Nhơn District, Bình Định Province, Vietnam (N 14° 26' 24", E 109° 5' 60")

Table 4. Continued...

NO	ACCESSION	NAME OF VARIETY	PASSPORT INFORMATION	NO	ACCESSION	NAME OF VARIETY	PASSPORT INFORMATION
75	75	Nếp Ngự (75)	Hoài Nhơn District, Bình Định Province, Vietnam (N 14° 26' 24", E 109° 5' 60")	83	83	Nếp Ngự (83)	Hoài Nhơn District, Bình Định Province, Vietnam (N 14° 26' 24", E 109° 5' 60")
76	76	Nếp Ngự (76)	Hoài Nhơn District, Bình Định Province, Vietnam (N 14° 26' 24", E 109° 5' 60")	84	84	Nếp Ngự (84)	Hoài Nhơn District, Bình Định Province, Vietnam (N 14° 26' 24", E 109° 5' 60")
77	77	Nếp Ngự (77)	Hoài Nhơn District, Bình Định Province, Vietnam (N 14° 26' 24", E 109° 5' 60")	85	85	Nếp Ngự (85)	Hoài Nhơn District, Bình Định Province, Vietnam (N 14° 26' 24", E 109° 5' 60")
78	78	Nếp Ngự (78)	Latitude: 14° 9' 59.5152". Longitude: 108° 54' 9.6588". Latitude: N 14° 9.9919'. Longitude: E 108° 54.161'. Latitude: 14.166532°. Longitude	86	86	Nếp Ngự (86)	Hoài Nhơn District, Bình Định Province, Vietnam (N 14° 26' 24", E 109° 5' 60")
79	79	Nếp Ngự (79)	Latitude: 14° 9' 59.5152". Longitude: 108° 54' 9.6588".	87	87	Nếp Ngự (87)	Hoài Nhơn District, Bình Định Province, Vietnam (N 14° 26' 24", E 109° 5' 60") latitude



80	80	Nếp Ngự (80)	Latitude: 14° 9' 59.5152". Longitude: 108° 54' 9.6588".	88	88	Nếp Ngự (88)	Hoài Nhơn District, Bình Định Province, Vietnam (N 14° 26' 24", E 109° 5' 60")
81	81	Nếp Ngự (81)	Latitude: 14° 9' 59.5152". Longitude: 108° 54' 9.6588".	89	89	Nếp Ngự (89)	Hoài Nhơn District, Bình Định Province, Vietnam (N 14° 26' 24", E 109° 5' 60")
82	82	Nếp Ngự (82)	Hoài Nhơn District, Bình Định Province, Vietnam (N 14° 26' 24", E 109° 5' 60")	90	90	Nếp Ngự (90)	Hoài Nhơn District, Bình Định Province, Vietnam (N 14° 26' 24", E 109° 5' 60")

Table 5. Continued....

NO	ACCESSION	NAME OF VARIETY	PASSPORT INFORMATION	NO	ACCESSION	NAME OF VARIETY	PASSPORT INFORMATION
91	91	Nếp Ngự (91)	Latitude: 14° 9' 59.5152". Longitude: 108° 54' 9.6588".	97	97	Nếp Ngự (97)	Hoài Nhơn District, Bình Định Province, Vietnam (N 14° 26' 24", E 109° 5' 60"), saline soil
92	92	Nếp Ngự (92)	Latitude: 14° 9' 59.5152". Longitude: 108° 54' 9.6588". Longitude: E 108° 54.161'. Latitude: 14.166532°. Longitude	98	98	Nếp Ngự (98)	Hoài Nhơn District, Bình Định Province, Vietnam (N 14° 26' 24", E 109° 5' 60") 00 N, 100 00 E
93	93	Nếp Ngự (93)	Latitude and longitude coordinates: 109.04532, 14.4666386	99	99	Nếp Ngự (99)	Latitude: 14° 9' 59.5152". Longitude: 108° 54' 9.6588". Latitude: N 14° 9.9919'. Longitude: E 108° 54.161'. Latitude: 14.166532°. Longitude
94	94	Nếp Ngự (94)	Lua nuoc troi, Latitude and longitude coordinates: 109.04532, 14.4666386	100	100	100 (Nếp Ngự Quảng Ngãi)	District on the north. Latitude: 15° 06' 60.00" N Longitude: 108° 47'
95	95	Nếp Ngự (95)	Lua nuoc troi, Latitude and longitude coordinates: 109.04532, 14.4666386	101	101	IR 29	IRRI
96	96	Nếp Ngự (96)	Latitude and longitude coordinates: 109.04532, 14.4666386	102	102	HATRI 04 nếp	HATRI
97	97	Nếp Ngự (97)	Latitude and longitude coordinates: 109.04532, 14.4666386				

**Quantitative traits**

1. Panicle length (cm)-length of panicle at maturity measured from the base to the tip of the panicle (from 10 randomly selected primary panicles per accession per replication).
2. Panicles per plant (number)-total number of panicles per plant (from 10 randomly selected primary panicles per accession per replication).
3. 1000-grain weight (gram)-weight of 1000 well-developed grains at 14% MC (from 5 randomly selected primary panicles per accession per replication).
4. Days to maturity-days from seeding when 80% of the grains are fully ripened on a per replication basis.
5. Filled grains (number)-obtained from counts of total number of filled grains per panicle (from 5 randomly selected primary panicles per accession per replication).
6. Unfilled grains (number) - obtained from counts of total number of unfilled grains per panicle (from 5

randomly selected primary panicles per accession per replication).

- Yield-obtained from the harvested plants in each replication. Harvested grains were threshed, cleaned, dried, and weighed for each accession per replication. Moisture content (MC) per plot was determined immediately after weighing using a moisture meter.

Yield = wt. of harvest (g)/ no. of hills harvest x no. of possible hills x MF

where:  $MF = \frac{100 - MC}{100}$  of the harvest grains

- Biomass-weight of 10 plants harvested from each accession per replication. Harvested plants were dried before weighing.

**Data Analysis**

**Analysis of variance.** The agro-morphological data collected were initially analyzed through analysis of variance to verify genetic variation in the traits measured. The few traits with insignificant genetic variation, based on the F-test, were not considered for further analyses.

**Shannon-Weaver diversity Index.** Diversity indices for the various traits were computed using the following formula:

$$H' = \frac{-\sum pi * \log_2(pi)}{\log_2 n}$$

where: *n* is the number of phenotypic classes for a character and

*pi* is the portion of the total number of entires belonging to the *i* class. The Shannon -Weaver diversity index was standardized by dividing *H'* by the  $\log_2$  of the total number of phenotypic classes. To have an estimate of the phenotypic diversity of the varieties, *H'* was computed in the MS-Excel for each of the morpho-agronomic descriptors. The mean phenotypic diversity index was computed for the pooled diversity estimates per descriptor. The standardized value ranged from 0 to 1, with 1 indicating maximum diversity.

**Correlation analysis.** Correlation coefficient (*r*) is a measure of the association between two or more variables. It is a measure of symmetrical association between variables and does not measure the dependence of one variable over other. Correlation among agro-morphological traits was calculated by using SAS program.

**Distance matrix.** Distance matrix was calculated by means of Euclidean Distance Coefficient (Sneath and Sokal, 1973):

$$Eij = [\sum_k (X_{ki} - X_{kj})^2]^{1/2}$$

where: *Eij* = 0 to ∞, the larger the value, the more distant the degree of relationship

*Xi* and *Xj* are the standardized values for the *i*th and *j*th characters in *k*th varieties.

**Cluster analysis.** Cluster analysis was carried out for agro-morphology-based genetic distance matrix using UPGMA clustering method in the NTSYS program. The results of the UPGMA were used to draw the dendrogram of the 102 traditional varieties.

**Principal component analysis.** The main function of PCA was to explain variance with the linear combination of the variables. Principal component analysis was done using NTSYS and SAS programs.

Molecular-based characterization and analysis using SSR DNA extraction. The 102 varieties were grown in pots. Maximum protection was employed to ensure healthy and disease-free seedlings. The leaves were collected 2-3 weeks after planting for DNA extraction. Standard molecular grade chemicals and general techniques for preparing stock solutions, buffers, reagents, and equipment were followed according to Lang 2002. Molecular work was conducted at the Genetics and Plant Breeding Department of the Hight Aricultural technology Insitute, Cantho, Vietnam (HATRI). DNA suitable for PCR analysis was prepared using a simplified procedure (McCouch et al., 1988). A piece of a young rice leaf (2 cm) was collected and placed in a labeled 1.5 ml centrifuge tube in ice. The leaf was ground using a polished glass rod in a well of a spot test plate (Thomas Scientific) after adding 400 µl of extraction buffer. Grinding was done until the buffer turned green, an indication of cell breakage and release of chloroplasts and cell contents. Another 400 µl of extraction buffer was added into the well by pipetting. Around 400 µl of the lysate was transferred to the original tube of the leaf sample. The lysate was deproteinized using 400 µl of chloroform. The aqueous supernatant was transferred to a new 1.5 ml tube and DNA was precipitated using absolute ethanol. DNA was air-dried and resuspended in 50 µl of TE buffer (Lang., 2002). DNA quality checks used 1% agarose by melting 3 g of agarose in 300 ml of TAE buffer. The mixture was heated in a microwave for 5-6 min and then cooled to around 55-60 0 C. This was then poured on a previously prepared electrophoresis box with combs. Gels were prepared and the combs removed after about 45 min. Seven microliters of DNA sample plus 3 µl of loading buffer (Tris 1 M pH = 8.0, glycerol, EDTA 0.5 M pH = 8.0, xylene cyanol 0.2%, bromphenol blue 0.2%, and distilled

water) was run at 70-80 v, 60 mA for 45 min or until the loading buffer dye moved far away from the wells. The gel was then taken out and stained with ethidium bromide, after which it was observed under UV light.

Microsatellite analysis :the whole microsatellite analysis included PCR assay, polyacrylamide gel electrophoresis, and band detection and scoring. PCR assay Microsatellite primers were used to survey polymorphism on the samples. These were randomly selected from the 135 microsatellite primer pairs currently available for rice (Temnykh et al., 2000).

**The PCR reaction was as follows:** Reactions were overlaid with mineral oil and processed in a programmable thermal controller set for 35 cycles of 1 min at 94 0 C, 1 min at 55 0 C, and 2 min at 72 0 C, with a final extension at 75 0 C for 5 min. After amplification, 10 µl of stop solution was added to the PCR product, which was then denatured at 94 0 C for 2 min. Eight microliters of each reaction were run on polyacrylamide gel. Band detection and scoring Plates were separated using a plastic wedge and were removed from the tank. The acrylamide gel was soaked in ethidium bromide staining solution for 15 to 20 min. Bands in the ethidium bromide-stained gels were detected and photographed under UV light. Allelic bands were scored as 1 (present) or 0 (absent), respectively. Data were entered directly into an Excel spreadsheet. Data analysis Pairwise comparisons of lines based on the presence of unique and shared polymorphic products were used to calculate the genetic similarity coefficients. These coefficients were calculated using Nei and Li's distance measure (Nei and Li, 1979) in the NTSYS-PC Numerical Taxonomy and Multivariate Analysis System (Rohlf, 1990). The lines were clustered on the basis of similarity coefficients using the unweighted pair group method-arithmetic average (UPGMA) clustering algorithm.

**III. RESULTS AND DISCUSSION**

**Polymorphism of microsatellite markers**

To overcome this, an assessment of genetic diversity of initial material sources is necessary. PCR amplification was performed with DNA samples extracted from 102

traditional Nep Ngu rice varieties. Several representative DNA samples were used as template in the PCR amplification reaction using SSR markers as 135 primers on 12 chromosome , but only 62 primers were polymorphic. Amplified PCR products were electrophoresed on 3% agarose gel with 1X TBE buffer solution, stained with ethidium bromide, then observed under UV-transilluminator. In the amplification of genomic DNA of the 102 rice genotypes using 135 primers, 62 were found to be polymorphic. The number of amplified fragments ranged from 2 to 4. All of the primer pairs used in this study generated polymorphic bands among the genotypes. A total of 62 loci were assigned to the 62 microsatellite primer pairs. A total of 178 alleles were detected among the 102 rice genotypes with an average of 1.26 alleles per locus (Table 3). The number of alleles per locus ranged from 2 to 5 (in RM11125). The total alleles identified in the 102 genotypes were classified into 3 categories: The PIC values for the microsatellite loci ranged from 0.16 to 0.87 with an average of 0.57 (Table 2). The low PIC values were observed among the primers of RM228 (0.16) RM26212(0.22); the PIC value high such as primers S11049 (0.74), RM115 (0.87). High PIC values indicate that the selected microsatellite markers are efficient at evaluating a large number of genetic resources. In this study, the mean PIC value of the microsatellite markers used to assess the diversity of rice genetic resources was 0.57, which was much lower than the PIC values of microsatellite markers used in other studies (Surapaneni et al .,2016; Jae-Ryoung et al.,2019).

A dendrogram based on cluster analysis using UPGMA with the module of SAHN in the NTSYS-pc package was created. Cluster analysis showed significant genetic variation among the landrace rice varieties studied, with genetic distance ranging from 0 to 0.84 (Figure 1). With a genetic distance of 0.63, the cluster revealed 3 major groups, A, B, and C, in the Binh Dinh Nep Ngu rice varieties. Group A was divided into sub-clusters A1 and A2 (27%); Group B and Group C (70.58%); and Group C consisted of 3 traditional varieties (2.94%) such as Line 52 , Line 81 and line 44.

Table 2: Primers and Chromosome, PIC values for survival 102 varieties from Binh Dinh VietNam.

STT	Primer	Chromosome location	No. of allele	Size (bp)	PIC VALUES
1	RM228	9	2	240-250	0.16
2	RM26212	4	2	200-220	0.22
3	RM243	1	2	190-210	0.41
4	RM10649	1	2	180-210	0.45
5	RM24	1	3	200-205	0.63
6	RM7643	1	3	205-220	0.66
7	RM472	1	3	210-242	0.64

8	RM11125	1	5	160-200	0.79
9	RM10843	1	4	180-200	0.73
10	RM3412b	1	3	190-200	0.64
11	RM10793	1	3	210-220	0.63
12	Salt 1	1	4	200-220	0.74
13	Salt 2	1	2	210-220	0.45
14	RM 152	8	3	175-200	0.63
15	RM5806	10	3	210-230	0.66
16	RM110	11	2	230-210	0.67
17	RM211	2	3	200-250	0.65
18	RM17	12	5	160-190	0.79
19	RM310	8	4	200-210	0.72
20	RM27877	12	3	215-240	0.63
21	RM221	2	3	220-230	0.66
22	RM28746	12	3	200-210	0.63
23	RM5436	7	4	200-210	0.73
24	RM3867	3	4	210-230	0.74
25	RM6329	3	3	220-230	0.61
26	RM249	5	3	210-230	0.56
27	RM5626	3	5	200-210	0.78
28	RM18	7	3	190-200	0.64
29	RM21	11	5	210-220	0.27
30	RM163	5	2	255-260	0.45
31	S11049	11	4	200-210	0.74
32	RM140	1	3	190-200	0.61
33	RM169	5	4	240-250	0.73
34	RM9	1	2	230-240	0.49
35	RM10852	1	3	220-230	0.64
36	RM10890	1	3	205-210	0.66
37	RM10927	1	2	240-245	0.40
38	RM154	2	2	160-180	0.45
39	RM231	3	3	200-210	0.67
40	RM21539	7	2	205-210	0.45
41	RM122	5	3	205-230	0.64
42	RM510	6	2	220-230	0.42
43	RM547	8	2	200-210	0.49
44	RM23662	9	3	210-220	0.64
45	RM219	9	3	200-215	0.65
46	RM24013	9	2	215-220	0.42
47	RM3	6	2	220-225	0.50
48	RM223	8	2	200-210	0.46
35	RM10852	1	3	220-230	0.64
36	RM10890	1	3	205-210	0.66

37	RM10927	1	2	240-245	0.40
38	RM154	2	2	160-180	0.45
39	RM231	3	3	200-210	0.67
40	RM21539	7	2	205-210	0.45
41	RM122	5	3	205-230	0.64
42	RM510	6	2	220-230	0.42
43	RM547	8	2	200-210	0.49
44	RM23662	9	3	210-220	0.64
45	RM219	9	3	200-215	0.65
46	RM24013	9	2	215-220	0.42
47	RM3	6	2	220-225	0.50
48	RM223	8	2	200-210	0.46
49	RM315	1	2	210-230	0.49
50	RM13	5	3	190-210	0.63
51	RM166	2	3	190-200	0.65
52	RM140	1	3	200-210	0.63
53	RM220	1	3	210-220	0.64
54	RM227	3	3	200-220	0.65
55	RM148	3	2	190-210	0.43
56	FMU1-2	8	3	190-210bp	0.52
57	RM115	6	2	210-300	0.87
58	Indel 5	7	2	213-250	0.23
59	RM106	2	2	300-350	0.56
60	RM244	10	3	250-230	0.31
61	RM105	9	2	210-215	0.27
62	RM10115	1	2	240-250	0.72
	Total		178		0.57

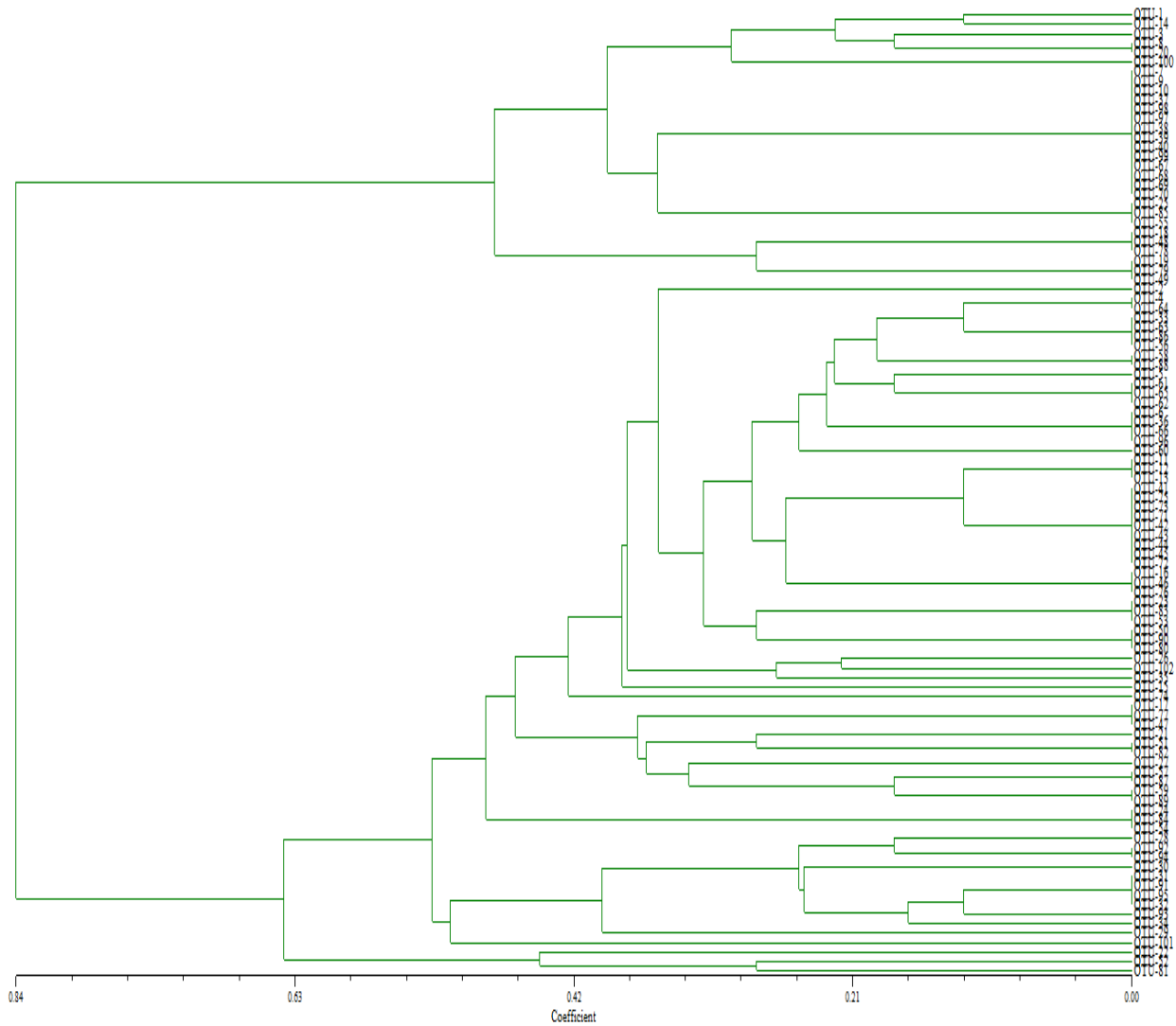


Fig 1. Classification of rice varieties based on genetic distance calculated from 62 microsatellite markers of 102 rice varieties

Table 3: Mean number of alleles based on microsatellite markers on different rice chromosomes

Group	Sub group	Mean of allele No. per SSR markers												Mean
		Chromosome												
		1	2	3	4	5	6	7	8	9	10	11	12	
<b>A</b>	1	1.23	1.56	1.42	0	1.42	0.92	1.74	1.17	1.24	1.53	1.82	1.48	1.29
	2	1.35	1.72	1.39	0	1.56	0.83	1.65	1.03	1.3	1.83	1.83	1.62	1.34
	<i>Mean</i>	1.29	1.64	1.4	0	1.49	0.87	1.69	1.1	1.27	1.68	1.83	1.55	1.31
<b>B</b>	1	1.52	1.68	1.65	0	1.74	1.12	1.78	1.46	1.75	1	2.92	1.64	1.52
	2	1.27	1.77	1.53	0	1.52	0.89	1.08	1.17	1.65	1.28	2.19	1.78	1.34
	3	1.33	1.25	1.58	0	1.65	0.1	1.55	1.32	1.42	1.79	2.36	1.98	1.36
	<i>Mean</i>	1.37	1.56	1.58	0	1.63	0.7	1.47	1.31	1.6	1.36	2.49	1.8	1.4

<b>C</b>	1	1.74	1.56	1.65	1.2	1.76	1.11	1.63	1.47	1.12	1.58	2.8	1.56	1.59
	<i>Mean</i>	1.74	1.56	1.65	1.2	1.76	1.11	1.63	1.47	1.12	1.58	2.8	1.56	1.59
<b>Total</b>	<i>Mean</i>	1.46	1.58	1.54	1.2	1.62	0.89	1.58	1.29	1.33	1.54	2.37	1.63	1.43

Mean of allele number per locus and each chromosome reveal much lower in the 1.43 (Table 3). The mean of allele number per locus group A is 1.34. The mean number of alleles per locus observed was group B is 1.40 similar with sub group C is 1.59.

Table 4. Mean and range of different quantitative traits used in measuring genetic distances among 102 landrace varieties.

	<b>Max</b>	<b>Min</b>	<b>Mean</b>	<b>CV</b>	<b>P</b>	<b>h<sup>2</sup></b>
<b>Plant height (cm)</b>	155.70	120.05	137.87	0.75	**	0.74
<b>No. of panicle/ hill</b>	30.22	5.69	15.89	3.07	**	0.68
<b>Panicle length (cm)</b>	28.06	17.19	22.62	3.17	**	0.81
<b>Percentage of fertile grain (%)</b>	130.74	55.35	93.05	0.56	**	0.71
<b>Percentage of unfertile grain (%)</b>	30.38	5.94	18.16	0.73	**	0.89
<b>1000grain Weight (gram)</b>	30.77	20.47	25.62	2.00	**	0.84
<b>Duration (days)</b>	155.78	120.00	139.39	0.52	**	0.84
<b>Biomass(gram)</b>	100.00	16.00	58.33	1.23	**	0.87
<b>Yield (gram/hill)</b>	56.52	16.15	36.33	1.40	**	0.89

Morphological table diversity analysis, using the analysis of agromorphological features of variance. For each of the 10 quantitative characteristics, the mean, range (maximum and minimum), standard deviation, coefficient of variation (CV), mean standard error, and F-value were calculated (Table 4).

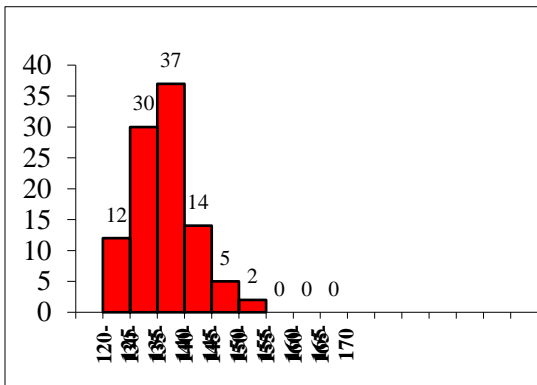
Frequency distribution of the varieties with respect to maturity, panicles per plant, number of filled grains, number of unfilled grains, 1000-g weight, yield, biomass harvest index and survival day affters stress NaCl showed the diversity of traditional varieties. These quantitative characters were found to be significant at 1% and all measurements were not too far from normal distribution (Figures 2a-h).

Hight plant showed normal distributions (figure 2a). Distribution of varieties for the number of filled grains was slightly skewed to the right with only a few varieties near the maximum value (Figure 2d) while distribution of varieties for the number of unfilled grains was slightly skewed to the left with only a few varieties near the maximum value Figure figure 2e. For traits like 1000 grain weight, yield and panicles per plant, unimodal distributions were observed with most varieties skewed to the left of the curve. Such distribution is favorable particularly with respect to number of unfilled grains because lower number of unfilled grains would mean higher yield. This is an

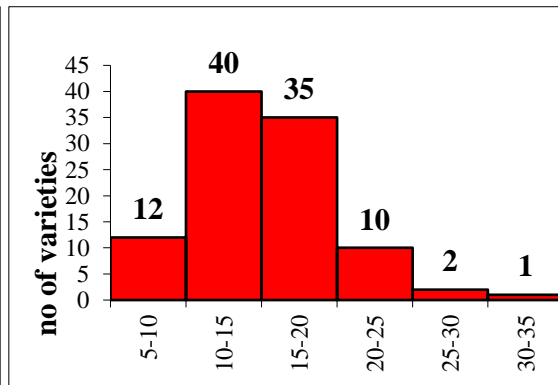
important objective for most plant breeders in improving present day varieties.

Yield showed near normal distributions, was slightly skewed to the right with only a few varieties near the maximum value (Figures 2h). With regards to maturity, almost half of the varieties investigated exhibited long maturity duration. Analysis of variance (ANOVA) showed high variability among the varieties in terms of number of unfilled grains, yield, number of filled grains, The results showed that most quantitative characteristics vary widely. For maturity, the earliest maturity genotype matures after 130 days while the maximum number of days to maturity is 140 days. The maximum value obtained in terms of yield (56.52g / hill).

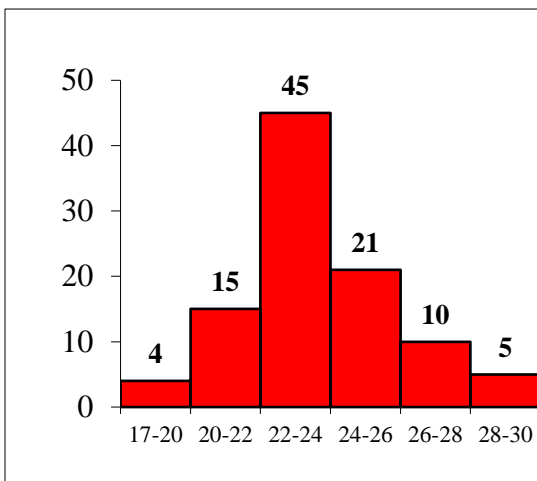
With regard to maturation, most varieties mature in 130-140 days. The challenge still exists for breeders to develop shorter duration varieties without sacrificing yields. In general, morphological characteristics show that most traditional varieties have a higher number of filled seeds, a lower number of unfilled seeds, late maturity, tall with wider leaves, a higher weight of 1000 grain, and late maturity. The variation in agricultural morphological features discussed above can be explained by genetic variability between the tested varieties. This change can be used as a raw material for plant breeders to improve rice for better crop grade, better grain quality, and higher photosynthesis efficiency( Lang et al 2014).



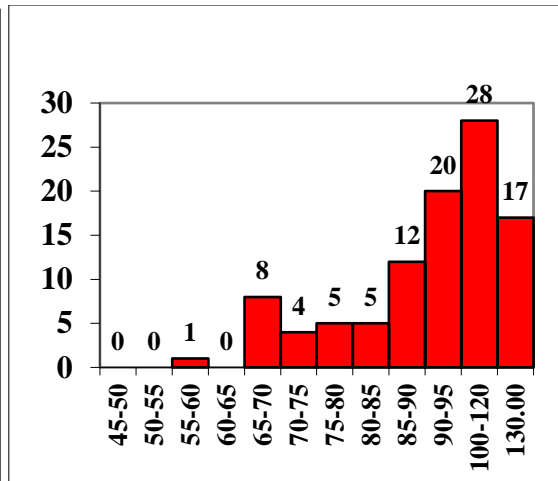
a. Plant height



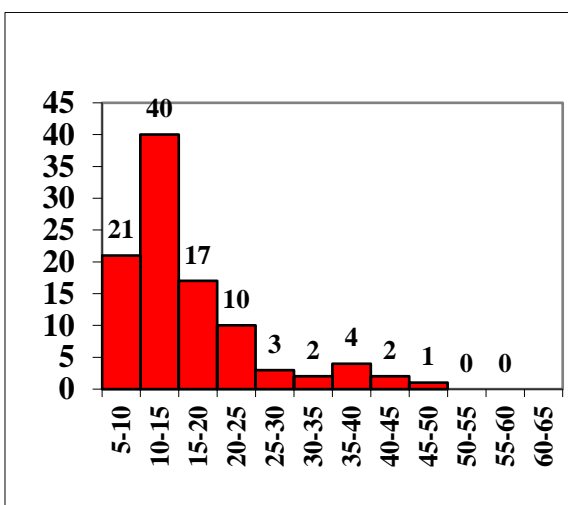
b. Panicle/ Hill



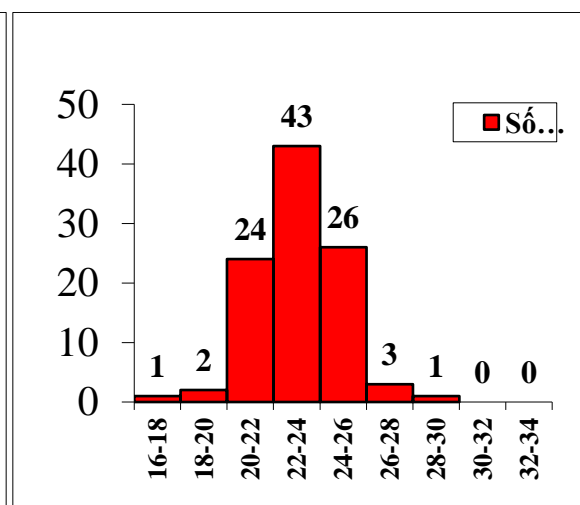
c. Length Panicle



d. Filling distribution



e. unfilling distribution



f. 1000 grain weight



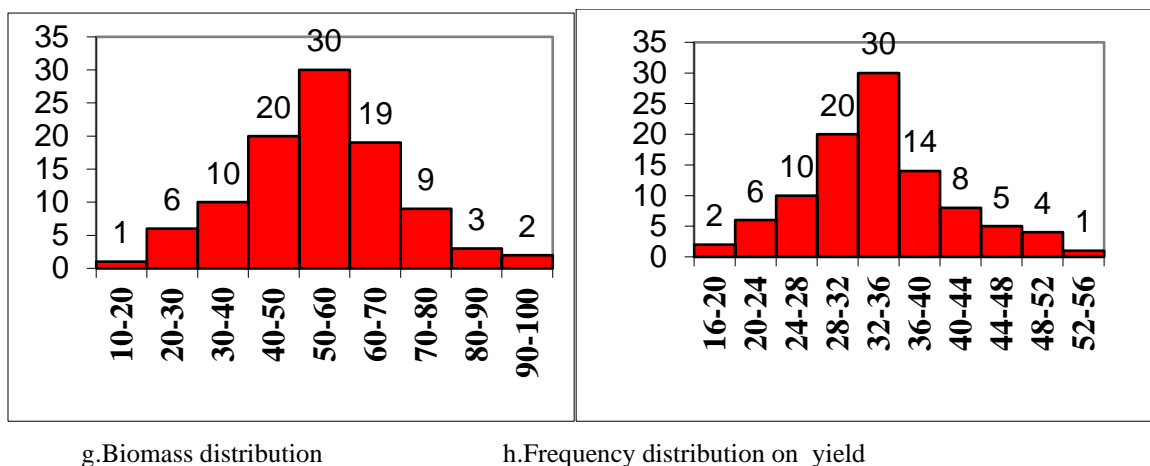


Fig.2: Frequency distribution of the varieties base on a/height plant duration, b/ panicles per plant, c/Length Panicle, d/number of filled grains, e/ number of unfilled grains, f/1000-g weight, f/biomass and g/yield, showed the diversity of landrace Nep Ngu varieties of Binh Dinh.

### Correlation Among Agro-morphological Traits

Correlation between agricultural morphological features. The correlation coefficients between the measured traits are shown in Table 5. The number of strong filling per plant was significantly correlated with yield ( $r = 0.623^{**}$ ) and biomass ( $r = 0.725^{**}$ ) suggesting that varieties with more also had higher yields. Significant correlations were also found between panicle length plant height ( $r = 0.425^{*}$ ), duration time ( $r = 0.474^{*}$ ) which can be explained by the principle of morphological compatibility in rice architecture. Other characteristics are strongly correlated

with the length of panicle. Weight 1000 g, closely related to yield ( $r = 0.795^{**}$ ) and biomass ( $r = 0.715$ ). Yield correlates greatly with biomass ( $r = 0.856^{**}$ ) but moderately correlated with duration ( $r = 0.017ns$ ). Other traits that were found to be poorly correlated with other agro-morphological traits. It exhibited negative correlation with panicle length and filling grain ( $-0.025$ ), Weight gran 1000 ( $0.135ns$ ). Some late maturing varieties had negative with yield ( $r = -0.043$ ). The result the difference with Lang et al 2014 explain for landrace varieties with Nep Ngu at Binh Dinh.

Table 5: Correlation coefficients among 9 agro-morphological traits of 102 Nep Ngu rice varieties

	Plant height	Duration	Length of panicle	Filling grain	Unfilled grain	Weight 1000	Yield	Biomass
Plant height	<b>1.000</b>							
Duration	0.223ns	<b>1.000</b>						
Panicle length	0.435*	0.474*	<b>1.000</b>					
Filling grain	-0.064ns	-0.117ns	-0.025ns	<b>1.000</b>				
Unfilled grain	0.275ns	0.176	0.198ns	-0.064ns	<b>1.000</b>			
Weight grain 1000	0.125ns	-0.167ns	0.135ns	0.084ns	-0.015ns	<b>1.000</b>		
Yield	0.457*	0.355	0.188	<b>0.623</b>	<b>0.751</b>	<b>0.795</b>	<b>1.000</b>	
Biomass	0.073ns	0.017	0.060	0.725	-0.033	0.715	<b>0.856</b>	<b>1.000</b>



#### IV. CONCLUSIONS

Agro-morphological characters and PCR based markers have provided valuable information about genetic diversity of rice collection in Binh Dinh, VietNam. In molecular-based analysis, results showed that SSR markers were very useful and effective in characterizing and estimating the extent and distribution of genetic variation in the 102 rice landraces. Clustering of the varieties based on genetic distance (0.63) allowed grouping of the 102 varieties into three clusters

In general, both morphological and SSR markers were able to group the varieties into ecotypes, rainfed and landrace rice.

Quantitative agro-morphological characters and molecular markers of 102 accessions were analyzed using clustering, correlation coefficient, principal component analysis and analysis of variance. Diversity of the collection was analyzed using Shannon-Weaver diversity index. The objective of the study was to determine the extent of diversity using agro-morphological and molecular markers (SSRs).

Using quantitative agro-morphological characters, ANOVA showed highly significant differences among the traits of the 102 rice landraces except panicles per plant and yield. Correlation coefficients showed that all the traits were significantly correlated with each other except yield, which was only slightly correlated with other traits. The diversity indices for quantitative descriptors were high ranging from  $H' = 0.68$  to  $0.79$ . Mean diversity index for all traits among the 102 traditional varieties was high ( $H' = 0.7$ ).

From these results, the following recommendations are presented:

1. Diversity analysis based on agro-morphological traits of rice landraces need to be continued to further confirm relationships among them.

2. Extensive molecular marker analysis may be conducted by considering more primers for its relevant application and efficient attainment of breeding objectives in rice improvement.

3. Continue analysis for the rest of the traits from difference traits such as grain quality and tolerance with biotic and biotic stress to Identification of novel resistance gene in rice germplasm for 102 lines Nep Ngu at Binh Dinh.

This paper presents findings from "Application of biotechnology to determine the endemism of glutinous rice varieties in Hoai Son commune, Hoai Nhon town, Binh Dinh province 'project'. We thanks Binh Dinh People's Committees and Department of Science and Technology for supported this project and We also acknowledge the support of and gene bank of the plant breeding and genetic division at HATRI.

#### REFERENCES

- [1] Botstein D, White RL, Skolnick M, Davis RW (1980). Construction of a genetic linkage map in man using restriction fragment length polymorphisms. *Am. J. Hum. Genet* 32: 314–331.
- [2] JARVIS, D.I., L. MYER, H. KLEMICK, L. GUARINO, M. SMALE, A.H.D. BROWN, M. SADIKI, B. STHAPIT and T. HODGKIN. 2000. A training guide for *in situ* conservation on farm. Version 1. International Plant Genetic Resources Institute, Rome, Italy. 68p.
- [3] Jae-Ryoung Park, Won-Tae Yang, Yong-Sham Kwon, Hyeon-Nam Kim, Kyung-Min Kim, and Doh-Hoon Kim 2019. Assessment of the Genetic Diversity of Rice Germplasm Characterized by Black-Purple and Red Pericarp Color Using Simple Sequence Repeat Markers. *Plants* 2019, 8(11), 471
- [4] Lang NT (2002). Protocol for basics of biotechnology. Agricultural Publishing House, Ho Chi Minh, Vietnam.
- [5] Lang (NT), Pham Thi Be Tu, Nguyen Chi Thanh, Bui Chi Buu and Ismail A (2009). Genetic diversity of salt-tolerant rice landraces in Vietnam. *J. Plant Breed. Crop Sci.* 1(5): 230-243
- [6] Lang Thi Nguyen, Bui Phuoc Tam, Nguyen Van Hieu, Chau Thanh Nha, Abdelbagi Ismail, Russell Reinke and Bui Chi Buu. 2014. Evaluation Of Rice Landraces In Vietnam Using Ssr Markers And Morphological Characters. *Sabrao Journal of Breeding and Genetics* 46 (1) 1-20, 2014.
- [7] McCouch SR (1988). Molecular mapping of rice chromosomes. *Theor. Appl. Genet.* 76: 815- 829.
- [8] Ni J, Colowit PM and MacKill DJ (2002). Evaluation of genetic diversity in rice subspecies using microsatellite markers. *Crop Sci.* 42: 601- 607.
- [9] Nei M and Wen-Hsiung LI (1979). Mathematical model for studying genetic variation in terms of restriction endonucleases. *Proc. Natl. Acad. Sci. USA* 76 (10): 5269-5273.
- [10] Nei M (1973). Analysis of gene diversity in subdivided populations. *Proc. Natl. Acad. Sci. USA.* 70: 395-401.
- [11] Newbury HJ and Ford Lloyd BV (1993). The use of RAPD in accessing variation in plants. *Plant Growth Reg.* 12: 45-51.

#### ACKNOWLEDGEMENTS

- [12] Rohlf FJ (1990). NTSYS-pc. Numerical taxonomy and multivariate analysis system. Applied Biostatistics Inc., New York. 175 p.
- [13] Surapaneni, M.; Balakrishnan, D.; Mesapogu, S.; Raju, A.K.; Rao, Y.V.; Neelamraju, S. 2016. Genetic characterization and population structure of Indian rice cultivars and wild genotypes using core set markers. *3 Biotech* **2016**, *6*, 95.
- [14] SAS Institute (1999). SAS/STAT: user's guide: version 8. SAS Institute, Cary.
- [15] Shinada H, Yamamoto T, Yamamoto E, Hori K, Yonemaru J, Matsuba S, Fujino K. Historical changes in population structure during rice breeding programs in the northern limits of rice cultivation. *Theor Appl Genet.* 2014;127:995–1004.
- [16] SuksonTonapha, Pusadee, ChanakanProm-uthai, Benjavanerkasem, and Sansanee Jamjod. 2021. Diversity of Purple Rice (*Oryza sativa* L.) Landraces in Northern Thailand. *Agronomy* 2021, *11*(10), 2029.
- [17] Temnykh S, Park WD, Ayres N, Cartinhour S, Hauck N, Lipovich L, Cho YG, Ishii T and McCouch SR (2000). Mapping and genome organization of microsatellite sequences in rice (*Oryza sativa* L.). *Theor. Appl. Genet.* 100: 697-712.
- [18] Yadav S, Singh A, Singh M, Goel N, Vinod KK, Mohapatra T, Singh AK. Assessment of genetic diversity in Indian rice germplasm (*Oryza sativa* L.): use of random versus trait-linked microsatellite markers. *J Genet.* 2013;92(3):545–557. doi: 10.1007/s12041-013-0312-5.
- [19] WILLIAMS, J.G.K., A.R. KUBELIK, K.J. LIVAK, J.A. RAFALSKI, and S.V. TINGEY. 1990. DNA polymorphism amplified by arbitrary primers is useful as genetic markers. *Nucleic Acids Res.* 18: 6531–6535.



# Search for a suitable substrate for mass propagation of a local strain of *Trichoderma harzianum* (ThTab) isolated in Burkina Faso

Tobdem Gaston DABIRE\*, Masséni Yasmine OUOLOGUEME, Schémaéza BONZI and Irénée SOMDA

<sup>1</sup>Université Nazi BONI, Ecole Doctorale Sciences Naturelles et Agronomie, Laboratoire des Systèmes Naturels, Agrosystèmes et de l'Ingénierie de l'Environnement (Sy. N. A. I. E.), 01 P.O Box 1091, Bobo-Dioulasso 01, Burkina Faso

\*Corresponding author: drdabiretoo@gmail.com

Received: 02 Nov 2023; Received in revised form: 08 Dec 2023; Accepted: 17 Dec 2023; Available online: 24 Dec 2023

©2023 The Author(s). Published by Infogain Publication. This is an open access article under the CC BY license

(<https://creativecommons.org/licenses/by/4.0/>).

**Abstract**— A strain of *Trichoderma harzianum* Pers. isolated in Burkina Faso showed significant antagonistic properties against phytopathogenic fungi in vitro and in the greenhouse. The aim of this study was to identify an effective, available and inexpensive medium for its multiplication and large-scale use. Thus, various organic substrates identified as carbon sources were supplemented with others identified as nitrogen sources and then tested using the solid-state fermentation method. An inoculum of the fungus was fermented on these slightly humified substrates for 07 days at room temperature (22-25°C). The number of micropropagules produced per substrate was then evaluated in Colony Forming Units per gram of substrate (CFU/gos). The use of maize bran supplemented with soy flour as a substrate resulted in an average micropropagule production of  $1045.5 \cdot 10^8$  CFU/gos, i.e. a 5228-fold multiplication of the initial inoculum. Maize bran was the best carbon source, with an average contribution of  $297,10^8$  CFU/gos whatever the nitrogen supplement, and soy flour the best nitrogen supplement, with an average contribution of  $113.7,10^8$  CFU/gos whatever the carbon source. The development of a formulation based on maize bran and soy flour for the mass multiplication of this strain is envisaged.



**Keywords**— *Trichoderma harzianum*, Micro propagules, Maize bran, Burkina Faso, Substrate

## I. INTRODUCTION

Until now, the control of crop pests has focused on the application of prophylactic measures (crop rotation, fallowing of infested land, seed and soil disinfection, etc.), the use of resistant and/or tolerant varieties and the use of chemical pesticides (Shahnaz *et al.*, 2013).

However, the adoption of certain prophylactic measures remains ill-suited to large farms, and is also hampered by land pressure (Traoré *et al.*, 2020). The low availability of varieties resistant to several pests also limits the use of genetic control (Gary & Hebbbar, 2015). The use of synthetic chemical pesticides is still the most widely used control method, as it delivers results very quickly (Schiffers & Wainwright, 2011). However, given the risks of damage to

the health of producers, consumers and agrosystems, and the rapid emergence of resistance within pathogen or pest populations, chemical control is increasingly discouraged and heavily regulated (Son *et al.*, 2018; Besmer *et al.*, 2022).

In view of all these limitations, the development of alternative control methods that are effective, sustainable and safe for both man and the environment is a major concern for agricultural research institutions. Biological control, used as an alternative to the use of chemicals, is an ecologically sound approach that involves the use of specific organisms to protect plants against their bio-aggressors (Sargin *et al.*, 2013). Biological control agents including yeasts, bacteria and fungi have been successfully

tested, and some formulations based on biological control agents are encountered commercially today (Dal Bello *et al.*, 2002; Bardin *et al.*, 2003; Trebicka *et al.*, 2012).

Among the biological control agents used, telluric fungi of the *Trichoderma* genus occupy an important place (Gary & Hebbbar, 2015). *Trichoderma* are telluric filamentous fungi of the Phylum Ascomycetes, family Hypocreales that are well known and used for their antagonism against several soil phytopathogens involving fungi, bacteria and invertebrates (Cowper *et al.*, 2013) and for their plant growth-promoting properties (Bacon *et al.*, 2001; John *et al.*, 2010; Abdel-Monaim, 2014). According to recent studies, these fungi use several modes of action such as mycoparasitism, competition and antibiosis, root stimulation, solubilization of plant fertilizing minerals and stimulation of plant natural defenses and soil bioremediation (Verma *et al.*, 2007, Cowper & Renaud, 2013).

*Trichoderma* spp are cosmopolitan fungi, characterized by their rapid growth, ability to use a variety of substrates and resistance to harmful chemical agents (Luz *et al.*, 2019). They are present on decaying wood and in soils at concentrations ranging from 10 to 10,000 propagules per gram of soil (Cowper & Renaud, 2013). One of the most frequently encountered species in biological control agent formulations worldwide is *Trichoderma harzianum* Pers. This species has been the subject of several research activities and has been shown to have proven antagonistic properties against several plant pathogens and to promote plant growth (Caron *et al.*, 2002; Souna *et al.*, 2012; Mahalakshmi & Yesu Raja, 2013; Abdel-Monaim *et al.*, 2014; Ferrigo *et al.*, 2014; Akrami & Yousefi, 2015; Gautam *et al.*, 2015). In Burkina Faso, a local strain of *Trichoderma harzianum* (ThTab) was isolated from the rhizosphere of an onion plot in the village of Tabtenga.

This strain was tested in vitro and in the greenhouse against *Fusarium* spp. and *Aspergillus niger*, respectively responsible for fusarium rot and black rot of onion (Dabiré

*et al.*, 2016a). It also exhibited an important growth-promoting property in greenhouse onions (Dabiré *et al.*, 2016b). The research question that emerged from this work was how to multiply and conserve this strain for large-scale use in market garden agrosystems. The literature indicates that one of the most suitable methods for successful multiplication of *T. harzianum* is its solid-state fermentation on moistened organic substrates without free water (Sargin *et al.*, 2013). The aim of the present study was to evaluate locally available and inexpensive agro-industrial by-products as natural organic substrates for mass production of micro propagules of this local strain of *T. harzianum* under solid-state fermentation conditions inspired by Sargin *et al.* (2013).

## II. MATERIALS AND METHODS

### 2.1 Microorganisms used

The fungal material used was a strain of *Trichoderma harzianum* ThTab, isolated from a soil sample taken from the rhizosphere of an onion plot in the village of Tabtenga, east of the city of Ouagadougou, Burkina Faso. The strain was sequenced and stored in the mycotheque of the Earth and Life Institute (ELI) of the *Université Catholique de Louvain (UCL)* under accession number 8129-THBFA.

### 2.2 Agro-industrial by-products used

Various local by-products, mainly of plant origin, were used as organic substrates for mushroom propagation (Table 1). These by-products were collected in the villages of Boni, Kodéni and Nasso, at the *Institut de l'Environnement et de Recherches Agricoles (INERA)* station in Farako-Bâ and in the industrial zone of Bobo-Dioulasso.

After collection, the organic materials were suitably crushed using an electric grinder, then sieved to obtain a fine, homogeneous powder. They were then oven-dried (0% moisture content). Moisture levels were checked using a RADWAG® moisture meter.

Table 1 Organic substrates (carbon and nitrogen sources) tested in this study

Source	Type	Scientific name	Provenance
Carbon sources	Acacia bark	<i>Faidherbia albida</i>	Boni
	Maize raids	<i>Zea mays</i>	Farako-bâ
	Eucalyptus sawdust	<i>Eucalyptus camaldulensis</i>	Bobo-Dioulasso
	Maize bran	<i>Zea mays</i>	Bobo-Dioulasso
	Rice bran	<i>Oryza sativa</i>	Kodéni
	Maize and rice bran (g/g)	<i>Z. mays</i> et <i>O. sativa</i>	Kodéni
	Millet stalks	<i>Pennisetum glaucum</i>	Farako-bâ
	Sorghum stalks	<i>Sorghum bicolor</i>	Nasso
Sorghum and millet stalks (g/g)	<i>P. glaucum</i> , <i>S. bicolor</i>	Farako-bâ et Nasso	

	Cottonseed cake	<i>Gossypium hirsutum</i>	Bobo-Dioulasso
Nitrogen sources	Acacia pods	<i>Faidherbia albida</i>	Bobo-Dioulasso
	Soy flour	<i>Glycine max</i>	Bobo-Dioulasso
	Moringa leaves	<i>Moringa oleifera</i>	Bobo-Dioulasso
	Cowpea hulls	<i>Vigna unguiculata</i>	Bobo-Dioulasso
	Peanut hulls	<i>Arachis hypogaea</i>	Bobo-Dioulasso
	Synthetic culture medium	Peptone	Bobo-Dioulasso

### 2.3 Inoculum preparation and strain mass production

To prepare the inoculum, the strain was cultured in Petri dishes containing PDA (Potato Dextrose Agar) medium, then incubated at 25°C under an alternating cycle of near-ultraviolet light and darkness (12h/12h) for 5 days. From a culture of the fungus, a conidial suspension was prepared with distilled water supplemented with Tween 80 (0.1%) under aseptic conditions on the colony in a Petri dish. After shaking, the resulting solution was filtered, its concentration assessed and adjusted to 10<sup>8</sup> conidia/ml using a Fuch-Rosental cell. This suspension was used as inoculum.

*T. harzianum* micropropagules were produced in 200 ml glass vials containing a mixture of 5 g of each carbon source + 50 mg of each nitrogen source (weight/weight ratio 1%). A control containing the carbon source with no nitrogen source was set up. The mixtures were first sterilized at 120°C for 20 minutes before being moistened with distilled water at 70% humidity. The substrates thus prepared were inoculated with the fungus by introducing 1 ml of the previously prepared inoculum into each flask, giving an initial concentration of 0.2 conidia per gram of substrate (0.2 conidia/gos). After inoculation, the vials were lightly resealed (to allow aeration) and then incubated at laboratory room temperature (approx. 22°C) for 7 days.

### 2.4 Evaluation of micropropagule production

At the end of the culture period, 40 ml of distilled water with a drop of tween 80 was added to the contents of each flask.

The contents were then vortexed for 3 min to obtain a mixture of conidia and mycelial fragments. Serial dilutions were made with each mixture, and the number of dilutions (aliquots) was a function of the initial concentration of the mixture (100-fold or 1000-fold).

Micropropagules were counted on a Dichloran-Glycerol (DG 18) agar-based culture medium as recommended by NF EN ISO 11133 (2014). For its preparation, 15 g of DG18 were suspended in 500 ml of distilled water. The suspension was brought to the boil with constant stirring until completely dissolved. After dissolution, 85 ml of glycerol were added, and the whole mixture was autoclaved at 120°C for 30 min. After cooling to approximately 50°C, the medium was dispensed into Petri dishes. Once the medium had solidified, 500 µl of each aliquot from the serial dilution was added to each Petri dish, at a rate of five (05) Petri dishes per aliquot. Ces dernières ont ensuite été mises en incubation à 25°C pendant huit (08) jours. Les colonies développées ont été comptées quotidiennement pendant les huit (08) jours. Les résultats ont été exprimés en Unités Formant des Colonies par gramme de substrat (UFC/gos).

### 2.5 Experimental design

For the fungi cultivation, the different nitrogen sources were tested with each organic substrate in a Randomized Complete Block design. For each carbon source, seven (7) treatments (Table 2) were carried out in five replicates.

Table 2 Treatments used for each substrate

Codes	Traitements
T0	Carbon source without nitrogen supplement
T1	CSS* with peanut hull powder
T2	CSS* with acacia pod powder
T3	CSS* with moringa leaf powder
T4	CSS* with cowpea hull powder
T5	CSS* with peptone
T6	CSS* with soy flour

CSS\*: Carbon source supplemented; CSS\* = Acacia barks; Maize raids; Eucalyptus sawdust; Maize bran; Rice bran; Millet stalks; Sorghum stalks; Maize and rice bran; Millet and sorghum stalks; Cottonseed cake.

## 2.6 Data processing

The data collected were first recorded and then the averages calculated using Excel software. The averages obtained were compared by an analysis of variance using the Student-Newman-Keuls multiple comparison test at the 5% threshold, performed with IBM SPSS version 22 software.

### III. RESULTS

The results obtained are grouped according to carbon sources based on maize and rice by-products, carbon sources based on millet and sorghum by-products and other carbon sources. The contribution of carbon sources to micropropagule production, irrespective of nitrogen supplement, and that of nitrogen supplements, irrespective of carbon source, were also presented.

#### 3.1 Multiplication of *T. harzianum* on carbon sources based on rice and maize by-products

The production of micropropagules per gram of substrate consisting of rice bran, maize bran, the mixture of rice bran plus maize bran and maize cobs in the presence of the various nitrogen supplements is shown in Table 3. The table shows that harvest levels varied according to the nitrogen supplements used, over a range from 3.2,10<sup>8</sup> to 19.6,10<sup>8</sup> CFU/gos for rice bran. For this organic substrate,

Table 3 Production of *T. harzianum* ThTab micropropagules on rice bran, maize bran, rice+maize bran and maize raids supplemented with the various nitrogen sources

Nitrogen supplements	Number of micropropagules (CFU/gos) X 10 <sup>8</sup>			
	Rice bran	Maize bran	Rice+Maize bran	Maize raids
No supplement	3.2 <sup>a</sup>	85.5 <sup>a</sup>	76.0 <sup>b</sup>	13.6 <sup>a</sup>
Peanut hulls	6.7 <sup>b</sup>	101.4 <sup>a</sup>	47.5 <sup>ab</sup>	14.3 <sup>a</sup>
Acacia pods	7.0 <sup>b</sup>	190.1 <sup>a</sup>	55.1 <sup>ab</sup>	9.8 <sup>a</sup>
Moringa leaves	4.4 <sup>ab</sup>	193.3 <sup>a</sup>	72.9 <sup>b</sup>	4.4 <sup>a</sup>
Cowpea hulls	19.6 <sup>c</sup>	285.1 <sup>a</sup>	57.7 <sup>b</sup>	19.6 <sup>a</sup>
Peptone	9.2 <sup>c</sup>	177.4 <sup>a</sup>	47.5 <sup>ab</sup>	13.0 <sup>a</sup>
Soy flour	12.7 <sup>d</sup>	1045.5 <sup>b</sup>	27.2 <sup>a</sup>	20.9 <sup>b</sup>
<b>F value</b>	<b>38.000</b>	<b>37.013</b>	<b>105.752</b>	<b>10.752</b>
<b>P value</b>	<b>0.000</b>	<b>0.000</b>	<b>0.000</b>	<b>0.000</b>

Means in the same column affected by the same alphabetical letter are not significantly different at the 5% threshold according to the Student-Newman-Keuls multiple comparison test. CFU/gos: Colony Forming Units per gram of substrate; F: Fisher's coefficient; P: Probability

The results of growing *T. harzianum* on the mixture (half/half) of rice bran and maize used as a carbon source in the presence of various nitrogen supplements are presented in Table 3. Micropropagule production levels varied according to nitrogen supplementation, from 27.2.10<sup>8</sup> CFU/gos for soybean meal to 76.0.10<sup>8</sup> CFU/gos for the treatment without nitrogen supplementation. The use of

supplementation with cowpea hull powder yielded the highest level of micropropagule harvest. All treatments produced harvest levels that were statistically different from the treatment without nitrogen supplementation, which presented the lowest harvest level. Apart from peanut hulls and acacia pods, which produced similar results, the other supplements were significantly different from each other (Table 3). Soy flour, which comes in second place after cowpea hulls, had a very good harvest.

For corn bran, analysis of the table shows that production levels varied according to nitrogen supplementation, from 85.5.10<sup>8</sup> to 1045.5.10<sup>8</sup> CFU/gos. The use of soy flour as a nitrogen supplement resulted in the highest number of micro-propagules, significantly different from other nitrogen supplements (Table 3). Cowpea hulls are the second most effective nitrogen supplement after soybean meal, although statistical analysis does not distinguish them significantly from other nitrogen supplements. The treatment without nitrogen supplements recorded the lowest number of micro-propagules, but this was not statistically different from the numbers obtained with the other nitrogen supplements. The use of maize bran as a carbon source resulted in significantly higher production levels than all other carbon sources (Table 3).

cowpea tops and moringa leaves, however, resulted in production levels statistically similar to those of the treatment without supplements, i.e. 2.9.10<sup>8</sup> CFU/gos and 57.7.10<sup>8</sup> CFU/gos respectively (Table 3). Supplementing this substrate with peanut hulls, acacia pods, peptone and soy flour did not significantly promote fungal multiplication on this carbon source.

Maize raids powder, used as a carbon source for *T. harzianum* multiplication in the presence of various nitrogen supplements, produced varying levels of micropropagule production. The numbers of micropropagules obtained for the different treatments range from  $4.4 \cdot 10^8$  CFU/gos for the use of moringa leaves as a nitrogen supplement to  $20.9 \cdot 10^8$  CFU/gos for soy flour used as a nitrogen supplement.

### 3.2 Multiplication of *T. harzianum* on carbon sources based on millet and sorghum by-products

The production of micropropagules on sorghum and millet stalk powder and their mixture, supplemented with different nitrogen sources, is recorded in Table 4.

Shredded millet stalks, supplemented with various nitrogen sources, enabled *T. harzianum* to multiply with varying levels of micro-propagule harvest depending on the type of supplement (Table 4). Micropropagule production levels according to nitrogen source ranged from  $0.6 \cdot 10^8$  to  $1.3 \cdot 10^8$  CFU/gos. On this carbon source, peptone culture medium, acacia pods and moringa leaves showed significantly similar and significantly different production levels to the

other supplements. Supplementing this carbon source with soy flour significantly and negatively affected the level of fungal multiplication (Table 4).

In sorghum stalks, the number of micro-propagules obtained for each nitrogen supplement ranged from  $2.4 \cdot 10^8$  CFU/gos (for Peptone) to  $3.6 \cdot 10^8$  CFU/gos (for peanut hulls). Soy flour and peanut hulls produced the best results, statistically distinguishing themselves from other nitrogen supplements. The other supplements did not produce results significantly different from the unsupplemented control.

Finally, Table 4 shows the average micropropagule counts obtained using a mixture (half/half) of sorghum and millet stalk powder in the presence of the various nitrogen supplements. The table shows that the averages, depending on the different treatments, range from  $4.8 \cdot 10^8$  to  $13.6 \cdot 10^8$  CFU/gos. Soy flour recorded the highest number of micro-propagules and the unsupplemented control the lowest. Soy flour and moringa leaves produced significantly higher averages than the other nitrogen supplements. The combination (millet stalks + sorghum stalks) produced more micropropagules than each carbon source taken separately.

Table 4 Production of *T. harzianum* *ThTab* micropropagules on millet stalks, sorghum stalks, millet+sorghum stalks supplemented with the various nitrogen sources

Nitrogen supplements	Number of micropropagules (CFU/gos) X $10^8$		
	Millet stalks	Sorghum stalks	Millet+sorghum stalks
No supplement	0.7 <sup>a</sup>	3.1 <sup>ab</sup>	4.8 <sup>a</sup>
Peanut hulls	1.0 <sup>ab</sup>	3.6 <sup>b</sup>	6.7 <sup>ab</sup>
Acacia pods	1.2 <sup>b</sup>	3.0 <sup>ab</sup>	9.5 <sup>bc</sup>
Moringa leaves	1.2 <sup>b</sup>	3.0 <sup>ab</sup>	12.7 <sup>c</sup>
Cowpea hulls	1.0 <sup>ab</sup>	2.9 <sup>ab</sup>	6.3 <sup>ab</sup>
Peptone	1.3 <sup>b</sup>	2.4 <sup>a</sup>	10.5 <sup>bc</sup>
Soy flour	0.6 <sup>a</sup>	3.5 <sup>b</sup>	13.6 <sup>c</sup>
<b>F value</b>	<b>05.976</b>	<b>03.347</b>	<b>09.373</b>
<b>P value</b>	<b>0.000</b>	<b>0.013</b>	<b>0.000</b>

Means in the same column affected by the same alphabetical letter are not significantly different at the 5% threshold according to the Student-Newman-Keuls multiple comparison test. CFU/gos: Colony Forming Units per gram of substrate; F: Fisher's coefficient; P: Probability

### 3.3 Multiplication of *T. harzianum* on acacia bark, eucalyptus sawdust and cottonseed cake as carbon sources

Micropropagule production levels per gram of substrate consisting of acacia bark, white sawdust and cottonseed cake in the presence of the various nitrogen supplements are presented in Table 5.

For acacia bark, harvest levels varied according to the nitrogen supplements used, from  $6.7 \cdot 10^8$  to  $15.5 \cdot 10^8$  CFU/gos. Supplementation with acacia pod powder produced significantly more micro-propagules than the other supplements. The unsupplemented control produced significantly more micropropagules than the other nitrogen supplements apart from cowpea tops.

The numbers of *T. harzianum* micropropagules produced on white sawdust powder in the presence of various nitrogen



sources varied from  $2.7.10^8$  to  $7.5. 10^8$  CFU/gos and all treatments were significantly different. The use of cowpea husk powder as a nitrogen supplement yielded the highest number of micropropagules, and groundnut husk powder the lowest. Apart from groundnut hulls, the other nitrogen supplements significantly improved the number of micro-propagules compared with the unsupplemented control.

Cottonseed cake, used as an organic substrate in the presence of various nitrogen supplements, was used to

multiply *T. harzianum*. Analysis of Table 5 shows that micro-propagule production levels varied with nitrogen supplementation from  $0.1.10^8$  to  $0.6.10^8$  CF/gos. The highest number of micropropagules was recorded in the untreated control and acacia pods. This indicates that supplementation with the other nitrogen sources significantly reduced the multiplication of the fungus. Regardless of the supplement used, the number of micro-propagules obtained using cottonseed cake as a carbon source was lower than with other carbonaceous substrates.

Table 5 Production of *T. harzianum* ThTab micropropagules on Acacia barks, Eucalyptus sawdust and Cottonseed cake supplemented with the various nitrogen sources

Nitrogen supplements	Number of micropropagules (CFU/gos) X $10^8$		
	Acacia barks	Eucalyptus sawdust	Cottonseed cake
No supplement	12,0 <sup>b</sup>	3,1 <sup>ab</sup>	0,6 <sup>e</sup>
Peanut hulls	07,3 <sup>a</sup>	2,7 <sup>a</sup>	0,4 <sup>d</sup>
Acacia pods	15,5 <sup>c</sup>	3,7 <sup>b</sup>	0,6 <sup>e</sup>
Moringa leaves	07,6 <sup>a</sup>	6,6 <sup>e</sup>	0,2 <sup>b</sup>
Cowpea hulls	09,8 <sup>ab</sup>	7,5 <sup>f</sup>	0,3 <sup>c</sup>
Peptone	06,7 <sup>a</sup>	5,8 <sup>d</sup>	0,1 <sup>a</sup>
Soy flour	08,2 <sup>a</sup>	4,4 <sup>c</sup>	0,3 <sup>c</sup>
<b>F value</b>	<b>10,422</b>	<b>59,063</b>	<b>100,653</b>
<b>P value</b>	<b>0,000</b>	<b>0,000</b>	<b>0,000</b>

Means in the same column affected by the same alphabetical letter are not significantly different at the 5% threshold according to the Student-Newman-Keuls multiple comparison test. CFU/gos: Colony Forming Units per gram of substrate; F: Fisher's coefficient; P: Probability

### 3.4 Contribution of carbon sources to the production of *T. harzianum* micropropagules

The contribution of carbon sources to micro-propagule production, whatever the nitrogen supplement, is summarized in Table 8. Analysis of the table shows that, depending on the source, micropropagule production varied from  $0.3.10^8$  to  $297.0.10^8$  CFU/gos.

The highest production was obtained using corn bran as substrate, and the lowest with cottonseed cake. Apart from

corn bran, statistical analysis revealed no significant difference between the other substrates (Table 6).

Harvesting of the fungus grown on maize raids powder was very significantly lower than that obtained with maize bran powder (Table 6).

The combination of maize and rice bran significantly reduced the level of micropropagule production compared with maize bran taken in isolation (Table 6).

Table 6 Production of *T. harzianum* ThTab micropropagules on various carbon sources

Carbon sources	Number of micropropagules (CFU/gos) X $10^8$
Rice bran	09.0 <sup>a</sup>
Maize bran	297.0 <sup>b</sup>
Maize raids	13.6 <sup>a</sup>
Rice+Maize bran	54.9 <sup>a</sup>
Sorghum stalks	03.1 <sup>a</sup>

Millet stalks	01.0 <sup>a</sup>
Sorghum+Millet stalks	09.1 <sup>a</sup>
Acacia barks	09.6 <sup>a</sup>
Eucalyptus sawdust	04.8 <sup>a</sup>
Cottonseed cake	00.3 <sup>a</sup>
<b>F value</b>	<b>25.938</b>
<b>P value</b>	<b>0.000</b>

Means in the same column affected by the same alphabetical letter are not significantly different at the 5% threshold according to the Student-Newman-Keuls multiple comparison test. CFU/gos: Colony Forming Units per gram of substrate; F: Fisher's coefficient; P: Probability

### 3.5 Contribution of nitrogen supplements to the production of *T. harzianum* micropropagules

The average harvests of micropropagules obtained for all treatments of the same nitrogen supplement, irrespective of the organic substrate, are shown in Table 7.

Average *T. harzianum* micropropagule production varied between nitrogen supplements, from 19.1.10<sup>8</sup> to 113.7.10<sup>8</sup> CFU/gos. Statistical analysis revealed no significant differences between supplements, with the exception of soy flour, which recorded the highest concentration (113.7.10<sup>8</sup> CFU/gos) (Table 7).

Table 7 Production of *T. harzianum* ThTab micropropagules on various nitrogen sources

Nitrogen supplements	Number of micropropagules (CFU/gos) X 10 <sup>8</sup>
No supplement	20,3 <sup>a</sup>
Peanut hulls	19,1 <sup>a</sup>
Acacia pods	29,5 <sup>a</sup>
Moringa leaves	31,5 <sup>a</sup>
Cowpea hulls	40,0 <sup>a</sup>
Peptone	27,4 <sup>a</sup>
Soy flour	113,7 <sup>b</sup>
<b>F value</b>	<b>03,063</b>
<b>P value</b>	<b>0,006</b>

Means in the same column affected by the same alphabetical letter are not significantly different at the 5% threshold according to the Student-Newman-Keuls multiple comparison test. CFU/gos: Colony Forming Units per gram of substrate; F: Fisher's coefficient; P: Probability

## IV. DISCUSSION

The genus of fungus most exploited in the biopesticide industry is *Trichoderma*, formulations of which are developed on various substrates through solid or liquid fermentation technologies (Gary & Hibbar, 2015). However, the main problem encountered by farmers and manufacturers regarding the bioproduct developed is its instability under different environmental conditions (Prakash & Basu, 2020). Added to this is the adaptation of the fungus strains to climatic conditions and the availability and cost elements of these carriers (Gary & Hibbar, 2015).

The general objective of this study was to evaluate the capacity of certain organic substrates, essentially agricultural by-products that are inexpensive and easily accessible in Burkina Faso, to massively and simply reproduce propagules of the local strain of *T. harzianum* (ThTab) with a view to developing a formulation for large-scale use.

The results of this experiment show that, with the exception of the "cotton cake supplemented with peptone and moringa leaves" treatments, all the other treatments multiplied the initial inoculum by factors ranging from 1, 5 times (for the cotton cake treatment supplemented with soybean meal) to

5228 times (for the maize bran treatment supplemented with soybean meal) in eight days of incubation, based on an initial substrate concentration of 0.2 conidia/gos).

These results indicate that solid-state fermentation is an effective method for the simple and massive reproduction of *T. harzianum* strains. This confirms the work of Sargin *et al.*, (2013) who massively reproduced micro propagules of a *T. harzianum* strain by solid-state fermentation with wheat bran. Long before, Nkaya (2007) had indicated that fermentation in a submerged (liquid) medium was more suitable for the multiplication of bacteria, and that solid-state fermentation, taking place on a surface of solid matter that could absorb or contain water, with or without soluble nutrients, was more suitable for the growth of fungal microorganisms.

*Trichoderma* species are filamentous fungi, and solid-state fermentation is better suited to the growth of this group of fungi than fermentation in liquid media (Duchiron & Legin-copinet, 2019). This is because these fungi have strong cell wall structures at the ends of colonizing hyphae that are able to penetrate solid substrates for nutrients (Duchiron & Legin-Copinet, 2019).

However, Sargin *et al.* (2013) also demonstrated that spore production levels were variable depending on the initial substrate humidity, but also on other characteristics such as incubation temperature and medium pH, parameters that were not considered in our study. It would therefore make sense to continue research by varying these different parameters with a view to optimizing solid-state fermentation.

Several agro-industrial by-products, including wheat bran, rice husks and bran, cotton cake, bran, corn grains and cobs, glucose, cowpea hulls, yeast extracts, etc., have long been tested as potential carriers for mass propagation of *Trichoderma harzianum* (Roussos, 1985; Lakshimi & Chandra, 2004; Verma *et al.*, 2005; Baghat & Sitansu, 2007; Calvacante, 2007; Rini & Sulochana, 2007; Onidule, 2012; Sargin *et al.*, 2013; Rajput *et al.*, 2014; Rai & Tewari, 2016; Mohiddin *et al.*, 2017; Siddhartha *et al.*, 2017; Sey-Amole *et al.*, 2018). Even if the evaluation method was not always the same, our results are mostly within the range of multiplication levels obtained by these authors.

The different carbon sources tested in this experiment showed variable levels of *T. harzianum* multiplication. This variability could be explained by the ease with which the fungus degrades the carbohydrates contained in each substrate. The enzymes released by *T. harzianum* (amylases, endo and exo cellulase,  $\beta$ -glucosidase, etc.) can rapidly and totally degrade disaccharides such as starch (contained in maize bran) and more difficultly and partially degrade polysaccharides such as cellulose (contained in

millet and sorghum stalks) and lignin in acacia bark and eucalyptus sawdust.

Maize bran was the most effective in producing *T. harzianum* micropropagules in contrast to cottonseed cake, which was the least effective. This result is in line with those of Mohiddin *et al.*, (2017) who tested several substrates and found that corn kernels enabled better multiplication of *T. harzianum*. According to these authors, this result obtained with maize can be explained by its high starch content as well as high water retention capacity. In fact, the maize shelling process under Burkina Faso conditions produces a residue consisting of a mixture of bran and kernel pieces. This mixture could have a high water-holding capacity and contain a significant quantity of starch that is easily degraded by *Trichoderma*, compared with the ground stalks of sorghum, millet, etc., which consist essentially of cellulose that is more difficult to degrade. Calvacante *et al.* (2007) have also pointed out that corn bran has a higher water retention capacity than rice bran.

While the low production levels obtained with other carbonaceous substrates can be explained by their high lignin content, which is very difficult to degrade, the result obtained with cottonseed cake can be explained by its high fat content, which reduces the fungus' development. Cottonseed cake also contains volatile aldehydes with an antifungal effect, which could prove toxic to *T. harzianum* (Zeringue, 1996).

Sargin *et al.* (2013) obtained more micro propagules using cotton cake. This was not the case in this study. This could be justified by a difference in the fat and gossypol contents of the oilcakes used.

In terms of nitrogen sources, soy flour was, on average, significantly more suitable as a supplement (113.7.108 CFU/gos) even if, depending on the carbon source, it was not always the best performer. This result is in line with those of Sargin *et al.* (2013), who obtained good micropropagule production using flour as a supplement to wheat bran. Cowpea hulls were the second most interesting nitrogen supplement, unlike peanut hulls, which did not promote fungal growth. This variability could be explained by the difference in nitrogen content of each supplement. However, it was noted that the contribution of nitrogen supplements seems to depend on the carbon source used. Soy flour was not always the best performer, depending on the carbon source used.

Supplementing maize bran with soybean and cowpea meal significantly increased the level of micropropagule production compared with the unsupplemented control. These results are all interesting because these agricultural by-products are accessible to farmers in Burkina Faso.

Maize is an annual plant grown as a cereal for its starch-rich grains for human consumption (Sanou *et al.*, 2022). In Burkina Faso, maize ranks second among cereal crops, with national production estimated at 1,700,127 tonnes (DGESS/MAAH, 2019). Apart from the Sahel and Northern regions, where maize production is low, all other regions of Burkina Faso produce and consume maize.

Maize flour is used by both urban and rural populations to prepare the dough commonly known as "Tô". Before this flour can be obtained, the kernels are shelled, so that in both rural and urban areas, maize bran is widely available and financially accessible to small-scale producers. Soya and cowpea are legumes also grown on a large scale in Burkina Faso as food crops.

According to 2019 statistics, soybean and cowpea production reached 31,314 tonnes and 683,174 tonnes respectively (DGESS/MAAH, 2019). These production levels make it possible to appreciate the availability of cowpea haulms and soybeans for the implementation of this technology.

These production levels show that the availability and affordability of these agricultural by-products in Burkina Faso are not objective barriers. Although maize bran and cowpea haulms are used for livestock feed, and soybeans are used in the manufacture of various dishes, the quantities to be used in this technology do not call into question the competitive use of these by-products. The results of this study are therefore very encouraging and point to interesting avenues for the development of a *Trichoderma* formulation that is easy for growers to prepare themselves.

## V. CONCLUSION

This study assessed the ability of various organic substrates to efficiently multiply a local strain of *Trichoderma harzianum* isolated in Burkina Faso. All the substrates tested by the solid-state fermentation method multiplied the fungus, but to varying degrees. Corn bran, supplemented with soy flour and cowpea powder respectively, multiplied the initial inoculum of the fungus by 5228 and 1426 times respectively.

As maize bran, soya beans and cowpea tops are widely available and accessible to farmers, this result opens up the prospect of developing a low-cost formulation that could be used as a seed coating or to increase *Trichoderma* levels in plots and nurseries (by spraying or watering) to initiate protection of targeted crops against telluric pest problems.

But first, in order to optimize the fermentation method, it seems important to continue investigations on the following points:

(i) Evaluate the maize-soybean or maize-cowpea hulls

combination by varying parameters such as substrate moisture content, pH, incubation temperature and proportion (nitrogen source / carbon source);

(ii) Evaluate the viability of micropropagules in harvested biomass;

(iii) Carry out on-farm tests to assess the most appropriate and economical method of use.

## ACKNOWLEDGEMENTS

The authors would like to express their sincere thanks to the staff of the Laboratoire des Systèmes Naturels, Agrosystèmes et de l'Ingénierie de l'Environnement (Sy. N. A. I. E.) for their great contribution in carrying out the activities. They are also grateful to the PRD Program of ARES-Belgium for funding the activities of the PRD-ProDuRe project (Bobo-Dioulasso, Burkina Faso).

## REFERENCES

- [1] Abdel-Monaim, M.F., Abdel-Gaid, M.A., Zayan, S.A., & Nassef, D.M.T. (2014). Enhancement of growth parameters and yield components in eggplant using antagonism of *Trichoderma* spp. against *Fusarium* wilt disease. *International Journal of Phytopathology*, 03(01), 33-40. DOI: [10.33687/phytopath.003.01.0510](https://doi.org/10.33687/phytopath.003.01.0510)
- [2] Akrami, M. & Yousefi, Z. (2015). Biological Control of *Fusarium* wilt of Tomato (*Solanum lycopersicum*) by *Trichoderma* spp. as Antagonist Fungi. *Biological Forum – An International Journal*, 7(1), 887-892.
- [3] Nkaya, G.D.(2007). La fermentation à l'état solide. Retrieved from : <http://agrogroun.unblog.fr/2007/04/28/fermentation-en-milieu-solide/>
- [4] Bacon, C.W., Yates, I.E., Hinton, D.M., & Meredith, F. (2001). Biological control of *Fusarium moniliforme* in maize. *Environmental Health Perspectives*, 109(2), 325–332. DOI: [10.1289/ehp.01109s2325](https://doi.org/10.1289/ehp.01109s2325)
- [5] Bardin, S.D., & Huang, H. (2003). Efficacy of stickers for seed treatment with organic matter or microbial agents for the control of damping-off of sugar beet. *Plant Pathology Bulletin*, 12, 19-26.
- [6] Besmer, R.A., Sawadogo, W.M., Dabiré, T.G., Kambiré, F.C., Bokonon-Ganta, A.H., Somda, I., & Verheggen, F.J. (2022). Susceptibility of fall armyworm *Spodoptera frugiperda* (JE Smith) to microbial and botanical bioinsecticides and control failure likelihood estimation. *Biotechnol. Agron. Soc. Environ*, 26(3), 136-143. DOI: [10.25518/1780-4507.19793](https://doi.org/10.25518/1780-4507.19793)
- [7] Bhagat, S., & Sitansu, P. (2007). Mass multiplication of *Trichoderma harzianum* on agricultural byproducts and their evaluation against seedling blight (*Rhizoctonia solani*) of mungbean and collar rot (*Sclerotium rolfsii*) of groundnut. *Indian Journal of Agricultural Sciences*, 77(9), 583-8. <https://epubs.icar.org.in/index.php/IJAgs/article/view/3186>
- [8] Cavalcante, R.S., Lima, L.S.H., Pinto, G.A.S., Gava, C.A.T., & Rodrigues, S. (2008). Effect of moisture on *Trichoderma*

- conidia production on corn and wheat bran by solid state fermentation. *Food Bioprocess Tech*, 1, 100–104. <https://doi.org/10.1007/s11947-007-0034-x>
- [9] Caron, J., Laverdière, L., Thibodeau, P.O., & Bélanger, R.R. (2002). Utilisation d'une souche indigène de *Trichoderma harzianum* contre cinq agents pathogènes chez le concombre et la tomate de serre au Québec. *Phytoprotection*, 83, 73-87. DOI: <https://doi.org/10.7202/706230ar>
- [10] Cowper, J.R., Canaguier, R.H., & Reynaud, H. L. (2013). Procédé de multiplication de micro-organismes phyto-bénéfiques. Organisation Mondiale de la Propriété Intellectuelle. Numéro de publication internationale WO 2013/079887. Al. <https://patents.google.com/patent/WO2013079887A1/fr>
- [11] Dabiré, T.G., Bonzi, S., Somda, I., & Legrève, A. (2016a). Evaluation in vitro de l'action antagoniste d'isolats de *Trichoderma harzianum* contre trois espèces fongiques pathogènes de l'oignon au Burkina Faso. *Tropicicultura*, 34(3), 313-322. <https://popups.uliege.be/2295-8010/>
- [12] Dabiré, T.G., Bonzi, S., Somda, I., & Legrève, A. (2016b). Evaluation of the potential of *Trichoderma harzianum* as a plant growth promoter and biocontrol agent against *Fusarium damping-off* in onion in Burkina Faso. *Asian Journal of plant pathology*, 10, 49-60. <https://scialert.net/abstract/?doi=ajppaj.2016.49.60>
- [13] Dal Bello, G.M., Monaco, C.I., & Simon, M.R. (2002). Biological control of seedling blight of wheat caused by *Fusarium graminearum* with beneficial rhizosphere microorganisms. *World Journal of Microbiology & Biotechnology*, 18, 627–636. <https://doi.org/10.1023/A:1016898020810>
- [14] DGESS/MAAH. (2019). Résultats définitifs de la campagne agropastorale 2018/2019, de la situation alimentaire et nutritionnelle du pays et perspectives. <https://sisabf/wp-content/uploads/2021/07/Rapport-General-Resultats-definitifs-2018-2019-1-2.pdf>
- [15] Duchiron, F., Legin-Copinnet, E. (2019) "Fermentation en milieu solide (FMS)" In Techniques de l'Ingénieur. <https://www.techniques-ingenieur.fr/base-documentaire/archives-th12/archives-bioprocédés-et-bioproductions-tiabi/archive-1/fermentation-en-milieu-solide-fms-bio620/>
- [16] Ferrigo, D., Raiola, A., Rasera, R., & Causin, R. (2014). *Trichoderma harzianum* seed treatment controls *Fusarium verticillioides* colonization and fumonisin contamination in maize under field conditions. *Crop Protection*, 65, 51-56. <https://doi.org/10.1016/j.cropro.2014.06.018>
- [17] Gary, J.S., & Hebbbar, P.K. (2015). *Trichoderma*. Identification and agricultural applications. The American Phytopathological Society press. 3340 Pilot Knob road. St Paul, Minnesota 55121 USA. Library of Congress Control number: 2015908956. International Standard book n°: 978-0-89054-484-6.
- [18] Gautam, S.S., Kanchan, K., & Satsangi, G.P. (2015). Effect of *Trichoderma* species on germination and growth of Mungbean (*Vigna radiata* L.) and its antagonistic effect against fungal pathogens. *International Journal of Advanced Research*, 3(2), 153-158. <http://www.journalijar.com/>
- [19] John, R.P., Tyagi, R.D., Prévost, D., Brar, S.K., Pouleur, S., & Surampalli, R.Y. (2010). Mycoparasitic *Trichoderma viride* as a biocontrol agent against *Fusarium oxysporum* f. sp. adzuki and *Pythium arrhenomanes* and as a growth promoter of soybean. *Crop Protection*, 29,1452-1459. <https://doi.org/10.1016/j.cropro.2010.08.004>
- [20] Lakshmi, T., & Chandra, B. (2004). Evaluation of agro-industrial wastes for conidia-based inoculum production of bio-control agent: *Trichoderma harzianum*. *Journal of Scientific and Industrial Research*, 63, 807-812.
- [21] Luz, T., Franco, A., Zanuzzi, V., & Ballini, E. (2019). Biological control using *Trichoderma*. Retrieved from <http://agrosys.fr/wp-content/uploads/2019/10/Modes-daction-de-TRichoderma.pdf>
- [22] Mahalakshmi, P., & Raja I.Y., 2015. Biocontrol potential of *Trichoderma* species against wilt disease of carnation (*Dianthus caryophyllus* L.) caused by *Fusarium oxysporum* f.sp. dianthi. *Journal of Biopesticides*, 6(1), 32-36.
- [23] Mohiddin, F.A., Bashir, I., Shahid, A.P., & Burhan, H. (2017). Evaluation of different substrates for mass multiplication of *Trichoderma* species. *Journal of Pharmacognosy and Phytochemistry*, 6(6), 563-569. <https://www.phytojournal.com/archives/2017.v6.i6.2133/evaluation-of-different-substrates-for-mass-multiplication-of-trichoderma-species>
- [24] Onilude, A.A., Adebayo-Tayo, B.C., Odeniyi, A.O., Banjo, D., & Garuba, E. O. (2012). Comparative mycelial and spore yield by *Trichoderma viride* in batch and fed-batch cultures. *Annals Microbiology*, 10, 547-553. <https://doi.org/10.1007/s13213-012-0502-z>
- [25] Prakash, V., & Basu, K. (2020). Mass Multiplication of *Trichoderma* in Bioreactors. In: Manoharachary, C., Singh, H.B., Varma, A. (eds) *Trichoderma: Agricultural Applications and Beyond*. Soil Biology, vol 61. Springer, Cham. [https://doi.org/10.1007/978-3-030-54758-5\\_5](https://doi.org/10.1007/978-3-030-54758-5_5)
- [26] Rai, D. & Tewari, A.K. (2016). Evaluation of different carbon and nitrogen sources for better growth and sporulation of *T. harzianum* (Th14). *Journal of Agricultural Biotechnology and Sustainable Development*, 8(8), 67-70. DOI: [10.5897/JABSD2016.0262](https://doi.org/10.5897/JABSD2016.0262)
- [27] Rajput, A.Q., Khanzada, M.A., & Shahzad, S. (2014). Effect of Different Organic Substrates and Carbon and Nitrogen Sources on Growth and Shelf Life of *Trichoderma harzianum*. *J. Agr. Sci. Tech*, 16, 731-745. <http://www.fspublishers.org/>
- [28] Rini, C.R., & Sulochana, K.K. (2007). Substrate evaluation for multiplication of *Trichoderma* spp. *Journal of Tropical Agriculture*, 45(1-2), 58–60.
- [29] Roussos, S. (1985). Croissance de *Trichoderma harzianum* par fermentation en milieu solide : Physiologie, sporulation et production de cellulase. Thèse de Doctorat en sciences naturelles : Université de Provence (France).
- [30] Sanou, A., Yonli, D., Séré, I., & Traoré, H. (2022). Influence de la fertilisation azotée et de la concurrence monospécifique de *Rottboellia cochinchinensis* (Lour.) W. Clayton sur le maïs dans l'Ouest du Burkina Faso. *Tropicicultura*, 40(1). DOI: [10.25518/2295-8010.1980](https://doi.org/10.25518/2295-8010.1980). <https://popups.uliege.be/2295-8010/index.php?id=1980>

- [31] Sargin, S., Gezgin, Y., Eltem, R., & Vardar, F. (2013). Micropropagule production from *Trichoderma harzianum* EGE-K38 using solid-state fermentation and a comparative study for drying methods. *Turkish Journal of Biology*, 37, 139-146. DOI: [10.3906/biy-1206-32](https://doi.org/10.3906/biy-1206-32)
- [32] Schiffers, B & Wainwright, H., 2011. La lutte Biologique et protection intégrée. Pour un Développement durable des filières fruits et légumes ACP. COLEACP Eds., Bruxelles. Manuel N° 10. 126 p. file:///C:/Users/UTILISATEUR/Downloads/coleacp-manuel-10-fr.pdf.
- [33] Shahnaz, E., Razdan, V.K., Rizvi, S.E.H., Rather, T.R., Gupta, S., & Andrabi, M. (2013). Integrated Disease Management of Foliar Blight Disease of Onion: A Case Study of Application of Confounded Factorials. *Journal of Agricultural Science*, 5(1), 17-22. DOI: [10.5539/jas.v5n1p17](https://doi.org/10.5539/jas.v5n1p17)
- [34] Sey-Amole, O.D., & Onilude, A.A. (2018). Influence of carbon and nitrogen sources on the spore yield of *Trichoderma harzianum* in fed-batch culture. *International journal of microbiology and mycology*, 7(1), 18-23.
- [35] Siddhartha, N.S., Amara, K.V., Ramya, Mol K.A., Saju, K.A., Harsha, K.N., Sharanappa, P., & Pradip, K. K. (2017). Evaluation of Substrates for Mass Production of *Trichoderma harzianum* and its Compatibility with Chlorpyrifos + Cypermethrin. *Int. J. Curr. Microbiol. App. Sci.*, 6(8), 3628-3635. <https://doi.org/10.20546/ijemas.2017.607.437>
- [36] Son, D., Zerbo, K.B.F., Bonzi, S., Legreve, A., Somda, I., & Schiffers, B. (2018). Assessment of Tomato (*Solanum lycopersicum* L.) Producers Exposure Level to Pesticides, in Kouka and Toussiana (Burkina Faso). *International Journal of Environmental Research. And Public Health*, 15(2), 204. DOI: [10.3390/ijerph15020204](https://doi.org/10.3390/ijerph15020204)
- [37] Traoré, O., Wonni, I., Boro, F., Somtoré, E., Zombré, C. T., Dianda, O. Z., Wicker, E., Ilboudo, P., Ouedraogo, L. S., & Somda, I. (2013). Evaluation of the 19 varieties and accessions of tomato against bacterial wilt in Bobo-Dioulasso, Burkina Faso. *Int. J. Biol. Chem. Sci.*, 14(8), 2870-2879. DOI : <https://dx.doi.org/10.4314/ijbcs.v14i8.17>
- [38] Trebicka, A., Oelmüller, R., Sherameti, I., Noghri, P.L., & Johnson, J.M. (2012). Utilization of root-colonizing fungi for improved performance of agricultural crops. *Albanian Journal of Agricultural science*, 11, 9-16.
- [39] Verma, M., Brar, S.K., Tyagi, R.D., Surampalli, R.Y., & Valéro, J.R. (2005). Wastewater sludge as a potential raw material for antagonistic fungus (*Trichoderma* sp.): Role of pre-treatment and solids concentration. *Water Res*, 39, 3587–3596. <https://doi.org/10.1016/j.watres.2005.07.001>
- [40] Verma, M., Brar, S.K., Tyagi, R.D., Surampalli, R.Y. & Valéro, J.R. (2007). Antagonistic fungi, *Trichoderma* spp.: Panoply of biological control. *Biochemical Engineering Journal*, 37, 1–20. <https://doi.org/10.1016/j.bej.2007.05.012>
- [41] Zeringue, H.J. (1996). Possible involvement of lipoxigenase in a defense response in aflatoxigenic *Aspergillus* – cotton plant interactions. *Canadian Journal of Botany*, 74 (1), 98-102. <https://doi.org/10.1139/b96-014>



# Extracting chromium-free protein hydrolysate from leather tanning wastes

Sameh Taha Kassem\*, Khaled Aly El-Shemy

Wool Production and Technology Department, Animal and Poultry Production Division, Desert Research Center, Cairo, Egypt.  
Correspondence email: sameh\_ta2000@yahoo.com

Received: 07 Nov 2023; Received in revised form: 09 Dec 2023; Accepted: 18 Dec 2023; Available online: 24 Dec 2023  
©2023 The Author(s). Published by Infogain Publication. This is an open access article under the CC BY license  
(<https://creativecommons.org/licenses/by/4.0/>).

**Abstract**— Leather tanning produces a variety of solid wastes, the most common of which is chrome shaving waste (CSW), which accounts for about one-third of the total solid waste produced from leather tanning. The biggest problem with this waste is that it contains chromium, which is a pollutant to the environment if the waste is disposed of by traditional methods such as landfilling or incineration. Therefore, the study aims to convert CSW into a proteinaceous material that does not contain chromium, so that it can be used in various applications with added value. In this study, chromium was removed from CSW using either an acid method or an alkaline oxidative method. In the acid method, sulfuric acid (1 molar) was used, while the other method was performed using a mixing ratio of 5:0.2:0.5:1 of CSW: potassium bicarbonate: hydrogen peroxide: water, respectively. The resulting protein was then hydrolyzed using acetic acid (1.5 molar). A chemical analysis of the CSW was performed to determine the percentage of chromium removed from both methods. The percentage of protein hydrolysis was also determined, as well as chromatographic analysis and amino acid analysis of the resulting proteins. The removed chromium was also reused in the tanning of sheepskin samples. The results showed that the alkaline oxidative method for chromium removal was better than using sulfuric acid, with a chromium removal percentage of 94.8% compared to 70.5%. The chromium removed was used in the tanning of leather without any differences in the properties of the resulting leather compared to traditional chrome tanning. The resulting hydrolyzed proteins were found to be collagenous proteins with an amino acid composition that can be used in various applications such as plant fertilizers. Therefore, the treatment and use of CSW achieves economic and environmental benefits for the leather tanning industry, thus achieving sustainability.



**Keywords**— chrome removal, collagen, leather tanning, sustainability

## I. INTRODUCTION

Chrome tanning is a widely employed method for leather tanning worldwide because it offers cost-effective production of high-quality leather. However, it is also recognized as the most environmentally harmful method due to the generation of solid and liquid waste containing significant levels of trivalent chromium (Huffer and Taeger, 2004; Kolomaznik *et al.*, 2008).

Among the various pollutants resulting from leather tanning, chrome shaving waste (CSW) is a prominent contributor, accounting for approximately one-third of the total solid waste produced. The disposal of CSW through incineration or landfilling poses risks as it introduces toxic

chromium salts into the soil. These contaminants can permeate the groundwater or be directly absorbed by plants and animals, thereby posing ecological concerns. Additionally, incineration emits harmful gases, and the conversion of trivalent chromium to its carcinogenic hexavalent form can occur (Beltrán-Prieto, *et al.*, 2012).

Consequently, the conversion of CSW into environmentally friendly materials becomes imperative to harness its potential for alternative beneficial applications. Previous research has explored various treatment methods and systems to utilize chromium leather waste, such as energy and protein hydrolysate production, panel manufacturing, and the generation of value-added products (Pati *et al.*, 2014).

Recent studies have specifically focused on the production of proteinaceous materials from leather waste, which holds promise as a valuable product for different purposes (Rajabimashhadi *et al.*, 2023; Maistrenko *et al.*, 2022; Parisi *et al.*, 2021). However, the challenge lies in the extraction of chromium salts from the waste. Chemical treatments have been predominantly employed to achieve this objective, involving the dissolution of chromium salts from leather waste or extracted ash. Although alkaline hydrolysis is more popular than acid hydrolysis using mineral acids for chrome shaving dust, the latter is commonly utilized due to its ease of use and cost-effectiveness (Rahaman *et al.*, 2017; Pantazopoulou and Zouboulis, 2020; Kokkinos, *et al.*, 2021). The extracted chromium can then be reused within the tanning industry (Nasr *et al.*, 2022; Sharaf *et al.*, 2013; Rao *et al.* 2002).

This study aligns with Egypt's 2030 strategy to mitigate environmental pollution and maximize waste utilization by transforming it into value-added materials. The primary objectives of this study are to produce chromium-free protein suitable for various applications and to facilitate the recycling of chromium extracted from CSW for reuse in chrome tanning.

## II. MATERIAL AND METHODS

### - Chrome shaving wastes:

The chrome shaving wastes used in this study were supplied by Elshafei Sons' Tannery, El-Max region, Alexandria, Egypt. CSW was dried at  $25\pm 3^{\circ}\text{C}$  for five days in an open and shaded place without the use of any of thermal drying methods. Characterization of CSW was determined. Volatile matter, ash, fat, total Kjeldahl nitrogen, chrome contents, total energy and pH values of CSW were determined according to (ASTM, 2014).

### - Removing chrome from CSW:

Chrome removal from chrome shaving waste (CSW) was accomplished using two primary methods: alkaline oxidative hydrolysis or acid hydrolysis.

### - Alkaline oxidative hydrolysis

CSW was mechanically treated with leaching solution using occasional stirring for 45 min at ambient temperature. According to Nasr (2023), leaching solution was prepared using CSW, potassium carbonate, hydrogen peroxide, and water in a ratio (w/w) of 1:0.5:0.2:5 (w/w), respectively. After treating with leaching solution, CSW was filtered and rinsed twice with water. De-chromed shaving wastes were obtained after rinsing by pressing, whereas the filtrate, containing chromium salts were collected for subsequent chromium sulfate preparation.

### - Acid hydrolysis

According to Nasr *et al.* (2022), 10 grams of CSW were precisely weighed and transferred to a beaker. Subsequently, 100 ml of sulfuric acid (1M) solution was added to the beaker. The beaker was then placed on a hot plate and maintained at  $50^{\circ}\text{C}$  for three hours, with continuous stirring at 500 rpm. This hydrolysis step facilitated the precipitation of chromium present in the CSW as  $\text{Cr}(\text{OH})_3$ . The  $\text{Cr}(\text{OH})_3$  precipitate was separated from the solution by filtration using Whatman filter paper. The filtered  $\text{Cr}(\text{OH})_3$  was then dried and weighed. The remaining supernatant solution was centrifuged multiple times at 15,000 rpm to remove any residual impurities and subsequently stored.

### - Preparation of protein hydrolysates

The protein hydrolysates were prepared from de-chromed shaving wastes that prepared previously by alkaline oxidative and acid hydrolysis. The process was carried out according to Selvaraj *et al.* (2019), using 2.5 g of the sample, which was separately dissolved in 100 mL of 1.5 M acetic acid solution. The solutions were then stirred at  $80^{\circ}\text{C}$  for 6 hours. Afterward, the solutions were centrifuged at 10,000 rpm for 30 minutes. The supernatant was collected, and the residue was dried at  $80^{\circ}\text{C}$  to remove moisture content. Figure 1 shows the protein hydrolysates from CSW after removing chromium by acid and alkaline oxidative methods.

Hydrolysis percentage, FTIR and amino acid analysis were determined for protein hydrolysate to evaluate its properties for using in varied purposes. Hydrolysis percentage was calculated according to Selvaraj *et al.* (2019) based on the residual weight of the chrome shaving waste, using the following formula.

$$\text{Hydrolysis percentage} = \frac{\text{Initial weight taken} - \text{Residual weight}}{\text{Initial weight taken}} \times 100$$

The spectrophotometer (Bruker Varian 70 transform infrared using Platinum ATR unit) was used to analyze the chemical structure and the fingerprint of CSW or protein hydrolysates. Small quantity of the sample was used and scanned directly on the instrument stage.

The polypeptides acquired from CSW and protein hydrolysates were analyzed for amino acid composition. The amounts of different amino acids present were also estimated after hydrolysis using Sykam amino acid analyzer SW.



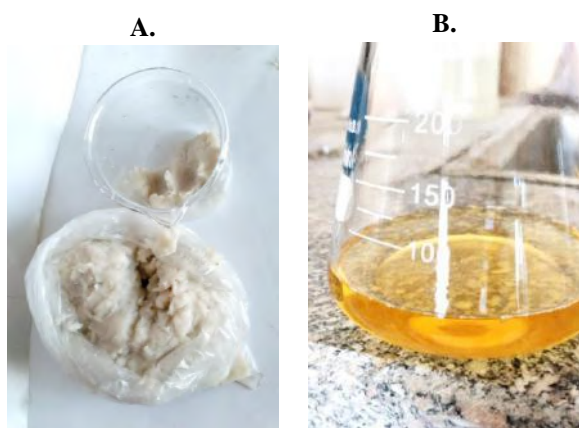


Fig. 1: Protein hydrolysate after removing chromium (A. oxidative alkaline, B. Acid hydrolysis)

- Re-using extracted chromium in leather tanning.

According to Sharaf *et al.* (2013), the chromium sulfate (33% basicity) was prepared from exhausted solution by adding concentrated sulfuric acid as an acid catalyst agent and table sugar as a reducing agent in the reaction. 25 g of chrome shaving ash were mixed with 62.5 ml water in a beaker; 23 g of concentrated sulfuric acid (Sp. Gr. 1.84) were added carefully and stirred well. The beaker was under cooling with continuous stirring while 6.25 g of table sugar were added slowly in 10 lots over three hours. During the reaction the color of the liquor changed gradually from orange to green and finally to bluish green indicating the completion of the reduction. The prepared chromium sulfate was used in tanning pieces of pickled sheep samples (20 cm × 20 cm) and compared with other samples tanned with normally commercial 33% basicity of chromium sulfate.

Tanned leathers' samples were assessed physically and chemically for thickness, tensile strength, elongation, split tear strength, water absorption, permeability to water vapor, pH, and contents of ash, chrome and moisture were analyzed according to (ASTM, 2014).

- Statistical analysis:

Data were analyzed using GLM procedure of SAS (2008) to evaluate the differences among different treatments. The fixed model that used in the analysis of removing chrome.

$$Y_{ij} = \mu + A_i + e_{ij}$$

Where  $Y_{ij}$  is the observation taken (k),  $\mu$  is an overall mean,  $A_i$  is a fixed effect of the (i) de-chroming method (alkaline oxidative or acid hydrolysis),  $e_{ij}$  is a random error assumed to be normally distributed with mean=0 and variance= $\sigma^2e$ .

### III. RESULTS AND DISCUSSION

Chrome shaving wastes (CSW) characteristics:

Results for CSW analysis are presented in Table (1). High concentration of nitrogen (12.28%) was found in CSW as a protein substance consisting mainly of collagen fibers. Low fat content (0.31%), low pH (3.92 ml mol/L) and high chromium content (3.68%) were found in CSW due to tanning processing steps, in which the fat is removed by the action of alkalis in unhairing step to facilitate the access of tanning material into collagen fibers, which usually react to the chromium sulfate at low value of pH. The total ash content was 10.28% due to the different elements in collagen fibers such as carbon, nitrogen and sulfur, in addition to other elements comes from different chemical used in tanning especially chromium salts. These obtained values of CSW properties were in accordance with previous investigations (Pati *et al.*, 2014; Scopel *et al.*, 2018).

Protein hydrolysates characteristics.

Table 2 demonstrates the influence of the chromium removal method on chrome shaving waste (CSW) and the subsequent hydrolysis rate of the resulting product. The results reveal a significant impact of the chromium removal method on both the residual chromium content ( $P < 0.05$ ) in the final waste and the recovered chromium content ( $P < 0.01$ ).

Table 1: Chemical properties of chrome shaving waste (CSW).

Parameter	CSW	ASTM
Volatile matter (%)	23.8	D-6403
Fat (%)	0.31	D-3495
Total Kjeldahl nitrogen (TKN)	12.28	D-2868
Total ash (%)	10.28	D-2617
Cr (%)	3.68	D-6714
pH (ml mol/L)	3.92	D-2810

The alkaline oxidative method proved superior to the acid method in removing chromium. The recovered chromium content reached 94.84% compared to 70.56% for the alkaline oxidative and acid methods, respectively. Similarly, the residual chromium content in the waste after chromium removal was significantly lower for the alkaline oxidative method (0.19%) compared to the acid method (1.08%).

Comparing the findings of this study with those of previous studies, Nasr *et al.* (2022) and Rahaman *et al.* (2017) demonstrated a positive correlation between the concentration of sulfuric acid and the amount of chromium removed. In Nasr *et al.* (2022) study, chromium removal reached 74% at a sulfuric acid concentration of 1 molar,

closely aligning with the results of this study. However, Rahaman *et al.* (2017) study reported a lower chromium removal rate (55.5%) at a sulfuric acid concentration of 5 molar compared to the value obtained in this study.

Table 2: Effect of hydrolysis method on removing chrome from chrome shaving waste and percentage of hydrolysis.

Hydrolysate group	Cr in residual (%)	Cr recovery (%)	Percentage of hydrolysis (%)
Acid hydrolysis	1.08 <sup>a</sup>	70.56 <sup>b</sup>	59.33 <sup>b</sup>
Alkaline oxidative hydrolysis	0.19 <sup>b</sup>	94.84 <sup>a</sup>	81.61 <sup>a</sup>
Over all of means	0.64	82.70	70.47
SEM	0.21	5.61	4.99
Significance	**	**	**

Significance: \*\* P<0.01.

Means in the same column having different superscripts are significantly different (P<0.05).

Despite limited utilization in previous studies, the alkaline oxidative method employed in this study yielded chromium removal rates comparable to those reported in previous studies of Nasr (2023) and Siska (1993), which were 95.43% and 98%, respectively.

Conversely, the hydrolysis rate of the resulting proteinaceous material was higher (P<0.05) in the waste obtained from chromium removal using the alkaline oxidative method (81.61%) compared to the acid method (59.33%). The hydrolysis percentages obtained in this study are in the range reported by Selvaraj *et al.* (2019), who used different concentrations of acetic acid from 0.5 molar to 2.5 molar, which gave hydrolysis percentages in the range of 48% to 87.5% with increasing acid concentration.

Therefore, the alkaline oxidative method emerged as the most suitable approach for achieving a proteinaceous material with exceptionally low chromium content.

Fourier-transform infrared (FTIR) spectroscopy was utilized to examine the impact of hydrolysis on changes in functional groups during the hydrolysis process. Figure 2 displays the FTIR spectra of CSW (chrome shaving waste) and its hydrolysates. The spectra demonstrate a reduction in the peak intensity of the amide I band, located at approximately 1610 cm<sup>-1</sup>, which corresponds to C=O stretching. A prominent peak is observed in the amide II region, around 1540 cm<sup>-1</sup>, representing the out-of-phase combination of -CN stretching and -NH bending. Additionally, a moderately intense peak is detected in the amide III region, around 1260 cm<sup>-1</sup>, associated with the in-phase combination of -CN stretching and -NH bending. The specific peak positions are summarized in Table 3.

Interestingly, the amide I peak, found at approximately 1608 cm<sup>-1</sup>, exhibits minimal variations under different hydrolysis conditions. Since the amide I peak is highly sensitive to the secondary structure of proteins, alterations in hydrolysis methods or waste sources have negligible influence on the conformation of the polypeptide chains present in the protein hydrolysate.

On the other hand, the amide II and III peaks consistently appear at approximately 1542 cm<sup>-1</sup> and 1260 cm<sup>-1</sup>, respectively, with relatively little variation observed across different hydrolysis groups.

Table 4 presents the amino acid analysis of CSW and the protein hydrolysates derived from CSW. The three hydrolysates exhibited comparable amino acid profiles, with a high abundance of glycine, proline, alanine, and hydroxyproline. The amino acid composition of the hydrolysates aligns with previous studies (Ammasi *et al.*, 2020; Aftab *et al.*, 2006), supporting their suitability for diverse applications, including encompassing cosmetics, adhesives, printing, and photography. The release of hydroxyproline indicates that amino acids are also produced during the degradation process, potentially opening up avenues for their purification and utilization in poultry feed.

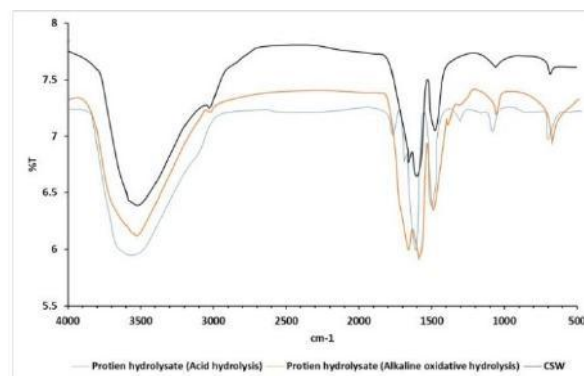


Fig 2: FTIR spectra of CSW and their hydrolysates.

Table 3: Peak positions of protein hydrolysate from chrome shaving and raw trimming wastes.

Group		Amide I (cm <sup>-1</sup> )	Amide II (cm <sup>-1</sup> )	Amide III (cm <sup>-1</sup> )
Protein hydrolysate	Acid hydrolysis	1609	1543	1248
	Alkaline oxidative hydrolysis	1612	1544	1278
Chrome shaving waste (CSW)		1614	1540	1280

The results of FTIR and amino acid analysis showed that the proteinaceous material produced after chromium

removal and hydrolysis is a collagenous material, as its results agreed with previous research.

Therefore, the liquid form of the protein that obtained from acid hydrolysis could serve as a plant fertilizer or undergo electrospinning to produce nano-filters for medical applications, such as wound dressings. In its solid form that obtained from alkaline oxidative hydrolysis, the protein can act as an absorbent for dyes, fats, or heavy metals generated by the leather tanning industry, contributing to environmental protection and industry sustainability.

Using extracted chromium in leather tanning

Table 4: Amino acids compositions of chrome shaving wastes (CSW) and their proteins hydrolysates.

Amino acid	Protein hydrolysate		CSW
	Acid hydrolysis	Alkaline oxidative hydrolysis	
	mg/gm	mg/gm	
Glycine	127.12	116.25	123.43
Proline	50.31	46.22	51.43
Alanine	46.09	40.53	45.82
Hydroxyproline	36.1	33.06	34.85
Glutamic acid	29.19	26.66	30.19
Arginine	19.97	18.49	20.89
Aspartic	17.67	16.35	17.31
Serine	11.91	11.02	12.72
Leucine	8.45	8.89	10.54
Lysine	9.6	9.95	10.11
Valine	6.53	8.18	8.95
Theronine	6.91	5.69	6.07
Isoleucine	4.22	4.27	4.98
Phenylalanine	4.22	4.62	5.91
Methionine	3.84	2.13	3.03
Histidine	1.15	1.78	1.59
Tyrosine	0.77	1.42	1.17
Total	384.06	355.5	389

Figures 3 and 4 show the results of physical and chemical properties of tanned leather samples produced using traditional vs. recovered chromium sulfate. There are insignificant differences between the two groups. This trend was found in previous studies that done by Nasr *et al.* (2022) and Rao *et al.* (2002). Thus, the usage of recovered chromium did not degrade the properties of produced leather which had similar properties to that tanned with

traditional basic chrome sulfate tanning. Therefore, recycling chrome from CSW could be a promised practice to achieve additional environmental and economic benefits.

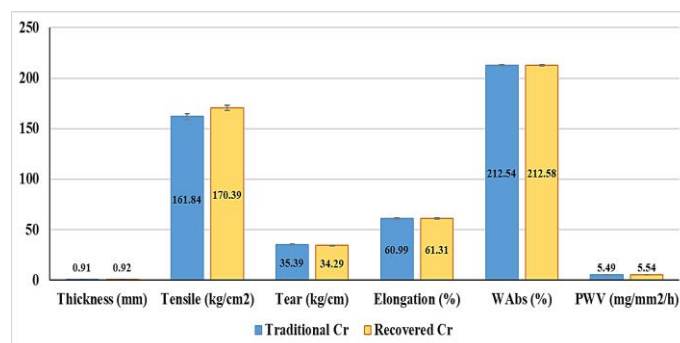


Fig. 3: Physical properties of tanned leather samples produced using traditional vs. recovered chromium sulfate

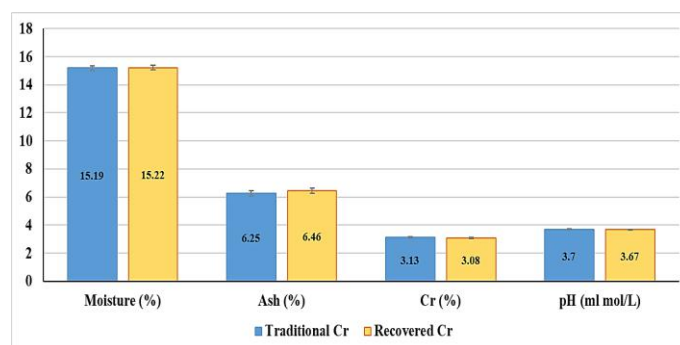


Fig. 4: Physical properties of tanned leather samples produced using traditional vs. recovered chromium sulfate.

#### IV. CONCLUSION

The study suggests that chrome shaving waste (CSW) from leather tanning is a proteinaceous material that can be reused after chromium removal, and that chromium can be recycled for reuse in leather tanning. Chromium can be removed from CSW using either acid hydrolysis or alkaline oxidative methods. The alkaline oxidative method was found to be the most effective method for chromium removal, with a removal percentage of about 95%. The proteinaceous material produced after chromium removal and hydrolysis is collagenous, and can be used in a variety of other applications, such as plant fertilizers and adhesives, printing, and photography. This approach can help to maximize the value of CSW, reduce environmental pollution from leather tanning, and achieve sustainability.

#### FUNDING

This research was supported financially by the Academy of Scientific Research and Technology (ASRT), Ministry of Scientific Research (MoSR), Egypt.

### ACKNOWLEDGMENT

The present document was achieved in the frame of project titled "Nanotechnological interventions to convert tannery solid waste into value added nanofibrous membrane", supported by the Academy of Scientific Research and Technology (ASRT), Ministry of Scientific Research (MoSR), Egypt with Desert Research Center, in cooperation with Department of Science & Technology (DST), Ministry of Science and Technology, India.

### REFERENCES

- [1] S. Huffer and T. Taeger, "Sustainable leather manufacturing: A topic with growing importance," vol. 99, no. 10, pp. 423-428, 2004.
- [2] K. Kolomaznik, M. Adamek, I. Andel and M. Uhlirova, "Leather waste—Potential threat to human health, and a new technology of its treatment," Journal of Hazardous Materials, vol. 160, pp. 514-520, 2008.
- [3] J. Beltrán-Prieto, R. Veloz-Rodríguez, M. Pérez-Pérez, J. Navarrete-Bolaños, E. Vázquez-Nava, H. Jiménez-Islas and J. Botello-Álvarez, "Chromium recovery from solid leather waste by chemical treatment and optimisation by response surface methodology.," Chemistry and Ecology, vol. 28, no. 1, pp. 89-102, 2012.
- [4] Pati, R. Chaudhary and S. Subramani, "A review on management of chrome-tanned leather shavings: a holistic paradigm to combat the environmental issues," Environ Sci Pollut Res, vol. 21, pp. 11266-11282, 2014.
- [5] Z. Rajabimashhadi, N. Gallo, L. Salvatore and F. Lionetto "Collagen Derived from Fish Industry Waste: Progresses and Challenges" Polymers, vol.15, no. 544, pp. 1-28, 2023.
- [6] L. Maistrenko, O. Iungin, P. Pikus, I. Pokholenko, O. Gorbatiuk, O. Moshynets, O. Okhmat, T. Kolesnyk, G. Potters and O. Mokrousova "Collagen Obtained from Leather Production Waste Provides Suitable Gels for Biomedical Applications " Polymers, vol.14, no. 4749, pp. 1-12, 2022.
- [7] M. Parisi, A. Nanni and M. Colonna "Recycling of Chrome-Tanned Leather and Its Utilization as Polymeric Materials and in Polymer-Based Composites: A Review " Polymers, vol.13, no. 429, pp. 1-23, 2021.
- [8] A. Rahaman, D. Islam and M. Raihan, "Recovery of chromium from chrome shaving dust," EUROPEAN ACADEMIC RESEARCH, vol. 5, no. 11, pp. 9441-9448, 2017.
- [9] E. Pantazopoulou and A. Zouboulis, "Chromium recovery from tannery sludge and its ash, based on hydrometallurgical methods," Waste Management & Research, vol. 38, no. 1, pp. 19-26, 2020.
- [10] E. Kokkinos, A. Banti, I. Mintsouli, A. Touni, S. Sotiropoulos and A. Zouboulis, "Combination of Thermal, Hydrometallurgical and Electrochemical Tannery Waste Treatment for Cr(III) Recovery." Applied Sciences, vol. 11, no. 532, pp. 1-14, 2021.
- [11] A. I. Nasr, M. A. El-Shaer, and M. A. Abd-Elraheem "Converting Leather Chrome Shaving Waste Into Free-Chrome Char As A Fuel " Egyptian Journal of Chemistry, vol. 65, no. 13, pp. 1291-1300, 2022.
- [12] S. A. Sharaf, G. A. Gasmeeled and A. E. Musa, "Extraction of chromium six from chrome shavings," Journal of Forest Products and Industries, vol. 2, no. 2, pp. 21-26, 2013.
- [13] J. R. Rao, P. Thanikaivelan, K. J. Sreeram and B. U. Nair, "Green Route for the Utilization of Chrome Shavings (Chromium-Containing Solid Waste) in Tanning Industry," Environmental Science Technology, vol. 36, pp. 1372-1376, 2002.
- [14] ASTM, Books of standards Vol.15.04, USA: American Society for Testing and Materials, 2014.
- [15] A. I. Nasr "Conversion of Chromium Shaving Waste from Leather Processing into Activated Carbon " Textile & Leather Review, vol. 6, pp. 343-359, 2023.
- [16] S. Selvaraj, V. Jeevan, R. Rao and N. N. Fathima "Conversion of tannery solid waste to sound absorbing nanofibrous materials: A road to sustainability" Journal of Cleaner Production, vol. 213, pp. 375-383, 2019.
- [17] SAS, SAS/STAT 9.2 User's guide, 2th edition ed., SAS Institute Inc., Cary, NC, 2008.
- [18] B. S. Scopel, C. Baldasso, A. Dettmer and R. M. C. Santana, "Hydrolysis of Chromium Tanned Leather Waste: Turning Waste into Valuable Materials – A Review," JALCA, vol. 113, pp. 122-129, 2018.
- [19] J. Z. Siska "Removal of chromium from chrome-tanned leather wastes" European Patent Application. Publication number 0567671A1. 1993.
- [20] R. Ammasi, J. S. Victor; R. Chellan and M. Chellappa "Amino Acid Enriched Proteinous Wastes: Recovery and Reuse in Leather Making" Waste and Biomass Valorization, vol. 11, pp. 5793-5807, 2020.
- [21] M. N. Aftab, Abdul Hameed, Ikram-ul-Haq, CHEN Runsheng "Biodegradation of Leather Waste by Enzymatic Treatment " The Chinese Journal of Process Engineering, vol. 6, no.3, pp. 462-465, 2006.



# Characterization, therapeutic applications, structures, and futures aspects of marine bioactive peptides

Azqa Ashraf<sup>1</sup>, Aiman Salah Ud Din<sup>2</sup>, Mudassar Hussain<sup>3</sup>, Imad Khan<sup>3</sup>, Farazia Hassan<sup>4</sup>, Adnan Ahmad<sup>5</sup>, Waleed AL-Ansi<sup>3</sup>, Zaixiang Lou\*

<sup>1</sup>Faculty of Food Science and Nutrition, Bahauddin Zakariya University, Multan Pakistan.

<sup>2</sup>Faculty of Food and Home Sciences, Muhammad Nawaz Sharif University of Agriculture, Multan Pakistan.

<sup>3</sup>State Key Laboratory of Food Science and Resources, National Engineering Research Center for Functional Food, National Engineering Research Center of Cereal Fermentation and Food Biomanufacturing, Collaborative Innovation Center of Food Safety and Quality Control in Jiangsu Province, School of Food Science and Technology, Jiangnan University, 1800 Lihu Road, Wuxi 214122, Jiangsu, China.

<sup>4</sup>Department of Bioinformatics, Faculty of Science and Technology, Virtual University of Pakistan, Samundri Pakistan.

<sup>5</sup>Karachi Institute of Medical Sciences Malir Cantt, Karachi Pakistan.

\*Corresponding author: Zaixiang Lou

Received: 05 Nov 2023; Received in revised form: 08 Dec 2023; Accepted: 16 Dec 2023; Available online: 26 Dec 2023

©2023 The Author(s). Published by Infogain Publication. This is an open access article under the CC BY license

(<https://creativecommons.org/licenses/by/4.0/>).

**Abstract**— Bioactive peptides from marine species have gained attention due to their promising biological features, and the disciplines of pharmaceutical, cosmeceutical, nutraceutical, and biomedical product development have increased recently. Their molecular mass, immunity, and natural abilities that they evolved are essential for host defense mechanisms. Marine bioactive peptides have extremely complex and diverse structures that vary greatly depending on the sources from which they are obtained. They frequently have secondary structures and can be cyclic in the form of depsi-peptides. Bioactive peptide purification from marine sources can be achieved via chromatography techniques, including reverse-phase high-performance liquid chromatography, gel filtration chromatography, and ion exchange chromatography, which is a current technique to extract biologically active peptides. Studies of marine plants, microbes, and animals over the last several eras have revealed a huge variety of structurally varied and bioactive secondary metabolites. With a particular focus on the conversion of nutraceutical and pharmaceutical research into commercially available products, this review summarizes current findings in marine peptide research as well as emerging patterns, and its promising directions are briefly reviewed. The use of active peptides derived from the sources mentioned earlier their health advantages and bioactivities are also focused. Along with safety concerns, their possible usages in the processed food industry, wound healing, feed, cosmetic, and pharmaceutical industries, for the growth of efficient goods, are highlighted.



**Keywords**— Bioactive peptide, functional food, pharmaceutical, sources, therapeutic applications

## I. INTRODUCTION

Protein fragments known as bioactive peptides are beneficial to various bodily functions and general human health. Most bioactive peptides have molecular masses between 0.4 and 2 kDa and contain two (dipeptides) to twenty amino acid residues (Zaky et al, 2022). There have also been a few components of longer peptides being reported. One peptide with anti-cancer and hypocholesterolemic effects is called lunatic, which is

made of 43 amino acids and is obtained from soy (Ulug, et al., 2021). From marine microorganisms, algae, fungi, mollusks, crustaceans, and marine byproducts like inferior muscles, viscera, skins, trimmings, and shell, bioactive peptides with antihypertensive, antioxidant, antidiabetic, anti-cancer, and anti-allergic effects were identified (Wang, et al., 2017). Despite the fact that marine peptides have just recently received the attention that is well-deserved (particularly when compared to peptides from

other plant/animal sources) and they have the potential to produce classes of peptides with intriguing features, such as antituberculosis, antiaging, anticoagulant, and antidiabetic and making them prospective agents not just in medicine and pharmacy. (Mayer et al., 2013; Rangel et al., 2017), as well as in the cosmetics sector (Corinaldesi et al., 2017; Kim & Wijesekara, 2010). Additionally, efforts have also been made to use biopolymers and nutraceuticals synthesized from microalgae (Charoensiddhi et al., 2017). The widespread usage of peptides generated from marine sources still faces several challenges that have not yet been resolved: this needs to identify ideal conditions for peptide isolation and consistent production from specific sources.; correlating structural and bioavailability; indicating the peptide's consistency and efficiency in vivo; and, in most situations, enhancing their availability and production rates. For example, microalgae is a common source of marine bioactive peptides. However, there are many challenges associated with both the availability of the source material and the effectiveness of peptide extraction. Seaweed cell walls contain polymers that limit peptide extraction (Admassu et al., 2018). However, these differences between the structures and functions of marine peptides are significantly more evident due to the vast biodiversity of the five basic classes of aquatic creatures that are used as food, including fishes, microalgae, bivalves, crustaceans, and cephalopods, which span four kingdoms of biological organisms (Phyo et al., 2018; Shinnar et al., 2003) Nutraceuticals can originate from a variety of marine creatures, including sponges, marine plants, and microbes. Each of these sources has distinctive biomolecules that help them to thrive and survive in aquatic surroundings. Seaweed is being investigated as a superior source of antioxidants due to its high amount of bioactive peptides (Shahidi & Ambigaipalan, 2015). The development of novel glucosidase inhibitors by marine microorganisms may provide an alternative to traditionally used diabetes treatments (Trang et al., 2021). Dieticians and food technologists have recently become interested in the vast range of purposes that marine and freshwater mollusks might serve as food and nutraceutical resources due to their tremendous biodiversity and abundance. The phyla of mollusks with the most bioactive properties and nutraceutical applications were Cephalopoda, Bivalvia, and Gastropodia (Chakraborty and Joy, 2020). Aquatic food intake has increased globally in recent years due to greater knowledge of their health benefits and a good attitude toward seafood. Due to the variety of their environments, marine creatures have evolved distinctive

traits and bioactive substances compared to terrestrial sources. Functional food ingredients have long been recognized for their value in promoting health and lowering illness risk (Shahidi and Ambigaipalan, 2015). Seaweed is a potential crop because of its anticancer, anti-inflammatory, anti-bacterial, antioxidant, anti-obesity, and anti-coagulant effects. The discovery of more sensitive and the development of new bioactive substances has been enhanced by omics technologies, including nuclear magnetic resonance, liquid chromatography-mass spectrometry (NMR-LC/MS), and next-generation high-throughput sequencing. (Rosic, 2021). Several aquatic invertebrate species can be located everywhere in the atmosphere, which include the deep ocean and the intertidal zone. Some taxonomic families include Cnidaria (corals, jellyfish), Porifera (sponges), Annelida (marine worms), and echinoderms (sea cucumbers, sea urchins, and starfish) and mollusks (oysters, crayfish, and prawns). Marine invertebrates have long been used in coastal community's diets and for therapeutic purposes (Ganesan et al., 2020). This article aims to provide a comprehensive overview of the origins, applications, and relevance of bioactive compounds derived from different marine animal species. Using marine bioactive compounds in the pharmaceutical and food industries. Multiple reviews on marine bioactive chemicals have been conducted in the past few years. In marine bioactive peptides domain several reviews explain bioactivities like as antioxidant, antimicrobial, antihypertensive. Additionally, most of the reviews concentrate on a specific source of bioactive peptide such as algae, fish, or mussels. This study gathers current and comprehensive knowledge about bioactive peptides from marine sources, concentrating on their biological activities, functional properties, and industrial uses that are already exploited.

## II. MARINE BIOACTIVE PEPTIDES SOURCES

Crabs, mollusks, and echinodermata are examples of edible marine invertebrates that can be exploited as organically derived biopolymers for a range of applications. Humans have used these biopolymers, which are comprised of protein, as food and supplement ingredients for decades to cure a variety of illnesses. Microalgal biomass are used in animal feed and have anti-bacterial, wound-healing, anti-inflammatory, anti-cancer, and antimicrobial properties **Fig. 1** (Ganesan et al., 2020).

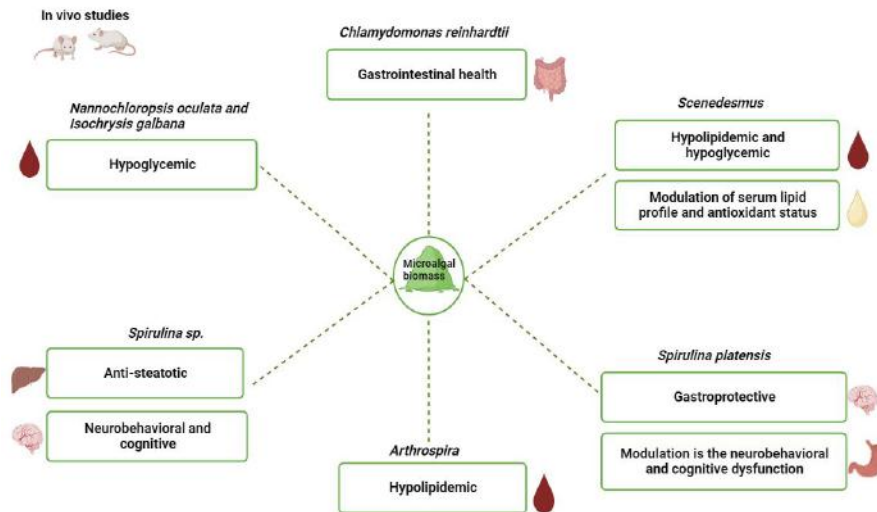


Fig. 1: Applications of microalgal biomass

It is well-acknowledged that sponges contain a lot of bioactive substances that have antimicrobial effects. Bioactive compounds have also been extracted from bryozoans. A marine *Polychaete* (phylum *Annelida*) has proven to be efficient in treating many pathophysiological conditions, such as bone cancer osteoporosis, and arthritis, among others. The marine annelid *arenicola marina* was used to separate bioactive substances. Several bioactive chemicals have also been produced by marine arthropods. The most well-known bioactive compound derived from marine arthropods is tachypleus, amoebocyte, and amoebocyte lysate from limulus lysate. (John et al., 2018). The bioactive substance pisulosine has antileukemic properties and is obtained from the hawaiian mollusk *elysia rufescens*. The synthetic equivalents of synthadotin dolstatin, and Soblidotin, which were derived from the mollusk species *D. auricularia* and are presently being studied for their potential as medicines, are synthadotin soblidotin. It has been discovered that the mollusk *dolabella auricularia* produces several aolastatins, which are cytotoxic and anticancer substances (Papon et al., 2022). The most prevalent bioactive substances that can be found in echinoderm metabolites are saponins. Among other things, sea urchins, sea cucumbers and starfish contain these sterol compounds are called asterosaponin's, but it has been declared that sea cucumber saponins are derived from terpenoids (Datta et al., 2015). From the marine snail *neptunea arthritica cumingii*, two newly multifunctional peptides were discovered. Both peptides had anti-inflammatory, ACE-inhibitory, and anti-diabetic properties (Li, et al., 2019). Each conus species venom contains a unique variety of neurophysiologically active peptides (Neves et al., 2019). The sea cucumber protein

hydrolysates were used to isolate ACE-inhibitory peptides using a plastein reaction (Ovchinnikova, 2019). Two new effective ACE-inhibitory peptides were isolated and discovered from *Acaudina molpadioidea* (sea cucumber). These compounds may be used to create hypertension medications (Li, et al., 2018). Gram-positive bacteria called actinomycetes are widely known for producing a wide range of antibiotics. Although most actinomycetes in nature are free-living organisms, some of them can be dangerous. With many different plants and animals, they develop symbiotic connections. Moreover, actinomycetes are symbiotic with a range of marine macrofauna, such as ecologically significant fora-like insects, cone snails, marine sponges, and invertebrates (*Haliclona*, *Axinella polypoides* etc.) are included. (Mahapatra et al., 2020). The main biologically active components used as functional foods come from marine sources such as peptides. Fish oils and microalgae are highly poly-saturated fatty acids that can help to enhance the nutritional profile of diets (Prabha et al., 2019).

## 2.1 Bioactive peptides from chelicerata and crustacea

Antimicrobial peptides have many physiological components that are active in the hemolymph of marine invertebrate chelicerate and crustacea. These substances typically produce pores in membranes and have modest molecular weights (less than 10 kDa) (Tincu & Taylor, 2004). The amphipathic nature of these peptides makes it easier for them to cling to, disrupt, and/or permeate the cytoplasmic membrane of bacteria. The horseshoe crab *limulus polyphemus* is the source of the 2-18 residue peptides known as polyphemusins I and II, which inhibit the development of both Gram-negative and Gram-positive bacteria. Peptides with antibacterial activity are also

present in the hemolymph of *Charybdis lucifera* and *thalamita crenata* (Rameshkumar et al., 2009; Rameshkumar et al., 2009). A 37-amino-acid antimicrobial peptide that are rich in proline and arginine was identified from the spider, *Hya Araneus*, crab, hemocytes. Arasin 1 is a peptide with two disulfide bonds at its C-terminus and a proline and arginine-rich N-terminal region. (Stensyng et al., 2008).

## 2.2 Fishes

There has not been much research done on marine vertebrates as a source of proteins and peptides with living activity. Fish have a defense mechanism that prevents dangerous microorganisms from penetrating their skin barrier. *Pleuronectes americanus* the winter flounder produces a peptide antibacterial in the skin mucus (Haefner 2003; Lazcano et al., 2012). Antifreeze polypeptides are produced by a variety of marine species e.g fish as a defense against freezing in chill saltwater environment. Longhorn sculpin (*Myoxocephalus octodecemspinosus*) skin has been used to isolate type I and type IV anti-freezing proteins (Low et al., 2001). From the epidermal tissues of the cunner *Tautogolabrus adspersus* and the Atlantic snailfish (*Liparis atlanticus*) have been discovered and partially characterized more anti-freezing proteins. (Evans & Fletcher 2004). The red sea bream's *Chrysophrys* gills contain a novel, C-terminally amidated peptide with three distinct isoforms (Iijima et al. 2003). Peptides with 20–25 amino acids make up *Chrysopsin-1*, *Chrysopsin-2*, and *Chrysopsin-3*. They are extremely cationic and have an odd Arg-Arg-Arg-His order at the C-terminus. The secondary structures of the *chrysopsin* peptides were used to predict their  $\alpha$ -helical topologies, which were then verified by CD spectroscopy. Fish proteins that have experienced hydrolysis-induced modification are target of bioactivity identification. The peptides produced during hydrolysis are highly dependent on the specialty of the proteolytic enzymes, the hydrolysis depends on temperature, the pH, and the enzyme/substrate ratio (Otte et al., 2007). Many hydrolysates are the product of successive hydrolysis with an endopeptidase (a peptidase that does not break peptides into single amino acids) followed by an exopeptidase (a peptidase that will break the peptides into small amino acid residues from the end of peptide chains) (Hamada 2000).

## 2.3 Seaweed derived peptides

### 2.3.1 Glycoproteins

A diverse group of algae species have different protein and sugar ratios in their GPs; for example, GPs-rich fractions in *Ulva* species demonstrated a protein content of high to 33.4 percent (Wijesekara, et al., 2017), GPs with MWs of 48 kDa are present in *Codium decorticated*, where

the protein content is 60% (Thangam, et al. 2014). Mannose appears to be the main constituent of the prosthetic portion in seaweed GPs (Yoshiie, et al., 2012). Various oligosaccharide chains are covalently bonded to these glycoproteins and make them substances called glycans. O-glycosylated and N-glycosylated chains are the two main forms of sugar chains found in GPs (Charoensiddh et al., 2017). The two functions of GPs are intercellular contacts and recognition, which can be found either free, after secretion, on the cell surface, or on the cell wall (Yoshiie et al., 2012).

### 2.3.2 Lectins proteins

Lectins are GPs with extraordinary traits in their binding to specific mono or oligosaccharides. Red seaweed is an excellent source of high and low-MW lectins (Barre, et al., 2019). Lectins serve a variety of purposes, including gamete identification, reproductive cell fusion, and pathogen protection (Barre, et al. 2019; Frenkel, et al, 2014). The four major categories of lectins are chitin-binding lectins, legume lectins, lectins, type-2 ribosome-inactivating proteins, and mannose-binding (Van Damme, et al., 2007). Many of these proteins bind mannose because mannose-binding glycans make up the majority of the glycans in seaweed. (Yoshiie et al. 2012). Relevant seaweed lectins exhibit a strong affinity for these residues similar to pertinent mannose-specific lectins. (Ambrosio et al., 2003). Like bacterial, viral, or eukaryotic cell surface GPs, they can "agglutinate" particles that contain these residues because of this characteristic (Wu et al. 2016). For instance, *griffithsin*, which is derived from red *Griffithsia* sp. seaweeds and possesses a variety of biological features has been described (Gunaydn, et al., 2019). Due to pharmacological characteristics, research in molecular biology, biochemistry, and medicine is concentrated on characterizing and isolating these compounds. Although seaweed lectins have been chemically characterized more carefully, more data is still required to fully comprehend their binding affinities, molecular structures, and potential biochemical activities for future implementations (Fontenelle, et al., 2018).

## 2.4 Macroalgae and seaweeds

Seaweed, commonly referred to as macroalgae, is a diverse group comprising around 10,000 species (Makkar et al., 2016). Green algae (*Chlorophyceae*), Brown algae (*Phaeophyceae*), and Red algae (*Rhodophyceae*), are the three major phyla of algae (*Chlorophyceae*). Fresh sea algae have a high water content, which can make up to 94% of the biomass (Holdt and Kraan, 2011). Microalgae have been cited in the literature as being excellent sources of bioactive peptides for usage in functional meals due to the characteristics of the aquatic environment and other



conditions which is salt content, temperature, and lighting conditions. (Gallego et al., 2019).

As previously indicated, many factors affect the protein content of seaweed. Furthermore, it is difficult to compare the protein content of algae due to different methodologies, particularly when extracting proteins, and the vast variety of species identified (Lourenço et al., 2002). Although the protein content of brown seaweed is typically lower than that of green or red seaweed, Pereira, Barbarino, Lourenço, De-Paula, and Marquez. (Schiener et al., 2015) found that the protein content of the species *Padina gymnospora*, *Dictyota menstrualis*, *Chnoospora minima*, and *Sargassum vulgare* was relatively high, ranging between 10 and 15 percent. *Fucus vesiculosus*, *Ascophyllum nodosum*, *Laminaria digitata*, and *Himantalia elongata* are examples of common brown seaweed. *Laminaria digitata* has an average protein content of 6.8%, with the lowest and highest protein levels occurring in the first and third quarters of the year, accordingly (Schiener et al., 2015). This result was comparable to that of Peinado, Girón, Koutsidis, and Ames (2014), who estimated *Laminaria digitata*'s protein concentration to be 5.8%. As previously mentioned, algae are known to contain significant amounts of high-quality vitamins, minerals, polysaccharides, and bioactive substances such as proteins, lipids, and various polyphenols (Holdt and Kraan, 2011). There are very few structurally and functionally effective peptides produced from seaweed. Currently, a variety of functional foods, primarily in Japan, are being promoted that contain peptides produced from seaweed. Foods for Specified Health Uses (FOSHU) are foods with specific health purposes that have been authorized by the law of the Japanese Ministry of Health and Welfare (Arai, 2000). Nori peptides (Shirako Co., Ltd., Tokyo, Japan) and Wakame peptide jelly (Riken Vitamin Co., Ltd., Tokyo, Japan) are two products containing seaweed-derived peptides with FOSHU-approved claims for lowering blood pressure (Fukami, 2010).

### III. CHARACTERIZATION OF MARINE BIOACTIVE PEPTIDES

#### 3.1 Preparation and purification

The bioactive peptides significantly differed on the basis of species, amino acid compositions and sequences, and they could be created by using various techniques. The bioactivities of peptides are also impacted by specific techniques (Agyei et al., 2016).

#### 3.2 Organic synthesis

The use of organic synthesis in marine natural products rise with the advancement of technology and structural elucidation methods (Pindur & Lemster, 2001). Marine biological compounds have produced many therapeutic applications due to their unique bioactivities. The target peptides are typically obtained through batch synthesis in organic production techniques utilizing a variety of solvents in the solid phase. In order to batch synthesize target peptides as a result of low production, organic synthesis is always used, starting from cyclic peptides to simple peptides (Zhou, 2014). Mass spectrometry is used to detect the final result to check the consistency of ultimate molecular mass. Its confirmed bioactivity would also be continued. The target peptides might be produced in large quantities because of organic synthesis. Nevertheless, the organic synthesis method is costly, time-consuming, and unsustainable. Targeting peptides with a distinct sequence is also required for this method. As researchers may need to determine the peptides compositions therefore better extraction procedures are recommended. Utilizing a variety of purification and isolation technologies (Wang et al., 2017).

#### 3.3 Chemical hydrolysis

Proteins can be hydrolyzed chemically by cleavage peptide bonds either with alkali or acid. This technology has been extensively utilized by the industry due to its low cost and simplicity. However, this method has significant limitations, including a difficult-to-control procedure and a tendency to produce mutated amino acids (Vijaykrishnaraj & Prabhasankar, 2015) and manufacturing products with varying functional and chemical qualities. Acidic hydrolysis is a substantial chemical transformation that can strongly alter the functional and structural characteristics of peptides (Lee & Jeffries, 2011). Because of its simplicity and efficiency, acid hydrolysis is favored over alternative pretreatments (Loow et al., 2016). Sulfuric acid (H<sub>2</sub>SO<sub>4</sub>) is the most prevalent kind of utilized diluted acid. However, research has also been done on hydrochloric acid (HCl), nitric acid (HNO<sub>3</sub>), phosphoric acid (H<sub>3</sub>PO<sub>4</sub>), and other acids (Xu & Huang, 2014). Maleic and oxalic acids hydrolyzed biomass better than H<sub>2</sub>SO<sub>4</sub> (Lee & Jeffries, 2014). Scales of bluefish, mackerel, salmon, and scup were assimilated by adding 25% to 0.4 M HCl (Richard et al., 2011). Acidic hydrolysate demands high temperatures and produces salty hydrolysates. Moreover, desalination in the subsequent experiment is complicated. Furthermore, acid hydrolysis can degrade tryptophan, an important amino acid. However, some study has been done on alkali hydrolysis using samples from Cod. Nevertheless, alkali hydrolysis

frequently leads to poor functioning and low nutrient content (Wang et al., 2017). Alkali treatment also results in increased solubility of collagen (Huang et al., 2016; Cho et al., 2004; Da Trindade Alfaro et al., 2009). In other words, whereas acidic hydrolysis might lead to the simple degradation of peptide bonds and yield a high output of peptides, it is unsecured and environment unfriendly. Hence, it is primarily utilized for industrial manufacturing.

### 3.4 Enzymatic hydrolysis

Recent investigations have demonstrated that enzymatic hydrolysis release the majority of peptide sequences encoded in dietary proteins and gives bioactive characteristics (Qilong et al., 2013). Proteins are often modified in the food industry through enzymatic cleavage of certain peptide couplings with proteolytic enzyme preparation. Although many other methods exist for increasing the value of the target peptides, animal sources and proteolytic enzymes from plants have been explored broadly or documented by multiple researchers over the last 60 years (Wang et al., 2017). Commercially available enzymes derived from bacteria, such as neutrase (Je et al., 2009; Foh et al., 2010), alcalase (Je et al., 2007; Sila et al., 2014), and flavour enzyme (Klompong et al., 2007; Liu et al., 2015), including from plants and animals, such as pepsin (Ko et al., 2012; Moreda-Piñeiro et al., 2011), trypsin (Alemán et al., 2011; Wu et al., 2015), subtilisin (Mbatia et al., 2010; Salampessy et al., 2015), papain (Liu et al., 2010; tripoteau et al., 2015), and bromelain (García-Moreno et al., 2016; Wang, Yu, Xing, & Li, 2017), are favored. Moreover, the usage of external enzymes may improve the control and reproducibility of the hydrolytic process. Enzymatic hydrolysis involves five distinct factors, each of which affects the process differently: extraction temperature, enzyme concentration, extraction time, water/material ratio, and pH (Wang, Yu, Xing, Chen, et al., 2017). For instance, (Bhaskar et al., 2008) employed an alcalase enzyme hydrolyze the intestinal excess catla proteins of (Catla catla) and produced a greater hydrolysate under optimal conditions, with an enzyme-to-substrate concentration 1.5 percent and a total hydrolysis time 135 minutes, the degree of hydrolysis approaches 50%. To get hydrolysis with the maximum amount of peptide, another study employed protamex to hydrolyze blue shake skin at the ideal pH of 7.1, a substrate-to-enzyme ratio of 4% is required, and a temperature of 51 C (Wang, Yu, Xing, & Li, 2017). Pepsin hydrolysis was also investigated by (Song et al., 2012), Who employed an 1100 U/g enzyme-to-substrate ratio, a pH of 2.0, at 2.4-hour average reaction time, and a 4:1 (v/w) water-to-substrate ratio. In a broad sense, many scientists have emphasized the hydrolysis of enzymes because of how conveniently it can be replicated and manipulated

(Wang, Yu, Xing, & Li, 2017). Additionally, enzymatic processes do not involve any unwanted byproducts and do not compromise the proteins nutritional content. Inorganic mass, such as salt, may be added when the pH is adjusted with acid or alkali, which may be difficult and expensive to remove afterward.

## IV. PURIFICATION OF MARINE BIOLOGICALLY ACTIVE PEPTIDES

The bioactivities of the peptides are reliant on their amino acid sequences and structures, which typically range from 3 to 20 residues. According to recent research, 95% of peptide sequences that are contained in dietary proteins offer bioactive characteristics after being released by hydrolysis of enzymes (Agyei & Danquah, 2011). Then, it is essential to determine the peptide structures, that is why there are several researchers who have studied peptide decontamination. An average approach for the identification of aquatic bioactive peptides is produced by isolating peptides from aquatic species, screening them for certain bioactivities, separating them using MTT assay fractionation techniques, and then purifying each individual bioactive peptide. To design an effective purification procedure, it is also required to conduct extensive research on techniques such as membrane filtering systems, gel filtration chromatography, ion exchange chromatography, and reverse-phase high-performance liquid chromatography (HPLC). Before purifying peptides, the researcher must carefully analyze the advantages and downsides of each purification technique.

### 4.1 Membrane filtration

A few years ago, several scientists used membrane filter as the first stage in the purifying process. For instance, (Cho et al., 2003), the galacturonic acid concentration in pectin raised from 68 to 72.2 percent using cross-flow membrane filtering. When Hoki (*Johnius belengerii*) protein hydrolysates were extracted by membrane filtering, it was shown that HPH-III, with a molar mass of 3-5 kDa, had the best anti-oxidant activity (Kim et al., 2007). In addition, with ultrafiltration membrane, the most efficient 1,1-diphenyl-2-picrylhydrazyl radical-scavenging peptide was identified with a molecular mass below 3 kDa (Wang et al., 2015). According to (Tonon et al., 2016), Shrimp ultrafiltration and hydrolysis were combined to produce protein hydrolysate, whereas filtration membranes (Roblet et al., 2016) used for the purification and electro dialysis of Atlantic salmon protein hydrolysate.

### 4.2 Cation-exchange chromatography IEX

In recent years IEX techniques has gained tremendous significance for the extraction, structural characterization, and detection of short sequences peptides. (Levison, 2003). IEX medium contain positive-charged hydroxyl functional-groups that bind electrostatically charged atoms. Bound molecules are dislocated and precipitated from the solvent by increasing concentrations of an identically polarized molecule. Proteins contain many hydroxyl groups with either positive or negative charges. Protein separation is achieved by adjusting the mobile phase's pH or ionic makeup. IEX is used for high-resolution separation to remove the heavy impurities from a high-volume solution, or to extract a specific protein as a preliminary filtration process or as a final purification step. Numerous researchers have utilized various IEX mediums to purify the target product based on the qualities described above to separate chitooligomers, for example, utilized C-25 Sephadex CM with (0-2 M)-HAc NaCl buffers eluted successively at 3 mL/min and a range of HAc-NaAc buffer (50 mM, pH = 4.8) (Li et al., 2012). The antioxidant peptide was isolated from hydrolysate blue mussel (*Mytilus edulis*) by using modified cation exchange C-25 SP-Sephadex, 50 mm acetate buffer (pH=4.0) (Park et al., 2016). Additionally, several studies use SP-Sephadex C-25 to isolate the desired peptide (Jun et al., 2004; S. Wang et al., 2014). Moreover, several media were used for marine organism purification, including Sepharose fast flow formulations, fast flow CM Sepharose (Hsieh et al., 2008; Song et al., 2015), fast flow DEAE Sepharose (Kumar et al., 2011; L. Wang et al., 2014; Ye et al., 2012), fast flow Q Sepharose (Hui et al., 2004), fast flow SP Sepharose (Beaulieu et al., 2010; Wang, Yu, Xing, & Li, 2017), and others.

#### 4.3 Gel filtration chromatography

Initially, the sample is subjected to gel filtration chromatography, then finally reversed phase C18 HPLC for further purification (Jai Ganesh et al., 2011; Zhang et al., 2012). For instance using DEAE Sepharose and Superdex 200 fast flow, increase and established with excellent resolution, high recovery, and low run times, as primary goals. (Huang et al., 2016). From the leaves of *Clinacanthus nutans* Lindau, an innovative peptide with a molar mass of 9.17 10<sup>4</sup> Da was identified (Qian et al., 2016). Similarly, Using Superdex 200 isolates an enzyme

that breaks down fish scales was found to have a molar weight of 1.19 10<sup>6</sup> Da (Pan et al., 2010). Superdex prep grades, and Sephacryl are employed for high-throughput, separation with high recovery in the research laboratory or production areas (Wang, Yu, Xing, & Li, 2017; Shen et al., 2015; Wang, Yu, Xing, & Li, 2017). Yellowfin Tuna roe (*Thunnus Albacores*) trypsin inhibitor was isolated, initiated by column chromatography on, Sephacry S200, DEAE-cellulose, Sephadex G-50, and its apparent molecular weight was determined to be 7 10<sup>4</sup> Da (Wu et al., 2016). Moreover Sephadex is often used in the filtration of aquatic organisms and is suggested for fast group separations, such as exchange of buffers desalination (Bougatef et al., 2010; Hsu, 2010) (Vijaykrishnaraj et al., 2016). Internal organs of *Parastromateus niger* and the flavor of the mussel were separated in order to conform using Sephadex G-25 (Jai Ganesh et al., 2011). Sephadex G-7 marine yeast purification was also examined. Sephadex G-75 marine yeast purification was also examined (Ma et al., 2007).

#### 4.4 High performance liquid chromatograph (HPLC)

The most well-known technique for identifying, classifying, and purifying biologically active substances is HPLC (Singh et al., 2014). The primary features of this technique are its simplicity of operating, sensitivity, and high resolution as well as the short time required to obtain elution spectra in comparison to the IEX and GFC which require twenty to twenty-five hours. Many scientists have utilized HPLC to purify marine organisms in recent years, including Thornback ray (Lassoued et al., 2015) cyanobacterium (Lopez et al., 2016), marine Snail (Dolashka et al., 2011), enteromorpha (Pan et al., 2016), abalone (Pan et al., 2016), sponge (Youssef et al., 2014), tuna (Seo et al., 2014), and others. Recently, HPLC has frequently been coupled with analytical tools like high performance liquid chromatography and mass spectrometry (MS), followed by (LC-MS/MS) tandem mass spectrometric detection, which has evolved the industrial level characterizing amino acid sequences (Vijaykrishnaraj & Prabhasankar, 2015), It has revolutionized protein and peptide structure elucidation but is expensive and time-consuming (Mann & Jensen, 200; Careri & Mangia, 2003). **Table 2** showed the different sequences of marine bioactive peptides.

Table 1: Sequence of Marine Bioactive peptides

Name	Biological activity	Sequence	References
Alaska Pollack	ACE inhibitory	FGASTRGA	(je, park, kwon, & kim, 2004)
Oyster	Anti-HIV	LLEYSL, LLEYSI	(Lee & Maruyama, 1998)
Marine Snail	Antifungal	SRSELIVHQR	Lopez-Abarrategui, Alba & silva, 2012)

Spirulina Maxima	Antiatherosclerotic	LDAVNR, MMLDF	(Voo & kim, 2013)
Yellow Catfish	Antimicrobial	GKLNFLSRLE	(Su, 2011)
Jumbo Squid	Antioxidant	FDSGPAGVL, NGPLQAGQGER	(Mendis, Rajapakse, Byun, & Kim 2005)
Sole	Antihypertensive	MIFPGAGGPEL	(jung, Mendis, & je 2006)
Hoki	Antioxidant	ESTVPERTHPA CPDFN	(Kim, Je, & Kim 2007)
Porphyra haitanesis	Anti-cancer	-----	(Marqus, et al., 2017)
shellfish	Anti-cancer	Ala-Phe-Asn-Ile-His-AsnArg-Asn-Leu-Leu	(Kim, et al., 2012)
koshikamides	Anti-HIV	-----	(Al-Khayri, et al., 2022)
Prawn	Antioxidant	IKK, FKK, FIKK	(Zhou, et al., 2012)
Sea cucumber	ACE inhibitors	MEGAQEAQGD	(Zhao, et al., 2009)
Tuna	Anti-hypertensive	GDLGKTTTVS NWSPPKYKDTP	(Lee, et al., 2010)
Yellow catfish	Anti-microbial	GKLNFLSRLE ILKLFVGAL	(Su, 2011)

## V. THERAPEUTIC APPLICATIONS

### 5.1 Antibacterial activity

Antibacterial peptides, which are typically 20–40 amino acids long, are used by a variety of organisms as a defense against infection. Most can quickly eradicate a variety of microorganisms. Large microbial peptides (>100 amino acids) usually serve as proteins that are lytic, nutrient-binding, or that specifically target bacterial cell membranes to fail or cease functioning as planned. Humans have been found many antibacterial proteins that are phagocytes, multicellular epithelial layer. Antimicrobial peptides (AMP) are endogenous antibiotics that also aid in wound healing, inflammation and the control of the defense mechanism (Da Costa, et al., 2015; Kang, et al., 2015). The scyphoid jellyfish's mesoglea is responsible for producing the AMP aurelin. *Auricula aurita* that is made up of 40 amino acid residues and aurelin was the name of the peptide which performed activity towards gram-positive bacteria and gram-negative bacteria. *Aurelin* reported to inhibit the growth of microorganisms under low salt conditions. The available therapies for various disorders, such as type-1 diabetes, Alzheimer's disease, other forms of arthritis and rheumatoid arthritis, cardiac disease, asthma allergies, Parkinson's disease, cancer, and irritable bowel syndrome many others are prohibited, and after a dosage, certain

medications have major side effects on patients' health. Consequently, Numerous approaches for treating these persistent bacterial infections need further study. Natural remedies have long been considered a potential kind of treatment for illnesses and antimicrobial therapy (Suleria et al., 2016). The *Actinomadura sp.* TP-A0878 can produce a nomimicin spirotetrone complex from polyketide source with the value of MIC 6.3, 12.5, and 12.5 g/ml, nomimicin showed strong antibacterial activity against *Candida albicans*, *Micrococcus luteus*, and *Kluyveromyces fragilis* (Karthikeyan et al., 2022). *Zunyimycins C* and *B* extracted from *Streptomyces sp.* FJS31-2 displayed antibacterial activity with MICs between 3.7 and 8.14 g/ml and 0.94 g/ml against MRSA isolates (methicillin-resistant *S. aureus*) (Lü et al., 2017). Strains of *Tetracenediones Streptomyces formicae* KY5 can synthesize the polyketides formicamycins A–L, which are able to restrict the MRSA with a minimum inhibitory concentration (MIC) of 0.41 g/ml and vancomycin-resistant *Enterococcus faecium* (VRE) with a MIC of 0.80 g/ml (Qin et al., 2017). Epinecidin-1, an antibacterial peptide group of fish (*Epinephelus coioides*), showed bacterial medication efficacy against *Vibrio vulnificus*, *Staphylococcus coagulase*, *pseudomonas aeruginosa*, and *staphylococcus coagulase*. Electroporation was used to introduce plasmid DNA into decapsulated *Artemia* cysts that code for a

cytomegalovirus (CMV) promoter-driven expression of the EGFP-epinecidin-1 fusion protein. Zebrafish with better resistance to *V. vulnificus* and a greater mortality were fed transgenic artemia generating CMV-gfp-epi in addition to commercial feed. The resultant protein, EGFP-epinecidin-1, decreased the proliferation of *V. vulnificus*. Immune-responsive gene expression and the immunomodulatory in reaction to *V. vulnificus* (204) infection were also impacted by feeding zebrafish transgenic artemia. These results imply that transgenic to have antimicrobial effects on fish larvae without introducing medication residues or creating bacterial drug resistance, artemia expressing CMVgfp-epi can be given (Jheng, et al., 2015 ; Qin, et al., 2014).

### 5.2 Anti-HIV activity

Marine sponges provide diverse habitats regarding a variety of marine organisms. They are filter feeding, soft-structured, aquatic invertebrate parazoans with a high concentration of bioactive components (Anjum, et al., 2016). Sponges are made up of a variety of biomolecules with different chemical and structural properties and a range of bioactive properties (Vitali, 2018). This is demonstrated by the fact that four of the nine marine medications with FDA approval came from sponges (Wu, et al., 2019). According to research studies, there are numerous bioactive substances that have been found from sponges and produce functional enzyme clusters. (Kang, et al., 2015). According to reports, the koshikamides found in *Theonella sp.* sponges have anti-HIV properties. When evaluated infectivity of HIV-1 in a single round experiment with respect to a viral envelope that uses CCR5, comparing their linear equivalents to their cyclic counterparts, the IC50 values of the koshikamides F and H decreased HIV entrance to 2.3 and 5.5 M, respectively (Agrawal, et al., 2016; Al-Khayri, et al., 2022). Depsipeptides, also known as cyclodepsipeptides, are powerful compounds discovered from different marine sponge species that are particularly interesting for therapeutic development against HIV. Their structure comes from pre-loaded with peculiar non-proteinogenic amino acid combinations. (Wu, et al., 2019). It has also been demonstrated that neamphamide A and callipeltin A, which are both derived from the plants *Callipelta sp.* and *Latrunculia sp.*, inhibit the replication of HIV (Kang, et al., 2018). For many years, sponges have been recognized for providing novel bioactive metabolites, including, polyethers, macrolides terpenoids, nucleoside derivatives, alkaloids, and many other chemical substances. An anticancer substance *Cytosine Arabinoside*, was subsequently create the synthetic analogues of the C-nucleosides pongouridine and pongothymidine that were discovered from a Caribbean sponge (Aneiros, and Garateix, 2004). Photosynthetic microorganisms called

marine cyanobacteria are widely found in nature (Silipo, et al., 2010). In addition to a wide range of toxins, they also contain several bioactive substances that may have properties including anticancer, antitumor, antifungal, antibacterial, protease inhibition and anti-inflammatory. An 11 kDa protein Cyanovirin-N (CV-N), obtained from the *Nostoc ellipsosporum* cyanobacterium, has undergone preclinical testing as an anti-HIV medication. (Fidor, et al., 2019).

### 5.3 Anti-cancer activity

Cancers are the deadliest and feared diseases worldwide. Drugs to treat cancer and tumors are being developed quickly by pharmaceutical corporations. Additionally, oncology research has made significant advances and has helped us to understand tumors better over time (Noguchi, et al., 2012). An effective starting point for the production of anticancer peptides is food protein hydrolysate. Protein hydrolysates from soy and rice have been shown to have anticancer properties in the past. Alcalase breaks down the proteins in rice bran to produce anticancer peptides in rice (Kannan, et al., 2010). The shellfish proteins contained Ala-Phe-Asn-Ile-His-Asn-Arg-Asn-AsnLeu-Leu is a different anticancer peptide that was effective in killing prostate, breast, and lung cancer cells while sparing healthy liver cells (Kim, et al., 2012). Peptides can pass through cell membranes because of their small size and chemical makeup; unlike proteins and antibodies, they do not accumulate to hazardous quantities. While having little interactions with other medicinal treatments, these molecules have demonstrated great affinity and specificity. While these substances often have limited oral bioavailability, which leads to quick clearance of the peptides, there are still issues with their utilization that must be resolved. These issues are primarily connected to the peptide delivery method (Marqus, et al., 2017). Proteins from *Porphyra haitanensis* were hydrolyzed by trypsin to create peptides that have anti-proliferation properties. Five human cancer cell lines were used to test the peptides produced from this source: HepG2 for liver cancer, HT-29 for colon cancer, MCF-7 for breast cancer, A549 for lung cancer and SGC-7901 for gastric cancer. The fluorouracil (5-FU) an chemotherapeutic agent was used as a control (Marqus, et al., 2017).

### 5.4 Antioxidant activity

A free radical is a chemical compound that has one or more orbital electrons that are unpaired and exist independently. It can form naturally in cells during normal cellular metabolism or because of external factors like radiation or pollution. The phenomenon of oxidative stress occurs when the body produces an excessive number of free radicals that cannot be effectively eliminated over

sometimes (Lafarga et al., 2020). Tumour formation and responses to anticancer therapy are both influenced by the level of oxidative stress present in the body (Gorrini et al., 2013). Antioxidants can be obtained endogenously or exogenously to reduce oxidative stress (via dietary means). Furthermore, as previously stated, seaweed has the potential to possess a significant amount of protein. These proteins derived from seaweed can be utilized in the production of antioxidant-hydrolyzed products and peptides. Several enzymatic hydrolysates were obtained from *Porphyra columbiana* byproducts through the utilization of alcalase, trypsin, and a combination of both enzymes (Cian et al., 2012). Furthermore, the enzymatic hydrolysate of *Palmaria palmata* was produced by Harnedy, O'Keeffe, and FitzGerald (2017) utilizing the Corolase PP, a food-grade enzyme. SDITRPGNM displayed the maximum hydroxyl radical scavenging capacity (ORAC) and ferric lowering free radical scavenging power (FRAP) activity among the peptides produced, with measured values of 152.43 2.73 and 21.23 0.08 nmol TE/mol peptide, correspondingly. The hydrolysate that was produced underwent a series of fractionation techniques, including reversed-phase semi-preparative high-performance liquid chromatography (RP-HPLC) and solid-phase extraction. Antioxidant peptides availability has also been measured, after a simulated gastrointestinal digestion was performed the antioxidant activity of *Pyropia columbina* peptides was found to increase (Cian et al., 2015).

### 5.5 Anti-inflammatory activity

In reaction to damage inflammation is an inherent component of the body's defense mechanism, characterized by a self-regulating nature. However, some diseases in which the inflammatory response persists, can result in chronic inflammation. Chronic inflammation is a factor in the pathogenesis of numerous infections, including, rheumatoid arthritis, cardiovascular disorders, autoimmune diseases, diabetes, asthma, pulmonary diseases, Alzheimer's disease, and cancer atherosclerosis (Y. S. Kixxm, Ahn, & Je, 2016). Macrophages play a crucial part in immunological responses since they are capable of secreting various mediators of inflammation, like nitric oxide (NO), prostaglandin E2 (PGE2), and cytokines including tumour necrosis factor (TNF- $\alpha$ ), interleukin-1 (IL-1), and interleukin-6 (IL-6) interleukin-1 (IL-1), in response to stimuli (Ahn, Cho, & Je, 2015). Macrophages can be stimulated through various means, including the presence of pro-inflammatory cytokines, interferon-gamma (IFN $\gamma$ ) such as IL-1b, IL-6, and TNF- $\alpha$  and, as well as lipopolysaccharides of bacteria (LPS) derived by Gram-negative microorganism (Ahn et al., 2015). NO has been associated to both inflammation and the development of

cancer, making its suppression is crucial for treatment (E. K. Kim, Kim, Hwang, Kang, et al., 2013). Numerous peptides from fish and mussels have been reported to have NO inhibiting action. A significant proportion of anti-inflammatory peptides was discovered in molluscs. Insufficient facts are available about the peptides that have already been isolated from fish, crustaceans, and algae. Peptides that reduce inflammation were recovered by flavour enzyme, alcalase, and protamex hydrolysis from the bivalves *Crassostrea gigas*, *Ruditapes philippinarum* and *Mytilus coruscus* (E. K. Kim, Kim, Hwang, Kang, et al., 2013) (Lee et al., 2012), (Hwang et al., 2012). These three peptides exhibited in vitro inhibition of LPS-induced mouse macrophage (RAW264.7) cell line NO generation. Using pepsin hydrolysis, an anti-inflammatory peptide containing the amino acid order Pro-Ala-Tyr was derived from salmon pectoral fin. These peptides demonstrated numerous advantageous anti-inflammatories response in LPS-stimulated macrophage cells RAW264.7, including inhibition of NO and PGE2 synthesis (63.80 percent and 45.33 percent, respectively), cyclooxygenase-2 protein expression, suppression of inducible NO synthase and, and reduction of proinflammatory cytokine (IL-1b, TNF-, and IL-6,) synthesis (Ahn et al., 2015). The anti-inflammatory effects of aquatic lectins are attributed to their carbohydrate-binding domain (Cheung, Wong et al. 2015). To effectively create lectin, green seaweed *Caulerpa cupressoides* are injected into the left temporomandibular joint zymosan before half an hour. For example, rats exhibit less zymosan-induced arthritis and mechanical hypernociception. In addition, there is a suppression of leukocyte accumulation in synovial fluid. However, the activity of the lectin decreased when it was treated with naloxone or ZnPP-IX an opioid receptor antagonist. However, lectin inhibited leukocyte infiltration and the expression of IL-1beta and TNF-alpha in the joint of temporomandibular, illustrating that lectin damaging the temporomandibular joint's hyper nociception and inflammation ultimately it based on the inhibition of TNF-alpha and IL-1beta (da Conceição Rivanor et al., 2014).

### 5.6 Antihypertensive activity

In the developed world, Cardiovascular-disease (CVD) is a leading cause of death. One of the main causes of CVDs is hypertension, which is sometimes Recognized as the "fatal disease." since this could take several years without showing any symptoms before causing a stroke or a heart attack (Sheih, Fang, & Wu, 2009). The system of renin-angiotensin (RAS) is crucial in the emergence of high blood pressure it regulates the body's water, electrolytes, and blood, (Fitzgerald et al., 2012). The enzyme angiotensin-converting-I (ACE-I) regulates

hypertension after stimulating Angiotensin II production, a potent vasopressor, bradykinin metabolism, and a vasodilator (Cao et al., 2017). Therefore, renin and ACE-I, two limiting enzymes involved in the RAS, can be inhibited or control excessive blood pressure (Fitzgerald et al., 2012). According to Riordan (2003), many anti-hypertensive medications with ACE inhibitory activity perform by increasing the bioavailability of bradykinin and lowering angiotensin II production (Samarakoon et al., 2013). However, they have a number of negative adverse reactions, including flavor loss, chronic cough, kidney disease, and angioneurotic edema (Cao et al., 2017). Finding natural compounds with antihypertensive effectiveness by suppression of ACE-I or enzymes for renin while avoiding unexpected effects became critical. Numerous ACE-inhibiting peptides have been investigated in various natural resources since the 1990s, including bovine whey, mushrooms, almonds, containing others (Cao et al., 2017). Peptides that lower blood pressure have been investigated in fish, mussels, and algae from marine sources (Samaranayaka et al., 2010; Neves et al., 2016; Cao et al., 2017; Chen et al., 2020). The algae *Chlorella vulgaris* obtained peptide VECYGPNRPQF (Sheih, Fang, & Wu, 2009), *Gracilariaopsis lemaneiformis* derived peptides TGAPCR and FQIN [M(O)] CILR (Deng et al., 2018), the peptides derived from *Undaria pinnatifida* YH, KY, FY, I, YNKL, IY, and IW has shown the ACE inhibited activity in vitro with values of IC<sub>50</sub> 23.94, 5.1, 7.7, 3.7, 2.7, 29.6, 9.64, 21.0, 6.1, and 1.5 M, respectively. The YH, KY, FY, and IY were derived using hot water and temperature, whereas the remaining peptides were all acquired through hydrolysis using trypsin or pepsin. Isolated peptides from *Mytilus edulis* and *Crassostrea gigas* fermented sauce showed IC<sub>50</sub> values of in vitro 87.40 g/mL and 19.34 g/mL, respectively, suggesting that these two species may be potential sources of ACE inhibitory peptides (Sara Alexandra Cunha, Manuela Estevez Pintado 2022).

### 5.7 Anti-allergic activity

As a defense mechanism against environmental chemicals, the immune system produces allergic reactions. It is common to see an overabundance of basophils, eosinophils, mast cells, and lymphocytes during an allergic reaction. In the pathophysiology of allergic disorders, mast cells are significant as they are triggered by IgE-mediated reactions to allergens (Ko et al. (2016). Several intracellular processes are triggered when mast cells become active, including the tyrosinase kinase activation ROS formation, which increases intracellular the production of cytokines calcium ion (Ca<sup>2+</sup>), degranulation, and the polymerization of microtubules, (Vo, Ngo, Kang, Park, & Kim, 2014) (Cunha and Pintado, 2021). One of the most crucial phases in allergic reactions is mast cell

degranulation since it triggers the release of inflammatory cytokines, proteases, histamine, and mediators in lipids, that can be in charge of a number of typical allergic reaction events (mucous production, airway constriction, among others). Histamine is a key modulator of the acute inflammatory response and is linked to a number of adverse consequences, including vascular hyperpermeability, angioedema, vasodilation, mucus formation, bronchoconstriction, and hypothermia. As a result, mast cell degeneration and histamine production are inhibited by anti-allergic medications (Vo et al., 2014). The antiallergic activities of aquatic peptides produced from microalgae *Spirulina* already have been investigated in vitro. After antigen induction, the LDAVNR (P1) and MMLDF (P2) peptides that were produced by the enzymatic hydrolysis of *Spirulina maxima* demonstrated dose-dependent anti-allergic function they could decrease the release of histamine and increasing intracellular Ca<sup>2+</sup> levels, thus preventing mast cell inflammatory reactions (verified by structural studies). While the P2 peptide blocked the activation of phospholipase C and the production of ROS, the peptide P1 functioned in the calcium and was dependent on microtubule signaling pathways (Cheung, Ng, & Wong, 2015; Vo et al., 2014). The ability to derive a peptide with a MW of 1175.5 Da from the *Haliotis discus hannai* mussel to reduce the release of histamine and the production of pro-inflammatory cytokines, such as IL-1, TNF-, and IL-6 in human mast cells after antigen initiation demonstrated its potential as an in vitro antiallergic (Ko et al., 2016). Researchers are now devoting their attention to developing anti-allergic chemicals from aquatic sources to combat the issues of food-induced allergies. Many plants have been shown to be anti-food allergic in numerous papers, and these plants contain terpenes, flavonoids, and other anti-food allergic substances. Enhancing Th1 immune function, inhibiting the development of Th2, preventing basophil degranulation and mast cell, lowering cytokine production, and controlling intracellular calcium concentration are just a few of the mechanisms that active substances of aquatic-derived have been found to use to release aversions (Wang K. et al., 2020).

### 5.8 Anti-microbial activity

In contrast to vertebrates, marine invertebrates lack adaptive immunity. Bivalves only exhibit the innate response to create defense mechanism against viruses and microorganisms, in order to adapt their frequently changing environment. Their susceptibility to infections is also enhanced by their filtering action (Nam et al., 2015). The sequence of antimicrobial peptides (AMPs) which range in length from 12 to 50 amino acids, is short, cationic, and amphipathic. They serve as the primary line of defense against diseases in both plants and animals (Cunha and

Pintado, 2021) (Semreen et al., 2018) (Costa et al., 2017). Antimicrobial peptides are often divided into four different classes based on the makeup of their amino acid sequence: (A) Linear basic peptides devoid of cysteine residues and with amphipathic  $\alpha$ -helices; (B) AMPs containing intramolecular disulfide linkages and cysteine residues; (C) AMPs with an excess of proline, arginine, glycine, or tryptophan, (D) antimicrobial Peptides generated by hydrolysate of huge amounts of inert protein (Cheng-Hua, Jian-Min, & Lin-Sheng, 2009). In this taxonomic arrangement, AMPs are typically defined in terms of hydrophobic and cationic amino acid groups (Silva, Sarmiento, & Pintado, 2013). In contrast to other bivalves, such as clams and oysters, mussels are less susceptible to infectious and inflammatory parasites, suggesting that these organisms have stronger defenses. (Novoa et al., 2016). Numerous studies show the antimicrobial action of peptides found in mussels, and it has been found that mussels are the primary source of the majority of marine antimicrobial peptides. Seven groups of marine mussel AMPs have been identified: large defensin, myticusin, myticins, mytilins, and mytimycin (Qin et al., 2014). Antibacterial properties of myticalins were established against both Gram-negative and Gram-positive microbes (Leoni et al., 2017). It also include that the isolation of defensins from *Crassostrea gigas* and *Haliotis discus* (Cunha, S. A., & Pintado, M. E., 2022)(De Zoysa et al., 2010). The hemolymph and hemoglobin of mussels contain a number of antimicrobial peptides that have been identified. Myticin C peptides from the mediterranean mussel *Mytilus galloprovincialis* have shown their antiviral attack against one ostreid herpesvirus (OsHV-1). A modified myticin-derived peptide that are nano encapsulated displayed in vitro antibacterial activity against HSV-1 and HSV-2 human herpes virus (Novoa et al., 2016). Both myticusin-1, and mytichitin-CB, are able to suppress the Gram-positive bacteria *Sarcina luteus*, *Staphylococcus*, *Bacillus subtilis*, and *Megaterium Bacillus* with MICs less than 5 mm, these compounds were isolated from the *Mytilus coruscus* (Liao et al., 2013) (Qin et al., 2014). These peptides did not have promising results against Gram-negative bacteria. Two types of yeast *Candida albicans* and *Monilia albicans* were also examined, and both showed potential at concentrations above 5 mm (Liao et al., 2013; Qin et al., 2014). According to a literature review, peptides extracted from mollusks show antibacterial efficacy against both Gram-negative and Gram-positive bacteria. Gram-positive bacteria had MECs ranging from 0.8 to 31.3 g/mL, whereas Gram-negative bacteria had MECs between 0.4 and 15.0 g/mL. Several other research found on algae AMPs demonstrated action against *E. coli*, *S. aureus*, and MRSA (Guzman'et al.,

2019; Jiao et al., 2019; Sedighi, Jalili, Ranaei-Siadat, & Amrane, 2016). Despite recent research shown promising findings anti-*S. aureus*, anti-*E. coli*, and anti-MRSA, algal peptides are not frequently investigated for their antimicrobial capabilities (Guzman et al., 2019). This demonstrates that algae could also be a potential source of AMPs. Therefore, it would have been highly beneficial to investigate this characteristic in algae in order to determine and test new AMPs for possible industrial uses. *Euphausia superba*, a kind of crustacean, has an AMP that can prevent *S. aureus* with a MIC of 5 mg/mL (Zhao, Yin, Liu, & Cao, 2013).

#### Mechanism:

The capacity of AMPs to bind to lipopolysaccharides (LPS) can produce gaps in microbial membranes, which results in cell death. In contrast, AMPs may be unable to cross membranes, in this case, they can hinder essential cellular functions once they have passed the helix (Semreen et al., 2018). AMPs tend to act in the cell membrane, however they can sometimes act inside cells (for instance, DNA/RNA, protein targets, mitochondria, or protein synthesis,). The danger of genetic variations and resistance to bacteria must be considered when specific targets are presumed (Bechinger & Gorr, 2017).

#### 5.9 Applications in pharmacology and nutraceuticals

The antihypertensive, antithrombotic, antimicrobial, and antioxidant characteristics of peptides may aid in the treatment or prevention of diseases. Many of the current studies are in vitro-based. However, several marine-derived peptides are increasingly being introduced into clinical practices. Therefore, in vivo testing is required to determine the efficacy of peptides before moving further with their use as nutraceuticals and medications. For instance, antihypertensive peptides are being extracted from a variety of marine sources, but additional in-vivo experiments and studies on pharmacokinetics are required to validate their effectiveness in lowering blood pressure (Chen et al., 2020). Due to their diverse bioactivities, several isolated peptides; one example is the BCP-A peptide (Trp-Pro-Pro, MW = 398.44 Da), which was extracted from the muscle of *Tegillarca granulosa*, may also be intriguing for a broader activity. BCP-A demonstrated DPPH, O<sub>2</sub>, OH, and ABTS+ show greater radical scavenging activity as well as the capacity to suppress lipid peroxidation. Due to its cytotoxicity in contradiction of the HeLa cell lines and DU-145, PC-3, H.1299, this peptide also shows a dose-dependent anticancer effect. These results suggest that this peptide may be significant for the pharmaceutical sector, both in terms of reducing excessive ROS and in terms of cancer



treatment (Chi, Hu, Wang, Li, & Ding, 2015). Since type II diabetes is a major concern worldwide, peptides with anti-diabetic action may have potential as nutraceuticals if it can be demonstrated that they sustain their function. However, several Peptides obtained from the marine are increasingly being examined in clinical studies (Ketnawa, Suwal, Huang, & Liceaga, 2019). Furthermore, very few of these peptides have been authorized by the FDA due to a lack of high-quality research (Rivero-Pino et al., 2020a). To introduce nutraceuticals with anti-diabetic qualities, more research is therefore required.

**5.10 Cosmetic industry applications**

Peptides with antioxidant properties might be very useful for cosmetics. Oxidative are one of the leading causes of skin age, thus they can be used to prevent cutaneous illnesses and age spots (Kammeyer & Luiten, 2015). Some wrinkles and hair care cosmetics, including

shampoo, body lotion, hair coloring hair restorers, agents, cleansers, and others, may comprise polypeptides derived from specific microalgae (Ariede et al., 2017). Besides anti-aging experimental animals such caenorhabditis elegans and drosophila melanogaster, marine species' proteins, carbohydrates, pigments, flavonoids, fatty acids, and phenols were utilized to illustrate their mechanism and action. Amino acids like mycosporine were found in marine, microalgae, macroalgae, bacteria, and molds, where they could absorb ultraviolet light after being reformed by amino acids and cyclohexenone (Wang X. et al., 2021).

**Fig 2.** Explains the advantages of microalgae peptides from processing to chromatographic techniques and in silico analysis. It also shows how microalgae peptides can be useful for cosmetical applications as well as good for human health.

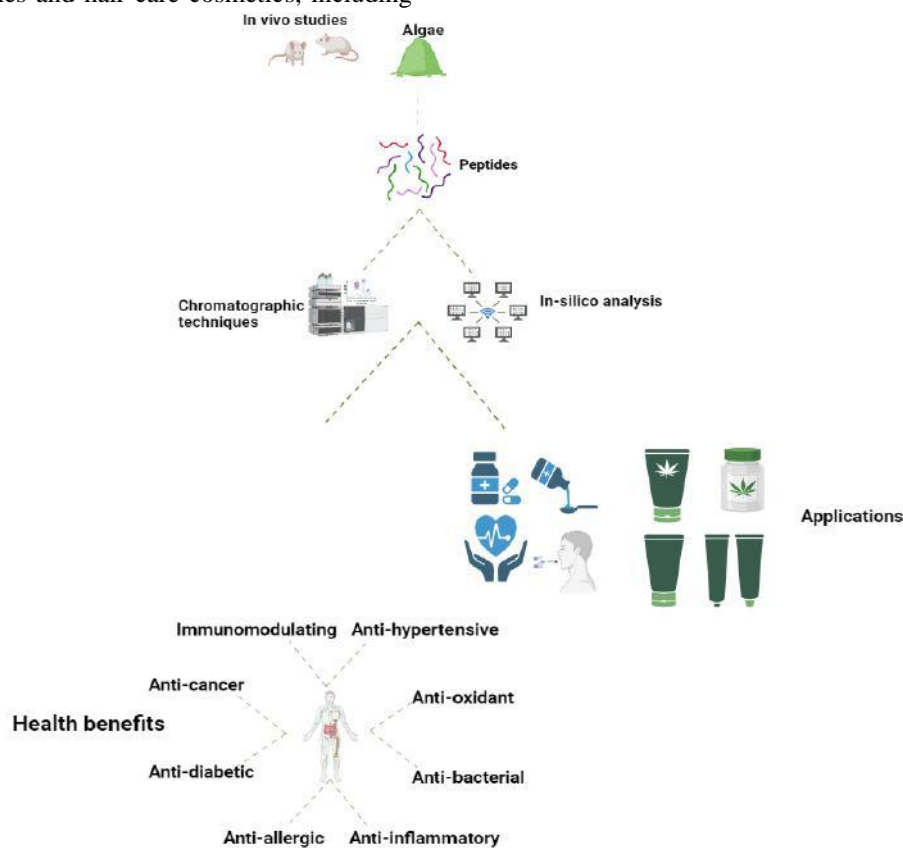


Fig 2: Applications of bioactive peptides

**VI. FDA-APPROVED MBPs AND CLINICAL TRIALS**

Many MBPs have obtained FDA approval due to their distinctive structural and multifunctional characteristics, which have already been described by a wide verity of bioactivities, including antimicrobial (antifungal and antibacterial), antiviral, antioxidant,

anticancer, anticoagulant, antithrombotic, antihypertensive, cholesterol-lowering and immunomodulatory and activities. the products on the market. In order to create MBP-based products that are suitable for medical, nutraceutical, and pharmaceutical uses a special mix of pristine counterparts and compositional alternation was used. Diverse materials and

techniques have been used for extractions, modifications, and purifications for several BPs from marine resources. However, a very small percentage of these bioactive peptides have already been approved for experimental phase evaluation, and indeed fewer have made it access to market. FDA-approved marine bioactive peptides are summarized to avoid redundancy in the literature (**Table. 3**). Many other biologically active substances and products

Table 2: Food and Drug Administration-approved MBPs.

Name of Compound	Chemical Formula	Molecular Mass	CAS Number	Source	Derivatives	Legal Presence	Availability	Half-life Elimination	Application
(intrathecal - ziconotide) Ziconotide	C102H172N36O32 S7	2639.14 (g/mol)	1074 52-89-1	Spiral Snail	Organic Substance	Prescription only	50%	2.9 to 6.6 h	Analgesics
(Brentuximab vedotin) Adcetris	C6476H9930N169 O02030S40	149.2–151.8 (kg/mol)	9140 88-09-8	Dolabella auricularia	Derivative	Prescription only	50–80%	Approximately 4 to 6 days	Cancer therapy, specifically for those suffering from cutaneous T-cell lymphoma
Bacitracin (Baciim)	C66H103N17O16S	1422.71 (g/mol)	1405 -87-4	A. subtilis (Bacillus)	Organic Substance	Only-Prescription for injection and OTC	unavailable	Not Available	Localized skin diseases, both acute and chronic
(Avodart) Dutasteride	C27H30F6N2O2	528.539 (g/mol)	1646 56-23-9		Synthetic	Only-Prescription	60%	5 Weeks	Hormone therapy for enlarged prostate and prostate cancer
A Curacin	C23H35NOS	373.60 (g/mol)	1552 33-30-0	A majuscula Lyngbya	Organic Substance	unavailable	unavailable	unavailable	treatment for Cancer
Eribulin (Halaven)	C40H59NO11	729.908 (g/mol)	2531 28-41-5	Sponge		Only-Prescription	unavailable	40 h	treatment for Cancer
(Yondelis) Trabectedin	C39H43N3O11S	761.84 (g/mol)	1148 99-77-3	Tunicate		Only-Prescription	unavailable	181 h	Chemotherapy drugs used to treat advanced cases of ovarian cancer and

with aquatic origins, such as *Hemiasterlin*, *Salinosporamide F*, *Pliditepsin*, *Spisulosine*, *Tetrodotoxin*, *PM00104 Plinabulin*, *Conotoxin G, A*, *Kahalalide*, *Bryostatin 1*, and, *Pseudopterosin A* are currently undergoing clinical trials (phases I–III) (Alves et al., 2018; Anjum et al., 2017; Ghareeb et al., 2020; Ucak et al., 2021; Zhang et al., 2021).

Dactinomy cin	C62H86N12O16	1255.438 (g/mol)	50- 76-0	parvul lus	Derivat ive	Only- Prescri ption	unavail able	37 h	soft-tissue sarcoma  Treatment for several types of cancer, such as GTN, WT1, RMS, RMS, and Ewing's sarcoma,
------------------	--------------	---------------------	-------------	---------------	----------------	---------------------------	-----------------	------	---

### 6.1 Clinical trials phase II drugs derived from marine sources

*Pseudopterosin H* was found from aquatic coral *Pseudoptero- gorgia elisabethae*. The medicinal efficiency of *pseudopterosin H* PC-3 cell line at varied proportions was evaluated in vitro utilizing the LDH, NBT and MTT tests, and also AO/EB fluorescence. As a result of causing apoptotic cell death and decreasing production of reactive oxygen species, *Pseudopterosin H* therapy decreases PC-3 cell proliferation, according to the outcomes. The PC-3 cells' chemosensitivity to *Pseudopterosin H* medication suggests that it may be used to treat and prevent metastatic castration-resistance the prostate cancer. PsH decreases PC-3 cell growth by inducing apoptosis and decreasing ROS levels. In order to reduce ROS, PsH may either simultaneously affect enzymes that promote oxidation or indirectly disrupt the pro-inflammatory mechanism, NF. Pharmacological features of PsH may effectively treat prostate cancer (Karthikeyan et al. 2022) (Bowers et al., 2021). Marine-derived bryostatin 1 exhibited procognitive and anti - depressive effects in animals and is being examined in humans for Alzheimer's disease (AD). Because of how well it improves retention of information, has been linked to the effects of bryostatin 1 on the structure and operation of hippocampal neurons. According to Calvin et al., bryostatin 1 encourages cortical synaptogenesis employing a variety of biochemical markers and pharmacologic antagonists and able to decrease dendritic spine density in a protein kinase C (PKC)-dependent approach. A unique pharmaceutical strategy for increasing memory by improving the signal-to-noise ratio in the nervous system may involve substances that improve synaptic density while also inducing the breakdown of immature dendritic spines brain (Ly et al., 2020). In both cell lines, calyculin-A boosted PP2A Y307 phosphorylation without reducing oral cancer cell growth. The available findings suggested that elevated p-PP2A expression caused by aberrant mechanisms may increase the proliferation of OSCC. The cell cycle, metabolism, migration, and viability are all directed by cell cycle

regulation in which PP2A plays an important role. Calyculin-A therapy was known to increase GSK-3 $\beta$  (Ser9) and AKT (Ser 473) cancer cell phosphorylation, indicating PP2A inactivation. The results indicate that CLA reduced GSK-3 $\beta$  expression through disabling PP2A. (Velmurugan et al., 2018).

### 6.2 Phase III clinical trials drugs derived from marine sources

Cyclic depsipeptide plitidepsin is generated from the aquatic tunicate *albicans apidium* that is chemically associated with didemnins, most of which possess antiviral properties. (Karthikeyan, A., Joseph, A., & Nair, B. G. (2022). In vitro models of SARSCoV-2 infection, plitidepsin performed better than other medicines, due to its strong antiviral efficacy and favorable therapeutic index such as remdesivir, in preclinical studies. Remarkably, plitidepsin has a significant in vitro antimicrobial activities effect on the SARS-CoV-2 B.1.1.7 diversity, which is known to contain several mutations that change the viral spike protein, which facilitates virus infection by associating in conjunction with the human ACE2 receptors (Reuschl et al., 2021). A neurotoxin called tetrodotoxin (TTX) is largely found in the puffer fish and other aquatic and the terrestrial animals. Voltage-gated Sodium channels that are obstructed by TTX (VGSCs). Many TTX-sensitive VGSCs are extremely expressed by major neuronal pathways and are important in the signaling of pain. Clinical trials are currently testing TTX for neuropathic pain brought on by radiotherapy and pain associated with cancer. The effectiveness and favorable safety profile of tetrodotoxin in treating pain brought on by neuropathies or cancer have been explored in both clinical and preclinical settings (González-Cano et al., 2021).

## VII. FUTURE INDUSTRIAL APPLICATION

It is fascinating to learn about the research on marine peptides and the various important activities that have been discovered so far. It seems like there is still much untapped potential framework to be explored and

developed. Due to their abundance, efficiency of production, large biomass, protein content, and algae may be one of the most intriguing bioactive peptides from marine sources. Indeed, while considering the production range, it is comparatively simpler to acquire a greater quantity of proteins from microalgae in comparison to more prevalent crops like wheat and soybean. The identification of numerous advantageous peptides derived from algae serves to underscore their considerable opportunities for industrial exploitation. Beside this, a significant challenge in the synthesis of peptides from microalgae is reported fluctuations in protein contents, which are influenced by factors that include changes in the seasons, variations in temperature, and the specific site of algae growth. Therefore, the quantity of peptides that may be separated may vary if the protein content changes. A cyanobacterium known as spirulina has also been investigated as a source of marine bioactive organisms, with bioactivities including antibacterial, antihypertensive, and antiallergic, described. All essential amino acid is present in spirulina, which has a high protein concentration (53-62 percent of its dry weight). Compared to other species, this marine species' bioactive peptides have received fewer investigations than those of other species. Therefore, Spirulina could be a fascinating and potential marine source for bioactive peptide production. Marine seaweed is a promising and relatively unexplored novel compound for usage in functional products and nutraceuticals, such as carbohydrates and bioactive peptides. Because they are more readily available and have less side effects than chemical-based produced formulations, natural marine-derived bioactive compounds should be preferred. The use of marine organisms for the manufacture of biologically active peptides may promote significant contributions and could also represent economic benefits. The most significant future challenge will be integrating bioactive components into human health and nutrition, as the majority of research remains in vivo models because of time and expense constraints. In the coming years, study should be conducted on the enhancement of beneficial marine foods so that, their regular incorporation into the human diet may reduce the occurrence and severity of different diseases. Focus on ensuring the upcoming economic growth of marine natural organism's health and their specialty to innovative pharmaceutical agents, that can significantly contribute in order to the treatment of human pathological conditions, risk reduction of chronic disease, medical cost savings, new advancements, and effective connections between academic knowledge and manufacturing sectors will be required. For the development of new medications in the upcoming years, more details on bioactive peptides derived

from marine origins is essential. A maximum degree of inventions in the area of seaweeds will lead to the development and successful innovation of marine nutraceuticals, providing us with the cause to expect that marine natural organisms will constitute a rising with the passage of time.

## VIII. CONCLUSION

This review examined the potential of marine-derived bioactive peptides from various sources, highlighting their features and possible therapeutic applications in pharmaceutical, food, nutraceutical, and cosmetic industries. To further understand peptide uses, we also explored bioavailability and toxicity. Additionally, purifying methods have improved in recent years and numerous ways have been discovered and enhanced. As expenses continue to rise, they are still limited by their poor yield. The use of marine organisms for the creation of bioactive peptides may potentially lead to significant financial benefits because the marine ecology includes around half of the world's biodiversity, and there is a large amount of waste associated with marine exploration. There are significant resources of biologically active compounds that promotes drug discovery. The functionality of marine natural substances as pharmacological pathways is dependent on technological advancements such as sequencing techniques, nanotechnology, NMR for structural analysis, total medicinal chemistry, genetic modification, and biosynthesis.

## REFERENCES

- [1] Al-Khayri, J. M., Asghar, W., Khan, S., Akhtar, A., Ayub, H., Khalid, N., ... & Shehata, W. F. (2022). Therapeutic Potential of Marine Bioactive Peptides against Human Immunodeficiency Virus: Recent Evidence, Challenges, and Future Trends. *Marine Drugs*, 20(8), 477.
- [2] Agrawal, S., Adholeya, A., & Deshmukh, S. K. (2016). The pharmacological potential of nonribosomal peptides from marine sponge and tunicates. *Frontiers in pharmacology*, 7, 333.
- [3] Ambrosio, A. L., Sanz, L., Sánchez, E. I., Wolfenstein-Todel, C., & Calvete, J. J. (2003). Isolation of two novel mannan-and L-fucose-binding lectins from the green alga *Enteromorpha prolifera*: biochemical characterization of EPL-2. *Archives of biochemistry and biophysics*, 415(2), 245-250.
- [4] Aneiros, A., & Garateix, A. (2004). Bioactive peptides from marine sources: pharmacological properties and isolation procedures. *Journal of Chromatography B*, 803(1), 41-53.
- [5] Anjum, K., Abbas, S. Q., Shah, S. A., Akhter, N., Batool, S., & ul Hassan, S. S. (2016). Erratum to "Marine Sponges

- as a Drug Treasure”[Biomol. Ther. 24 (2016) 347–362]. *Biomolecules & Therapeutics*, 24(5), 559.
- [6] Barre, A., Simplicien, M., Benoist, H., Van Damme, E. J., & Rougé, P. (2019). Mannose-specific lectins from marine algae: diverse structural scaffolds associated to common virucidal and anticancer properties. *Marine drugs*, 17(8), 440.
- [7] Beppu, F., Niwano, Y., Tsukui, T., Hosokawa, M., & Miyashita, K. (2009). Single and repeated oral dose toxicity study of fucoxanthin (FX), a marine carotenoid, in mice. *The Journal of toxicological sciences*, 34(5), 501-510.
- [8] Berteau, O., & Mulloy, B. (2003). Sulfated fucans, fresh perspectives: structures, functions, and biological properties of sulfated fucans and an overview of enzymes active toward this class of polysaccharide. *Glycobiology*, 13(6), 29R-40R.
- [9] Brinkman, D. L., Aziz, A., Loukas, A., Potriquet, J., Seymour, J., & Mulvenna, J. (2012). Venom proteome of the box jellyfish *Chironex fleckeri*. *PLoS one*, 7(12), e47866.
- [10] Chakraborty, K., and Joy, M. (2020). High-value compounds from the molluscs of marine and estuarine ecosystems as prospective functional food ingredients: an overview. *Food Res. Int.* 137:109637.
- [11] Charoensiddhi, S., Conlon, M. A., Franco, C. M., & Zhang, W. (2017). The development of seaweed-derived bioactive compounds for use as prebiotics and nutraceuticals using enzyme technologies. *Trends in Food Science & Technology*, 70, 20-33.
- [12] D’Orazio, N., Gammone, M. A., Gemello, E., De Girolamo, M., Cusenza, S., & Riccioni, G. (2012). Marine bioactives: Pharmacological properties and potential applications against inflammatory diseases. *Marine drugs*, 10(4), 812-833.
- [13] Da Costa, J. P., Cova, M., Ferreira, R., & Vitorino, R. (2015). Antimicrobial peptides: an alternative for innovative medicines?. *Applied microbiology and biotechnology*, 99, 2023-2040.
- [14] Datta, D., Talapatra, S. N., & Swarnakar, S. (2015). Bioactive compounds from marine invertebrates for potential medicines-an overview. *International Letters of Natural Sciences*, (07).
- [15] Dembitsky, V. M., & Maoka, T. (2007). Allenic and cumulenilic lipids. *Progress in lipid research*, 46(6), 328-375.
- [16] Elbandy, M.; Shinde, P.B.; Hong, J.; Bae, K.S.; Kim, M.A.; Lee, S.M.; Jung, J.H.  $\alpha$ -pyrones and yellow pigments from the sponge-derived fungus *paecilomyces lilacinus*. *Bull. Korean Chem. Soc.* 2009, 30, 188–192.
- [17] Ellis, A., & Bennett, D. L. H. (2013). Neuroinflammation and the generation of neuropathic pain. *British journal of anaesthesia*, 111(1), 26-37.
- [18] Evans, R. P., & Fletcher, G. L. (2004). Isolation and purification of antifreeze proteins from skin tissues of snailfish, cunner and sea raven. *Biochimica et Biophysica Acta (BBA)-Proteins and Proteomics*, 1700(2), 209-217.
- [19] Fidor, A., Konkel, R., & Mazur-Marzec, H. (2019). Bioactive peptides produced by cyanobacteria of the genus *Nostoc*: A review. *Marine drugs*, 17(10), 561.
- [20] Fontenelle, T. P. C., Lima, G. C., Mesquita, J. X., de Souza Lopes, J. L., de Brito, T. V., Júnior, F. D. C. V., ... & Freitas, A. L. P. (2018). Lectin obtained from the red seaweed *Bryothamnion triquetrum*: Secondary structure and anti-inflammatory activity in mice. *International journal of biological macromolecules*, 112, 1122-1130.
- [21] Frenkel, J., Vyverman, W., & Pohnert, G. (2014). Pheromone signaling during sexual reproduction in algae. *The plant journal*, 79(4), 632-644.
- [22] Galasso, C., Corinaldesi, C., & Sansone, C. (2017). Carotenoids from marine organisms: Biological functions and industrial applications. *Antioxidants*, 6(4), 96.
- [23] Gallego, R., Bueno, M., and Herrero, M. (2019). Sub- and supercritical fluid extraction of bioactive compounds from plants, food-by-products, seaweeds and microalgae – an update. *TrAC-Trends Anal. Chem.* 116, 198–213.
- [24] Gammone, M. A., Riccioni, G., & D’Orazio, N. (2015). Marine carotenoids against oxidative stress: effects on human health. *Marine Drugs*, 13(10), 6226-6246.
- [25] Ganesan, A. R., Mohanram, M. S. G., Balasubramanian, B., Ho Kim, I., Seedeivi, P., Mohan, K., et al. (2020a). Marine invertebrates’ proteins: a recent update on functional property. *J. King Saud Univ. Sci.* 32, 1496–1502. doi: 10.1016/j.jksus.2019.12.003
- [26] Ganesan, A. R., Saravana Guru, M., Balasubramanian, B., Mohan, K., Chao Liu, W., Valan Arasu, M., et al. (2020b). Biopolymer from edible marine invertebrates: a potential functional food. *J. King Saud Univ. Sci.* 32, 1772–1777. doi: 10.1016/j.jksus.2020.01.015
- [27] Günaydin, G., Edfeldt, G., Garber, D. A., Asghar, M., Noël-Romas, L., Burgener, A., ... & Broliden, K. (2019). Impact of Q-Griffithsin anti-HIV microbicide gel in non-human primates: In situ analyses of epithelial and immune cell markers in rectal mucosa. *Scientific reports*, 9(1), 18120.
- [28] Gupta, S., & Abu-Ghannam, N. (2011). Bioactive potential and possible health effects of edible brown seaweeds. *Trends in Food Science & Technology*, 22(6), 315-326.
- [29] Haefner, B. (2003). Drugs from the deep: marine natural products as drug candidates. *Drug discovery today*, 8(12), 536-544.
- [30] Holdt, S. L., & Kraan, S. (2011). Bioactive compounds in seaweed: functional food applications and legislation. *Journal of applied phycology*, 23, 543-597.
- [31] Iijima, N., Tanimoto, N., Emoto, Y., Morita, Y., Uematsu, K., Murakami, T., & Nakai, T. (2003). Purification and characterization of three isoforms of chrysopsin, a novel antimicrobial peptide in the gills of the red sea bream, *Chrysophrys major*. *European Journal of Biochemistry*, 270(4), 675-686.
- [32] Jheng, Y. H., Lee, L. H., Ting, C. H., Pan, C. Y., Hui, C. F., & Chen, J. Y. (2015). Zebrafish fed on recombinant *Artemia* expressing epinecidin-1 exhibit increased survival and altered expression of immunomodulatory genes upon *Vibrio vulnificus* infection. *Fish & Shellfish Immunology*, 42(1), 1-15.

- [33] Jiao, G., Yu, G., Zhang, J., & Ewart, H. S. (2011). Chemical structures and bioactivities of sulfated polysaccharides from marine algae. *Marine drugs*, 9(2), 196-223.
- [34] John, B. A., Nelson, B. R., Sheikh, H. I., Cheung, S. G., Wardiatno, Y., Dash, B. P., ... & Pati, S. (2018). A review on fisheries and conservation status of Asian horseshoe crabs. *Biodiversity and conservation*, 27, 3573-3598.
- [35] Kang, H. K., Choi, M. C., Seo, C. H., & Park, Y. (2018). Therapeutic properties and biological benefits of marine-derived anticancer peptides. *International journal of molecular sciences*, 19(3), 919.
- [36] Kang, H. K., Seo, C. H., & Park, Y. (2015). Marine peptides and their anti-infective activities. *Marine drugs*, 13(1), 618-654.
- [37] Kannan, A., Hettiarachchy, N. S., Lay, J. O., & Liyanage, R. (2010). Human cancer cell proliferation inhibition by a pentapeptide isolated and characterized from rice bran. *Peptides*, 31(9), 1629-1634.
- [38] Kim, E. K., Joung, H. J., Kim, Y. S., Hwang, J. W., Ahn, C. B., Jeon, Y. J., ... & Park, P. J. (2012). Purification of a novel anticancer peptide from enzymatic hydrolysate of *Mytilus coruscus*. *Journal of microbiology and biotechnology*, 22(10), 1381-1387.
- [39] Koyande, A. K., Chew, K. W., Manickam, S., Chang, J. S., and Show, P. L. (2021). Emerging algal nanotechnology for high-value compounds: a direction to future food production. *Trends Food Sci. Technol.* 116, 290–302.
- [40] Lazcano-Pérez, F., A Roman-Gonzalez, S., Sánchez-Puig, N., & Arreguin-Espinosa, R. (2012). Bioactive peptides from marine organisms: A short overview. *Protein and Peptide Letters*, 19(7), 700-707.
- [41] Lee, A., Shin, H. Y., Park, J. H., Koo, S. Y., Kim, S. M., & Yang, S. H. (2021). Fucoxanthin from microalgae *Phaeodactylum tricornutum* inhibits pro-inflammatory cytokines by regulating both NF- $\kappa$ B and NLRP3 inflammasome activation. *Scientific reports*, 11(1), 1-12.
- [42] Li, J., Gong, C., Wang, Z., Gao, R., Ren, J., Zhou, X., ... & Zhao, Y. (2019). Oyster-derived zinc-binding peptide modified by plastein reaction via zinc chelation promotes the intestinal absorption of zinc. *Marine drugs*, 17(6), 341.
- [43] Li, J., Liu, Z., Zhao, Y., Zhu, X., Yu, R., Dong, S., & Wu, H. (2018). Novel natural angiotensin converting enzyme (ACE)-inhibitory peptides derived from sea cucumber-modified hydrolysates by adding exogenous proline and a study of their structure–activity relationship. *Marine Drugs*, 16(8), 271.
- [44] Low, W. K., Lin, Q., Stathakis, C., Miao, M., Fletcher, G. L., & Hew, C. L. (2001). Isolation and characterization of skin-type, type I antifreeze polypeptides from the longhorn sculpin, *Myoxocephalus octodecemspinosus*. *Journal of Biological Chemistry*, 276(15), 11582-11589.
- [45] Lee, S. H., Qian, Z. J., & Kim, S. K. (2010). A novel angiotensin I converting enzyme inhibitory peptide from tuna frame protein hydrolysate and its antihypertensive effect in spontaneously hypertensive rats. *Food Chemistry*, 118(1), 96-102.
- [46] Marqus, S., Pirogova, E., & Piva, T. J. (2017). Evaluation of the use of therapeutic peptides for cancer treatment. *Journal of biomedical science*, 24(1), 1-15.
- [47] Neves, J. L., Imperial, J. S., Morgenstern, D., Ueberheide, B., Gajewiak, J., Antunes, A., ... & Olivera, B. M. (2019). Characterization of the first conotoxin from *Conus ateralbus*, a vermivorous cone snail from the Cabo Verde archipelago. *Marine drugs*, 17(8), 432.
- [48] Noguchi, T., Kato, T., Wang, L., Maeda, Y., Ikeda, H., Sato, E., ... & Nishikawa, H. (2012). Intracellular tumor-associated antigens represent effective targets for passive immunotherapy. *Cancer research*, 72(7), 1672-1682.
- [49] Ovchinnikova, T. V. (2019). Structure, function, and therapeutic potential of marine bioactive peptides. *Marine drugs*, 17(9), 505.
- [50] Papon, N., Copp, B. R., & Courdavault, V. (2022). Marine drugs: Biology, pipelines, current and future prospects for production. *Biotechnology Advances*, 54, 107871.
- [51] Peng, J., Yuan, J. P., Wu, C. F., & Wang, J. H. (2011). Fucoxanthin, a marine carotenoid present in brown seaweeds and diatoms: metabolism and bioactivities relevant to human health. *Marine drugs*, 9(10), 1806-1828.
- [52] Pomin, V. H. (2009). An overview about the structure–function relationship of marine sulfated homopolysaccharides with regular chemical structures. *Biopolymers: Original Research on Biomolecules*, 91(8), 601-609.
- [53] Prabha, S. P., Nagappan, S., Rathna, R., Viveka, R., & Nakkeeran, E. (2020). Blue biotechnology: a vision for future marine biorefineries. In *Refining Biomass Residues for Sustainable Energy and Bioproducts* (pp. 463-480). Academic Press.
- [54] Qin, C. L., Huang, W., Zhou, S. Q., Wang, X. C., Liu, H. H., Fan, M. H., ... & Liao, Z. (2014). Characterization of a novel antimicrobial peptide with chitin-binding domain from *Mytilus coruscus*. *Fish & shellfish immunology*, 41(2), 362-370.
- [55] Rameshkumar, G., Aravindhan, T., & Ravichandran, S. (2009). Antimicrobial proteins from the crab *Charybdis lucifera* (Fabricius, 1798). *Middle-East Journal of Scientific Research*, 4(1), 4043.
- [56] Rameshkumar, G., Ravichandran, S., Kaliyavarathan, G., & Ajithkumar, T. T. (2009). Antimicrobial peptide from the crab, *Thalamita crenata* (Latreille, 1829). *World J Fish Mar Sci*, 1(2), 74-79.
- [57] Rosic, N. N. (2021). Recent advances in the discovery of novel marine natural products and mycosporine-like amino acid UV-absorbing compounds. *Applied Microbiology and Biotechnology*, 105, 7053-7067.
- [58] Shahidi, F., and Ambigaipalan, P. (2015). Novel functional food ingredients from marine sources. *Curr. Opin. Food Sci.* 2, 123–129.
- [59] Shenkarev, Z. O., Pantelev, P. V., Balandin, S. V., Gizatullina, A. K., Altukhov, D. A., Finkina, E. I., ... & Ovchinnikova, T. V. (2012). Recombinant expression and solution structure of antimicrobial peptide aurelin from jellyfish *Aurelia aurita*. *Biochemical and biophysical research communications*, 429(1-2), 63-69.

- [60] Silipo, A., Molinaro, A., Molteni, M., Rossetti, C., Parrilli, M., & Lanzetta, R. (2010). Full structural characterization of an extracellular polysaccharide produced by the freshwater cyanobacterium *oscillatoria planktothrix* fp1.
- [61] Stensvåg, K., Haug, T., Sperstad, S. V., Rekdal, Ø., Indrevoll, B., & Styrvold, O. B. (2008). Arasin 1, a proline-arginine-rich antimicrobial peptide isolated from the spider crab, *Hyas araneus*. *Developmental & Comparative Immunology*, 32(3), 275-285.
- [62] Synytsya, A., Kim, W. J., Kim, S. M., Pohl, R., Synytsya, A., Kvasnička, F., ... & Park, Y. I. (2010). Structure and antitumour activity of fucoidan isolated from sporophyll of Korean brown seaweed *Undaria pinnatifida*. *Carbohydrate polymers*, 81(1), 41-48.
- [63] Su, Y. (2011). Isolation and identification of pelteobagrin, a novel antimicrobial peptide from the skin mucus of yellow catfish (*Pelteobagrus fulvidraco*). *Comparative Biochemistry and Physiology Part B: Biochemistry and Molecular Biology*, 158(2), 149-154.
- [64] Thangam, R., Senthilkumar, D., Suresh, V., Sathuvan, M., Sivasubramanian, S., Pazhanichamy, K., ... & Sivaraman, J. (2014). Induction of ROS-dependent mitochondria-mediated intrinsic apoptosis in MDA-MB-231 cells by glycoprotein from *Codium decortatum*. *Journal of agricultural and food chemistry*, 62(15), 3410-3421.
- [65] Tincu, J. A., & Taylor, S. W. (2004). Antimicrobial peptides from marine invertebrates. *Antimicrobial agents and chemotherapy*, 48(10), 3645-3654.
- [66] Trang, N. T. H., Tang, D. Y. Y., Chew, K. W., Linh, N. T., Hoang, L. T., Cuong, N. T., et al. (2021). Discovery of  $\alpha$ -Glucosidase inhibitors from marine microorganisms: optimization of culture conditions and medium composition. *Mol. Biotechnol.* 63, 1004–1015.
- [68] Ulug, S. K., Jahandideh, F., & Wu, J. (2021). Novel technologies for the production of bioactive peptides. *Trends in Food Science & Technology*, 108, 27-39.
- [69] Van Damme, E. J., Culerrier, R., Barre, A., Alvarez, R., Rougé, P., & Peumans, W. J. (2007). A novel family of lectins evolutionarily related to class V chitinases: an example of neofunctionalization in legumes. *Plant physiology*, 144(2), 662-672.
- [70] Vitali, A. (2018). Antimicrobial peptides derived from marine sponges. *Am J Clin Microbiol Antimicrob.* 2018; 1(1), 1006.
- [71] Wang, X., Yu, H., Xing, R and Li, P. (2017). Characterization, Preparation, and Purification of Marine Bioactive Peptides: Hindawi BioMed Research International, 1-16.
- [72] Wijesekara, I., Lang, M., Marty, C., Gemin, M. P., Boulho, R., Douzenel, P., ... & Bourgoignon, N. (2017). Different extraction procedures and analysis of protein from *Ulva* sp. in Brittany, France. *Journal of applied phycology*, 29, 2503-2511.
- [73] Wijesekara, I., Pangestuti, R., & Kim, S. K. (2011). Biological activities and potential health benefits of sulfated polysaccharides derived from marine algae. *Carbohydrate polymers*, 84(1), 14-21.
- [74] Wu, M., Tong, C., Wu, Y., Liu, S., & Li, W. (2016). A novel thyroglobulin-binding lectin from the brown alga *Hizikia fusiformis* and its antioxidant activities. *Food chemistry*, 201, 7-13.
- [75] Wu, Q., Nay, B., Yang, M., Ni, Y., Wang, H., Yao, L., & Li, X. (2019). Marine sponges of the genus *Stelletta* as promising drug sources: Chemical and biological aspects. *Acta Pharmaceutica Sinica B*, 9(2), 237-257.
- [76] Yoshiie, T., Maeda, M., Kimura, M., Hama, Y., Uchida, M., & Kimura, Y. (2012). Structural features of N-glycans of seaweed glycoproteins: predominant occurrence of high-mannose type N-glycans in marine plants. *Bioscience, biotechnology, and biochemistry*, 76(10), 1996-1998.
- [77] Zaky, A. A., Simal-Gandara, J., Eun, J. B., Shim, J. H., & Abd El-Aty, A. M. (2022). Bioactivities, applications, safety, and health benefits of bioactive peptides from food and by-products: A review. *Frontiers in Nutrition*, 8, 815640.
- [78] Zhou, D. Y., Zhu, B. W., Qiao, L., Wu, H. T., Li, D. M., Yang, J. F., & Murata, Y. (2012). In vitro antioxidant activity of enzymatic hydrolysates prepared from abalone (*Haliotis discus hannai* Ino) viscera. *Food and Bioprocess Technology*, 90(2), 148-154.
- [79] Zhao, Y., Li, B., Dong, S., Liu, Z., Zhao, X., Wang, J., & Zeng, M. (2009). A novel ACE inhibitory peptide isolated from *Acaudina molpadioidea* hydrolysate. *Peptides*, 30(6), 10281033.
- [80] H.P. Makkar, G. Tran, V. Heuzé, S. Giger-Reverdin, M. Lessire, F. Lebas, P. Ankers, Seaweeds for livestock diets: a review, *Anim. Feed Sci. Technol.* 212 (2016) 1–17
- [81] S.L. Holdt, S. Kraan, Bioactive compounds in seaweed: functional food applications and legislation, *J. Appl. Phycol.* 23 (2011) 543–597.
- [82] S.O. Lourenço, E. Barbarino, J.C. De-Paula, L.O.d.S. Pereira, U.M.L. Marquez, Amino acid composition, protein content and calculation of nitrogen-to-protein conversion factors for 19 tropical seaweeds, *Phycol. Res.* 50 (2002) 233–241.
- [83] P. Schiener, K.D. Black, M.S. Stanley, D.H. Green, The seasonal variation in the chemical composition of the kelp species *Laminaria digitata*, *Laminaria hyperborea*, *Saccharina latissima* and *Alaria esculenta*, *J. Appl. Phycol.* 27 (2015) 363–373.
- [84] Peinado, J. Girón, G. Koutsidis, J. Ames, Chemical composition, antioxidant activity and sensory evaluation of five different species of brown edible seaweeds, *Food Res. Int.* 66 (2014) 36–44.
- [85] S. Arai, Functional food science in Japan: state of the art, *Biofactors* 12 (2000) 13–16.
- [86] H. Fukami, Functional foods and biotechnology in Japan, *Biotechnology in Functional Foods and Nutraceuticals*, 2010, p. 29.
- [87] L.A. Pham-Huy, H. He, C. Pham-Huy, Free radicals, antioxidants in disease and health, *International journal of biomedical science: IJBS* 4 (2008) 89.
- [88] C. Gorrini, I.S. Harris, T.W. Mak, Modulation of oxidative stress as an anticancer strategy, *Nat. Rev. Drug Discov.* 12 (2013) 931.

- [89] S.-J. Heo, E.-J. Park, K.-W. Lee, Y.-J. Jeon, Antioxidant activities of enzymatic extracts from brown seaweeds, *Bioresour. Technol.* 96 (2005) 1613–1623.
- [90] R.E. Cian, O. Martínez-Augustin, S.R. Drago, Bioactive properties of peptides obtained by enzymatic hydrolysis from protein byproducts of *Porphyra columbina*, *Food Res. Int.* 49 (2012) 364–372.
- [91] R.E. Cian, A.G. Garzón, D.B. Ancona, L.C. Guerrero, S.R. Drago, Hydrolyzates from *Pyropia columbina* seaweed have antiplatelet aggregation, antioxidant and ACE I inhibitory peptides which maintain bioactivity after simulated gastrointestinal digestion, *LWT-Food Science and Technology* 64 (2015) 881–888.
- [92] L. Smart, S. Gaisford, A. W. Basit, *Expert Opin. Drug Deliv.* 2014, 11, 1323.
- [93] Aneiros, A., & Garateix, A. (2004). Bioactive peptides from marine sources: pharmacological properties and isolation procedures. *Journal of Chromatography B*, 803(1), 41–53.
- [94] B. Wang, N. Xie, B. Li, *J. Food Biochem.* 2019, 43, 1.
- [95] J. S. Hamada, *J. Food Sci.* 2000, 65, 305.
- [96] N. H. Cho, J. E. Shaw, S. Karuranga, Y. Huang, J. D. da Rocha Fernandes, A. W. Ohlrogge, B. Malanda, *Diabetes Res. Clin. Pract.* 2018, 138, 271.
- [97] Suleria HAR, Gobe G, Masci P, Osborne SA (2016) Marine bioactive compounds and health promoting perspectives; innovation pathways for drug discovery. *Trends Food Sci Technol* 50:44–55
- [98] Igarashi Y, Iida T, Oku N, Watanabe H, Furihata K, Miyanouchi K (2012) Nomimicin, a new spirotetronate-class polyketide from an actinomycete of the genus *Actinomadura*. *J Antibiot (Tokyo)* 65:355–359
- [99] Lü Y, Shao M, Wang Y, Qian S, Wang M, Wang Y, Li X, Bao Y, Deng C, Yue C, Liu D, Liu N, Liu M, Huang Y, Chen Z, Hu Y (2017) Zunymycins B and C, New chloroanthrabenoxocinones antibiotics against methicillin-resistant *Staphylococcus aureus* and *Enterococci* from *Streptomyces* sp. FJS31-2. *Molecules (Basel, Switzerland)* 22:251
- [100] Qin Z, Munnoch JT, Devine R, Holmes NA, Seipke RF, Wilkinson KA, Wilkinson B, Hutchings MI (2017) Formicamycins, antibacterial polyketides produced by *Streptomyces formicae* isolated from African *Tetraponera* plant-ants. *Chem Sci* 8:3218–3227
- [101] Kim, Y. S., Ahn, C. B., & Je, J. Y. (2016). Anti-inflammatory action of high molecular weight *Mytilus edulis* hydrolysates fraction in LPS-induced RAW264.7 macrophage via NF- $\kappa$ B and MAPK pathways. *Food Chemistry*, 202, 9–14. <https://doi.org/10.1016/j.foodchem.2016.01.114>
- [102] Ahn, C. B., Cho, Y. S., & Je, J. Y. (2015). Purification and anti-inflammatory action of tripeptide from salmon pectoral fin byproduct protein hydrolysate. *Food Chemistry*, 168, 151–156. <https://doi.org/10.1016/j.foodchem.2014.05.112>
- [103] Kim, E. K., Hwang, J. W., Kim, Y. S., Ahn, C. B., Jeon, Y. J., Kweon, H. J., et al. (2013). A novel bioactive peptide derived from enzymatic hydrolysis of *Ruditapes philippinarum*: Purification and investigation of its free-radical quenching potential. *Process Biochemistry*, 48(2), 325–330. <https://doi.org/10.1016/j.procbio.2012.10.016>
- [104] Lee, S. J., Kim, E. K., Kim, Y. S., Hwang, J. W., Lee, K. H., Choi, D. K., et al. (2012). Purification and characterization of a nitric oxide inhibitory peptide from *Ruditapes philippinarum*. *Food and Chemical Toxicology*, 50(5), 1660–1666. <https://doi.org/10.1016/j.fct.2012.02.021>
- [105] Kim, E. K., Hwang, J. W., Kim, Y. S., Ahn, C. B., Jeon, Y. J., Kweon, H. J., et al. (2013). A novel bioactive peptide derived from enzymatic hydrolysis of *Ruditapes philippinarum*: Purification and investigation of its free-radical quenching potential. *Process Biochemistry*, 48(2), 325–330. <https://doi.org/10.1016/j.procbio.2012.10.016>
- [106] Hwang, J. W., Lee, S. J., Kim, Y. S., Kim, E. K., Ahn, C. B., Jeon, Y. J., et al. (2012). Purification and characterization of a novel peptide with inhibitory effects on colitis induced mice by dextran sulfate sodium from enzymatic hydrolysates of *Crassostrea gigas*. *Fish & Shellfish Immunology*, 33(4), 993–999. <https://doi.org/10.1016/j.fsi.2012.08.017>
- [107] Ahn, C. B., Cho, Y. S., & Je, J. Y. (2015). Purification and anti-inflammatory action of tripeptide from salmon pectoral fin byproduct protein hydrolysate. *Food Chemistry*, 168, 151–156. <https://doi.org/10.1016/j.foodchem.2014.05.112>
- [108] Cheung RC, Wong JH, Pan W, Chan YS, Yin C, Dan X, Ng TB (2015) Marine lectins and their medicinal applications. *Appl Microbiol Biotechnol* 99:3755–3773 48.
- [109] Da Conceicao Rivanor RL, Chaves HV, Do Val DR, De Freitas AR, Lemos JC, Rodrigues JA, Pereira KM, De Araujo IW, Bezerra MM, Benevides NM (2014) A lectin from the green seaweed *Caulerpa cupressoides* reduces mechanical hyper-nociception and inflammation in the rat temporomandibular joint during zymosan-induced arthritis. *Int Immunopharmacol* 21:34–43
- [110] Sheih, I. C., Fang, T. J., & Wu, T. K. (2009). Isolation and characterisation of a novel angiotensin I-converting enzyme (ACE) inhibitory peptide from the algae protein waste. *Food Chemistry*, 115(1), 279–284. <https://doi.org/10.1016/j.foodchem.2008.12.019>
- [111] Fitzgerald, C., Mora-Soler, L., Gallagher, E., O'Connor, P., Prieto, J., Soler-Vila, A., et al. (2012). Isolation and characterization of bioactive pro-peptides with in Vitro renin inhibitory activities from the macroalga *Palmaria palmata*. *Journal of Agricultural and Food Chemistry*, 60(30), 7421–7427. <https://doi.org/10.1021/jf301361c>
- [112] Cao, D., Lv, X., Xu, X., Yu, H., Sun, X., & Xu, N. (2017). Purification and identification of a novel ACE inhibitory peptide from marine alga *Gracilariopsis lemaneiformis* protein hydrolysate. *European Food Research and Technology*, 243(10), 1829–1837. <https://doi.org/10.1007/s00217-017-2886-2>
- [113] Samarakoon, K. W., O-Nam, K., Ko, J. Y., Lee, J. H., Kang, M. C., Kim, D., et al. (2013). Purification and identification of novel angiotensin-I converting enzyme (ACE) inhibitory peptides from cultured marine microalgae (*Nannochloropsis oculata*) protein hydrolysate. *Journal of*



- Applied Phycology, 25(5), 1595–1606. <https://doi.org/10.1007/s10811-013-9994-6>
- [114] Samaranayaka, A. G. P., Kitts, D. D., & Li-Chan, E. C. Y. (2010). Antioxidative and angiotensin-I-converting enzyme inhibitory potential of a pacific hake (merluccius productus) fish protein hydrolysate subjected to simulated gastrointestinal digestion and caco-2 cell permeation. *Journal of Agricultural and Food Chemistry*, 58(3), 1535–1542. <https://doi.org/10.1021/jf9033199>
- [115] Neves, A. C., Harnedy, P. A., & FitzGerald, R. J. (2016). Angiotensin converting enzyme and dipeptidyl peptidase-IV inhibitory, and antioxidant activities of a blue mussel (*Mytilus edulis*) meat protein extract and its hydrolysates. *Journal of Aquatic Food Product Technology*, 25(8), 1221–1233. <https://doi.org/10.1080/10498850.2015.1051259>
- [116] Chen, J., Tan, L., Li, C., Zhou, C., Hong, P., Sun, S., et al. (2020). Mechanism analysis of a novel angiotensin-I-converting enzyme inhibitory peptide from *isochrysis zhanjiangensis* microalgae for suppressing vascular injury in human umbilical vein endothelial cells. *Journal of Agricultural and Food Chemistry*, 68(15), 4411–4423. <https://doi.org/10.1021/acs.jafc.0c00925>
- [117] Sheih, I. C., Fang, T. J., & Wu, T. K. (2009). Isolation and characterisation of a novel angiotensin I-converting enzyme (ACE) inhibitory peptide from the algae protein waste. *Food Chemistry*, 115(1), 279–284. <https://doi.org/10.1016/j.foodchem.2008.12.019>
- [118] Deng, Z., Liu, Y., Wang, J., Wu, S., Geng, L., Sui, Z., et al. (2018). Antihypertensive effects of two novel angiotensin i-converting enzyme (ace) inhibitory peptides from *gracilariopsis lemaneiformis* (Rhodophyta) in spontaneously hypertensive rats (SHRs). *Marine Drugs*, 16(9). <https://doi.org/10.3390/md16090299>
- [119] Cunha, S. A., & Pintado, M. E. (2022). Bioactive peptides derived from marine sources: Biological and functional properties. *Trends in Food Science & Technology*, 119, 348–370.
- [120] Ko, S. C., Lee, D. S., Park, W. S., Yoo, J. S., Yim, M. J., Qian, Z. J., et al. (2016). Antiallergic effects of a nonameric peptide isolated from the intestine gastrointestinal digests of abalone (*Haliotis discus hannai*) in activated HMC-1 human mast cells. *International Journal of Molecular Medicine*, 37(1), 243–250. <https://doi.org/10.3892/ijmm.2015.2420>
- [121] Vo, T. S., Ngo, D. H., Kang, K. H., Park, S. J., & Kim, S. K. (2014). The role of peptides derived from *Spirulina maxima* in downregulation of FcεRI-mediated allergic responses. *Molecular Nutrition & Food Research*, 58(11), 2226–2234. <https://doi.org/10.1002/mnfr.201400329>
- [122] Vo, T. S., Ryu, B. M., & Kim, S. K. (2013). Purification of novel anti-inflammatory peptides from enzymatic hydrolysate of the edible microalgal *Spirulina maxima*. *Journal of Functional Foods*, 5(3), 1336–1346. <https://doi.org/10.1016/j.jff.2013.05.001>
- [123] Cheung, R. C. F., Ng, T. B., & Wong, J. H. (2015). Marine peptides: Bioactivities and applications. *Marine Drugs*, 13(7), 4006–4043. <https://doi.org/10.3390/md13074006>
- [124] Ko, S. C., Lee, D. S., Park, W. S., Yoo, J. S., Yim, M. J., Qian, Z. J., et al. (2016). Antiallergic effects of a nonameric peptide isolated from the intestine gastrointestinal digests of abalone (*Haliotis discus hannai*) in activated HMC-1 human mast cells. *International Journal of Molecular Medicine*, 37(1), 243–250. <https://doi.org/10.3892/ijmm.2015.2420>
- [125] Cunha, S. A., and Pintado, M. E. (2021). Bioactive peptides derived from marine sources: biological and functional properties. *Trends Food Sci. Technol.* 119, 348–370. doi: 10.1016/j.tifs.2021.08.017
- [126] Wang, X., Yuen, K. F., Wong, Y. D., and Li, K. X. (2020). How can the maritime industry meet sustainable development goals? an analysis of sustainability reports from the social entrepreneurship perspective. *Transp. Res. Part D Transp. Environ.* 78:102173.
- [127] Nam, B. H., Seo, J. K., Lee, M. J., Kim, Y. O., Kim, D. G., An, C. M., et al. (2015). Functional analysis of Pacific oyster (*Crassostrea gigas*) β-thymosin: Focus on antimicrobial activity. *Fish & Shellfish Immunology*, 45(1), 167–174. <https://doi.org/10.1016/j.fsi.2015.03.035>
- [128] Semreen, M. H., El-Gamal, M. I., Abdin, S., Alkhazraji, H., Kamal, L., Hammad, S., et al. (2018). Recent updates of marine antimicrobial peptides. *Saudi Pharmaceutical Journal*, 26(3), 396–409. <https://doi.org/10.1016/j.sjps.2018.01.001>
- [129] Costa, J., Silva, N., Sarmento, B., & Pintado, M. (2017). Delivery systems for antimicrobial peptides and proteins: Towards optimization of bioavailability and targeting. *Current Pharmaceutical Biotechnology*, 18(2), 108–120. <https://doi.org/10.2174/1389201017666161207112244>
- [130] Silva, N. C., Sarmento, B., & Pintado, M. (2013). The importance of antimicrobial peptides and their potential for therapeutic use in ophthalmology. *International Journal of Antimicrobial Agents*, 41(1), 5–10. <https://doi.org/10.1016/j.ijantimicag.2012.07.020>
- [131] Novoa, B., Romero, A., Alvarez, A. L., Moreira, R., Pereira, P., Costa, M. M., et al. (2016). Antiviral activity of myticin C peptide from mussel: An ancient defense against herpesviruses. *Journal of Virology*, 90(17), 7692–7702. <https://doi.org/10.1128/jvi.00591-16>
- [132] Qin, C. L., Huang, W., Zhou, S. Q., Wang, X. C., Liu, H. H., Fan, M. H., et al. (2014). Characterization of a novel antimicrobial peptide with chitin-binding domain from *Mytilus coruscus*. *Fish & Shellfish Immunology*, 41(2), 362–370. <https://doi.org/10.1016/j.fsi.2014.09.019>
- [133] Leoni, G., De Poli, A., Mardirossian, M., Gambato, S., Florian, F., Venier, P., et al. (2017). Myticalins: A novel multigenic family of linear, cationic antimicrobial peptides from marine mussels (*Mytilus* spp.). *Marine Drugs*, 15(8). <https://doi.org/10.3390/md15080261>
- [134] De Zoysa, M., Whang, I., Lee, Y., Lee, S., Lee, J. S., & Lee, J. (2010). Defensin from disk abalone *Haliotis discus discus*: Molecular cloning, sequence characterization and immune response against bacterial infection. *Fish & Shellfish Immunology*, 28(2), 261–266. <https://doi.org/10.1016/j.fsi.2009.11.005>

- [135] Cunha, S. A., & Pintado, M. E. (2022). Bioactive peptides derived from marine sources: Biological and functional properties. *Trends in Food Science & Technology*, 119, 348-370.
- [136] Liao, Z., Wang, X., chao, L., hui, H., Fan, M., hua, S., et al. (2013). Molecular characterization of a novel antimicrobial peptide from *Mytilus coruscus*. *Fish & Shellfish Immunology*, 34(2), 610-616. <https://doi.org/10.1016/j.fsi.2012.11.030>
- [137] Guzmán, F., Wong, G., Román, T., Cardenas, C., Alvarez, C., Schmitt, P., et al. (2019). Identification of antimicrobial peptides from the microalgae *tetraselmis suecica* (kylin) butcher and bactericidal activity improvement. *Marine Drugs*, 17(8), 453. <https://doi.org/10.3390/md17080453>
- [138] Sedighi, M., Jalili, H., Ranaei-Siadat, S. O., & Amrane, A. (2016). Potential health effects of enzymatic protein hydrolysates from *Chlorella vulgaris*. *Applied Food Biotechnology*, 3(Issue 3). <https://doi.org/10.22037/afb.v3i3.11306>
- [139] Jiao, K., Gao, J., Zhou, T., Yu, J., Song, H., Wei, Y., et al. (2019). Isolation and purification of a novel antimicrobial peptide from *Porphyra yezoensis*. *Journal of Food Biochemistry*, 43(7), Article e12864. <https://doi.org/10.1111/jfbc.12864>
- [140] Zhao, L., Yin, B., Liu, Q., & Cao, R. (2013). Purification of antimicrobial peptide from Antarctic Krill (*Euphausia superba*) and its function mechanism. *Journal of Ocean University of China*, 12(3), 484-490. <https://doi.org/10.1007/s11802-013-2180-2>
- [141] Bechinger, B., & Gorr, S. U. (2017). Antimicrobial peptides: Mechanisms of action and resistance. *Journal of Dental Research*, 96(3), 254-260. <https://doi.org/10.1177/0022034516679973>
- [142] Wang, X., Zhang, Z., Zhang, S., Yang, F., Yang, M., Zhou, J., et al. (2021). Antiaging compounds from marine organisms. *Food Res. Int.* 143:110313. doi: 10.1016/j.foodres.2021.110313
- [143] Kammeyer, A., & Luiten, R. M. (2015). Oxidation events and skin aging. *Ageing Research Reviews*, 21, 16-29. <https://doi.org/10.1016/j.arr.2015.01.001>
- [144] Chen, J., Tan, L., Li, C., Zhou, C., Hong, P., Sun, S., et al. (2020). Mechanism analysis of a novel angiotensin-I-converting enzyme inhibitory peptide from *isochrysis zhanjiangensis* microalgae for suppressing vascular injury in human umbilical vein endothelial cells. *Journal of Agricultural and Food Chemistry*, 68(15), 4411-4423. <https://doi.org/10.1021/acs.jafc.0c00925>
- [145] Chi, C. F., Hu, F. Y., Wang, B., Li, T., & Ding, G. F. (2015). Antioxidant and anticancer peptides from the protein hydrolysate of blood clam (*Tegillarca granosa*) muscle. *Journal of Functional Foods*, 15, 301-313. <https://doi.org/10.1016/j.jff.2015.03.045>
- [146] Ketnawa, S., Suwal, S., Huang, J. Y., & Liceaga, A. M. (2019). Selective separation and characterisation of dual ACE and DPP-IV inhibitory peptides from rainbow trout (*Oncorhynchus mykiss*) protein hydrolysates. *International Journal of Food Science and Technology*, 54(4), 1062-1073. <https://doi.org/10.1111/ijfs.13939>
- [147] Rivero-Pino, F., Espejo-Carpio, F. J., & Guadix, E. M. (2020a). Antidiabetic food-derived peptides for functional feeding: Production, functionality and in vivo evidences. In , Vol. 9. *Foods*. MDPI Multidisciplinary Digital Publishing Institute. <https://doi.org/10.3390/foods9080983>. Issue 8.
- [148] Ucak, I.; Afreen, M.; Montesano, D.; Carrillo, C.; Tomasevic, I.; Simal-Gandara, J.; Barba, F.J. Functional and bioactive properties of peptides derived from marine side streams. *Mar. Drugs* 2021, 19, 71. [CrossRef] [PubMed]
- [149] Zhang, Q.T.; Liu, Z.D.; Wang, Z.; Wang, T.; Wang, N.; Wang, N.; Zhang, B.; Zhao, Y.F. Recent Advances in Small Peptides of Marine Origin in Cancer Therapy. *Mar. Drugs* 2021, 19, 115. [CrossRef] [PubMed]
- [150] Reuschl AK, Thorne LG, Zuliani-Alvarez L, Bouhaddou M, Obernier K, Soucheray M, Turner J, Fabius JM, Nguyen GT, Swaney DL, Rosales R (2021) Host-directed therapies against early-lineage SARS-CoV-2 retain efficacy against B.1.1.7 variant. *BioRxiv*
- [151] González-Cano R, Ruiz-Cantero MC, Santos-Caballero M, Gómez-Navas C, Tejada MA, Nieto FR (2021) Tetrodotoxin, a potential drug for neuropathic and cancer pain relief? *Toxins* 13:483
- [152] Karthikeyan, A., Joseph, A., & Nair, B. G. (2022). Promising bioactive compounds from the marine environment and their potential effects on various diseases. *Journal of Genetic Engineering and Biotechnology*, 20(1), 1-38.
- [153] Koyande, A. K., Chew, K. W., Manickam, S., Chang, J. S., and Show, P. L. (2021). Emerging algal nanotechnology for high-value compounds: a direction to future food production. *Trends Food Sci. Technol.* 116, 290-302. doi: 10.1016/j.tifs.2021.07.026
- [154] Hosseini, S. F., Rezaei, M., and McClements, D. J. (2020). Bioactive functional ingredients from aquatic origin: a review of recent progress in marine-derived nutraceuticals. *Crit. Rev. Food Sci. Nutr.* doi: 10.1080/10408398.2020.1839855 [Epub ahead of print].
- [155] Qin, Y. (2018a). 6 - Applications of Bioactive Seaweed Substances in Functional Food Products. Cambridge, MA: Academic Press.
- [156] Ganesan, A. R., Saravana Guru, M., Balasubramanian, B., Mohan, K., Chao Liu, W., Valan Arasu, M., et al. (2020b). Biopolymer from edible marine invertebrates: a potential functional food. *J. King Saud Univ. Sci.* 32, 1772-1777. doi: 10.1016/j.jksus.2020.01.015
- [157] D. Agyei, C. M. Ongkudon, C. Y. Wei, A. S. Chan, and M. K. Danquah, "Bioprocess challenges to the isolation and purification of bioactive peptides," *Food and Bioproducts Processing*, vol. 98, pp. 244-256, 2016.
- [158] Y. Zhou, "The potential biomedical application of cyclopeptides from marine natural products," *Current Organic Chemistry*, vol. 18, no. 7, pp. 918-924, 2014.
- [159] Wang, X., Yu, H., Xing, R., & Li, P. (2017). Characterization, preparation, and purification of marine bioactive peptides. *BioMed research international*, 2017.

- Characterization, preparation, and purification of marine bioactive peptides. *BioMed research international*, 2017.
- [160] M. Vijaykrishnaraj and P. Prabhasankar, "Marine protein hydrolysates: their present and future perspectives in food chemistry—a review," *RSC Advances*, vol. 5, no. 44, pp. 34864–34877, 2015.
- [161] J. Lee and T. W. Jeffries, "Efficiencies of acid catalysts in the hydrolysis of lignocellulosic biomass over a range of combined severity factors," *Bioresource Technology*, vol. 102, no. 10, pp. 5884–5890, 2011.
- [162] Y.-L. Loow, T. Y. Wu, J. M. Jahim, A. W. Mohammad, and W. H. Teoh, "Typical conversion of lignocellulosic biomass into reducing sugars using dilute acid hydrolysis and alkaline pretreatment," *Cellulose*, vol. 23, no. 3, Article ID A1491, pp. 1491–1520, 2016.
- [163] Z. Xu and F. Huang, "Pretreatment methods for bioethanol production," *Applied biochemistry and biotechnology*, vol. 174, no. 1, pp. 43–62, 2014.
- [164] L. Wang, Y. Zou, and B. Jiang, "Process and Kinetic Models of Hydrochloric Acid-Extracted Collagen from Bighead Carp Scale," in *Proceedings of the 5th International Conference on Information Engineering for Mechanics and Materials*, AERAdvances in Engineering Research, pp. 476–482, Huhhot, Inner Mongolia, July 2015.
- [165] Wang, X., Yu, H., Xing, R., & Li, P. (2017). Characterization, preparation, and purification of marine bioactive peptides. *BioMed research international*, 2017.
- [166] C.-Y. Huang, J.-M. Kuo, S.-J. Wu, and H.-T. Tsai, "Isolation and characterization of fish scale collagen from tilapia (*Oreochromis sp.*) by a novel extrusion-hydro-extraction process," *Food Chemistry*, vol. 190, pp. 997–1006, 2016.
- [167] Da Trindade Alfaro, C. Simoes Da Costa, G. Graciano ~ Fonseca, and C. Prentice, "Effect of extraction parameters on the properties of gelatin from king weakfish (*Macrodon ancylodon*) Bones," *Food Science and Technology International*, vol. 15, no. 6, pp. 553–562, 2009.
- [168] D. Agyei and M. K. Danquah, "Industrial-scale manufacturing of pharmaceutical-grade bioactive peptides," *Biotechnology Advances*, vol. 29, no. 3, pp. 272–277, 2011.
- [169] Q. Ren, H. Xing, Z. Bao et al., "Recent advances in separation of bioactive natural products," *Chinese Journal of Chemical Engineering*, vol. 21, no. 9, pp. 937–952, 2013.
- [170] C.-W. Cho, D.-Y. Lee, and C.-W. Kim, "Concentration and purification of soluble pectin from mandarin peels using crossflow microfiltration system," *Carbohydrate Polymers*, vol. 54, no. 1, pp. 21–26, 2003.
- [171] R. V. Tonon, B. A. dos Santos, C. C. Couto, C. Mellinger-Silva, A. I. S. Brígida, and L. M. C. Cabral, "Coupling of ultrafiltration and enzymatic hydrolysis aiming at valorizing shrimp wastewater," *Food Chemistry*, vol. 198, pp. 20–27, 2016.
- [172] S.-Y. Kim, J.-Y. Je, and S.-K. Kim, "Purification and characterization of antioxidant peptide from hoki (*Johnius belengerii*) frame protein by gastrointestinal digestion," *Journal of Nutritional Biochemistry*, vol. 18, no. 1, pp. 31–38, 2007.
- [173] X. Wang, R. Xing, S. Liu et al., "Purification and characterization of novel antioxidant peptides of different molecular weights from mackerel *Pneumatophorus japonicus* protein hydrolysate," *Chinese Journal of Oceanology and Limnology*, vol. 33, no. 1, pp. 159–168, 2014.
- [174] C. Roblet, M. J. Akhtar, S. Mikhaylin et al., "Enhancement of glucose uptake in muscular cell by peptide fractions separated by electrodialysis with filtration membrane from salmon frame protein hydrolysate," *Journal of Functional Foods*, vol. 22, pp. 337–346, 2016.
- [175] P. R. Levison, "Large-scale ion-exchange column chromatography of proteins: Comparison of different formats," *Journal of Chromatography B: Analytical Technologies in the Biomedical and Life Sciences*, vol. 790, no. 1-2, pp. 17–33, 2003
- [176] K. Li, R. Xing, S. Liu et al., "Separation of chito-oligomers with several degrees of polymerization and study of their antioxidant activity," *Carbohydrate Polymers*, vol. 88, no. 3, pp. 896–903, 2012.
- [177] S. Y. Park, Y.-S. Kim, C.-B. Ahn, and J.-Y. Je, "Partial purification and identification of three antioxidant peptides with hepatoprotective effects from blue mussel (*Mytilus edulis*) hydrolysate by peptic hydrolysis," *Journal of Functional Foods*, vol. 20, pp. 88–95, 2016.
- [178] S. Wang, J. Zhao, L. Chen, Y. Zhou, and J. Wu, "Preparation, isolation and hypothermia protection activity of antifreeze peptides from shark skin collagen," *LWT—Food Science and Technology*, vol. 55, no. 1, pp. 210–217, 2014.
- [179] S.-Y. Jun, P.-J. Park, W.-K. Jung, and S.-K. Kim, "Purification and characterization of an antioxidative peptide from enzymatic hydrolysate of yellowfin sole (*Limanda aspera*) frame protein," *European Food Research and Technology*, vol. 219, no. 1, pp. 20–26, 2004.
- [180] R. Song, R.-B. Wei, G.-Q. Ruan, and H.-Y. Luo, "Isolation and identification of antioxidative peptides from peptic hydrolysates of half-fin anchovy (*Setipinna taty*)," *LWT—Food Science and Technology*, vol. 60, no. 1, pp. 221–229, 2015.
- [181] M.-S. Hsieh, L.-J. Yin, and S.-T. Jiang, "Purification and characterization of the amylase from a small abalone *Haliotis sieboldii*," *Fisheries Science*, vol. 74, no. 2, pp. 425–432, 2008.
- [182] L. Wang, Y. Qu, X. Fu, M. Zhao, S. Wang, and L. Sun, "Isolation, purification and properties of an R-phycoyanin from the phycobilisomes of a marine red macroalga *Polysiphonia urceolata*," *PLoS ONE*, vol. 9, no. 2, Article ID e87833, 2014.
- [183] L. Beaulieu, J. Thibodeau, M. Desbiens, R. Saint-Louis, C. Zatylny-Gaudin, and S. Thibault, "Evidence of antibacterial activities in peptide fractions originating from snow crab (*Chionoecetes opilio*) by-products," *Probiotics and Antimicrobial Proteins*, vol. 2, no. 3, pp. 197–209, 2010.

- [184] W. S. Huang, K. J. Wang, M. Yang, J. J. Cai, S. J. Li, and G. Z. Wang, "Purification and part characterization of a novel antibacterial protein Scygonadin, isolated from the seminal plasma of mud crab, *Scylla serrata* (Forsk., 1775)," *Journal of Experimental Marine Biology and Ecology*, vol. 339, no. 1, pp. 37–42, 2006.
- [185] Y. Zhang, X. Duan, and Y. Zhuang, "Purification and characterization of novel antioxidant peptides from enzymatic hydrolysates of tilapia (*Oreochromis niloticus*) skin gelatin," *Peptides*, vol. 38, no. 1, pp. 13–21, 2012.
- [186] R. Jai ganesh, R. A. Nazeer, and N. S. Sampath Kumar, "Purification and identification of antioxidant peptide from black pomfret, *Parastromateus niger* (Bloch, 1975) viscera protein hydrolysate," *Food Science and Biotechnology*, vol. 20, no. 4, pp. 1087–1094, 2011.
- [187] D. Huang, Y. Li, F. Cui, J. Chen, and J. Sun, "Purification and characterization of a novel polysaccharide-peptide complex from *Clinacanthus nutans* Lindau leaves," *Carbohydrate Polymers*, vol. 137, pp. 701–708, 2016.
- [188] L. Qian, Y. Zhang, and F. Liu, "Purification and characterization of a ~43 kDa antioxidant protein with antitumor activity from *Pholiota nameko*," *Journal of the Science of Food and Agriculture*, vol. 96, no. 3, pp. 1044–1052, 2016.
- [189] M.-H. Pan, M.-L. Tsai, W.-M. Chen et al., "Purification and characterization of a fish scale-degrading enzyme from a newly identified *Vogesella* sp.," *Journal of Agricultural and Food Chemistry*, vol. 58, no. 23, pp. 12541–12546, 2010.
- [190] G. Iberer, H. Schwinn, D. Josic, A. Jungbauer, and A. Buchacher, "Improved performance of protein separation by continuous annular chromatography in the size-exclusion mode," *Journal of Chromatography A*, vol. 921, no. 1, pp. 15–24, 2001.
- [191] J. G. Joyce, J. C. Cook, C. T. Przysiecki, and E. Dale Lehman, "Chromatographic separation of low-molecular-mass recombinant proteins and peptides on Superdex 30 prep grade," *Journal of Chromatography B: Biomedical Sciences and Applications*, vol. 662, no. 2, pp. 325–334, 1994.
- [192] M.-J. Cao, K. Osatomi, K. Hara, and T. Ishihara, "Identification of a myofibril-bound serine proteinase (MBSP) in the skeletal muscle of lizard fish *Saurida wanieso* which specifically cleaves the arginine site," *Comparative Biochemistry and Physiology - B Biochemistry and Molecular Biology*, vol. 125, no. 2, pp. 255–264, 2000.
- [193] J.-D. Shen, Q.-F. Cai, L.-J. Yan et al., "Cathepsin L is an immune-related protein in Pacific abalone (*Haliotis discus hannai*)—Purification and characterization," *Fish and Shellfish Immunology*, vol. 47, no. 2, pp. 986–995, 2015.
- [194] J.-L. Wu, S.-Y. Ge, Z.-X. Cai et al., "Purification and characterization of a gelatinolytic matrix metalloproteinase from the skeletal muscle of grass carp (*Ctenopharyngodon idellus*)," *Food Chemistry*, vol. 145, pp. 632–638, 2014.
- [195] K.-C. Hsu, "Purification of antioxidative peptides prepared from enzymatic hydrolysates of tuna dark muscle by-product," *Food Chemistry*, vol. 122, no. 1, pp. 42–48, 2010.
- [196] C. Ma, X. Ni, Z. Chi, L. Ma, and L. Gao, "Purification and characterization of an alkaline protease from the marine yeast *Aureobasidium pullulans* for bioactive peptide production from different sources," *Marine Biotechnology*, vol. 9, no. 3, pp. 343–351, 2007.
- [197] M. Vijaykrishnaraj, B. S. Roopa, and P. Prabhasankar, "Preparation of gluten free bread enriched with green mussel (*Perna canaliculus*) protein hydrolysates and characterization of peptides responsible for mussel flavour," *Food Chemistry*, vol. 211, pp. 715–725, 2016.
- [198] Bougatef, N. Nedjar-Arroume, L. Manni et al., "Purification and identification of novel antioxidant peptides from enzymatic hydrolysates of sardinelle (*Sardinella aurita*) by-products proteins," *Food Chemistry*, vol. 118, no. 3, pp. 559–565, 2010.
- [199] P. Singh, S. Vij, and S. Hati, "Functional significance of bioactive peptides derived from soybean," *Peptides*, vol. 54, pp. 171–179, 2014.
- [200] S. Pan, S. Wang, L. Jing, and D. Yao, "Purification and characterisation of a novel angiotensin-I converting enzyme (ACE)- inhibitory peptide derived from the enzymatic hydrolysate of *Enteromorpha clathrata* protein," *Food Chemistry*, vol. 211, pp. 423–430, 2016.
- [201] J. A. V. Lopez, S. S. Al-Lihaibi, W. M. Alarif et al., "Wewakazole B, a Cytotoxic Cyanobactin from the Cyanobacterium *Moorea producens* Collected in the Red Sea," *Journal of Natural Products*, vol. 79, no. 4, pp. 1213–1218, 2016.
- [202] Lassoued, L. Mora, A. Barkia, M.-C. Aristoy, M. Nasri, and F. Toldra, "Bioactive peptides identified in thornback ray skin's gelatin hydrolysates by proteases from *Bacillus subtilis* and *Bacillus amyloliquefaciens*," *Journal of Proteomics*, vol. 128, pp. 8–17, 2015.
- [203] D. T. A. Youssef, L. A. Shaala, G. A. Mohamed, J. M. Badr, F. H. Bamanie, and S. R. M. Ibrahim, "Theonellamide G, a potent antifungal and cytotoxic bicyclic glycopeptide from the red sea marine sponge *Theonella swinhoei*," *Marine Drugs*, vol. 12, no. 4, pp. 1911–1923, 2014.
- [204] J.-K. Seo, M. J. Lee, H.-G. Jung, H.-J. Go, Y. J. Kim, and N. G. Park, "Antimicrobial function of SH  $\beta$ AP, a novel hemoglobin  $\beta$  chain-related antimicrobial peptide, isolated from the liver of skipjack tuna, *Katsuwonus pelamis*," *Fish and Shellfish Immunology*, vol. 37, no. 1, pp. 173–183, 2014.
- [205] V.-T. Nguyen, Z.-J. Qian, B. Ryu et al., "Matrix metalloproteinases (MMPs) inhibitory effects of an octameric oligopeptide isolated from abalone *Haliotis discus hannai*," *Food Chemistry*, vol. 141, no. 1, pp. 503–509, 2013.
- [206] P. Dolashka, V. Moshtanska, V. Borisova et al., "Antimicrobial proline-rich peptides from the hemolymph of marine snail *Rapana venosa*," *Peptides*, vol. 32, no. 7, pp. 1477–1483, 2011.
- [207] M. Careri and A. Mangia, "Analysis of food proteins and peptides by chromatography and mass spectrometry," *Journal of Chromatography A*, vol. 1000, no. 1-2, pp. 609–635, 2003.

- [208] M. Mann and O. N. Jensen, "Proteomic analysis of posttranslational modifications," *Nature Biotechnology*, vol. 21, no. 3, pp. 255–261, 2003.
- [209] M. Vijaykrishnaraj and P. Prabhasankar, "Marine protein hydrolysates: their present and future perspectives in food chemistry—a review," *RSC Advances*, vol. 5, no. 44, pp. 34864–34877, 2015.
- [210] Bleakley, S., & Hayes, M. (2017). Algal proteins: Extraction, application, and challenges concerning production. *Foods*, 6(5), 33. <https://doi.org/10.3390/foods6050033>
- [211] Ejike, C. E. C. C., Collins, S. A., Balasuriya, N., Swanson, A. K., Mason, B., & Udenigwe, C. C. (2017). Prospects of microalgae proteins in producing peptide-based functional foods for promoting cardiovascular health. *Trends in Food Science & Technology*, 59, 30–36. <https://doi.org/10.1016/j.tifs.2016.10.026>
- [212] Ovando, C. A., Carvalho, J. C., de Vinicius de Melo Pereira, G., Jacques, P., Soccol, V. T., & Soccol, C. R. (2018). Functional properties and health benefits of bioactive peptides derived from *Spirulina*: A review. In *Food reviews international*. Taylor and Francis Inc, 34(Issue 1), 34–51. <https://doi.org/10.1080/87559129.2016.1210632>
- [213] Messina, C.M.; Manuguerra, S.; Arena, R.; Renda, G.; Ficano, G.; Randazzo, M.; Fricano, S.; Sadok, S.; Santulli, A. In Vitro Bioactivity of Astaxanthin and Peptides from Hydrolysates of Shrimp (*Parapenaeus longirostris*) By-Products: From the Extraction Process to Biological Effect Evaluation, as Pilot Actions for the Strategy "From Waste to Profit". *Mar. Drugs* 2021, 19, 216. [CrossRef]
- [214] Dahiya, R.; Rampersad, S.; Ramnansingh, T.G.; Kaur, K.; Kaur, R.; Mourya, R.; Chennupati, S.V.; Fairman, R.; Jalsa, N.K.; Sharma, A.; et al. Synthesis and Bioactivity of a Cyclopolypeptide from Caribbean Marine Sponge. *Iran. J. Pharm. Res. IJPR* 2020, 19, 156.
- [215] Leisch, M.; Egle, A.; Greil, R. Plitidepsin: A potential new treatment for relapsed/refractory multiple myeloma. *Future Oncol.* 2019, 15, 109–120. [CrossRef]
- [216] Nowruzi, B.; Blanco, S.; Nejadstattari, T. Chemical and molecular evidences for the poisoning of a duck by anatoxin-a, nodularin and cryptophycin at the coast of Lake Shoormast (Mazandaran province, Iran). *Int. J. Algae* 2018, 20, 359–376. [CrossRef]
- [217] Nowruzi, B.; Haghighat, S.; Fahimi, H.; Mohammadi, E. Nostoc cyanobacteria species: A new and rich source of novel bioactive compounds with pharmaceutical potential. *J. Pharm. Health Serv. Res.* 2018, 9, 5–12. [CrossRef]
- [218] Li, B.; Gao, M.H.; Zhang, X.C.; Chu, X.M. Molecular immune mechanism of C-phycocyanin from *Spirulina platensis* induces apoptosis in HeLa cells in vitro. *Biotechnol. Appl. Biochem.* 2006, 43, 155–164.
- [219] Ahmed, I., Asgher, M., Sher, F., Hussain, S. M., Nazish, N., Joshi, N., ... & Iqbal, H. M. (2022). Exploring marine as a rich source of bioactive peptides: Challenges and opportunities from marine pharmacology. *Marine drugs*, 20(3), 208.
- [220] Lachia, M.; Moody, C.J. The synthetic challenge of diazonamide A, a macrocyclic indole bis-oxazole marine natural product. *Nat. Prod. Rep.* 2008, 25, 227–253. [CrossRef] [PubMed]
- [221] Barry CE III, Slayden RA, Sampson AE, Lee RE (2000) Use of genomics and combinatorial chemistry in the development of new antimycobacterial drugs. *Biochem Pharm* 59:221–231
- [222] Oja T, San Martin Galindo P, Taguchi T, Manner S, Vuorela PM, Ichinose K, Metsa-Ketela M, Fallarero A (2015) Effective antibiofilm polyketides against *Staphylococcus aureus* from the pyranonaphthoquinone biosynthetic pathways of *Streptomyces* species. *Antimicrob Agents Chemother* 59:6046–6052
- [223] Meijer L, Thunnissen AM, White A, Garnier M, Nikolic M, Tsai L, Walter J, Cleverley K, Salinas P, Wu Y, Biernat J (2000) Inhibition of cyclin-dependent kinases, GSK-3 $\beta$  and CK1 by hymenialdisine, a marine sponge constituent. *Chem Biol* 7:51–63
- [224] Yu Y, Wu J, Lei F, Chen L, Wan W, Hai L, Guan M, Wu Y (2013) Design, synthesis and anticancer activity evaluation of diazepam derivatives. *Lett Drug Des Disc* 10:369–373
- [225] Jensen PR, Williams PG, Oh DC, Zeigler L, Fenical W (2007) Species-specific secondary metabolite production in marine actinomycetes of the genus *Salinispora*. *Appl Environ Microbiol* 73:1146–1152
- [226] Itoh T, Kinoshita M, Aoki S, Kobayashi M (2003) Komodoquinone A, a novel neurotoxic anthracycline, from marine *Streptomyces* sp. KS3. *J Nat Prod* 66:1373–1377
- [227] Phan LY, Jian T, Chen Z, Qiu YL, Wang Z, Beach T, Polemropoulos A, Or YS (2004) Synthesis and antibacterial activity of a novel class of 4'-substituted 16-membered ring macrolides derived from tylosin. *J Med Chem* 47:2965–2968
- [228] Rao M, Wei W, Ge M, Chen D, Sheng X (2013) A new antibacterial lipopeptide found by UPLC-MS from an actinomycete *Streptomyces* sp. HCCB10043. *Nat Prod Res* 27:2190–2195
- [229] Ramalingam V, Varunkumar K, Ravikumar V, Rajaram R (2018) p53 mediated transcriptional regulation of long non-coding RNA by 1-hydroxyl-norresistomycin triggers intrinsic apoptosis in adenocarcinoma lung cancer. *Chem Biol Interact* 287:1–12
- [230] Brana AF, Sarmiento-Vizcaino A, Osset M, Perez-Victoria I, Martin J, De Pedro N, De la Cruz M, Diaz C, Vicente F, Reyes F, Garcia LA, Blanco G (2017) Lobophorin K, a new natural product with cytotoxic activity produced by *Streptomyces* sp. M-207 associated with the deep-sea coral *Lophelia pertusa*. *Mar Drugs* 15(5):144
- [231] Abdelkader MSA, Philippon T, Asenjo JA, Bull AT, Goodfellow M, Ebel R, Jaspars M, Rateb ME (2018) Asenjonamides A-C, antibacterial metabolites isolated from *Streptomyces asenjonii* strain KNN 42.f from an extreme-hyper arid Atacama Desert soil. *J Antibiot (Tokyo)* 71:425–431

- [232] Hou J, Liu P, Qu H, Fu P, Wang Y, Wang Z, Li Y, Teng X, Zhu W (2012) Gilvocarcin HE: a new polyketide glycoside from *Streptomyces* sp. *J Antibiot (Tokyo)* 65:523–526
- [233] Lü Y, Shao M, Wang Y, Qian S, Wang M, Wang Y, Li X, Bao Y, Deng C, Yue C, Liu D, Liu N, Liu M, Huang Y, Chen Z, Hu Y (2017) Zunyimycins B and C, New chloroanthrabenoxocinones antibiotics against methicillinresistant *Staphylococcus aureus* and *Enterococci* from *Streptomyces* sp. FJS31-2. *Molecules (Basel, Switzerland)* 22:251
- [234] Qin Z, Munnoch JT, Devine R, Holmes NA, Seipke RF, Wilkinson KA, Wilkinson B, Hutchings MI (2017) Formicamycins, antibacterial polyketides produced by *Streptomyces formicae* isolated from African *Tetraponera* plant-ants. *Chem Sci* 8:3218–3227
- [235] Cruz JC, Mafoli SI, Bernasconi A, Brunati C, Gaspari E, Sosio M, Wellington E, Donadio S (2017) Allocyclinones, hyperchlorinated angucyclinones from *Actinoallomurus*. *J Antibiot (Tokyo)* 70:73–78
- [236] Cheng C, Othman EM, Reimer A, Grüne M, Kozjak-Pavlovic V, Stopper H, Hentschel U, Abdelmohsen UR (2016) Ageloline A, new antioxidant and antichlamydia quinolone from the marine sponge-derived bacterium *Streptomyces* sp. SBT345. *Tetrahedron Lett* 57:2786–2789
- [237] Liu LL, Xu Y, Han Z, Li YX, Lu L, Lai PY, Zhong JL, Guo XR, Zhang XX, Qian PY (2012) Four new antibacterial xanthenes from the marine-derived actinomycetes *Streptomyces caelestis*. *Mar Drugs* 10:2571–2583
- [238] Mahajan G, Thomas B, Parab R, Patel ZE, Kuldharan S, Yemparala V, Mishra PD, Ranadive P, D'Souza L, Pari K, Sivaramkrishnan H (2013) In vitro and in vivo activities of antibiotic PM181104. *Antimicrob Agents Chemother* 57:5315–5319
- [239] Moon K, Chung B, Shin Y, Lee SK, Oh KB, Shin J, Oh DC (2015) Discovery of new bioactive secondary metabolites from bacteria in extreme habitats. *Planta Med* 81(11):PT24
- [240] Flora DO, Adeyemi AI, George WP (2015) Himalomycin A and cycloheximide-producing marine actinomycete from Lagos Lagoon soil sediment. *J Coast Life Med* 3:361–365
- [241] Phan LY, Jian T, Chen Z, Qiu YL, Wang Z, Beach T, Polemeropoulos A, Or YS (2004) Synthesis and antibacterial activity of a novel class of 4'-substituted 16-membered ring macrolides derived from tylosin. *J Med Chem* 47:2965–2968
- [242] Igarashi M, Sawa R, Yamasaki M, Hayashi C, Umekita M, Hatano M, Fujiwara T, Mizumoto K, Nomoto A (2017) Kribellosides, novel RNA 5'-triphosphatase inhibitors from the rare actinomycete *Kribbella* sp. MI481-42F6. *J Antibiot (Tokyo)* 70:582–589
- [243] Bister B, Bischof, Strobele M, Riedlinger J, Reicke A, Wolter F, Bull AT, Zahner H, Fiedler HP, Sussmuth RD (2004) Abyssomicin C-A polycyclic antibiotic from a marine *Verrucospora* strain as an inhibitor of the p-aminobenzoic acid/tetrahydrofolate biosynthesis pathway. *Angew Chem Int Ed Engl* 43:2574–2576
- [244] Bruntner C, Binder T, Pathom-aree W, Goodfellow M, Bull AT, Potterat O, Puder C, Horer S, Schmid A, Bolek W, Wagner K, Mihm G, Fiedler HP (2005) Frigocyclinone, a novel angucyclinone antibiotic produced by a *Streptomyces griseus* strain from Antarctica. *J Antibiot (Tokyo)* 58:346–349
- [245] Lu Y, Dong X, Liu S, Bie X (2009) Characterization and identification of a novel marine *Streptomyces* sp. produced antibacterial substance. *Mar Biotechnol (NY)* 11:717–724
- [246] Maskey RP, Helmke E, Kayser O, Fiebig HH, Maier A, Busche A, Laatsch H (2004) Anti-cancer and antibacterial trioxacarcins with high anti-malaria activity from a marine *Streptomyces* and their absolute stereochemistry. *J Antibiot* 57:771–779
- [247] Manam RR, Teisan S, White DJ, Nicholson B, Grodberg J, Neuteboom ST, Lam KS, Mosca DA, Lloyd GK, Potts BC (2005) Lajollamycin, a nitrotetraene spiro-beta-lactone-gamma-lactam antibiotic from the marine actinomycete *Streptomyces nodosus*. *J Nat Prod* 68:240–243
- [248] Gunasekera SP, McCarthy PJ, Kelly-Borges M, Lobkovsky E, Clardy J (1996) Dysidiolide: a novel protein phosphatase inhibitor from the Caribbean sponge *Dysidea etheria* de Laubenfels. *J Am Chem Soc* 118:8759–8760
- [249] Nagle DG, Zhou YD, Mora FD, Mohammed KA, Kim YP (2004) Mechanism targeted discovery of antitumor marine natural products. *Curr Med Chem* 11:1725–1756
- [250] Loukaci S, Le Saout I, Samadi M, Leclerc S, Damiens E, Meijer L, Debitus C, Guyot M (2001) Coscinosulfate, a CDC25 phosphatase inhibitor from the sponge *Coscinoderma mathewsi*. *Bioorg Med Chem* 9:3049–3054
- [251] Skropeta D, Pastro N, Zivanovic A (2011) Kinase inhibitors from marine sponges *Mar. Drugs* 9:2131–2154
- [252] Cherigo L, Lopez D, Martinez-Luis S (2015) Marine natural products as breast cancer resistance protein inhibitors. *Mar Drugs* 13:2010–2029
- [253] Losada AA, Cano-Prieto C, Garcia-Salcedo R, Brana AF, Mendez C, Salas JA, Olano C (2017) Caboxamycin biosynthesis pathway and identification of novel benzoxazoles produced by cross-talk in *Streptomyces* sp. NTK 937. *Microb Biotechnol* 10:873–885
- [254] Malloy KL, Choi H, Fiorilla C, Valeriote FA, Matainaho T, Gerwick WH (2012) Hoiamide D, a marine cyanobacteria-derived inhibitor of p53/MDM2 interaction. *Bioorg Med Chem Lett* 22:683–688
- [255] Kato H, Nehira T, Matsuo K, Kawabata T, Kobashigawa Y, Morioka H, Losung F, Mangindaan RE, De Voogd NJ, Yokosawa H (2015) Niphateolide A: isolation from the marine sponge *Niphates olemda* and determination of its absolute configuration by an ECD analysis. *Tetrahedron* 71:6956–6960
- [256] Tsukamoto S, Yoshida T, Hosono H, Ohta T, Yokosawa H (2006) Hexylitaconic acid: a new inhibitor of p53-HDM2 interaction isolated from a marine-derived fungus, *Arthrinium* sp. *Bioorg Med Chem Lett* 16:69–71
- [257] Clement JA, Kitagaki J, Yang Y, Saucedo CJ, O'Keefe BR, Weissman AM, McKee TC, McMahon JB (2008) Discovery of new pyridoacridine alkaloids from *Lissoclinum cf. badium* that inhibit the ubiquitin ligase activity of Hdm2 and stabilize p53. *Bioorg Med Chem* 16:10022–10028

- [258] Tsukamoto S, Hirota H, Imachi M, Fujimuro M, Onuki H, Ohta T, Yokosawa H (2005) Himeic acid A: a new ubiquitin-activating enzyme inhibitor isolated from a marine-derived fungus, *Aspergillus* sp. *Bioorg Med Chem Lett* 15:191–194
- [259] Tsukamoto S, Yamashita K, Tane K, Kizu R, Ohta T, Matsunaga S, Fusetani N, Kawahara H, Yokosawa H, Bulletin P (2004) Girolline, an antitumor compound isolated from a sponge, induces G2/M cell cycle arrest and accumulation of polyubiquitinated p53. *Biol Pharm Bul* 27:699–701
- [260] Tsukamoto S, Takeuchi T, Rotinsulu H, Mangindaan RE, Van Soest RW, Ukai K, Kobayashi H, Namikoshi M, Ohta T, Yokosawa H (2008) Leucettamol A: a new inhibitor of Ubc13-Uev1A interaction isolated from a marine sponge, *Leucetta* af. *Microrhaphis* *Bioorg Med Chem Lett* 18:6319–6320
- [261] Takahashi A, Kurasawa S, Ikeda D, Okami Y, Takeuchi T (1989) Altemicidin, a new acaricidal and antitumor substance. *J Antibiot* 42:1556–1561
- [262] Shin HJ, Jeong HS, Lee HS, Park SK, Kim HM, Kwon HJ (2007) Isolation and structure determination of streptochlorin, an antiproliferative agent from a marine-derived *Streptomyces* sp. 04DH110. *J Microbiol Biotechnol* 17:1403–1406
- [263] Boonlarpradab C, Kaufman CA, Jensen PR, Fenical W (2008) Marineosins A and B, cytotoxic spiroaminals from a marine-derived actinomycete. *Org Lett* 10:5505–5508
- [264] Pan E, Oswald NW, Legako AG, Life JM, Posner BA, Macmillan JB (2013) Precursor-directed generation of amidine containing ammosamide analogs: ammosamides E-P. *Chem Sci* 4:482–488
- [265] Mitchell SS, Nicholson B, Teisan S, Lam KS, Potts BC (2004) Aureoverticillactam, a novel 22-atom macrocyclic lactam from the marine actinomycete *Streptomyces aureoverticillatus*. *J Nat Prod* 67:1400–1402
- [266] Stritzke K, Schulz S, Laatsch H, Helmke E, Beil W (2004) Novel caprolactones from a marine streptomycete. *J Nat Prod* 67:395–401
- [267] Li F, Maskey RP, Qin S, Sattler I, Fiebig H, Maier A, Zeeck A, Laatsch H (2005) Chinikomycins A and B: isolation, structure elucidation, and biological activity of novel antibiotics from a marine *Streptomyces* sp. isolate M045. *J Nat Prod* 68:349–353
- [268] Malet-Cascon L, Romero F, Espliego-Vazquez F, Gravalos D, FernandezPuentes JL (2003) IB-00208, a new cytotoxic polycyclic xanthone produced by a marine-derived *Actinomadura*. I. Isolation of the strain, taxonomy and biological activities. *J Antibiot (Tokyo)* 56:219–225
- [269] Beer LL, Moore BS (2007) Biosynthetic convergence of salinosporamides A and B in the marine actinomycete *Salinispora tropica*. *Org Lett* 9:845–848
- [270] Ganesan S, Velsamy G, Sivasudha T, Manoharan N (2013) MALDI-TOF mass spectrum profiling, antibacterial and anticancer activity of marine *Streptomyces fradiae* BDMS1. *World J Pharm Pharm Sci* 2:5148–5165
- [271] Leet JE, Schroeder DR, Golik J, Matson JA, Doyle TW, Lam KS, Hill SE, Lee MS, Whitney JL, Krishnan BS (1996) Himastatin, a new antitumor antibiotic from *Streptomyces hygroscopicus*. III. Structural elucidation. *J Antibiot (Tokyo)* 49:299–311
- [272] Asolkar RN, Jensen PR, Kaufman CA, Fenical W (2006) Daryamides A-C, weakly cytotoxic polyketides from a marine-derived actinomycete of the genus *Streptomyces* strain CNQ-085. *J Nat Prod* 69:1756–1759
- [273] Kim SK, Hoang VL, Kim MM (2006) Bioactive compounds derived from marine bacteria: anti-cancer activity. *J Mar Biosci Biotechnol* 1:232–242
- [274] Martin GD, Tan LT, Jensen PR, Dimayuga RE, Fairchild CR, RaventosSuarez C, Fenical W (2007) Marmycins A and B, cytotoxic pentacyclic C-glycosides from a marine sediment-derived actinomycete related to the genus *Streptomyces*. *J Nat Prod* 70:1406–1409
- [275] Smith WC, Xiang L, Shen B (2000) Genetic localization and molecular characterization of the nonS gene required for macrotetrolide biosynthesis in *Streptomyces griseus* DSM40695. *Antimicrob Agents Chemother* 44:1809–1817
- [276] Butler MS (2008) Natural products to drugs: natural product-derived compounds in clinical trials. *Nat Prod Rep* 25:475–516
- [277] J.-Y. Je, P.-J. Park, J. Y. Kwon, and S.-K. Kim, “A novel angiotensin I converting enzyme inhibitory peptide from Alaska pollack (*Theragra chalcogramma*) frame protein hydrolysate,” *Journal of Agricultural and Food Chemistry*, vol. 52, no. 26, pp. 7842–7845, 2004
- [278] T.-G. Lee and S. Maruyama, “Isolation of HIV-1 proteaseinhibiting peptides from thermolysin hydrolysate of oyster proteins,” *Biochemical and Biophysical Research Communications*, vol. 253, no. 3, pp. 604–608, 1998.
- [279] C. Lopez-Abarrategui, A. Alba, O. N. Silva et al., “Functional characterization of a synthetic hydrophilic antifungal peptide derived from the marine snail *Cenchritis muricatus*,” *Biochimie*, vol. 94, no. 4, pp. 968–974, 2012.
- [280] T.-S. Vo and S.-K. Kim, “Down-regulation of histamineinduced endothelial cell activation as potential anti-atherosclerotic activity of peptides from *Spirulina maxima*,” *European Journal of Pharmaceutical Sciences*, vol. 50, no. 2, pp. 198–207, 2013.
- [281] S.-Y. Kim, J.-Y. Je, and S.-K. Kim, “Purification and characterization of antioxidant peptide from hoki (*Johnius belengerii*) frame protein by gastrointestinal digestion,” *Journal of Nutritional Biochemistry*, vol. 18, no. 1, pp. 31–38, 2007.
- [282] E. Mendis, N. Rajapakse, H.-G. Byun, and S.-K. Kim, “Investigation of jumbo squid (*Dosidicus gigas*) skin gelatin peptides for their in vitro antioxidant effects,” *Life Sciences*, vol. 77, no. 17, pp. 2166–2178, 2005.
- [283] Y. Su, “Isolation and identification of pelteobagrins, a novel antimicrobial peptide from the skin mucus of yellow catfish (*Pelteobagrus fulvidraco*),” *Comparative Biochemistry and Physiology Part B: Biochemistry and Molecular Biology*, vol. 158, no. 2, pp. 149–154, 2011.
- [284] W.-K. Jung, E. Mendis, J.-Y. Je et al., “Angiotensin I-converting enzyme inhibitory peptide from yellowfin sole (*Limanda aspera*) frame protein and its antihypertensive

- effect in spontaneously hypertensive rats,” *Food Chemistry*, vol. 94, no. 1, pp. 26–32, 2006.
- [285] Admassu, H., Gasmalla, M. A. A., Yang, R., & Zhao, W. (2018). Bioactive peptides derived from seaweed protein and their health benefits: antihypertensive, antioxidant, and antidiabetic properties. *Journal of Food Science*, 83(1), 6-16.
- [286] Charoensiddhi, S., Conlon, M. A., Franco, C. M., & Zhang, W. (2017). The development of seaweed-derived bioactive compounds for use as prebiotics and nutraceuticals using enzyme technologies. *Trends in Food Science & Technology*, 70, 20-33.
- [287] Corinaldesi, C., Barone, G., Marcellini, F., Dell’Anno, A., & Danovaro, R. (2017). Marine microbial-derived molecules and their potential use in cosmeceutical and cosmetic products. *Marine drugs*, 15(4), 118.
- [288] Kim, S.-K., & Wijesekara, I. (2010). Development and biological activities of marine-derived bioactive peptides: A review. *Journal of Functional foods*, 2(1), 1-9.
- [289] Mayer, A. M., Rodríguez, A. D., Taglialatela-Scafati, O., & Fusetani, N. (2013). Marine pharmacology in 2009–2011: Marine compounds with antibacterial, antidiabetic, antifungal, anti-inflammatory, antiprotozoal, antituberculosis, and antiviral activities; affecting the immune and nervous systems, and other miscellaneous mechanisms of action. *Marine drugs*, 11(7), 2510-2573.
- [290] Phyo, Y. Z., Ribeiro, J., Fernandes, C., Kijjoa, A., & Pinto, M. M. (2018). Marine natural peptides: Determination of absolute configuration using liquid chromatography methods and evaluation of bioactivities. *Molecules*, 23(2), 306.
- [291] Rangel, M., José Correia de Santana, C., Pinheiro, A., Dos Anjos, L., Barth, T., Rodrigues Pires Júnior, O., Fontes, W., & S Castro, M. (2017). Marine depsipeptides as promising pharmacotherapeutic agents. *Current Protein and Peptide Science*, 18(1), 72-91.
- [292] Shinnar, A. E., Butler, K. L., & Park, H. J. (2003). Cathelicidin family of antimicrobial peptides: proteolytic processing and protease resistance. *Bioorganic chemistry*, 31(6), 425-436.
- [293] Bowers, Z., Caraballo, D., & Bentley, A. (2021). Therapeutic potential of pseudopterosin H on a prostate cancer cell line. *J Cancer Prev Curr Res*, 12(3), 82-91.
- [294] Ly, C., Shimizu, A. J., Vargas, M. V., Duim, W. C., Wender, P. A., & Olson, D. E. (2020). Bryostatin 1 promotes synaptogenesis and reduces dendritic spine density in cortical cultures through a PKC-dependent mechanism. *ACS chemical neuroscience*, 11(11), 1545-1554.
- [295] Velmurugan, B. K., Lee, C. H., Chiang, S. L., Hua, C. H., Chen, M. C., Lin, S. H., Yeh, K. T., & Ko, Y. C. (2018). PP2A deactivation is a common event in oral cancer and reactivation by FTY720 shows promising therapeutic potential. *Journal of Cellular Physiology*, 233(2), 1300-1311.





# Temperature and pH-sensitive chitosan-collagen hydrogels for antimicrobial and wound healing applications

Aiman Salah Ud Din<sup>1</sup>, Azqa Ashraf<sup>2</sup>, Mudassar Hussain<sup>3</sup>, Adnan Ahmad<sup>4</sup>, Imad Khan<sup>3</sup>, Waleed AL-Ansi<sup>3</sup>, Xiaoqiang Zou\*

<sup>1</sup>Faculty of Food and Home Sciences, Muhammad Nawaz Sharif University of Agriculture, Multan Pakistan.

<sup>2</sup>Faculty of Food Science and Nutrition, Bahauddin Zakariya University, Multan Pakistan.

<sup>3</sup>State Key Laboratory of Food Science and Resources, National Engineering Research Center for Functional Food, National Engineering Research Center of Cereal Fermentation and Food Biomanufacturing, Collaborative Innovation Center of Food Safety and Quality Control in Jiangsu Province, School of Food Science and Technology, Jiangnan University, 1800 Lihu Road, Wuxi 214122, Jiangsu, China.

<sup>4</sup>Karachi Institute of Medical Sciences Malir Cantt, Karachi Pakistan.

\*Corresponding author: Xiaoqiang Zou

Received: 10 Nov 2023; Received in revised form: 11 Dec 2023; Accepted: 18 Dec 2023; Available online: 26 Dec 2023

©2023 The Author(s). Published by Infogain Publication. This is an open access article under the CC BY license

(<https://creativecommons.org/licenses/by/4.0/>).

**Abstract**— Hydrogels have proven to be of great value because of their useful properties and functions. Temperature and pH-sensitive chitosan-collagen-based hydrogels have drawn research interest in the area of wound care. Their unique mechanism allows them to release antimicrobial agents in response to changes in the environment and aids in efficient healing of wounds. The current review aims to describe various composite hydrogels of chitosan and collagen, their temperature and pH sensitivity, the antimicrobial effect of chitosan-collagen hydrogels and their applications in wound healing. Sources and properties of chitosan and collagen have also been stated in order to highlight their importance in these hydrogels. The main focus revolves around the potential of chitosan-collagen hydrogels as antimicrobial biomaterials for healing wounds in an efficient manner.



**Keywords**— Antibacterial, hydrogels, pH, temperature, wound healing

## I. INTRODUCTION

Hydrogels' unique properties make them essential vehicles for specific medications. This is because of their well-known capacities to keep the wound interface moist, suppress infectious activity, eradicate surplus exudates from the wound, encourage wound healing, and have a reasonable level of biocompatibility with cell tissues (Vaneau et al., 2007). Hydrogel dressings are therefore recommended for wound healing (Li et al., 2016). Moreover, it is crucial to incorporate biocompatible macromolecular components into degradable hydrogel wound dressings (Jie Zhu et al., 2019).

Hydrogel dressings can be used to keep a wound wet and absorb tissue exudates. Next, as the wound area is cooled, the dressing allows oxygen to permeate and provides pain relief (Dong et al., 2014). Finally, the usage

of hydrogel dressing was more strongly linked with the characteristics of in-situ encapsulating medicines, wound sites filling, and adhesion to wounds (Tran et al., 2011). Similar to how hydrogels work as barriers against microbes, using hydrogel as a wound dressing has been a popular choice in studies.

They also provide 3-D structures for cell adhesion and development and preserve wet surroundings at the wound interface (Kokabi et al., 2007). The polymer chitosan is derived from chitin, which is the second most abundant polymer in nature. It exhibits remarkable qualities such as making it an indispensable biomaterial that is attracting significant industrial interest as a potential replacement for synthetic polymers in the future (Kurakula, 2020).

All of the body's numerous connective tissues, such as the skin, bones, ligaments, tendons, and cartilage, include

collagen, the most prevalent structural protein. Collagen is another essential element in the wound-healing process. Collagen is essential for every stage of wound healing, including hemostasis, inflammation, proliferation, and (Liu et al., 2019). Collagen serves as the natural structural foundation for the synthesis and growth of new tissue. Collagen, the most structural protein found in the extracellular matrix of the body's connective tissues, including skin, bones, ligaments, tendons, and cartilage, is crucial for wound healing. Collagen is essential for all phases of wound healing, including hemostasis, inflammation, proliferation, and remodeling. It acts as a natural structural basis for the development of new tissue (Gu et al., 2019).

In hydrogels, there exist both synthetic and natural polymer chains (Ahmad et al., 2022). Agarose, alginate, chitosan, collagen, gelatin, hyaluronic acid, and cellulose derivatives are examples of natural polymers frequently employed in hydrogel formulations (Gasperini et al., 2014)). These polymers are useful for biological applications because of their inherent biocompatibility and biodegradability. It is possible to create hydrogels with certain properties by adjusting the chemical and physical properties of synthetic polymers (Almajed et al., 2022). To join the polymer chains and create the hydrogel's network structure, crosslinking agents are used. These substances might be chemical or physical. Physical crosslinking, including reversible connections like hydrogen bonds or physical entanglement, can be brought on by changes in pH, temperature, or other environmental factors. Covalent bonds between polymer chains are formed via chemical crosslinking, which is commonly accomplished through chemical processes like condensation or free radical polymerization (Ertl et al., 2020).

Here, we will review about pH and temperature sensitive chitosan and collagen based hydrogel systems and

explore their properties with different natural and synthetic polymers by using different crosslinking methods while simultaneously discussing the application of antibacterial and wound healing along with other biomedical materials that the hydrogels can be used with some recent advancements.

## II. PROPERTIES OF CHITOSAN AND COLLAGEN AS BIOMATERIALS

### 2.1 Chitosan

Chitosan is produced by partially deacetylating naturally occurring insoluble chitin (Martínez-Ruvalcaba et al., 2007) found in the exoskeletons of insects, fungi (Merzendorfer, 2011), and crustaceans (Khor & Lim, 2003). Because of the hydrogen interactions between hydroxyl and acetamide groups, chitin has a hard crystalline structure. A higher concentration of amino groups and improved water solubility are obtained when chitin undergoes partial deacetylation and transforms into chitosan. Chitosan deacetylation is increased proportionately, and biocompatibility and biodegradability are improved (Murakami et al., 2010).

#### 2.1.1. Sources of chitosan

Although other species including lobster, crayfish, and oysters have also been used, prawns and crabs are the most frequently mentioned sources (Fig. 1) in the literature when discussing the raw materials used to prepare chitosan (Rizeq et al., 2019). The weight percentage (wt%) of chitin varies depending on the organism. For example, the waste from crustacean shells typically contains 30% to 50% calcium carbonate and 20% to 30% chitin. However, in certain lobster genera, like *Nephrops* sp. and *Homarus* sp., the chitin content of the shells ranges from 60% to 75%, which is the highest of all chitin-containing species (Arbia et al., 2013).

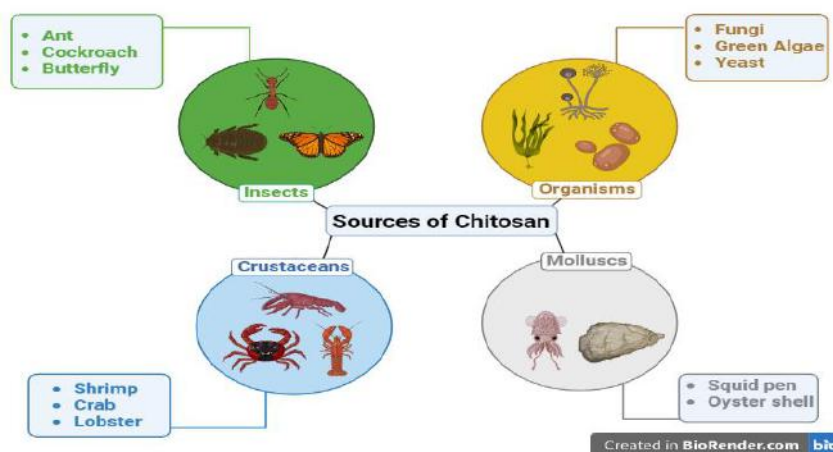


Fig. 1: Sources of Chitosan

Studies that have already been conducted on the extraction of chitin or chitosan from crustacean byproducts that contain 20% (wt%) or more of chitin have produced encouraging results when used as industrial feedstocks for the synthesis of chitosan. For example, *Procambarus clarkii* (crayfish) by-products, which included the entire animal body, thorax, and claws, have been found to contain roughly 20% to 23% (by weight) of chitin. Because this source is readily available and inexpensive, it already justifies its use as an economically viable source for chitin production on an industrial scale (Bautista et al., 2001).

The economic and environmental benefits of using these crustacean sources for chitosan preparation have also been suggested by previous research. This is because 40–50% of the mass of crustaceans that are harvested for human consumption is wasted, and the majority of this waste is disposed of in the sea, where it causes serious pollution (Vázquez et al., 2013). Consequently, it is possible to identify byproducts of crustacea, such as lobster

cephalothorax, as a good source for the industrial synthesis of chitosan.

### 2.1.2. Chemical structure of chitosan

Chitosan (CS) is a naturally occurring cationic polymer that is derived from chitin through a process of alkaline deacetylation (**Fig. 2**). It shares structural similarities with glycosaminoglycan, a component of the extracellular matrix (Raj et al., 2018). Covalent bonding between the chitosan macromers results in chemically cross-linked hydrogels; this bond formation is irreversible. Chitosan cross-linked system, hybrid polymer networks (HPN), interpenetrating polymer networks (IPN), and semi-interpenetrating polymer networks (SIPN) are the four states of creation of chemical cross-linked hydrogels. The second chain in the derivation may resemble or differ from the first structural unit (Shi et al., 2018). Chemical cross-linking is caused by hydroxyl groups and amines on chitosan chains. Chemical cross-linking can happen through photopolymerization reactions or cross-linkers (Fidalgo et al., 2018).

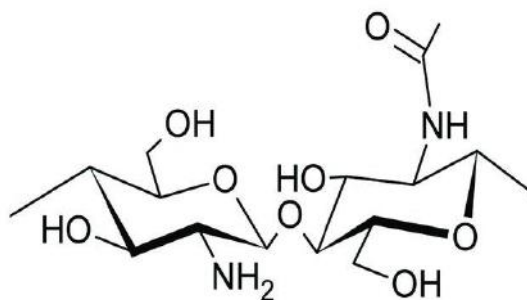


Fig.2: Chemical Structure of Chitosan

It is common to see hydrogen bonds form between the functional groups of chitosan and polyurethane chains. In order to improve the interaction between the two components, this is significant (Mohraz et al., 2019). The FTIR spectra of the composites studied confirmed the presence of distinct absorption bands for PUR and Chit (Qin & Wang, 2019). The addition of Chit to the PUR matrix resulted in a shift in the C=O wave number from about 1700  $\text{cm}^{-1}$  to 1640  $\text{cm}^{-1}$ , as well as an increase in the band of –O–H and –N–H stretching vibration at around 3500  $\text{cm}^{-1}$  to 3400  $\text{cm}^{-1}$ . These unambiguously showed that PUR and Chit in the third composite formed hydrogen bonds (Hernández-Martínez et al., 2017).

FTIR scans showed a comparable shift in the carbonyl band to a lower wavenumber as Chit in composites increased (Gupta & Kim, 2019) (**Fig 3**). The study analyzed six composites with varying chitosan flakes percentages, revealing a uniform nanoflake structure. Monitoring changes in polyurethane structure was challenging due to

similar functional groups. The absence of a urea peak in FTIR spectra suggests no secondary reaction or covalent bond formation (Garnica-Palafox & Sánchez-Arévalo, 2016).

It is possible to insert chitosan into the polyurethane framework after lowering its size to the nanoscale, as verified by FTIR (Gupta & Kim, 2019). Even if there isn't a distinct continuous phase (matrix) and filler, the materials that were created were nevertheless referred to as biocomposites. Nevertheless, compared to traditional composites, the material's trend of changing properties is distinct. Adding chitosan to the polyurethane framework increased the material's mechanical strength by increasing cross-linking. ATR-FTIR analysis of eight composites revealed that PUR chains were present on the surface of the samples, while Chit particles were submerged in the bulk of the matrix (Brzeska et al., 2019).

### 2.1.3. Properties of chitosan

Chitosan is a naturally occurring polysaccharide that is renewable, non-toxic, biodegradable, and biocompatible (Croisier & Jérôme, 2013). The solubility of chitosan is attributed to the protonation of the amino group (NH<sub>2</sub>) on its chains into a positively charged group (NH<sub>3</sub><sup>+</sup>) at pH values lower than its pK<sub>a</sub> (pH < 6.2). Numerous applications, including tissue engineering, drug delivery, water treatment, biosensors, and water treatment (Teotia et al., 2015), are made possible by soluble chitosan (Kim & Kim, 2017). Chitosan amino groups can be neutralized to produce physical chitosan hydrogels (Ladet et al., 2008). Nevertheless, chitosan has a low mechanical strength, particularly when it is wet (Latza et al., 2015).

3D printing of a chitosan physical hydrogel was described to construct the structure on a three-axis positioning platform. This involved directly depositing the ink in air (Fig. 4). By dissolving chitosan in an acidic combination, a low concentration (8 wt%) 3D-printable chitosan ink was created. This ink was directly converted into three-dimensional scaffolds layer by layer by solvent evaporation after being extruded through micronozzles (Wu et al., 2017). The inks' rheological characteristics are crucial to the extrusion-based 3D printing techniques. Researchers looked on apparent viscosity related to the process in order to find the right concentration of polymer for solvent-assisted 3D printing (Guo et al., 2013).

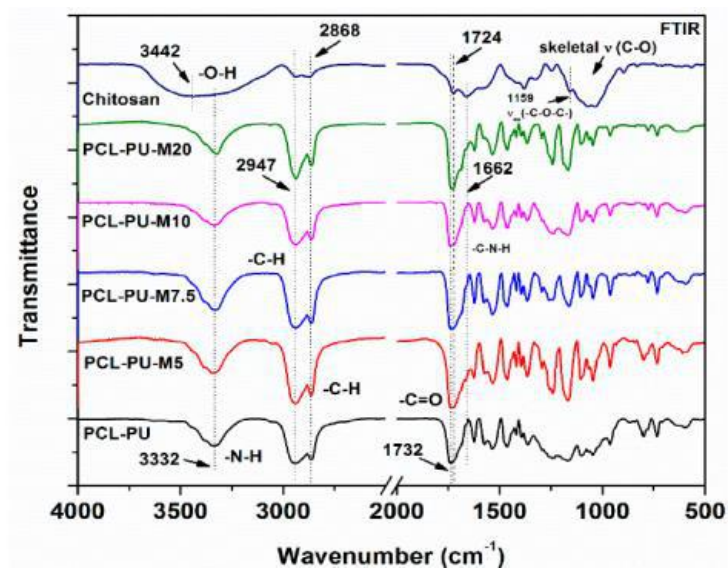


Fig.3: Chitosan FTIR Spectra with 6 composites

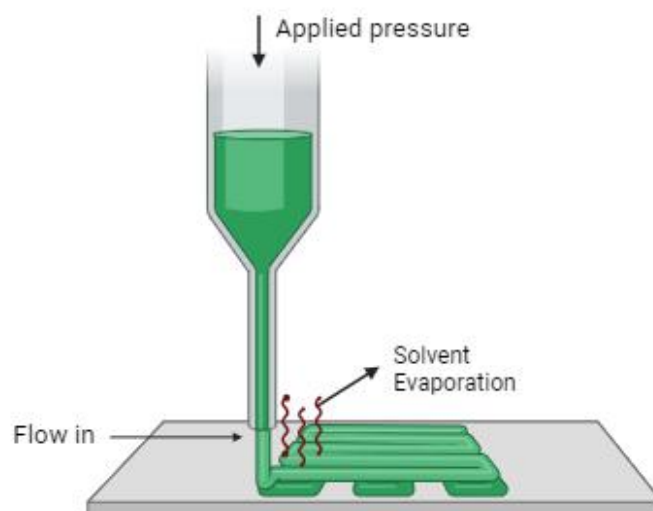


Fig.4:3D printing process diagram and key process parameters

A wide range of investigations have been undertaken to examine the rheological properties of solutions derived from chitosan, encompassing physical chitosan hydrogel, thermosensitive chitosan-glycerol-phosphate solutions, and chitosan blends (Cho et al., 2005). Scientists have been examining chitosan closely to solve a variety of problems. Chitosan is a polysaccharide derived from chitin by the process of deacetylation (Ali & Ahmed, 2018). It is characterized by its relatively low cost and high yield. It is the second most abundant natural biopolymer (Tripathy et al., 2018). However, because of their excellent biodegradability, biocompatibility, immunogenicity, and low toxicity, chitosan hydrogels have previously been used in a wide range of disciplines, including material science (Fu et al., 2016) and biomedicine (G. Chen et al., 2017). Thus, chitosan has been the subject of numerous prior research and among the several techniques that have been suggested, solubilizing chitosan in an acidic aqueous media has historically been the most widely used technique for creating chitosan hydrogels (Bhattarai et al., 2010).

Nevertheless, the limited mechanical properties of chitosan hydrogels impose restrictions on their potential uses (Wang et al., 2016). Several approaches have been employed thus far to enhance the of chitosan hydrogel's mechanical properties (Cao et al., 2018). These methods encompass chemical crosslinking, incorporation of nanofillers possessing superior mechanical properties, and blending with other polymers (Li et al., 2018). While there are moderate enhancements in the mechanical qualities, the inherent characteristics of chitosan are compromised. Moreover, it was discovered that several of the crosslinking agents exhibited toxicity or resulted in undesirable interactions with the bioactive components (Oryan et al., 2018). Consequently, improving mechanical properties of chitosan hydrogel has emerged as a prominent area of research. A unique solvent system was proposed by utilizing alkali-urea aqueous solutions for the synthesis of chitosan hydrogel. This approach resulted in notable improvements in both hardness and toughness, all achieved without the need of any cross-linking agents (Cao et al., 2018).

Alkali-urea solution system was employed for the synthesis of chitosan hydrogel. The research incorporated Ag nanoparticles as both a filling and secondary reinforcing material in order to enhance the mechanical properties of chitosan hydrogel. The objective was to develop a chitosan hydrogel with exceptionally high mechanical properties (Zhao et al., 2018). The primary design principle is utilizing the amino groups present in chitosan as a chelating agent for Ag ions through coordination interactions, hence enhancing the mechanical strength. The secondary objective of incorporating Ag nanoparticles into the chitosan hydrogel is

to enhance its antibacterial properties, hence mitigating the risk of wound infection (Fan et al., 2014). Silver is a frequently utilized antimicrobial agent owing to its broad-spectrum antibacterial activity against aerobic and anaerobic microorganisms (Wang et al., 2018).

Furthermore, chitosan possesses the advantageous characteristic of being a biocompatible polyelectrolyte. This property enables it to function as a stabilizing ligand, so restricting the toxicity of silver metal while yet permitting its antimicrobial activity for infection control purposes (Fan et al., 2014). Subsequently, varying proportions of Ag ions are introduced into the structured hydrogel to form chelation complexes with chitosan (Yi et al., 2003). The reductive silver nanoparticles were incorporated into the system using trisodium citrate as a green reducing agent. The objective was to create a chitosan-Ag nanoparticles hydrogel that would exhibit enhanced mechanical properties, increased antibacterial activity, and accelerated wound healing abilities. The hydrogels were subjected to a comprehensive evaluation of their mechanical properties, swelling characteristics, antibacterial activity, and wound healing impact which were found to be satisfactory (Thomas et al., 2007).

#### **2.1.4. Role of chitosan in wound healing**

Extensive research has been conducted on chitosan-based materials, with particular focus on wound dressings, due to their diverse range of properties such as antibacterial, anti-inflammatory, and biomedical applications. The antibacterial and anti-inflammatory properties of chitosan have shown promise in the field of wound healing, positioning it as a potential biomaterial (Ahmed & Ikram, 2016). Optimal qualities tailored to specific wound types, cost-effectiveness, and minimal patient inconvenience are key considerations for the development of effective dressings. Chitosan has various applications in multiple domains along with concurrent researches in the field of wound healing. Chitosan has antimicrobial properties which makes it a suitable material for clinical utilization and biomedical applications. It has an important role in wound healing procedures. Wound healing is enhanced by chitosan and synthetic/natural polymer scaffolds. The utilization of chitosan-based scaffolds immobilized with oil for wound healing purposes is now under investigation. Drug loaded scaffolds with chitosan as a base material for wound healing is an area of interest around the world. Chitin and chitosan are known to stimulate wound healing, with research showing their potential to expedite the process. These materials are used in various forms, including nano fibers, gels, scaffolds, membranes, filaments, powders, granules, sponges, and composites. Their primary biochemical functions include

activating polymorphonuclear cells, stimulating fibroblast activity, creating cytokines, migrating giant cells, and stimulating the synthesis of type IV collagen (Mezzana, 2008).

Nano-fiber matrices are promising for tissue engineering in skin substitutes due to their ability to facilitate oxygen diffusion, high porosity, diverse pore sizes, and

morphological resemblance to the skin's extracellular matrix. These properties enhance cell adhesion, migration, and proliferation (**Fig. 5**). Progress in chitin and chitosan nanofibril materials has also improved flexibility and utility for creating novel bio-related products. The field of process chemistry has made significant progress in producing these materials (Mattioli-Belmonte et al., 2007).

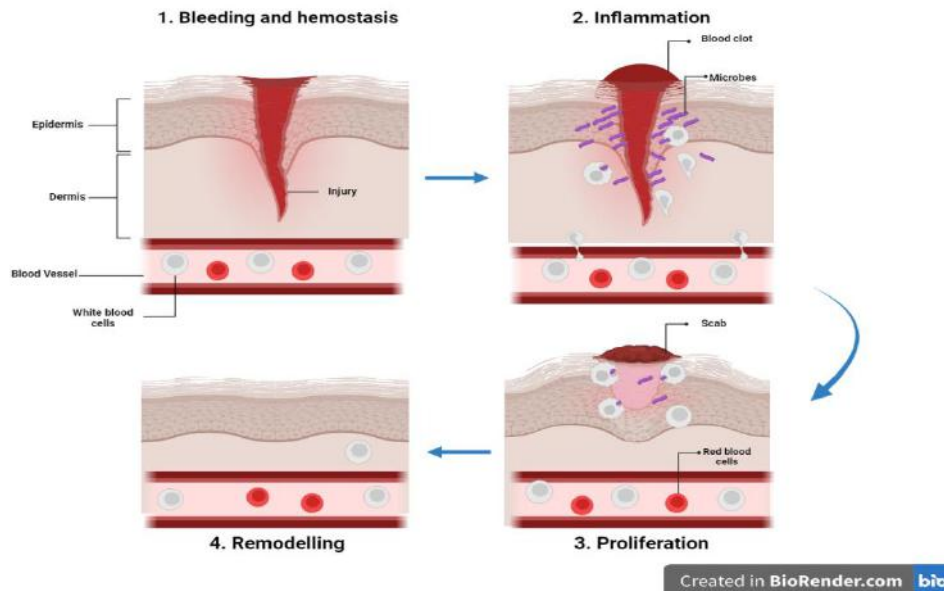


Fig.5: Mechanism of wound healing with diagram

## 2.2. Collagen

Collagen is a highly prevalent protein synthesized within the human body. The process under consideration is responsible for maintaining the integrity and strength of bodily tissues through the formation of supportive networks that span across cellular structures. Over time, the structural integrity of the fiber deteriorates, resulting in several consequences, one of which is the development of wrinkles on the skin (Chang et al., 2012). It has been empirically demonstrated that the consumption of hydrolyzed protein can facilitate the replacement of damaged fibers with new ones. Consequently, the promotion of collagen creation ensued, so facilitating the process of healing and enhancing the overall appearance of the tissue (Schagen, 2017).

Collagen, as reported by the Protein Data Bank, is the predominant structural protein found in the human body. It provides essential support to a variety of tissues, including tendons, skin, and teeth (with collagen being connected to mineral crystals). Collagen fibers are frequently observed to possess a white coloration, exhibiting an opaque appearance, and are easily identifiable within various tissue samples. Collagen is classified as a viscoelastic substance, characterized by its notable tensile strength and limited extensibility. It is widely recognized for its low immunogenicity, hence reducing the likelihood of rejection

whether administered orally or by injection into a foreign entity. The fractions that are capable of inducing an immunological response are specifically situated inside the helical area of the chains and the telopeptide region (Kumar et al., 2014).

### 2.2.1. Sources of Collagen

Collagen, a naturally occurring polymer present mostly in fibril forming proteins within the cartilage, bone, tendon and skin, exhibits versatile applications in several industries such as food, cosmetics, and medicines (Wang et al., 2013). The extraction of commercial collagen from several wild species has been extensively investigated because to its significant economic value. While it is true that mammals possess collagen protein, non-mammals are also of significant interest due to their likeness to the human body and their potential as abundant economic resources. Collagen is sourced from several origins, encompassing fish, avian species, bovines, marine organisms, kangaroo tails, chicken feet, horse tendons, frog bones and skin, rat-tail tendons, sheepskin, and sporadically even human sources (Silvipriya et al., 2015). However, the use of pig skin for collagen extraction is prohibited in certain countries with a mostly Muslim population (Wang et al., 2014). Since the 1930s, pig skins and bovine have been the primary sources of collagen in commercial applications, while fish

scales are used in religious practices to reduce exposure to infections. Research has been conducted to find alternative collagen sources, with the industry focusing on mammalian collagen. Type I collagen from fish scales has similar properties to mammalian collagen, and marinated or salted skins have lower protein content compared to cold-water fishes (Rawat et al., 2021).

Collagen utilized in industrial settings primarily comes from mammalian sources, like pig and cow collagen.

Since these collagens are associated with several problems, such as an outbreak of foot-and-mouth disease (FMD), an outbreak of bovine spongiform encephalopathy (BSE), and religious prohibitions, it is imperative to find a new source (Duan et al., 2009). Numerous marine species have been identified as potential safe and alternative sources for collagen extraction. These species include eels, cuttlefish, seaweed pipe fish, squid, catfish, and ocellate puffer fish (Veeruraj et al., 2013).

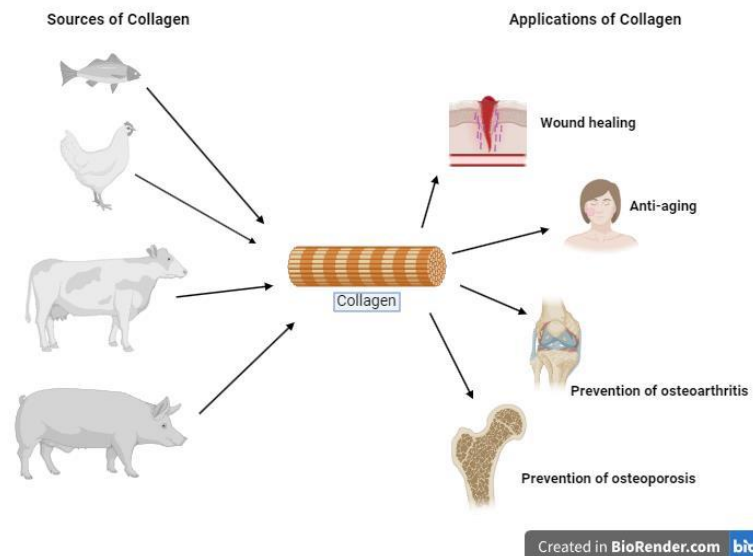


Fig. 6: Sources and Applications of Collagen

In addition, compared to collagen from mammals, that from marine creatures is less immunogenic, less poisonous, and has a higher collagen concentration. The skin, scales, bones, and fins of freshwater and marine fish species are the primary suppliers of collagen. Furthermore, skin, scale, and bone—all of which have a high collagen content—make up almost 30% of the wastes produced by the fishing industry during the processing of fish (Wang et al., 2008). Fish skin typically has a lot of collagen that can be harvested and utilized (Liu et al., 2008). The finest solutions for effective waste management and the creation of value-added goods that boost the fishing industries' profits may be found in the environmentally friendly extraction of collagen from these wastes (Kittiphattanabawon et al., 2005). Fish collagen has a number of drawbacks, including low mechanical strength, low amino acid content, quick biodegradation, and melting point. Fish collagen can be functionally modified and combined with other synthetic or natural polymers to solve these issues (Subhan et al., 2015).

There are many other sources of collagen, but at the moment, animal collagen is the most common type used in collagen products, the majority of which are made

from raw materials like cow's milk (Silvipriya et al., 2015). Numerous skin fragments from pigs and cows are used to make the majority of collagen products. Collagen makes up up to 85% of the protein in tendons and makes up one-third of the protein mass in cows. Immunological, zoonotic, and religious sensitivities restrict the use of collagen obtained from animals (Kisling et al., 2019). To prevent FMD (foot and mouth disease) and mad cow disease, researchers are working to find a safer source of collagen. In contrast to the adverse inflammatory and immunological reactions in terrestrial animals as well as pandemic health problems, research is being done on marine sources (Maschmeyer et al., 2020). There are many other sources of marine collagen, such as various marine sources, particularly microalgae, and marine vertebrates. At the moment, marine fish, jellyfish, sponges, and other creatures are the primary subjects of collagen extraction research from marine organisms for tissue engineering biomaterials. Collagen is abundant in the epidermis, muscles, and cartilage tissue of these aquatic creatures (Smith et al., 2023).

The amino acid composition and biocompatibility of collagen derived from marine sources are similar to

those of traditional terrestrial mammalian collagen. However, marine collagen offers additional benefits over mammalian collagen, such as easy extraction, abundant sources, which are particularly useful in the fishing and fish processing industries (Ge et al., 2020). Fish are actually widely available, have no religious limitations, and pose little risk of spreading disease, which makes their skin an excellent choice for type I collagen extraction (Lim et al., 2019). Interestingly, it has been observed that certain

collagens derived from marine sources can denature at temperatures below the typical physiological temperature of humans. Some collagen-derived biomaterials are practically challenging because of this thermal instability, primarily when employed for human medical purposes (Felician et al., 2018).

### 2.2.2. Chemical structure of collagen

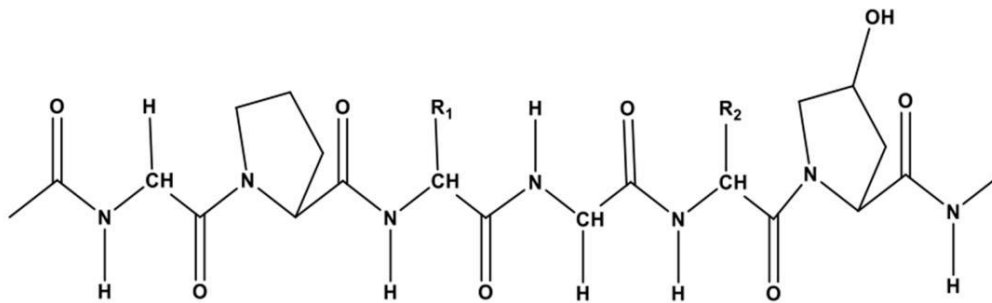


Fig.7: Chemical Structure of Collagen

### 2.2.3. Properties of collagen

Collagen exhibits a distinct structural characteristic in the form of elongated fibrous arrangements, setting it apart from globular protein enzymes. The process involves catabolic activity driven by collagenolytic enzymes and phagocytosis, which is the outer element of the ECM, forming collagen, which supports cells or tissue and has tensile strength. Collagen is primarily composed of ligaments, muscles, bones, skin, the lens, and the cornea. Findings indicate that collagen fibrils in aged skin display signs of fragmentation and uneven distribution, in contrast to the plentiful, dense, and orderly arrangement of collagen fibrils observed in youthful skin (Shin et al., 2019).

Collagen is a versatile and biodegradable material with desirable features such as biocompatibility, accessibility, versatility, cell compatibility, water affinity, high tensile strength, and body absorbability. Its bioactive properties enable it to create gum or gel-like substances, facilitating cellular healing. Collagen plays a crucial role in wound healing, regulating tissue structure and restoring strength in compromised skin. Skin scarring from burns, surgeries, and physical trauma strains the healthcare system, especially for children with significant scars. Type I and type III collagen are the predominant components of scar tissue (Toshniwal et al., 2019).

TGF- $\beta$  regulates collagen type I synthesis, promoting scar formation and fibrosis during remodeling. Scar tissue has a unique unidirectional cross-linking pattern, resulting in lower functional quality compared to normal

collagen. However, many tissues, like bone, can heal without damaging their structure or function. Collagen has enhanced biocompatibility characteristics and a reduced cytotoxic impact, making it a potential candidate for healing processes. Overall, collagen's unique characteristics make it a promising candidate for repairing and repairing damaged tissues (Agarwal et al., 2016).

Collagen in the human body is adaptable and can be used in bioactive coated platforms to enhance the integration of implantable scaffolds. Hyphapatite (HA) is used for tissue regeneration, and certain fish skin has bioactive properties, making it suitable for human skin treatment. The skin contains eight forms of collagen, each maintaining the skin's smoothness, firmness, and resilience. Enzymatic hydrolysis of triple helix structures generates oligopeptides, which are then converted into bioactive di- and tripeptides. Collagen accumulation on the skin forms a bio-matrix (Bolke et al., 2019).

Being one of the most prevalent structural proteins in the mammalian extracellular matrix (ECM), collagen has unique properties that promote the rapid healing of damaged skin tissue. The primary constituent of connective tissues is collagen type I. Short analogs have also been produced for tissue engineering applications, such as controlling the wound healing response, and they are easily synthesized and purified. The impact of various collagen implants on the promotion of skin and corneal wound healing is covered in this review. These include hydrogels and sponges made of collagen as well as films and membranes (Sklenářová et al., 2022).



Currently, the inclusion of collagen fibers with 50-200 nanometer diameter contributes to the assessment of mechanical properties, owing to their resemblance to protein-like structures. Nevertheless, while considering the perspective of scientists, the mechanical characteristics of collagen remain uncertain. However, it is worth noting that the primary drawback lies in its restricted mechanical properties. The significance of its duty necessitates the utmost importance of its exceptional mechanical qualities (Haaparanta et al., 2014).

Collagen nanofiber mats are being used in scaffolds for organ tissue enhancement due to their exceptional mechanical qualities and flexibility. These biomaterials provide temporary support to damaged organs, enhance cell adhesion and proliferation, and are influenced by factors like material creation, porosity, thickness, and diameter. Synthetic compounds and natural polymers are used to enhance mechanical strength and low wear strength in transplantation procedures. Collagen impacts cellular processes like chemotaxis, adhesion, migration, and morphogenesis, and polymeric aggregations of collagen-platelets contribute to hemostatic effects in human body cells (Golieskardi et al., 2020).

#### 2.2.4. Contribution of collagen in tissue regeneration

The current evaluation of fish-derived extracts as dietary supplements for their ability to facilitate skin regeneration is limited (Lapi et al., 2021). Tissue engineering can be achieved through two distinct methodologies. Two types of biomaterials can facilitate tissue regeneration: biomaterials that only promote tissue regeneration, and biomaterials that incorporate growth factors and supportive cells to further increase tissue regeneration. In the context of skin injury treatment, Cinzia and her research team propose the utilization of sea urchins as a source of native collagen in the development of collagen-based skin-like scaffolds (CBSS). Specifically, they suggest employing sea urchin food waste to construct bilayer CBSS, which consists of both two-dimensional (2D) and three-dimensional (3D) components. The present study describes a methodology centered around the isolation of collagen that is abundant in fibrillar glycosaminoglycan (GAG) from discarded sea urchin gonads (Dong & Lv, 2016).

The characteristics of sea urchin-sourced chondroitin sulfate-based biomaterials were examined, focusing on their microstructure, mechanical stability, water permeability, and ability to prevent bacterial infiltration and promote fibroblast proliferation. Results showed that a 2D collagen membrane effectively mitigates water evaporation and protein diffusion, while three-dimensional collagen scaffolds mimic the dermal layer

structure and function, facilitating fibroblast infiltration. These findings suggest potential environmental sustainability and economic feasibility for tissue regeneration (Ferrario et al., 2020).

To generate collagen sponges possessing hemostatic characteristics, the process involves the crosslinking of collagen type I derived from the jellyfish *R. esculentum* using 1-ethyl-3-(3-dimethyl aminopropyl) carbodiimide (EDC). Research conducted on animal subjects has demonstrated that the utilization of sponges composed of EDC collagen exhibits a notable ability to rapidly absorb blood. This can be attributed to their substantial capacity for water absorption, as well as their facilitation of blood cell aggregation at the location of a recent lesion (Cheng et al., 2017). Biomaterials derived from collagen sourced from marine sponges belonging to the *Hexactinellida* class exhibit notable efficacy in the context of bone regeneration. In addition to possessing silicon, calcium, and spongin as constituents of their spicules, these sponges also can undergo regeneration. The primary roles of these structures are to provide structural support for the organism during its growth and development, as well as to provide as a means of protection against potential predators. The chondrogenic properties of collagen isolated from jellyfish, specifically *Rhopilema esculentum*, have been seen to resemble those of human collagen I in animal tests. This suggests that jellyfish collagen could potentially serve as a viable alternative to traditional swine collagen I scaffolds in the field of cartilage regeneration (Felician et al., 2018).

#### 2.3. Hydrogel preparation by different crosslinking methods

Collagen-based hydrogels are created by self-assembling collagen fibers in aqueous solvents. However, their properties decrease during extraction and application, necessitating modification for biological uses. Changes in solvent conditions, external additives, and crosslinking mechanisms can influence the structure and properties of these hydrogels, modulating collagen molecule self-assembly (Cheng et al., 2019).

##### 2.3.1 Solution Condition

Collagen-based hydrogels are subject to the effect of multiple parameters, including solution conditions such as collagen concentration, polymerization temperature, and polymerization pH (Freytes et al., 2008). There exists a causal relationship between the self-assembly of the collagen base and the concentration of collagen (Stepanovska et al., 2021). Studies show a correlation between collagen concentration and hydrogel mechanical properties. An increase in collagen concentration reduces pore size in collagen-based hydrogels, potentially impacting

cell inoculation and viability. The manufacturing process of collagen hydrogels is significantly influenced by temperature. Most gelation occurs at 37°C, but some studies use 25°C or cryogenic conditions. The process can A causal

relationship exists also occur under cryogenic conditions, characterized by temperatures below zero degrees Celsius (Carvalho et al., 2022).

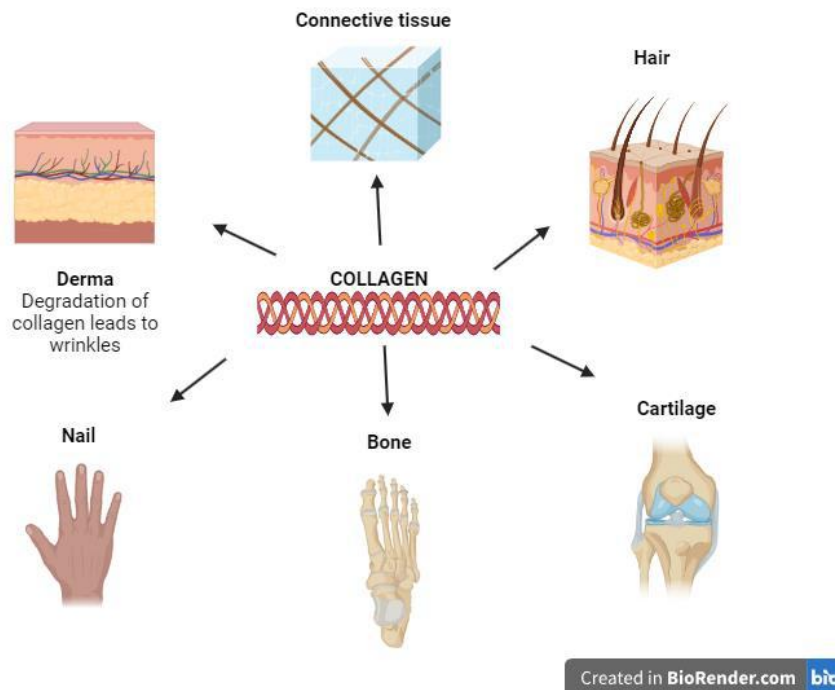


Fig. 8: Role of collagen in tissue regeneration

### 2.3.2 Physical Crosslinking

Physical crosslinking is a process that creates a three-dimensional network structure of collagen using physical stimuli like UV light,  $\gamma$ -ray irradiation, heating, and freeze-drying. This creates a viscoelastic gel system without introducing harmful chemicals. Dehydrothermal (DHT) treatment is another technique, subjecting collagen molecules to high temperatures in a vacuum environment. However, DHT results in collagen deformation, which can take several days to occur. Ultraviolet radiation can induce unpaired electrons in aromatic amino acid residues, specifically chromic acid and phenylalanine. The irradiation of collagen molecules can result in the generation of ions, which in turn can facilitate the creation of crosslinking between nearby collagen molecules (Bax et al., 2019). Nevertheless, collagen exhibits sensitivity towards UV radiation. Collagen degeneration can occur because of very elevated temperatures and prolonged periods of exposure. The processes of crosslinking and denaturation are in opposition to one other when exposed to UV irradiation. The ultimate equilibrium of these two processes has an impact on the ultimate mechanical characteristics and degradation of collagen biomaterials (Sionkowska et al., 2020).

Crosslinking, a complex process involving physics and chemistry, has garnered significant interest from researchers due to its complex nature and difficulty in precise transformation (L. Xu et al., 2022). Typically, this method entails the interaction between the photosensitizer and ultraviolet (UV) radiation, resulting in the formation of intra- and intermolecular connections inside the collagen fibers. The crosslinking reaction of collagen caused by UV-riboflavin or UV-GelMA is a widely employed method in the field of skin tissue treatment (Yang et al., 2022).

### 2.3.3 Chemical Crosslinking

Chemical crosslinking is a method used to improve the properties of biomaterials by altering functional groups within collagen. This process results in the formation of a desirable collagen hydrogel by crosslinking polymer chains. Crosslinking facilitates the conversion of 1-ethyl-3-(3-dimethylaminopropyl) carbodiimide (EDC) into urea derivatives that are soluble in water, while ensuring that they are not released into the collagen matrix (Grabska-Zielińska et al., 2022).

EDC/HNS (N-hydroxysuccinimide) shows a reduced level of cytotoxicity, while significantly improving the physicochemical characteristics of collagen (Feng et al., 2020). The collagen scaffold possesses several active groups, including hydroxyl and ester bonds, which have the

capability to directly interact with amino acids or proteins. Dialdehyde starch (DAS), a polymeric aldehyde compound, is synthesized through a chemical interaction between native starch and periodate. It initiates a crosslinking reaction with collagen's amino and imino groups, preserving its fundamental structure and enhancing its biological stability. DAS is characterized by minimal toxicity, biodegradability, antiviral capabilities, and mechanical properties (L. Xu et al., 2022).

### 2.3.4 Enzymatic Crosslinking

Enzymatic crosslinking is preferred over physical and chemical methods due to its advantages such as mild reaction conditions, absence of byproducts, exceptional specificity, and enhanced catalytic efficiency. It uses specialized enzymes like LOX (lysyl oxidase), MTG (glutamine transaminase), and HRP (horseradish peroxidase) to modify amino groups and produce protofibril connections (Ying et al., 2019). The observed phenomenon demonstrates a notable level of catalytic efficiency and a desirable degree of response to the surrounding environment. In physiological circumstances, the stability of collagen is achieved through enzymatic processes that occur after the translation of its protein sequence. This mechanism facilitates the preservation of collagen's structural integrity, flexibility, and physiological functionality (Zhao et al., 2016). Glutamine transaminase (MTG) has emerged as a prevalent enzyme employed for enhancing the mechanical strength of collagen (Lei et al., 2020).

The enzyme glutamine transaminase is responsible for the conversion of glutamine residues in collagen's  $\gamma$ -hydroxylamine group into an acyl receptor. Subsequently, the acyl transfer process facilitates the formation of an isopeptide bond, leading to the establishment of a covalent cross linkage inside the collagen structure (Jiang et al., 2019). Horseradish peroxidase (HRP) is a plant peroxidase that has been extensively utilized in commercial applications. The enzyme known as horseradish peroxidase (HRP) facilitates the synthesis of polymers rich in phenolic compounds through the utilization of hydrogen peroxide ( $H_2O_2$ ) as an oxidizing agent (Frayssinet et al., 2020). Collagen comprises several tyrosine residues that can undergo oxidation by the HRP- $H_2O_2$  system, resulting in the production of active free radicals. These radicals can then engage in polymerization processes with collagen (Cao et al., 2020). Laccase, often known as LAC, is an oxidase that contains multiple copper ions. Evidence for the enhanced stability of collagen by crosslinking with LAC has been noticed (L. Xu et al., 2022).

## 2.4 Hydrogel preparation via chitosan crosslinking

Chitosan's polysaccharide chains are anchored by hydrogen bonding, hydrophobic interactions, and ionic interactions, as per intermolecular forces. The molecular weight and ionic strength have been shown to exert an influence on these interactions. The process of cross-linking chitosan polymers is imperative for enhancing chitosan's inherent characteristics, particularly its stability and endurance, with the ultimate objective of facilitating drug delivery. The categorization of chitosan-based hydrogel networks is determined by the method employed for chitosan cross-linking and manufacturing (Qun & Ajun, 2006).

### 2.4.1 Preparation of chitosan hydrogels via chemical cross-linking

Chemically cross-linked hydrogels are produced by covalently linking chitosan macromers, leading to the development of bonds that cannot be reversed. Chemical cross-linked hydrogels can be classified into four unique states of formation, namely: a) chitosan cross-linked system, b) hybrid polymer networks (HPN), c) interpenetrating polymer networks (IPN), and d) semi interpenetrating polymer networks (SIPN).

The phenomenon of chemical cross-linking in chitosan chains can be linked to the presence of amines and hydroxyl groups. Chemical cross-linking can be accomplished through the utilization of cross-linkers or by means of a photopolymerization reaction (Sheng et al., 2019).

### 2.4.2 Physical cross-linking

Another type of crosslinking involves the use of physical interactions to create chitosan-based hydrogel networks. Ionic interactions can give rise to the formation of ionically cross-linked chitosan hydrogels and polyelectrolyte complexes. Additionally, secondary interactions can occur within networks known as grafted chitosan hydrogels and entangled chitosan hydrogels (Berger et al., 2004).

### 2.4.3 Chemical versus physical cross-linking

Hydrogel stability depends on the cross-linking mechanism used. Covalent cross-linked hydrogels have resilience against environmental conditions but require additional purification to remove harmful agents. Physically cross-linked hydrogels have higher biocompatibility due to the absence of chemical cross-linkers, making them more bearable. However, these materials may have restricted mechanical stability and are susceptible to environmental changes like pH, temperature, or ionic strength fluctuations. Therefore, it's crucial to incorporate extra purification procedures for these systems (Berger et al., 2004). The unique characteristic of physically cross-linked hydrogels is

highly advantageous in the development of stimuli-responsive systems that exhibit sensitivity to environmental conditions. These systems have the potential to be utilized for targeted medication administration under specific circumstances (Zhang et al., 2009).

### III. CHITOSAN AND COLLAGEN COMPOSITE HYDROGELS PREPARATION USING DIVERSE POLYMERS

#### 3.1. Chitosan and collagen based composite hydrogels with natural polymers

Natural polymer hydrogels exhibit a diminished antigenicity, favorable biocompatibility, and a reduced likelihood of eliciting immunological rejection. In addition, some natural polymer hydrogels possess intrinsic antibacterial characteristics, including chitosan and cellulose. Nevertheless, the antimicrobial characteristics exhibited by these natural polymers are insufficient for their application in clinical settings. Previous research has demonstrated the incorporation of antibiotics and antibacterial agents, including metal nanoparticles and conventional drugs, into hydrogels (Zhong et al., 2020). Furthermore, sophisticated techniques have been employed to fabricate diverse multifunctional hydrogels that exhibit notable characteristics such as potent antibacterial activity and controlled release of therapeutic agents under specific conditions (e.g., pH-responsive hydrogels, photo-controlled release hydrogels, thermoresponsive gels) (Trombino et al., 2019). Numerous natural polymers serve as biomaterials in the formulation of hydrogels; however, their utility is hindered by inherent drawbacks such as inadequate stability, mechanical characteristics, and vulnerability to degradation. Synthetic polymers are commonly used in hydrogel wound dressings due to their superior stability, mechanical characteristics, and ability to address mechanical and viscoelastic challenges, making them a popular choice (Raus et al., 2021).

##### 3.1.1. Alginate

Alginate, a marine biopolymer derived from brown seaweed, is widely used in medical dressings due to its biocompatibility, non-toxicity, hydrophilicity, and hemostatic properties (Gunes & Ziylan Albayrak, 2021). Injectable hydrogels are extensively utilized in various applications due to their notable characteristics, including high solubility in aqueous solutions, fast gelation, exceptional flexibility, and biocompatibility (Zhao et al., 2020). A new composite hydrogel was prepared from double net xanthan gum (XG) and dopamine-modified oxidized sodium alginate (OSA-DA), specifically designed for wound dressing and skin simulation sensing. Hydrogel possesses the advantageous characteristics of self-healing

and injectability, which allow it to effectively fill wounds of various shapes and sizes, as well as provide a suitable covering for the skin surface to facilitate monitoring. The hydrogel's capacity to function as a sensor establishes a basis for investigating a novel hydrogel dressing that combines biological and sensing functionalities, thereby facilitating human health monitoring. Reactive oxygen species (ROS) in the vicinity of injured tissue can cause potential DNA and protein impairment impede tissue regeneration (Zhao & Yuan, 2022).

It has been observed that cannabidiol (CBD) possesses the capacity to impede the production of superoxide free radicals originating from oxidase enzymes NOX1 and NOX4, along with oxidase enzyme XO. Furthermore, it has been observed that CBD exhibits the ability to reduce the production of reactive oxygen species (ROS) (Atalay et al., 2019). Zn<sup>2+</sup> exhibits antibacterial capabilities across a wide range of bacterial strains. Additionally, it has been found that Zn<sup>2+</sup> has the ability to modulate the expression of the vascular growth factor (VEGF) gene and facilitate the process of angiogenesis (Atalay et al., 2019). A novel hydrogel composed of zinc alginate (AlgZn) infused with cannabidiol (CBD) was prepared. This was achieved by incorporating CBD and Zn<sup>2+</sup> ions into a pre-existing sodium alginate hydrogel matrix. The findings from *in vitro* investigations on hydrogels shown that CBD/Alg-Zn hydrogels had remarkable attributes in terms of anti-inflammatory, antioxidant, and antibacterial effects. Thus, these hydrogels hold promise as innovative wound dressings with multifunctional capabilities for facilitating wound healing (Zheng et al., 2022). Furthermore, the integration of mineral constituents into the polymer matrix has the potential to induce the inherent proliferation of living tissue and facilitate the restoration of compromised anatomical structures. This issue poses significant complexities within the field of regenerative medicine (Ma & Yu, 2021). A PVP-HA-SA hydrogel membrane was developed by adding hydroxyapatite (HA) *in-situ*. This enhanced adhesion, decreased cytotoxicity, and encouraged tissue growth and wound healing. Experiments showed that higher concentrations of PVP can improve the hydrogel membranes' adhesion properties, mitigating HA-induced toxicity. The membranes exhibit robust adhesion and minimal toxicity, facilitating cell tissue growth and potentially serving as a bandage for wounds on the human body (Fadeeva et al., 2021).

##### 3.1.2. Hyaluronic Acid (HA)

Hyaluronic acid, a natural polymer with biocompatibility, degradability, high hydrophilicity, moisturizing properties, and wound healing capabilities, is

widely used in the biomedical domain. Additionally, it is frequently employed in the fabrication of hydrogel dressings (Alven & Aderibigbe, 2021). The natural deep eutectic solvent (DES) exhibits favorable biocompatibility and has significant efficacy in facilitating the process of wound healing. As a result, it holds considerable promise for utilization within the domain of innovative hydrogel wound dressings (Y. Wang et al., 2020). An innovative antibacterial material called DES-DASH@Ag hydrogel wound dressing, was introduced. This material was prepared by filling a deep eutectic solvent (DES) with lyophilized solute. The DES was then combined with a DASH polymer network, resulting in the formation of the antibacterial material. Glucose and choline chloride exhibit properties that facilitate skin tissue regeneration and mitigate the risk of wound infection (Li et al., 2021). The DES-DASH@Ag hydrogel wound dressing, made of AgNPs synthesized through dopamine reduction and sodium hyaluronate coating, shows significant antibacterial and biocompatibility properties, with cellular activity exceeding 80%. Its sponge-like structure facilitates water absorption and interception, creating a moist environment for wound healing (Qian et al., 2020). Photo crosslinking, a technique used in wound dressings, has shown significant potential in clinical medicine due to its rapid crosslinking rate, minimal invasiveness, and ability to manage the process duration. This advancement in in situ hydrogels is gaining interest (Pang et al., 2021). Nevertheless, the light initiator utilized in the photocrosslinking reaction often exhibits drawbacks such as limited solubility in water and potential harm to living cells. The absence of initiators during UV treatment in the crosslinking reaction of hydrogels has been seen to result in the non-generation of hazardous chemicals. The dual network structure exhibits remarkable mechanical strength and toughness simultaneously, hence endowing the produced hydrogels with a diverse range of exceptional functionalities (Sun et al., 2020). A dual network hydrogel (CMC-AZ/HANB) was developed with various functionalities, composed of azide-functionalized CMC (CMC-AZ) and o-nitrobenzyl modified HA (HA-NB). The hydrogel's mechanical properties were enhanced, and the use of amoxicillin as a medicine within hydrogels showed significant wound healing efficacy (Mao et al., 2022).

### 3.1.3. Gelatin

The low mechanical strength of chitosan can be efficiently addressed by blending its biopolymer with other polymers (Hong et al., 2019). A covalently antibacterial alginate-chitosan hydrogel dressing that incorporated gelatin microspheres loaded with tetracycline hydrochloride was developed. This was achieved through the utilization of the emulsion crosslinking approach, with the purpose of

enhancing wound healing. The microspheres containing antibiotics are integrated into the gel scaffolds, resulting in both sustained drug release and improved mechanical qualities. The principal objective was to augment the mechanical characteristics and drug administration capacities of hydrogels obtained from natural sources (H. Chen et al., 2017).

The application of antibacterial composite hydrogel dressings has been shown to effectively enhance wound healing by addressing and treating infections. To provide a visual representation, the experiment demonstrated the phenomenon of growth inhibition in relation to *Escherichia coli* and *Staphylococcus aureus* (Sudheesh Kumar et al., 2012). Novel wound dressing materials were developed using gelatin and gelatin-based chitosan bilayers. Gelatin's biocompatibility and biodegradability make it ideal for medicine and pharmaceuticals. The study used an ex vivo model to investigate biocompatibility. The cross-linked gelatin provides mechanical support to hydro-films, while a porous structural matrix shows swelling capacity. No cytotoxicity was found during in vitro testing. The bilayer hydrofilm in human skin showed satisfactory biocompatibility, indicating its potential for wound healing (Garcia-Orue et al., 2019).

A multifunctional hydrogel, the Gel/TA (Gelatin-Tannic Acid) hydrogel, was synthesized using gelatin and tannic group functional groups. This hydrogel has the potential to be used in full-thickness wound management and release active compounds within wound settings. The hydrogel's cytocompatible properties, ability to induce ECM regeneration, and promotion of cell adhesion and proliferation have been shown to improve wound healing processes. The gel-based composite hydrogel has potential for clinical management of full-thickness wounds (Ahmadian et al., 2021).

The antioxidative action of the Gel/TA hydrogel is attributed to TA, which possesses a polyphenolic structure and contains many hydroxyl (OH) groups (Jimoh et al., 2016). Nevertheless, research indicates that the process of gelation in hydrogel formation involves the occurrence of hydrogen bonding cross-linking (Kamoun et al., 2017). In contrast, the impact of adding 2-hydroxyethyl methacrylate (HEMA) and poly (ethylene glycol) methyl ether methacrylate (PEGMA) to Gel-N-acetylcysteine hydrogels was studied. These polymers enhance wound healing and blood clotting abilities. The antioxidant activity of these hydrogels is attributed to the conversion of amino groups into amides through dehydrothermal cross-linking treatment. The study also found a decline in antioxidant cross-linking in hydrogels derived from N-acetylcysteine

due to decreased amino group accessibility. This suggests that dehydrothermal crosslinking significantly enhances the antioxidation ability of gel-based hydrogels (Gomez-Aparicio et al., 2021).

#### 3.1.4. Agarose

Agarose, a linear polysaccharide, is widely used in biological investigations due to its minimal interaction with biomolecules, robust properties, and ability to form gels. Its high biocompatibility makes it an attractive biomaterial for tissue engineering and medicine delivery, as tissue regeneration relies on biocompatibility and biodegradability. Its application in electrophoresis and bacterial cell culture is also significant (Yamada et al., 2020). Agarose-based hydrogels show potential in regenerative medicine, especially in producing human skin and organs. Agarose, an injectable polymer, is gaining attention due to its in-situ polymerization, reduced invasiveness, on-site shape ability, and potential for targeted cell and signaling molecule delivery (Irastorza-Lorenzo et al., 2021). The utilization of agarose scaffolds has demonstrated enhanced surgical outcomes and improved consistency in cell phenotypic. Although agarose is widely recognized as a highly effective medium for facilitating tissue regeneration, there has been limited investigation into its application inside three-dimensional tumor models (Salati et al., 2020).

The thermal crosslinking method is the predominant technique employed for the manufacture of agarose scaffolds. This approach entails employing the gelation procedure, which the utilization of microwave radiation can execute. A thermal crosslinking technique was used to fabricate an agarose scaffold. The process involved dissolving agarose (1.5% weight) in aqueous solvent using microwave heating, with temperatures ranging from 60 °C to ambient temperature. The cooling rate was set at 30°C/min. The blending of agarose with other polymers resulted in an augmentation of cellular activity and cell regeneration (Varoni et al., 2012).

A composite material combining agarose and silk for cartilage regeneration was developed. The presence of the silk/agarose scaffold also increased the expression of cartilage-specific marker genes, such as aggrecan, sox-9, and collagen Type II, which improved the agarose microenvironment for chondrocyte culture (Singh et al., 2016).

CHO-agarose hydrogels and peptide-agarose microgel scaffolds were developed using oxidizing 2,2,6,6-(tetramethylpiperidin-1-yl)oxyl. The peptide-agarose microgel scaffold-based 3D cell culture system demonstrated its efficacy as a biomaterial for tissue engineering, enhancing cell proliferation in a three-

dimensional environment (Yamada et al., 2020). A nanocomposite of agarose-gelatin-glass nanoparticles was developed using freeze gelation. The compound was dissolved in distilled water, then glass nanoparticles were added to the gelatin mixture. Lyophilization allowed for the formation of a scaffold, which could be used in treating osteomyelitis by enhancing the hydroxyapatite layer in bodily fluids, thereby promoting tissue regeneration. The scaffolds have potential applications in various medical applications (Ali et al., 2021). The utilization of agarose-based scaffolds offers several notable advantages, including robust physical crosslinking, responsiveness to changes in temperature, and enhanced stability even at lower concentrations (Utech & Boccaccini, 2016).

#### 3.1.5.

#### Dextran

Dextran, an exopolysaccharide, is produced by lactic acid bacteria using sucrose as a primary substrate, consisting of a linear chain of D-glucopyranose units linked by  $\alpha$  (1 $\rightarrow$ 6) bonds. Additionally, there are varying numbers of branching connections, such as  $\alpha$ -(1 $\rightarrow$ 2),  $\alpha$ -(1 $\rightarrow$ 3), and  $\alpha$ -(1 $\rightarrow$ 4), present within the molecule. The molecular weights of these molecules typically range around 40 kDa (Díaz-Montes, 2021). The compound possesses chemically reactive hydroxyl groups, which enable its modification with various functional groups, resulting in the formation of spherical, tubular, and three-dimensional networks. Dextran-based scaffolds that are biodegradable have the ability to serve as carriers for bioactive protein biomolecules, enabling controlled release and facilitating tissue regeneration. Dextran hydrogels have the potential to serve as a matrix for bioartificial cardiac tissue (BCT) in in-vitro regeneration. These hydrogels offer unique benefits for soft tissue engineering due to their resistance to protein adsorption and cell adhesion, enabling the creation of targeted recognition sites (Banerjee et al., 2021). The creation of a crosslinked network of dextran hydrogels through radical methacrylate group polymerization, resulting in macroporous scaffolds with a beaded-wall morphology due to the lack of miscibility between the dextran matrix and poly(ethylene glycol). These scaffolds demonstrated the ability to effectively handle liquid-liquid phase separations and exhibited enhanced cell penetration and nutrient diffusion capabilities (Lévesque et al., 2005). These carriers could serve as bioactive agents for various protein biomolecules that possess inherent biodegradability. However, it has been noted that these carriers are more expensive and exhibit lower bioavailability (Varghese et al., 2020).

#### 3.2. Chitosan and collagen-based composite hydrogels with synthetic polymers

Numerous natural polymers serve as biomaterials in the formulation of hydrogels; however, their utility is hindered by inherent drawbacks such as inadequate stability, mechanical characteristics, and vulnerability to degradation. On the other hand, synthetic polymers exhibit enhanced stability, superior mechanical characteristics, and the ability to manipulate their structure and properties, and they effectively address the mechanical and viscoelastic challenges associated with hydrogels. Consequently, hydrogel wound dressings frequently incorporate them in their formulation (Raus et al., 2021).

### 3.2.1. Polyvinyl alcohol (PVA)

PVA's superior water solubility, biocompatibility, biodegradability, non-carcinogenicity, mechanical qualities, and ease of processing have led to substantial research on the material's potential for wound healing (Su et al., 2021). Nevertheless, the elasticity of PVA hydrogels is insufficient, and their hydrophilicity is also limited, hence constraining their standalone application as polymer materials for wound dressings. The utilization of intricate combinations comprising both natural and synthetic polymers is significant in enhancing the mechanical and physicochemical characteristics of PVA hydrogel dressings. Hence, several composite polymers have been employed in the fabrication of wound dressings based on polyvinyl alcohol (PVA). The careful selection and manufacturing techniques of these composites are of utmost significance, as the characteristics of PVA hydrogels are contingent upon the properties of the incorporated ingredients (Radulescu et al., 2022).

Polyvinyl alcohol (PVA) is a promising material for hydrogel dressings due to its bioactivity, which prevents cell growth. Composite materials like chitosan and alginate can increase PVA's bioactivity. These dressings have shown promise in medication delivery systems and wound dressings, expediting wound healing by releasing therapeutic agents like medicines, DNA, growth factors, nanoparticles, and proteins. An experimental study aimed to develop PVA hydrogels with zinc oxide nanoparticles and mesoporous silica nanoparticles to create effective treatments for infected wounds using cephalexin antibiotics (Nikdel et al., 2021). Furthermore, there is a growing body of research exploring the utilization of electrospinning as an alternative manufacturing method to produce nanofiber hydrogels, specifically for the delivery of wound-healing active materials. This approach aims to replace conventional manufacturing methods now in use. Propolis nanoparticles are being utilized in wound healing and tissue regeneration by being incorporated into wound dressings composed of cross-linked polyvinyl alcohol (PVA) and propolis polymer nanofibers (Alberti et al., 2020).

### 3.2.2. Poly (N-isopropylacrylamide)

Poly (N-isopropylacrylamide) (PNIPAM) is a thermos reversible hydrogel with a low critical solution temperature (LCST) of 32°C. Its cross-linked gels exhibit expansion and contraction phenomena, allowing continuous medication delivery based on physiological signals. PNIPAM has been extensively researched as a controlled drug delivery system (Sun et al., 2019). Thermosensitive polyvinyl alcohol (PVA) hydrogels were fabricated by using SA-g-N-isopropyl acrylamide, a thermosensitive copolymer, for wound management. The polymer was synthesized using redox co-polymerization, achieving a drug release rate of 65% at ambient temperature and 35% at temperatures above the human body's normal range (Montaser et al., 2019).

### 3.2.3. Polyethylene Glycol (PEG)

Polyethylene glycol (PEG) is a water-soluble, amphiphilic polyether with both hydrophilic and hydrophobic properties. As a transparent, colorless liquid, PEG is highly compatible with biological systems and exhibits exceptional biocompatibility and biodegradability. A bilayer dressing was developed using PVA-CMC-PEG hydrogels using a freeze-thaw technique. They manipulated the hydrogel's pore size, resulting in a thorough combination of two layers. The double-layer dressing had favorable mechanical qualities, impeding germ infiltration, and regulating moisture loss from the wound. This created a moist environment leading to enhancing wound healing (Y. Li et al., 2019). A semi-interpenetrating hydrogel dressing was developed using PEG diacrylate, PVA, and gum tragacanth. The addition of PVA increased swelling rate and reduced porosity. Increased PEG diacrylate increased cell adhesion and network elongation. Reduction in PEG diacrylate reduced network disintegration. The dressing is non-toxic and has antibacterial efficacy (Hemmatgir et al., 2022).

### 3.2.4. Poly (lactic-co-glycolic acid)

Poly (lactic-co-glycolic acid) (PLGA) is a FDA-approved synthetic polymer widely used in pharmaceuticals and tissue engineering due to its biocompatibility, adjustable mechanical properties, and manageable degradation rate. It can be easily manufactured by adjusting the copolymer ratio between lactic acid and glycolic acid (Sezlev Bilecen et al., 2019). Periodontal tissue regeneration requires materials that meet the necessary requirements. Synthetic polymers have favorable mechanical and biological attributes but lack biocompatibility. Natural polymers have hydrophilicity and biocompatibility but lack the necessary mechanical features. Research groups are developing periodontal materials for guided tissue regeneration (GTR) and guided

bone regeneration (GBR) by combining natural polymers with inorganic or synthetic polymers to achieve the necessary characteristics (Forero et al., 2017). The combination of PLGA and CS can be readily achieved using diverse methodologies to form nanoparticles. The utilization of PLGA nanoparticles (nPLGA) and CS nanoparticles (nCS) as drug delivery systems has been widely employed in many applications. Nano-sized materials are commonly preferred in periodontal surgery, making it necessary to synthesize nanoparticles. This study aims to synthesize periodontal tissue regeneration materials by combining nPLGA, nCS, and nAg. The objective is to develop a biocompatible substance that promotes cellular mineralization and reduces periodontal disease relapse. The research involved synthesizing nanoparticles of PLGA, CS, and Ag, and investigating their cytotoxicity and impact on cell calcification. After understanding the characteristics of the materials, they were mixed and evaluated for their cytological properties. This is the first research on this combination (Ma et al., 2018).

#### IV. EFFECT OF TEMPERATURE AND pH ON CHITOSAN-COLLAGEN HYDROGELS

The effects of temperature on hydrogels can either be positive or negative. If gel material swells with the rise in temperature and pH then it is a positive response. If shrinks, then it is a negative response (Huang et al., 2019).

##### 4.1. Temperature-sensitive nature of hydrogels

Temperature-sensitive hydrogels can be categorized into two types based on their structure: negatively thermo-sensitive hydrogels and positively thermo-sensitive hydrogels. Polymers having LCST can negatively generate temperature sensitive hydrogels, the polymers shrink along with the temperature increases. At reduced temperatures, the prevalence of hydrogen bonding between hydrophilic groups within the polymer chain and water molecules becomes prominent, resulting in the solubility of the polymer in water. Nevertheless, as the temperature rises, the hydrophobic contacts between hydrophobic groups are enhanced, whilst the strength of hydrogen bonding diminishes, resulting in the phenomenon of gelation. Hydrogels that exhibit a positive temperature sensitivity demonstrate an increase in their solubility in water as the temperature rises, hence exhibiting an upper critical solution temperature (UCST) (Huang et al., 2019).

##### 4.2. pH-sensitive behavior of hydrogels

pH-responsive polymers (PRPs) exhibit a capacity to undergo structural and property modifications in response to fluctuations in environmental pH. These alterations encompass changes in surface activity, chain

structure, conformation, solubility, and configuration. pH-sensitive polymers are characterized by the presence of acidic or basic functional groups, which exhibit the ability to either take or donate protons in response to changes in the surrounding pH conditions. PRP types are present and can be differentiated based on categorization criteria, including distinguishing weak bases from weak acids, as well as differentiating biopolymers and degradable polymers from synthetic polymers. Nanoparticles are utilized in several fields, such as medicine delivery, gene delivery, actuation and sensing/biosensing, and separation techniques, among others (Wei et al., 2017).

Chitosan demonstrates pH-sensitive characteristics as a weak polybase owing to the abundant presence of amino groups along its molecular chain. Chitosan has great solubility in acidic conditions; however, it retains its insoluble nature when exposed to alkaline pH levels. The process of pH-sensitive swelling is initiated by the protonation of the amine groups when exposed to low-pH circumstances. Protonation induces chain repulsion, resulting in the diffusion of protons, counter ions, and water inside the gel matrix, as well as the dissociation of secondary connections. The phenomenon of pH sensitivity has been documented in the context of drug delivery applications (Woraphatphadung et al., 2018). Successful production of pH-sensitive nanocomposites composed of chitosan and silica was documented, with the incorporation of curcumin. The researchers exhibited a release of curcumin that was dependent on pH. The researchers reached a conclusion regarding the adjustable release profile of the active chemical by utilizing the pH of the release medium (Gaware et al., 2019). Other researchers have also demonstrated the pH-dependent release of drugs utilizing polymeric polymers based on chitosan (Ata et al., 2020). A novel chitosan-based film was developed that exhibits pH-dependent color-changing properties, thereby demonstrating its potential as a creative application. Alizarin was integrated into the formulation for the purpose of enhancing the functionality and intelligence of food packaging materials. The composite film exhibited a discernible alteration in color, transitioning from a faint yellow hue to a vibrant purple shade, in response to fluctuations in pH within the range of 4 to 10. The film composed of chitosan and alizarin exhibited antibacterial, antioxidant, and color-changing characteristics in response to changes in pH (Ezati & Rhim, 2020).

##### 4.3. Advantages of temperature and pH-sensitive hydrogels in wound care

Temperature-sensitive hydrogels have demonstrated exceptional potential as carriers for the delivery of diverse biotherapeutic compounds, offering

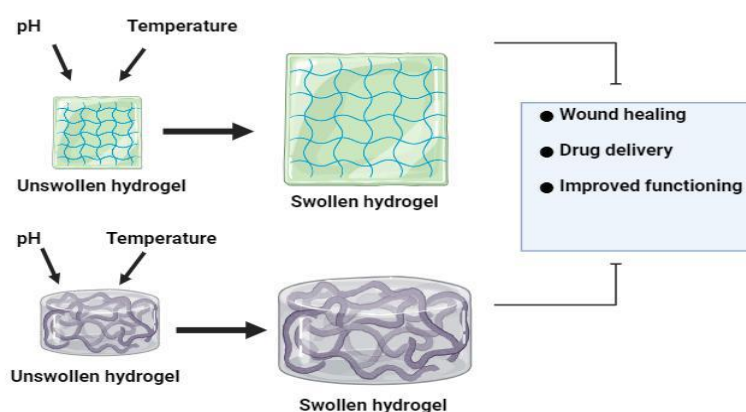


several notable advantages: (i) Temperature-sensitive hydrogels have the ability to undergo gelation at physiological temperatures, making them more practical for administration purposes. (ii) The hydrogel matrix that is formed can provide protection for delicate drugs and cells that are incorporated within it. (iii) The controlled release of biotherapeutic molecules from hydrogels allows for enhanced efficacy and a reduction in potential side effects. The obstacles and constraints associated with the use of temperature-sensitive hydrogels as delivery vehicles for biotherapeutic compounds include the mechanical strength of the swelling gel, its low temperature sensitivity, and the biocompatibility of the polymers (Huang et al., 2019).

#### 4.3.1 Effect of temperature and pH sensitivity of chitosan-collagen hydrogels

Thermo and pH-responsive hydrogels were developed and loaded with doxorubicin (DOX) with potential therapy of breast cancer. Swelling studies of hydrogels and their morphology implied the porous structure, high water content with rapid swelling/deswelling rate in response to abrupt changes of pH and temperature. The release investigation of DOX at different concentration, temperature and pH values confirmed the accelerated release of DOX in lower concentration and acidic condition at 37 °C as compared to neutral pH and the temperature of 40 °C.

The proliferation of MCF-7 cells on the prepared hydrogel and DOX-loaded hydrogel was evaluated by 4',6-diamidino-2-phenylindole (DAPI) staining which further demonstrated the potential of developed hydrogels for local therapy of breast cancer (Fathi et al., 2019).



Created in BioRender.com 

Fig: 9. Effect of temperature and pH on hydrogels

Injectable hydrogels have shown great potential in cell therapy and drug delivery. They can easily fill in any irregular-shaped defects and remain in desired positions after implantation using minimally invasive strategies. Here, we developed hydrogels prepared from tilapia skin collagen and chitosan (HCC). The residual mass rate of HCC was affected by the pH at the time of preparation, which was 29.1 % at pH 7 in 36 h. By comparison, the residual mass ratios of HCC at pH values of 6 and 5 were only approximately 8.4 % and 0, respectively. In addition, the stability of HCC was also affected by the concentration of these two components. HCC10 catalyzed by 10 mg mL<sup>-1</sup> tilapia skin collagen and 10 mg mL<sup>-1</sup> chitosan was more stable than HCC5 catalyzed by 5 mg mL<sup>-1</sup> tilapia skin collagen and 10 mg mL<sup>-1</sup> chitosan; therefore, we

studied the ability of HCC10 to deliver two model nanobodies: 2D5 and KPU. As the concentration of nanobodies increased, the cumulative release rate of 2D5 decreased, and the release rate of KPU increased. Meanwhile, the cumulative release rate of 2D5 was the highest (68.3 %) at pH 5.5, followed by pH 6.8 (56.4 %) and 7.4 (28.4 %). However, the cumulative release rates of KPU were similar at pH 5.5 (45.1 %), 6.8 (46.5 %), and 7.4 (44.9 %). HCC is biodegradable and can facilitate the release nanobodies; thus, HCC could be developed into an intelligent responsive tumor treatment matrix for use in cancer therapy (Maturavongsadit et al., 2020).

Dapsone (DAP) is a bactericidal agent used in the treatment of leprosy caused by *Mycobacterium leprae*. Despite its therapeutic potential, DAP has low solubility,

which results in allow therapeutic index and a high microbial resistance. Recently, new approaches were used to increase the DAP solubility. In particular, the use of interpenetrating polymer network (IPN)-hydrogels based chitosan (CS) for the controlled release of DAP provides some advantages because they can modify their swelling properties and network structures as a response to environmental stimuli. The aim of this study was to synthesize and physicochemically characterize pH-responsive chitosan/polymer hydrogels to control the release of DAP. For this reason, different combinations of polymers, such as polyvinyl pyrrolidone, polyethylene glycol and hydroxypropyl methylcellulose, and concentrations of the cross-linking agents (glutaraldehyde) were used and then blended to the CS. The resulting hydrogels were evaluated in terms of physicochemical and swelling properties, rheological analysis, and in vitro release of DAP at different pHs (1.2–6.8). Hydrogels were further characterized by Fourier transformed infrared (FT-IR) spectroscopy and scanning electron microscopy (SEM) analysis. pH-responsive DAP-loaded hydrogels may represent the set-up for developing potential oral formulations for the treatment of leprosy caused by *Mycobacterium leprae* (Chaves et al., 2019).

Fucoidans, sulfated polysaccharides from brown algae, possess multiple bioactivities regarding osteogenesis, angiogenesis, and inflammation, all representing key molecular processes for successful bone regeneration. To utilize fucoidans in regenerative medicine, a delivery system is needed that temporarily immobilizes the polysaccharide at the injured site. Hydrogels have become increasingly interesting biomaterials for the support of bone regeneration. Their structural resemblance with the extracellular matrix, their flexible shape, and capacity to deliver bioactive compounds or stem cells into the affected tissue make them promising materials for the support of healing processes. Injectable hydrogels stand out due to their minimal invasive application. In the current study, we developed an injectable thermosensitive hydrogel for the delivery of fucoidan based on chitosan, collagen, and  $\beta$ -glycerophosphate ( $\beta$ -GP). Physicochemical parameters such as gelation time, gelation temperature, swelling capacity, pH, and internal microstructure were studied. Further, human bone-derived mesenchymal stem cells (MSC) and human outgrowth endothelial cells (OEC) were cultured on top (2D) or inside the hydrogels (3D) to assess the biocompatibility. We found that the sol-gel transition occurred after approximately 1 min at 37 °C. Fucoidan integration into the hydrogel had no or only a minor impact on the mentioned physicochemical parameters compared to hydrogels which did not contain fucoidan. Release assays showed that 60% and 80% of the fucoidan was released

from the hydrogel after two and six days, respectively. The hydrogel was biocompatible with MSC and OEC with a limitation for OEC encapsulation. This study demonstrates the potential of thermosensitive chitosan-collagen hydrogels as a delivery system for fucoidan and MSC for the use in regenerative medicine (Ohmes et al., 2022).

Mandible defects are a difficult issue in dental surgery owing to limited therapeutic options. Recombinant human bone morphogenetic protein-2 (rhBMP2) is osteoinductive in bone regeneration. This article prepared chitosan/collagen hydrogels with rhBMP2-incorporated gelatin microsphere (GMs) for a sustained release of rhBMP2 to induce bone regeneration in rabbits. The rhBMP2 release profiles in vitro were investigated within a period of 4 weeks. The test groups were hydrogels+10  $\mu$ g rhBMP2, GMs+10  $\mu$ g rhBMP2, and hydrogels/GMs+10  $\mu$ g rhBMP2. These delivery systems were suspended in 2 mL of PBS (pH 7.4) and incubated at 37°C with shaking at 80 rpm for 4 weeks. At predetermined time points, 50  $\mu$ L of supernatants were harvested and then 50  $\mu$ L of fresh PBS (pH 7.4) was supplemented. The concentrations of released rhBMP2 in the harvests were detected using the rhBMP2 ELISA kit (R&D Systems, Shanghai, China). The cumulative release of rhBMP2 was computed. Chitosan/collagen hydrogels with rhBMP2- incorporated GMs exhibited an ideal releasing profile of rhBMP2 in vitro. These composite scaffolds had a better capacity to heal mandible defects than the other two hydrogel scaffolds. Chitosan/collagen hydrogels with rhBMP2-incorporated GMs might be potential carriers of rhBMP2 for accelerating the repair of bone defect (Song et al., 2016).

This introduces a novel type of injectable temperature-sensitive chitosan/glycerophosphate/collagen (C/GP/Co) hydrogel that possesses great biocompatibility for the culture of adipose tissue-derived stem cells. The C/GP/Co hydrogel is prepared by mixing 2.2% (v/v) chitosan with 50% (w/w)  $\beta$ -glycerophosphate at different proportions and afterwards adding 2 mg/ml of collagen. The gelation time of the prepared solution at 37°C was found to be around 12 min. The inner structure of the hydrogel presented a porous spongy structure, as observed by scanning electron microscopy. Moreover, the osmolality of the medium in contact with the hydrogel was in the range of 310–330 mmol kg<sup>-1</sup>. These analyses have shown that the C/GP/Co hydrogels are structurally feasible for cell culture, while their biocompatibility was further examined. Human adipose tissue-derived stem cells (ADSCs) were seeded into the developed C/GP and C/GP/Co hydrogels (The ratios of C/GP and C/GP/Co were 5:1 and 5:1:6, respectively), and the cellular growth was periodically observed under an inverted microscope. The proliferation of ADSCs was detected using cck-8 kits, while cell apoptosis was

determined by a Live/Dead Viability/Cytotoxicity kit. After 7 days of culture, cells within the C/GP/Co hydrogels displayed a typical adherent cell morphology and good proliferation with very high cellular viability. It was thus demonstrated that the novel C/GP/Co hydrogel herein described possess excellent cellular compatibility, representing a new alternative as a scaffold for tissue engineering, with the added advantage of being a gel at the body's temperature that turns liquid at room temperature (Song et al., 2010).

Thermo and pH responsive chitosan–collagen (CHT–CLG) scaffolds were prepared using a non-residue strategy. CHT–CLG scaffolds (pH sensitive) were produced by freeze drying method, cross-linked with glutaraldehyde, and coated with poly (N,N-diethylacrylamide) (PDEAAM) in supercritical media to confer the thermoresponsive behavior. This green and integrated process generated a wide range of porous structures with different mechanical properties, reversible swelling ability and controlled biodegradability, depending on the scaffold composition and cross-linking degree. The ability of these dual sensitive structures to control the release of a low molecular weight drug (ibuprofen, Ibu) and a model protein (BSA) was investigated. Small portions of the native and PDEAAM coated scaffolds (around 20 mg) were placed inside a 50 mL of buffer solutions at different pH (5.5 or 7.4) and temperatures (20 and 37 °C). 1 mL aliquots were withdrawn periodically from the solutions and collected in eppendorfs. The release medium was refreshed with buffer solution (1 mL) after sampling. In order to determine the ibuprofen and BSA released, the samples were analyzed in a Helius Alpha DoubleBeam UV/VIS spectrophotometer at 265 and 280 nm, respectively. In order to design a completely clean strategy to develop potential pH and thermo ON–OFF devices with controlled morphological and mechanical properties for drug delivery, chitosan and collagen-based scaffolds were prepared by freeze drying method and coated with PDEAAM in scCO<sub>2</sub>. By varying the scaffold composition as well as the cross-linking degree, it was possible to tune the morphological and mechanical properties of the blended matrices. The efficiency of the hydrogel coating was evaluated by investigating the mean pore size of the matrices, the swelling–deswelling ability, the biodegradability, cytotoxicity, and mechanical behavior of the PDEAAM-coated scaffolds. Owing to the promising morphological, biological, and mechanical features, the native scaffolds also proved to have a defined pH-sensitive behavior, and the PDEAAM-coated ones showed an effective dual (pH and thermo) sensitive conduct. Moreover, the BSA release profile was revealed to be significantly dependent on pH and temperature effects (higher release profiles at pH 7.4 and 20 °C), while the Ibu

release behavior demonstrated to be mainly reliant on morphological and mechanical properties of the scaffolds (higher release profiles using CLG scaffolds cross-linked with 1% of GA). Herein it was developed an integrated sustainable strategy comprising scaffold preparation, drug loading, cross-linking process and coating in scCO<sub>2</sub> to produce dual thermo and pH responsive chitosan–collagen scaffolds for sustained drug delivery; future work will extend the strategy to generate highly regulated dual sensitive porous networks able to release therapeutic antibodies, growth factors, genes and enzymes which are also essential biomolecules for tissue regeneration (Barroso et al., 2014).

In situ 3D printing technologies is a new frontier for highly personalized medicine, which requires suitable bioink with rheology, biocompatibility, and gelation kinetics to support the right shape and mechanical properties of the printed construct. To this end, a facile design of thermo/photo dual cure composite hydrogel was proposed using MHBC and soluble collagen in this study. M/C composite hydrogel exhibited rapid thermo-induced sol-gel transition and contraction, tunable mechanical properties, proper microstructure, and biodegradability for 3D cell culture, as well as improve cyto-compatibility, all of which were dependent upon the methacrylation degree of MHBC and M/C ratios. The printability of the optimal formulation (3% MHBC/1% collagen) was validated by its mild printing condition, rapid gelation of bioink at 37 °C and simple postprocessing manipulation. Both desirable printability and cyto-compatibility enable M/C composite hydrogel, a potential candidate as bioink to be applied for in situ 3D bioprinting (Liu et al., 2021).

Chitosan and collagen are natural biomaterials that have been used extensively in tissue engineering, both separately and as composite materials. Most methods to fabricate chitosan/collagen composites use freeze drying and chemical crosslinking to create stable porous scaffolds, which subsequently can be seeded with cells. In this study, we directly embedded human bone marrow stem cells (hBMSC) in chitosan/collagen materials by initiating gelation using b-glycerophosphate at physiological temperature (37°C) and pH (7.3-7.4). We further examined the use of glyoxal, a dialdehyde with relatively low toxicity, to crosslink these materials and characterized the resulting changes in matrix and cell properties. The cytocompatibility of glyoxal and the crosslinked gels were investigated in terms of hBMSC metabolic activity, viability, proliferation, and osteogenic differentiation. These studies revealed that glyoxal was cytocompatible at concentrations below about 1 mM for periods of exposure up to 15 h, though the degree of cell spreading, and proliferation were dependent on matrix composition. Glyoxal-crosslinked matrices were

stiffer and compacted less than uncrosslinked controls. It was further demonstrated that hBMSC can attach and proliferate in three-dimensional matrices composed of 50/50 chitosan/collagen, and that these materials supported osteogenic differentiation in response to stimulation. Such glyoxal-crosslinked chitosan/collagen composite materials may find utility as cell delivery vehicles for enhancing the repair of bone defects (Wang & Stegemann, 2011).

Chitosan and collagen type I are naturally derived materials used as cell carriers because of their ability to mimic the extracellular environment and direct cell function. In this study beta-glycerophosphate (b-GP), an osteogenic medium supplement and a weak base, was used to simultaneously initiate gelation of pure chitosan, pure collagen, and chitosan-collagen composite materials at physiological pH and temperature. Adult human bone marrow-derived stem cells (hBMSC) encapsulated in such hydrogels at chitosan/collagen ratios of 100/0, 65/35, 25/75, and 0/100 wt% exhibited high viability at day 1 after encapsulation, but DNA content dropped by about half over 12 days in pure chitosan materials while it increased twofold in materials containing collagen. Collagen-containing materials compacted more strongly and were significantly stiffer than pure chitosan gels. In monolayer culture, exposure of hBMSC to b-GP resulted in decreased cell metabolic activity that varied with concentration and exposure time but washing effectively removed excess b-GP from hydrogels. The presence of chitosan in materials resulted in higher expression of osterix and bone

sialoprotein genes in medium with and without osteogenic supplements. Chitosan also increased alkaline phosphatase activity and calcium deposition in osteogenic medium. Chitosan–collagen composite materials have potential as matrices for cell encapsulation and delivery or as in situ gel-forming materials for tissue repair (Wang & Stegemann, 2010).

## V. CHITOSAN-COLLAGEN HYDROGELS ANTI-BACTERIAL AND WOUND-HEALING PROPERTIES

The conjugation of chitosan biopolymer with other polymers might successfully address the difficulty of chitosan's low mechanical strength (Garnica-Palafox & Sánchez-Arévalo, 2016). Using an emulsion crosslinking approach, a hydrogel dressing was prepared with antibacterial properties through covalent bonding and gelatin microspheres that transport tetracycline hydrochloride, aiding wound healing. These microspheres, infused with antibiotics, are inserted into gel scaffolds, ensuring continuous drug release, and enhancing mechanical properties. The study aimed to improve the mechanical and drug transport characteristics of natural hydrogels, enhancing wound healing, and addressing infections. The dressings effectively inhibit the growth of *E. coli* and *S. aureus*, which often multiply after infections (H. Chen et al., 2017). Examples of the antibacterial activity of chitosan-based hydrogels are shown in **Table 1**.

Table 1: Different types of chitosan-based hydrogels for antibacterial activity.

Bacterial Species	Hydrogel Type	References
<i>E. coli</i>	PEG–Chitosan Hydrogel	(Sharma et al., 2019)
<i>E. coli</i> and <i>S. aureus</i>	Chitosan/Alginate Hydrogel Dressing Loaded FGF/VE-Cadherin	(Wei et al., 2022)
<i>E. coli</i> , <i>S. aureus</i> and <i>P. aeruginosa</i>	PVA/Starch/Chitosan Hydrogel Membranes with Nano Zinc oxide	(Baghaie et al., 2017)
<i>E. coli</i> and <i>S. aureus</i>	Polyvinyl alcohol (PVA)/N–succinyl chitosan (NSCS)/lincomycin hydrogels	(Qing et al., 2021)
<i>S. aureus</i>	Chitosan/PVA-Based Hydrogel Films	(Mohite et al., 2023)

Innovative wound dressing materials were developed by combining gelatin and chitosan in a bilayer structure. Gelatin is widely used in medical and pharmaceutical applications due to its biocompatibility and biodegradability (**Fig. 10**). The materials can be used for wound healing due to their mechanical reinforcement and swelling capacity. The porous structural matrix showed no in vitro cytotoxicity, ensuring the hydro-film's mechanical integrity. The bilayer hydrofilm in human skin showed

significant biocompatibility (Garcia-Orue et al., 2019). Researchers are now exploring hydrogen-bonded extracellular matrix-mimicking hydrogels for wound treatment. A hydrogel was made mimicking the extracellular matrix (ECM) using gelatin and tannic groups. The Gel/TA hydrogel is suitable for full-thickness wound treatment, releasing active chemicals and promoting wound healing through cytocompatibility, regeneration, and cell adhesion. The antioxidation action of the Gel/TA hydrogel

is attributed to the polyphenolic structure of TA and the abundance of OH groups it contains (Ahmadian et al., 2021). Investigations have shown that hydrogen bonding cross-linking takes place throughout the process of hydrogel formation, leading to gelation (Kamoun et al., 2017). Gel-

N-acetylcysteine hydrogels were enhanced with HEMA and PEGMA, enhancing wound healing and blood clotting. The antioxidant activity decreases with dehydrothermal cross-linking, affecting the antioxidation capabilities more than uncross-linked polymers (Gomez-Aparicio et al., 2021).

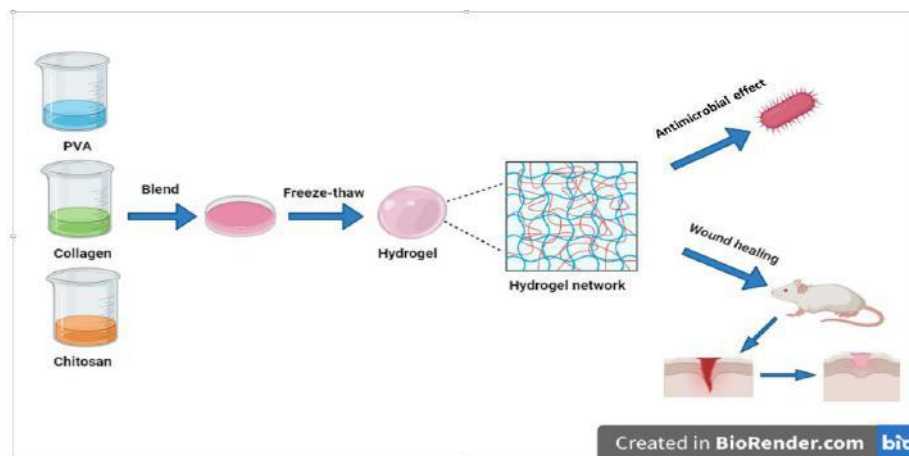


Fig.10: Chitosan-collagen have antimicrobial and wound healing effects

Skin diseases are a significant and critical clinical concern. Hydrogels, which mimic the human body's extracellular matrix, can be used as regenerative scaffolds to address skin defects. Synthesized by blending hyaluronic acid (HA) and carboxylated chitosan (CCS) with human-like collagen (HLC), these hydrogels have been tested for their biocompatibility. The hydrogels significantly enhanced the adhesion, proliferation, and migration of L929 cells, validating their biocompatibility. In vivo experiments showed they inhibited microorganism infiltration into wounds and facilitated wound healing. Subcutaneous implantation experiments showed hydrogels degrade over time and restricted inflammatory responses, indicating their compatibility with body tissues (Zhu et al., 2018).

### 5.1. Bacterial growth inhibition

The antibacterial activity of chitosan-collagen nanoparticle suspension with ZnO was tested using the adapted diffusimetric method by measuring the widths of the zones of inhibition. The best antibacterial activity against *S. aureus* was achieved for the CS-Coll-ZnO, with the materials formed by precipitation in the presence of NaOH showing a substantial improvement (Tiplea et al., 2021). A mucous adhesive polymeric membrane wound dressing containing hydroethanolic red propolis extract (HERP) was created. Membranes were developed employing a casting method that included collagen, chitosan, polyethylene glycol (15, 20, and 30v %), and a hydroethanolic extraction of EtOH-H<sub>2</sub>O 70v% - 30v% (v/v) of HERP (0.5, 1.0, and 1.5%). Membranes demonstrated substantial bacterial inhibition, implying that the 0.5% HERP with chitosan and collagen membrane has the

potential for future wound application research. (Loureiro et al., 2020). Silver nanoparticles carrying fibrillar collagen-chitosan hydrogel matrix was developed by biomimetic methodology by mixing silver nanoparticles, collagen fibril and chitosan hydrogel followed by cross-linking and bio mineralization. Antibacterial activity research revealed that *S. aureus* and *E. coli* were inhibited by roughly 27% and 37% of their growth, respectively. In its native state, the developed composite would contain silver nanoparticles loaded with collagen fibril and the resulting bio mineral would be identical to bone mineral. Therefore, the properties and potential of such hydrogel composites could be harnessed for developing biomaterials for applications in bone tissue engineering (Socrates et al., 2019).

### 5.2. Biocompatible properties

Tissue engineering hydrogels commonly consist of biopolymers due to their distinctive structure and characteristics. The features encompassed are minimal antigenicity and inflammation, strong affinity for water, sufficient cytotoxic effects, compatibility with living tissues, ability to degrade naturally, and a tendency to adhere to mucous membranes (Mozafari et al., 2019). Hydrogels have been found to be effective biomaterials for soft tissue regeneration. Because of its great biocompatibility, Collagen is the primary material used in hydrogel development, but its mechanical strength, temperature resistance, and pH vulnerability make it necessary to explore other options. Collagen and polysaccharides can enhance hydrogel characteristics. Hybrid hydrogels with different collagen/chitosan ratios show comparable physicochemical and microstructural

characteristics, enhancing thermomechanical capabilities and cell viability. This makes them suitable biomaterials for tissue engineering purposes. Hence, the synergism between collagen and chitosan resulted in enhanced hydrogel properties, demonstrating good thermomechanical properties and cell survival for application as promising biomaterials for tissue engineering (Sánchez-Cid et al., 2022). Diabetes mellitus is one of the most common diseases, and it is frequently accompanied by diabetic ulcers. Chitosan, a biopolymer with biodegradability, biocompatibility, and low toxicity, has been used to create hydrogels for diabetic wound treatment. These hydrogels, made of chitosan, collagen, and silver nanoparticles, have been found to have antibacterial, cytotoxic, and swelling properties. In mice with diabetes caused by alloxan, the hydrogels increased the expression of VEGF, TGF- $\beta$ 1, IL-1 $\beta$ , and TIMP1 genes, leading to faster wound healing. The hydrogels also facilitated collagen deposition, hair follicle repair, and sebaceous gland formation. However, clinical trials are needed to fully evaluate the effectiveness of these hydrogels, as animal models do not fully represent the entire diabetic pathology (Shagdarova et al., 2022). Hydrogels made from natural polymers like chitosan and collagen are popular for soft tissue engineering due to their hydrophilicity and softness. However, their mechanical properties require crosslinking techniques like small molecules or synthetic polymers. FTIR-ATR spectra confirmed the expected structure, while scanning electron microscopy showed a porous morphology with interconnected pores. These hydrogels are crucial for soft tissue engineering. Furthermore, swelling degree assay revealed a tunable behavior in natural polymers that was associated with composition. Finally, in vitro biodegradability and biocompatibility experiments demonstrated that the material performed well in simulated biologically living environments with interconnected pores (Duceac et al., 2019). Injectable thermosensitive hydrogels made of chitosan, collagen, and  $\beta$ -GP were used, which can form a gel at body temperature and are suitable for treating uneven surface wounds. These hydrogels offer a cell-friendly environment like the extracellular matrix (ECM) in cell-based therapies and are compatible with living tissues. Collagen in the hydrogel facilitates cell adhesion, migration, survival, and proliferation, and encourages gel remodeling. The hydrogel, combined with 3D MSC spheroids, significantly influenced the growth and release of paracrine factors, enhancing its effectiveness in healing deep skin wounds by stimulating the growth of new blood vessels and skin regeneration (Yang et al., 2020).

### 5.3. Wound healing in moist environments

Hydrogels, which are classified as advanced dressings, possess the ability to sustain a moist environment

at the specific location of application. This characteristic, attributed to their high-water content, renders hydrogels very suitable for the purpose of wound treatment. Hydrogels have the potential to be utilized in the treatment of both exudating and dry necrotic wounds (Gupta et al., 2019). Moist conditions are crucial in the management of wound healing acceleration. In contrast to scaffolds of diverse compositions, hydrogels possess the ability to sustain a wet environment within the wound region. Cross-linked hydrophilic polymeric networks that bear resemblance to natural soft tissues and extracellular matrix are present (Li et al., 2020). The process of wound healing is a multifaceted biological phenomenon that encompasses the regeneration of damaged tissue. Conventional wound dressings exhibit a lack of moisture retention, hence impeding the creation of an optimal moist environment conducive to wound healing. Additionally, these dressings demonstrate limited efficacy in terms of their antibacterial capabilities. Hydrogels possess the ability to retain substantial quantities of water, hence facilitating the establishment of a moist healing environment. At present, phototherapies have demonstrated significant potential in the realm of bacterial illness treatment. Hence, the integration of hydrogels with phototherapy presents a viable solution to address the limitations associated with conventional approaches to wound management. This combination exhibits considerable promise in promoting wound healing due to its notable efficacy, little irritability, and favorable antibacterial properties (Y. Xu et al., 2022).

### 5.4. Hemostasis

Development of a composite sponge made of halloysite, chitosan, and collagen using directed freeze-drying techniques was studied. The sponge was then coated with a hydrophobic polydimethylsiloxane layer to enhance its hemostatic properties. The sponge's channel structure, with a pore size of 30  $\mu$ m, facilitates blood transportation. The sponge's morphology and spectrum analysis show that chitosan and collagen adsorb onto the external surface of HNTs due to hydrogen bonding and electrostatic attraction. The directional freeze-dried sponge showed faster blood absorption rates than its non-directional counterpart. The composite sponges also showed significant antibacterial efficacy against *Escherichia coli* and *Staphylococcus aureus*, were non-cytotoxic to mouse fibroblasts, and showed excellent compatibility with blood cells. The use of the hemostatic dressing effectively mitigated superfluous blood loss due to its exceptional capacity for excessive blood absorption. The efficacy of the asymmetric sponges in promoting quick clotting and minimizing blood loss was validated in in vivo trials on rats. The study highlights the potential of this dressing in wound healing (Lin et al., 2023). Numerous chemicals have been identified as potential

hemostatic agents, although their efficacy is contingent upon the specific nature of the bleeding event and the anatomical site of the laceration or injury. Although there are numerous effective hemostatic materials available for treating superficial wounds that can be compressed, managing internal vascular and surgical bleeding continues to pose challenges. The difficulties about strong adherence in wet environments and applications in complex conditions, such as cutaneous, cardiac, and liver lesions, have been effectively addressed by recent advancements in wet-adhesive hydrogels. These hydrogels can also be biocompatible, antimicrobial, and high blood pressure resistant, outperforming certain conventional products (Han & Wang, 2023). The utilization of hydrogel bio adhesion technology has presented remarkable prospects in the field of minimally-invasive operations, which are commonly conducted with the aim of mitigating postoperative complications, shortening recovery periods, and alleviating patient suffering. Current hydrogel-based adhesives have challenges due to their limited ability to adhere in wet and dynamic environments, as well as potential immunological adverse effects, particularly in the case of synthetic hydrogel bio adhesives. A novel class of synthetic hydrogel bio adhesives derived from diverse polymer precursors have been presented. These bio adhesives exhibit rapid creation of a durable bio interface, enabling effective adherence to moist and resilient biological tissues with significant mobility. Furthermore, the elimination of monomers in the process of hydrogel manufacturing ensures that these hydrogel adhesives do not elicit an inflammatory response when used for in vivo wound sealing. This property has great potential for the prompt healing of vascular defects and surgical hemostasis. Furthermore, these materials could potentially function as interfaces between humans and electronic devices, facilitating the integration of bioelectronics implants for the purpose of monitoring physiological and clinical data in real-time (Zhang et al., 2022).

## VI. ANTI-MICROBIAL AND WOUND HEALING APPLICATIONS OF CHITOSAN-COLLAGEN BASED HYDROGELS

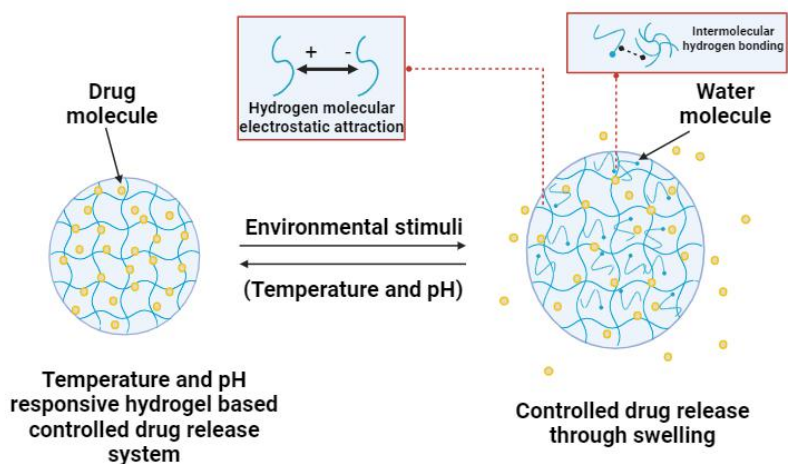
### 6.1. Controlled release of antimicrobials and drugs

Researchers aimed to create composite hydrogels by combining blue crab chitosan (CS) with bluefin tuna collagenous protein (BTCP) at different concentrations. The hydrogels showed improved porosity and swelling degree

with increased BTCP concentration. The hydrogels also showed enhanced elasticity and mechanical strength, particularly in hydrogels with 50% BTCP. The pH of the surrounding medium impacted the release of phycocyanin, a biologically active chemical. The study suggests that pH-sensitive Cs-BTTPC composite hydrogels may provide a favorable environment for encapsulation and delivery of medicinal drugs. The study presents a new method for promoting maritime industries by focusing on the utilization and economic significance of marine by-products, known as the blue economy. The chitosan-collagen combination is recognized as a highly effective substrate for developing materials with significant potential in tissue engineering and drug delivery applications. The physicochemical properties of the hydrogels were assessed using Fourier Transform Infrared Spectroscopy, X-ray Diffraction, and Scanning Electron Microscopy (Azaza et al., 2023).

As discussed previously, hydrogels can be formulated to deliver drugs using passive and active mechanisms, and hydrogel coatings can use these strategies to provide local and sustained release of antibacterial compounds to prevent implant infections. For example, the porosity of hydrogel coatings can be tuned to create “active” coatings that release small molecules or particles embedded in the scaffold. One strategy being explored clinically is the encapsulation of intrinsically antimicrobial silver nanoparticles into polyacrylamide-based hydrogels to prevent infections from *E. coli* and *S. aureus* (Qasim et al., 2018).

Thermosensitive hydrogels called bTCP-chitosan/collagen-quercetin hydrogels were prepared by combining beta-tricalcium phosphate (bTCP) nanoparticles and quercetin with a chitosan/collagen composite. These hydrogels undergo a sol-gel transformation triggered by beta-glycerophosphate (bGP) and changes in temperature, aligning with typical body temperature and pH conditions (Fig. 11). The hydrogels showed a porous structure with interconnected pore architecture. The addition of 3% bTCP improved the hydrogels' mechanical characteristics, decreased swelling and degradation rates, and improved pore size, permeability, and quercetin release rate. The hydrogels were biocompatible and showed the ability to support cell encapsulation. The consistent and ongoing release pattern of quercetin from the 3% bTCP-hydrogel suggests it could be an effective carrier for delivering natural flavonoids for bone repair (Sareethammanuwat et al., 2021).



Created in BioRender.com bio

Fig.11: Controlled drug release

Biopolymer hydrogels were created by combining hyaluronic acid, hydrolyzed collagen, and chitosan with caffeic acid as an antioxidant agent. The hydrogels were characterized using X-ray diffraction, differential scanning calorimetry, and thermogravimetric analysis. The hydrogels showed no structural or thermal changes, and their swelling behavior was superior due to high hyaluronic acid concentration. The initial rapid release of caffeic acid was around 70% within 60 minutes, followed by a slow release of up to 80% by 480 minutes. The antioxidant activity of the hydrogels was demonstrated through DPPH, ABTS<sup>+</sup>, and FRAP tests, suggesting their potential as dressings (Chusinuan et al., 2020).

Hydrogel composites made of collagen and chitosan were synthesized using a solvent casting method, with caffeic acid (CA) as a crosslinking agent. The hydrogel's structural characteristics were studied using FTIR spectroscopy. The presence of CA impeded the molecular chain mobility of chitosan and collagen, causing cracking and dimensional stability issues. The addition of CA reduced swelling properties and degrading behavior. The drug release profile showed a progressive pattern over 8 hours, influenced by CA quantity. The composite hydrogel's antioxidant activity was evaluated, indicating its potential in drug release and cosmetic research (Thongchai et al., 2020).

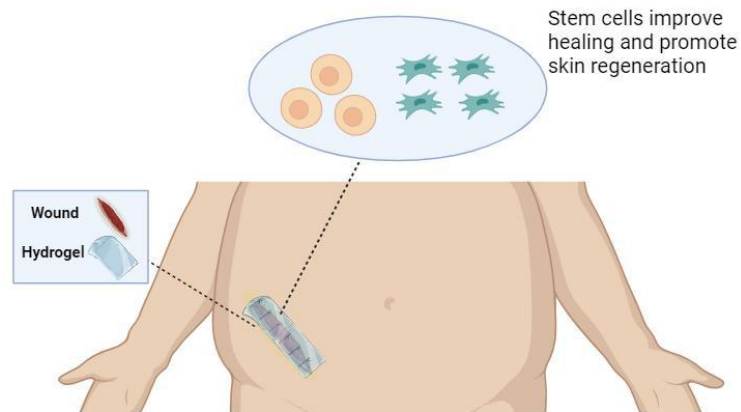
A porous bio-sponge for oral mucositis treatment was developed by blending collagen with chitosan. The impact of blending on crystallinity structure and thermal behavior of both polymers was evaluated. In vitro studies

showed a semi-crystalline structure in the collagen-chitosan film, which significantly impacts drug release. FT-IR analysis revealed electrostatic interactions and hydrogen bonding between collagen and chitosan, as well as between dexamethasone and the polymers. The collagen-chitosan (1:1) blend formulation effectively regulated medication release within a 10-hour timeframe, compared to the collagen sponge's completion time of 16 hours (Alagha et al., 2020).

## 6.2. Surgical site dressings

Hydrogel coatings provide novel strategies to combat one of the biggest challenges for implantable devices infections. In 2011 alone, the United States saw nearly 185,000 cases of hospital-acquired infections associated with medical devices (Magill et al., 2014). The use of mesh in hernia repair procedures relates to a significant risk known as surgical-site infection (**Fig. 12**). Triclosan-infused absorbable suture materials are used to reduce the occurrence of infections. To enhance the therapeutic efficacy, an experiment was conducted whereby the efficacy of using meshes coated with chitosan gel containing triclosan was examined to prevent and treat mesh infections in a rat model. A model of mesh infection was established using simultaneous and 24-hour *Staphylococcus aureus* injection. The rats were then monitored for a duration of 8 days to assess the occurrence of surgical-site infections. According to the findings, grafts that were covered with chitosan gel containing triclosan shown effective preventative benefits against graft infection (Çakmak et al., 2009).





Created in BioRender.com bto

Fig.12: Use of hydrogels as surgical dressing for appendicitis surgery wound

The adhesion of laser-activated chitosan films in a mixed in-vitro and animal setting was investigated. The purpose of this investigation was to explore the potential applicability of these films for suture-less tissue fixation. Sheep intestine was affixed with chitosan films, which were in the form of flexible and insoluble strips. This bonding process was carried out utilizing laser energies of varying intensities, specifically at a wavelength of 808 nm. In addition, genipin, a natural cross-linker, was incorporated into the film to assess its impact on tissue restoration strength in comparison to the films that were plain. The dressing was also applied in vivo to the sciatic nerves of rat models, and the resulting thermal damage caused by the laser was assessed four days post-surgery. The experimental findings provided evidence that the application of chitosan adhesives effectively facilitated the restoration of intestinal tissue, with the highest level of strength of repair observed at a 120-mW laser power. The chitosan gel loaded with n showed effective preventative benefits against graft infection (Lauto et al., 2007).

A composite dressing made of collagen, chitosan, and alginate was developed to improve wound healing and resist seawater immersion. The CCA cushion was fabricated using paint coat and freeze-drying methods and attached to a polyurethane material. The dressing showed favorable water absorption and mechanical properties, resulting in a higher wound healing ratio in rats compared to gauze or chitosan treatment. The dressing also showed increased fibroblast cells, intact re-epithelialization, and increased levels of EGF, bFGF, TGF- $\beta$ , and CD31. The dressing showed no harmful effects on cells and showed positive compatibility with blood (Xie et al., 2018).

The chitosan/ $\beta$ GP hydrogel is made and subsequently combined with a liposomal formulation of diethyldithiocarbamate and copper ions for the purpose of treating surgical site infections. The injectable gel has a high efficacy in eradicating 98.7% of methicillin-resistant *Staphylococcus aureus* and effectively inhibiting 99.9% of biofilm formation caused by *Staphylococcus epidermidis* within a 48-hour timeframe (Kaul et al., 2022).

A surgical wound refers to a deliberate cut created by a qualified physician. The delayed process of surgical wound healing has the potential to result in the development of chronic wounds, which can pose a significant health concern. This research aims to improve the healing process of surgical wounds by developing liposomes containing curcumin within a hydrogel made of lysine and collagen. The liposomal formulation was prepared using the thin-film hydration method and characterized for size, shape, encapsulation efficiency, and in vitro release. The hydrogel matrix was created, followed by the infusion of curcumin-loaded liposomes, resulting in formulations F1, F2, and F3. Safety, stability, swelling index, pH, rheological characteristics, and in vivo wound healing assay were used to characterize all formulations. The histology and histomorphometry of tissue samples from the wound area were also analyzed to assess the effects of the formulations, as well as the control group. This suggests how collagen hydrogel address the potential health concerns associated with delayed surgical wound healing (Cardoso-Daodu et al., 2022).

Surgical infections can lead to delayed wound healing, oxidative stress, and tissue ischemia. Hydrogels, non-antibiotic wound dressings, have potential to address these issues. A reductionism methodology has been

developed to produce bioactive hydrogels with antibacterial, antioxidant, pro-angiogenic, and hemostatic properties. These hydrogels, made from extracts from *Cirsium setosum* (CE) and carboxymethyl chitosan (CS), have been tested in three models. The hydrogels showed significant efficacy in mitigating bleeding and enhancing vascularization for skin flap regeneration, demonstrating the potential of these hydrogels. In general, the integration of bioactive CECS hydrogels with a straightforward and scalable assembly technique, as well as their inherent biological activities without the need for antibiotics, holds promise for their application as multifunctional wound dressings in surgical anti-infection procedures (Geng et al., 2022).

### 6.3. Burn care.

Burn injuries are a common and severe type of trauma that necessitates comprehensive medical attention for patients. The prompt administration of medical

intervention for burn injuries has been shown to have a substantial positive impact on the process of wound healing. The effectiveness of amnion and collagen-based hydrogels in promoting the healing of cutaneous burn wounds in rats was studied. A unique cell-free hydrogel was formulated using a combination of human amnion, rabbit collagen, carboxymethyl cellulose sodium salt, citric acid, methyl paraben, propyl paraben, glycerin, and triethanolamine. The wound dressing material was created using a combination of rabbit collagen and chitosan derived from prawn shells. The hydrogels were found to be non-cytotoxic and compatible with human blood cells. The gels accelerated wound healing, with complete re-epithelialization occurring within  $16.75 \pm 0.96$  days and wound closure via contraction reaching  $72 \pm 3.27\%$  when a wound dressing membrane was applied. The sprayable hydrogel with a covering membrane was more effective (**Fig. 13**). This suggests a potential alternative for treating cutaneous injuries, addressing issues like high costs and logistical intricacies (Rana et al., 2020).

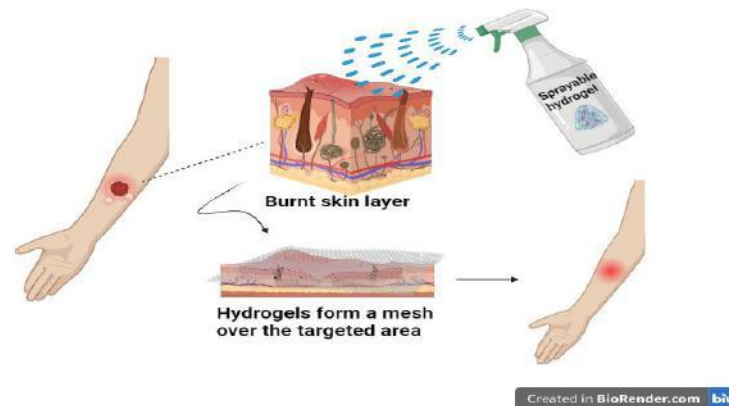


Fig.13: Burn wound healing

A study was conducted on the effectiveness of the HemCon™ bandage in treating burn infections in mice. The study found that the bacterial population in untreated burns increased by about 1000-fold from day 0 to day 3. However, in burns treated with silver dressing or chitosan acetate bandage, the bacterial luminescence signal decreased on day 1. The chitosan acetate bandage had a higher survival rate for *Pseudomonas aeruginosa* infections, with a survival rate of 73.3%. The chitosan acetate bandage was found to be effective in managing bacterial growth in burn wounds and preventing systemic sepsis, as confirmed by quantitative analysis of bacterial luminescence signals and blood culture results (Dai et al., 2009).

Utilizing a rat model to examine and compare the impact of chitosan and heparin on the first expansion of burn injuries, a study was conducted (Jin et al., 2007). A study on rats showed that chitosan powder, heparin powder, and a combination of chitosan and heparin were used to

induce burns. The results showed that chitosan had a lower severity of burns and a significant preventive effect on the initial phase, while heparin did not. However, concurrent administration of chitosan and heparin reduced chitosan's protective efficacy. The efficiency of chitosan in promoting wound healing in rat burn injuries was assessed (Burkatovskaya et al., 2006).

Lysostaphin was investigated against MRSA-induced burn infection in New Zealand White rabbits by combining it with a chitosan-collagen hydrogel (CCHL). The scientists created third-degree burn wounds ( $3 \times 3$  cm) using an electronic temperature controller set to  $80^\circ\text{C}$  for 15 seconds. Two days after the burning, the eschar was removed, and each wound contained MRSA (200 L of  $1 \times 10^9$  CFU/mL bacterial solution). When compared to groups treated with chitosan-collagen hydrogel without lysostaphin or animals treated with saline, the animals treated with CCHL should exhibit improvements in lesion healing

coupled with a decrease in MRSA burden. Additionally, after therapy, the administration of CCHL resulted in better repair of tissue architecture (Cui et al., 2011).

A chitosan hydrogel was developed for use as a wound dressing for burn wounds in rats. The hydrogel facilitated cell adhesion and proliferation and showed no harmful effects. The wound beds of the treated animals were significantly smaller than the untreated control group. Histological examination showed no inflammatory responses in the skin lesions treated with the hydrogel, and no pathological abnormalities were observed in the organs retrieved during necropsy. These findings suggest the biomaterial's compatibility at both local and systemic levels (Ribeiro et al., 2020).

The effect of a thermosensitive hydrogel made from chitosan, collagen, and  $\beta$ -glycerophosphate ( $\beta$ -GP) and a conditioned medium from human umbilical cord mesenchymal stem cells (MSC-CM) on mice with third-degree burns was examined. The hydrogel was stored at 4°C and applied to the wounds of the mice. The mice were divided into three groups and treated with different treatments: unconditioned MSC medium, MSC-conditioned medium, or a combination of unconditioned medium with chitosan, collagen, and  $\beta$ -GP thermosensitive hydrogels. Skin tissue samples were collected at different time points and analyzed using hematoxylin and eosin staining and Ki-67 staining. A comparative analysis was conducted to assess the rates and durations of wound healing within the four experimental groups. The use of MSC-CM/hydrogel showed several beneficial effects, including reduced healing time, inflammation restriction, epithelialization facilitation, well-vascularized granulation tissue development, and mitigating the creation of fibrotic and hypertrophic scar tissue. In summary, the use of MSC-CM/hydrogel shows significant efficacy in facilitating wound healing in mice with third-degree burns (Zhou et al., 2019).

Marine organisms yield natural compounds that contain biologically active substances, such as collagen, which serve as a significant reservoir of compounds with medical potential. These compounds have been found to be particularly useful in wound dressing applications, especially when used in conjunction with other natural or synthetic materials, since they expedite the wound healing process. This study evaluates the capacity of collagen derived from *Rutilus kutum* skin combined with chitosan in a collagen-chitosan gel for facilitating the recovery of second-degree burn injuries in rats. Collagen and chitosan were extracted from discarded skin and shells of prawns, and their subunit composition was evaluated using SDS-PAGE. High-performance liquid chromatography (HPLC)

was used to analyze amino acids, and different Col-CH gel formulations were prepared in different ratios. The results showed a significant reduction in wound size in Col-CH treated animals compared to silver sulfadiazine ointment. Histological examination showed an enhancement in epithelial cell growth and blood vessel growth, and a decrease in inflammatory cells. The data suggests that the Col-CH gel combination effectively cures burn wounds, surpassing silver sulfadiazine ointment (Naderi Gharegheshlagh et al., 2021).

The effects of collagen-chitosan gel from *Scomberomorus guttatus* and prawn skin on second-degree burn healing in rats was investigated. Results showed that Col-CH (3:1) treatment significantly decreased wound size and increased epithelialization, collagen content, and fibroblast cell presence. It also reduced inflammatory cell infiltration. The study concluded that Col-CH gel showed superior effectiveness in promoting burn wound healing on the 25th day after the burn, compared to sulfadiazine (Fatemi et al., 2021).

Chronic wounds can lead to limb amputation, and researchers have explored pro-angiogenic agents like cerium oxide and cerium peroxide nanoparticles. These nanoparticles were incorporated into chitosan and collagen hydrogel matrices, and their pro-angiogenic characteristics were investigated using in-vivo CAM tests. The study found that the presence of cerium peroxide in the hydrogels significantly enhanced angiogenesis, compared to cerium oxide-loaded materials. This suggests that cerium peroxide incorporated chitosan and collagen hydrogels have potential for facilitating the healing process of chronic ulcers and burn wounds (Zubairi et al., 2022).

The demand for wound dressings for partial-thickness burns is increasing, and hydrogels have potential as materials for sustaining hydration and facilitating tissue elimination. A study incorporated tilapia peptides and hydroxyapatite into a chitosan system to create novel hydrogels. These hydrogels showed exceptional water absorption, minimal hemolysis, and antibacterial efficacy against bacteria. They also promoted skin regeneration by decreasing TNF- $\alpha$  and IL-6 expression (Qianqian et al., 2021).

#### 6.4. Wound dressings and wound healing

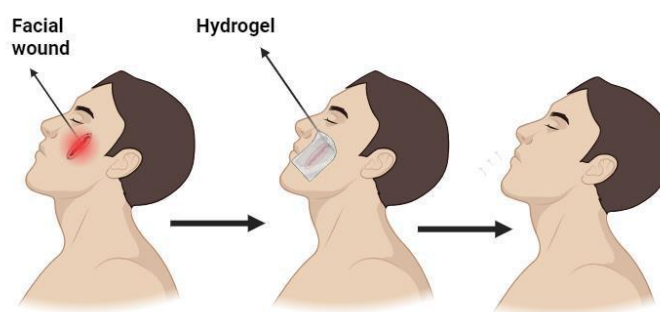
The impact of collagen on chitosan/gelatin hydrogels, specifically their growth and attachment of fibroblasts for wound dressing applications was studied. The hydrogels were synthesized using chitosan and collagen biopolymers, with varying ratios. The hydrogels showed improved mechanical properties, reduced swelling ratio, and superior water vapor transmission rate. Collagen also resulted in a uniform and interconnected architecture,

leading to higher cell survival and attachment rates. These findings suggest the potential of chitosan/collagen hydrogels for wound dressing applications (Mousavi et al., 2019).

One of the most appealing options for a wound dressing is hydrogel because, in addition to acting as a barrier against microorganisms, it also maintains a moist environment at the wound interface, offering three-dimensional structures that support cell adhesion and proliferation and permit the exchange of gases, nutrients, and metabolic waste products (Lakshmanan et al., 2013). A study involving water-soluble carboxymethyl-chitosan (CMCS) crosslinked with genipin was conducted to investigate its impact on wound healing properties. The CMCS was divided into hydrogel, membrane, and sponge dressings. The sponge dressing showed superior water absorption, gas permeability, hemostatic performance, and promotes skin fibroblast proliferation. It also induced

matrix metalloproteinase-1 production. The sponge dressing was effective in wound closure and expedited healing in in-vivo settings. The hydrogel and membrane showed biocompatibility, hemostatic characteristics, and wound healing facilitation. (D. Wang et al., 2020).

A novel chitosan-collagen sponge (CCS) was developed with the intention of exploring its application as a biomaterial for wound dressings. Wound dressing was prepared by using a combination consisting of 3.0% chitosan and 1.0% type I collagen in a ratio of 7:3 (w/w). This mixture was subjected to the freeze-drying process. Subsequently, the dressing was made to assess its qualities via a sequence of tests. The newly developed dressing exhibited its ability to ensure the safety of NIH3T3 cells. The study found that chitosan-collagen wound dressing showed significant improvement in healing after a surgical procedure (**Fig. 14**), indicating its potential as a viable option for future wound treatments. (Zhang et al., 2021).



Created in BioRender.com bio

Fig.14: Hydrogels are used in faster healing of facial wounds

The equine distal limb wound healing model, similar to human wound healing, is used for investigating biomaterials with potential applications in veterinary and human medical fields. A study found significant differences in functional and structural aspects of unwounded and injured skin across different locations on the distal limb. The study also examined the impact of a collagen-chitosan hydrogel modified with peptides on wound healing. The Q-peptide hydrogel increased wound closure and modulated the biomechanical properties of the healed tissue, resulting in a more compliant structure (Sparks et al., 2021).

The use of alginate dialdehyde (ADA) as a crosslinker was explored to improve the mechanical properties of collagen-chitosan (COL-CS) membranes. The resulting COL-CS-ADA films showed improved thermal stability and mechanical characteristics, increased cross-

linking with higher oxidation levels, and no harmful effects on fibroblasts. Additionally, the ADA film significantly improved wound healing and biocompatibility (Yang et al., 2019).

Wound dressings, including hydrogels, films, wafers, nanofibers, foams, and transdermal patches, are used to treat both acute and chronic wounds. The utilization of chitosan and cellulose, two biopolymers, in the formulation of hydrogels was examined with the aim of enhancing wound management. Hydrogels have unique properties like a damp environment, moisture retention, and bacterial protection. Biopolymers, like cellulose and chitosan, are used due to their non-toxic, biodegradable, and biocompatible properties. These hydrogels accelerate wound healing, mimic skin structure, and facilitate skin

regeneration. Antibacterial compounds also help prevent microorganism entry. (Alven & Aderibigbe, 2020).

A collagen and chitosan composite gel was developed, incorporating oligoarginine (R8) as a cell penetrating peptide. The gel was examined for its physical and chemical properties using various techniques. Results showed that the gel effectively inhibited *Staphylococcus aureus* proliferation and promoted wound healing. The gel showed the highest healing rate and rapid speed compared to other treatments. It also enhanced skin wound healing by facilitating granulation tissue formation, collagen accumulation, and angiogenesis (M. Li et al., 2019).

The properties and compatibility of a hydrogel made from collagen, chitosan, and dialdehyde starch, Col/Ch/DAS were investigated. The hydrogels were created by combining collagen and chitosan, with a cross-linker called DAS. The hydrogels showed high swelling and biodegradability and were suitable for wound dressings. A collagen and chitosan composite gel was also created, which inhibited *Staphylococcus aureus* proliferation and promoted wound healing. The gel showed remarkable healing rates and speed, enhancing skin wound healing by facilitating granulation tissue formation and collagen accumulation (Valipour et al., 2023).

Wound healing dressings and scaffolds were introduced, which were composed of single layers in the form of electrospun sheets and hydrogels. A bilayer scaffold consisting of chitosan/gelatin hydrogel and co-electrospun PCL/PVA was developed. The uniqueness of the product stemmed from the utilization of the freeze-gelation technique to attain a porous structure within the hydrogel component of the bilayer configuration. The qualities of the product and its performance in wound healing were evaluated by various methods, including scanning electron microscopy, MTT proliferation assay, swelling analysis, tensile strength testing, and in vivo assessments (Kamali & Shamloo, 2020).

### 6.5. Regeneration of tissues

The utilization of hydrogels derived from various materials has emerged as a novel strategy within the biomedical domain, namely in the realm of regenerative medicine (Catoira et al., 2019). Nerve regeneration using a chitosan-collagen hydrogel neural conduit (CCN) encapsulating Schwann cells (SC) in a rat model with sciatic nerve defects was investigated. The CCN+ group showed enhanced motor functional recovery, axonal regeneration, and myelination compared to the CCN- and silicone+ groups. The use of SC-encapsulated CCNs demonstrates a collaborative impact on peripheral nerve regeneration, promoting the development of axons and remyelination of host SCs. This suggests SC-encapsulated CCNs could be a

viable strategy for addressing extensive peripheral nerve deficits (Takeya et al., 2023).

The production of porous chitosan/collagen composite scaffolds for peripheral nerve tissue engineering applications was studied. The scaffolds were examined using various analytical techniques, including shape, porosity, liquid absorption capacity, swelling behavior, composition, mechanical properties, and degrading behavior. The composite scaffolds showed surface morphology resembling fibers and internal porosity, with chitosan reducing pore size, liquid absorption capacity, and rate of degradation. The physicochemical features were suitable for the proposed use, and the composite scaffolds exhibited cytocompatibility without any harmful effects. The study also demonstrated the composite scaffolds' ability to enhance Schwann cell adhesion, movement, and replication. The chitosan/collagen composite scaffolds have considerable potential for peripheral nerve regeneration (Fig. 15) (Si et al., 2019).

The investigation focused on the potential application of hydrogels composed of chitosan and collagen in the field of skin tissue engineering. Three amino acids (arginine, alanine, and phenylalanine) were incorporated into chitosan/collagen hydrogels, ACC hydrogels. The ACC hydrogels were synthesized using freeze drying and assessed for their angiogenic capabilities using the chorioallantoic membrane assay. ACC hydrogels loaded with arginine had the highest porosity and the highest formation of blood vessels. CH-Arg hydrogels showed higher efficacy in promoting angiogenesis compared to control materials (Aleem et al., 2019).

Fucoidans, sulfated polysaccharides from brown algae, are essential for bone regeneration. To use them in regenerative medicine, a delivery system that temporarily immobilizes the polysaccharide at the injury site is crucial. Hydrogels, which are less invasive, have gained attention for their ability to facilitate healing processes. This study aimed to develop an injectable thermosensitive hydrogel for fucoidan delivery using chitosan, collagen, and  $\beta$ -glycerophosphate. The hydrogel showed compatibility with mesenchymal stem cells (MSC) and endothelial cells (OEC), demonstrating their potential in regenerative medicine. Collagen and chitosan are also recognized biomaterials with their inherent characteristics, functional properties, and environmental friendliness. A study on Col/Ch/DAS hydrogels found that the composition of DAS significantly influenced swelling ratio and biodegradability. The gel composite showed antibacterial characteristics, indicating its therapeutic effectiveness in wound healing (Ohmes et al., 2022).

A hydrogel composite scaffold was created using chitosan-collagen hydrogel, 3D printed poly(lactic acid) struts and nanofibrous cellulose. The scaffolds, which were shaped into micro- and nano-sized topographical features, were designed to enhance cellular activities and mechanical characteristics. The scaffolds, which were applied with

different concentrations of genipin, showed an interconnected microporous architecture, a swelling ratio of 400%, and a compressive strength of approximately 32 kPa. The scaffold showed minimal cytotoxicity towards rabbit mesenchymal stem cells and facilitated cellular attachment, proliferation, and migration (Gunes et al., 2022).

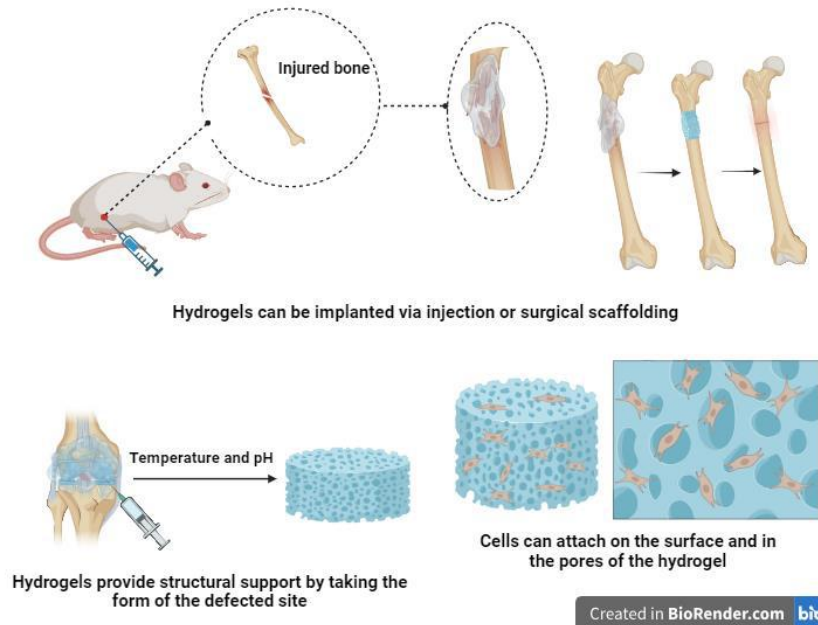


Fig.15: Hydrogels help in bone and tissue repair

The use of crosslinking strategies in creating polymeric biomaterial scaffolds was examined. It focuses on a collagen-chitosan hydrogel film created using tannic acid and genipin simultaneously. The film's porosity and strength were evaluated using infrared analysis spectroscopy, scanning electron microscopy, and thermogravimetric analysis. The dual crosslinking process significantly influences the films' strength and adhesion and multiplication of cells. This technique has gained widespread use in ophthalmology for temporary corneal injuries and skin tissue regeneration (Shah et al., 2019).

The hydrogel nanocomposites were fabricated using chitosan/collagen and chitosan/collagen/nano-hydroxyapatite (nHAP) from Persian Gulf shrimp wastes and rat tail tendons. The porous scaffolds were assessed using various techniques like SEM, FTIR, water content, STA, and AFM nanoindentation. The results showed significant promise for cartilage tissue engineering, suggesting the hydrogels could be a viable candidate (Kaviani et al., 2019).

The skin is a multilayered organ that acts as the primary barrier between the inside tissues or cells and the outside environment, protecting them. To achieve the desired mechanical qualities of artificial skin, it is imperative to prioritize the considerations of

biocompatibility and biodegradability. In contrast to other living organisms, humans have exhibited limited tissue regeneration due to genetic variability. Furthermore, hydrogel scaffolds have gained a growing interest for the purpose of repairing and regenerating skin tissue. This is primarily due to their remarkable capacity to undergo self-renewal and promote the proliferation of the specific cell populations that play a crucial role in the regeneration of skin tissue. Additionally, an investigation was conducted on the intelligent healing capabilities of hydrogel scaffolds loaded with peptides and growth factors for the purpose of regeneration in skin tissues (Kalai Selvan et al., 2020).

ColChHAmoD (Collagen-Chitosan-Hyaluronic acid) hydrogels, made from genipin crosslinked collagen, chitosan, and lysine-modified hyaluronic acid, are a novel material for injection applications. These hydrogels have unique properties, such as interaction with living organisms and multiple functions. By adding primary amine groups through lysine attachment, HAmoD can form covalent links with other hydrogel components, resulting in structurally robust and clear hydrogels. The hydrogels can be controlled for bone tissue regeneration and have varying physicochemical properties. In vitro cell culture experiments confirmed their biocompatible surfaces and

antibacterial activity against *Escherichia coli* (Gilarska et al., 2020).

Use of alkaline phosphatase (ALP) in nanotubes made of halloysite (HAL) and incorporated into hydrogel scaffolds made of chitosan (CH) and chitosan-collagen (C-CH) to promote bone regeneration was studied. The addition of 30% HAL-ALP significantly increased the swelling ratio of chitosan-based scaffolds, while collagen enhanced porosity. The biomineralization process was more effective in hydrogels with collagen. C-CH scaffolds, particularly those with biomineralization, showed enhanced cell attachment and proliferation properties. The C-CH scaffolds with a 30% concentration of HAL-ALP showed the highest capacity for bone regeneration (Pietraszek et al., 2020).

Biomineralization is crucial for bone repair, where calcium and phosphate ions are deposited into the extracellular matrix (ECM). To mimic this process, a composite hydrogel made of chitosan and collagen has been created. The hydrogel contains black phosphorus coated with mesenchymal stem cell membranes, which activates osteoblast recruitment through near-infrared light. This leads to the formation of hydroxyapatite, which stimulates osteoblast movement and bone formation. The hydrogel therapy, when implanted into cranial defects of lab rats, improved local bone density and new bone generation. This research has significant implications for bone healing and treating cranial abnormalities in clinical settings (Tan et al., 2022).

### 6.6. Management and healing of ulcers

A porous cross-linked hydrogel was developed for treating persistent skin ulcers, combining collagen and chitosan. Cross-linking techniques like UV irradiation, tannic acid, and ultrasonication were used. The hydrogel's composition, chitosan concentration, and ratio were crucial for its effectiveness. Stable systems were achieved through freeze-drying. The Design of Experiments methodology was used to determine the optimal hydrogel composition. The scaffold's biocompatibility, biomimicry, and safety were tested in vitro and in vivo (Valentino et al., 2023).

Diabetic foot ulcers (DFUs) represent a highly widespread concern commonly observed in individuals diagnosed with diabetes mellitus. Diabetic foot ulcers (DFUs) are enduring lesions that frequently result in non-traumatic amputations of the lower extremities, primarily due to persistent infection and other adverse effects associated with ulcers. Furthermore, these issues pose a substantial financial strain on the healthcare system due to the necessity of costly medical interventions. Furthermore, the existing clinical interventions for diabetic foot ulcers (DFUs) have demonstrated only modest efficacy,

highlighting the urgent requirement for the development of innovative approaches to enhance the treatment outcomes of DFUs. Hydrogels are complex structures that can be produced using a combination of natural and/or synthetic polymers. These materials have undergone substantial research for many biological applications, such as drug delivery and tissue engineering, due to their distinctive adaptability, tunability, and hydrophilic characteristics (Güiza-Argüello et al., 2022).

Based on data provided by the World Health Organization, an estimated annual fatality counts of 180,000 has been attributed to burn-related incidents. Chronic wounds affect 6.5 million Americans, requiring advanced therapeutic strategies. Biodegradable polymeric wound dressings have been developed over the past 50 years, eliminating the need for frequent replacements, and reducing immune response risk. These polymers come from natural or synthetic sources, with natural polymers preferable due to biocompatibility and mechanical capabilities (Miguel et al., 2021).

Diabetic foot ulcers (DFU) frequently exhibit a challenging healing process, even when conventional care protocols are implemented. The effectiveness of novel collagen matrix dressings was assessed using chitosan-collagen hydrogel in comparison to conventional dressing, for the purpose of promoting wound healing in individuals with a chronic diabetic foot ulcer (DFU). The study involved 61 patients with neuropathic diabetic foot ulcers. The study group received a collagen matrix dressing from Tebaderm, while the control group received gauze. The study group showed a higher reduction in DFU size at four weeks and a higher percentage of full healing at 20 weeks. Collagen matrix dressings can expedite wound healing, potentially reducing the duration needed for full recovery (Djavid et al., 2020).

Corneal disease is the second leading cause of blindness, with around 10 million people worldwide experiencing visual impairment. Research on wound dressings for corneal coverage has shown potential for optimal healing. A chitosan coating was applied to an electrospun membrane made of collagen, hyaluronic acid, and PEO, with glutaraldehyde as a crosslinking agent. The coating enhanced membrane transparency but did not significantly change it. The pore diameter of the membrane decreased with increased chitosan coating concentration. The membrane's cell viability was non-toxic, and the coating showed antibacterial properties, particularly against *Pseudomonas aeruginosa*. In summary, the incorporation of a chitosan coating has been found to enhance the properties of the electrospun membrane utilized for wound dressing in cases of corneal ulcers (Putra et al., 2020).

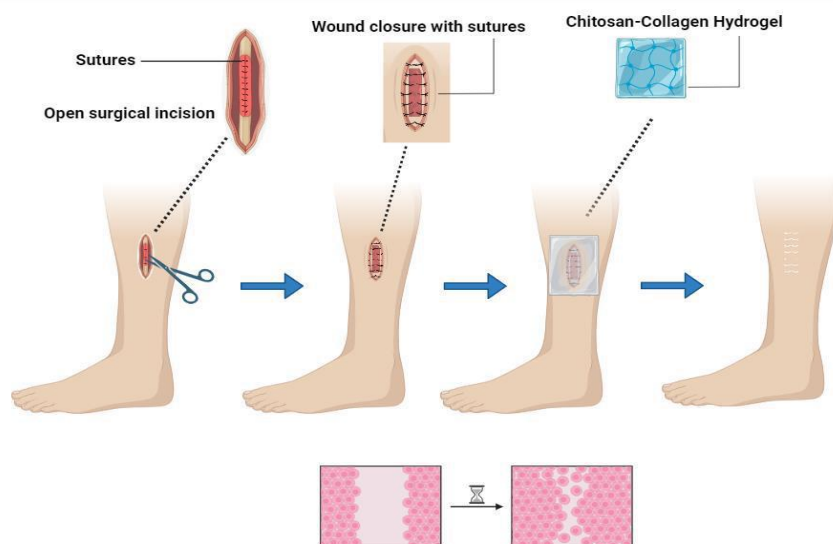
The most effective delivery strategy for mesenchymal stem cells secretome as a diabetic wound dressing is a film-forming spray composed of a hydrogel matrix including carboxymethyl chitosan, hyaluronic acid, and collagen tripeptide (CCHACTP). The application of a chitosan/collagen hydrogel patch resulted in the expedited healing of diabetic foot ulcers (Umar et al., 2022). Chitosan-based hydrogels and membranes are used for managing cutaneous injuries like wounds, burns, and ulcers. They improve wound healing by boosting immunomodulatory, antimicrobial, and local cell proliferative activity. They stimulate cellular metabolism and reduce scar size. Chitosan-based membranes have favorable characteristics, making them suitable for chronic wound management. Changes to chitosan can improve its physicochemical properties, creating multilayer membranes and self-healing hydrogels. Other formulations include sponges, topical gels, and coatings (Kim et al., 2023). Studies have been conducted on chitosan biomaterials for the purpose of treating wounds with diverse causes, such as burn wounds and pressure ulcers. These biomaterials are utilized in the development of dressing materials. (Zavalyova et al., 2021).

### 6.7. Closure of surgical wounds

Traditionally, conventional methods for closing surgical wounds have involved the utilization of sutures, staples, or wires. Nevertheless, the use of these methodologies, specifically in relation to parenchymatous tissues like the lung, liver, or kidney, may result in necrosis and wound dehiscence. In addition to this, surgical operations frequently elicit significant health issues

associated with haemorrhage. Minimally invasive procedures encounter notable challenges associated with bleeding, such as the potential impairment of eyesight during ocular treatments. Consequently, surgical sealants, possessing the twin capability of hemostasis and wound closure, have emerged as a crucial element in the surgical repertoire for the purpose of controlling persistent bleeding. (Chiara et al., 2018). Currently, within the domain of sutureless surgical techniques, a diverse array of protein-based adhesives (such as fibrin, collagen, and gelatin), polysaccharide-based adhesives (including chitosan and alginate), as well as cyanoacrylate-based adhesives, are employed for a multitude of clinical wound closure purposes (Baghdasarian et al., 2022).

Sutures are the primary surgical wound closure method, but they can cause foreign body reactions and atypical collagen accumulation, leading to hypertrophic scars. The development of suture materials that can effectively suppress inflammation and minimize scar formation is of paramount clinical importance. The S@LC@CGTP suture material was developed which was a combination of a conventional 3-0 PPDO (poly(p-dioxanone)) suture and two additional layers, showed promising sustained-drug release characteristics in vitro and in vivo. The drug-loaded layer contained curcumin, while the electroactive layer was made of oligochitosan-gelatin/tannic acid/polypyrrole. Collectively, S@LC@CGTP suture material possesses significant promise in promoting ideal, scar-free wound healing following surgical incisions (Han et al., 2023).



Created in BioRender.com bio

Fig.16: Chitosan-collagen hydrogels accelerate surgical wound closure and healing



Composite hydrogels referred to as Gel-ZBG consisting of ZBG (zinc doped bioactive glass), SCS (succinyl chitosan), and OAL (oxidized alginate) have been developed. These were designed specifically for use as wound dressings, with the aim of promoting faster wound closure in **Fig. 16**. The incorporation of Schiff-based connections into composite hydrogels has been implemented to create a moist microenvironment that promotes cell growth at wound sites. The composite hydrogels were shown to possess remarkable antibacterial capabilities, as

evidenced by the *in vitro* antibacterial assays. The presence of  $\text{Si}^{4+}$  and  $\text{Ca}^{2+}$  ions is crucial in promoting the secretion of beneficial factors by fibroblasts, hence facilitating the processes of angiogenesis and wound closure (Jiangying Zhu et al., 2019).

The primary hazards contributing to casualties in catastrophes are extensive bleeding and wound infection resulting from tissue trauma, which demand first-aid provisions that can successfully facilitate wound closure, as well as efficiently manage haemorrhage and infection. The hemostatic and antibacterial properties of current tissue adhesives are often limited. A liquid bandage (LBA) called NB-CMC/CMC hydrogel is an *in-situ* imine crosslinking-based photoresponsive chitosan hydrogel. The modified carboxymethyl chitosan (CMC) demonstrates enhanced tissue adhesive performance. Furthermore, it demonstrates favorable biocompatibility, biodegradability, and the potential to augment the wound healing process and for wound closure (Ma et al., 2020).

Suture lines have been used for wound healing for millennia, with polysaccharides like celluloses, starches, and glycogens being common. Cotton is a popular suture material, but regenerated celluloses and hydrogel polysaccharide materials like chitosan and alginate are also used in modern medical practice (Peng et al., 2020). The experimental findings indicate that the groups treated with the hydrogels exhibited accelerated wound recovery and earlier healing compared to the control groups. This advocates a considerable advancement in the use of hydrogels for wound repair and closure of wounds (Pan et al., 2019).

## VII. CHALLENGES IN THE DEVELOPMENT AND USE OF INNOVATIONS FOR THE BETTERMENT

A hydrogel must meet application-specific design criteria to suitably treat a medical condition. Broadly, these design criteria can be defined as either physical, chemical, or biological. Despite the success of hydrogel-based delivery systems, key technological challenges including

chemistry, manufacturing and controls, defined regulatory guidelines, and practical adaptability remain as major roadblocks in their successful clinical translation (Mandal et al., 2020). Since hydrogel fabrication is complex and varies between hydrogel systems, the development costs through clinical translation range in estimation from \$50 million up to \$800 million (Li & Mooney, 2016). Despite being a well-known biopolymer with various biomedical applications, chitosan also has some limitations such as small specific surface area and void fraction that should be overcome (Esquerdo et al., 2014). While collagen could control drug release from hydrogels and could induce cell growth (Ghasemiyeh & Mohammadi-Samani, 2019).

Chemical and physical crosslinking methods using glutaraldehyde (GA) and ammonium hydroxide (AH), respectively, were utilized to prepare chitosan (CS) and chitosan/collagen (CS-Co) hydrogels; these materials were then subjected to freeze-drying process to obtain 3D porous scaffolds. Physically crosslinked scaffolds exhibited a homogeneous morphology with higher pore size and interconnectivity in comparison to other prepared scaffolds; also, these samples, showed a good biocompatibility. Scaffolds derived from hydrogels treated with acetone (AC) showed shrinkage, smaller pore size and higher degradation rates; finally, materials chemically crosslinked with glutaraldehyde presented cytotoxicity and exhibited a heterogeneous morphology (Reyna-Urrutia et al., 2019).

The collagen–chitosan material was more resistant to enzymatic degradation and was better able to maintain its form over time. Ideally, the degradation rate of the biomaterial matches the regeneration rate of the host tissue and the collagen–chitosan degradation rate can be regulated by adjusting the ratio of collagen to chitosan. The ability to control degradation and structural integrity should prevent a sudden loss of mechanical properties that may occur from materials with more rapid degradation rates. It is likely that the addition of chitosan conferred these improved physical properties, at least in part, through the provision of additional amino groups, which would serve to increase the crosslinking density and reinforce the hydrogel (Deng et al., 2010).

Graphene oxide (GO) a nanostructure with high surface area and high surface functional groups enhances the biological properties of collagen hydrogel scaffold for neural stem/precursor cells (NS/PCs). Addition of 1%–1.5% GO to collagen hydrogel (by weight of collagen) provided a hydrogel in which nNS/PCs could survive and migrate more in comparison with control (poly-L-lysine coated well) and pure collagen. Also, GO modulates elasticity of collagen hydrogels and makes it favorable for neural stem cells (Rezaei et al., 2021). A composite

hydrogel was developed consisting of photocrosslinkable methacrylated glycol chitosan (MeGC) and semi-interpenetrating collagen (Col) with a riboflavin photoinitiator under blue light. The incorporation of Col in MeGC hydrogels enhanced the compressive modulus and slowed the degradation rate of the hydrogels. MeGC–Col composite hydrogels significantly enhanced cellular attachment, spreading, proliferation and osteogenic differentiation of mouse bone marrow stromal cells (BMSCs) seeded on the hydrogels compared with pure MeGC hydrogels, as observed by upregulated alkaline phosphatase (ALP) activity as well as increased mineralization (Arakawa et al., 2017).

### VIII. CONCLUSION

In conclusion, temperature- and pH-sensitive chitosan-collagen hydrogels have a variety of applications in wound healing along with effective antimicrobial potential. The combined beneficial effects of chitosan and collagen in composite hydrogels have enabled health professionals to treat wounds that were hard to heal in the past with traditional dressings. Chitosan helps in the release of antimicrobial agents in response to changes in temperature and pH, while collagen plays a role in wound healing by promoting tissue regeneration. Chitosan-collagen hydrogels stimulate advanced wound healing compared to commercial dressings, proving their potential as dressings for full-thickness skin wound healing. Their temperature and pH sensitivity make them able to perform their activity in the desired manner. The composite chitosan-collagen hydrogels have improved hydrophilicity, which prevents the immediate dissolution of the hydrogel in an aqueous solution. Combining chitosan and collagen results in hydrogels with higher mechanical strength in comparison to mere chitosan or collagen hydrogels. A moist environment appropriate for wound healing is efficiently maintained by chitosan-collagen hydrogels, along with a slow degradation rate. These novel biomaterials have not only the exceptional attributes of chitosan and collagen but also the ability to respond to temperature and pH changes, which makes them important defense equipment against infections and promotes wound healing. The biocompatibility of temperature- and pH-sensitive chitosan-collagen hydrogels make them an innovative solution for healing chronic wounds and controlling infections. Further research in this domain can unlock more opportunities for cheaper production of these biomaterials for the treatment of a variety of health complications.

### REFERENCES

- [1] Agarwal, V., Toshniwal, P., Smith, N. E., Smith, N. M., Li, B., Clemons, T. D., Byrne, L. T., Kakulas, F., Wood, F. M., & Fear, M. (2016). Enhancing the efficacy of cation-independent mannose 6-phosphate receptor inhibitors by intracellular delivery. *Chemical communications*, 52(2), 327-330.
- [2] Ahmad, Z., Salman, S., Khan, S. A., Amin, A., Rahman, Z. U., Al-Ghamdi, Y. O., Akhtar, K., Bakhsh, E. M., & Khan, S. B. (2022). Versatility of hydrogels: from synthetic strategies, classification, and properties to biomedical applications. *Gels*, 8(3), 167.
- [3] Ahmadian, Z., Correia, A., Hasany, M., Figueiredo, P., Dobakhti, F., Eskandari, M. R., Hosseini, S. H., Abiri, R., Khorshid, S., & Hirvonen, J. (2021). A hydrogen-bonded extracellular matrix-mimicking bactericidal hydrogel with radical scavenging and hemostatic function for pH-responsive wound healing acceleration. *Advanced Healthcare Materials*, 10(3), 2001122.
- [4] Ahmed, S., & Ikram, S. (2016). Chitosan based scaffolds and their applications in wound healing. *Achievements in the life sciences*, 10(1), 27-37.
- [5] Alagha, A., Nourallah, A., & Hariri, S. (2020). Characterization of dexamethasone loaded collagen-chitosan sponge and in vitro release study. *Journal of Drug Delivery Science and Technology*, 55, 101449. <https://doi.org/https://doi.org/10.1016/j.jddst.2019.101449>
- [6] Alberti, T. B., Coelho, D. S., de Prá, M., Maraschin, M., & Veleirinho, B. (2020). Electrospun PVA nanoscaffolds associated with propolis nanoparticles with wound healing activity. *Journal of Materials Science*, 55(23), 9712-9727.
- [7] Aleem, A. R., Shahzadi, L., Tehseen, S., Alvi, F., Chaudhry, A. A., Rehman, I. u., & Yar, M. (2019). Amino acids loaded chitosan/collagen based new membranes stimulate angiogenesis in chorioallantoic membrane assay. *International Journal of Biological Macromolecules*, 140, 401-406. <https://doi.org/https://doi.org/10.1016/j.ijbiomac.2019.08.095>
- [8] Ali, A., & Ahmed, S. (2018). A review on chitosan and its nanocomposites in drug delivery. *International Journal of Biological Macromolecules*, 109, 273-286. <https://doi.org/https://doi.org/10.1016/j.ijbiomac.2017.12.078>
- [9] Ali, A. F., Ahmed, M. M., El-Kady, A. M., Abd El-Hady, B. M., & Ibrahim, A. M. (2021). Synthesis of gelatin-agarose scaffold for controlled antibiotic delivery and its modification by glass nanoparticles addition as a potential osteomyelitis treatment. *Silicon*, 13, 2011-2028.
- [10] Almajed, A., Lemboye, K., & Moghal, A. A. B. (2022). A critical review on the feasibility of synthetic polymers inclusion in enhancing the geotechnical behavior of soils. *Polymers*, 14(22), 5004.
- [11] Alven, S., & Aderibigbe, B. A. (2020). Chitosan and Cellulose-Based Hydrogels for Wound Management. *International Journal of Molecular Sciences*, 21(24), 9656. <https://www.mdpi.com/1422-0067/21/24/9656>

- [12] Alven, S., & Aderibigbe, B. A. (2021). Hyaluronic acid-based scaffolds as potential bioactive wound dressings. *Polymers*, 13(13), 2102.
- [13] Arakawa, C., Ng, R., Tan, S., Kim, S., Wu, B., & Lee, M. (2017). Photopolymerizable chitosan–collagen hydrogels for bone tissue engineering. *Journal of Tissue Engineering and Regenerative Medicine*, 11(1), 164-174. <https://doi.org/https://doi.org/10.1002/term.1896>
- [14] Arbia, W., Arbia, L., Adour, L., & Amrane, A. (2013). Chitin extraction from crustacean shells using biological methods—a review. *Food Technology and Biotechnology*, 51(1), 12-25.
- [15] Ata, S., Rasool, A., Islam, A., Bibi, I., Rizwan, M., Azeem, M. K., & Iqbal, M. (2020). Loading of Cefixime to pH sensitive chitosan based hydrogel and investigation of controlled release kinetics. *International Journal of Biological Macromolecules*, 155, 1236-1244.
- [16] Atalay, S., Jarocka-Karpowicz, I., & Skrzydlewska, E. (2019). Antioxidative and anti-inflammatory properties of cannabidiol. *Antioxidants*, 9(1), 21.
- [17] Azaza, Y. B., van der lee, A., Li, S., Nasri, M., & Nasri, R. (2023). Chitosan/collagen-based hydrogels for sustainable development: Phycocyanin controlled release. *Sustainable Chemistry and Pharmacy*, 31, 100905. <https://doi.org/https://doi.org/10.1016/j.scp.2022.100905>
- [18] Baghaie, S., Khorasani, M. T., Zarrabi, A., & Moshtaghian, J. (2017). Wound healing properties of PVA/starch/chitosan hydrogel membranes with nano Zinc oxide as antibacterial wound dressing material. *Journal of Biomaterials Science, Polymer Edition*, 28(18), 2220-2241.
- [19] Baghdasarian, S., Saleh, B., Baidya, A., Kim, H., Ghovvati, M., Sani, E. S., Haghniaz, R., Madhu, S., Kanelli, M., Noshadi, I., & Annabi, N. (2022). Engineering a naturally derived hemostatic sealant for sealing internal organs. *Materials Today Bio*, 13, 100199. <https://doi.org/https://doi.org/10.1016/j.mtbio.2021.100199>
- [20] Banerjee, S., Szepes, M., Dibbert, N., Rios-Camacho, J.-C., Kirschning, A., Gruh, I., & Dräger, G. (2021). Dextran-based scaffolds for in-situ hydrogelation: Use for next generation of bioartificial cardiac tissues. *Carbohydrate Polymers*, 262, 117924.
- [21] Barroso, T., Viveiros, R., Casimiro, T., & Aguiar-Ricardo, A. (2014). Development of dual-responsive chitosan–collagen scaffolds for pulsatile release of bioactive molecules. *The Journal of Supercritical Fluids*, 94, 102-112.
- [22] Bautista, J., Jover, M., Gutierrez, J., Corpas, R., Cremades, O., Fontiveros, E., Iglesias, F., & Vega, J. (2001). Preparation of crayfish chitin by in situ lactic acid production. *Process biochemistry*, 37(3), 229-234.
- [23] Bax, D. V., Davidenko, N., Hamaia, S. W., Farnedale, R. W., Best, S. M., & Cameron, R. E. (2019). Impact of UV-and carbodiimide-based crosslinking on the integrin-binding properties of collagen-based materials. *Acta biomaterialia*, 100, 280-291.
- [24] Berger, J., Reist, M., Mayer, J., Felt, O., Peppas, N., & Gurny, R. (2004). Structure and interactions in covalently and ionically crosslinked chitosan hydrogels for biomedical applications. *European journal of pharmaceuticals and biopharmaceutics*, 57(1), 19-34.
- [25] Bhattarai, N., Gunn, J., & Zhang, M. (2010). Chitosan-based hydrogels for controlled, localized drug delivery. *Advanced drug delivery reviews*, 62(1), 83-99.
- [26] Bolke, L., Schlippe, G., Gerß, J., & Voss, W. (2019). A collagen supplement improves skin hydration, elasticity, roughness, and density: Results of a randomized, placebo-controlled, blind study. *Nutrients*, 11(10), 2494.
- [27] Brzeska, J., Tercjak, A., Sikorska, W., Kowalczyk, M., & Rutkowska, M. (2019). Morphology and physicochemical properties of branched polyurethane/biopolymer blends. *Polymers*, 12(1), 16.
- [28] Burkatovskaya, M., Tegos, G. P., Swietlik, E., Demidova, T. N., Castano, A. P., & Hamblin, M. R. (2006). Use of chitosan bandage to prevent fatal infections developing from highly contaminated wounds in mice. *Biomaterials*, 27(22), 4157-4164.
- [29] Çakmak, A., Çirpanli, Y., Bilensoy, E., Yorgancı, K., Çaliş, S., Saribaş, Z., & Kaynaroğlu, V. (2009). Antibacterial activity of triclosan chitosan coated graft on hernia graft infection model. *International journal of pharmaceuticals*, 381(2), 214-219.
- [30] Cao, J., Wang, P., Liu, Y., Zhu, C., & Fan, D. (2020). Double crosslinked HLC-CCS hydrogel tissue engineering scaffold for skin wound healing. *International Journal of Biological Macromolecules*, 155, 625-635.
- [31] Cao, J., You, J., Zhang, L., & Zhou, J. (2018). Homogeneous synthesis and characterization of chitosan ethers prepared in aqueous alkali/urea solutions. *Carbohydrate Polymers*, 185, 138-144.
- [32] Cardoso-Daodu, I. M., Ilomuanya, M. O., & Azubuike, C. P. (2022). Development of curcumin-loaded liposomes in lysine–collagen hydrogel for surgical wound healing. *Beni-Suef University Journal of Basic and Applied Sciences*, 11(1), 100. <https://doi.org/10.1186/s43088-022-00284-2>
- [33] Carvalho, D. N., Gonçalves, C., Oliveira, J. M., Williams, D. S., Mearns-Spragg, A., Reis, R. L., & Silva, T. H. (2022). A design of experiments (DoE) approach to optimize cryogel manufacturing for tissue engineering applications. *Polymers*, 14(10), 2026.
- [34] Catoira, M. C., Fusaro, L., Di Francesco, D., Ramella, M., & Boccafroschi, F. (2019). Overview of natural hydrogels for regenerative medicine applications. *Journal of Materials Science: Materials in Medicine*, 30(10), 115. <https://doi.org/10.1007/s10856-019-6318-7>
- [35] Chang, S.-W., Shefelbine, S. J., & Buehler, M. J. (2012). Structural and mechanical differences between collagen homo-and heterotrimers: relevance for the molecular origin of brittle bone disease. *Biophysical journal*, 102(3), 640-648.
- [36] Chaves, L. L., Silveri, A., Vieira, A. C. C., Ferreira, D., Cristiano, M. C., Paolino, D., Di Marzio, L., Lima, S. C., Reis, S., Sarmiento, B., & Celia, C. (2019). pH-responsive chitosan based hydrogels affect the release of dapson: Design, set-up, and physicochemical characterization. *International Journal of Biological Macromolecules*, 133, 1268-1279.

- <https://doi.org/https://doi.org/10.1016/j.ijbiomac.2019.04.178>
- [37] Chen, G., Ren, J., Deng, Y., Wu, X., Huang, J., Wang, G., Zhao, Y., & Li, J. (2017). An injectable, wound-adapting, self-healing hydrogel for fibroblast growth factor 2 delivery system in tissue repair applications. *Journal of biomedical nanotechnology*, 13(12), 1660-1672.
- [38] Chen, H., Xing, X., Tan, H., Jia, Y., Zhou, T., Chen, Y., Ling, Z., & Hu, X. (2017). Covalently antibacterial alginate-chitosan hydrogel dressing integrated gelatin microspheres containing tetracycline hydrochloride for wound healing. *Materials Science and Engineering: C*, 70, 287-295.
- [39] Cheng, S., Wang, W., Li, Y., Gao, G., Zhang, K., Zhou, J., & Wu, Z. (2019). Cross-linking and film-forming properties of transglutaminase-modified collagen fibers tailored by denaturation temperature. *Food chemistry*, 271, 527-535.
- [40] Cheng, X., Shao, Z., Li, C., Yu, L., Raja, M. A., & Liu, C. (2017). Isolation, characterization and evaluation of collagen from jellyfish *Rhopilema esculentum* Kishinouye for use in hemostatic applications. *PloS one*, 12(1), e0169731.
- [41] Chiara, O., Cimbanassi, S., Bellanova, G., Chiarugi, M., Mingoli, A., Olivero, G., Ribaldi, S., Tugnoli, G., Basilicò, S., & Bindi, F. (2018). A systematic review on the use of topical hemostats in trauma and emergency surgery. *BMC surgery*, 18(1), 1-20.
- [42] Cho, J., Heuzey, M.-C., Bégin, A., & Carreau, P. J. (2005). Physical Gelation of Chitosan in the Presence of  $\beta$ -Glycerophosphate: The Effect of Temperature. *Biomacromolecules*, 6(6), 3267-3275. <https://doi.org/10.1021/bm050313s>
- [43] Chuysinuan, P., Thanyacharoen, T., Thongchai, K., Techasakul, S., & Ummartyotin, S. (2020). Preparation of chitosan/hydrolyzed collagen/hyaluronic acid based hydrogel composite with caffeic acid addition. *International Journal of Biological Macromolecules*, 162, 1937-1943. <https://doi.org/https://doi.org/10.1016/j.ijbiomac.2020.08.139>
- [44] Croisier, F., & Jérôme, C. (2013). Chitosan-based biomaterials for tissue engineering. *European Polymer Journal*, 49(4), 780-792.
- [45] Cui, F., Li, G., Huang, J., Zhang, J., Lu, M., Lu, W., Huan, J., & Huang, Q. (2011). Development of chitosan-collagen hydrogel incorporated with lysostaphin (CCHL) burn dressing with anti-methicillin-resistant *Staphylococcus aureus* and promotion wound healing properties. *Drug delivery*, 18(3), 173-180.
- [46] Dai, T., Tegos, G. P., Burkatovskaya, M., Castano, A. P., & Hamblin, M. R. (2009). Chitosan acetate bandage as a topical antimicrobial dressing for infected burns. *Antimicrobial agents and chemotherapy*, 53(2), 393-400.
- [47] Deng, C., Zhang, P., Vulesevic, B., Kuraitis, D., Li, F., Yang, A. F., Griffith, M., Ruel, M., & Suuronen, E. J. (2010). A collagen-chitosan hydrogel for endothelial differentiation and angiogenesis. *Tissue Engineering Part A*, 16(10), 3099-3109.
- [48] Díaz-Montes, E. (2021). Dextran: sources, structures, and properties. *Polysaccharides*, 2(3), 554-565.
- [49] Djavid, G. E., Tabaie, S. M., Tajali, S. B., Totouchi, M., Farhoud, A., Fateh, M., Ghafghazi, M., Koosha, M., & Taghizadeh, S. (2020). Application of a collagen matrix dressing on a neuropathic diabetic foot ulcer: a randomised control trial. *Journal of Wound Care*, 29(Sup3), S13-S18. <https://doi.org/10.12968/jowc.2020.29.Sup3.S13>
- [50] Dong, C., & Lv, Y. (2016). Application of collagen scaffold in tissue engineering: recent advances and new perspectives. *Polymers*, 8(2), 42.
- [51] Dong, Y., Hassan, W. U., Kennedy, R., Greiser, U., Pandit, A., Garcia, Y., & Wang, W. (2014). Performance of an in situ formed bioactive hydrogel dressing from a PEG-based hyperbranched multifunctional copolymer. *Acta biomaterialia*, 10(5), 2076-2085.
- [52] Duan, R., Zhang, J., Du, X., Yao, X., & Konno, K. (2009). Properties of collagen from skin, scale and bone of carp (*Cyprinus carpio*). *Food chemistry*, 112(3), 702-706.
- [53] Duceac, I. A., Lobiuc, A., Coseri, S., & Verestiuc, L. (2019, 21-23 Nov. 2019). Tunable Hydrogels based on Chitosan, Collagen and Poly(Acrylic Acid) for Regenerative Medicine. 2019 E-Health and Bioengineering Conference (EHB).
- [54] Ertl, P., Altmann, E., & McKenna, J. M. (2020). The most common functional groups in bioactive molecules and how their popularity has evolved over time. *Journal of medicinal chemistry*, 63(15), 8408-8418.
- [55] Esquerdo, V. M., Cadaval Jr, T., Dotto, G., & Pinto, L. (2014). Chitosan scaffold as an alternative adsorbent for the removal of hazardous food dyes from aqueous solutions. *Journal of colloid and interface science*, 424, 7-15.
- [56] Ezati, P., & Rhim, J.-W. (2020). pH-responsive chitosan-based film incorporated with alizarin for intelligent packaging applications. *Food Hydrocolloids*, 102, 105629.
- [57] Fadeeva, I. V., Trofimchuk, E. S., Forsyenkova, A. A., Ahmed, A. I., Gnezdilov, O. I., Davydova, G. A., Kozlova, S. G., Antoniac, A., & Rau, J. V. (2021). Composite polyvinylpyrrolidone-sodium alginate-Hydroxyapatite hydrogel films for bone repair and wound dressings applications. *Polymers*, 13(22), 3989.
- [58] Fan, Z., Liu, B., Wang, J., Zhang, S., Lin, Q., Gong, P., Ma, L., & Yang, S. (2014). A novel wound dressing based on Ag/graphene polymer hydrogel: effectively kill bacteria and accelerate wound healing. *Advanced Functional Materials*, 24(25), 3933-3943.
- [59] Fatemi, M. J., Garahgheshlagh, S. N., Ghadimi, T., Jamili, S., Nourani, M. R., Sharifi, A. M., Saberi, M., Amini, N., Sarmadi, V. H., & Yazdi-Amirkhiz, S. Y. (2021). Investigating the Impact of Collagen-Chitosan Derived from *Scomberomorus Guttatus* and Shrimp Skin on Second-Degree Burn in Rats Model. *Regenerative Therapy*, 18, 12-20. <https://doi.org/https://doi.org/10.1016/j.reth.2021.03.001>
- [60] Fathi, M., Alami-Milani, M., Geranmayeh, M. H., Barar, J., Erfan-Niya, H., & Omid, Y. (2019). Dual thermo-and pH-sensitive injectable hydrogels of chitosan/(poly(N-isopropylacrylamide-co-itaconic acid)) for doxorubicin delivery in breast cancer. *International Journal of Biological Macromolecules*, 128, 957-964.

- <https://doi.org/https://doi.org/10.1016/j.ijbiomac.2019.01.122>
- [61] Felician, F. F., Xia, C., Qi, W., & Xu, H. (2018). Collagen from marine biological sources and medical applications. *Chemistry & biodiversity*, 15(5), e1700557.
- [62] Feng, X., Zhang, X., Li, S., Zheng, Y., Shi, X., Li, F., Guo, S., & Yang, J. (2020). Preparation of aminated fish scale collagen and oxidized sodium alginate hybrid hydrogel for enhanced full-thickness wound healing. *International Journal of Biological Macromolecules*, 164, 626-637.
- [63] Ferrario, C., Rusconi, F., Pulaj, A., Macchi, R., Landini, P., Paroni, M., Colombo, G., Martinello, T., Melotti, L., & Gomiero, C. (2020). From food waste to innovative biomaterial: Sea urchin-derived collagen for applications in skin regenerative medicine. *Marine Drugs*, 18(8), 414.
- [64] Fidalgo, C., Rodrigues, M., Peixoto, T., Lobato, J., Santos, J., & Lopes, M. (2018). Development of asymmetric resorbable membranes for guided bone and surrounding tissue regeneration. *Journal of Biomedical Materials Research Part A*, 106(8), 2141-2150.
- [65] Forero, J. C., Roa, E., Reyes, J. G., Acevedo, C., & Osses, N. (2017). Development of useful biomaterial for bone tissue engineering by incorporating nano-copper-zinc alloy (nCuZn) in chitosan/gelatin/nano-hydroxyapatite (Ch/G/nHAp) scaffold. *Materials*, 10(10), 1177.
- [66] Frayssinet, A., Petta, D., Illoul, C., Haye, B., Markitantova, A., Eglin, D., Mosser, G., D'este, M., & H elary, C. (2020). Extracellular matrix-mimetic composite hydrogels of cross-linked hyaluronan and fibrillar collagen with tunable properties and ultrastructure. *Carbohydrate Polymers*, 236, 116042.
- [67] Freytes, D. O., Martin, J., Velankar, S. S., Lee, A. S., & Badylak, S. F. (2008). Preparation and rheological characterization of a gel form of the porcine urinary bladder matrix. *Biomaterials*, 29(11), 1630-1637.
- [68] Fu, G., Chen, Y., Cui, Z., Li, Y., Zhou, W., Xin, S., Tang, Y., & Goodenough, J. B. (2016). Novel hydrogel-derived bifunctional oxygen electrocatalyst for rechargeable air cathodes. *Nano letters*, 16(10), 6516-6522.
- [69] Garcia-Orue, I., Santos-Vizcaino, E., Etxabide, A., Uranga, J., Bayat, A., Guerrero, P., Igartua, M., de la Caba, K., & Hernandez, R. M. (2019). Development of bioinspired gelatin and gelatin/chitosan bilayer hydrofilms for wound healing. *Pharmaceutics*, 11(7), 314.
- [70] Garnica-Palafox, I., & S anchez-Ar evalo, F. (2016). Influence of natural and synthetic crosslinking reagents on the structural and mechanical properties of chitosan-based hybrid hydrogels. *Carbohydrate Polymers*, 151, 1073-1081.
- [71] Gasperini, L., Mano, J. F., & Reis, R. L. (2014). Natural polymers for the microencapsulation of cells. *Journal of the royal society Interface*, 11(100), 20140817.
- [72] Gaware, S. A., Rokade, K. A., & Kale, S. (2019). Silica-chitosan nanocomposite mediated pH-sensitive drug delivery. *Journal of Drug Delivery Science and Technology*, 49, 345-351.
- [73] Ge, B., Wang, H., Li, J., Liu, H., Yin, Y., Zhang, N., & Qin, S. (2020). Comprehensive assessment of Nile tilapia skin (Oreochromis niloticus) collagen hydrogels for wound dressings. *Marine Drugs*, 18(4), 178.
- [74] Geng, H., Zhang, P., Liu, L., Shangguan, Y., Cheng, X., Liu, H., Zhao, Y., Hao, J., Li, W., & Cui, J. (2022). Convergent architecting of multifunction-in-one hydrogels as wound dressings for surgical anti-infections. *Materials Today Chemistry*, 25, 100968. <https://doi.org/https://doi.org/10.1016/j.mtchem.2022.100968>
- [75] Ghasemiyeh, P., & Mohammadi-Samani, S. (2019). Hydrogels as drug delivery systems; pros and cons. *Trends in Pharmaceutical Sciences*, 5(1), 7-24.
- [76] Gilarska, A., Lewandowska-Łańcucka, J., Guzdek-Zaj ac, K., Karczewska, A., Horak, W., Lach, R., W ojcik, K., & Nowakowska, M. (2020). Bioactive yet antimicrobial structurally stable collagen/chitosan/lysine functionalized hyaluronic acid – based injectable hydrogels for potential bone tissue engineering applications. *International Journal of Biological Macromolecules*, 155, 938-950. <https://doi.org/https://doi.org/10.1016/j.ijbiomac.2019.11.052>
- [77] Golieskardi, M., Satgunam, M., Ragurajan, D., Hoque, M. E., & Ng, A. M. H. (2020). Microstructural, Tribological, and Degradation Properties of Al<sub>2</sub>O<sub>3</sub>-and CeO<sub>2</sub>-Doped 3 mol.% Yttria-Stabilized Zirconia Bioceramic for Biomedical Applications. *Journal of Materials Engineering and Performance*, 29, 2890-2897.
- [78] Gomez-Aparicio, L. S., Bern aldez-Sarabia, J., Camacho-Villegas, T. A., Lugo-Fabres, P. H., D iaz-Mart inez, N. E., Padilla-Camberos, E., Licea-Navarro, A., & Castro-Cese na, A. B. (2021). Improvement of the wound healing properties of hydrogels with N-acetylcysteine through their modification with methacrylate-containing polymers. *Biomaterials Science*, 9(3), 726-744.
- [79] Grabska-Zielińska, S., Pin, J. M., Kaczmarek-Szczepańska, B., Olewnik-Kruszkowska, E., Sionkowska, A., Monteiro, F. J., Steinbrink, K., & Kleszczyński, K. (2022). Scaffolds Loaded with Dialdehyde Chitosan and Collagen—Their Physico-Chemical Properties and Biological Assessment. *Polymers*, 14(9), 1818.
- [80] Gu, L., Shan, T., Ma, Y.-x., Tay, F. R., & Niu, L. (2019). Novel biomedical applications of crosslinked collagen. *Trends in biotechnology*, 37(5), 464-491.
- [81] G uiza-Arg uello, V. R., Solarte-David, V. A., Pinz on-Mora, A. V.,  vila-Quiroga, J. E., & Becerra-Bayona, S. M. (2022). Current Advances in the Development of Hydrogel-Based Wound Dressings for Diabetic Foot Ulcer Treatment. *Polymers*, 14(14), 2764. <https://www.mdpi.com/2073-4360/14/14/2764>
- [82] Gunes, O. C., Kara, A., Baysan, G., Bugra Husemoglu, R., Akokay, P., Ziylan Albayrak, A., Ergur, B. U., & Havitcioglu, H. (2022). Fabrication of 3D Printed poly(lactic acid) strut and wet-electrospun cellulose nano fiber reinforced chitosan-collagen hydrogel composite scaffolds for meniscus tissue engineering. *Journal of Biomaterials Applications*, 37(4), 683-697. <https://doi.org/10.1177/08853282221109339>

- [83] Gunes, O. C., & Ziylan Albayrak, A. (2021). Antibacterial Polypeptide nisin containing cotton modified hydrogel composite wound dressings. *Polymer Bulletin*, 78, 6409-6428.
- [84] Guo, S. Z., Gosselin, F., Guerin, N., Lanouette, A. M., Heuzey, M. C., & Therriault, D. (2013). Solvent-cast three-dimensional printing of multifunctional microsystems. *Small*, 9(24), 4118-4122.
- [85] Gupta, A., & Kim, B. S. (2019). Shape memory polyurethane biocomposites based on toughened polycaprolactone promoted by nano-chitosan. *Nanomaterials*, 9(2), 225.
- [86] Gupta, A., Kowalczyk, M., Heaselgrave, W., Britland, S. T., Martin, C., & Radecka, I. (2019). The production and application of hydrogels for wound management: A review. *European Polymer Journal*, 111, 134-151. <https://doi.org/https://doi.org/10.1016/j.eurpolymj.2018.12.019>
- [87] Haaparanta, A.-M., Järvinen, E., Cengiz, I. F., Ellä, V., Kokkonen, H. T., Kiviranta, I., & Kellomäki, M. (2014). Preparation and characterization of collagen/PLA, chitosan/PLA, and collagen/chitosan/PLA hybrid scaffolds for cartilage tissue engineering. *Journal of Materials Science: Materials in Medicine*, 25, 1129-1136.
- [88] Han, H., Tang, L., Li, Y., Li, Y., Bi, M., Wang, J., Wang, F., Wang, L., & Mao, J. (2023). A multifunctional surgical suture with electroactivity assisted by oligochitosan/gelatin-tannic acid for promoting skin wound healing and controlling scar proliferation. *Carbohydrate Polymers*, 320, 121236. <https://doi.org/https://doi.org/10.1016/j.carbpol.2023.121236>
- [89] Han, W., & Wang, S. (2023). Advances in Hemostatic Hydrogels That Can Adhere to Wet Surfaces. *Gels*, 9(1), 2. <https://www.mdpi.com/2310-2861/9/1/2>
- [90] Hemmatgir, F., Koupaei, N., & Poorazizi, E. (2022). Characterization of a novel semi-interpenetrating hydrogel network fabricated by polyethylene glycol diacrylate/polyvinyl alcohol/tragacanth gum as a wound dressing. *Burns*, 48(1), 146-155.
- [91] Hernández-Martínez, A. R., Molina, G. A., Jiménez-Hernández, L. F., Oskam, A. H., Fonseca, G., & Estevez, M. (2017). Evaluation of inulin replacing chitosan in a polyurethane/polysaccharide material for Pb<sup>2+</sup> removal. *Molecules*, 22(12), 2093.
- [92] Hong, Y., Zhou, F., Hua, Y., Zhang, X., Ni, C., Pan, D., Zhang, Y., Jiang, D., Yang, L., & Lin, Q. (2019). A strongly adhesive hemostatic hydrogel for the repair of arterial and heart bleeds. *Nature communications*, 10(1), 2060.
- [93] Huang, H., Qi, X., Chen, Y., & Wu, Z. (2019). Thermo-sensitive hydrogels for delivering biotherapeutic molecules: A review. *Saudi Pharmaceutical Journal*, 27(7), 990-999.
- [94] Irastorza-Lorenzo, A., Sánchez-Porrás, D., Ortiz-Arrabal, O., de Frutos, M. J., Esteban, E., Fernández, J., Janer, A., Campos, A., Campos, F., & Alaminos, M. (2021). Evaluation of marine agarose biomaterials for tissue engineering applications. *International Journal of Molecular Sciences*, 22(4), 1923.
- [95] Jiang, H., Zheng, M., Liu, X., Zhang, S., Wang, X., Chen, Y., Hou, M., & Zhu, J. (2019). Feasibility study of tissue transglutaminase for self-catalytic cross-linking of self-assembled collagen fibril hydrogel and its promising application in wound healing promotion. *ACS Omega*, 4(7), 12606-12615.
- [96] Jimoh, T. O., Ogunmoyole, T., Aladejana, E. A., & Kade, I. J. (2016). Antioxidant potentials of tannic acid on lipid peroxidation induced by several pro-oxidants in cerebral and hepatic lipids. *International Journal of Ethnopharmacology*, 2 (1), 014-020.
- [97] Jin, Y., Ling, P.-X., He, Y.-L., & Zhang, T.-M. (2007). Effects of chitosan and heparin on early extension of burns. *Burns*, 33(8), 1027-1031.
- [98] Kalai Selvan, N., Shanmugarajan, T. S., & Uppuluri, V. N. V. A. (2020). Hydrogel based scaffolding polymeric biomaterials: Approaches towards skin tissue regeneration. *Journal of Drug Delivery Science and Technology*, 55, 101456. <https://doi.org/https://doi.org/10.1016/j.jddst.2019.101456>
- [99] Kamali, A., & Shamloo, A. (2020). Fabrication and evaluation of a bilayer hydrogel-electrospinning scaffold prepared by the freeze-gelation method. *Journal of Biomechanics*, 98, 109466. <https://doi.org/https://doi.org/10.1016/j.jbiomech.2019.109466>
- [100] Kamoun, E. A., Kenawy, E.-R. S., & Chen, X. (2017). A review on polymeric hydrogel membranes for wound dressing applications: PVA-based hydrogel dressings. *Journal of advanced research*, 8(3), 217-233.
- [101] Kaul, L., Grundmann, C. E., Köll-Weber, M., Löffler, H., Weiz, A., Zannettino, A. C., Richter, K., & Süß, R. (2022). A thermosensitive, chitosan-based hydrogel as delivery system for antibacterial liposomes to surgical site infections. *Pharmaceutics*, 14(12), 2841.
- [102] Kaviani, A., Zebarjad, S. M., Javadpour, S., Ayatollahi, M., & Bazargan-Lari, R. (2019). Fabrication and characterization of low-cost freeze-gelated chitosan/collagen/hydroxyapatite hydrogel nanocomposite scaffold. *International Journal of Polymer Analysis and Characterization*, 24(3), 191-203. <https://doi.org/10.1080/1023666X.2018.1562477>
- [103] Khor, E., & Lim, L. Y. (2003). Implantable applications of chitin and chitosan. *Biomaterials*, 24(13), 2339-2349.
- [104] Kim, M. Y., & Kim, J. (2017). Chitosan microgels embedded with catalase nanozyme-loaded mesocellular silica foam for glucose-responsive drug delivery. *ACS Biomaterials Science & Engineering*, 3(4), 572-578.
- [105] Kim, Y., Zharkinbekov, Z., Razyieva, K., Tabyldiyeva, L., Berikova, K., Zhumagul, D., Temirkhanova, K., & Saporov, A. (2023). Chitosan-Based Biomaterials for Tissue Regeneration. *Pharmaceutics*, 15(3), 807. <https://www.mdpi.com/1999-4923/15/3/807>
- [106] Kislíng, A., Lust, R. M., & Katwa, L. C. (2019). What is the role of peptide fragments of collagen I and IV in health and disease? *Life sciences*, 228, 30-34.
- [107] Kittiphattanabawon, P., Benjakul, S., Visessanguan, W., Nagai, T., & Tanaka, M. (2005). Characterisation of acid-

- soluble collagen from skin and bone of bigeye snapper (*Priacanthus tayenus*). *Food chemistry*, 89(3), 363-372.
- [108] Kokabi, M., Sirousazar, M., & Hassan, Z. M. (2007). PVA-clay nanocomposite hydrogels for wound dressing. *European Polymer Journal*, 43(3), 773-781.
- [109] Kumar, V. A., Taylor, N. L., Jalan, A. A., Hwang, L. K., Wang, B. K., & Hartgerink, J. D. (2014). A nanostructured synthetic collagen mimic for hemostasis. *Biomacromolecules*, 15(4), 1484-1490.
- [110] Kurakula, M. (2020). Prospection of recent chitosan biomedical trends: Evidence from patent analysis (2009–2020). *International Journal of Biological Macromolecules*, 165, 1924-1938.
- [111] Ladet, S., David, L., & Domard, A. (2008). Multi-membrane hydrogels. *Nature*, 452(7183), 76-79.
- [112] Lapi, I., Kolliniati, O., Aspevik, T., Deiktakis, E. E., Axarlis, K., Daskalaki, M. G., Dermitzaki, E., Tzardi, M., Kampranis, S. C., & Marsni, Z. E. (2021). Collagen-containing fish sidestream-derived protein hydrolysates support skin repair via chemokine induction. *Marine Drugs*, 19(7), 396.
- [113] Latza, V., Guerette, P. A., Ding, D., Amini, S., Kumar, A., Schmidt, I., Keating, S., Oxman, N., Weaver, J. C., & Fratzl, P. (2015). Multi-scale thermal stability of a hard thermoplastic protein-based material. *Nature communications*, 6(1), 8313.
- [114] Lauto, A., Stoodley, M., Marcel, H., Avolio, A., Sarris, M., McKenzie, G., Sampson, D., & Foster, L. (2007). In vitro and in vivo tissue repair with laser-activated chitosan adhesive. *Lasers in Surgery and Medicine: The Official Journal of the American Society for Laser Medicine and Surgery*, 39(1), 19-27.
- [115] Lei, H., Zhu, C., & Fan, D. (2020). Optimization of human-like collagen composite polysaccharide hydrogel dressing preparation using response surface for burn repair. *Carbohydrate Polymers*, 239, 116249.
- [116] Lévesque, S. G., Lim, R. M., & Shoichet, M. S. (2005). Macroporous interconnected dextran scaffolds of controlled porosity for tissue-engineering applications. *Biomaterials*, 26(35), 7436-7446.
- [117] Li, J., & Mooney, D. J. (2016). Designing hydrogels for controlled drug delivery. *Nature Reviews Materials*, 1(12), 1-17.
- [118] Li, J., Yu, F., Chen, G., Liu, J., Li, X.-L., Cheng, B., Mo, X.-M., Chen, C., & Pan, J.-F. (2020). Moist-Retaining, Self-Recoverable, Bioadhesive, and Transparent in Situ Forming Hydrogels To Accelerate Wound Healing. *ACS Applied Materials & Interfaces*, 12(2), 2023-2038. <https://doi.org/10.1021/acsami.9b17180>
- [119] Li, J., Zhai, D., Lv, F., Yu, Q., Ma, H., Yin, J., Yi, Z., Liu, M., Chang, J., & Wu, C. (2016). Preparation of copper-containing bioactive glass/eggshell membrane nanocomposites for improving angiogenesis, antibacterial activity and wound healing. *Acta biomaterialia*, 36, 254-266.
- [120] Li, M., Han, M., Sun, Y., Hua, Y., Chen, G., & Zhang, L. (2019). Oligoarginine mediated collagen/chitosan gel composite for cutaneous wound healing. *International Journal of Biological Macromolecules*, 122, 1120-1127. <https://doi.org/https://doi.org/10.1016/j.ijbiomac.2018.09.061>
- [121] Li, S., Wang, L., Yu, X., Wang, C., & Wang, Z. (2018). Synthesis and characterization of a novel double cross-linked hydrogel based on Diels-Alder click reaction and coordination bonding. *Materials Science and Engineering: C*, 82, 299-309.
- [122] Li, W., Zhao, X., Huang, T., Ren, Y., Gong, W., Guo, Y., Wang, J., & Tu, Q. (2021). Preparation of sodium hyaluronate/dopamine/AgNPs hydrogel based on the natural eutectic solvent as an antibacterial wound dressing. *International Journal of Biological Macromolecules*, 191, 60-70.
- [123] Li, Y., Zhu, C., Fan, D., Fu, R., Ma, P., Duan, Z., Li, X., Lei, H., & Chi, L. (2019). A Bi-Layer PVA/CMC/PEG Hydrogel with Gradually Changing Pore Sizes for Wound Dressing. *Macromolecular bioscience*, 19(5), 1800424.
- [124] Lim, Y.-S., Ok, Y.-J., Hwang, S.-Y., Kwak, J.-Y., & Yoon, S. (2019). Marine collagen as a promising biomaterial for biomedical applications. *Marine Drugs*, 17(8), 467.
- [125] Lin, X., Feng, Y., He, Y., Ding, S., & Liu, M. (2023). Engineering design of asymmetric halloysite/chitosan/collagen sponge with hydrophobic coating for high-performance hemostasis dressing. *International Journal of Biological Macromolecules*, 237, 124148. <https://doi.org/https://doi.org/10.1016/j.ijbiomac.2023.124148>
- [126] Liu, H., Li, D., & Guo, S. (2008). Rheological properties of channel catfish (*Ictalurus punctatus*) gelatine from fish skins preserved by different methods. *LWT-Food Science and Technology*, 41(8), 1425-1430.
- [127] Liu, X., Zheng, C., Luo, X., Wang, X., & Jiang, H. (2019). Recent advances of collagen-based biomaterials: Multi-hierarchical structure, modification and biomedical applications. *Materials Science and Engineering: C*, 99, 1509-1522.
- [128] Liu, Y., Luo, X., Wu, W., Zhang, A., Lu, B., Zhang, T., & Kong, M. (2021). Dual cure (thermal/photo) composite hydrogel derived from chitosan/collagen for in situ 3D bioprinting. *International Journal of Biological Macromolecules*, 182, 689-700. <https://doi.org/https://doi.org/10.1016/j.ijbiomac.2021.04.058>
- [129] Loureiro, K. C., Barbosa, T. C., Nery, M., Chaud, M. V., da Silva, C. F., Andrade, L. N., Corrêa, C. B., Jaguer, A., Padilha, F. F., & Cardoso, J. C. (2020). Antibacterial activity of chitosan/collagen membranes containing red propolis extract. *Die Pharmazie-An International Journal of Pharmaceutical Sciences*, 75(2-3), 75-81.
- [130] Ma, M.-Z., & Yu, Y. (2021). Research and Application Progress of Chitosan-based Hemostatic Materials---Review. *Zhongguo shi yan xue ye xue za zhi*, 29(5), 1685-1689.
- [131] Ma, X.-Y., Feng, Y.-F., Wang, T.-S., Lei, W., Li, X., Zhou, D.-P., Wen, X.-X., Yu, H.-L., Xiang, L.-B., & Wang, L. (2018). Involvement of FAK-mediated BMP-2/Smad pathway in mediating osteoblast adhesion and

- differentiation on nano-HA/chitosan composite coated titanium implant under diabetic conditions. *Biomaterials Science*, 6(1), 225-238.
- [132] Ma, Y., Yao, J., Liu, Q., Han, T., Zhao, J., Ma, X., Tong, Y., Jin, G., Qu, K., Li, B., & Xu, F. (2020). Liquid Bandage Harvests Robust Adhesive, Hemostatic, and Antibacterial Performances as a First-Aid Tissue Adhesive. *Advanced Functional Materials*, 30(39), 2001820. <https://doi.org/https://doi.org/10.1002/adfm.202001820>
- [133] Magill, S. S., Edwards, J. R., Bamberg, W., Beldavs, Z. G., Dumyati, G., Kainer, M. A., Lynfield, R., Maloney, M., McAllister-Hollod, L., & Nadle, J. (2014). Multistate point-prevalence survey of health care-associated infections. *New England Journal of Medicine*, 370(13), 1198-1208.
- [134] Mandal, A., Clegg, J. R., Anselmo, A. C., & Mitragotri, S. (2020). Hydrogels in the clinic. *Bioengineering & Translational Medicine*, 5(2), e10158. <https://doi.org/https://doi.org/10.1002/btm2.10158>
- [135] Mao, H., Zhao, S., He, Y., Feng, M., Wu, L., He, Y., & Gu, Z. (2022). Multifunctional polysaccharide hydrogels for skin wound healing prepared by photoinitiator-free crosslinking. *Carbohydrate Polymers*, 285, 119254.
- [136] Martínez-Ruvalcaba, A., Chornet, E., & Rodrigue, D. (2007). Viscoelastic properties of dispersed chitosan/xanthan hydrogels. *Carbohydrate Polymers*, 67(4), 586-595.
- [137] Maschmeyer, T., Luque, R., & Selva, M. (2020). Upgrading of marine (fish and crustaceans) biowaste for high added-value molecules and bio (nano)-materials. *Chemical Society Reviews*, 49(13), 4527-4563.
- [138] Mattioli-Belmonte, M., Zizzi, A., Lucarini, G., Giantomassi, F., Biagini, G., Tucci, G., Orlando, F., Provinciali, M., Carezzi, F., & Morganti, P. (2007). Chitin nanofibrils linked to chitosan glycolate as spray, gel, and gauze preparations for wound repair. *Journal of bioactive and compatible polymers*, 22(5), 525-538.
- [139] Maturavongsadit, P., Paravyan, G., Shrivastava, R., & Benhabbour, S. R. (2020). Thermo-/pH-responsive chitosan-cellulose nanocrystals based hydrogel with tunable mechanical properties for tissue regeneration applications. *Materialia*, 12, 100681. <https://doi.org/https://doi.org/10.1016/j.mtla.2020.100681>
- [140] Merzendorfer, H. (2011). The cellular basis of chitin synthesis in fungi and insects: common principles and differences. *European journal of cell biology*, 90(9), 759-769.
- [141] Mezzana, P. (2008). Clinical efficacy of a new chitin nanofibrils-based gel in wound healing. *Acta chirurgiae plasticae*, 50(3), 81-84.
- [142] Miguel, S. P., Ribeiro, M. P., & Coutinho, P. (2021). Biomedical Applications of Biodegradable Polymers in Wound Care. In P. Kumar & V. Kothari (Eds.), *Wound Healing Research: Current Trends and Future Directions* (pp. 509-597). Springer Singapore. [https://doi.org/10.1007/978-981-16-2677-7\\_17](https://doi.org/10.1007/978-981-16-2677-7_17)
- [143] Mohite, P., Rahayu, P., Munde, S., Ade, N., Chidrawar, V. R., Singh, S., Jayeoye, T. J., Prajapati, B. G., Bhattacharya, S., & Patel, R. J. (2023). Chitosan-Based Hydrogel in the Management of Dermal Infections: A Review. *Gels*, 9(7), 594.
- [144] Mohraz, M., Golbabaee, F., Yu, I., Mansournia, M., Zadeh, A., & Dehghan, S. (2019). Preparation and optimization of multifunctional electrospun polyurethane/chitosan nanofibers for air pollution control applications. *International Journal of Environmental Science and Technology*, 16, 681-694.
- [145] Montaser, A., Rehan, M., & El-Naggar, M. E. (2019). pH-Thermosensitive hydrogel based on polyvinyl alcohol/sodium alginate/N-isopropyl acrylamide composite for treating re-infected wounds. *International Journal of Biological Macromolecules*, 124, 1016-1024.
- [146] Mousavi, S., Khoshfetrat, A. B., Khatami, N., Ahmadian, M., & Rahbarghazi, R. (2019). Comparative study of collagen and gelatin in chitosan-based hydrogels for effective wound dressing: Physical properties and fibroblastic cell behavior. *Biochemical and Biophysical Research Communications*, 518(4), 625-631. <https://doi.org/https://doi.org/10.1016/j.bbrc.2019.08.102>
- [147] Mozafari, M., Sefat, F., & Atala, A. (2019). *Handbook of tissue engineering scaffolds: Volume one*. Woodhead Publishing.
- [148] Murakami, K., Aoki, H., Nakamura, S., Nakamura, S.-i., Takikawa, M., Hanzawa, M., Kishimoto, S., Hattori, H., Tanaka, Y., & Kiyosawa, T. (2010). Hydrogel blends of chitin/chitosan, fucoidan and alginate as healing-impaired wound dressings. *Biomaterials*, 31(1), 83-90.
- [149] Naderi Gharehgheshlagh, S., Fatemi, M. J., Jamili, S., Nourani, M. R., Sharifi, A. M., Saberi, M., Amini, N., & Ganji, F. (2021). A Dermal Gel Made of Rutilus Kutum Skin Collagen-Chitosan for Deep Burn Healing. *International Journal of Peptide Research and Therapeutics*, 27(1), 317-328. <https://doi.org/10.1007/s10989-020-10082-y>
- [150] Nikdel, M., Rajabinejad, H., Yaghoubi, H., Mikaeiliagh, E., Cella, M. A., Sadeghianmaryan, A., & Ahmadi, A. (2021). Fabrication of cellulosic nonwoven material coated with polyvinyl alcohol and zinc oxide/mesoporous silica nanoparticles for wound dressing purposes with cephalixin delivery. *ECS Journal of Solid State Science and Technology*, 10(5), 057003.
- [151] Ohmes, J., Saure, L. M., Schütt, F., Trenkel, M., Seekamp, A., Scherließ, R., Adelung, R., & Fuchs, S. (2022). Injectable Thermosensitive Chitosan-Collagen Hydrogel as A Delivery System for Marine Polysaccharide Fucoidan. *Marine Drugs*, 20(6), 402. <https://www.mdpi.com/1660-3397/20/6/402>
- [152] Oryan, A., Kamali, A., Moshiri, A., Baharvand, H., & Daemi, H. (2018). Chemical crosslinking of biopolymeric scaffolds: Current knowledge and future directions of crosslinked engineered bone scaffolds. *International Journal of Biological Macromolecules*, 107, 678-688.
- [153] Pan, H., Fan, D., Duan, Z., Zhu, C., Fu, R., & Li, X. (2019). Non-stick hemostasis hydrogels as dressings with bacterial barrier activity for cutaneous wound healing. *Materials Science and Engineering: C*, 105, 110118. <https://doi.org/https://doi.org/10.1016/j.msec.2019.110118>



- [154] Pang, L., Tian, P., Cui, X., Wu, X., Zhao, X., Wang, H., Wang, D., & Pan, H. (2021). In situ photo-cross-linking hydrogel accelerates diabetic wound healing through restored hypoxia-inducible factor 1-alpha pathway and regulated inflammation. *ACS Applied Materials & Interfaces*, *13*(25), 29363-29379.
- [155] Peng, X., Liu, G., Zhu, L., Yu, K., Qian, K., & Zhan, X. (2020). In vitro and in vivo study of novel antimicrobial gellan-polylysine polyion complex fibers as suture materials. *Carbohydrate Research*, *496*, 108115. <https://doi.org/https://doi.org/10.1016/j.carres.2020.108115>
- [156] Pietraszek, A., Ledwójcik, G., Lewandowska-Lańcucka, J., Horak, W., Lach, R., Łatkiewicz, A., & Karczewicz, A. (2020). Bioactive hydrogel scaffolds reinforced with alkaline-phosphatase containing halloysite nanotubes for bone repair applications. *International Journal of Biological Macromolecules*, *163*, 1187-1195. <https://doi.org/https://doi.org/10.1016/j.ijbiomac.2020.07.045>
- [157] Putra, A. P., Fahmadiyah, E., Hikmawati, D., & Aminatun, A. (2020). Chitosan-Coated Collagen-Hyaluronic Acid-Poly Ethylene Oxide-Based Electrospun Membrane for Corneal Ulcers Wound Dressing Candidate. *Walailak Journal of Science and Technology (WJST)*, *17*(11), 1230-1240. <https://doi.org/10.48048/wjst.2021.6319>
- [158] Qasim, M., Udomluck, N., Chang, J., Park, H., & Kim, K. (2018). RETRACTED ARTICLE: Antimicrobial activity of silver nanoparticles encapsulated in poly-N-isopropylacrylamide-based polymeric nanoparticles. *International journal of nanomedicine*, 235-249.
- [159] Qian, C., Higashigaki, T., Asoh, T.-A., & Uyama, H. (2020). Anisotropic conductive hydrogels with high water content. *ACS Applied Materials & Interfaces*, *12*(24), 27518-27525.
- [160] Qianqian, O., Songzhi, K., Yongmei, H., Xianghong, J., Sidong, L., Puwang, L., & Hui, L. (2021). Preparation of nano-hydroxyapatite/chitosan/tilapia skin peptides hydrogels and its burn wound treatment. *International Journal of Biological Macromolecules*, *181*, 369-377. <https://doi.org/https://doi.org/10.1016/j.ijbiomac.2021.03.085>
- [161] Qin, H., & Wang, K. (2019). Study on preparation and performance of PEG-based polyurethane foams modified by the chitosan with different molecular weight. *International Journal of Biological Macromolecules*, *140*, 877-885.
- [162] Qing, X., He, G., Liu, Z., Yin, Y., Cai, W., Fan, L., & Fardim, P. (2021). Preparation and properties of polyvinyl alcohol/N-succinyl chitosan/lincomycin composite antibacterial hydrogels for wound dressing. *Carbohydrate Polymers*, *261*, 117875.
- [163] Qun, G., & Ajun, W. (2006). Effects of molecular weight, degree of acetylation and ionic strength on surface tension of chitosan in dilute solution. *Carbohydrate Polymers*, *64*(1), 29-36.
- [164] Radulescu, D.-M., Neacsu, I. A., Grumezescu, A.-M., & Andronescu, E. (2022). New insights of scaffolds based on hydrogels in tissue engineering. *Polymers*, *14*(4), 799.
- [165] Raj, R. M., Priya, P., & Raj, V. (2018). Gentamicin-loaded ceramic-biopolymer dual layer coatings on the Ti with improved bioactive and corrosion resistance properties for orthopedic applications. *Journal of the mechanical behavior of biomedical materials*, *82*, 299-309.
- [166] Rana, M. M., Rahman, M. S., Ullah, M. A., Siddika, A., Hossain, M. L., Akhter, M. S., Hasan, M. Z., & Asaduzzaman, S. M. (2020). Amnion and collagen-based blended hydrogel improves burn healing efficacy on a rat skin wound model in the presence of wound dressing biomembrane. *Bio-Medical Materials and Engineering*, *31*(1), 1-17.
- [167] Raus, R. A., Nawawi, W. M. F. W., & Nasaruddin, R. R. (2021). Alginate and alginate composites for biomedical applications. *Asian Journal of Pharmaceutical Sciences*, *16*(3), 280-306.
- [168] Rawat, P., Zhu, D., Rahman, M. Z., & Barthelat, F. (2021). Structural and mechanical properties of fish scales for the bio-inspired design of flexible body armors: A review. *Acta biomaterialia*, *121*, 41-67.
- [169] Reyna-Urrutia, V. A., Mata-Haro, V., Cauch-Rodriguez, J. V., Herrera-Kao, W. A., & Cervantes-Uc, J. M. (2019). Effect of two crosslinking methods on the physicochemical and biological properties of the collagen-chitosan scaffolds. *European Polymer Journal*, *117*, 424-433. <https://doi.org/https://doi.org/10.1016/j.eurpolymj.2019.05.010>
- [170] Rezaei, A., Aligholi, H., Zeraatpisheh, Z., Gholami, A., & Mirzaei, E. (2021). Collagen/chitosan-functionalized graphene oxide hydrogel provide a 3D matrix for neural stem/precursor cells survival, adhesion, infiltration and migration. *Journal of bioactive and compatible polymers*, *36*(4), 296-313.
- [171] Ribeiro, D. M. L., Carvalho Júnior, A. R., Vale de Macedo, G. H. R., Chagas, V. L., Silva, L. d. S., Cutrim, B. d. S., Santos, D. M., Soares, B. L. L., Zagnignan, A., de Miranda, R. d. C. M., de Albuquerque, P. B. S., & Nascimento da Silva, L. C. (2020). Polysaccharide-Based Formulations for Healing of Skin-Related Wound Infections: Lessons from Animal Models and Clinical Trials. *Biomolecules*, *10*(1), 63. <https://www.mdpi.com/2218-273X/10/1/63>
- [172] Rizeq, B. R., Younes, N. N., Rasool, K., & Nasrallah, G. K. (2019). Synthesis, bioapplications, and toxicity evaluation of chitosan-based nanoparticles. *International Journal of Molecular Sciences*, *20*(22), 5776.
- [173] Salati, M. A., Khazai, J., Tahmuri, A. M., Samadi, A., Taghizadeh, A., Taghizadeh, M., Zarrintaj, P., Ramsey, J. D., Habibzadeh, S., & Seidi, F. (2020). Agarose-based biomaterials: Opportunities and challenges in cartilage tissue engineering. *Polymers*, *12*(5), 1150.
- [174] Sánchez-Cid, P., Jiménez-Rosado, M., Rubio-Valle, J. F., Romero, A., Ostos, F. J., Rafii-El-Idrissi Benhnia, M., & Perez-Puyana, V. (2022). Biocompatible and Thermoresistant Hydrogels Based on Collagen and Chitosan. *Polymers*, *14*(2), 272. <https://www.mdpi.com/2073-4360/14/2/272>
- [175] Sareethammanuwat, M., Boonyuen, S., & Arpornmaeklong, P. (2021). Effects of beta-tricalcium phosphate nanoparticles on the properties of a thermosensitive chitosan/collagen hydrogel and controlled release of

- quercetin. *Journal of Biomedical Materials Research Part A*, 109(7), 1147-1159. <https://doi.org/https://doi.org/10.1002/jbm.a.37107>
- [176] Schagen, S. K. (2017). Topical peptide treatments with effective anti-aging results. *Cosmetics*, 4(2), 16.
- [177] Sezlev Bilecen, D., Uludag, H., & Hasirci, V. (2019). Development of PEI-RANK siRNA complex loaded PLGA nanocapsules for the treatment of osteoporosis. *Tissue Engineering Part A*, 25(1-2), 34-43.
- [178] Shagdarova, B., Konovalova, M., Zhuikova, Y., Lunkov, A., Zhuikov, V., Khaydapova, D., Il'ina, A., Svirshchevskaya, E., & Varlamov, V. (2022). Collagen/Chitosan Gels Cross-Linked with Genipin for Wound Healing in Mice with Induced Diabetes. *Materials*, 15(1), 15. <https://www.mdpi.com/1996-1944/15/1/15>
- [179] Shah, R., Stodulka, P., Skopalova, K., & Saha, P. (2019). Dual Crosslinked Collagen/Chitosan Film for Potential Biomedical Applications. *Polymers*, 11(12), 2094. <https://www.mdpi.com/2073-4360/11/12/2094>
- [180] Sharma, P. K., Halder, M., Srivastava, U., & Singh, Y. (2019). Antibacterial PEG-chitosan hydrogels for controlled antibiotic/protein delivery. *ACS applied bio materials*, 2(12), 5313-5322.
- [181] Sheng, C., Zhou, Y., Lu, J., Zhang, X., & Xue, G. (2019). Preparation and characterization of chitosan based hydrogels chemical cross-linked by oxidized cellulose nanowhiskers. *Polymer Composites*, 40(6), 2432-2440.
- [182] Shi, Q., Rondon-Cavano, E.-P., Dalla Picola, I. P., Tiera, M. J., Zhang, X., Dai, K., Benabdoune, H. A., Benderdour, M., & Fernandes, J. C. (2018). In vivo therapeutic efficacy of TNF $\alpha$  silencing by folate-PEG-chitosan-DEAE/siRNA nanoparticles in arthritic mice. *International journal of nanomedicine*, 387-402.
- [183] Shin, J.-W., Kwon, S.-H., Choi, J.-Y., Na, J.-I., Huh, C.-H., Choi, H.-R., & Park, K.-C. (2019). Molecular mechanisms of dermal aging and antiaging approaches. *International Journal of Molecular Sciences*, 20(9), 2126.
- [184] Si, J., Yang, Y., Xing, X., Yang, F., & Shan, P. (2019). Controlled degradable chitosan/collagen composite scaffolds for application in nerve tissue regeneration. *Polymer Degradation and Stability*, 166, 73-85. <https://doi.org/https://doi.org/10.1016/j.polymdegradstab.2019.05.023>
- [185] Silvipriya, K., Kumar, K. K., Bhat, A., Kumar, B. D., & John, A. (2015). Collagen: Animal sources and biomedical application. *Journal of Applied Pharmaceutical Science*, 5(3), 123-127.
- [186] Singh, Y. P., Bhardwaj, N., & Mandal, B. B. (2016). Potential of agarose/silk fibroin blended hydrogel for in vitro cartilage tissue engineering. *ACS Applied Materials & Interfaces*, 8(33), 21236-21249.
- [187] Sionkowska, A., Lewandowska, K., & Adamiak, K. (2020). The influence of UV light on rheological properties of collagen extracted from Silver Carp skin. *Materials*, 13(19), 4453.
- [188] Sklenářová, R., Akla, N., Latorre, M. J., Ulrichová, J., & Franková, J. (2022). Collagen as a biomaterial for skin and corneal wound healing. *Journal of Functional Biomaterials*, 13(4), 249.
- [189] Smith, I. P., Domingos, M., Richardson, S. M., & Bella, J. (2023). Characterization of the Biophysical Properties and Cell Adhesion Interactions of Marine Invertebrate Collagen from *Rhizostoma pulmo*. *Marine Drugs*, 21(2), 59.
- [190] Socrates, R., Prymak, O., Loza, K., Sakthivel, N., Rajaram, A., Epple, M., & Narayana Kalkura, S. (2019). Biomimetic fabrication of mineralized composite films of nanosilver loaded native fibrillar collagen and chitosan. *Materials Science and Engineering: C*, 99, 357-366. <https://doi.org/https://doi.org/10.1016/j.msec.2019.01.101>
- [191] Song, K., Qiao, M., Liu, T., Jiang, B., Macedo, H. M., Ma, X., & Cui, Z. (2010). Preparation, fabrication and biocompatibility of novel injectable temperature-sensitive chitosan/glycerophosphate/collagen hydrogels. *Journal of Materials Science: Materials in Medicine*, 21(10), 2835-2842. <https://doi.org/10.1007/s10856-010-4131-4>
- [192] Song, W.-Y., Liu, G.-M., Li, J., & Luo, Y.-G. (2016). Bone morphogenetic protein-2 sustained delivery by hydrogels with microspheres repairs rabbit mandibular defects. *Tissue engineering and regenerative medicine*, 13, 750-761.
- [193] Sparks, H. D., Sigaeva, T., Tarraf, S., Mandla, S., Pope, H., Hee, O., Di Martino, E. S., Biernaskie, J., Radisic, M., & Scott, W. M. (2021). Biomechanics of Wound Healing in an Equine Limb Model: Effect of Location and Treatment with a Peptide-Modified Collagen-Chitosan Hydrogel. *ACS Biomaterials Science & Engineering*, 7(1), 265-278. <https://doi.org/10.1021/acsbiomaterials.0c01431>
- [194] Stepanovska, J., Otahal, M., Hanzalek, K., Supova, M., & Matejka, R. (2021). pH modification of high-concentrated collagen bioinks as a factor affecting cell viability, mechanical properties, and printability. *Gels*, 7(4), 252.
- [195] Su, J., Li, J., Liang, J., Zhang, K., & Li, J. (2021). Hydrogel preparation methods and biomaterials for wound dressing. *Life*, 11(10), 1016.
- [196] Subhan, F., Ikram, M., Shehzad, A., & Ghafoor, A. (2015). Marine collagen: An emerging player in biomedical applications. *Journal of food science and technology*, 52, 4703-4707.
- [197] Sudheesh Kumar, P., Lakshmanan, V.-K., Anilkumar, T., Ramya, C., Reshmi, P., Unnikrishnan, A., Nair, S. V., & Jayakumar, R. (2012). Flexible and microporous chitosan hydrogel/nano ZnO composite bandages for wound dressing: in vitro and in vivo evaluation. *ACS Applied Materials & Interfaces*, 4(5), 2618-2629.
- [198] Sun, H., Zhang, M., Liu, M., Yu, Y., Xu, X., & Li, J. (2020). Fabrication of double-network hydrogels with universal adhesion and superior extensibility and cytocompatibility by one-pot method. *Biomacromolecules*, 21(12), 4699-4708.
- [199] Takeya, H., Itai, S., Kimura, H., Kurashina, Y., Amemiya, T., Nagoshi, N., Iwamoto, T., Sato, K., Shibata, S., Matsumoto, M., Onoe, H., & Nakamura, M. (2023). Schwann cell-encapsulated chitosan-collagen hydrogel nerve conduit promotes peripheral nerve regeneration in rodent sciatic nerve defect models. *Scientific Reports*, 13(1), 11932. <https://doi.org/10.1038/s41598-023-39141-2>

- [200] Tan, L., Hu, Y., Li, M., Zhang, Y., Xue, C., Chen, M., Luo, Z., & Cai, K. (2022). Remotely-activatable extracellular matrix-mimetic hydrogel promotes physiological bone mineralization for enhanced cranial defect healing. *Chemical Engineering Journal*, 431, 133382. <https://doi.org/https://doi.org/10.1016/j.cej.2021.133382>
- [201] Teotia, R. S., Kalita, D., Singh, A. K., Verma, S. K., Kadam, S. S., & Bellare, J. R. (2015). Bifunctional polysulfone-chitosan composite hollow fiber membrane for bioartificial liver. *ACS Biomaterials Science & Engineering*, 1(6), 372-381.
- [202] Thomas, V., Yallapu, M. M., Sreedhar, B., & Bajpai, S. (2007). A versatile strategy to fabricate hydrogel-silver nanocomposites and investigation of their antimicrobial activity. *Journal of colloid and interface science*, 315(1), 389-395.
- [203] Thongchai, K., Chuysinuan, P., Thanyacharoen, T., Techasakul, S., & Ummartyotin, S. (2020). Characterization, release, and antioxidant activity of caffeic acid-loaded collagen and chitosan hydrogel composites. *Journal of Materials Research and Technology*, 9(3), 6512-6520. <https://doi.org/https://doi.org/10.1016/j.jmrt.2020.04.036>
- [204] Tiplea, R. E., Lemnar, G.-M., Trusca, R., Holban, A., Kaya, M. G. A., Dragu, L. D., Ficai, D., Ficai, A., & Bleotu, C. (2021). Antimicrobial films based on chitosan, collagen, and znO for skin tissue regeneration. *Biointerface Res. Appl. Chem*, 11, 11985-11995.
- [205] Toshniwal, P., Nguyen, M., Guédin, A., Viola, H., Ho, D., Kim, Y., Bhatt, U., Bond, C. S., Hool, L., & Hurley, L. H. (2019). TGF- $\beta$ -induced fibrotic stress increases G-quadruplex formation in human fibroblasts. *FEBS letters*, 593(22), 3149-3161.
- [206] Tran, N. Q., Joung, Y. K., Lih, E., & Park, K. D. (2011). In situ forming and rutin-releasing chitosan hydrogels as injectable dressings for dermal wound healing. *Biomacromolecules*, 12(8), 2872-2880.
- [207] Tripathy, A., Pahal, S., Mudakavi, R. J., Raichur, A. M., Varma, M. M., & Sen, P. (2018). Impact of Bioinspired Nanotopography on the Antibacterial and Antibiofilm Efficacy of Chitosan. *Biomacromolecules*, 19(4), 1340-1346. <https://doi.org/10.1021/acs.biomac.8b00200>
- [208] Trombino, S., Servidio, C., Curcio, F., & Cassano, R. (2019). Strategies for hyaluronic acid-based hydrogel design in drug delivery. *Pharmaceutics*, 11(8), 407.
- [209] Umar, A. K., Luckanagul, J. A., Zothantluanga, J. H., & Sriwidodo, S. (2022). Complexed Polymer Film-Forming Spray: An Optimal Delivery System for Secretome of Mesenchymal Stem Cell as Diabetic Wound Dressing? *Pharmaceutics*, 15(7), 867. <https://www.mdpi.com/1424-8247/15/7/867>
- [210] Utech, S., & Boccaccini, A. R. (2016). A review of hydrogel-based composites for biomedical applications: enhancement of hydrogel properties by addition of rigid inorganic fillers. *Journal of Materials Science*, 51, 271-310.
- [211] Valentino, C., Vigani, B., Zucca, G., Ruggeri, M., Boselli, C., Icaro Cornaglia, A., Malavasi, L., Sandri, G., & Rossi, S. (2023). Formulation development of collagen/chitosan-based porous scaffolds for skin wounds repair and regeneration. *International Journal of Biological Macromolecules*, 242, 125000. <https://doi.org/https://doi.org/10.1016/j.ijbiomac.2023.125000>
- [212] Valipour, F., Rahimabadi, E. Z., & Rostamzad, H. (2023). Preparation and characterization of wound healing hydrogel based on fish skin collagen and chitosan cross-linked by dialdehyde starch. *International Journal of Biological Macromolecules*, 253, 126704. <https://doi.org/https://doi.org/10.1016/j.ijbiomac.2023.126704>
- [213] Vaneau, M., Chaby, G., Guillot, B., Martel, P., Senet, P., Téot, L., & Chosidow, O. (2007). Consensus panel recommendations for chronic and acute wound dressings. *Archives of dermatology*, 143(10), 1291-1294.
- [214] Varghese, S. A., Rangappa, S. M., Siengchin, S., & Parameswaranpillai, J. (2020). Natural polymers and the hydrogels prepared from them. In *Hydrogels based on natural polymers* (pp. 17-47). Elsevier.
- [215] Varoni, E., Tschon, M., Palazzo, B., Nitti, P., Martini, L., & Rimondini, L. (2012). Agarose gel as biomaterial or scaffold for implantation surgery: characterization, histological and histomorphometric study on soft tissue response. *Connective tissue research*, 53(6), 548-554.
- [216] Vázquez, J. A., Rodríguez-Amado, I., Montemayor, M. I., Fraguas, J., del Pilar González, M., & Murado, M. A. (2013). Chondroitin sulfate, hyaluronic acid and chitin/chitosan production using marine waste sources: Characteristics, applications and eco-friendly processes: A review. *Marine Drugs*, 11(3), 747-774.
- [217] Veeruraj, A., Arumugam, M., & Balasubramanian, T. (2013). Isolation and characterization of thermostable collagen from the marine eel-fish (*Evenchelys macrura*). *Process biochemistry*, 48(10), 1592-1602.
- [218] Wang, B., Wang, Y.-M., Chi, C.-F., Luo, H.-Y., Deng, S.-G., & Ma, J.-Y. (2013). Isolation and characterization of collagen and antioxidant collagen peptides from scales of croceine croaker (*Pseudosciaena crocea*). *Marine Drugs*, 11(11), 4641-4661.
- [219] Wang, D., Yang, H., Zhou, Z., Zhao, M., Chen, R., & Reed, S. H. (2018). XPF plays an indispensable role in relieving silver nanoparticle induced DNA damage stress in human cells. *Toxicology Letters*, 288, 44-54.
- [220] Wang, D., Zhang, N., Meng, G., He, J., & Wu, F. (2020). The effect of form of carboxymethyl-chitosan dressings on biological properties in wound healing. *Colloids and Surfaces B: Biointerfaces*, 194, 111191. <https://doi.org/https://doi.org/10.1016/j.colsurfb.2020.111191>
- [221] Wang, L., An, X., Yang, F., Xin, Z., Zhao, L., & Hu, Q. (2008). Isolation and characterisation of collagens from the skin, scale and bone of deep-sea redfish (*Sebastes mentella*). *Food chemistry*, 108(2), 616-623.
- [222] Wang, L., Liang, Q., Chen, T., Wang, Z., Xu, J., & Ma, H. (2014). Characterization of collagen from the skin of Amur sturgeon (*Acipenser schrenckii*). *Food Hydrocolloids*, 38, 104-109.

- [223] Wang, L., & Stegemann, J. P. (2010). Thermogelling chitosan and collagen composite hydrogels initiated with  $\beta$ -glycerophosphate for bone tissue engineering. *Biomaterials*, *31*(14), 3976-3985. <https://doi.org/https://doi.org/10.1016/j.biomaterials.2010.01.131>
- [224] Wang, L., & Stegemann, J. P. (2011). Glyoxal crosslinking of cell-seeded chitosan/collagen hydrogels for bone regeneration. *Acta biomaterialia*, *7*(6), 2410-2417.
- [225] Wang, Y., Zhang, Y., Su, J., Zhang, X., Wang, J., & Tu, Q. (2020). Preparation of a multifunctional wound dressing based on a natural deep eutectic solvent. *ACS Sustainable Chemistry & Engineering*, *8*(37), 14243-14252.
- [226] Wang, Z., Nie, J., Qin, W., Hu, Q., & Tang, B. Z. (2016). Gelation process visualized by aggregation-induced emission fluorogens. *Nature communications*, *7*(1), 12033.
- [227] Wei, L., Tan, J., Li, L., Wang, H., Liu, S., Chen, J., Weng, Y., & Liu, T. (2022). Chitosan/alginate hydrogel dressing loaded FGF/VE-cadherin to accelerate full-thickness skin regeneration and more normal skin repairs. *International Journal of Molecular Sciences*, *23*(3), 1249.
- [228] Wei, M., Gao, Y., Li, X., & Serpe, M. (2017). Stimuli-Responsive Polymers and Their Applications. *Polym. Chem.* 2017, *8* (1), 127–143. In.
- [229] Woraphatphadung, T., Sajomsang, W., Rojanarata, T., Ngawhirunpat, T., Tonglairoum, P., & Opanasopit, P. (2018). Development of chitosan-based pH-sensitive polymeric micelles containing curcumin for colon-targeted drug delivery. *AAPS PharmSciTech*, *19*, 991-1000.
- [230] Wu, Q., Maire, M., Lerouge, S., Therriault, D., & Heuzey, M. C. (2017). 3D printing of microstructured and stretchable chitosan hydrogel for guided cell growth. *Advanced Biosystems*, *1*(6), 1700058.
- [231] Xie, H., Chen, X., Shen, X., He, Y., Chen, W., Luo, Q., Ge, W., Yuan, W., Tang, X., Hou, D., Jiang, D., Wang, Q., Liu, Y., Liu, Q., & Li, K. (2018). Preparation of chitosan-collagen-alginate composite dressing and its promoting effects on wound healing. *International Journal of Biological Macromolecules*, *107*, 93-104. <https://doi.org/https://doi.org/10.1016/j.ijbiomac.2017.08.142>
- [232] Xu, L., Liu, Y., Tang, L., Xiao, H., Yang, Z., & Wang, S. (2022). Preparation of recombinant human collagen III protein hydrogels with sustained release of extracellular vesicles for skin wound healing. *International Journal of Molecular Sciences*, *23*(11), 6289.
- [233] Xu, Y., Chen, H., Fang, Y., & Wu, J. (2022). Hydrogel Combined with Phototherapy in Wound Healing. *Advanced Healthcare Materials*, *11*(16), 2200494. <https://doi.org/https://doi.org/10.1002/adhm.202200494>
- [234] Yamada, Y., Yoshida, C., Hamada, K., Kikkawa, Y., & Nomizu, M. (2020). Development of three-dimensional cell culture scaffolds using laminin peptide-conjugated agarose microgels. *Biomacromolecules*, *21*(9), 3765-3771.
- [235] Yang, C., Dan, N., You, W., Huang, Y., Chen, Y., Yu, G., Dan, W., & Wen, H. (2019). Modification of collagen-chitosan membrane by oxidation sodium alginate and in vivo/ in vitro evaluation for wound dressing application. *International Journal of Polymer Analysis and Characterization*, *24*(7), 619-629. <https://doi.org/10.1080/1023666X.2019.1648637>
- [236] Yang, M., He, S., Su, Z., Yang, Z., Liang, X., & Wu, Y. (2020). Thermosensitive Injectable Chitosan/Collagen/ $\beta$ -Glycerophosphate Composite Hydrogels for Enhancing Wound Healing by Encapsulating Mesenchymal Stem Cell Spheroids. *ACS Omega*, *5*(33), 21015-21023. <https://doi.org/10.1021/acsomega.0c02580>
- [237] Yang, Y., Xu, R., Wang, C., Guo, Y., Sun, W., & Ouyang, L. (2022). Recombinant human collagen-based bioinks for the 3D bioprinting of full-thickness human skin equivalent. *International Journal of Bioprinting*, *8*(4).
- [238] Yi, Y., Wang, Y., & Liu, H. (2003). Preparation of new crosslinked chitosan with crown ether and their adsorption for silver ion for antibacterial activities. *Carbohydrate Polymers*, *53*(4), 425-430.
- [239] Ying, H., Zhou, J., Wang, M., Su, D., Ma, Q., Lv, G., & Chen, J. (2019). In situ formed collagen-hyaluronic acid hydrogel as biomimetic dressing for promoting spontaneous wound healing. *Materials Science and Engineering: C*, *101*, 487-498.
- [240] Zavyalova, O., Gajewska, S., Dąbrowska-Wislocka, D., & Sionkowska, A. (2021). Characteristics of physicochemical and rheological properties of chitosan hydrogels based on selected hydroxy acids. *Engineering of Biomaterials*, *24*(161).
- [241] Zhang, J., Xie, R., Zhang, S.-B., Cheng, C.-J., Ju, X.-J., & Chu, L.-Y. (2009). Rapid pH/temperature-responsive cationic hydrogels with dual stimuli-sensitive grafted side chains. *Polymer*, *50*(11), 2516-2525.
- [242] Zhang, K., Chen, X., Xue, Y., Lin, J., Liang, X., Zhang, J., Zhang, J., Chen, G., Cai, C., & Liu, J. (2022). Tough Hydrogel Bioadhesives for Sutureless Wound Sealing, Hemostasis and Biointerfaces. *Advanced Functional Materials*, *32*(15), 2111465. <https://doi.org/https://doi.org/10.1002/adfm.202111465>
- [243] Zhang, M.-X., Zhao, W.-Y., Fang, Q.-Q., Wang, X.-F., Chen, C.-Y., Shi, B.-H., Zheng, B., Wang, S.-J., Tan, W.-Q., & Wu, L.-H. (2021). Effects of chitosan-collagen dressing on wound healing in vitro and in vivo assays. *Journal of Applied Biomaterials & Functional Materials*, *19*, 2280800021989698. <https://doi.org/10.1177/2280800021989698>
- [244] Zhao, H., Huang, J., Li, Y., Lv, X., Zhou, H., Wang, H., Xu, Y., Wang, C., Wang, J., & Liu, Z. (2020). ROS-scavenging hydrogel to promote healing of bacteria infected diabetic wounds. *Biomaterials*, *258*, 120286.
- [245] Zhao, L., Li, X., Zhao, J., Ma, S., Ma, X., Fan, D., Zhu, C., & Liu, Y. (2016). A novel smart injectable hydrogel prepared by microbial transglutaminase and human-like collagen: Its characterization and biocompatibility. *Materials Science and Engineering: C*, *68*, 317-326.
- [246] Zhao, N., & Yuan, W. (2022). Functionally integrated bioglass microspheres-composited double-network hydrogel with good tissue adhesion and electrical conductivity for efficient wound treatment and health detection. *Composites Part B: Engineering*, *242*, 110095.

- [247] Zhao, X., Zhou, L., Riaz Rajoka, M. S., Yan, L., Jiang, C., Shao, D., Zhu, J., Shi, J., Huang, Q., & Yang, H. (2018). Fungal silver nanoparticles: synthesis, application and challenges. *Critical reviews in biotechnology*, 38(6), 817-835.
- [248] Zheng, Z., Qi, J., Hu, L., Ouyang, D., Wang, H., Sun, Q., Lin, L., You, L., & Tang, B. (2022). A cannabidiol-containing alginate based hydrogel as novel multifunctional wound dressing for promoting wound healing. *Biomaterials Advances*, 134, 112560.
- [249] Zhong, Y., Xiao, H., Seidi, F., & Jin, Y. (2020). Natural polymer-based antimicrobial hydrogels without synthetic antibiotics as wound dressings. *Biomacromolecules*, 21(8), 2983-3006.
- [250] Zhou, P., Li, X., Zhang, B., Shi, Q., Li, D., & Ju, X. (2019). A human umbilical cord mesenchymal stem cell-conditioned medium/chitosan/collagen/ $\beta$ -glycerophosphate thermosensitive hydrogel promotes burn injury healing in mice. *BioMed research international*, 2019.
- [251] Zhu, C., Lei, H., Fan, D., Duan, Z., Li, X., Li, Y., Cao, J., Wang, S., & Yu, Y. (2018). Novel enzymatic crosslinked hydrogels that mimic extracellular matrix for skin wound healing. *Journal of Materials Science*, 53(8), 5909-5928. <https://doi.org/10.1007/s10853-017-1956-y>
- [252] Zhu, J., Han, H., Li, F., Wang, X., Yu, J., Chu, C.-C., & Wu, D. (2019). Self-assembly of amino acid-based random copolymers for antibacterial application and infection treatment as nanocarriers. *Journal of colloid and interface science*, 540, 634-646.
- [253] Zhu, J., Jiang, G., Song, G., Liu, T., Cao, C., Yang, Y., Zhang, Y., & Hong, W. (2019). Incorporation of ZnO/Bioactive Glass Nanoparticles into Alginate/Chitosan Composite Hydrogels for Wound Closure. *ACS Applied Bio Materials*, 2(11), 5042-5052. <https://doi.org/10.1021/acsabm.9b00727>
- [254] Zubairi, W., Tehseen, S., Nasir, M., Anwar Chaudhry, A., Ur Rehman, I., & Yar, M. (2022). A study of the comparative effect of cerium oxide and cerium peroxide on stimulation of angiogenesis: Design and synthesis of pro-angiogenic chitosan/collagen hydrogels. *Journal of Biomedical Materials Research Part B: Applied Biomaterials*, 110(12), 2751-2762. <https://doi.org/https://doi.org/10.1002/jbm.b.35126>



# The synergistic effect of non-thermal techniques and modified atmosphere packaging in food preservation

Farazia Hassan<sup>1</sup>, Sehar Anwar<sup>2</sup>, Mukesh<sup>2</sup>, Hafiz Abdul Munam<sup>3</sup>, Muhammad Arslan Asjad<sup>2</sup>, Mudassar Hussain<sup>2</sup>, Zahra batool<sup>3</sup>, Nauman Khan<sup>4</sup>, Muhammad Umair Khalid<sup>2\*</sup>

<sup>1</sup>Department of Bioinformatic, Faculty of Science and Technology, Virtual University of Pakistan, Samundri Campus, Pakistan

<sup>2</sup>State Key Laboratory of Food Science and Technology, Jiangnan University Wuxi 214122, Jiangsu, China

<sup>3</sup>National institute of Food Science and Technology, University of Agriculture Faisalabad, Pakistan

<sup>4</sup>Department of biotechnology, University of Malakand dir (L) KPK Pakistan 18800

Email : [ch.umairfst@gmail.com](mailto:ch.umairfst@gmail.com)

Received: 05 Nov 2023; Received in revised form: 09 Dec 2023; Accepted: 17 Dec 2023; Available online: 26 Dec 2023

©2023 The Author(s). Published by Infogain Publication. This is an open access article under the CC BY license

(<https://creativecommons.org/licenses/by/4.0/>).

**Abstract**— Consumer's demand for food products that retain the natural properties and microbiologically safer food has promoted the use of non-thermal techniques for the reduction of microbial load and inactivation of enzymatic activity. However, the bacterial spores and some enzymes show high resistance against non-thermal techniques. Therefore, the application of non-thermal techniques with modified atmosphere packaging (MAP) represents an emerging method to increase the shelf life of food products. These combined preservation techniques reduced the microbial load, increase the shelf life without effecting the sensory attributes of food products. The surface of food products would benefit from the preservative effect of both non-thermal techniques and MAP. These integrated techniques are more energy efficient and better preservative effect than the single preservation technique. The use of MAP with non-thermal techniques reduces the intensity of nonthermal treatments required to achieve the desirable results. This review discusses the advantages that may be derived from the combined use of non-thermal techniques and MAP in the preservation of food.



**Keywords**— Food Safety, Innovative Technology, Modified Atmosphere packaging, non-thermal processing, Quality Control.

## I. INTRODUCTION

The fresh fruits and vegetables should consume within 7 to 8 days after harvesting because they have a limited shelf life up to 5 days [1]. After harvesting of food products different physical, chemical, enzymatic, and microbiological changes get started at a higher rate that reduced the quality attributes of fresh products. The washing of fruits or vegetables after harvesting removes the soil residues and plant debris but it has less effectiveness for microbial decontamination. The use of preservation techniques improves the quality deterioration and extending the shelf life of food products by inactivating the microorganisms and enzymes that are responsible for the spoilage [2]. The best preservation technique is one which improves the quality of food products without changing the nutrient

contents and sensory attributes. Non-thermal preservation techniques improve the shelf life and microbiological safety of food without affecting the freshness of fruit juice, while thermal techniques negatively affect the freshness, nutrient contents and sensory attributes of food products. Food industries prefer those preservation techniques that retain the freshness of food products because consumer likes natural and fresh food products [3].

Thermal techniques are mostly use in the preservation of food products. Although they increase the shelf life of food products, the use of high-temperature negatively affects the quality attributes like reduction in the nutrient contents, sensory attributes, inactivation of enzymes and coagulation of proteins [4]. It's the need of the hour to find a technique that fulfills the requirements of consumers in terms of better

sensory attributes, food safety and less harmful effect on the health of consumer [5]. Therefore, the application of non-thermal techniques in the processing and preservation of food products gaining popularity. Nonthermal techniques are the best alternative for the processing and preservation of food products, but they have a certain limit due to the resistance of some bacterial spores and certain enzymes. Sometimes, the use of single preservation does not inactivate all the spoilage causing agents. To get a better result for food preservation, application of non-thermal techniques is applied in combination with other food preservation techniques. A combination of different preservation techniques is preferred because the synergic effect of combined preservation techniques inactive all the microorganisms and reduced the time of processing. The integration of non-thermal techniques with other preservation techniques give better results in terms of the inactivation of enzymes and the destruction of bacterial

spores [2]. Application of non-thermal techniques together with modified atmosphere packaging (MAP) in the preservation of food reduced the loss of nutrient contents retains better sensory attributes and extends the shelf life as compared to the use of a single non-thermal preservation technique. The integration of preservation method has been used successfully in different countries for centuries without the proper scientifically understanding like a combination of heat, water activity and storage conditions [6, 7].

The use of non-thermal techniques with other preservation techniques is not always beneficial. Sometimes treatments of food with a combination of processing techniques increase the harmful effects. Reduction in the intensity of nonthermal techniques is needed when they are applied together with MAP [2].

*Table:1 Summary of deteriorative changes in food products responsible for spoilage of food*

Deteriorative changes	Reason behind deteriorative changes	Consequences	Citation
Enzymatic changes	Phenolase, Amylase, pectin methyl esterase Phenylalanine ammonia lyase Polyphenol Oxidase Peroxide	Oxidation of phenolic compounds, Conversion of sugar to starch, post-harvest demethylation of pectin is responsible for the softening and ripening of tissue.	[8]
Sensory changes	Lipid oxidation enzymatic browning.	Essential fatty acid loss, production of toxic substance.	[9]
Change in color	Loss of Chlorophyll due to phenophytinisation or photo-oxidation. Loss of Anthocyanin at high pH. Loss of Carotenoids due to oxidation.	Green color lost, loss of reddish color	[9]
Flavor change	Hydrolysis, lipolysis, and proteolysis	Off-flavor mainly due to aldehydes and ketones (rancid taste).	[9]
Nutritional changes	Light, temperature, water activity and temperature are responsible for the degradation of nutrients such as ascorbic acid.	Loss of ascorbic acid,	[9]
Physical changes	Bruising, absorption of moisture, dehydration, moisture migration, starch gelatinization, chill injury, crystal growth and emulsion breakdown are different physical factors affect the shelf life of food products.	Economic losses, loss in weight, increase in senescence, sugar bloom, fat bloom, phase separation	[9]

Microbial changes	Bacteria yeast, mold and fungus are responsible for the microbial spoilage of food.	They reduced the shelf life by accelerating the decay process and its results in loss of nutritional quality and sensory attributes [9]
Microbiological changes	Insects and rodents	They cause considerable off flavor, acceleration of decay process and nutritional quality. [10]

## II. MODIFIED ATMOSPHERE PACKAGING (MAP)

Modified atmosphere is helpful in the preservation of food while at the same time retain the fresh attributes of food products [11]. In a modified atmosphere packag (MAP), the atmosphere of gases around the foods in packaging material is altered to extend the shelf life and maintain the quality of foods. MAP is not a new concept in the food industry [12]. The use of MAP for the preservation of food is started in the 1930s when research was done on the modification of atmosphere gases for the preservation of food. Active modified atmosphere and passive modified atmosphere are two different types. In active MAP, the desired atmosphere in the package is produced by displacing the air with a mixture of desired gases (inert gas and active gas) [13]. In passive MAP, the desired atmosphere is produced by the respiration of food in the package and the diffusion of gases produced by respiration from the packaging barrier [14]. A high concentration of carbon dioxide in the MAP a preservative effect by inhibiting the growth of spoilage microorganism. The shelf life of food products is limited in the presence of air because a high concentration of oxygen in the air increases the growth of aerobic microorganisms and oxidation of fat [13].

The normal level of nitrogen in the atmosphere is 78% while the oxygen percentage is 21% and the carbon dioxide percentage in the atmosphere is 0.03%. Food products kept in the air have limited shelf life due to a reduction in the quality attributes caused by microorganisms and oxygen reactions. MAP is used to protect the food products from quality reduction by altering the gas composition within the packaging. Modification of atmosphere within the packaging is done by decreasing the level of oxygen and increasing the content of carbon oxide or nitrogen. The level of oxygen is kept low because it is responsible for the rapid growth of aerobic microbes and some enzymatic reactions like oxygenation of myoglobin and oxidation of unsaturated fats. In some exceptional cases, a high level of oxygen within the packaging is needed for the respiration of fruits, vegetables and red color retention in meats [15]. The level of carbon dioxide is kept high within MAP because it

inhibits the growth of aerophilic bacteria that cause spoilage of food. The level of carbon dioxide applied in atmosphere packaging varied from 25% to 100% depending upon the type of food. Preservation of fats or hard cheeses requires a high level of carbon oxide within the MAP [16]. Nitrogen is inert gases used in the MAP in place of oxygen to control the rancidity and oxidation in fat-rich food products. It is also used as filler in packaging to control the collapse in the packaging of food products that absorbed carbon dioxide. Carbon monoxide is also used in MAP for the preservation of food, but it is a highly toxic gas and its use within modified packaging is not proved by authorities owing to its health hazards. Mostly a mixture of three gases is used in MAP to obtain the desire preservation effect [17].

MAP prevents the spoilage caused by bacteria in many food products, especially minimally processed fruits, or vegetables. Alteration in the gaseous components in the packaging atmosphere may increase the shelf life of food products by decreasing the rate of respiration [18]. The combination of MAP with non-thermal treatments increases the sensitivity of bacteria for non-thermal techniques [1].

## III. TYPES OF NON-THERMAL TECHNIQUES

There are many types of non-thermal processing methods are available that enhance the quality of food without the application of heat. These methods are sonication, radiation, ultra-high pressure, magnetic field. Pulsed electric field, pulsed light field and ozone [19].

### 3.1. Synergistic effect of ultrasonication in food preservation

#### 3.1.1. Inactivation of microbes

Microorganisms directly or indirectly enter the food and decrease the quality and safety of food products. The presence of a low level of microbial load on the minimally processed food product is an indicator of the long shelf life and high safety of food products. the ultrasound is used as an alternative to thermal techniques for the inactivation of microorganisms. The antimicrobial effect of ultrasound is due the cavitation phenomenon. The change in pressure and temperature during cavitation produce free radicals that



case disruption of microbial cell wall, DNA and cell membrane damage. The different types of bacteria due to their different membrane structure show different response against ultrasound [20, 21]. The behavior of gram positive and gram negative is different against ultrasonication waves. The certain microorganisms specially spores show resistance again ultrasound treatment [22]. Therefore, ultrasonication is used with MAP to inactivate the resistant microorganisms.

Storage of minimally processed food products under MAP reduces the risk of molds, yeast and aerobic bacterial counts. Treatment of food products with ultrasound before storage in MAP reduces the proliferation of food spoilage microbes. The level of decay of the untreated food product kept under air conditions was higher than the food treated with ultrasound and packaged in modified atmosphere [23].

Application of ultrasonication treatment to the beef samples kept under vacuum packaging and MAP reduced the load of lactic acid bacteria. The minimum increase in the LAB counts was seen on the beef sample treated with US-MAP than the control sample of beef after 8 weeks of storage [24].

Treatment of fresh-cut cucumber samples with ultrasound and kept under MAP reduce the total number of bacterial counts, yeast and mold after 15 days of storage. The total no of bacterial counts, mold and yeast of untreated fresh-cut cucumber was 6.72 CFU/g, 4.17, 3.85 and 3.69 log CFU/g respectively. The total number of colonies of fresh-cut cucumber samples treated with ultrasound for 5 min, 10 min and 15 min was 6.72, 5.98, 5.28 and 5.14 log CFU/g, respectively whereas mold and yeast of these treatments of fresh-cut cucumber were 4.17, 3.85 and 3.69 log CFU/g, respectively. Fresh-cut cucumber treated with ultrasonication treatment for 10 min with MAP was highly effective to inhibit the growth of bacteria, yeast and molds [25]. However, the application of combined treatment ultrasound and MAP to the Pakchoi did not show any reduction of microbial load during the storage [26].

### 3.1.2. Effect on enzymes

The changes induced by endogenous enzymes in plant tissue during storage may be desirable or undesirable. PAL, PPO and POD involved in the oxidation of phenolics compounds which result in browning of fruits or vegetables [27]. The Pectin methyl esterase involved in the autolysis of cell which result in increased the biosynthesis of ethylene. The Pectin methyl esterase also involves in demethylation of pectin result in softening of fruits and vegetables tissue.  $\alpha$ -amylase,  $\beta$ -amylase and starch phosphorylase degrade the starch into simple sugar which result in high concentration of reducing sugar, and low concentration of total sugar. The different factor that affect the activity of enzymes are temperature, moisture and storage time [28,

29]. The Pakchoi sample treated with UT-10min + MAP showed reduced activity of POD and PPO enzymes throughout the storage than the control sample. The pakchoi sample treated with US-10 min and kept under MAP showed the lowest activity of POD and PPO throughout the storage period [26]. [30] reported that the application of ultrasound to the Psidium guajava kept under MAP inactive the POD during storage.

### 3.1.3. Synergistic effect on the quality attributes of food

Total soluble solid is an important parameter for the measurement of the quality of fruits and vegetables. Total soluble contents in fruits were increased during the early period of storage due to the after-ripening of fruits and loss of water by evaporation. With the increase in the storage of fruits or vegetables total soluble solid decreased due to the consumption of nutrients for the maintenance of normal physiology, respiration and metabolic activities of fruits and vegetables [31]. The total soluble solid of fresh cut cucumber was decreased during storage due to senescence. The treatment of fresh cut cucumber with ultrasonication reduce the degradation of total soluble solid during storage. The fresh-cut cucumber treated with ultrasound for 10 min and kept under MAP was lower than untreated fresh-cut cucumber sample [25]. Application of ultrasound together with MAP to the Pakchoi delays the degradation of TSS than the control sample of Pakchoi. [32].

The ascorbic acid of fruits and vegetables were decreased during storage. When fruits and vegetables were treated with ultrasound for 10 minutes and packed in MAP, a high level of ascorbic acid was found at the end of storage. The decrease in the ascorbic acid contents of the control sample of fresh-cut cucumber was 49.55% whereas in cucumber treated with UT-5 min + MAP, UT-10 min + MAP and UT-15 min + MAP was 41.14%, 32.83% and 44.24% respectively at the end of storage. The reduction in ascorbic acid of fresh-cut cucumber treated with UT-10 min + MAP was lower than all other treatments during storage [25]. The application of ultrasound together with MAP reduce the decrease in content during storage. Different samples of Pakchoi were subjected to UT-5 min + MAP, UT-10min + MAP, UT-15 min + MAP and it was found that Pakchoi treated with UT-10min + MAP showed a higher level of ascorbic acid than all other treatment of Pakchoi at the end of storage [26]. [30] reported that ultrasound treatment with MAP reduced the loss of ascorbic acid of Psidium guajava during the 30 days of storage. The reduction in degradation of ascorbic acid in fruits and vegetables during storage is due to is due cavitation effect produced by ultrasound treatment and low level of dissolved oxygen in MAP [33].

Antioxidant activity of untreated fruit juices decreased due to the degradation of phenolics during storage. The fruit juices subjected to ultrasonication showed better antioxidant activity than untreated juice. The fruit juices treated with ultrasonication and packed in MAP showed high antioxidant activity. The combined application of Ultrasonication, anti-browning treatments to the fresh-cut apple Packed in MAP showed high antioxidant activity due to the low degradation of phenolics during storage. [34].

The formation of malondialdehyde compound is an indication of lipid peroxidation. The increase in the MDA content was observed during storage. The combined application of ultrasonication with modified atmosphere packaging reduced the formation MDA compound in fresh-cut cucumber. After 15 days of storage, production of MDA in the control sample of fresh-cut cucumber was 3.42 nmol/g whereas, in fresh-cut cucumber samples treated with US5min+MAP, US10min+MAP and US15min+MAP were 2.53 nmol/g, 2.15 nmol/g and 2.78 nmol/g respectively. The lowest MDA was produced in fresh-cut cucumber treated with US10+MAP. This is because US treatment of fresh-cut cucumber for 10 min and packaging under MAP maintain the integrity of the cell membrane and slowdown the senescence of fresh-cut cucumber [25] [26]. A similar type of effect of US treatment was seen in mushrooms where US treatment for 10 minutes decrease the MDA production in mushrooms kept under a relative humidity of 95% [35].

The high rate of respiration and loss of water increase the weight loss of fruits and vegetables during storage. The application of ultrasonication with modified atmosphere packaging reduced the weight loss of fresh-cut cucumber during storage. It was observed that application of ultrasonication for 10 minutes with MAP reduces the weight loss of fresh-cut cucumber by 8.63%. This is due to the protection of hydrogen bonds between molecules of water and macromolecules of fresh-cut cucumber [25]. Application of ultrasonication together with Modified atmosphere Packaing also reduce the weight loss of Pakchoi during storage. [26]. [24] reported that beef samples treated with ultrasonication and kept under modified atmosphere packaging also show less weight loss as compared to untreated sample. The *Psidium guajava* treated with US-10 min and kept under MAP showed a lower reduction in weight than the control sample during storage [30].

The water holding capacity of untreated beef decreased during storage. During the 3 to 6 days of storage, the water holding capacity of beef treated with US-MAP or US-VP was higher than the control sample [24].

Storage of fruits or vegetables without any treatment results in a change in the volatile compounds and deterioration of

the flavor quality. Fruits or vegetables treated with ultrasound combined with MAP have a better quality of the flavor at the end of storage. Fresh-cut cucumber treated with ultrasound for 10 minutes and kept under MAP maintain a high quality of flavor because ultrasound treatment with a modified atmosphere prevents the change in the aromatic compound responsible for the flavor. The changes in color and decrease in firmness of fresh-cut cucumber samples treated with ultrasound (10 min) and packed under MAP were less than untreated samples after 15 days of storage [25].

The application of ultrasonication with MAP reduces the increase in yellowness of leaves during storage. Pakchoi samples treated with ultrasonication for 10 min and kept under MAP showed the lowest yellowness of leaves than the control sample during the storage [26]. Ultrasonication treatment with MAP preserves the original flavor of *Psidium guajava* during the storage. [30] reported that The *Psidium guajava* treated with US-10 min and kept under MAP showed retain better flavor than the control sample during storage.

The integration of the ultrasound technique with MAP or vacuum packaging also retained the texture, color, and flavor of beef fresh as compared to beef sample without any treatment. The beef sample maintains its texture better in vacuum packaging as compared to MAP because bacteria yeast and mold are unable to grow in it the absence of oxygen [24].

### 3.2. Irradiation

#### 3.2.1. Synergistic effect of irradiation and MAP in food preservation

A combination of irradiation and MAP was proved effective to control all the aerobic bacteria and coliforms of Chinese cabbage than single preservation method. Gamma irradiation dose up to 0.5 kGy is applied to Chinese cabbage, reduced the initial load of aerobic bacteria up to 2–3 log CFU/g. Irradiation of Chinese cabbage packaged under MAP reduced the coliform counts to undetectable limits after 3 weeks of storage. Lactic acid bacteria continue to grow in the presence of a high level of carbon dioxide during storage, but irradiation of Chinese cabbage inhibits the growth of lactic acid bacteria in the presence of a high level of carbon dioxide. A dose of 1 kGy of irradiation with MAP reduced all the spoilage causing microbes and increasing the shelf life of Chinese cabbage [36]. Carrots treated with irradiation (2 kGy) improved the quality and shelf life by destroying the microbes that cause spoilage [37].

A combination of gamma irradiation (1.0, 1.5, and 2.0 kGy) with MAP was proved effective to reduce the microbial load of shiitake mushrooms. Small brown spots were developed

on the shiitake mushrooms after 4 days when alone modified atmosphere package was used for the preservation. After 8 days, small brown spots on the shiitake mushroom were changed into black spots due to the high microbial activity of pseudomonas. Black spots on the shiitake mushroom is an indication of decay of the mushroom and end of shelf life. The shelf life of shiitake mushrooms was increased by treating with gamma irradiation (1.0, 1.5, and 2.0 kGy) + MAP that prevents the development of black spots by inactivating the activity of pseudomonas [38].

The combined effect of gamma irradiation and MAP on the strawberry increase the shelf life from 5 days to 7 days without any evidence of fungal decay and any change in the sensory attributes. The spoilage agent of strawberry is *B. cinerea* that causes grey mold disease and decreases the shelf life of strawberry by changing the texture and appearance. After 7 days, mold decay of the non-irradiated strawberry stored under aerobic packaging was started. While strawberry sample irradiated by a dose of 1.0 kGy and stored under MAP showed not any sign of mold growth after 14 days of storage [39].

Irradiation of grated carrots stored under MAP reduced the *E. coli* from log 6 to log 2 while the reduction of *E. coli* of irradiated grated carrots stored under air was from 6 to 3 log. A difference of one log exists between the grated carrots stored under MAP and air conditions during 20 days of storage. There was not any *E. coli* colony detected on the grated carrots treated with irradiation at a dose greater than 0.3 kGy and stored under MAP. A 1–2 log CFU/g bacteria were seen on irradiated grated carrot samples stored under air between 5 days and 15 days. Complete elimination of bacteria in grated carrots require treatment with irradiation by dose 0.6 kGy under air and a dose of 0.3 kGy stored under MAP [40]. Irradiated cut romaine lettuce (0.15 and 0.35 kGy) kept under MAP reduced aerobic counts, yeasts and molds by 1 log during storage for 22 days [41].

Saffron treated with gamma irradiation decrease the microbial load while reduction of the microbial load was higher in irradiated saffron kept under MAP. The untreated saffron sample showed limited shelf life due to the high load of *E. coli*, mold, and yeast [39].

Irradiation of spices by doses of 12 kGy and 7 kGy reduced the microbial load (bacteria, mold and yeast) to an undetectable level. Although irradiation itself is effective to improve the shelf life of spices by destroying spoilage microorganisms but is a combination with a modified atmosphere that gives an extra benefit [42].

Figs treated with irradiation by dose 1 kGy packed under MAP exhibit the lowest microbial load then followed by fig samples treated with irradiation by dose 0.5 kGy packed

under MAP, irradiation alone by dose 1 kGy, 0.5 kGy and modified atmosphere package alone. The microbial load of figs samples treated with the irradiation (1 kGy) + MAP, (0.5 kGy) + MAP, only irradiation by dose 1 kGy, 0.5 kGy and non-irradiated figs sample packed under MAP was 2.56, 3.17, 3.42, 3.86, 4.17 CFU/g respectively. Figs sample without any treatment showed the highest microbial load of 4.71 CFU/g [43].

Microorganisms responsible for the quality deterioration of the chicken meat are LAB, *B. thermosphacta*, Enterobacteriaceae, *Pseudomonas* spp. and yeast. Irradiated chicken meat at dose 4 kGy and kept under MAP1 (30% CO<sub>2</sub>/70% N<sub>2</sub>) and MAP2 (70% CO<sub>2</sub>/30% N<sub>2</sub>) had low microbial load than all meat samples treated with irradiation or MAP1 only [44].

### 3.2.2. Synergistic effect on the quality attributes of food product

The Application of gamma irradiation (1.0, 1.5, and 2.0 kGy) and modified atmosphere packaging to Shiitake mushrooms lower the degradation of phenolic contents and MDA production during Storage [38].

. The increase in MDA level of Shiitake mushroom treated with irradiation (1, 1.5 and 2 kGy) and kept under MAP were increased upto 31.7%, 70.1 and 59.2 % respectively while MDA level of non-irradiated shiitake mushroom kept under MAP only was increased approximately 100% [45].

[46] reported that the Level of sweetness in the fruit or vegetables is indicated by TSS and it increases over time as the fruit mature to produce sweeter fruits. The concentration of total soluble sugar is considered the predominant indicator of postharvest losses in harvested fruits and vegetables. The concentration of total soluble sugar increase in shiitake mushroom samples treated with irradiation + MAP at the same rate as in the MAP during the first 12<sup>th</sup> day. However higher increase in the sugar level was observed in the shiitake mushrooms treated with irradiation (1.0 kGy) and MAP during whole storage while a small increase in sugar was observed in the shiitake mushrooms sample kept under MAP only [45].

After harvesting, TSS values of fruits and vegetables increase over time due to the respiration. The increase in TSS was slow in the fig samples treated with combined preservation methods irradiated (0.5, 1 kGy) + MAP and alone MAP. Intergradation of Irradiation with MAP or alone MAP reduced the rate of respiration and metabolic changes in harvested figs result in less increase of TSS during storage. Irradiation of figs by dose 0.5 kGy and MAP was found effective to reduce the increase in TSS of fruits or vegetables during storage [43].

The high value of titratable acidity of fruits or vegetables means the presence of a high concentration of total acid within fruits or vegetables [47]. TA of all fruits or vegetables was decreased over time due to the consumption of organic acid for the production of new compounds and as a substrate for respiration during ripening [48]. Treatment of fresh fruits or vegetables with irradiation decreases the TA due to the irradiation injury [49]. Irradiated figs by dose 1 kGy had a low value of TA while irradiated figs by dose 0.5 kGy. Small changes in TA of figs sample treated with irradiation and kept under MAP were observed than fig samples treated with irradiation or MAP only [43]. Titratable acidity of salted Chinese cabbage was increased during storage due to the growth of lactic acid bacteria. Irradiation of Chinese cabbage packaged under MAP delay the change of titratable acidity for 3 weeks by reducing the growth of lactic acid bacteria. MAP did not have any effect on the TA of Chinese cabbage [36].

The weight loss of shiitake mushroom depends on the water loss by transpiration and the rate of respiration. The weight losses were increased over time during the storage. Fruits or vegetables lost their freshness if weight loss increases up to 3-10% during storage. The gamma irradiation (1.0, 1.5, and 2.0 kGy) with MAP reduced the weight loss of shiitake mushroom during storage of 8 days. The weight loss of non-irradiated shiitake mushroom kept under MAP was 4.4% after 20 days of storage. Gamma irradiation with MAP reduced the weight loss of shiitake mushroom to 2.7% throughout the whole storage [38]. Irradiation of fig samples by dose 0.5 kGy and 1 kGy kept under MAP reduced the weight loss of figs during storage of 15 days. The loss in the weight of irradiated fig samples kept under MAP was 3% during storage of 15 days. The weight loss of the control sample was 3.39% and fig samples kept under MAP was 3.12% [43].

The combined preservation techniques were proved better in the preservation of sensory attributes of food products than the single preservation technique. The sensory attributes of mushrooms (color, flavor, dark zones, gill and cap uniformity) were decreased during storage. Mushrooms treated with gamma irradiation (1.0, 1.5 and 2.0 kGy) + MAP showed better sensory properties during storage. The deterioration in color and appearance of mushrooms are associated with the browning of mushrooms tissues. Application of Irradiation with MAP inactivate the microorganisms that cause browning of mushrooms during storage [45].

Irradiated strawberry stored under active MAP retains better sensory attributes (appearance, texture, aroma and overall acceptance) than the non-irradiated strawberry samples or irradiated strawberry samples stored under air conditions.

Irradiated strawberry kept under active MAP shows better appearance and texture than non-irradiated strawberry samples packed under air conditions after 7 days of storage. The sensory attributes of irradiated strawberry stored in active MAP remained acceptable even after 14 days. The score of non-irradiated strawberry kept under air conditions was below the acceptability limit for all the sensory attributes [39]. [41] reported that the treatment of Irradiation to the cut romaine kept under MAP decreased the firmness while color, flavor and visual appearance remained unaffected.

The sensory attributes (aroma, color, and flavor) of saffron treated with gamma irradiation stored under MAP score higher than the non-irradiated saffron samples kept under MAP or atmosphere packaging. The shelf life of saffron treated with irradiation (2 kGy) and stored under MAP increased from 30 days to 60 days [39].

Irradiation increase the discoloration in spices (rosemary and black pepper), MAP decreased the discoloration of spices caused by irradiation. Therefore, the MAP for spices is preferred to prevent the loss of color before the treatment of spices with irradiation [42].

The appearance and aroma of the untreated fig sample deteriorated after 5 days. Irradiated Fig samples kept under MAP received the highest score for appearance, aroma and overall acceptance than fig samples treated with irradiation or MAP only on the day 5 and 10 during storage [43]. Irradiation of meat at dose 4 kGy stored under MAP score best for all the sensory attributes than irradiated meat under air conditions. The acceptability limit for the taste and odor of a meat sample treated with a combination of irradiation (4 kGy) and MAP2 (70%/30% CO<sub>2</sub>/N<sub>2</sub>) was increased from 6 days to 18 -19 days. Non-irradiated meat samples kept under MAP had an acceptability limit of 9–10 days [44].

Color parameters ( $L^*$ ,  $a^*$  and  $b^*$  value) of all fig samples were changed during storage at a temperature of 5 °C for 15 days. Irradiated fruits at dose 1 kGy show lower  $L^*$ ,  $a^*$  and  $b^*$  values during storage than irradiated fruits at dose 1 kGy. Irradiated fruits showed a lower  $L^*$  value (lightness) for all samples than the irradiated fruits sample kept under MAP during storage. Irradiation of some fruits like figs was unable to preserve the natural color due to the oxidation of anthocyanin. A combination of irradiation by dose 0.5 kGy and MAP was found effective in preserving the color of figs. A decrease in  $a^*$  and  $b^*$  values of the irradiated sample treated kept under MAP were lower than figs samples treated with irradiation or MAP only [43]. Irradiation treated poultry meat did not have any effect on the  $L^*$  and  $b^*$  values while irradiation of poultry meat by dose 4 kGy increased the  $a^*$  values. The increase in redness of irradiated chicken meat was due to the formation of CO-

myoglobin. A small effect of MAP was observed on the  $L^*$  values of poultry meat [44].

During storage of minimally processed fruits or vegetable, softening of tissue occur due to the degradation of the cell wall by the bacterial enzymes and increase the activity of endogenous enzymes. Integration of gamma irradiation + MAP reduces the softness of tissue by inactivating the enzymes. The shiitake mushrooms treated with Gamma irradiation (1.0 and 1.5 kGy) + MAP showed a higher level of firmness as compared to mushrooms sample treated with irradiation only [45].

Irradiated strawberry kept in MAP had more firmness than the irradiated fresh strawberry kept in atmosphere packaging. The Firmness of fruits in MAP is associated with a high concentration of carbon dioxide. The reason behind the firmness of strawberry tissue due to the increasing concentration of carbon dioxide is still unknown. The firmness of fruit tissue may change due to the loss of water by respiration and transpiration [39].

The firmness of figs decreases with the increase in the storage in all irradiated figs, figs kept under MAP and figs treated with combined treatments. The firmness of figs decreased with the increase in irradiation dose. The decrease in firmness of irradiated figs was due to the degradation of pectin and destruction of cell wall caused by a high dose of irradiation. The decreased in the firmness of figs treated with irradiation by dose 2, 3 and 4 KGy was more than figs samples treated with irradiation by dose 1 KGy or untreated figs during 20 days of storage. A high dose of Irradiation also increased the softness in kiwifruit [50], peach [51] and gala apple [52]. The firmness of the figs treated with combined preservation methods (irradiation + MAP) was higher than the firmness of irradiated figs kept under air conditions. Among all the irradiated samples, figs treated with irradiation (0.5 kGy) and MAP showed the best firmness during the storage [43].

### 3.3. Ultraviolet treatment

#### 3.3.1. Synergistic effect of UV-C and MAP in food preservation

Integration of UV-C and MAP are useful to increase the shelf-life food products by reducing the microbial contamination. The application of UV-C in combination with MAP or MAP individually improve the shelf life of trout fillets by reducing the mesophilic and psychotropic microbial counts. This is because UV-C inactive the microbes present on the surface of food and unable to penetrate the depth of food products entirely. The UV-C induce changes in the biochemical composition of food products that potentially enhance the nutrient's availability and promote the growth of remaining microorganisms. The MAP contains a high concentration of carbon dioxide that

reduced the microbial load of trout fillet. The bacteriostatic activity of carbon dioxide is due to its ability to penetrate the cell membrane, change in the functions of the cell membrane, inactivation of enzymes and changes in the protein properties of bacteria. MAP was effective against mesophilic bacteria while MAP+ UV-C was effective against total mesophilic and psychotropic counts [53]. The ultraviolet irradiation, and MAP extend the shelf life up to 2-5 days of tilapia fillets by reducing the growth of *S. typhimurium* and *E. coli* [54].

Microbial load on the harvested fruits or vegetables increased sharply with time throughout the storage. An increase in the *S. Typhimurium* was seen sharply on the untreated cherry tomatoes kept at 20 °C. After 3 days of storage, reduction in the *S. Typhimurium* counts of 4.32 log CFU/g were seen on the cherry tomatoes treated with UV-C and kept under active MAP at 4 °C. After 6 days of storage, *S. Typhimurium* counts in the samples kept under active MAP were reduced to 1.05 log CFU/g as compared to untreated fresh samples kept under air conditions. After 9 days of storage, *S. Typhimurium* was decreased to 3.74 log CFU/g on the cherry potatoes treated with UV-C and kept under active MAP while the decrease in the *S. Typhimurium* counts was 5.22 log CFU/g in the cherry tomatoes without UV-C kept under MAP at 4 °C [55]. The combination of UV-C and MAP were found effective to reduce the microbial of 'Red Oak Leaf' lettuce by controlling the growth of psychotropic bacteria, coliform and yeast growth. UV-C did not have any effect on the growth of lactic acid bacteria because gram-positive bacteria show high resistance against UV-C [56].

Combined treatment UV-C+MAP reduced the initial microbial load of mesophilic, psychophilic, enterobacteria, yeast and molds. However, the increases in the microbial growth on the processed rocket leaves treated with UV-C and kept under MAP was less than the untreated sample. The low microbial growth on the fresh-cut rocket leaves treated with UV-C and kept under MAP during storage increase the shelf life up to 8 days. The untreated fresh-cut rocket leaves had shelf life of only 4 days due to the spoilage caused by microbes [57].

The Treatment of minimally processed pomegranate arils with UV-C and MAP reduced the growth of mesophilic, psychotropic, lactic acid and *Enterobacteriaceae* counts during storage while yeast and mold remained unaffected [58].

#### 3.3.2. Synergistic effect on the quality attributes of food products

The antioxidant capacity of fruits or vegetables treated with UV-C + MA was higher than untreated fresh fruits or vegetables. UV-C improve the antioxidant activity by

enhancing the aggregating the phenolics in tomato fruits [59]. [60] reported that UV-C treatment increases the antioxidant activity of the blueberries. UV-C improve the antioxidant activity of tomatoes by increasing the phenolic contents and flavonoids [61]. with the antioxidant of tomatoes treated with UV-C and MAP was higher as compared to untreated tomatoes. The reduction in the antioxidant activity was observed with time due to a decrease in some antioxidants like ascorbic acid. The application of UV-C inactivates the enzyme (ascorbate oxidase) responsible for the oxidation of ascorbic acid. MAP alone or in combination with UV-C decrease the oxygen responsible for the degradation of ascorbic acid. Antioxidant activity of UV-C treated fruits was significantly similar to the antioxidant activity of fruits sample treated with UV-C + MA but the antioxidant activity of fresh, control or MAP treated fruits samples were significantly different [62].

The rate of respiration of the fruits or vegetables relies on the ripening level, temperature, and oxygen to carbon dioxide ratio in air. UV treatment speed up the rate of respiration in fruits and vegetables like in tomatoes [56]. The rate of respiration of tomatoes samples treated with MAP was slower as compared to the samples treated with UV-C + MAP. The MAP slows down the rate of respiration and ethylene due to the low level of oxygen (3.1%) and a higher level of carbon dioxide (11.3%). More the production of ethylene gas higher the rate of respiration. The rate of respiration of fruits sample kept under MA was slow because the ethylene gas has been eliminated through MAP films [62]. The UV-C with MAP did not have any significant effect on the rate of respiration of fresh-cut arils of pomegranate during storage [58].

Antioxidant activity was reduced in the presence of a high concentration of oxygen due to the degradation of ascorbic acid-induced by oxygen [63]. UV-C treated samples kept under MAP showed higher antioxidant activity than UV-C treated samples kept under atmosphere conditions because of a low level of oxygen assists in controlling the degradation of ascorbic acid. Higher the rate of respiration in tomatoes, the lower the antioxidant activity as respiration negatively affects the antioxidant activity. UV-C + MA increases the antioxidant activity of tomatoes samples by increasing the accumulation of phenolic acid, lowering the rate of respiration and degradation of ascorbic acid [62]. The combined treatment UV-C + MAP did not show any effect on the antioxidant activity of fresh-cut rocket leaves [57]. The antioxidant activity of treated fresh-cut rocket and untreated rocket remained unchanged at the end of storage. The application of combined treatment UV-C and MAP did not affect the antioxidant activity of minimally processed pomegranate arils during storage [58].

The weight loss of food products results in a reduction of shelf life and economic value [64]. [65] reported that Fruits or vegetable with weight loss of more than 5% lose their freshness. The improper storage condition, long storage time, high rate of transpiration and respiration are responsible for the high loss in the weight of fresh food products. The weight loss of cherry tomatoes treated with UV-C and kept under passive or active MAP was 0.45% whereas the weight loss of cherry tomatoes without UV-C was 0.64% for 9 days storage at 4 and 20 °C. there was not any large difference exist in a weight loss of all treatments [66].

High %TSS is present in fresh fruits, and it reduces overtime throughout the storage. The reason behind the decrease in TSS is the degradation of sugar. A decrease in TSS in Cherry tomato kept under MAP was reduced due to the high concentration of carbon dioxide [67]. UV+ MA treatment reduces the decrease in % TSS in tomatoes than fresh fruits or vegetable [62].

The color change of fruits is the important property for estimating the degrees of maturity. The color changes in untreated fruits are more than UV-C + MA treated fruits. The changes in the color of fruits depend on the ripening, senescence, duration of storage and conditions of storage [68]. The changes in the color of fruits treated with UV and kept under MAP or fruit samples kept under MAP is slower than the untreated sample or sample treated with UV only. The slower color changes in tomato kept under MAP is due to the presence of a low concentration of oxygen and a higher level of carbon dioxide. The main pigment responsible for the color in tomato is lycopene and its activity depends on oxygen [62].

The analysis of the external quality of cherry tomatoes was done by determining the changes in color throughout the storage. UV-C + MA treatments maintain the visual appearance of cherry tomatoes by delaying the change in the color of cherry tomatoes. The redness of cherry tomatoes increases with the increase in the lycopene throughout the storage. The change in color of untreated cherry tomatoes sample were more than cherry tomatoes treated with the combination of UV-C + MA or kept under MAP only [55]. [54] reported that MAP/UV and MAP decreased the redness and increased the yellowness of tilapia fillets during storage of 10 days. The UV-C treatment with MAP did not affect the  $L^*$ , Chroma and Hue values during the storage [57].

The firmness of fruits or vegetables is one of the important attributes that affect consumer acceptability. The firmness of fruits or some vegetables reduces during storage due to an increase in the respiration rate and enzyme activity. Fruits treated with UV+ MA had high firmness than the fruits without any treatment. A higher concentration of

carbon dioxide in the MAP maintains high firmness in tomatoes. A high rate of respiration and mass loss negatively affects the firmness. The rate of respiration and weight loss was lower in tomato samples treated with UV and kept under MAP. High moisture in fruits maintains a higher firmness than the samples with low moisture content. The firmness of tomato is decreased during ripening, enzymes start to be degrading the pectin and cause softening of the cell wall. UV treatment reduced the enzyme activity responsible for the degradation of the cell wall of tomatoes. Tomato samples kept under UV+MAP showed better firmness than samples treated with UV only. The MAP contribution to improving the firmness of tomato samples was more while UV has little contribution to improve the firmness. UV-C improved the firmness of cherry tomatoes by suppressing the production of ethylene gas. The higher the production of ethylene gas, the lower the firmness of tomatoes. UV+MAP treatment treatments retain the moisture of food products and removed the ethylene gas [37].

### 3.4. Cold Plasma

#### 3.4.1 Synergistic effect of Cold Plasma and MAP in food preservation

Microbial flora reduced the shelf life of fresh produce by degrading the quality attributes of fresh fruits and vegetables. The consumption of food products contaminated with the toxins produced by microorganisms can harm the health of consumers. Different thermal and novel non-thermal techniques were applied to destroy the microorganisms and improve food safety [69]. The integration of cold plasma and MAP are very beneficial in term of reducing the microbial load while retaining the critical quality attributes of the strawberry. Atmospheric cold plasma reduces the mesophilic bacteria yeasts and molds on the strawberry samples kept under MAP (65 % O<sub>2</sub> + 16 % N<sub>2</sub> + 19 % CO<sub>2</sub>) and MAP (90 % N<sub>2</sub> + 10 % O<sub>2</sub>). MAP with different gases mixture has a different effect on the microorganism. MAP containing gas mixture high in N<sub>2</sub> (90 %) reduced mesophilic bacteria, yeasts and molds counts to 3.7 and 3.3 log whereas MAP containing gas mixture high in oxygen content O<sub>2</sub> (65 %) reduced the bacteria and yeast or mold to 3.1 and 3.4 logs. The reduction of mesophilic bacterial counts was more kept under MAP while the reduction of yeast counts was less [70]. Fungi are more sensitive to cold plasma as compared to mesophilic bacteria. Plasma produces UV radiation that penetrates in fungi and destroys the cell membrane of yeast by reacting with the cellular matrix inside fungi cell [71]. The rate of microbial inactivation depends on the current microbial population present on the food surface, the type of food products and its internal attributes [72]. A large population

of bacteria, yeasts and molds are present on the surface of strawberry [73].

#### 3.4.2. Synergistic effect on the quality attributes of food product

Several biochemical changes include respiration and transpiration. continue to proceed in harvested fruits and vegetables. The rate of respiration increases in harvested fruits or vegetables due to physiological stress [74]. The shelf life of fresh produce becomes limited with a high rate of respiration. The rate of respiration in fresh produce kept under MAP decrease due to a low level of oxygen and a high level of carbon dioxide. The effect of Cold plasma and MAP on the respiration rate depends on the fruits or vegetable's maturity, degree of fruits ripeness, gases percentage in the atmosphere, time, and temperature of storage [1]. It was observed that the firmness of untreated fruits or vegetable decreases during storage as tissue become soft over time. Highly perishable fruits like strawberry are soft in nature and more prone to loss of firmness. All strawberry samples treated with atmosphere cold plasma or untreated showed a decrease in firmness with 24 hours. Strawberry kept under atmosphere high in oxygen retain the best firmness whereas high nitrogen in MAP reduces the firmness [75]. Greatest retention of firmness was seen in strawberry treated with atmosphere cold plasma and kept under MAP (65 % O<sub>2</sub> + 16 % N<sub>2</sub> + 19 % CO<sub>2</sub>). Consumer likes the bright red color of strawberry. Strawberry treated with atmosphere cold plasma and kept under MAP (65 % O<sub>2</sub> + 16 % N<sub>2</sub> + 19 % CO<sub>2</sub>) turned brighter whereas strawberry treated with atmosphere cold plasma and kept under MAP (65 % O<sub>2</sub> + 16 % N<sub>2</sub> + 19 % CO<sub>2</sub>) showed a decrease in brightness [76].

### 3.4. Pulse Electric Field

#### 3.4.1. Synergistic effect of pulse of electric field and MAP in food preservation

The microbial load on the fresh meat surface was 4.63 log CFU/g which increase with time after 9 days microbial load was exceeded to 6 log CFU/g considered to be the microbial threshold index for the fresh meat. After 18 days, it was seen that the pork meat sample treated with the moderate electric field and kept under MAP showed low values of TVC (less than 6 logs CFU/g) during storage. MEF inactivate the microorganisms by inducing an electric field across the cell membrane which leads to the breakdown of the structure of the cell membrane [8].

#### 3.4.2. Synergistic effect on the quality attributes

Low water-holding capacity costs the food industry millions of dollars each year. Water loss from the meat increased with the increase in storage time. [77] reported that High

drip loss was recorded in 50% of products of Pork meat. Purge loss results in a decrease in the weight of meat and loss of some water-soluble proteins [78]. Different techniques were applied to suppress the drip loss of meat. Application of moderate electric field with high oxygen MAP was approved highly effective to improve the water holding capacity of meat. After 6 days unacceptable cooking losses were observed in untreated pork meat whereas cooking losses were decreased in pork meat treated with moderate electric field kept under high oxygen moderate atmosphere. The moderate electric field improves the water holding capacity by polarizing the dipoles of water molecules and arranging in the direction of the electric field within muscle tissue [79]. Polarization and arrangement of water molecules influence the compartmentalization of water [80].

Food tenderness is generally recognized as one of the most important indicators of the quality of meat. The amount of intramuscular connective tissue, the length of the sarcomere and also the proteolytic ability of the muscle affect the meat tenderness [81]. The storage of meat high in oxygen results in a decrease in tenderness and juiciness of meat whereas the storage of meat is high in oxygen atmosphere after treatment with a moderate electric field increases the softness of meat [82]. Meat treated with moderate electric field and MAP had high water holding capacity than meat samples kept under MAP only. Meat tenderness increase with the increase in the water holding capacity of meat during storage. More the water holding capacity, the higher the tenderness [8]. Combine treatment of moderate electric field and MAP retain the color of meat better than the meat sample treated with moderate electric field or MAP only.  $L^*$ ,  $a^*$ , and  $b^*$  values were used for the measurement of meat color. It was observed that  $L^*$  (lightness) increased in all meat samples throughout the storage whereas  $a^*$  (redness) of meat samples treated with the moderate electric field and kept under MAP increased. Redness of meat sample kept under MAP was higher than the meat sample treated with MEF-MAP on days six and nine while lower on days 15 and 18. Meat samples kept under MAP after treatment with moderate electric field retained a brighter color of meat sample for a longer time than meat samples kept under MAP only [8].

### 3.5. High-Pressure Processing

#### 3.5.1. Synergistic effect of HHP and MAP in preservation

The shelf life of meat is affected by aerobic mesophilic counts and lactic acid bacteria. The increase in aerobic mesophilic counts on the surface of meat samples kept in control air conditions was more than the meat samples kept under MAP during the storage. [83] reported that the

aerobic mesophilic bacteria consume oxygen for the respiration in control air package result in high mesophilic counts at the end of storage. It was observed that the increase in lactic acid bacteria counts was similar to the meat samples kept under controlled air and MAP because LAB is a facultative anaerobic bacterium that can grow in the presence or absence of oxygen and the presence of carbon dioxide. HPP treatment of 500 MPa inactive the growth of both aerobic mesophilic bacteria and lactic acid bacteria in MAP and controlled air. A reduction of microbial counts on the meat samples treated with HPP+MAP was more than the meat samples treated with HPP and kept in controlled air conditions. Aerobic mesophilic counts on the meat samples treated with HPP and kept under air conditions and MAP were decreased to  $2.60 \log \text{cfu} \cdot \text{g}^{-1}$  and  $2.35 \log \text{cfu} \cdot \text{g}^{-1}$  respectively. While lab counts were under the detection limit on the meat samples treated with HPP kept under controlled air or MAP during 22 days of storage [84]. The pseudomonads, Yeasts, lactic acid bacteria (LAB) and hydrogen sulfide-producing bacteria (presumably *S. putrefaciens*) are responsible for the spoilage of salmon. The application of high pressure reduced the microbial counts of salmon to 100/g. The threshold values for the microbial contamination of salmon are 7.0–7.2 log CFU/g. After 7 days of storage, High counts of *S. putrefaciens*. were the observed result in spoilage of salmon. The application of high pressure and MAP reduced the total microbial load of the salmon. The HPP reduced the reduced growth of *S. putrefaciens* whereas MAP was effective against the LAB. The application of pressure in the range of 150 MPa-200 MPa for 30- and 60-min results in the reduction of spoilage microorganisms present on the surface of salmon [85].

#### 3.5.2. Synergistic effect on quality attributes

The meat samples kept under air high in oxygen are more prone to oxidation. Higher the rate of lipid oxidation lowers the shelf life of meat because lipid produces undesirable flavor and off-color. The ground meat is more prone to oxidation because disruption of muscle calls exposes the unsaturated fats to oxidation. The oxidative stability of meat samples stored under the control air package after treatment with HPP was less than the meat samples kept under MAP. The presence of oxygen in a controlled air package induces oxidation of unsaturated fat of the meat samples. HPP treatment to the meat samples did not inhibit the oxidation of fat if oxygen was present in the package [84]. Oxidative stability of salmon was improved when treated with high pressure 150 MPa and kept under MAP [85]. The high intensity of HPP increases the  $L^*$  (lightness) values of salmon during storage. Application of high pressure of 50 MPa for 60 min or 200 MPa for 10 min results in the opaque color of salmon. While the application of high pressure with



MAP (50% O<sub>2</sub>+50% CO<sub>2</sub>) results in acceptable L\* (lightness) of salmon. The redness values of salmon samples treated with high pressure and compressed gases (50% O<sub>2</sub> + 50% CO<sub>2</sub>) were decreased after 14 days of storage whereas salmon treated with high pressure and kept under vacuum packaging had acceptable values for redness after 14 days of storage [85].

#### IV. CONCLUSION

Nonthermal techniques have been used to inactivate the microorganisms and enzymes as an alternative approach to the thermal techniques from the last two decades. Nonthermal techniques are ideal preservation techniques that extend the shelf life of food products without effecting the nutrient contents and sensory attributes. However, certain bacterial spores and enzymes showed high resistance against nonthermal techniques. Therefore, the integration of nonthermal techniques with MAP is an effective approach to inactivate all microbial spores and enzymes that cause spoilage. The combination of different non-thermal techniques like ultrasound, irradiation, ultraviolet irradiation, cold plasma, pulse electric field and high-pressure processing with MAP increase the shelf life by protecting the food products different deteriorative reactions such as oxidation, water loss, texture loss, loss of sensory attributes and accumulation of malodialdehyde.

#### REFERENCES

- [1] Lacroix, M. and R. Lafortune, *Combined effects of gamma irradiation and modified atmosphere packaging on bacterial resistance in grated carrots (Daucus carota)*. Radiation Physics and Chemistry, 2004. **71**(1-2): p. 79-82.
- [2] Raso, J. and G.V. Barbosa-Cánovas, *Nonthermal preservation of foods using combined processing techniques*. 2003.
- [3] Zárate-Rodríguez, E., E. Ortega-Rivas, and G.V. Barbosa-Cánovas, *Effect of membrane pore size on quality of ultrafiltered apple juice*. International journal of food science & technology, 2001. **36**(6): p. 663-667.
- [4] Lado, B.H. and A.E. Yousef, *Alternative food-preservation technologies: efficacy and mechanisms*. Microbes and infection, 2002. **4**(4): p. 433-440.
- [5] Ortega-Rivas, E. and I. Salmerón-Ochoa, *Nonthermal food processing alternatives and their effects on taste and flavor compounds of beverages*. Critical reviews in food science and nutrition, 2014. **54**(2): p. 190-207.
- [6] Abadias, M., et al., *Growth potential of Escherichia coli O157: H7 on fresh-cut fruits (melon and pineapple) and vegetables (carrot and escarole) stored under different conditions*. Food Control, 2012. **27**(1): p. 37-44.
- [7] Sandhya, *Modified atmosphere packaging of fresh produce: Current status and future needs*. LWT-Food Science and Technology, 2010. **43**(3): p. 381-392.
- [8] Hu, H., et al., *Effects of the combination of moderate electric field and high-oxygen modified atmosphere packaging on pork meat quality during chill storage*. Journal of Food Processing and Preservation, 2020. **44**(1): p. e14299.
- [9] Kong, F. and R. Singh, *Chemical deterioration and physical instability of foods and beverages, in The stability and shelf life of food*. 2016, Elsevier. p. 43-76.
- [10] Mason, L.J., *Effect and control of insects, molds and rodents affecting corn quality, in Corn*. 2019, Elsevier. p. 213-234.
- [11] Narasimha Rao, D. and N. Sachindra, *Modified atmosphere and vacuum packaging of meat and poultry products*. Food Reviews International, 2002. **18**(4): p. 263-293.
- [12] Oliveira, M., et al., *Application of modified atmosphere packaging as a safety approach to fresh-cut fruits and vegetables—A review*. Trends in Food Science & Technology, 2015. **46**(1): p. 13-26.
- [13] Horev, B., et al., *The effects of active and passive modified atmosphere packaging on the survival of Salmonella enterica serotype Typhimurium on washed romaine lettuce leaves*. Food Research International, 2012. **45**(2): p. 1129-1132.
- [14] Charles, F., C. Guillaume, and N. Gontard, *Effect of passive and active modified atmosphere packaging on quality changes of fresh endives*. Postharvest biology and Technology, 2008. **48**(1): p. 22-29.
- [15] Mullan, M. and D. McDowell, *Modified atmosphere packaging in Food Packaging Technology*. Modified atmosphere packaging, in Food and Beverage Packaging Technology, 2003.
- [16] Devlieghere, F. and J. Debevere, *Influence of dissolved carbon dioxide on the growth of spoilage bacteria*. LWT-Food Science and Technology, 2000. **33**(8): p. 531-537.
- [17] Parry, R., *Principles and applications of modified atmosphere packaging of foods*. 2012: Springer Science & Business Media.
- [18] Severino, R., et al., *Antimicrobial effects of modified chitosan based coating containing nanoemulsion of essential oils, modified atmosphere packaging and gamma irradiation against Escherichia coli O157: H7 and Salmonella Typhimurium on green beans*. Food control, 2015. **50**: p. 215-222.
- [19] Morris, C., A.L. Brody, and L. Wicker, *Non-thermal food processing/preservation technologies: A review with packaging implications*. Packaging Technology and Science: An International Journal, 2007. **20**(4): p. 275-286.
- [20] Huang, H., et al., *UV-C treatment affects browning and starch metabolism of minimally processed lily bulb*. Postharvest Biology and Technology, 2017. **128**: p. 105-111.
- [21] Wu, T., et al., *Ultrasonic disruption of yeast cells: underlying mechanism and effects of processing parameters*. Innovative Food Science & Emerging Technologies, 2015. **28**: p. 59-65.
- [22] Dehghani, M.H., *Effectiveness of ultrasound on the destruction of E. coli*. American journal of environmental sciences, 2005. **1**(3): p. 187-189.
- [23] Caleb, O.J., et al., *Modified atmosphere packaging of pomegranate fruit and arils: a review*. 2012. **5**(1): p. 15-30.
- [24] Abdalhai, M.H., et al., *Effect of ultrasound treatment prior to vacuum and modified atmosphere packaging on microbial and physical characteristics of fresh beef*. Journal of Food and Nutrition Research, 2014. **2**(6): p. 312-320.
- [25] Fan, K., M. Zhang, and F.J.U.s. Jiang, *Ultrasound treatment to modified atmospheric packaged fresh-cut cucumber: influence on microbial inhibition and storage quality*. 2019. **54**: p. 162-170.
- [26] Zhang, X.-t., et al., *Effect of Combined Ultrasonication and Modified Atmosphere Packaging on Storage Quality of Pakchoi (Brassica chinensis L.)*. Food and Bioprocess Technology, 2019. **12**(9): p. 1573-1583.
- [27] O'donnell, C., et al., *Effect of ultrasonic processing on food enzymes of industrial importance*. Trends in food science & technology, 2010. **21**(7): p. 358-367.

- [28] Barbagallo, R., M. Chisari, and G. Spagna, *Enzymatic browning and softening in vegetable crops: studies and experiences*. Italian journal of food science, 2009. **21**(1).
- [29] Huang, G., et al., *Effects of ultrasound on microbial growth and enzyme activity*. Ultrasonics sonochemistry, 2017. **37**: p. 144-149.
- [30] Zhang, F., et al., *Effects of ultrasonic treatment combining modified atmosphere package on quality and physiological changes of Psidium guajava during postharvest storage*. Journal of Southern Agriculture, 2017. **48**(3): p. 493-498.
- [31] Brummell, D.A. and M.H. Harpster, *Cell wall metabolism in fruit softening and quality and its manipulation in transgenic plants, in plant cell walls*. 2001, Springer. p. 311-340.
- [32] Cansino, N., et al., *Ultrasound processing on green cactus pear (Opuntia ficus indica) juice: physical, microbiological and antioxidant properties*. 2013. **4**(9).
- [33] Bhat, R., et al., *Sonication improves kasturi lime (Citrus microcarpa) juice quality*. 2011. **18**(6): p. 1295-1300.
- [34] Putnik, P., et al., *Effects of modified atmosphere, anti-browning treatments and ultrasound on the polyphenolic stability, antioxidant capacity and microbial growth in fresh-cut apples*. 2017. **40**(5): p. e12539.
- [35] Li, N., et al., *Improved postharvest quality and respiratory activity of straw mushroom (Volvariella volvacea) with ultrasound treatment and controlled relative humidity*. Scientia Horticulturae, 2017. **225**: p. 56-64.
- [36] Ahn, H.-J., et al., *Combined effects of irradiation and modified atmosphere packaging on minimally processed Chinese cabbage (Brassica rapa L.)*. Food Chemistry, 2005. **89**(4): p. 589-597.
- [37] Chervin, C. and P. Boisseau, *Quality maintenance of "ready-to-eat" shredded carrots by gamma irradiation*. Journal of Food Science, 1994. **59**(2): p. 359-361.
- [38] Jiang, T., et al., *Effect of integrated application of gamma irradiation and modified atmosphere packaging on physicochemical and microbiological properties of shiitake mushroom (Lentinus edodes)*. Food Chemistry, 2010. **122**(3): p. 761-767.
- [39] Jouki, M. and N. Khazaei, *Effects of low-dose  $\gamma$ -irradiation and modified atmosphere packaging on shelf-life and quality characteristics of saffron (Crocus Sativus Linn) in Iran*. Food Science and Biotechnology, 2013. **22**(3): p. 687-690.
- [40] Lacroix, M., et al., *The influence of atmosphere conditions on Escherichia coli and Salmonella typhi radiosensitization in irradiated ground beef containing carvacrol and tetrasodium pyrophosphate*. Radiation Physics and Chemistry, 2004. **71**(1-2): p. 61-64.
- [41] Prakash, A., et al., *Effects of low-dose gamma irradiation on the shelf life and quality characteristics of cut romaine lettuce packaged under modified atmosphere*. Journal of Food Science, 2000. **65**(3): p. 549-553.
- [42] Kirkin, C., et al., *Combined effects of gamma-irradiation and modified atmosphere packaging on quality of some spices*. Food Chemistry, 2014. **154**: p. 255-261.
- [43] Waghmare, R.B. and U.S. Annapure, *Integrated effect of radiation processing and modified atmosphere packaging (MAP) on shelf life of fresh fig*. Journal of food science and technology, 2018. **55**(6): p. 1993-2002.
- [44] Chouliara, E., et al., *Combined effect of irradiation and modified atmosphere packaging on shelf-life extension of chicken breast meat: microbiological, chemical and sensory changes*. European Food Research and Technology, 2008. **226**(4): p. 877-888.
- [45] Jiang, T., et al., *Influence of UV-C treatment on antioxidant capacity, antioxidant enzyme activity and texture of postharvest shiitake (Lentinus edodes) mushrooms during storage*. Postharvest Biology and Technology, 2010. **56**(3): p. 209-215.
- [46] Owureku-Asare, M., et al., *Effect of gamma irradiation treatment and storage on physico-chemical, microbial and sensory quality of minimally processed pineapple (Ananas comosus)*. Current Journal of Applied Science and Technology, 2014: p. 2752-2761.
- [47] Sadler, G.D. and P.A. Murphy, *pH and titratable acidity*, in *Food analysis*. 2010, Springer. p. 219-238.
- [48] Wani, A., et al., *Effect of gamma-irradiation and refrigerated storage on the improvement of quality and shelf life of pear (Pyrus communis L., Cv. Bartlett/William)*. Radiation Physics and Chemistry, 2008. **77**(8): p. 983-989.
- [49] Fan, X. and J.P. Mattheis, *1-Methylcyclopropene and storage temperature influence responses of 'Gala' apple fruit to gamma irradiation*. Postharvest Biology and Technology, 2001. **23**(2): p. 143-151.
- [50] Kim, J.-H., et al., *The combined effects of N<sub>2</sub>-packaging, heating and gamma irradiation on the shelf-stability of Kimchi, Korean fermented vegetable*. Food control, 2008. **19**(1): p. 56-61.
- [51] McDonald, H., et al., *Commercial scale irradiation for insect disinfestation preserves peach quality*. Radiation Physics and Chemistry, 2012. **81**(6): p. 697-704.
- [52] Fernandes, Â., et al., *Effects of gamma irradiation on physical parameters of Lactarius deliciosus wild edible mushrooms*. Postharvest Biology and Technology, 2012. **74**: p. 79-84.
- [53] Lázaro, C., et al., *Effects of ultraviolet light on biogenic amines and other quality indicators of chicken meat during refrigerated storage*. Poultry Science, 2014. **93**(9): p. 2304-2313.
- [54] Lázaro, C.A., M.L.G. Monteiro, and C.A. Conte-Junior, *Combined Effect of Modified Atmosphere Packaging and UV-C Radiation on Pathogens Reduction, Biogenic Amines, and Shelf Life of Refrigerated Tilapia (Oreochromis niloticus) Fillets*. Molecules, 2020. **25**(14): p. 3222.
- [55] Choi, D.S., et al., *The combined effects of ultraviolet-C irradiation and modified atmosphere packaging for inactivating Salmonella enterica serovar Typhimurium and extending the shelf life of cherry tomatoes during cold storage*. Food packaging and shelf life, 2015. **3**: p. 19-30.
- [56] Allende, A. and F. Artés, *Combined ultraviolet-C and modified atmosphere packaging treatments for reducing microbial growth of fresh processed lettuce*. LWT-Food Science and Technology, 2003. **36**(8): p. 779-786.
- [57] Gutierrez, D.R. and S.d.C. Rodriguez, *Combined effect of UV-C and modified atmosphere packaging for keeping antioxidant compounds and extend to shelf-life of fresh-cut rocket leaves*. International Journal of New Technology and Research, 2017. **3**(6).
- [58] López-Rubira, V., et al., *Shelf life and overall quality of minimally processed pomegranate arils modified atmosphere packaged and treated with UV-C*. Postharvest biology and technology, 2005. **37**(2): p. 174-185.
- [59] Srilaong, V. and Y. Tatsumi, *Changes in respiratory and antioxidative parameters in cucumber fruit (Cucumis sativus L.) stored under high and low oxygen concentrations*. Journal of the Japanese Society for Horticultural Science, 2003. **72**(6): p. 525-532.
- [60] Perkins-Veazie, P., J.K. Collins, and L. Howard, *Blueberry fruit response to postharvest application of ultraviolet radiation*. Postharvest Biology and Technology, 2008. **47**(3): p. 280-285.
- [61] Castagna, A., et al., *Effect of post-harvest UV-B irradiation on polyphenol profile and antioxidant activity in flesh and*

- peel of tomato fruits. Food and bioprocess technology, 2014. **7**(8): p. 2241-2250.
- [62] Vunnam, R., et al., *Physico-chemical changes in tomato with modified atmosphere storage and UV treatment*. Journal of food science and technology, 2014. **51**(9): p. 2106-2112.
- [63] Rojas-Graü, M.A., et al., *The use of packaging techniques to maintain freshness in fresh-cut fruits and vegetables: a review*. International Journal of Food Science & Technology, 2009. **44**(5): p. 875-889.
- [64] Kraśniewska, K., et al., *The use of pullulan coating enriched with plant extracts from *Satureja hortensis* L. to maintain pepper and apple quality and safety*. Postharvest Biology and Technology, 2014. **90**: p. 63-72.
- [65] Koide, S. and J. Shi, *Microbial and quality evaluation of green peppers stored in biodegradable film packaging*. Food Control, 2007. **18**(9): p. 1121-1125.
- [66] Vunnam, R., et al., *Physico-chemical changes in tomato with modified atmosphere storage and UV treatment*. Journal of food science and technology, 2014. **51**: p. 2106-2112.
- [67] Akbudak, B., et al. *The effect of harpin treatment on storage of cherry tomato cv. Naomi*. in *IV International Conference on Managing Quality in Chains-The Integrated View on Fruits and Vegetables Quality 712*. 2006.
- [68] Moneruzzaman, K., et al., *Effect of stages of maturity and ripening conditions on the physical characteristics of tomato*. American Journal of Biochemistry and Biotechnology, 2008. **4**(4): p. 329-335.
- [69] Kim, H.Y., et al., *Gas temperature effect on reactive species generation from the atmospheric pressure air plasma*. Plasma Processes and Polymers, 2013. **10**(8): p. 686-697.
- [70] Misra, N., et al., *Nonthermal plasma inactivation of food-borne pathogens*. Food Engineering Reviews, 2011. **3**(3-4): p. 159-170.
- [71] Park, B.J., et al., *Sterilization using a microwave-induced argon plasma system at atmospheric pressure*. Physics of Plasmas, 2003. **10**(11): p. 4539-4544.
- [72] Fernandez, A., E. Noriega, and A. Thompson, *Inactivation of *Salmonella enterica* serovar Typhimurium on fresh produce by cold atmospheric gas plasma technology*. Food Microbiology, 2013. **33**(1): p. 24-29.
- [73] Jensen, B., et al., *Characterization of microbial communities and fungal metabolites on field grown strawberries from organic and conventional production*. International journal of food microbiology, 2013. **160**(3): p. 313-322.
- [74] Rico, D., et al., *Extending and measuring the quality of fresh-cut fruit and vegetables: a review*. Trends in Food Science & Technology, 2007. **18**(7): p. 373-386.
- [75] Wszelaki, A. and E. Mitcham, *Effects of superatmospheric oxygen on strawberry fruit quality and decay*. Postharvest Biology and Technology, 2000. **20**(2): p. 125-133.
- [76] Misra, N., et al., *Cold plasma in modified atmospheres for post-harvest treatment of strawberries*. Food and bioprocess technology, 2014. **7**(10): p. 3045-3054.
- [77] Stetzer, A. and F. McKeith, *Benchmarking value in the pork supply chain: Quantitative strategies and opportunities to improve quality Phase I*. Savoy (IL): American Meat Science Association, 2003.
- [78] Huff-Lonergan, E. and S.M. Lonergan, *Mechanisms of water-holding capacity of meat: The role of postmortem biochemical and structural changes*. Meat science, 2005. **71**(1): p. 194-204.
- [79] Rayat, K. and F. Feyzi, *Influence of external electric field on the polarity of water droplets in water-in-oil emulsion phase transition*. Colloids and Surfaces A: Physicochemical and Engineering Aspects, 2011. **375**(1-3): p. 61-67.
- [80] Stadnik, J. and Z.J. Dolatowski, *Influence of sonication on Warner-Bratzler shear force, colour and myoglobin of beef (*m. semimembranosus*)*. European Food Research and Technology, 2011. **233**(4): p. 553.
- [81] Rawdkuen, S., M. Jaimakreu, and S. Benjakul, *Physicochemical properties and tenderness of meat samples using proteolytic extract from *Calotropis procera* latex*. Food chemistry, 2013. **136**(2): p. 909-916.
- [82] Lund, M.N., et al., *High-oxygen packaging atmosphere influences protein oxidation and tenderness of porcine longissimus dorsi during chill storage*. Meat Science, 2007. **77**(3): p. 295-303.
- [83] Patsias, A., et al., *Combined effect of freeze chilling and MAP on quality parameters of raw chicken fillets*. Food Microbiology, 2008. **25**(4): p. 575-581.
- [84] Lerasle, M., et al., *Combined use of modified atmosphere packaging and high pressure to extend the shelf-life of raw poultry sausage*. Innovative Food Science & Emerging Technologies, 2014. **23**: p. 54-60.
- [85] Amanatidou, A., et al., *Effect of combined application of high pressure treatment and modified atmospheres on the shelf life of fresh Atlantic salmon*. Innovative Food Science & Emerging Technologies, 2000. **1**(2): p. 87-98.



# The Effect of Eco Enzyme Concentration and NPK Fertilizer Dosage on the Growth and Yield of Sweet Potatoes (*Ipomoea batatas* L.) at the Urban Farming Planting System

Ferziana Nurmeilinda Dzikrika<sup>1</sup>, Sitawati<sup>2\*</sup>, Nurul Aini<sup>2</sup>, Dewi Ratih Rizki Damaiyanti<sup>2</sup>

Faculty of agriculture, University of Brawijaya, Indonesia

Received: 10 Nov 2023; Received in revised form: 12 Dec 2023; Accepted: 20 Dec 2023; Available online: 28 Dec 2023

©2023 The Author(s). Published by Infogain Publication. This is an open access article under the CC BY license

(<https://creativecommons.org/licenses/by/4.0/>).

**Abstract**— This research was conducted at Malang during rainy seasons from february until June 2023. The purpose of the study is to obtain optimum tuber yields by applying eco enzyme concentration and NPK fertilizer dosage through agronomic experiments in urban farming systems. The research used Factorial randomized block design. Eco enzyme concentration (E) as First factor:  $E_0 = 0 \text{ ml.l}^{-1}$ ,  $E_1 = 15 \text{ ml.l}^{-1}$ ,  $E_2 = 30 \text{ ml.l}^{-1}$ ,  $E_3 = 45 \text{ ml.l}^{-1}$ . The second factor, NPK = (P) NPK fertilizer dose, namely:  $P_1 = 3.75 \text{ g plant}^{-1}$  NPK,  $P_2 = 5.62 \text{ g plant}^{-1}$  NPK,  $P_3 = 7.50 \text{ g plant}^{-1}$  NPK. This research was repeated three times. The results showed Eco enzyme concentration treatment affects the dose of NPK fertilizer on sweet potato plants. At an NPK fertilizer dose of  $3.75 \text{ g plant}^{-1}$ , the highest fresh tuber weight was produced at an eco enzyme concentration of  $30 \text{ ml l}^{-1}$ . At NPK fertilizer doses of  $5.62$  and  $7.50 \text{ g plant}^{-1}$ , the fresh weight of tubers was the same at all eco enzyme concentrations. The optimum eco enzyme concentration in the NPK fertilizer dose treatment of  $3.75 \text{ g plant}^{-1}$  was  $27.05 \text{ ml l}^{-1}$ ,  $5.62 \text{ g plant}^{-1}$  was  $25.44 \text{ ml l}^{-1}$  and  $7.50 \text{ g plant}^{-1}$  was  $26.54 \text{ ml l}^{-1}$ . eco enzyme concentrations and NPK doses can increase the growth and yield of sweet potato plants, on the variables: leaf area, plant dry weight, tuber fresh weight, harvest index.

**Keywords**— eco enzyme, npk fertilizer, sweet potato, planter bag.

## I. INTRODUCTION

Sweet potato (*Ipomoea batatas* L.) or often called sweet potato is a food plant that is widely cultivated in Indonesia. However, the availability of sweet potatoes in Indonesia, especially in East Java, is decreasing from year to year. According to the Central Statistics Agency (2018), sweet potato production in East Java in 2015-2017 was 350,516 tons, 288,039 tons, 257,414 tons. Another obstacle faced by farmers is the insufficient availability of fertilizer. The impact of continuous use of inorganic fertilizers will result in a decrease in land quality, therefore the government makes government regulations so that farmers do not depend on inorganic fertilizers. Regarding the scarcity of fertilizer, it is necessary to reduce dependence on NPK fertilizer, by using household waste

in the form of Eco enzymes. Due to the scarcity of NPK fertilizer, its function is expected to improve soil properties and overcome the leaching of nutrients in the soil.

Limited agricultural land affects the ability of a region to meet the food needs of its population, thereby weakening food security conditions. Nutrient limitations also become an obstacle to agricultural productivity and weaken food security conditions. According to Sitawati et al. (2019) that limited land in urban areas occurs due to infrastructure development, which can reduce the area of agricultural land. Minimalist use of sleeping land and yards in urban areas can be done with verticulture or planting activities using polybags or planter bags.

To provide and meet food needs, urban farming can be done by farming, which is a farming activity carried out in urban areas or land. The decreasing amount of agricultural land in urban areas can be caused by the increasing population, so that land use for residential areas is also increasing. The availability of sufficient nutrients in the soil is one of the factors that supports plant growth and development. This can be done by utilizing household waste which can be used as eco enzymes in the form of liquids originating from the fermentation of household waste, namely fruit, vegetable, water and sugar residues. The role of eco enzymes as decomposers is very important in breaking down dead organic material and accelerating the nutrient cycle in the environment. According to Panataria *et al.*, (2022), Eco enzyme contains several enzymes such as amylase, protease, and lipase, which help break down carbohydrates, proteins, fats, and plant fibers into compounds that are simpler and easier for microorganisms to take up. According to Arifin *et al.*, (2009), the process of making eco enzymes which are fermented for 3 months, uses the formula 1:3:10, namely 1 part sugar, 3 parts fruit and vegetable waste, 10 parts air. Efforts to use eco enzymes in agriculture can speed up compound reactions and produce enzymes.

Urban farming practices can be a solution for providing food by utilizing planting containers, cow manure, and eco enzymes which have the status of household waste. It is estimated that there is an interaction between eco enzymes and NPK fertilizer, so that the use of eco enzymes can reduce the use of NPK fertilizer.

The basic information above stated is deemed necessary to carry out research regarding the provision of eco enzyme concentrations and doses of NPK fertilizer on the growth and yield of sweet potato plants (*Ipomoea batatas* L.) in urban farming systems.

## II. MATERIAL AND METHODS

The research was carried out from February to June 2023, located in Gading Kasri Village, Klojen District, Malang City, East Java.

Materials used in the research include: Cuttings of sweet potato varieties: Beta-2, Eco Enzyme (EE), NPK fertilizer (15:15:15), and cow manure. The research was conducted using two factors with a Factorial Randomized Block Design (RBD), placing Eco enzyme (E) concentration as the first factor and NPK fertilizer (P) as the second factor.

Based on the design used, the field experiment was repeated 3 (three) times so that there were 36 experimental units. These treatments are:

The first factor, Eco enzyme concentration (E) is:

1. E0 = No eco enzyme
2. E1 = 15 ml l<sup>-1</sup>
3. E2 = 30 ml l<sup>-1</sup>
4. E3 = 45 ml l<sup>-1</sup>

Second Factor, NPK Fertilizer Dosage (P), namely:

1. P1 = 3.75 g plant<sup>-1</sup>
2. P2 = 5.62 g plant<sup>-1</sup>
3. P3 = 7.50 g plant<sup>-1</sup>

Research activities include: Planting, Maintenance, and Harvest. Maintenance activities include replanting, watering, applying eco enzyme, controlling pests and diseases, and fertilizing. Sweet potato plants are harvested 16 weeks after planting. Research observation variables included: number of leaves, leaf area, fresh weight of plants, dry weight of plants, fresh weight of tubers, length of tubers, and number of tubers.

The collected data was analyzed using the analysis of variance (ANOVA) method at 5% level. If the observation data obtained is significantly different then proceed with the HSD Test (Honestly Significant Difference) level of 5% to determine the differences between treatments.

## III. RESULT AND DISCUSSION

### Leaf Area

Based on analysis of variations in leaf area at the observation ages 16 WAP, it showed that there are interaction between the eco enzyme concentration treatment and the NPK fertilizer dose treatment. The average leaf area influenced by eco enzyme concentration and NPK fertilizer dosage is presented in Table 1.

At the observation ages 16 WAP the leaf area patterns were the same (Table 1). In the treatment with an NPK fertilizer dose of 3.75 g plant<sup>-1</sup>, the highest leaf area produced in the treatment with an eco enzyme concentration of 15 and 30 ml l<sup>-1</sup>. By administering an NPK fertilizer dose of 5.62 g plant<sup>-1</sup>, the highest leaf area produced in the treatment with an eco enzyme concentration of 15 to 45 ml l<sup>-1</sup>. In the treatment with an NPK fertilizer dose of 7.50 g plant<sup>-1</sup>, leaf area are not significantly different at all eco enzyme concentrations.

Observing the number of sweet potato leaves is important to determine the growth of sweet potato plants, this is because the leaves are a place to produce food through the process of photosynthesis. Sweet potato plants tend to invest most of their initial growth in the form of

additional leaf area, due to the influence and use of solar radiation. This phase began since the plants are 8-17 weeks old. Between 8-12 weeks, the plant stops forming new tubers because it starts to grow the existing tubers. The characteristic of tuber plants is that they have a rapid tuber formation and growth, but the stem and leaf growth is decreased (Amao *et al.*, 2018). Leaves are the main

photosynthetic organs in plants in which the process of converting light energy into chemical energy and accumulating energy in the form of dry matter (Liu *et al.* 2021). Furthermore, Gong *et al.* (2013) stated that leaves can show the mechanisms of light radiation interception, transpiration, growth and crop yields.

Table 1. Interaction of Eco enzyme concentration treatment and NPK fertilizer dose on average leaf area

Plant Age (WAP)	NPK Fertilizer Dosage (g plant <sup>-1</sup> )	Leaf Area (cm <sup>2</sup> plant <sup>-1</sup> )			
		Eco Enzyme Concentration (ml l <sup>-1</sup> )			
		0	15	30	45
16	3.75	3006.33 a	3426.66 ab	4131.00 b	3051.00 a
		A	A	A	A
	5.62	2912.66 a	4086.00 b	3413.33 ab	3851.00 b
		A	A	A	A
	7.50	3120.66 a	3380.33 a	3993.33 a	3491.66 a
		A	A	A	A
HSD Eco Enzyme 5%		893.37			
HSD NPK Fertilizer 5%		927.79			

Note: Numbers followed by the same lowercase letter in the row and numbers followed by the same uppercase letter in the same row and column are not significantly different based on the 5% HSD test. WAP = week after planting.

### Plant dry weight

Based on analysis of variations in dry weight of plants aged 16 WAP, it showed that there was a significant interaction ( $p=0.05$ ) between the eco enzyme concentration treatment and the NPK fertilizer dose treatment. The average dry weight of plants which is influenced by the concentration of eco enzyme and the dose of NPK fertilizer is presented in Table 2.

At the observation age of 16 WAP, treatment without eco enzyme and eco enzyme concentrations of 15 and 45 ml l<sup>-1</sup> showed that the dry weight value of sweet potato plants is not significantly different at all doses of NPK fertilizer. Treatment with an eco enzyme concentration of 30 ml l<sup>-1</sup> at a fertilizer dose of 3.75 g plant<sup>-1</sup>, showed the highest dry weight of plants and experienced a decrease at NPK fertilizer doses of 5.62 and 7.50 g plant<sup>-1</sup>. Treatment with an NPK fertilizer dose of 3.75 g plant<sup>-1</sup> with the addition of an eco enzyme concentration of 30 ml l<sup>-1</sup> can increase the dry weight value of sweet potato plants. In the treatment with a fertilizer dose of 3.75 g plant<sup>-1</sup>, the treatment with an eco enzyme concentration of 15 ml l<sup>-1</sup> had plant dry weight values that were not significantly different from those without eco enzyme and an eco enzyme concentration of 45 ml l<sup>-1</sup>. In

the treatment with NPK fertilizer doses of 5.62 and 7.50 g ton<sup>-1</sup>, the dry weight of sweet potato plants was not significantly different at all eco enzyme concentrations.

The increase in plant growth rate is influenced by the total dry weight of plants produced per unit of time. Plant dry weight reflects the accumulation of organic compounds that plants successfully synthesize from inorganic compounds, especially water and carbon dioxide. Nutrients including eco enzymes that have been absorbed by the roots contribute to the increase in plant dry weight. According to Sitompul and Guritno (1995) the main reason for using total plant biomass is that plant dry matter is seen as a manifestation of all processes and events that occur in plant growth. Biomass measurement is the total dry weight of all plant parts and increases due to plants absorbing CO<sub>2</sub> from the air and converting this substance into organic material through the process of photosynthesis. If the dry matter produced by plants is low, then the assimilate produced by plants will also be low (Ogbonna and Nweze, 2012). When plants enter the reproductive phase, assimilation will be carried to reproductive parts such as leaves. Reproduction is the plant organ that absorbs the most assimilation compared to other places (Ravi and Saravanan, 2012).

Table 2. Interaction of Eco enzyme concentration treatment and NPK fertilizer dose on average plant dry weight

Plant Age (WAP)	NPK Fertilizer Dosage (g plant <sup>-1</sup> )	Plant dry weight (g plant <sup>-1</sup> )			
		Eco Enzyme Concentration (ml l <sup>-1</sup> )			
		0	15	30	45
16	3.75	168.83 a	234.48 a	407.35 b	248.81 a
		A	A	B	A
	5.62	190.83 a	262.51 a	280.65 a	235.32 a
		A	A	A	A
	7.50	201.78 a	242.41 a	260.93 a	236.72 a
		A	A	A	A
HSD Eco Enzyme 5%		82.12			
HSD NPK Fertilizer 5%		90.77			

Note: Numbers followed by the same lowercase letter in the row and numbers followed by the same uppercase letter in the same row and column are not significantly different based on the 5% HSD test. WAP = week after planting.

### Tuber fresh weight

Based on analysis of variations in fresh weight of tubers at 16 WAP, it showed that there is a significant interaction ( $p=0.05$ ) between the eco enzyme concentration treatment and the NPK fertilizer dose treatment. The average fresh weight of tubers which is influenced by the interaction between eco enzyme concentration and NPK fertilizer dose is presented in

Table 3. Interaction of Eco enzyme concentration treatment and NPK fertilizer dose on average tuber fresh weight

Plant Age (WAP)	NPK Fertilizer Dosage (g plant <sup>-1</sup> )	Plant dry weight (g plant <sup>-1</sup> )			
		Eco Enzyme Concentration (ml l <sup>-1</sup> )			
		0	15	30	45
16	3.75	671.00 a	994.87 a	1720.00 b	972.17 a
		A	A	B	A
	5.62	724.53 a	1062.13 a	1046.20 a	891.00 a
		A	A	A	A
	7.50	709.77 a	978.47 a	1033.80 a	880.93 a
		A	A	A	A
HSD Eco Enzyme 5%		314.25			
HSD NPK Fertilizer 5%		347.36			

Note: Numbers followed by the same lowercase letter in the row and numbers followed by the same uppercase letter in the same row and column are not significantly different based on the 5% HSD test. WAP = week after planting.

In the treatment fertilizer doses of 5.62 and 7.50 g plant<sup>-1</sup>, leaf area is not significantly different at all eco enzyme concentrations. who states that the growth of sweet potato plants requires different nutrient intake in

each growth phase. In the initial growth phase, balanced N, P, K nutrients are needed, then in the tuber formation phase an increased amount of N, P, K nutrients is needed from the initial growth phase. The tuber filling phase

requires a higher amount of nutrients than the initial growth phase, and lower than the tuber formation phase. This is supported by the statement of trimunghan (2016), who stated that the formation of tubers is influenced by the K nutrient in the growth and development of plant roots, the P nutrient has a role in cell division and plant tissue development.

Based on the results of the regression analysis, it shows that there is a high degree of relationship between the concentration of eco enzyme and the dose of NPK fertilizer. Treatment doses of NPK fertilizer 3.75, 5.62 and 7.5 g.plant<sup>-1</sup> respectively had quite large coefficient

of determination values, including 0.70, 0.97 and 1, which shows the suitability of the data with the quadratic regression model (Figure 1). In the treatment with NPK fertilizer doses of 3.75, 5.62 and 7.5 g.plant<sup>-1</sup> respectively the quadratic equation  $y = -1.1908x^2 + 64.443x + 577.29$ ,  $y = -0.5476x^2 + 27.863x + 735.24$ , and  $y = -0.4684x^2 + 24.871x + 710.03$ . From this equation, the optimum eco enzyme concentration requirement can be calculated. The optimum eco enzyme concentration in the NPK fertilizer dose treatment of 3.75 g.plant<sup>-1</sup> was 27.05 ml l<sup>-1</sup>, 5.62 g.plant<sup>-1</sup> was 25.44 ml l<sup>-1</sup> and 7.5 g.plant<sup>-1</sup> was 26.54 ml l<sup>-1</sup>.

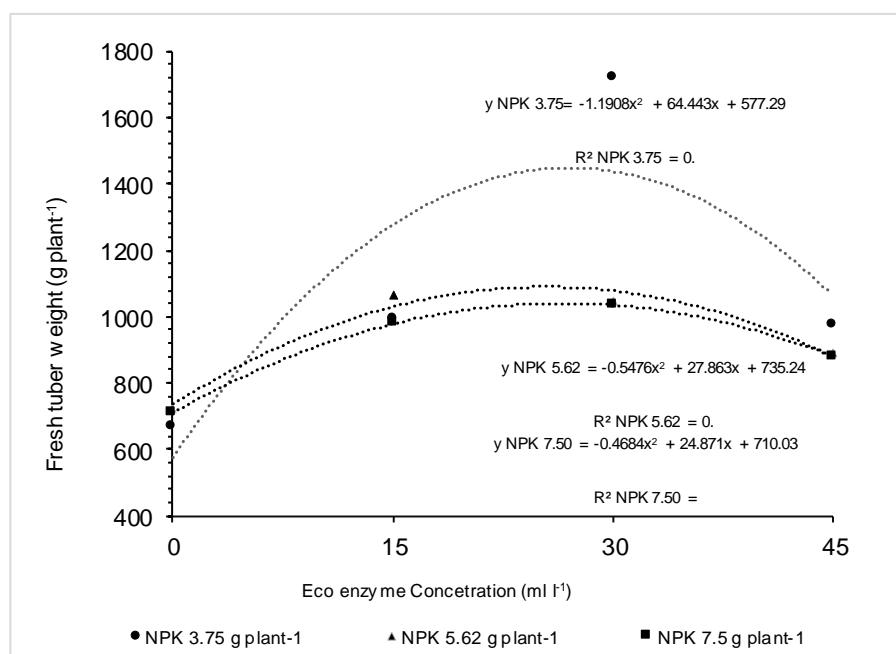


Fig 1. Regression of tuber fresh weight with eco enzyme concentration on NPK fertilizer dose

### Harvest index

Based on the analysis of various harvest index at 16 WAP, it shows that there is no significant interaction ( $p=0.05$ ) between the eco enzyme concentration treatment and the NPK fertilizer dose treatment. The harvest index of sweet potato plants only influenced by the eco enzyme concentration treatment (Figure 2). The results of observations of the harvest index at the age of 16 WAP showed that the treatment without eco enzyme have the lowest harvest index value. Treatments with eco enzyme concentrations of 15 and 30 ml l<sup>-1</sup> have the highest harvest index values and significantly different results compared to treatments without eco enzyme. Treatment with eco enzyme concentration of 15 to 45 ml l<sup>-1</sup> can increase the fresh weight of plants and have values that are not significantly different. The treatment without eco enzyme have a harvest index value that is not significantly

different from the treatment with a concentration of 45 ml l<sup>-1</sup>. The average harvest index which is influenced by eco enzyme concentration is presented in Figure 2.

Based on the results of the regression analysis, it shows that there is a high degree of relationship between the concentration of eco enzyme and the dose of NPK fertilizer. The control eco enzyme concentration treatment, 15 ml.l<sup>-1</sup>, 30 ml.l<sup>-1</sup>, 45 ml.l<sup>-1</sup> has a fairly large coefficient of determination value, namely 0.99, which shows the suitability of the data to the quadratic regression model (Figure 2). In the control eco enzyme concentration treatment, 15 ml.l<sup>-1</sup>, 30 ml.l<sup>-1</sup>, 45 ml.l<sup>-1</sup> has a quadratic equation  $y = -0.0325x^2 + 0.1795x + 0.6025$ . From this equation, it can be concluded that the optimum eco enzyme concentration is an eco enzyme concentration of 30 ml.l<sup>-1</sup>.



The results of the observations show that without giving eco enzyme the IP results are smaller than when giving eco enzyme. According to Jha (2012) that tuber yield is positively correlated with IP, weight of the entire plant and number of tubers per plant. A high IP indicates greater distribution of assimilate to the tuber while a low IP indicates greater distribution of assimilate to the top of

the plant. According to Gu *et al.*, (2021), the use of eco enzymes can regulate the growth pattern of sweet potato plants by maintaining a balance of vegetative and generative growth, so that competition for source utilization by vegetative and generative growth which results in low levels of assimilate distributed into the sink can be suppressed.

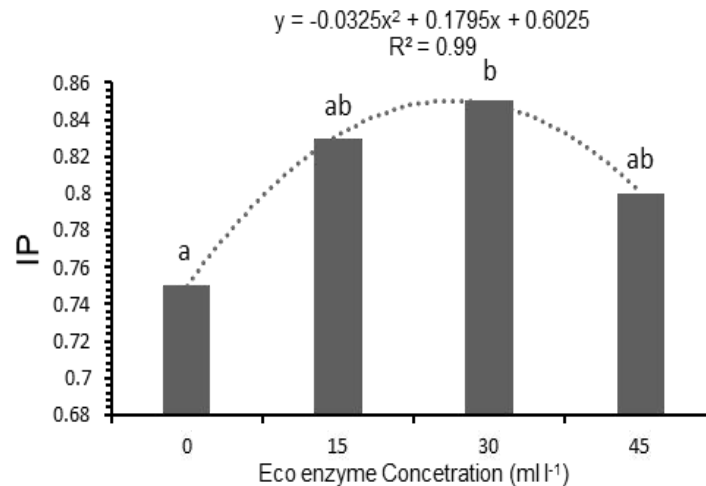


Fig 2. Regression of harvest index with eco enzyme concentration on NPK fertilizer dose

#### IV. CONCLUSION

Eco enzyme concentration treatment affects the dose of NPK fertilizer on sweet potato plants. At an NPK fertilizer dose of 3.75 g plant<sup>-1</sup>, the highest fresh tuber weight was produced at an eco enzyme concentration of 30 ml l<sup>-1</sup>. At NPK fertilizer doses of 5.62 and 7.50 g plant<sup>-1</sup>, the fresh weight of tubers was the same at all eco enzyme concentrations. The optimum eco enzyme concentration in the NPK fertilizer dose treatment of 3.75 g plant<sup>-1</sup> was 27.05 ml l<sup>-1</sup>, 5.62 g plant<sup>-1</sup> was 25.44 ml l<sup>-1</sup> and 7.5 g plant<sup>-1</sup> was 26.54 ml l<sup>-1</sup>. Eco enzyme concentrations and NPK doses can increase the growth and yield of sweet potato plants, on the variables: leaf area, plant dry weight, tuber fresh weight, and harvest index.

#### REFERENCES

- [1] Adeyeye, A.S., WB. Akanbi, O.O. Sobola, W.A. Lamidi, and K.K. Olalekan. 2016. Comparative effect of organic and In-organic fertilizer treatment on the growth and tuber yield of Sweet potato (*Ipomoea batatas* L.). *International Journal of Sustainable Agricultural Research*. 3 (3): 54-57.
- [2] Amao, P.A., S.O. Osunsanya, and A. M. Afolabi. 2018. Yield Evaluation and Assessment of Growth of Five Different Varieties of Sweet Potato (*Ipomoea batatas* (L.) Lam). *Journal of Agriculture and Ecological Research International*. 15 (1): 1-8.
- [3] Badan Pusat Statistik. 2018. Luas panen, produktivitas, dan produksi komoditi Ubi Jalar di Jawa Timur, 2002-2017.
- [4] Gong, A., X. Wu., Z. Qiu and Y. He. 2013. A handheld device for leaf area measurement. *Comput.Electron.Agric*.98:74-80.
- [5] Gu, S., Xu, D., Zhou, F., Chen, C., Liu, C., Tian, M., and Jiang, A. 2021. The garbage enzyme with chinese hoenylocust fruits showed better properties and application than when using the garbage enzyme alone. *Foods*. 10 (11): 1-14.
- [6] Hemalatha, M. and P. Visantini. 2020. Potential use of eco-enzyme for the treatment of metal based effluent. *IOP Conference Series: Materials Science and Engineering*. 716 (2020): 1-6.
- [7] Liu, C. W., Ling, R. L. Z., and Teo, S. S. 2021. Effective microorganisms in producing eco-enzyme from food waste for wastewater treatment. *Applied Microbiology: Theory & Technology*. 28-36.
- [8] Jha, G. 2012. Increasing productivity of sweet potato (*Ipomoea batatas* L.) through clonal selection of ideal genotypes from open pollinated seedling population. *International Journal of Farm Sciences*. 2 (2):17-27.
- [9] Ogbonna, P.E. and N.J. Nweze. 2012. Evaluation of growth and yield responses of cocoyam (*Colocasia esculenta*) cultivars to rates of NPK 15:15:15 fertilizer. *Afr. Journal. Agric. Res*. 7: 6553-6561.
- [10] Panataria, L.R., E. Sianipar, H. Sembiring, E. Sitorus, M. Saragih. 2022. Study of nutrient content in eco enzymes from various types of organic materials. *Journal Agric*. 1 (2): 90-95.
- [11] Sitawati., E. E. Nurlaelih, dan D. R. R. Damaiyanti. 2019. *Urban Farming Untuk Ketahanan Pangan*. UB Press, Malang.

- [12] Sitompul, S. dan B. Guritno. 1995. Analisis pertumbuhan tanaman. UGM Press, Yogyakarta.
- [13] Thirumurugan, P, and Mathivanan, K. 2016. Production and analysis of enzyme Bio-cleaners from fruit and vegetable wastes by using Yeast and Bacteria. Student project Report (DO Rc. No. 1082/2015A, pp. 4-6.



# The Symbolism of Double Consciousness in the Works of W.E.B. Du Bois and its Evolution in Contemporary Black Literature

Neethu S

Research Enthusiast, Devanandanam, Ernakulam, 682305, India

Received: 08 Nov 2023; Received in revised form: 13 Dec 2023; Accepted: 21 Dec 2023; Available online: 30 Dec 2023

©2023 The Author(s). Published by Infogain Publication. This is an open access article under the CC BY license

(<https://creativecommons.org/licenses/by/4.0/>).

**Abstract**— This research paper traverse into the concept of double consciousness as presented by W.E.B. Du Bois in his seminal work *The Souls of Black Folk* and explores how this theme has been redefined and adapted in contemporary black literature. The study examines the symbolic use of double consciousness in characters, narratives, and motifs, tracing its evolution as a literary device and its continued relevance in the portrayal of black identity and experience. Through an in-depth analysis of selected works spanning different periods, the research aims to shed light on the ways in which black writers have engaged with and transformed this concept to reflect the complexities of black life in diverse sociocultural contexts.



**Keywords**— *Black Literature, Contemporary, Double Consciousness, Identity, W.E.B. Du Bois.*

## I. INTRODUCTION

The concept of double consciousness, introduced by W.E.B. Du Bois in his seminal work *The Souls of Black Folk*, stands as a poignant and enduring exploration of the intricacies inherent in black identity. Du Bois, a pioneering African American sociologist, scholar, and writer, introduced this concept to articulate the unique internal conflict experienced by individuals of African descent. This research embarks on a comprehensive journey to unravel the symbolic manifestations of double consciousness in Du Bois's works, illuminating its profound implications for understanding the duality of black existence.

Du Bois's articulation of double consciousness resonates as a foundational concept, encapsulating the internal tug-of-war between an individual's self-perception and the societal perceptions that are often shaped by prevailing racial prejudices. The duality inherent in this concept reflects the tension between one's authentic self and the external expectations and stereotypes imposed by a racially stratified society. This internal conflict, as elucidated by Du Bois, becomes a powerful lens through

which to scrutinize the complexities of black identity formation.

To comprehensively investigate this concept, the study contextualizes Du Bois's writings within the historical and socio-cultural milieu of his time. Understanding the societal challenges and racial dynamics that influenced Du Bois's work provides a critical foundation for deciphering the nuanced layers of double consciousness. The historical context, encompassing the post-Reconstruction era and the Jim Crow South, elucidates the profound impact of systemic racism on the construction of black identity.

Moreover, this research positions itself as a bridge between historical foundations and contemporary expressions of black literature. By tracing the evolution of double consciousness, the study seeks to understand how contemporary black authors engage with and reinterpret this seminal concept in the context of the present day. This exploration paves the way for an in-depth analysis of the ways in which double consciousness continues to shape and be shaped by the evolving landscape of black literature, offering profound insights into the ongoing dialogue on race, identity, and cultural representation.

## II. METHOD

The methodological framework adopted for this research underscores a rigorous exploration of double consciousness through an analysis of primary texts, primarily centering on the works of W.E.B. Du Bois and selected contemporary black literature that prominently engages with the theme. This approach ensures a focused and nuanced examination of the symbolic manifestations of double consciousness.

The core of the methodology lies in the careful examination of primary texts, emphasizing Du Bois's writings, particularly *The Souls of Black Folk*, as foundational sources. These texts serve as the bedrock for understanding the historical origins and conceptual underpinnings of double consciousness. Additionally, the study incorporates a selection of contemporary black literary works known for their explicit exploration of double consciousness. This inclusive approach allows for a comprehensive analysis that spans historical and contemporary periods, facilitating a rich understanding of the evolution of this concept.

Textual analysis forms the backbone of the methodology, enabling a granular examination of how double consciousness is symbolically represented in literature. This involves a meticulous scrutiny of character development, narrative techniques, and recurring motifs within the chosen works. By dissecting the textual elements, the study aims to unearth the nuances and complexities embedded in the portrayal of double consciousness, shedding light on its varied expressions and implications.

The comparative method plays a pivotal role, allowing for a dynamic exploration of connections and distinctions between historical and contemporary portrayals of double consciousness. Through systematic comparison, the research aims to discern patterns, shifts, and innovations in the representation of this concept over time. This comparative lens facilitates a nuanced understanding of the evolution of double consciousness within the broader context of black literature.

By drawing on these methodological approaches, this research aspires to contribute not only to a deeper comprehension of double consciousness but also to the methodological toolkit of literary scholars. The intertwining of historical analysis, textual scrutiny, and comparative examination promises a comprehensive exploration that transcends the temporal boundaries of literary works, offering valuable insights into the ongoing narrative of black identity and the enduring resonance of double consciousness in the literary landscape.

## III. RESULT

The results section of this research unfolds as a rich tapestry, weaving together the intricate findings derived from a meticulous textual analysis of both W.E.B. Du Bois's seminal works and selected contemporary black literature. The focus is on elucidating the symbolic representations of double consciousness, unraveling the threads that connect the historical foundations laid by Du Bois to the contemporary reinterpretations of this profound concept.

In examining Du Bois's works, the results illuminate the multifaceted ways in which double consciousness is symbolically represented. Key themes emerge, reflecting the internal conflict and duality inherent in black existence. Du Bois employs literary devices such as symbolism, metaphor, and allegory to vividly depict the tensions between self-perception and societal expectations. The results underscore the enduring power of Du Bois's narrative craft in encapsulating the complexities of black identity during the post-Reconstruction and Jim Crow eras.

Subsequently, the results delve into the contemporary landscape of black literature, revealing how authors have reimagined and adapted the concept of double consciousness. Through a focused examination of specific examples, the study unveils the nuanced ways in which contemporary black authors engage with this enduring theme. From Toni Morrison to Ta-Nehisi Coates, the evolution of double consciousness is evidenced through diverse narrative strategies and stylistic choices.

The findings suggest that contemporary authors often expand upon Du Bois's groundwork, introducing new dimensions and perspectives to the concept. The results underscore the adaptability and resilience of double consciousness as a literary symbol, mirroring the ever-evolving nature of black identity in response to shifting socio-cultural landscapes.

Furthermore, the results emphasize the concept's continued relevance as a powerful and evolving symbol within the landscape of black literature. The dynamic interplay between historical foundations and contemporary reinterpretations serves as a testament to the enduring significance of double consciousness in articulating the complexities, struggles, and triumphs of black identity. This section thus contributes to a deeper understanding of the evolution of a central theme in black literature, transcending temporal boundaries and providing a lens through which to appreciate the ongoing narrative of black identity in literary expression.

#### IV. CONCLUSION

In essence, this research culminates in a resounding affirmation of the enduring significance of double consciousness as a potent and evolving literary symbol within the realm of black literature. The journey through the analyses of W.E.B. Du Bois's seminal works and contemporary literature has illuminated the rich tapestry of this concept, highlighting its nuanced representations and the profound ways in which it encapsulates the multifaceted nature of black identity.

The synthesis of findings from Du Bois's era to the contemporary landscape underscores the evolution of double consciousness as a dynamic and resilient symbol. From its inception as a response to the racial challenges of the post-Reconstruction period to its adaptation in the context of modern complexities, the concept has proven its adaptability. The research reveals how contemporary black authors have deftly reimagined and adapted double consciousness, infusing it with new layers of meaning and relevance that resonate with the contemporary sociocultural milieu.

Moreover, the conclusion emphasizes the broader implications of this research for the understanding of black literature and identity. It posits that the exploration of double consciousness serves as a mirror reflecting the ongoing struggles and triumphs of the black experience. The concept, as revealed through literary analysis, becomes a means through which scholars and readers alike can engage with the complexities of black identity, offering a deeper appreciation of the rich and diverse narratives within black literature.

As a call to action, the conclusion suggests avenues for future research, inviting scholars to delve further into the dynamic symbolism of double consciousness. The evolving landscape of black literary expression presents an opportunity for continued exploration, encouraging scholars to examine how this concept may continue to evolve, adapt, and resonate in response to ever-changing societal dynamics. By extending this research, scholars can contribute to the ongoing discourse on race, culture, and identity, enriching our understanding of the enduring narrative woven into the fabric of black literature. In this way, the conclusion serves not only as a summation of the research's findings but as an invitation to further illuminate the complex and evolving nature of black literary expression.

#### REFERENCES

[1] Adichie, C. N. (2003). *Purple Hibiscus*. Algonquin Books.

- [2] Angelou, M. (1969). *I Know Why the Caged Bird Sings*. Random House.
- [3] Baldwin, J. (1953). *Go Tell It on the Mountain*. Knopf.
- [4] Coates, T.-N. (2015). *Between the World and Me*. Spiegel & Grau.
- [5] Du Bois, W. E. B. (1903). *The Souls of Black Folk*. Oxford University Press.
- [6] Ellison, R. (1952). *Invisible Man*. Random House.
- [7] Hughes, L. (1926). *The Weary Blues*. Alfred A. Knopf.
- [8] Hurston, Z. N. (1937). *Their Eyes Were Watching God*. J.B. Lippincott.
- [9] Locke, A. (1925). *The New Negro: An Interpretation*. Albert and Charles Boni.
- [10] Marshall, P. (1959). *Brown Girl, Brownstones*. Random House.
- [11] Morrison, T. (1987). *Beloved*. Knopf.
- [12] Ngozi Adichie, C. (2006). *Half of a Yellow Sun*. Knopf.
- [13] Reed, I. (1972). *Mumbo Jumbo*. Doubleday.
- [14] Walker, A. (1982). *The Color Purple*. Harcourt Brace Jovanovich.
- [15] White, E. B. (1982). *Charlotte's Web*. Harper & Row.
- [16] Wright, R. (1940). *Native Son*. Harper & Brothers.



# Cultural Hybridity in Focus: Exploring Globalized Identities Through Jhumpa Lahiri's *The Namesake* and Alejandro González Iñárritu's *Babel*

Arjun K Anil

Research Scholar in English, PG and Research Dept. of English, Govt. Victoria College, Palakkad, India

Received: 11 Nov 2023; Received in revised form: 17 Dec 2023; Accepted: 22 Dec 2023; Available online: 31 Dec 2023

©2023 The Author(s). Published by Infogain Publication. This is an open access article under the CC BY license

(<https://creativecommons.org/licenses/by/4.0/>).

**Abstract**— This research paper focuses on the phenomenon of Cultural Hybridity within the realm of literature and film, honing in on specific works as case studies to illuminate the intricacies of cultural fusion in globalized societies. The chosen literary work here is Jhumpa Lahiri's *The Namesake*, while the film *Babel* directed by Alejandro González Iñárritu serves as a cinematic counterpart. Through a meticulous analysis of these culturally rich narratives, the study explores how the characters navigate their identities in the face of globalization. The paper traverses into the ways in which the authors and filmmakers employ narrative techniques, character development, and symbolic elements to depict the hybridization of cultures. It examines how these artistic creations serve as mirrors reflecting the broader issues of diaspora, immigration, and the clash of traditional and modern values. By dissecting the chosen literary and cinematic works, this research aims to unveil the unique ways in which Cultural Hybridity is portrayed and its implications on individual and collective identity. The formal analysis of *The Namesake* and *Babel* provides a lens through which scholars and enthusiasts can deepen their understanding of how cultural amalgamation is articulated in creative expressions, enriching the discourse on the intersection of art, culture, and globalization.



**Keywords**— *Babel*, Cultural Hybridity, Globalization, Identity, Jhumpa Lahiri.

## I. INTRODUCTION

The intricate dance of cultures in the face of globalization has given rise to a phenomenon known as Cultural Hybridity, a dynamic process of amalgamation that reshapes identities on both individual and societal levels. This research embarks on a nuanced exploration of Cultural Hybridity, with a specific focus on its portrayal in literature and film. By delving into the rich narratives of Jhumpa Lahiri's *The Namesake* and Alejandro González Iñárritu's *Babel*, this study seeks to unravel the complex threads of cultural fusion within the realms of storytelling and visual representation.

As the world becomes increasingly interconnected, the cultural tapestry that defines our global society undergoes a profound transformation. The chosen literary work, *The*

*Namesake*, provides a lens through which we can examine the experiences of characters caught between the gravitational pulls of their heritage and the currents of contemporary life. Simultaneously, *Babel*, a cinematic masterpiece, captures the mosaic of cultures converging and colliding on the screen, reflecting the interconnectedness of the modern world.

The intersection of literature and film allows us to explore how artists navigate the challenges and opportunities presented by Cultural Hybridity. The characters in *The Namesake* and the narrative arcs in *Babel* serve as microcosms of the broader issues of diaspora, immigration, and the negotiation of tradition in a globalized context. Through the meticulous analysis of these works, this research aims to contribute valuable

insights into the ways in which cultural identities are portrayed and negotiated in the creative realm.

By placing these specific cultural artifacts under the microscope, we aim to shed light on the unique ways in which Cultural Hybridity is articulated, offering a deeper understanding of its manifestations and implications. As we embark on this journey through the pages of literature and the frames of cinema, we strive to unravel the narratives that mirror the complexities of our interconnected world, paving the way for a comprehensive exploration of the interplay between culture, globalization, and artistic expression.

## II. METHOD

This research employs a comprehensive and multi-faceted approach to delve into the portrayal of Cultural Hybridity in Jhumpa Lahiri's *The Namesake* and Alejandro González Iñárritu's *Babel*. The chosen methodology combines literary analysis, film studies, and cultural critique to provide a thorough examination of the selected works, allowing for a nuanced exploration of the themes related to Cultural Hybridity.

The study initiates with an in-depth literary analysis of *The Namesake*, scrutinizing the narrative structure, character development, and thematic elements. This involves a close reading of the text to identify instances of cultural hybridization, exploring how Lahiri weaves the complexities of identity into the fabric of her storytelling. Key themes such as diaspora, generational shifts, and the clash of cultural norms are dissected to reveal the nuances of Cultural Hybridity in the literary realm.

Moving to the cinematic domain, the research engages in a meticulous examination of *Babel*. This involves a frame-by-frame analysis, considering visual elements, cinematography, and narrative techniques employed by Iñárritu. By dissecting the film's structure, character interactions, and visual symbolism, the study aims to uncover how Cultural Hybridity is visually represented on the screen. The integration of cultural elements, language, and the portrayal of diverse landscapes becomes focal points in this cinematic exploration.

To draw meaningful comparisons and contrasts between the literary and cinematic portrayals, a comparative analysis is conducted. This involves identifying commonalities and divergences in how Cultural Hybridity is articulated in the two mediums. The goal is to highlight the unique strengths of each art form in conveying the intricacies of cultural amalgamation.

The research incorporates a cultural critique lens, contextualizing the findings within broader discussions on

globalization, identity, and cultural exchange. This involves drawing on relevant theoretical frameworks and scholarly discourse to provide a theoretical foundation for the analysis.

Through this multi-methodological approach, the study aims to offer a comprehensive understanding of Cultural Hybridity as depicted in *The Namesake* and *Babel*, contributing to the discourse on culture, globalization, and artistic representation.

## III. RESULTS

The comprehensive examination of Jhumpa Lahiri's *The Namesake* and Alejandro González Iñárritu's *Babel* unveils a rich tapestry of Cultural Hybridity within the realms of literature and film. In *The Namesake*, Lahiri skillfully weaves a narrative that intricately explores the complexities of cultural identity. The characters, particularly Gogol Ganguli, navigate the delicate balance between their cultural heritage and the demands of a rapidly changing world. The diasporic experience is vividly depicted as characters grapple with the nuances of assimilation, generational shifts, and the preservation of cultural traditions. The literary analysis reveals how Lahiri employs narrative techniques to illustrate the fluid nature of cultural boundaries, portraying a dynamic process of identity formation.

In parallel, the film *Babel* provides a visual exploration of Cultural Hybridity on a global scale. The cinematography and narrative structure, spanning multiple continents and languages, encapsulate the interconnectedness of diverse cultures. Iñárritu masterfully intertwines individual stories to create a mosaic that reflects the complexities of human connection and miscommunication. The film serves as a visual metaphor for the interplay of cultures, emphasizing the challenges and beauty inherent in cross-cultural interactions. The visual elements, such as the use of landscapes and symbols, contribute to the portrayal of a world where cultures collide and converge.

The comparative analysis underscores the unique strengths of each medium in conveying Cultural Hybridity. While Lahiri's prose delves deep into the internal struggles of characters, Iñárritu's cinematic vision provides a panoramic view of cultural intersections. The juxtaposition of these works highlights the diverse ways in which artists articulate and represent the intricate process of cultural amalgamation.

This research contributes to the broader discourse on culture, globalization, and artistic expression by providing a nuanced understanding of how Cultural Hybridity is depicted in literature and film. The findings invite further

exploration into the intricate dynamics of identity negotiation in a world shaped by interconnected cultural influences.

#### IV. CONCLUSION

In the culmination of this research journey into Cultural Hybridity as depicted in Jhumpa Lahiri's *The Namesake* and Alejandro González Iñárritu's *Babel*, a nuanced understanding emerges of the intricate interplay between cultures in literature and film. Through the lens of literature, Lahiri's narrative delves deep into the internal struggles of characters negotiating their cultural identities. The portrayal of diaspora, generational shifts, and the clash between tradition and modernity serves as a literary mirror reflecting the complexities of Cultural Hybridity in individual lives.

In parallel, *Babel* provides a cinematic panorama that captures the mosaic of global cultures. Iñárritu's masterful storytelling, spanning multiple continents and languages, visually encapsulates the interconnectedness of diverse societies. The film becomes a visual metaphor for the challenges and beauty inherent in cross-cultural interactions, emphasizing the globalized nature of our contemporary world.

The comparative analysis underscores the unique strengths of each medium, demonstrating how literature and film offer distinct yet complementary perspectives on Cultural Hybridity. Lahiri's prose allows for an intimate exploration of characters' internal struggles, while Iñárritu's cinematic vision provides a broader, visual canvas that conveys the grand scale of cultural intersections.

As we reflect on these findings, it becomes evident that both literary and cinematic representations of Cultural Hybridity contribute to a richer understanding of the complexities of identity negotiation in a globalized context. The dynamics of assimilation, preservation, and transformation are unveiled, offering insights into the ways individuals and societies grapple with the evolving nature of culture.

In essence, this research extends an invitation for scholars, artists, and enthusiasts to further explore the multifaceted nature of Cultural Hybridity. The interplay between literature and film, as demonstrated through *The Namesake* and *Babel*, serves as a testament to the enduring power of storytelling in shaping our understanding of culture, identity, and the ever-evolving tapestry of the globalized world. Through these artistic expressions, we navigate the cultural landscape, recognizing the beauty and

challenges inherent in the fusion of diverse traditions and narratives.

#### REFERENCES

- [1] González Iñárritu, A. (Director). (2006). *Babel* [Film]. Paramount Pictures.
- [2] Lahiri, J. (2003). *The Namesake*. Houghton Mifflin Harcourt.
- [3] Appadurai, A. (1996). *Modernity at Large: Cultural Dimensions of Globalization*. University of Minnesota Press.
- [4] Featherstone, M. (1995). *Undoing Culture: Globalization, Postmodernism, and Identity*. SAGE Publications.
- [5] Hall, S. (1991). *The Local and the Global: Globalization and Ethnicity*. In A. D. King (Ed.), *Culture, Globalization, and the World-System* (pp. 19-39). Macmillan.
- [6] Hannerz, U. (1996). *Transnational Connections: Culture, People, Places*. Routledge.
- [7] Said, E. W. (1978). *Orientalism*. Vintage Books.
- [8] Tomalin, C., & Stainton, E. (2006). *Jhumpa Lahiri: The Namesake*. A&C Black.
- [9] Tomlinson, J. (1999). *Globalization and Culture*. University of Chicago Press.





# Study of Biological Factors Likely to Influence Sensitivity to Dry Ball Disease of Rubber Tree in Three Rubber Production Zones of Cote D'ivoire

Zoh Olivia Dominique<sup>1\*</sup>, Dolou Charlotte Tonessia<sup>2</sup>, Éric Francis Soumahin<sup>3</sup>, Kouamé Kouassi James Joseph<sup>4</sup>, Amadou Doumbia<sup>5</sup>

<sup>1,2,3,4</sup>Agricultural Production Improvement Laboratory, UFR-Agroforestry, University Jean Lorougnon Guédé BP 150 Daloa, Côte d'Ivoire

<sup>5</sup>EXAT rubber company (Exploitation Agricolaire Téhui) BP 2508 Abidjan, Côte d'Ivoire

\*Corresponding author

Received: 03 Nov 2023; Received in revised form: 09 Dec 2023; Accepted: 20 Dec 2023; Available online: 31 Dec 2023

©2023 The Author(s). Published by Infogain Publication. This is an open access article under the CC BY license

(<https://creativecommons.org/licenses/by/4.0/>).

**Abstract**—Rubber production in rubber trees is affected by dry notch disease, the cause of which has unfortunately not yet been fully elucidated. This study aims to evaluate the impact of biological factors on susceptibility to disease across agro-industrial companies in the West (Zagné), South-West (San-Pédro) and South-East (Anguédédou) zones of the Côte d'Ivoire. The method used is the recording of panel sick length (PSL) of rubber trees in relation to their clonal metabolisms and the attacks of the main pests of rubber trees such as *Corynespora* sp, *Fomes* sp and *Loranthaceae*. The results showed that the three cultivated clonal metabolic class were all affected by dry notch of rubber but at different levels with an average of  $34.65 \pm 1.77$  %. Regarding pests, the study revealed that they significantly influence ( $Pr < 0.05$ ) the sensitivity to dry notch. Rubber trees attacked by *Fomes* sp displayed a higher rate of diseased notch ( $50.56 \pm 20.30$  %) than that of non-attacked rubber trees ( $30.58 \pm 20$  %). Similarly, rubber trees parasitized by *Loranthaceae* displayed higher PSL ( $38.41 \pm 20.55$  %) than those of rubber trees free ( $30.16 \pm 21.62$  %). Only rubber trees attacked by *Corynespora* sp presented lower PSL ( $15.61 \pm 13.69$  %) than those of non-attacked rubber trees ( $39.76 \pm 20.22$  %). Depending on the different production zones, *Loranthaceae* infested rubber plantations more than the other two pests.



**Keywords**—Pest of crops, rubber tree, stoppage of latex flow, tropical country.

## I. INTRODUCTION

Rubber is a very popular cash crop in Côte d'Ivoire. It is certainly not the only rubber plant in the world, but almost all of the natural rubber used in industries comes from the rubber tree. This is also what makes natural rubber a strategic raw material and rubber growing a dynamic and expanding sector (Thaler, 2013). In 2021, with a production of nearly one million tonnes and a cultivated area of 700 000 hectares, Côte d'Ivoire rose to 4<sup>th</sup> place, behind the world giants (APROMAC, 2021).

However, it seems that this performance is more linked to the increase in cultivated areas rather than to the productivity of rubber trees. For good reason, in rubber

farms, a fairly recurring problem is observed during tapping. This is the phenomenon of dry notch of rubber trees, a disease which results in a partial or total cessation of the flow of latex after tapping (Okoma *et al.*, 2011). This syndrome, which is economically serious, has become a priority in rubber growing research programs. The efforts made by Ivorian researchers in 2011, in industrial plantations, reported a national average rate of dry notch of 9 % (Okoma *et al.*, 2009). Since then, an increasing evolution of dry notch has been noted in rubber plantations. Unfortunately, the real cause of this physiological dysfunction has not been fully elucidated (Okoma, 2008).

Knowing that the cultivation of rubber trees involves on the one hand, the clone whose sensitivity to dry notch follows a gradient identical to that of the metabolic activity (Okoma *et al.*, 2009) and on the other hand, that the attacks of pests constitute opening doors to dysfunctions in trees (Déon, 2012), this study aims to evaluate the impact of biological factors on the sensitivity to dry notch of rubber trees in main areas of Ivorian rubber production.

## II. MATERIALS AND METHODS

### Study sites

The study was carried out on the basis of surveys and empirical data collection in agro-industrial companies in the Anguédédou, San-Pédro and Zagné zones (Fig. 1). The characteristics of these zones are recorded in Table 1.

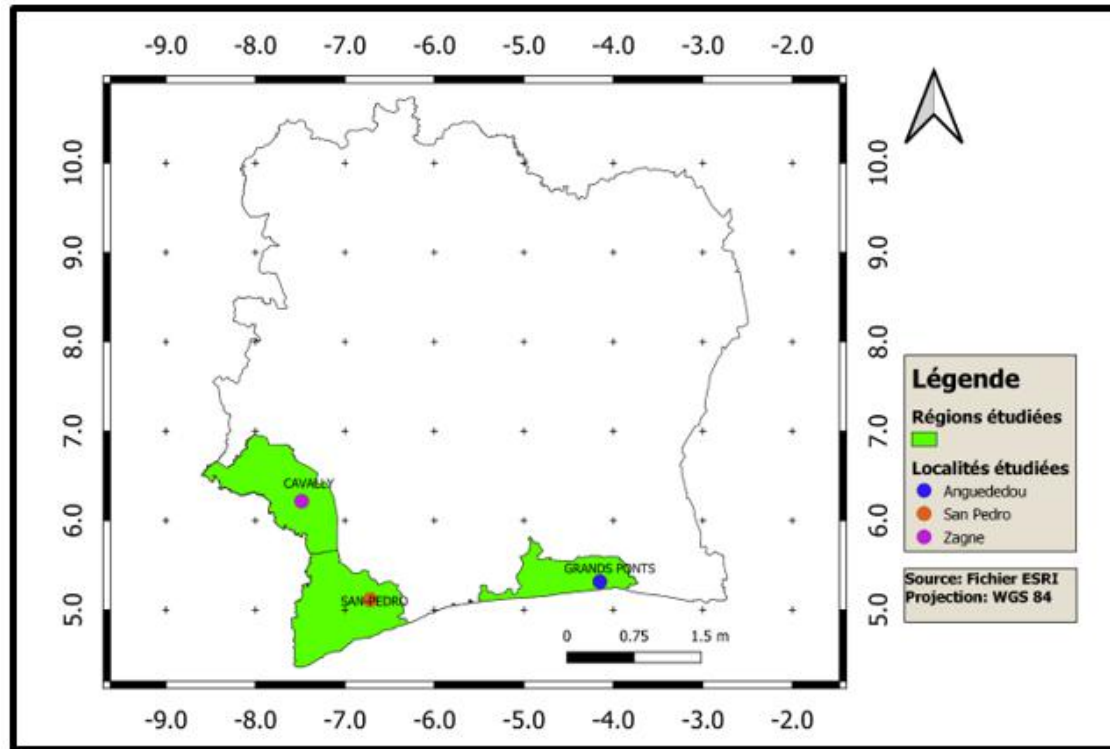


Fig. 1 : Presentation of the different survey sites

Table 1 : Characteristics of the study areas

Localities	Geographic coordinates	Vegetation	Floors	Precipitation (mm/year)	Average temperature (°C)	Insolation (hours/year)	Relative humidity (%)
Anguédédou	5°19'N and 4°09'W	Cleared rainforest	Highly desaturated ferralitic with little gravel content	1800-2000	26	2000-2100	90
San Pedro	4°45'N and 6°38'W	Dense evergreen humid forest	Highly desaturated ferralitic and gravelly	1800-2000	25	1700-1800	90
Zagné	6°13'N and 7°29'W	Dense, humid forest	Humus and ferruginous forestry poor in humus	1200	18-36	1200-1500	72-90

Sources : Brou (2005) and Neobot (2020).

### Plant material

The plant material used for this study consists of popularized *Hevea brasiliensis* clones, that is to say clones found both in village and industrial plantations. These clones were identified during surveys and prospections in the main rubber production areas of Côte d'Ivoire and are part of the three classes of metabolic activities.

### Data collection device

Surveys for data collection were carried out from October 2020 to February 2021 ; period which corresponds to the end of the 2020-2021 production campaign and which allows us to better appreciate the symptoms of dry notch and the main pests.

Field surveys were carried out taking into account the metabolic classes of the cultivated clones. From one plot to another, a tapper was retained to tap the trees of the chosen diagonal line, eliminating the border trees. The

tapping shares of the different tappers selected included an average of 500 trees ; which approximately corresponds to a plot of one hectare in a rural environment taking into account the 6 m x 3 m system which corresponds to 555 trees per hectare. Daily surveys began at 6 : 30 a.m. and ended around 12 p.m. with an average time of 30 minutes per tapper.

### Parameters measured

#### Dry notch survey of rubber trees

The determination of the actual length of notch which no longer produces latex at the level of a tree in operation, also called panel sick length (PSL), was done by visual assessment using the method rapid dry notch survey by Van De Sype (1984). The trees observed were rated on a scale of 0 to 6 depending on the flow of latex after tapping (Table 2). Then, the scores obtained were used to calculate the panel sick length (PSL) using the following formula :

$$PSL = [(0.1 n_1 + 0.3 n_2 + 0.5 n_3 + 0.7 n_4 + 0.9 n_5 + n_6) / N] \times 100$$

With PSL = Panel Sick Length ; N = total number of trees in the plot ; Coefficients 0.1; 0.3; 0.5; 0.7; 0.9 and 1 = class averages of non-latex producing kerf length percentage ; n1; n2; n3; n4; n5 and n6 = numbers of trees observed per percentage class of non-latex-producing bleed notch length.

Table 2 : Dry notch length rating scale (Van De Sype, 1984)

NOTE	(PSL %)	MEANING
0	0	Healthy trees
1	1 to 20	Trees affected by very low level dry notch
2	21 to 40	Trees affected by low level dry notch
3	41 to 60	Trees affected by mid-level dry notch
4	61 to 80	Trees affected by fairly high levels of dry notch
5	81 to 99	Trees affected by high level dry notch
6	100	Trees affected by total dry notch or dry trees

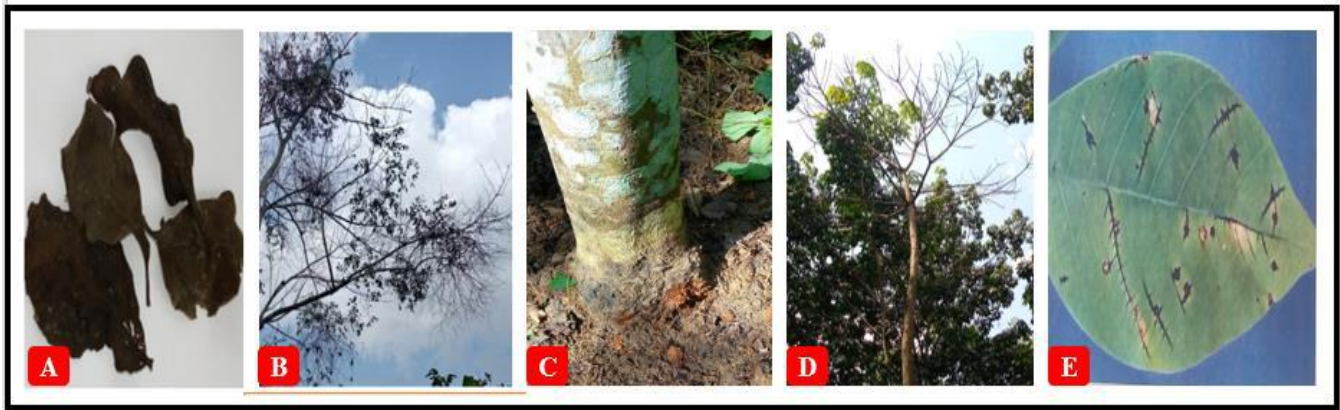
With PSL = Panel sick length

### Inventory of rubber tree pests

The inventory of the main pests of rubber trees such as *Corynespora sp* (responsible for leaf fall fungal disease), *Fomes sp* (responsible for root rot fungal disease) and *Loranthaceae* (parasitic plants) was made on the same trees of the chosen diagonal line. During the observations, stops at intervals of 5 to 10 min were marked to inspect the

trees using different identification keys derived from the Côte d'Ivoire agricultural advisor's guide (Fig. 2 ; FIRCA, 2013). For each tree observed, the presence (score 1) or absence (score 0) of the parasite was recorded. The impact of pests on rubber trees was assessed by calculating the attack rate (Ta) as follows :

$$Ta = \frac{\text{total number of rubber trees parasitized}}{\text{total number of rubber trees observed}} \times 100$$



A = Leaves of Loranthaceae ; B = Tufts of Loranthaceae ; C = Root attack of Fomes sp ; D = Defoliation linked to Fomes sp ; E = Leaf symptom of Corynespora sp.

**Statistical analysis**

All data was subjected to analysis of variance using STATISTICA version 7.1 software. The comparison of the means of the parameters studied was carried out using the parametric factorial ANOVA test at the 5 % threshold when the distribution followed a normal law. When the effect of the factor studied was significant, the post hoc Student-Newman-Keuls mean comparison test was used at the 5 % threshold.

**III. RESULTS AND DISCUSSION**

**3.1. Results**

**3.1.1. Characteristics and lengths of diseased notches in the plots visited**

Table 3 : Characteristics and lengths of diseased notches in the plots visited

PRODUCTION AREA	NUMBER OF PLOTS	AREAS (%)	PSL (%)
Zagné	90	51.90 ± 9.72a	34.33 ± 17.86b
San Pedro	131	22.79 ± 17.30b	33.07 ± 25.37c
Anguedou	60	23.28 ± 7.57b	36.56 ± 17.12a
TOTAL/AVERAGE	281	32.22 ± 19.09	34.65 ± 1.77
Pr	-	0.00	0.00

With PSL = Panel Sick Length ; In each column, the results assigned to the different letters are not significantly different (Newman-Keuls test at 5 %).

**3.1.2. Influence of clonal metabolism on sensitivity to dry notch**

In this study, nine popularized clones were identified, namely PB 217, PB 235, PB 260, IRCA 331, IRCA 230, IRCA 130, IRCA 41, GT1 and RRIC 100. Among these clones, only PB 217 belongs to the class slow metabolism.

The surveys carried out at the end of the 2020-2021 production campaign in Zagné, San-Pédro and Anguédedou made it possible to visit 281 plots. Depending on the different production areas, the number of plots varied depending on the clones present. The surveyed areas also differed significantly (Pr < 0.05) from one zone to another depending on the configuration of the plots visited. The average dry notch rate recorded on all sites was 34.65 ± 1.77 %. The Anguédedou plots were the sickest with an average panel sick length (PSL) of 36.56 ± 17.12 %. They were followed by the Zagné and San-Pédro plots with respective average PSL of 34.33 ± 17.86 % and 33.07 ± 25.37 % (Table 3).

GT1, IRCA 331, IRCA 41 and RRIC 100 belong to the intermediate metabolic class. PB 235, PB 260, IRCA 230 and IRCA 130 also belong to the rapid metabolic class (Table 4).

Overall, analyzes of variance revealed a significant difference (Pr < 0.05) between the panel sick lengths (PSL)

of the three clonal metabolisms. The metabolic class most sensitive to dry notch ( $42.71 \pm 17.47\%$ ) was that of rapid metabolism. It was followed by the class of slow and intermediate metabolisms with respectively average PSL of  $38.27 \pm 20.51\%$  and  $31.45 \pm 21.37\%$  (Table 5).

Depending on the different production areas, the three metabolic classes displayed statistically identical average PSL in Zagné. It is only in San-Pédro and Anguédedou that variable levels of sensitivity were recorded (Table 5).

Table 4 : Diseased notch lengths and metabolic class of the different clones identified

CLONES	METABOLIC CLASS	
	CLASS	AVERAGE PSL (%)
PB 217	Slow	$38.27 \pm 20.51ab$
GT1	Intermediate	$25.97 \pm 17.44bc$
RRIC 100	Intermediate	$53.91 \pm 29.72a$
IRCA 331	Intermediate	$18.37 \pm 23.60c$
IRCA 41	Intermediate	$39.39 \pm 17.80ab$
IRCA 130	Fast	$28.45 \pm 30.32bc$
IRCA 230	Fast	$40.88 \pm 29.90ab$
BP 235	Fast	$55.93 \pm 7.85a$
BP 260	Fast	$32.85 \pm 16.02bc$
AVERAGE	-	$34.65 \pm 1.77$
Pr	-	0.00

With PSL = Panel Sick Length ; BP = Prang Besar ; IRCA = Rubber Research Institute ; GT1 = Gondang Tapen 1 ; RRIC = Rubber Research Institute of Ceylon ; In each column, the results assigned the same letter are not significantly different (Newman-Keuls test at 5 %) ; (-) = not recorded.

Table 5 : Diseased notch lengths depending on the metabolic class of the clones identified in the different production areas

CLASS METABOLIC	DIFFERENT PRODUCTION ZONES			AVERAGE PSL (%)
	ZAGNE	SAN PEDRO	ANGUEDEDOU	
	PSL (%)	PSL (%)	PSL (%)	
Slow	$35.45 \pm 16.88abc$	$45.17 \pm 26.51ab$	$31.79 \pm 9.38bc$	$38.27 \pm 20.51b$
Intermediate	$34.33 \pm 17.63abc$	$26.57 \pm 22.87c$	$45.47 \pm 14.44ab$	$31.45 \pm 21.37c$
Fast	$38.52 \pm 16.05abc$	$51.73 \pm 17.94a$	$41.45 \pm 17.65abc$	$42.71 \pm 17.47a$
AVERAGE	$35.47 \pm 16.99b$	$33.32 \pm 25.30c$	$38.40 \pm 14.71a$	$35.22 \pm 20.96$
Pr	0.00	0.00	0.00	0.00

With PSL = Panel Sick Length ; In each column, the results assigned the same letter are not significantly different (Newman-Keuls test at 5 %).

### 3.1.3. Influence of the main pests of rubber trees on sensitivity to dry notch

#### 3.1.3.1. Influence of *Corynespora sp*

On a total of 281 visited plots, the analyzes of variance revealed a significant difference ( $Pr < 0.05$ ) between the panel sick lengths (PSL) of rubber trees and *Corynespora*

*sp* so that the clones parasitized by this disease had had lower average PSLs ( $15.61 \pm 13.69\%$ ) than non-parasitized clones ( $39.76 \pm 20.22\%$ ) (Table 6).

Furthermore, depending on the different study areas, it is only in San-Pédro that *Corynespora sp* attacks were noted. The effects of this rubber tree pest were particularly

intense on GT1 ( $81.03 \pm 39.54$  %) and PB 235 ( $100 \pm 0.00$  %) (Table 7).

Table 6 : Influence of *Corynespora* sp on sensitivity to dry notch

	Average PSL (%)	Pr
Absence of <i>Corynespora</i>	$39.76 \pm 20.22a$	
Presence of <i>Corynespora</i>	$15.61 \pm 13.69b$	0.00

With PSL = Panel Sick Length ; In each column, the results assigned the same letter are not significantly different (Newman-Keuls test at 5 %).

Table 7 : Influence of *Corynespora* sp on clonal sensitivity to dry notch according to different production zones

CLONES	DIFFERENT PRODUCTION ZONES		
	ZAGNE PSL (%)	SAN PEDRO PSL (%)	ANGUEDEDOU PSL (%)
PB 217	$0 \pm 0.00$	$29.41 \pm 46.25b$	$0 \pm 0.00$
GT1	$0 \pm 0.00$	$81.03 \pm 39.54a$	$0 \pm 0.00$
RRIC 100	$0 \pm 0.00$	$20 \pm 44.72b$	-
IRCA 331	-	$46.15 \pm 51.88b$	-
IRCA 41	$0 \pm 0.00$	$9.09 \pm 30.15b$	$0 \pm 0.00$
IRCA 130	-	$0 \pm 0.00$	-
IRCA 230	-	$0 \pm 0.00$	-
BP 235	$0 \pm 0.00$	$100 \pm 0.00a$	$0 \pm 0.00$
BP 260	$0 \pm 0.00$	-	$0 \pm 0.00$
AVERAGE	0.00	$50.38 \pm 50.19$	0.00
Pr	-	0.00	-

With PSL = Panel Sick Length ; BP = Prang Besar ; IRCA = Rubber Research Institute; GT1 = Gondang Tapen 1 ; RRIC = Rubber Research Institute of Ceylon ; In each column, the results assigned the same letter are not significantly different (Newman-Keuls test at 5 %) ; (-) = Clone not recorded.

### 3.1.3.2. Influence of *Fomes* sp

The table 8 shows the influence of *Fomes* sp on the sensitivity to dry notch of all the plots visited. From a general point of view, the results revealed that rubber trees attacked by *Fomes* sp have a higher rate of diseased notch ( $50.56 \pm 20.30$  %) than that of non-attacked rubber trees ( $30.58 \pm 20$  %).

Depending on the different production zones, San-Pédro and Anguédédou were the zones most sensitive to *Fomes* sp attacks with a higher prevalence among RRIC 100 clones ( $80 \pm 44.72$  %), IRCA 41 ( $72.72 \pm 46.70$  %), IRCA 130 ( $66.67 \pm 57.73$  %) and IRCA 230 ( $66.67 \pm 51.63$  %) (Table 9).

Table 8 : Influence of *Fomes* sp on sensitivity to dry notch

	Average PSL (%)	Pr
Absence of <i>Fomes</i>	$30.58 \pm 20b$	
Presence of <i>Fomes</i>	$50.56 \pm 20.30a$	0.00

With PSL = Panel Sick length ; In each column, the results assigned the same letter are not significantly different (Newman-Keuls test at 5 %).

Table 9 : Influence of *Fomes sp* on clonal sensitivity to dry notch according to different production zones

CLONES	DIFFERENT PRODUCTION ZONES		
	ZAGNE PSL (%)	SAN PEDRO PSL (%)	ANGUEDEDOU PSL (%)
PB 217	3.57 ± 18.89a	38.24 ± 49.32ab	33.33 ± 48.15b
GT1	11.76 ± 33.21a	1.72 ± 13.13b	6.25 ± 25b
RRIC 100	0 ± 0.00a	80 ± 44.72a	-
IRCA 331	-	15.38 ± 37.55ab	-
IRCA 41	5 ± 22.36a	72.72 ± 46.70ab	80 ± 44.72a
IRCA 130	-	66.67 ± 57.73ab	-
IRCA 230	-	66.67 ± 51.63ab	-
BP 235	0 ± 0.00a	0 ± 0.00b	20 ± 44.72b
BP 260	0 ± 0.00a	-	10 ± 31.62b
AVERAGE	4.44 ± 20.72b	25.95 ± 44.01a	25 ± 43.67a
Pr	0.65	0.00	0.00

With PSL = Panel Sick Length ; BP = Prang Besar; IRCA = Rubber Research Institute ; GT1 = Gondang Tapen 1 ; RRIC = Rubber Research Institute of Ceylon ; In each column, the results assigned the same letter are not significantly different (Newman-Keuls test at 5 %) ; (-) = Clone not recorded.

### 3.1.3.3. Influence of *Loranthaceae*

Analyzes of variance revealed a significant difference ( $Pr < 0.05$ ) between panel sick lengths (PSL) of rubber trees and *Loranthaceae*. Indeed, plots attacked by *Loranthaceae* displayed greater diseased notch lengths ( $38.41 \pm 20.55$  %)

than those of non-attacked plots ( $30.16 \pm 21.62$  %) (Table 10).

Generally speaking, the localities in this study were all sensitive to attacks by *Loranthaceae* with a prevalence in almost all of the clones present (Table 11).

Table 10 : Influence of *Loranthaceae* on susceptibility to dry notch

	Average PSL (%)	Pr
Absence of <i>Loranthaceae</i>	30.16 ± 21.62b	
Presence of <i>Loranthaceae</i>	38.41 ± 20.55a	0.00

With PSL = Panel Sick Length ; In each column, the results assigned the same letter are not significantly different (Newman-Keuls test at 5 %).

## 3.2. DISCUSSION

### 3.2.1. Features and lengths of diseased notches in the plots visited

Data collections carried out in agro-industrial plantations in the Zagné, San-Pédro and Anguédedou zones revealed an average diseased notch length (PSL) of  $34.65 \pm 1.77$  %. This result reflects the scale and complexity of managing dry notch of rubber trees on farms. For good reason, by extrapolation to the national average rate of 9 % noted by Okoma *et al.* in 2009, it can be said that the rate of dry notch has tripled in a decade although the rubber agro-industrialists know the requirements and the best options

for exploiting the rubber tree. Dryness of the notch therefore has not only causes, but also symptoms which can be very different (Jacob *et al.*, 1990) although leading to the same effects : dysfunction of the laticiferous system and reduction, otherwise the disappearance of latex production from the rubber tree. Among the direct or indirect causes of the disease, we must of course cite overexploitation due to the intensity of tapping or excessive stimulation (Van de Sype, 1984), but also to the season, drought, quality of certain soils (Commère *et al.*, 1989). Furthermore, the non-random dispersion of diseased trees has also directed studies towards the search for various pathogens, although the absence of current

results does not allow this hypothesis to be ruled out (Nandris *et al.*, 1991). Sensitivity to dry notch is also a clonal characteristic (Van de Sype, 1984, ; Sethuraj, 1990) which can be extremely marked ; thus clones PB 235 or PB 260 are very sensitive to this disease, while clones PB 217 or PR 107 are much less so. Symptomatic and evolutionary differences also made it possible to

distinguish several forms of dry notch. Some disappear after a fairly long suspension of tapping; they are therefore reversible (Van de Sype, 1984). Others, despite a long rest and sometimes a slight resumption of production, lead inexorably to total drought of the tree (De Faye *et al.*, 1989) ; they are therefore much more serious.

Table 11 : Influence of Loranthaceae on clonal sensitivity to dry notch according to different production zones

CLONES	DIFFERENT PRODUCTION ZONES		
	ZAGNE PSL (%)	SAN PEDRO PSL (%)	ANGUEDEDOU PSL (%)
PB 217	85.71 ± 35.63a	52.94 ± 50.66a	95.83 ± 20.41a
GT1	23.53 ± 43.72b	32.75 ± 47.34b	93.75 ± 25a
RRIC 100	12.50 ± 35.35b	0 ± 0.00b	-
IRCA 331	-	7.69 ± 27.73b	-
IRCA 41	45 ± 51.04b	18.18 ± 40.45b	100 ± 0.00a
IRCA 130	-	33.33 ± 57.73b	-
IRCA 230	-	50 ± 54.77a	-
BP 235	100 ± 0.00a	0 ± 0.00b	80 ± 44.72a
BP 260	7.17 ± 26.72b	-	100 ± 0.00a
AVERAGE	46.67 ± 50.16b	33.58 ± 47.41b	95 ± 21.97a
Pr	0.00	0.03	0.53

With PSL = Panel Sick Length ; BP = Prang Besar ; IRCA = Rubber Research Institute ; GT1 = Gondang Tapen 1 ; RRIC = Rubber Research Institute of Ceylon ; In each column, the results assigned the same letter are not significantly different (Newman-Keuls test at 5 %) ; (-) = Clone not recorded.

### 3.2.2. Influence of clonal metabolism on sensitivity to dry notch

In the industrial plantations visited, nine types of rubber clones were identified. These clones were all affected by rubber tree dry notch but to different degrees depending on their metabolic classes. The fast metabolic class was most susceptible to dry notch with a panel sick length (PSL) of  $42.71 \pm 17.47$  %. It was followed by the slow and intermediate metabolic classes with PSL of respectively  $38.27 \pm 20.51$  % and  $31.45 \pm 21.37$  %. These differences could be explained by the fact that clonal sensitivity to dry notch is linked to the metabolic activity of the clones. This hypothesis is further supported by the fact that the study by Chrestin (1985) showed that the dry notch rate increases with the frequency of stimulation. The latter being described as a process of activation of metabolism (Coupé & Chrestin, 1989). We therefore observe that the clones not very sensitive to dry notch have an inactive (or slow) metabolism, the moderately sensitive clones have an intermediate metabolism and the clones very sensitive to

this syndrome have a very active (or rapid) metabolism.(Okoma *et al.*, 2009). However, in this study, the slow metabolic class was more sensitive ( $38.27 \pm 20.51$  %) at the dry notch than the intermediate metabolic class ( $31.45 \pm 21.37$  %). This contrast could be explained by the fact that the low PSL ( $26.57 \pm 22.87$  %) clones GT1 and IRCA 331 noted in San-Pédro contributed to reducing the general average of the intermediate metabolic class for all the areas visited.

### 3.2.3. Influence of the main pests of rubber trees on sensitivity to dry notch

#### 3.2.3.1. Influence of *Corynespora* sp

The study of the influence of the pest *Corynespora* sp on sensitivity to dry notch revealed that clones parasitized by this fungal disease had lower diseased notch lengths (PSL) ( $15.61 \pm 13.69$  %) than non-parasitized clones ( $39.76 \pm 20.22$  %). It would therefore seem that the rubber trees parasitized by *Corynespora* sp, in this study, were at the start of infestation at the time of the dry notch survey,



which is why they produced more latex to defend themselves against the stimulus. Indeed, when we bleed the tree, we incise specialized cells (“laticiferous” cells) and these then release their contents, the latex. It is now believed that these cells constitute a defense system of the plant, the coagulation of the latex released during an incision, or wound, making it possible to quickly seal them and therefore facilitate healing (Hornus & Gohet, 2009). Furthermore, previous studies have shown that the kinetics of hydrogen peroxide production by the attacked rubber tree is very often used to distinguish hypersensitive type reactions from incompatible reactions (Dixon *et al.*, 1994). Generally, the first peak of H<sub>2</sub>O<sub>2</sub>, which is produced at the first contact between the elicitor and the receptor on the host cell, is common to compatible and incompatible reactions while the appearance of a second peak later would be characteristic of the hypersensitive reaction. These kinetics were studied during the interaction of the resistant clone GT1 with *Corynespora cassiicola* and revealed a single H<sub>2</sub>O<sub>2</sub> peak, which would reflect the absence of a hypersensitive reaction in the resistant clone to infection (Breton 1997). However, in our study, the GT1 clones grown in San-Pédro were particularly sensitive (81.03 ± 39.54 %) to the dry notch of the rubber tree following *Corynespora sp* attacks revealing, this time, their hypersensitivity to the disease.

### 3.2.3.2. Influence of *Fomes sp*

The demonstration of the effect of *Fomes sp* on the sensitivity to dry notch of the rubber tree showed that the rubber trees attacked by this fungal root disease had a higher rate of diseased notch (50.56 ± 20.30 %) to that of unattacked rubber trees (30.58 ± 20 %). This lignivorous soil fungus, by preferentially attacking the main pivot of the rubber tree, diverts its reserves for the benefit of its food (Obouayéba, 2005). It could therefore be that the rubber trees parasitized by the wood-eating fungus were at an advanced stage of the disease. The general yellowing of the leaves and the repeated defoliations (Okoma, 2008) which resulted forced these rubber trees to concentrate all their energy and their sugars (sucrose) on refoliation and defense against the stress suffered to the detriment of the production of the latex. All things which acted on the production performance of the rubber trees by causing dry notches (partial or total stoppage of the flow of the latex) to the extent that the sugar, raw material for the regeneration of the latex, was derived entirely from the defense. This hypothesis is all the more supported by the fact that the study by Hornus & Gohet (2009) showed that the parasitized tree uses its energy and its sugars for the needs of its defense. However, it is depending on the level of sugar available in the latex that we can have a fairly precise idea of the possibility of increasing yield.

### 3.2.3.3. Influence of *Loranthaceae*

In the industrial plantations visited, the plots attacked by *Loranthaceae* displayed longer panel sick lengths (PSL) than those of the non-attacked plots. This negative influence of this parasite on the production of the tree through the length of diseased notch of rubber trees could be explained by the fact that *Loranthaceae* are parasitic plants which, once fixed on the tree, take water and nutrients ; which weakens host trees and makes them more vulnerable to other types of attacks and diseases (Koffi *et al.*, 2014). As a result, the tree weakened by an attack by *Loranthaceae*, sees its production reduced until it stops completely in certain cases (Koffi *et al.*, 2014). The dry notch disease of rubber trees being the partial or total cessation of the flow of latex after tapping (Okoma *et al.*, 2011), it therefore seems normal that the rate of the disease increases simultaneously with the attack on *Loranthaceae* to the extent that the physiological stress resulting from parasitism significantly reduces the production capacities of the tree (Dibong *et al.*, 2010 ; Ahamedé *et al.*, 2017) at a more advanced stage of the attack. In fact, parasites divert the raw sap from rubber trees. Plant growth is then slowed and eventually fades. The ability of trees to produce leaves, flowers, fruits and latex is also reduced due to the diversion of nutrients and water (Koffi *et al.*, 2014).

## IV. CONCLUSION

At the end of this study, it appears that the dry notch disease of rubber trees continues to be prevalent in agro-industrial plantations in the areas of Zagné, San-Pédro and Anguédédou with a panel sick length (PSL) average of 34.65 ± 1.77 % and a high prevalence (42.71 ± 17.47 %) in clones with a fast metabolic class. Furthermore, the sensitivity of the disease is exacerbated by attacks from the main pests of the rubber tree.

Indeed, from one cultivation zone to another, the influence of pests on the sensitivity to dry notch of rubber trees differed significantly (Pr < 0.05). Rubber trees attacked by *Fomes sp*, which were at an advanced stage of the disease, displayed a higher rate of diseased notch (50.56 ± 20.30 %) than that of non-attacked rubber trees (30.58 ± 20 %). In addition, *Loranthaceae*, which were also the most widespread pests in rubber plantations unlike the other two, induced greater PSL (38.41 ± 20.55%) in rubber trees than in rubber trees they were parasitized (30.16% ± 21.62%). Only rubber trees attacked by *Corynespora sp* presented lower PSL (15.61 ± 13.69 %) than those of non-attacked rubber trees (39.76 ± 20.22 %) ; a sign that the attacked trees were at the beginning of an infestation and

that they generated a peak in rubber production to defend against the pest.

Faced with the persistence of the effects of dry notch, rubber growers are advised to plant clones with an intermediate metabolic class, in particular IRCA 331, which proved to be the least susceptible to the disease in this study.

Therefore, it would be more judicious to set up experiments to monitor the impact of biological factors on the evolution of rubber tree dry notch disease.

### ACKNOWLEDGMENTS

The authors thank :

- FIRCA / FCIAD which financed this work on behalf of the project "Improvement of tapping quality in rubber cultivation through the use of an innovative tapping knife" contract No. 1968 FIRCA/UJLoG/FADCI-FCIAD/2019-AV01 ;
- The agro-industrial companies EXAT-Agriculture (San-Pédro), SCASO (San-Pédro), TRCI (Anguédédou) and CHC (Zagné) for their good collaboration in the execution of surveys and data collection on their respective sites.

### REFERENCES

- [1] Ahamidé I. D. Y., Tossou M. G., Dassou H. G., Yedomonhan H., Houenon J. G., Akoegninou A. (2017). Usages des plantes parasites de la famille des Loranthaceae et variation du niveau de leur connaissance au Nord-Bénin : Implications pour la gestion durable des hémiparasites. *Afrique Science*, 13(5), 222-235.
- [2] APROMAC. (2021). Atelier sur les problèmes de la filière hévéa en Côte d'Ivoire. [www.apromac.ci](http://www.apromac.ci). Consulté le 21 Juillet 2021.
- [3] Breton F. (1997). Réactions de défense dans l'interaction *Hevea brasiliensis*/Corynespora cassiicola et implication d'une toxine dans le déterminisme de la réponse clonale. Université Montpellier 2, Montpellier. 128 p.
- [4] Brou Y.T. (2005). Climat, mutations socio-économiques et paysages en Côte d'Ivoire. Mémoire de synthèse des activités scientifiques présenté en vue de l'obtention de l'Habilitation à Diriger des Recherches. Universités des Sciences et Technologies de Lille, 213 p.
- [5] CIRAD. (1993). Recueil de fiches de clones HEVEA. Abidjan, Côte d'Ivoire : CIRAD-CP. 170 p.
- [6] D'Auzac J. (1996). L'oxygène "toxique" : une défense contre les pathogènes. Parcelles, Recherche, Développement 3 : 153-170 p.
- [7] De Faye (1981). Histologie comparée des écorces saines et pathologiques (maladie des encoches sèches) de l'*Hevea brasiliensis*. Thèse de Doctorat de 3ème Cycle, USTL, Montpellier II, 75 p.
- [8] Déon M. (2012). Importance de la cassiicoline en tant qu'effecteur de la Corynespora Leaf fall (CLF) chez l'hévéa. Développement d'outil pour le contrôle de la maladie. Thèse de Doctorat. Université Blaise pascal (France), Ecole doctorale Sciences de la vie, Santé, Agronomie, environnement. 179 p.
- [9] Dian K., (1997). Tapping Panel Dryness Research: List of questions. Institute of Rubber Research Development Board, (IRRDB). 1. Annual meeting, Ho Chi Minh City, Vietnam, 11-13 October 1997, 12 p.
- [10] Dibong S. D., Biyon B. N., Obiang N. E., Din N., Priso R. J., Taffouo V. D., Akoa A. (2010). Faut-il éradiquer les Loranthaceae sur les ligneux à fruits commercialisés de la région littorale du Cameroun ? *International Journal of Biological and Chemical Sciences*, 4 (3). 1991-8631.
- [11] Dixon R.A, Harrison M.J., Lamb C.J. (1994). Early events in the activation of plant defense responses. *Annual Review of Phytopathology* 32 : 479-501 p.
- [12] FIRCA (2013). Production de matériel végétal d'hévéa. FIRCA/APROMAC-Guide du conseiller agricole hévéa Tome 2, document interne, 56 p.
- [13] Gohet E., Lacrotte R., Obouayéba S., Commere J. (1991). Tapping systems recommended in West Africa West Africa. Proc. Rubb. Growers' Conf. Rubb. Res. Inst. Malaysia ; ed., Kuala Lumpur, Malaysia, 235-254 p.
- [14] Gohet E., Prévot J. C., Eschbach J. M., Clément A., Jacob J. L. (1996). Clone, croissance et stimulation, facteurs de la production de latex. Parcelle Recherche Développement, 3 (1) : 30-38 p.
- [15] Gohet E., Chatuma P., Lacote R., Obouayéba S., Dian K. (2003). Latex clonal typology of *Hevea brasiliensis* modelling of yield potential and clonal response to ethephon stimulation. In : Proceedings of the International Workshop on Exploitation technology, India, 199-217 p.
- [16] Jayasinghe C.K. (2000). Corynespora Leaf Fall: the most challenging rubber disease in Asian and African continents. Bulletin of the Rubber Research Institute of Sri Lanka 42 : 56-64 p.
- [17] Koffi A. A., Kouassi F. A., N'Goran S. B. K., Soro D. (2014). Les Loranthaceae, parasites des arbres et arbustes : cas du département de Katiola, au nord de la Côte d'Ivoire. *International Journal of Biological and Chemical Sciences*, 8(6), 2552-2559.
- [18] Neobot. (2020). Géolocalisation de Zagné. La carte topographique de Côte d'Ivoire, 4 p.
- [19] Newsam A. (1960). Plant Pathology Division Report. Rubber Research Institute of Malaysia, 63-70 p.
- [20] Okhuoya J.A. (1986). Seasonal and diurnal changes of two leaf pathogens of Rubber (*Hevea brasiliensis* Muell. Arg.) in the air of Iyanomo, Nigeria. *Acta Mycologica* 12 : 65-67 p.
- [21] Okoma K.M. (2008). Étude de la sensibilité au syndrome de l'encoche sèche chez *Hevea brasiliensis* Muell. Arg. (Euphorbiaceae). Thèse de Doctorat, UFR Biosciences, Université Félix Houphouët Boigny, (Abidjan, Côte d'Ivoire), 160p.
- [22] Okoma K.M, Dian K., Allou D., Sangaré A. (2009). Etude de la sensibilité des clones d'*Hevea brasiliensis* (Muell.

- Arg.) à l'encoche sèche. *Sciences & Nature* 6 (1) : 17-26.  
Rubber production. *Crop Protection* 20 : 581-590 p.
- [23] Okoma K.M., Dian K., Obouayéba S., Elabo A., Gnage M., Koffi E., Soumahin F., Doumbia S., Kéli J. (2011). Bien diagnostiquer l'encoche sèche chez l'hévéa en Côte d'Ivoire. Fiche technique N°2. 2 p.
- [24] Radzia N.Z., Sulong S.H., Hidir S. (1996). The epidemiology of *Corynespora* leaf fall disease of rubber in Malaysia - conidia dispersal pattern. Workshop on *Corynespora* Leaf Fall Disease of Hevea Rubber organised by the Indonesian Rubber Research Institute (Medan, Indonésie) : 26-27 p.
- [25] Ramakrishnan T.S & Pillay P.N.R. (1961). Leaf spot of rubber caused by *Corynespora cassiicola* (Berk & Curt) Wei. *Rubber Board Bulletin*, 5 : 32-35 p.
- [26] Thaler P. (2013). « Natural Rubber » : insustainable solutions for modern Economies, sous la direction de Rainer Hôfer, London (UK) RSC, 335-363 p.
- [27] Van De Sype H. (1984). The dry eut syndroms of *Hevea brasiliensis*, evolution, agronomical and physiological aspects. C. R. Coll. *Physiol. Amél. Hévéa.*, Ed., IRCA-CIRAD, Montpellier, France : 249-271 p.



# Pseudouridine in RNA: Enzymatic Synthesis Mechanisms and Functional Roles in Molecular Biology

Adil Khan<sup>1</sup>, Yu Dong Hu<sup>1</sup>, Salman Khan<sup>1</sup>, Sahibzada Muhammad Aqeel<sup>2</sup>, Imad Khan<sup>3</sup>, Mudassar Hussain<sup>3</sup>, Waleed AL-Ansi<sup>3</sup>, Guochao Xu<sup>1,4,\*</sup>

<sup>1</sup>Key Laboratory of Industrial Biotechnology, Ministry of Education, School of Biotechnology, Jiangnan University, Wuxi 214122, Jiangsu, China

<sup>2</sup>National Engineering Research Center for Cereal Fermentation and Food Biomanufacturing, Jiangnan University, Wuxi 214122, China

<sup>3</sup>State Key Laboratory of Food Science and Resources, National Engineering Research Center for Functional Food, National Engineering Research Center of Cereal Fermentation and Food Biomanufacturing, Collaborative Innovation Center of Food Safety and Quality Control in Jiangsu Province, School of Food Science and Technology, Jiangnan University, 1800 Lihu Road, Wuxi 214122, Jiangsu, China

<sup>4</sup>State Key Laboratory of Biocatalysis and Enzyme Engineering, School of Life Sciences, Hubei University, China, 430062

\* Corresponding author: Guochao Xu, email: guochaoxu@jiangnan.edu.cn, tel:13661841332

Received: 11 Nov 2023; Received in revised form: 12 Dec 2023; Accepted: 19 Dec 2023; Available online: 31 Dec 2023

©2023 The Author(s). Published by Infogain Publication. This is an open access article under the CC BY license

(<https://creativecommons.org/licenses/by/4.0/>).

**Abstract**—Pseudouridine, a common modified nucleotide, is prevalent in bacterial tRNA, rRNA, and snRNA. Initially identified in rRNA and tRNA, its presence extends to snRNA. Despite being the first identified and most prevalent RNA modification, its biosynthesis and diverse roles remain insufficiently understood. This extensively occurring modified nucleotide influences structural and functional attributes in various RNA categories. The isomerization process involves a carbon-carbon bond formation, and Puf family proteins (PUFs) are potential Ψ reader proteins. Pseudouridine, a ubiquitous constituent in structural RNAs, is notably absent in mRNA or viral RNAs. Its enzymatic isomerization occurs at the polynucleotide level, independently of cofactors. Compared to uridine, pseudouridine prefers the C3'-endo conformation, enhancing stability in specific structural motifs. Evolutionarily conserved in major spliceosomal snRNAs, it plays a crucial role in spliceosome assembly and splicing. Pseudouridine (ψ), comprising 0.2–0.6% of uridines in mammalian mRNA, is enzymatically generated by pseudouridine synthases. Five pseudouridine synthase families orchestrate its site-specific isomerization. In eukaryotic and archaeal organisms, specific synthases rely on noncoding RNAs, like box H/ACA small nucleolar/scaRNPs. These modifications contribute to RNA structural stabilization and functional efficacy. In pre-mRNA and mRNA they guide splicing processes and protect against degradation, acting as a defense mechanism against viral infections. This review delves into the detection, structure, functions, and applications of pseudouridine in RNA. Methodologies like High-performance liquid chromatography, mass spectrometry, thin layer chromatography, enzyme-linked Immunosorbent assay, capillary electrophoresis, northern blotting, reverse transcriptase polymerase chain reaction and RNA bisulfite sequencing, establish a robust framework. Pseudouridine's roles in reinforcing RNA structures, modulating translation, and its potential in mRNA.



**Keywords**— Enzyme, Pseudouridine, RNA modification, , Synthesis, Uridine.

## I. INTRODUCTION

Pseudouridine (ψ), constituting 0.2–0.6% of mammalian mRNA uridines, is enzymatically derived through pseudouridine synthases. Initially identified in rRNA and tRNA, it extends to snRNA (Riley, Sanford,

Woodard, Clerc, & Sumita, 2021). With over a hundred post-transcriptional RNA modifications shaping our understanding of biological processes, pseudouridine stands out as a prevalent and fundamental modification in living cells. Despite being the first RNA modification discovered

and the most abundant, the mechanisms governing its biosynthesis and multifaceted roles remain insufficiently elucidated since its recognition as the "fifth nucleoside" in RNA (Yu & Meier, 2014).

Pseudouridine, a widespread modified nucleotide, is abundant in various RNA types, including tRNA, rRNA, snRNA, and snoRNAs, significantly influencing their structural and functional characteristics. The isomeric transition of the glycosidic bond, shifting from N1 to C5 of uracil, enhances base rotation, potentially improving the thermodynamic stability of RNA duplexes through additional hydrogen bonding and stacking interactions (Riley et al., 2021). Pseudouridine's isomerization involves tethering uracil via a carbon-carbon bond, which is different from the conventional nitrogen-carbon glycosidic bond. While  $\Psi$  reader proteins remain unidentified, Pumilio family proteins (PUFs) are promising candidates (Corollo et al., 1999). This modification introduces an extra imino group, serving as an additional hydrogen bond donor, and enhances the stability of the carbon-carbon glycosidic bond compared to the prevalent nitrogen-carbon bond (Becker, Motorin, Sissler, Florentz, & Grosjean, 1997).

Pseudouridine is a widespread and mysterious element in structural RNAs, commonly found in tRNA, rRNA, and snoRNA, yet absent in mRNA or viral RNAs (Anderson et al., 2010). Its enzymatic isomerization from uridine occurs at the polynucleotide level, independently of cofactors or external energy sources. In *Escherichia coli*, the small subunit rRNA has one pseudouridine, while the large subunit rRNA boasts nine instances of this modification (Charette & Gray, 2000).

Compared to uridine, pseudouridine favors the C30-endo conformation of the ribose, aligning with the anti-conformational preferences of nucleobases (Yamauchi et al., 2016). It is prevalent in the T pseudouridine C loop of nearly all tRNAs and is often found in the D stem and/or the anticodon stem and loop (Mengel-Jørgensen & Kirpekar, 2002). Pseudouridine's inclusion significantly stabilizes specific structural motifs. Notably, it is evolutionarily conserved in major spliceosomal snRNAs (U6, U5, U4, U2, and U1), occupying crucial regions for RNA-RNA and RNA-protein interactions vital for spliceosome assembly and the splicing process. As a rotational isomer of uridine, pseudouridine stands out as the most abundant modified nucleotide, ubiquitously present in almost all tRNA, rRNA, and snRNA in bacteria. Its site-specific isomerization in tRNA and rRNA is orchestrated by five families of pseudouridine synthases (Kellner, Burhenne, & Helm, 2010).

In eukaryotes and archaea, a distinct group of pseudouridine synthases relies on noncoding RNAs for site-

specific isomerization of rRNA and snRNA (Morais, Adachi, & Yu, 2021). This unique mechanism involves box H/ACA sno/scaRNPs, consisting of four proteins and a box H/ACA RNA (Liang et al., 2009). The biological landscape features numerous post-transcriptional RNA modifications, with potential roles in stabilizing RNA strands and enhancing functional efficacy. Modifications in pre-mRNA and mRNA can guide splicing and protect RNAs from degradation by nucleases, acting as a defense against viral infections (Riley et al., 2021).

In the realm of natural modifications, methylation is prevalent, but pseudouridine ( $\Psi$ ) claims the distinction of being the most common and earliest identified modification (Becker et al., 1997).  $\Psi$ , an isomer of uridine with a C1'-C5 glycosidic bond, undergoes a substantial structural transformation during its isomerization (Penzo, Guerrieri, Zacchini, Treré, & Montanaro, 2017). This process involves cleaving the N1-C1' glycosidic bond and a 180° rotation of the base, and it is hypothesized to be facilitated by nucleophilic attack by arginine residues within pseudouridine synthases. The fundamental concept of this mechanism relies on enzymes stabilizing ribose sugars and uracil bases, allowing for the cleavage of the C-N glycosidic bond, leading to a 180° base flip, and the formation of a C-C glycosidic bond, resulting in  $\Psi$  as the final product (Riley et al., 2021).

## II. SIGNIFICANCE OF $\Psi$ IN RNA

Pseudouridylation, impacting over 100 specific uridines in rRNAs, is crucial for maintaining the proper functioning, folding, and conformational stability of rRNAs (Corollo et al., 1999). These modifications also affect interactions between rRNAs and ribosomal proteins, ensuring the catalytic activity of the ribosome. Changes in rRNA pseudouridylation directly influence interactions with tRNAs and mRNAs, modifying translational efficiency, gene expression patterns, and levels (Wang et al., 2023).

Despite being widespread in ribosomes,  $\Psi$ 's precise function remains elusive. In eukaryotes, especially in the critical core region of LSU and SSU RNAs,  $\Psi$  likely plays a role in optimal ribosome performance (Cortese, Kammen, Spengler, & Ames, 1974). Experimental verification of its direct contribution has proven challenging. Nature, synthesizing  $\Psi$  without energy expenditure, may have adapted it for diverse purposes (Kazimierczyk & Wrzesinski, 2021). Found exclusively in RNA molecules with functional tertiary structures,  $\Psi$ 's primary function could be molecular glue, fortifying and enhancing RNA conformations (Singh, Shyamal, & Panda, 2022). This proposition aligns with varying  $\Psi$  numbers

across species, the lack of correspondence in  $\Psi$  sites among organisms, and challenges in detecting effects upon individual  $\Psi$  removal. Measuring functional effects may prove more effective when considering multiple  $\Psi$  deletions (Pfeiffer, Ribar, & Nidetzky, 2023).

During translation, pseudouridine (W) is believed to modulate interactions between tRNA molecules and rRNAs, as well as with mRNAs. Pseudouridylation of tRNA does not disrupt overall three-dimensional tRNA structure, isn't essential for cell viability, and isn't universally required for amino acylation. However, pseudouridine does influence the local structure of the domains in which it is present (Vaidyanathan, AlSadhan, Merriman, Al-Hashimi, & Herschlag, 2017). W residues, occasionally located in the anticodon region, contribute to alternative codon usage. Additionally, there's consideration of a catalytic role for pseudouridine in rRNA during the peptidyl transfer process in translation.

Pseudouridine enhances the stability of RNA molecules, which is crucial for optimal functionality in processes like translation and splicing by influencing their secondary conformation. Pseudouridine actively shapes intricate folding patterns of RNA molecules, contributing to the delineation of distinct RNA structures essential for biological efficacy (Barbieri & Kouzarides, 2020). Non-random distribution of pseudouridine within RNA sequences, particularly in functionally significant regions, suggests its potential involvement in orchestrating diverse cellular processes. Ubiquitously present in various RNA species across diverse organisms, Pseudouridine's functional role offers insights into the complex landscape of RNA modifications and their multifaceted impact on cellular functionalities (Corollo et al., 1999).

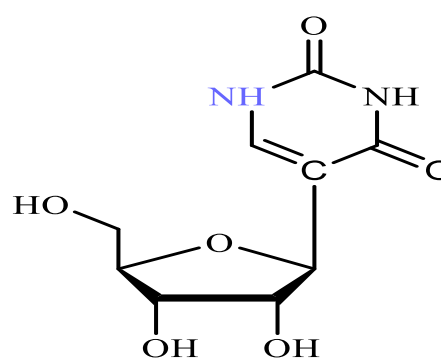
In vitro-transcribed mRNAs face challenges due to instability and immunogenicity. Integrating pseudouridines enhances mRNA stability and translational efficacy in mammalian cells and mice, reducing immunogenicity (Rintala-Dempsey & Kothe, 2017). Pseudouridine's strategic placement in loop-closing regions suggests roles in stabilization and conformational modulation. Its structural disparities amplify base stacking, introducing rigidity and bolstering stability in pseudouridylated duplexes (Cortese et al., 1974). This modification holds promise for modulating splicing, immunogenicity, and translation in vivo, responding to cellular stress and extending RNA half-life. Understanding pseudouridine's contributions to cellular processes is advanced by targeted disruptions of modification enzymes. This research sheds light on the potential therapeutic applications of pseudouridine-modified mRNA (Huang et al., 2021).

### III. PSEUDOURIDINE IN RNA

#### 3.1. Chemical structure of pseudouridine

Early hypotheses about pseudouridine in RNA focused on its unique physicochemical properties, setting it apart from its precursor, uridine (Nombela, Miguel-López, & Blanco, 2021). Pseudouridine's distinctiveness lies in its possession of a C-C glycosyl bond, deviating from the typical N-C bond connecting the base and sugar moieties (Huang et al., 2021). Anticipation stemmed from the idea that the C-C glycosyl bond, offering increased rotational freedom compared to the N-C glycosyl bond, might provide pseudouridine with greater conformational flexibility than uridine. Additionally, the free N1-H in pseudouridine, serving as an additional hydrogen bond donor, hinted at potential novel pairing interactions in RNA (Karikó et al., 2008). Speculation also revolved around the high group transfer potential for acyl moieties by the N1-H of pseudouridine (Lovejoy, Riordan, & Brown, 2014).

Conformational studies of free pseudouridine nucleosides revealed a subtle preference for the syn glycosyl conformation, differing from the anti-configuration adopted by uridine and other nucleosides. This led to the proposition that pseudouridine might serve as a conformational switch in RNA, given its low energy requirement for the syn/anti-transition and comparable hydrogen-bonding potential (Zhao & He, 2015). However, within polynucleotide chains, pseudouridine consistently adopts the anti-configuration. In these instances, it imparts rigidity rather than flexibility to both single- and double-stranded regions despite sharing the same basic topology in RNA as uridine. Insights from nuclear magnetic resonance, X-ray crystallography, and molecular dynamics simulations support this deduction, providing valuable perspectives on pseudouridine's nuanced impact on RNA structure (Penzo et al., 2017).



Pseudouridine( $\psi$ )

Fig.1. The structure of Pseudouridine

### 3.2. Unique features of Pseudouridine

Pseudouridine's unique characteristics, when compared to uridine, arise mainly from its additional hydrogen bonding capabilities. In the anti-conformation within RNA, pseudouridine provides a favorable geometry and distance for coordinating a water molecule between its N1-H and the 5' phosphates of both pseudouridine and the preceding residue (Cerneckis, Cui, He, Yi, & Shi, 2022). This constraint on base conformation and backbone mobility persists at the 5' site of pseudouridylation, regardless of the surrounding sequence or structural context, whether in a single- or double-strand configuration (Levi & Arava, 2021).

Pseudouridylation enhances local RNA stacking in single-stranded and duplex regions, favoring a 3'-endo ribose conformation and axial anti-base moiety alignment (Morais et al., 2021). This process involves a structured water molecule replacing a weak C5-H bond, stabilizing the pseudouridine moiety. The result is increased rigidity in the phosphodiester backbone, leading to cooperative enhancement of adjacent nucleoside stacking and reinforcing RNA structure. Pseudouridine's major contribution lies in amplifying base stacking (Koonin, 1996).

### 3.3. Distribution of Pseudouridine in different classes of RNA

#### 3.3.1. Transfer RNAs

$\Psi$ , prevalent in almost all tRNAs, notably as the near-universal  $\Psi55$ , extends across life domains and organelles like mitochondria and chloroplasts. Found in locations such as the D stem and anticodon regions,  $\Psi$ 's distribution follows domain-specific patterns. It crucially stabilizes structural motifs like the T $\Psi$ C loop ( $\Psi55$ ), D stem ( $\Psi13$ ), anticodon stem (with a strong closing base pair between  $\Psi39$  and A31), and anticodon loop (featuring noncanonical base-pairing between  $\Psi38$  and residue 32) (Morena, Argentati, Bazzucchi, Emiliani, & Martino, 2018).

#### 3.3.2. Small Nuclear and Nucleolar RNAs

Pseudouridine ( $\Psi$ ) is a widespread modification found in most transfer RNAs, prominently located at  $\Psi55$  in the T $\Psi$ C stem loop. Its presence is observed across all life domains, including archaea, bacteria, and eukaryotes, as well as in cellular organelles like mitochondria and chloroplasts (Tavakoli et al., 2023).  $\Psi$  is distributed in the D stem, anticodon stem, and loop, displaying domain-specific patterns. The intentional use of pseudouridine plays a crucial role in stabilizing key structural motifs within tRNA, such as the T $\Psi$ C loop at  $\Psi55$ , D stem at  $\Psi13$  and anticodon stem. Notably,  $\Psi$  contributes to the stability of

the anticodon loop, forming noncanonical base pairs with residues like  $\Psi38$  and 32. This strategic placement enhances the overall stability and functionality of essential tRNA structural elements (Zimna, Dolata, Szweykowska-Kulinska, & Jarmolowski, 2023).

In eukaryotes, pseudouridine ( $\Psi$ ) is notably present in major spliceosomal small nuclear RNAs (snRNAs) like U1, U2, U4, U5, and U6, as well as in minor variants associated with AU/AC intron splicing (U12, U4atac, and U6atac) (Westhof, 2019). While  $\Psi$  residues show phylogenetic conservation, subtle organism-specific variations add complexity. These modifications strategically occur in functionally critical regions, participating in vital RNA-RNA or RNA-protein interactions crucial for spliceosome assembly and operation (Riley et al., 2021). For example, a  $\Psi$ -A pair near the intron's branch site enhances stability in the U2 snRNA/pre-mRNA interaction, aiding the initial splicing reaction.  $\Psi$  residues are recurrent in U4/U6 snRNA interaction regions and between U1 snRNA and the 5' splice site. Beyond spliceosomal snRNAs,  $\Psi$  is found in small nucleolar RNAs (snoRNAs) like U3, U8, snR4, and snR8, presenting intriguing areas for further exploration of  $\Psi$  formation and functional implications (Morais et al., 2021).

#### 3.3.3. Ribosomal RNAs

Pseudouridine ( $\Psi$ ) is a prevalent component in the ribosomal RNAs (rRNAs) of both small (SSU) and large (LSU) subunits across eubacteria, archaeobacteria, and eukaryotes, including mitochondria and chloroplasts (Foster, Huang, Santi, & Stroud, 2000). It is also present in 5.8S and select 5S rRNAs. Through nucleotide-resolution mapping techniques,  $\Psi$  has been identified in LSU rRNA, notably in *Escherichia coli* and *Saccharomyces cerevisiae* (Koonin, 1996). The clustering of  $\Psi$  residues within crucial domains of LSU rRNA, such as Domain II (near the 5'-end), Domain IV (central), and Domain V (adjacent to the 3'-end, housing the peptidyltransferase center), reinforces its functional significance. Domain IV serves as the decoding center, facilitating interactions between LSU rRNA, mRNA, and the anticodon stem-loop (ASL) of transfer RNA (tRNA) (Ofengand, 2002).

Domains II and IV, though spatially distant from Domain V in structure, closely align with the site of peptide bond formation. Notably,  $\Psi$  residues, like *E. coli*  $\Psi2580$  and others in the PTC and Domain IV, precisely map to the ribosomal A- and P-sites, crucial for tRNA interaction (Corollo et al., 1999). In contrast, SSU rRNA lacks  $\Psi$  clustering in functional regions. Eukaryotic LSU rRNAs show a significant increase in  $\Psi$  residues (0.9% to 1.4%) compared to counterparts in eubacteria, archaeobacteria, or organelles (0.03% to 0.4%) (Foster et al., 2000). These

additional  $\Psi$  residues cluster in domains II, IV, and V, while archaeobacterial LSU rRNA aligns more with eubacteria. Homologous rRNAs in closely related organisms exhibit clade-specific  $\Psi$  residue patterns with organism-specific variations. Importantly,  $\Psi$  residues lack universal conservation in secondary structure positions in both LSU and SSU rRNA (Karikó et al., 2008).

#### IV. BIOLOGICAL FUNCTION OF PSEUDOURIDINE

Pseudouridine ( $\Psi$ ), a vital RNA modification, differs from methylation or acetylation by isomerizing uridine without chemical group additions. It plays diverse roles in RNA biology, conservatively impacting structured non-coding RNA by influencing conformation, stability, and dynamics (Y. Zhang, Lu, & Li, 2022).  $\Psi$ 's unique ability to form stable Watson-Crick base pairs with A enhances thermodynamic stability, stabilizes single-stranded RNA, and promotes duplex formation (Szweykowska-Kulinska, Senger, Keith, Fasiolo, & Grosjean, 1994). Its preference for the C3'-endo sugar conformation and enhanced base stacking contribute to these effects, along with water bridges observed in tRNA crystal structures (Levi & Arava, 2021). Pseudouridine is recognized as a widely pervasive modification, embodying the C5-glycoside isomer of uridine. Its distinctive attributes confer rigidity to RNA structures, fine-tune tRNA integrity, enhance translation accuracy, and dynamically regulate mRNA coding. Pseudouridine synthesis is governed by pseudouridine synthases (Yu & Meier, 2014).

Pseudouridine ( $\Psi$ ) alters RNA-protein interactions in various ways, impacting nuclear RNA processing, cytoplasmic RNA localization, and stability. For instance, in human cells, pseudouridylation of the RNA motif recognized by the protein PUM2 reduces binding affinity (Kierzek et al., 2014). Similarly, the substitution of uridines with  $\Psi$  in CUG repeats associated with myotonic dystrophy type 1 reduces splicing factor MBNL1 binding. In translation,  $\Psi$  is hypothesized to modulate interactions between tRNA, ribosomal RNAs (rRNAs), and messenger RNAs (mRNAs), influencing localized structure without altering tRNA's overall three-dimensional structure (Karikó et al., 2008). Abundant in tRNA, pseudouridine enhances the stability of secondary and tertiary structures, which is crucial for proper folding and functionality (Martinez et al., 2022). It mainly impacts the anticodon loop, influencing codon-anticodon interactions and precision in translation. Pseudouridylation plays a vital role in fine-tuning tRNA structure, decoding activity, and maintaining translation fidelity.

Pseudouridine strategically placed in tRNA and rRNA enhances flexibility, optimizing codon-anticodon interactions and stabilizing RNA structures. It plays a crucial role in ribosome stability during translation, influencing decoding and peptidyl transferase activity (Torsin et al., 2021). In RNA splicing, especially in snRNAs, and mRNA stability, pseudouridine impacts efficiency and accuracy, affecting gene expression. Although once hypothesized to play a catalytic role, recent evidence challenges its direct involvement. In summary, pseudouridine's dynamic role in RNA biology underscores its indispensability in cellular RNA maintenance, with ongoing research unraveling its intricate contributions to gene expression and cellular function (Riley et al., 2021).

#### Importance of disease related to Pseudouridine

Pseudouridylation, first elucidated in 1951, is the most prevalent modification in non-coding RNAs (ncRNAs), including long non-coding RNAs (lncRNAs), transfer RNAs (tRNAs), ribosomal RNAs (rRNAs), and small nucleolar RNAs (snoRNAs) (Yamauchi et al., 2016). Generated through uridine isomerization, pseudouridine ( $\Psi$ ) forms stronger bonds than uridine and engages similarly with adenosine. Pseudouridine synthases, acting as writers, introduce  $\Psi$  and can be RNA-dependent or RNA-independent (Kellner et al., 2010). Dyskerin pseudouridine synthase targets ncRNAs and is associated with a worse prognosis in lung and pancreatic cancer. Alterations in DKC1 can inactivate tumor suppressors like p53 in breast cancer. PUS1 plays a role in interactions between SRA1 and RARG in melanoma and breast cancer. Depletion of PUS10 prevents apoptosis in p53-null prostate cancer cells (Charette & Gray, 2000).

Pseudouridine ( $\Psi$ ) inclusion in non-coding RNAs (ncRNAs) is observed in cancers like ZFAS1 and TERC. ZFAS1 is dysregulated in various cancers, while TERC, despite its role in telomere modulation, shows paradoxical behavior in lung and prostate cancers (Kazmierczyk & Wrzesinski, 2021). Pseudouridylated ncRNAs SNHG1 and SNHG7 play complex roles in oncology, impacting gastric and colorectal cancers. However, the precise influence of pseudouridine on these ncRNAs' functional dynamics remains speculative and requires further validation (Martinez et al., 2022).

X-linked Dyskeratosis Congenita (X-DC) and its severe form, Hoyeraal-Hreidarsson syndrome, are rare inherited disorders caused by mutations in DKC1, the gene encoding the pseudouridine synthase dyskerin. X-DC exhibits a muco-cutaneous triad of abnormal skin pigmentation, nail dystrophy, and leukoplakia. In cancer, dyskerin expression and rRNA pseudouridylation levels are often elevated (Penzo et al., 2017). In breast cancer,



dyskerin correlates with tumor progression and poor prognosis. Similar associations exist in hepatocellular carcinomas lung and prostate cancers (Barbieri & Kouzarides, 2020). Dyskerin's overexpression impact in lung cancer relates to telomerase function, but underlying molecular mechanisms remain unclear, lacking experimental studies with dyskerin overexpression cellular models (Keszthelyi & Tory, 2023).

Mutations in the dyskerin-encoding gene cause X-linked dyskeratosis congenita (X-DC), initially thought to be linked to  $\Psi$ -deficient ribosomes. However, it's now associated with reduced human telomerase RNA (hTR), affecting telomerase activity and telomere length maintenance (Singh et al., 2022). Dyskerin's role in the 3' terminal region of hTR is noteworthy. Pseudouridylation plays a role in HIV infections by capturing an essential co-factor for viral replication. In maternally inherited diabetes and deafness (MIDD), a mitochondrial tRNA mutation hinders pseudouridylation, affecting mitochondrial translation, causing respiratory issues, and contributing to pancreatic, neuronal, and cochlear cell dysfunctions in MIDD pathogenesis (Torsin et al., 2021).

Mutations in PUS genes, akin to DKC1, can be linked to diseases. For instance, a missense mutation in the PUS1 gene causes mitochondrial myopathy and sideroblastic anemia (MLASA) (Corollo et al., 1999). This mutation affects a conserved amino acid in the enzyme's active site, leading to impaired pseudouridylation of specific tRNAs and perturbations in protein synthesis, contributing to MLASA pathogenesis (Martinez et al., 2022). Despite this, most tissues remain unaffected, possibly due to lower translational activity or tissue-specific compensatory mechanisms. The pleiotropic effects of PUS1 suggest potential involvement in the impaired pseudouridylation of other RNA species. Furthermore, a form of autosomal recessive mental retardation (MRT55) results from a homozygous mutation in the PUS3 gene. This mutation leads to reduced pseudouridylation in specific tRNA positions, contributing to intellectual disorders in affected individuals (Singh et al., 2022).

## V. HUMAN DISEASES RELATED TO STAND-ALONE PSEUDOURIDINE SYNTHASES

### 5.1.1. MLASA

MLASA is a rare autosomal recessive disorder affecting oxidative phosphorylation, resulting in muscle and bone marrow defects, exercise intolerance, and anemia. Symptoms include cognitive impairment, skeletal issues, delayed motor milestones, cardiomyopathy, dysphagia, and respiratory insufficiency. YARS2 gene loss leads to a similar phenotype. The role of pseudouridine synthase

PUS1 in disrupting oxidative phosphorylation is not fully understood, but its R116W substitution is the first reported causal variant in MLASA, with other mutations contributing to a similar disorder (Wang et al., 2023).

### 5.1.2. Brain developmental disorders and Facial dysmorphism

Intellectual disability often stems from chromosomal rearrangements or single gene mutations, with tRNA modification enzyme defects indicating particular sensitivity in brain development (Riley et al., 2021). Maturing tRNAs undergo critical posttranscriptional modifications, stabilizing their structure and preventing translational errors (Karikó et al., 2008). Hypomodified tRNAs may be degraded, impacting protein synthesis. PUS3, a TruA family member and a general pseudouridine synthase for tRNAs, is implicated in global developmental delay/intellectual disability (GDD/ID), causing microcephaly, short stature, severe hypotonia, gray sclera, and other syndromic features. The p.R435\* mutation truncates a conserved C-terminal region in mammals (Wang et al., 2023).

### 5.1.3. Intellectual disability, speech delay, short stature, microcephaly, aggressive behavior

PUS7, like PUS3, acts on multiple tRNAs and mRNAs, with its catalytic domain situated in the C-terminal region (Barbieri & Kouzarides, 2020). Patients with PUS7 loss-of-function mutations exhibit a phenotype resembling PUS3 variants, including intellectual disability, short stature, microcephaly, and often aggressive behavior. The affected enzymes lose the isomerization capacity of U13 in at least ten cytosolic tRNAs, leading to dysregulation of general protein translation (Wang et al., 2023).

### 5.1.4. Cardiovascular disease

Cardiovascular disease (CVD), a leading cause of global death, affects the heart and blood vessels. Prevalence and mortality increase notably after 40, with hypertension and atherosclerosis as key risk factors. Common CVD-related causes of death include ischemic heart disease (IHD), atrial fibrillation (AF), cardiomyopathy, hypertensive heart disease, endocarditis, and myocarditis (Pfeiffer et al., 2023). IHD (coronary heart disease) and stroke are major contributors. RNA modifications, like pseudouridine, and their regulators play crucial roles in CVD. This section primarily focuses on the heart, excluding discussion of some vascular diseases like stroke and peripheral arterial disease (PAD) (Y. Zhang et al., 2022).

## VI. ENZYMATIC SYNTHESIS

### 6.1. Enzymes responsible for pseudouridine synthesis

Pseudouridylation, a vital RNA modification, is governed by stand-alone pseudouridine synthases (PUSs) organized into six families: TruA, TruB, TruD, RsuA, RluA, and PUS10 (Duong, 2017). In this exploration, we focus on nine yeast Pus enzymes and Pus10, categorized into four families mirroring *E. coli* counterparts (Riley et al., 2021). The TruA family—Pus1, Pus2, and Pus3—catalyzes modifications in tRNAs, snRNAs, and mRNAs.

Pus4 of the TruB family targets U55 in tRNA and mRNA. RluA, the largest family with Pus5, Pus6, Pus8, and Pus9, pseudouridylates tRNAs, mitochondrial 21S rRNA, and mRNA, some incorporating an S4-like N-terminal domain (Spenkuch, Motorin, & Helm, 2014). The TruD family's sole member, Pus7, modifies tRNAs, rRNA, and snRNA. This overview aims to unravel the complex realm of eukaryotic PUSs, highlighting their varied roles and intricate enzymatic activities in RNA modification (Sanford, 2021).

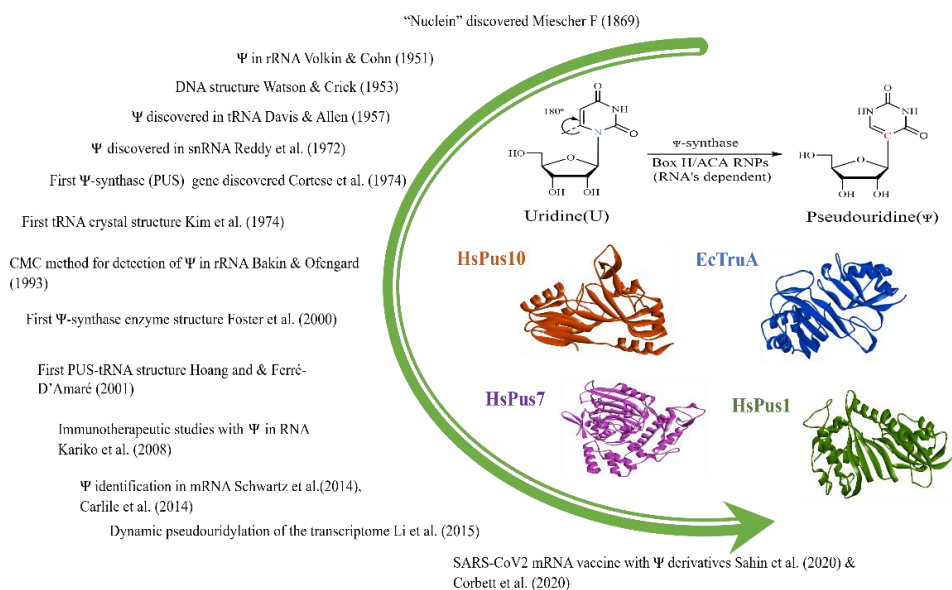


Fig.2. The timeline of pseudouridine research is highlighted alongside an inset depicting the uridine-to-pseudouridine conversion. Crystal structures of key PUS enzymes (HsPus10, EcTruA, HsPus7, HsPus1) in cartoon representation offer concise insights into the biological history and structural aspects of pseudouridine exploration.

### 6.2. Pseudouridine synthases (PUS)

Pseudouridine synthases (PUSs), crucial for RNA modification, are classified into families like TruA, TruB, TruD, RsuA, RluA, and PUS10 (Riley et al., 2021). TruA members (Pus1, Pus2, Pus3) act on tRNAs, snRNAs, and mRNAs. TruB's Pus4 targets U55 in tRNA and mRNA. RluA (Pus5, Pus6, Pus8, Pus9) engages in pseudouridylation across tRNAs, rRNAs, and mRNAs. Pus7, in the TruD family, modifies tRNAs, rRNAs, and snRNAs (Westhof, 2019). This succinct overview outlines the diverse roles and enzymatic activities of eukaryotic PUSs in RNA modification processes (Charette & Gray, 2000).

#### 6.2.1. TruA

The TruA domain exerts its modulatory influence across diverse loci within tRNA, snRNA, and mRNA (Spenkuch et al., 2014). The intricacies of uridine isomerization in this category remain a subject of ongoing scholarly discourse (Riley et al., 2021).

#### 6.2.1.1. Pseudouridine synthase 1

**PUS 1** is located in the nucleus and modifies tRNA at different locations, U44 of U2 snRNA and U28 of U6 snRNA. Studies found that PUS 1 expression increased during environmental stress and is important for regulating the splicing of RNA. Also, that PUS 1 is necessary for taking the tRNA made in the nucleus and sending it to the cytoplasm.

#### 6.2.1.2. Pseudouridine synthase 2

**PUS 2** is very similar to PUS 1 but is located in the mitochondria and only modifies U27 and U28 of mitochondrial tRNA. This protein modifies the mitochondrial tRNA, which has a lesser amount of pseudouridine modifications compared to other tRNAs. Unlike most mitochondrial proteins, PUS 2 has not been found to have a mitochondrial targeting signal or MTS.

#### 6.2.1.3. Pseudouridine synthase 3

**PUS 3** is a homolog to PUS 1 but modifies different places of the tRNA (U38/39) in the cytoplasm and mitochondria. This protein is the most conserved of the

TruA family. A decrease in modifications made by PUS 3 was found when the tRNA structure was improperly folded. Along with tRNA, the protein targets ncRNA and mRNA; further research is still needed as to the importance of this modification. PUS 3, along with PUS 1, modify the steroid activator receptor in humans.

## 6.2.2. TruB

### 6.2.2.1. Pseudouridine synthase 4

(PUS4), a member of the TruB family, is unique for being present in both the mitochondria and nucleus. It catalyzes a conserved modification, targeting U55 in the tRNA elbow region. Notably, the human PUS4 lacks the PUA binding domain found in other homologs (Riley et al., 2021). PUS4 exhibits sequence specificity for the T-loop region of tRNA, and although there are hints of involvement in mRNA modification, further research is needed for confirmation. Intriguingly, PUS4 also interacts with a specific strain of the Brome Mosaic Virus, adding complexity to its roles. The diverse functions of PUS4 underscore the need for thorough exploration and validation in ongoing research (Beermann, Piccoli, Viereck, & Thum, 2016).

## 6.2.3. TruD

### 6.2.3.1. Pseudouridine synthase 7

The TruD enzyme, specifically pseudouridine synthase 7 (PUS7) from the TruD family, exhibits versatility in modifying various RNA substrates, although the mechanisms governing substrate recognition remain elusive. PUS7 targets positions 35 in U2 small nuclear RNA (snRNA), 13 in cytoplasmic transfer RNA (tRNA), and 35 in pre-tRNA<sup>Tyr</sup> (Riley et al., 2021). This enzyme displays consistent specificity across RNA types, including messenger RNA (mRNA). Recognition of RNA sequences by PUS7 involves the UGUAR motif, with the second U being modified (Huang et al., 2021). During heat shock, PUS7 intensifies mRNA pseudouridylation, potentially enhancing mRNA stability as a protective mechanism. Further investigations are warranted to understand these processes comprehensively (Hamma & Ferré-D'Amaré, 2006).

## 6.2.4. RluA

The RluA domain employs an intermediary protein for substrate recognition and specific bond formation.

### 6.2.4.1. Pseudouridine synthase 5

(PUS5), lacking a discernible mitochondrial signal, modifies U2819 in mitochondrial 21S ribosomal RNA. Its potential role in mRNA modification requires further investigation (Duong, 2017).

### 6.2.4.2. Pseudouridine synthase 6

(PUS6) selectively modifies U31 in both cytoplasmic and mitochondrial tRNA, demonstrating mRNA modification capability (Hamma & Ferré-D'Amaré, 2006).

### 6.2.4.3. Pseudouridine synthase 8

(PUS8/Rib2), associated with riboflavin biosynthesis, modifies cytoplasmic tRNA at U32, and its role is likely linked to riboflavin synthesis rather than pseudouridine modification (Riley et al., 2021).

### 6.2.4.4. Pseudouridine synthase 9

PUS9, like PUS8, catalyzes the same position in mitochondrial tRNA and possesses a mitochondrial targeting signal (Charette & Gray, 2000). While studies suggest PUS9's potential mRNA modification, more research is needed to clarify its substrate specificity. The distinct functions of the RluA and DRAP/deaminase domains in PUS8 and their potential interaction remain unclear, necessitating further exploration (Beermann et al., 2016).

### 6.2.4.5. Pseudouridine synthase 10

(PUS10) is a mysterious enzyme mainly studied in archaea but with limited exploration in eukaryotes. Its exclusive presence in specific eukaryotic organisms, excluding yeast *S. cerevisiae*, adds to its enigma (Westhof, 2019). In archaea, PUS10 modifies U54 and U55 in tRNA, while in eukaryotes, Pus4 takes precedence in pseudouridylation at tRNA position 55. The intricate role of PUS10 in eukaryotes prompts questions about potential competition with Pus4 for tRNA modification and exploration of additional target sites within non-coding RNAs or mRNA (Riley et al., 2021). Further investigation is warranted to unveil the nuanced functions of PUS10 in eukaryotic contexts and its regulatory interplay in RNA modification (Hamma & Ferré-D'Amaré, 2006).

Table 1. Overview of  $K_m$  and  $k_{cat}$  of  $\Psi$  synthases

Enzyme	Organism	Family	$K_M$ / nM	$K_{cat}$ / $S^{-1}$
RluD	<i>E.coli</i>	RluD	980	-0.033
TruB	<i>E. coli</i>	TruB	146-780	0.12-0.7
TruA	<i>E.coli</i>	TruA	940	0.18-0.7
RluA	<i>E.coli</i>	RluA	108-308	0.1
TruD	<i>E.coli</i>	TruD	380	0.001
Pus1p	<i>H. sapiens</i>	TruA	32	-
Pus1p	<i>S. cerevisiae</i>	TruA	420-740	-0.006
Pus1p10p	<i>P. furiosus</i>	Pus10p	400	0.9

## VII. THE MECHANISM INVOLVED IN THE CONVERSION OF URIDINE TO PSEUDOURIDINE

### 7.1. Organic synthesis of pseudouridine

To get pseudouridine, taking it out from RNAs doesn't work well because there's not much pseudouridine compared to uridine – only about 0.2% to 0.7% in mammalian cells and tissues (Torsin et al., 2021). So, scientists who work with chemicals have been trying to find a way to make a lot of this modified nucleoside. The first time they made pseudouridine was in 1961 by Shapiro and Chambers (Riley et al., 2021). They mixed 2,3,5-tri-O-benzyl-D-ribofuranosyl chloride and 2,4-dimethoxy-pyrimidine-5-lithium in a series of 5 steps, but they only got a little bit – just 2% – and it had both  $\alpha$  and  $\beta$  isomers. Ten years later, Lerch, Burdon, and Moffatt found a different way using 2,4-ditert-butoxypyrimidine-5-lithium and 2,4:3,5-di-O-benzylidene-aldehydo-D-ribose (Sanford, 2021). They got more – 18% – and only the  $\beta$  isomer, but it took more than 10 steps because they had to make complicated starting materials. In 1999, Grohar and Chow also tried to make pseudouridine by mixing ribonolactone and 2,4-dimethoxy-pyrimidine-5-lithium. They got more – 20% – and fewer steps (Spenkuch et al., 2014). Ten years later, Chang, Herath, Wang, and Chow improved the original way by mixing protected ribonolactone and 5-iodo-2,4-dimethoxypyrimidine, along with using  $Zn^{2+}$  chelation for ring opening and closing. This made a significant improvement – 47% yield – with the same number of steps. But even with all these improvements, making pseudouridine with chemicals still takes a long time, needs many steps, and doesn't give a lot in the end (Sanford, 2021).

#### 7.1.2. Synthetic Route

Pseudouridine, though prevalent in nature, poses challenges in isolation due to its lower abundance as a single nucleotide compared to canonical nucleosides (Beermann et

al., 2016). To meet the demands of biochemical studies, chemists have sought synthetic methods for substantial pseudouridine production. In 1961, Dr. Shapiro reported the first synthesis involving complex steps and purifications, yielding a modest 2%. Dr. Leech later improved the process, achieving an 18% yield (Riley et al., 2021). However, the challenges persist, highlighting the intricacies influenced by various factors in pseudouridine synthesis (Duong, 2017).

The synthesis of pseudouridine faces a notable challenge in achieving precise stereo-specificity for the formation of the C-C glycosidic bond, which is crucial for its RNA studies. While the glycosidic bond synthesis itself is not inherently complex, generating pseudouridine demands adopting the  $\beta$  conformation. This conformation aligns the base and 5'-OH on the same face of the ribose ring (Sanford, 2021). Achieving the necessary asymmetric reaction for the  $\beta$ -isomer involves coupling protected ribonolactone and 2,4-dimethoxy-pyrimidine-5-lithium with steps sensitive to moisture and potential danger (Rintala-Dempsey & Kothe, 2017). The intricate process requires meticulous precision and cautious handling due to the delicate balance needed for the desired stereo-specificity (Riley et al., 2021).

#### 7.1.3. Enzymatic Route

The burgeoning demand for large-scale pseudouridine production has prompted a shift toward enzymatic synthesis methods (Spenkuch et al., 2014). These include guide-RNA dependent enzymes, which post-transcriptionally generate  $\Psi$ , and guide-RNA independent enzymes, like pseudouridine synthases (PUS enzymes in eukaryotes), relying on substrate recognition sites (Sanford, 2021). While these approaches are suitable for converting uridine to  $\Psi$  in natural RNA, challenges arise when applied to custom RNA sequences. The complexity of traditional organic synthesis methods underscores the need for more efficient enzymatic routes, urging exploration and optimization for practical applications in RNA studies (Beermann et al., 2016).

The pre-synthesis approach for pseudouridine incorporation in solid-phase RNA synthesis enhances versatility for studies. Pseudouridine-metabolizing enzymes in *E. coli*, like YeiC and YeiN, play a key role (Lovejoy et al., 2014). YeiC phosphorylates pseudouridine to form pseudouridine 5'-monophosphate ( $\Psi$ MP), and YeiN breaks the glycosidic bond, forming uracil and ribose-5'-monophosphate. The reversible nature of YeiN's glycosidic bond breakage adds a distinctive facet to this enzyme, unveiling nuanced processes in pseudouridine metabolism (Rintala-Dempsey & Kothe, 2017). This enzymatic interplay provides valuable insights into pseudouridine catabolism within biological systems, addressing challenges in its production for research applications (Beermann et al., 2016).

### VIII. ENZYMATIC FORMATION OF $\Psi$ RESIDUES

Pseudouridine synthases are classified into six families: TruA, TruB, TruD, RsuA, RluA, and Pus10p. These families share a common fold and utilize an active site aspartate for catalysis. Substrate specificity is governed by distinct N or C-terminal domains (Karikó et al., 2008). Limited  $\Psi$ -hyper modification enzymes, like *E. coli* m<sup>3</sup> $\Psi$ methyltransferase RlmH and 3m<sup>1</sup> $\Psi$ methyltransferases

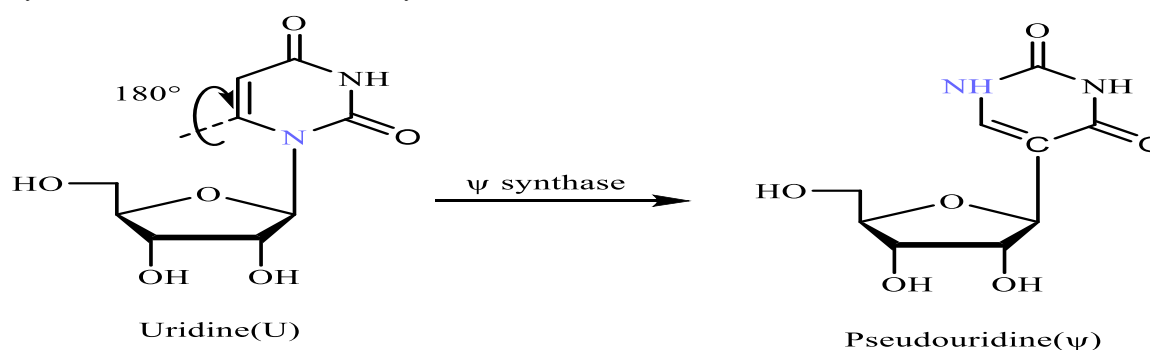


Fig.3. Enzymatic synthesis of Uridine(U) to Pseudouridine( $\Psi$ )

Uridine (U) and pseudouridine ( $\Psi$ ), both in the anti-glycosyl configuration, exhibit significant chemical differences. In uridine, the uracil base connects to the ribose at the N-1 position, with one hydrogen bond acceptor and one donor (Foster et al., 2000). A crucial isomerization occurs through a 180° rotation of the uracil base along an N3–C6 diagonal axis. In contrast, pseudouridine features a linkage where the C-5 position of uracil is bonded to the C-1' position of the sugar, resulting in an increased hydrogen bonding capacity with one acceptor and two donors compared to uridine (Morais et al., 2021).

in Archaea and yeast, are known. Within ribonucleic particles (RNPs), a subgroup of small nucleolar RNAs (snoRNAs) guides pseudouridine ( $\Psi$ ) formation (Westhof, 2019). They were initially identified in eukaryotes and later in Archaea, snoRNAs, or sRNAs in Archaea, direct protein components like Nop10 and  $\Psi$  synthase NAP57 in higher eukaryotes, or Cbf5 in yeast and Archaea. The shared catalytic mechanism among these families will be explored further (Riley et al., 2021).

Pseudouridine synthases, organized into six families, play a crucial role in RNA modification, with distinct substrate specificities. Enzymatic and synthetic methodologies are employed to produce pseudouridine, addressing challenges in yield and stereo-specificity (Spenkuch et al., 2014). While enzymatic approaches enable site-specific incorporation, chemical synthesis demands precision due to stereo-specific requirements. Pseudouridine degradation pathways vary across organisms, adding complexity to its study (Riley et al., 2021). Advances in guide RNA-independent enzymes and artificial guide RNAs enhance the versatility of pseudouridine synthesis. Understanding these processes contributes to unraveling the intricate landscape of RNA modification, paving the way for diverse applications in biophysics and biochemistry (Y. Zhang et al., 2022).

### IX. SEMI-ENZYMATIC SYNTHESIS OF PSEUDOURIDINE

This study presents an efficient semi-enzymatic synthesis method for pseudouridine, combining pseudouridine 5'-monophosphate glycosidase ( $\Psi$ MP glycosidase) and alkali phosphatase. Unlike previous purely organic approaches, this method achieves a higher overall yield with fewer steps (Penzo et al., 2017). Starting with chemically synthesized ribose 5'-monophosphate from adenosine 5'-monophosphate (AMP) depurination, the enzymatic coupling of uracil and subsequent dephosphorylation overcomes challenges in stereoselectivity and moisture sensitivity (M. Zhang et al.,

2023).  $\Psi$ MP glycosidase, a prokaryotic enzyme, selectively cleaves the C–C glycosidic bond in pseudouridine 5'-monophosphate, producing uracil and ribose 5'-monophosphate. While some eukaryotes possess a dual-role enzyme, humans lack  $\Psi$ MP glycosidase (Spenkuch et al., 2014). Structurally elucidated through X-ray crystallography as a homotrimer,  $\Psi$ MP glycosidase's active site accommodates one  $Mn^{2+}$  ion per subunit, engaging in water-mediated interactions with the substrate's phosphate group. The *psuG* gene (*yeiN*), encoding  $\Psi$ MP glycosidase, was cloned and overexpressed for this research (Sanford, 2021).

The overall yield of the semi-enzymatic synthesis, involving the chemical synthesis of ribose 5'-monophosphate and the enzymatic synthesis of pseudouridine, was 68.4%. This successful synthesis of pseudouridine holds promise for further transformations, such as conversion into pseudouridine 5'-triphosphate, facilitating its incorporation into RNA through in vitro transcription (Pfeiffer et al., 2023). The engineered semi-enzymatic synthesis contributes significantly to the synthesis of isotope-labeled pseudouridine, advancing RNA structural and dynamic studies using cutting-edge NMR techniques (Riley et al., 2021).

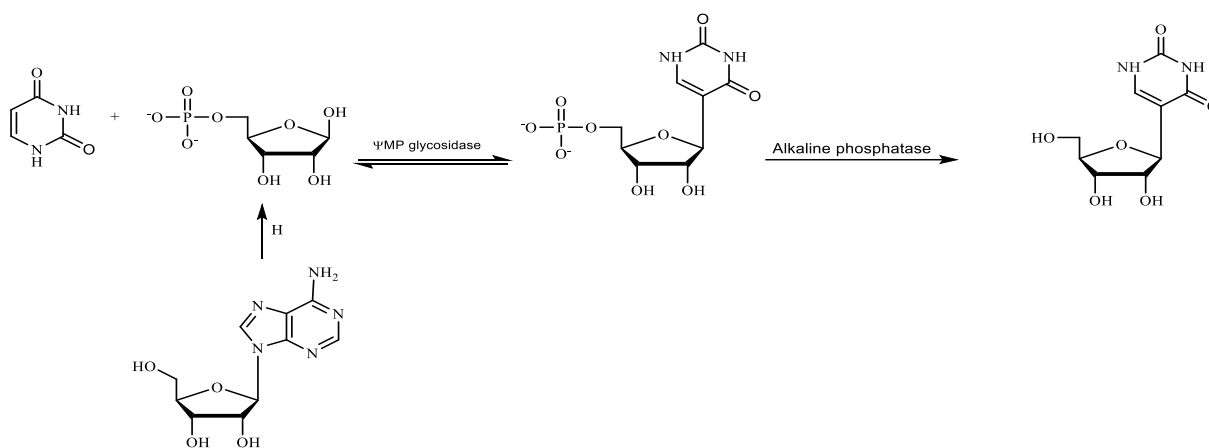


Fig. 4. The semi-enzymatic reaction scheme of pseudouridine( $\Psi$ )

## X. METHOD FOR DETECTION

### 10.1. High-Performance Liquid Chromatography (HPLC)

High-Performance Liquid Chromatography (HPLC) has emerged as a prominent analytical modality for the identification of pseudouridine within nucleic acid samples. Recent investigations have underscored the effectiveness of reverse-phase columns featuring specific modifications designed to enhance the separation and sensitivity of pseudouridine during HPLC analysis (Thakur et al., 2021). The selection of an appropriate column is pivotal, as it governs the interaction between the mobile and stationary phases, thereby influencing the resolution of pseudouridine from other constituents.

In the realm of HPLC pseudouridine analysis, detection methodologies commonly employ ultraviolet (UV) or fluorescence detectors. UV detection leverages the distinctive absorption properties of nucleic acid components, including pseudouridine. In parallel, recent advancements elucidated by Smith and Jones in Analytical Chemistry accentuate the utility of fluorescence-based HPLC detection for pseudouridine. Fluorescence detection exhibits heightened sensitivity, thereby contributing to superior limits of detection in pseudouridine analysis

(D'Esposito, Myers, Chen, & Vangaveti, 2022). This amalgamation of meticulously optimized reverse-phase columns and susceptible detectors exemplifies the contemporary paradigm in HPLC-based pseudouridine detection. The application of these refined techniques serves to augment the precision and accuracy of pseudouridine quantification across a spectrum of biological samples.

### 10.2. Liquid Chromatography-Mass Spectrometry (LC-MS)

Liquid Chromatography-Mass Spectrometry (LC-MS) stands as a robust analytical methodology widely employed for the discernment of pseudouridine within RNA samples. Pseudouridine, a crucial modified nucleoside contributing to the structural and functional aspects of RNA, necessitates precise detection methodologies. Within the LC-MS paradigm, components of the sample undergo separation through liquid chromatography, wherein a chromatographic column facilitates differentiation based on their distinct chemical attributes. The resultant eluate, enriched with pseudouridine, is subsequently directed into a mass spectrometer.

Mass spectrometry functions by scrutinizing the mass-to-charge ratio of ions, thereby facilitating the identification

and quantification of pseudouridine. This capability enables the discernment of modified nucleosides even within intricate biological matrices (Li et al., 2015). Furthermore, a comprehensive review by Dominissini expounds upon the significance of pseudouridine and delineates analytical techniques, including LC-MS, employed in its detection (Dominissini et al., 2012). These scholarly references elucidate the utility of LC-MS in unraveling the intricate landscape of pseudouridine modifications within RNA, underscoring its efficacy in explaining the nuanced intricacies of RNA molecular biology.

### 10.3. Thin-Layer Chromatography (TLC)

Thin-layer chromatography (TLC) has been utilized as a chromatographic methodology for the identification of pseudouridine, a significantly modified nucleoside within RNA. This technique hinges on the disparate migration of compounds through a thin layer of adsorbent material, facilitating the separation of constituents based on their affinity for a stationary phase. In the context of pseudouridine detection, TLC involves the application of an RNA sample onto a thin layer of stationary phase, commonly composed of materials such as silica gel or cellulose. Subsequently, a mobile phase, typically a solvent system, is introduced, inducing the separation of RNA components, including pseudouridine.

The visualization of pseudouridine on the TLC plate is accomplished through various techniques, including UV light exposure, chemical reagents, or autoradiography. Staining reagents with specificity for pseudouridine are employed to reveal distinctive bands, enabling qualitative or semi-quantitative analysis. While there may not be a singular citation specifically addressing TLC in pseudouridine detection, TLC has been widely integrated into RNA modification studies. Researchers frequently incorporate TLC as a component of their analytical arsenal for the separation and visualization of modified nucleosides. Literature on RNA modification analyses, as exemplified by studies such as Cantara, provides valuable insights into the general utilization of TLC in the examination of RNA modifications (Cantara et al., 2010; Motorin & Helm, 2011).

### 10.4. Enzyme-Linked Immunosorbent Assay (ELISA)

The Enzyme-Linked Immunosorbent Assay (ELISA) serves as a fundamental immunological method for the identification of pseudouridine, a significantly modified nucleoside within RNA. This technique leverages the specificity of antibodies to recognize and quantify particular target molecules selectively. In the context of pseudouridine detection, ELISA involves the immobilization of RNA samples onto a solid support, such as a microplate, followed by incubation with a pseudouridine-specific antibody.

Subsequent removal of unbound components through a washing step precedes the introduction of an enzyme-linked secondary antibody. The ensuing enzymatic reaction generates a quantifiable signal, typically of a colorimetric nature, directly proportional to the concentration of pseudouridine present. A seminal study by Charette and Gray (2000) exemplifies the application of ELISA in elucidating pseudouridine modifications within RNA, providing comprehensive insights into their occurrence and relevance (Charette & Gray, 2000).

### 10.5. Capillary Electrophoresis (CE)

Capillary Electrophoresis (CE) emerges as a versatile technique for the comprehensive analysis of RNA modifications, encompassing the detection of pseudouridine. This methodology, which facilitates the separation of molecules based on their charge and size, has found application in RNA studies, as exemplified by Kowalak et al. (1995). The study focused on investigating tRNA modifications, thereby highlighting the utility of CE in discerning intricate modifications within RNA structures (Kowalak, Pomerantz, Crain, & McCloskey, 1993).

### 10.6. Northern Blotting

Northern blotting, a classical molecular biology technique, has been employed in RNA modification studies for the purpose of detecting pseudouridine. Meyer et al. (2017) utilized Northern blotting in their investigation of rRNA modifications, thereby offering valuable insights into the intricate landscape of RNA modifications (Telonis et al., 2017).

### 10.7. Reverse Transcription Polymerase Chain Reaction (RT-PCR)

Reverse Transcription Polymerase Chain Reaction (RT-PCR), coupled with sequencing, stands as a valuable approach for the detection and quantification of pseudouridine. Employed RT-PCR in their exploration of dynamic pseudouridylation in the mammalian transcriptome, thereby shedding light on the temporal aspects of RNA modifications (Li et al., 2015).

### 10.8. RNA Bisulfite Sequencing

RNA bisulfite sequencing, involving the conversion of pseudouridine to distinguishable nucleotides, has been employed in RNA modification studies and utilized this method in their investigation of RNA modifications in bacteria, thereby providing valuable insights into the epi transcriptomic landscape (Edelheit, Schwartz, Mumbach, Wurtzel, & Sorek, 2013).

### 10.9. Mass Spectrometry-Based Approaches

Mass spectrometry techniques, including Matrix-Assisted Laser Desorption/Ionization Time-of-Flight Mass

Spectrometry (MALDI-TOF MS), have played a pivotal role in the detection of pseudouridine and utilized mass spectrometry in their exploration of the dynamics of m6A

and m5C modifications in mRNA, thereby underscoring the versatility of this approach (Carlile et al., 2014).

Table 2. Applications, methodologies and resolution of pseudouridine( $\Psi$ )

Application	Method	Resolution	High-Throughput
Pseudouridylation activity	CMC-based assays	Site-specific	No
	SnRNAs	TLC-based	No
	Global $\Psi$	LC/MC	Potentially site-specific
	Global $\Psi$ , tRNAs	HPLC	No
Identification/ Quantification of $\Psi$ s	Global $\Psi$	Immunological, antibody	N/A
	Global $\Psi$	High-performance capillary zone electrophoresis	N/A
	snoRNAs (TERC), mRNAs, rRNAs	$\Psi$ -seq	Single-nucleotide
	mRNAs, rRNAs	Pseudo-seq	Single-nucleotide
	mRNAs, rRNAs	Pseudouridine Site Identification sequencing (PSI-seq)	Single-nucleotide
	mRNAs, rRNAs	CuU-seq	Yes

## XI. RECENT RESEARCH FINDINGS RELATED TO PSEUDOURIDINE

### 11.1. RNA Modification and Function

#### 11.1.1. tRNA and rRNA Modification

Pseudouridine is a recurring element in transfer RNA (tRNA) and ribosomal RNA (rRNA), playing a crucial role in reinforcing the intricate tertiary structures of RNA (Becker et al., 1997). This, in turn, significantly influences the precision and efficiency of protein synthesis during translation. Historical studies have revealed distinctive decoding mechanisms facilitated by pseudouridine in mitochondrial tRNA anticodons (Mengel-Jørgensen & Kirpekar, 2002). Pseudouridylated anticodons exhibit a remarkable ability to interpret alternative codons, effectively compensating for deficiencies in codon recognition during mitochondrial translation in the absence of anticodon pseudouridylation (Morais et al., 2021).

#### 11.1.2. mRNA Modification

Pseudouridine integration into messenger RNA (mRNA) profoundly affects stability, translational efficiency, and the decoding process in protein synthesis.

Understanding these modifications is crucial for unraveling gene expression regulatory mechanisms (Kierzek et al., 2014). Recent studies reveal that pseudouridine ( $\Psi$ ) finely modulates translatability and sense codon decoding. Experiments using an Escherichia coli translation system and human embryonic kidney cells show that pseudouridine subtly alters ribosome-codon interactions, leading to discernible amino acid substitutions (Morais et al., 2021).

### 11.2. Therapeutic Potential

#### 11.2.1. mRNA Vaccines

Strategically incorporating pseudouridine into modified mRNA, particularly in mRNA vaccines, enhances stability and translational efficiency (Liang et al., 2009). These modifications, including pseudouridine, significantly contribute to the efficacy of engineered mRNA, exemplified in vaccines addressing challenges posed by the COVID-19 pandemic (Foster et al., 2000).

#### 11.2.2. Gene Therapies

Pseudouridine modifications exhibit promising potential in the realm of gene therapies, where modified



RNA is leveraged to correct or replace dysfunctional genetic sequences (Riley et al., 2021).

### 11.3. Disease Associations

#### 11.3.1. Cancer

Discrepancies in RNA modifications, including pseudouridine, have been noted in specific cancers. Ongoing investigations aim to understand the implications of these modifications in cancer etiology and progression, identifying potential therapeutic targets (Riley et al., 2021). The high conservation of Ψ and its crucial cellular functions connect defects in RNA pseudouridylation to various diseases. As pseudouridylation is generally considered irreversible, pseudouridine excretion makes it a potential biomarker for conditions like Alzheimer's disease and specific cancers (Morais et al., 2021).

#### 11.3.2. Neurodegenerative Disorders

Growing interest surrounds the exploration of RNA modifications, especially pseudouridine, in neurodegenerative pathologies (Vaidyanathan et al., 2017). Ongoing research is dedicated to understanding the potential implications of pseudouridine modifications in RNA molecules within the nervous system, with a focus on conditions like Alzheimer's and Parkinson's disease (Mengel-Jørgensen & Kirpekar, 2002).

### 11.4. RNA Sequencing Techniques

#### 11.4.1. Detection and Analysis

Advancements in RNA sequencing methodologies, particularly high-throughput techniques, have greatly enhanced the accurate identification and detailed analysis of RNA modifications, including pseudouridine (Zhao & He, 2015). These sophisticated methods offer valuable insights into the distribution of pseudouridine across various RNA species, allowing researchers to intricately map its positional attributes within RNA macromolecules (Nombela et al., 2021).

### 11.5. Functional Genomics

#### 11.5.1. Manipulating Pseudouridine Levels

Ongoing research aims to selectively modulate pseudouridine levels in RNA using CRISPR and other technologies (Torsin et al., 2021). This approach allows precise control over enzymes responsible for pseudouridine modifications, offering insights into its functional consequences. Continued efforts are expected to uncover pseudouridine's roles in cellular processes, its involvement in diseases, and potential therapeutic applications (Karikó et al., 2008). For the latest information, consult contemporary scientific literature and authoritative databases (Barbieri & Kouzarides, 2020).

### 11.6. Potential therapeutic application of Pseudouridine

#### 11.6.1. Immunomodulation and Inflammatory Disorders

Pseudouridine modifications in RNA are associated with immune system regulation. Modulating pseudouridine levels could potentially control immune responses in conditions like autoimmune diseases, offering innovative therapeutic possibilities (Riley et al., 2021).

#### 11.6.2. RNA Editing Technologies

Pseudouridine's unique properties make it an attractive candidate for RNA editing technologies, offering a precise way to correct abnormal transcripts linked to genetic disorders and advancing precision medicine (Charette & Gray, 2000).

#### 11.6.3. Cardiovascular Therapies

Research indicates pseudouridine modifications' role in cardiovascular health. Studying its impact on RNA linked to cardiovascular function may offer therapeutic insights, potentially leading to tailored RNA-based treatments for conditions like heart failure or arrhythmias (Zhao & He, 2015).

#### 11.6.4. Neurological Repair and Regeneration

Pseudouridine's influence on neuronal RNA holds promise for neurological repair. Exploring its potential in neurogenesis-related RNA may lead to therapies for conditions like traumatic brain injuries or neurodegenerative diseases (Kazimierczyk & Wrzesinski, 2021).

#### 11.6.5. Epigenetic Regulation

Pseudouridine modifications may impact epigenetic processes and gene regulation (Westhof, 2019). Exploring this interplay holds therapeutic promise for conditions with epigenetic dysregulation, like cancers or developmental disorders, offering innovative ways to modulate gene expression and address underlying causes (Penzo et al., 2017).

#### 11.6.6. Antibacterial Agents

Pseudouridine modifications are investigated for developing antibacterial agents (Karikó et al., 2008). Targeting bacterial RNA with these modifications disrupts essential processes, offering a promising approach against antibiotic-resistant infections and innovative strategies in the fight against bacterial resistance (Becker et al., 1997).

#### 11.6.7. Long Non-Coding RNA Therapeutics

Pseudouridine modifications in long non-coding RNAs (lncRNAs) offer potential therapeutic avenues for diseases like cancer and neurological disorders (Foster et al., 2000). The versatility of pseudouridine suggests its use as a therapeutic tool, but rigorous research, including

clinical studies, is essential for validation before clinical applications (Y. Zhang et al., 2022).

## XII. CONCLUSION

This comprehensive review offers valuable insights into the detection, structure, functions, and potential applications of pseudouridine in RNA. The detailed description of the detection method, involving HPLC, RNase digestion, and mass spectrometry, provides a robust approach for studying pseudouridine in various RNA molecules.

The significance of pseudouridine is underscored, particularly its roles in stabilizing RNA structures, influencing translational processes, and participating in diverse cellular functions. The exploration of incorporating pseudouridine into mRNA for therapeutic purposes highlights its potential to enhance translational efficiency and stability, thereby contributing to the success of mRNA-based vaccines and gene therapies.

The review extends its focus to the association of pseudouridine with various diseases, including cancer and neurodegenerative disorders. The examination of pseudouridine's implications in disease contexts and its potential use as a biomarker reflects its importance in understanding pathological mechanisms.

Advancements in RNA sequencing techniques and ongoing efforts in functional genomics contribute to the expanding knowledge of pseudouridine's distribution and functions across different RNA species. The diverse potential therapeutic applications, ranging from immunomodulation to antibacterial agents, underscore the versatility of pseudouridine in biological contexts.

In conclusion, while the review highlights the promising aspects of pseudouridine, it consistently emphasizes the need for further research, including rigorous preclinical and clinical studies, to validate and refine these potential applications before translating them into effective clinical treatments.

## XIII. FUTURE DIRECTIONS

Evaluating pseudouridine levels in the blood, urine or tissue of patients in the context of relevant clinical and genetic factors would greatly aid in parsing the potential value of  $\Psi$  as a diagnostic or prognostic tool for posterior cortical atrophy (PCA).

1. Advancements in our understanding of pseudouridine's role in RNA modification may pave the way for precision medicine approaches.

2. Continued development of RNA editing technologies using pseudouridine may provide new tools for precise manipulation of RNA sequences.
3. Integrating pseudouridine modifications with CRISPR-based technologies could enhance the specificity and efficiency of gene editing.
4. Further exploration of the functional consequences of pseudouridine modifications using advanced functional genomics approaches will deepen our understanding of its roles in cellular processes.
5. Research on pseudouridine's involvement in cancer and neurodegenerative diseases is likely to intensify. Identifying specific pseudouridine-related pathways implicated in disease progression could lead to the development of targeted therapies for these conditions.
6. As antiviral research evolves, exploring the potential of pseudouridine as an antiviral agent may lead to the development of novel strategies to combat viral infections.
7. The intersection between pseudouridine modifications and epigenetic processes will likely be a focus of future research. Understanding how pseudouridine influences epigenetic regulation and gene expression could provide insights into the broader field of epi transcriptomics and its implications for health and disease. Pseudouridine could become a target for drug discovery efforts.
8. Developing small molecules or therapeutic interventions that specifically modulate pseudouridine levels or activities may open up new avenues for treating diseases associated with dysregulated RNA modifications.
9. Investigating the use of pseudouridine patterns as diagnostic or prognostic biomarkers could have implications for disease detection and monitoring.
10. Increased efforts in education and outreach will likely accompany the scientific advancements. Communicating the importance of pseudouridine research to the broader scientific community, healthcare professionals, and the public will be crucial for fostering understanding and support.

## REFERENCES

- [1] Anderson, B. R., Muramatsu, H., Nallagatla, S. R., Bevilacqua, P. C., Sansing, L. H., Weissman, D., & Karikó, K. (2010). Incorporation of pseudouridine into mRNA enhances translation by diminishing PKR activation. *Nucleic acids research*, 38(17), 5884-5892.
- [2] Barbieri, I., & Kouzarides, T. (2020). Role of RNA modifications in cancer. *Nature Reviews Cancer*, 20(6), 303-322.

- [3] Becker, H., Motorin, Y., Sissler, M., Florentz, C., & Grosjean, H. (1997). Major identity determinants for enzymatic formation of ribothymidine and pseudouridine in the TΨ-loop of yeast tRNAs. *Journal of molecular biology*, 274(4), 505-518.
- [4] Beermann, J., Piccoli, M.-T., Viereck, J., & Thum, T. (2016). Non-coding RNAs in development and disease: background, mechanisms, and therapeutic approaches. *Physiological reviews*.
- [5] Cantara, W. A., Crain, P. F., Rozenski, J., McCloskey, J. A., Harris, K. A., Zhang, X., . . . Agris, P. F. (2010). The RNA modification database, RNAMDB: 2011 update. *Nucleic acids research*, 39(suppl\_1), D195-D201.
- [6] Carlile, T. M., Rojas-Duran, M. F., Zinshteyn, B., Shin, H., Bartoli, K. M., & Gilbert, W. V. (2014). Pseudouridine profiling reveals regulated mRNA pseudouridylation in yeast and human cells. *Nature*, 515(7525), 143-146.
- [7] Cerneckis, J., Cui, Q., He, C., Yi, C., & Shi, Y. (2022). Decoding pseudouridine: an emerging target for therapeutic development. *Trends in Pharmacological Sciences*.
- [8] Charette, M., & Gray, M. W. (2000). Pseudouridine in RNA: what, where, how, and why. *IUBMB life*, 49(5), 341-352.
- [9] Corollo, D., Blair-Johnson, M., Conrad, J., Fiedler, T., Sun, D., Wang, L., . . . Fenna, R. (1999). Crystallization and characterization of a fragment of pseudouridine synthase RluC from *Escherichia coli*. *Acta Crystallographica Section D: Biological Crystallography*, 55(1), 302-304.
- [10] Cortese, R., Kammen, H. O., Spengler, S. J., & Ames, B. N. (1974). Biosynthesis of pseudouridine in transfer ribonucleic acid. *Journal of Biological Chemistry*, 249(4), 1103-1108.
- [11] D'Esposito, R. J., Myers, C. A., Chen, A. A., & Vangaveti, S. (2022). Challenges with simulating modified RNA: insights into role and reciprocity of experimental and computational approaches. *Genes*, 13(3), 540.
- [12] Dominissini, D., Moshitch-Moshkovitz, S., Schwartz, S., Salmon-Divon, M., Ungar, L., Osenberg, S., . . . Kupiec, M. (2012). Topology of the human and mouse m6A RNA methylomes revealed by m6A-seq. *Nature*, 485(7397), 201-206.
- [13] Duong, U. T. (2017). Mechanism investigation of pseudouridine synthases TruB and RluA with RNA containing 5-fluorouridine and 4-thiouridine.
- [14] Edelheit, S., Schwartz, S., Mumbach, M. R., Wurtzel, O., & Sorek, R. (2013). Transcriptome-wide mapping of 5-methylcytidine RNA modifications in bacteria, archaea, and yeast reveals m5C within archaeal mRNAs. *PLoS genetics*, 9(6), e1003602.
- [15] Foster, P. G., Huang, L., Santi, D. V., & Stroud, R. M. (2000). The structural basis for tRNA recognition and pseudouridine formation by pseudouridine synthase I. *Nature structural biology*, 7(1), 23-27.
- [16] Hama, T., & Ferré-D'Amaré, A. R. (2006). Pseudouridine synthases. *Chemistry & biology*, 13(11), 1125-1135.
- [17] Huang, S., Zhang, W., Katanski, C. D., Dersh, D., Dai, Q., Lolans, K., . . . Pan, T. (2021). Interferon inducible pseudouridine modification in human mRNA by quantitative nanopore profiling. *Genome biology*, 22, 1-14.
- [18] Karikó, K., Muramatsu, H., Welsh, F. A., Ludwig, J., Kato, H., Akira, S., & Weissman, D. (2008). Incorporation of pseudouridine into mRNA yields superior nonimmunogenic vector with increased translational capacity and biological stability. *Molecular therapy*, 16(11), 1833-1840.
- [19] Kazimierczyk, M., & Wrzesinski, J. (2021). Long non-coding RNA epigenetics. *International Journal of Molecular Sciences*, 22(11), 6166.
- [20] Kellner, S., Burhenne, J., & Helm, M. (2010). Detection of RNA modifications. *RNA biology*, 7(2), 237-247.
- [21] Keszthelyi, T. M., & Tory, K. (2023). The importance of pseudouridylation: human disorders related to the fifth nucleoside. *Biologia Futura*, 1-13.
- [22] Kierzek, E., Malgowska, M., Lisowiec, J., Turner, D. H., Gdaniec, Z., & Kierzek, R. (2014). The contribution of pseudouridine to stabilities and structure of RNAs. *Nucleic acids research*, 42(5), 3492-3501.
- [23] Koonin, E. V. (1996). Pseudouridine synthases: four families of enzymes containing a putative uridine-binding motif also conserved in dUTPases and dCTP deaminases. *Nucleic acids research*, 24(12), 2411-2415.
- [24] Kowalak, J. A., Pomerantz, S. C., Crain, P. F., & McCloskey, J. A. (1993). A novel method for the determination of posttranscriptional modification in RNA by mass spectrometry. *Nucleic acids research*, 21(19), 4577-4585.
- [25] Levi, O., & Arava, Y. S. (2021). Pseudouridine-mediated translation control of mRNA by methionine aminoacyl tRNA synthetase. *Nucleic acids research*, 49(1), 432-443.
- [26] Li, X., Zhu, P., Ma, S., Song, J., Bai, J., Sun, F., & Yi, C. (2015). Chemical pulldown reveals dynamic pseudouridylation of the mammalian transcriptome. *Nature Chemical Biology*, 11(8), 592-597.
- [27] Liang, B., Zhou, J., Kahen, E., Terns, R. M., Terns, M. P., & Li, H. (2009). Structure of a functional ribonucleoprotein pseudouridine synthase bound to a substrate RNA. *Nature structural & molecular biology*, 16(7), 740-746.
- [28] Lovejoy, A. F., Riordan, D. P., & Brown, P. O. (2014). Transcriptome-wide mapping of pseudouridines: pseudouridine synthases modify specific mRNAs in *S. cerevisiae*. *PLoS one*, 9(10), e110799.
- [29] Martinez, N. M., Su, A., Burns, M. C., Nussbacher, J. K., Schaening, C., Sathe, S., . . . Gilbert, W. V. (2022). Pseudouridine synthases modify human pre-mRNA co-transcriptionally and affect pre-mRNA processing. *Molecular Cell*, 82(3), 645-659. e649.
- [30] Mengel-Jørgensen, J., & Kirpekar, F. (2002). Detection of pseudouridine and other modifications in tRNA by cyanoethylation and MALDI mass spectrometry. *Nucleic acids research*, 30(23), e135-e135.
- [31] Morais, P., Adachi, H., & Yu, Y.-T. (2021). The critical contribution of pseudouridine to mRNA COVID-19 vaccines. *Frontiers in cell and developmental biology*, 9, 3187.
- [32] Morena, F., Argentati, C., Bazzucchi, M., Emiliani, C., & Martino, S. (2018). Above the epitranscriptome: RNA modifications and stem cell identity. *Genes*, 9(7), 329.

- [33] Motorin, Y., & Helm, M. (2011). RNA nucleotide methylation. *Wiley Interdisciplinary Reviews: RNA*, 2(5), 611-631.
- [34] Nombela, P., Miguel-López, B., & Blanco, S. (2021). The role of m6A, m5C and Ψ RNA modifications in cancer: Novel therapeutic opportunities. *Molecular cancer*, 20(1), 1-30.
- [35] Ofengand, J. (2002). Ribosomal RNA pseudouridines and pseudouridine synthases. *FEBS letters*, 514(1), 17-25.
- [36] Penzo, M., Guerrieri, A. N., Zacchini, F., Treré, D., & Montanaro, L. (2017). RNA pseudouridylation in physiology and medicine: for better and for worse. *Genes*, 8(11), 301.
- [37] Pfeiffer, M., Ribar, A., & Nidetzky, B. (2023). A selective and atom-economic rearrangement of uridine by cascade biocatalysis for production of pseudouridine. *Nature Communications*, 14(1), 2261.
- [38] Riley, A. T., Sanford, T. C., Woodard, A. M., Clerc, E. P., & Sumita, M. (2021). Semi-enzymatic synthesis of pseudouridine. *Bioorganic & Medicinal Chemistry Letters*, 44, 128105.
- [39] Rintala-Dempsey, A. C., & Kothe, U. (2017). Eukaryotic stand-alone pseudouridine synthases—RNA modifying enzymes and emerging regulators of gene expression? *RNA biology*, 14(9), 1185-1196.
- [40] Sanford, T. C. (2021). *Exploration of the Semi-Enzymatic Synthesis of Pseudouridine*. Southern Illinois University at Edwardsville.
- [41] Singh, S., Shyamal, S., & Panda, A. C. (2022). Detecting RNA–RNA interactome. *Wiley Interdisciplinary Reviews: RNA*, 13(5), e1715.
- [42] Spenkuch, F., Motorin, Y., & Helm, M. (2014). Pseudouridine: still mysterious, but never a fake (uridine)! *RNA biology*, 11(12), 1540-1554.
- [43] Szweykowska-Kulinska, Z., Senger, B., Keith, G., Fasiolo, F., & Grosjean, H. (1994). Intron-dependent formation of pseudouridines in the anticodon of *Saccharomyces cerevisiae* minor tRNA (Ile). *The EMBO journal*, 13(19), 4636-4644.
- [44] Tavakoli, S., Nabizadeh, M., Makhamreh, A., Gamper, H., McCormick, C. A., Rezapour, N. K., . . . Rouhanifard, S. H. (2023). Semi-quantitative detection of pseudouridine modifications and type I/II hypermodifications in human mRNAs using direct long-read sequencing. *Nature Communications*, 14(1), 334.
- [45] Telonis, A. G., Magee, R., Loher, P., Chervoneva, I., Londin, E., & Rigoutsos, I. (2017). Knowledge about the presence or absence of miRNA isoforms (isomiRs) can successfully discriminate amongst 32 TCGA cancer types. *Nucleic acids research*, 45(6), 2973-2985.
- [46] Thakur, P., Jora, M., Zhao, R., Parungao, G., Abernathy, S., Limbach, P. A., & Addepalli, B. (2021). Mass Spectrometry-Based Methods for Characterization of Hypomodifications in Transfer RNA. *Epitranscriptomics*, 555-592.
- [47] Torsin, L. I., Petrescu, G. E., Sabo, A. A., Chen, B., Brehar, F. M., Dragomir, M. P., & Calin, G. A. (2021). Editing and chemical modifications on non-coding RNAs in cancer: a new tale with clinical significance. *International Journal of Molecular Sciences*, 22(2), 581.
- [48] Vaidyanathan, P. P., AlSadhan, I., Merriman, D. K., Al-Hashimi, H. M., & Herschlag, D. (2017). Pseudouridine and N6-methyladenosine modifications weaken PUF protein/RNA interactions. *RNA*, 23(5), 611-618.
- [49] Wang, C., Hou, X., Guan, Q., Zhou, H., Zhou, L., Liu, L., . . . Liu, H. (2023). RNA modification in cardiovascular disease: implications for therapeutic interventions. *Signal Transduction and Targeted Therapy*, 8(1), 412.
- [50] Westhof, E. (2019). Pseudouridines or how to draw on weak energy differences. *Biochemical and biophysical research communications*, 520(4), 702-704.
- [51] Yamauchi, Y., Nobe, Y., Izumikawa, K., Higo, D., Yamagishi, Y., Takahashi, N., . . . Taoka, M. (2016). A mass spectrometry-based method for direct determination of pseudouridine in RNA. *Nucleic acids research*, 44(6), e59-e59.
- [52] Yu, Y.-T., & Meier, U. T. (2014). RNA-guided isomerization of uridine to pseudouridine—pseudouridylation. *RNA biology*, 11(12), 1483-1494.
- [53] Zhang, M., Jiang, Z., Ma, Y., Liu, W., Zhuang, Y., Lu, B., . . . Yi, C. (2023). Quantitative profiling of pseudouridylation landscape in the human transcriptome. *Nature Chemical Biology*, 1-11.
- [54] Zhang, Y., Lu, L., & Li, X. (2022). Detection technologies for RNA modifications. *Experimental & Molecular Medicine*, 54(10), 1601-1616.
- [55] Zhao, B. S., & He, C. (2015). Pseudouridine in a new era of RNA modifications. *Cell research*, 25(2), 153-154.
- [56] Zimna, M., Dolata, J., Szweykowska-Kulinska, Z., & Jarmolowski, A. (2023). The expanding role of RNA modifications in plant RNA polymerase II transcripts: highlights and perspectives. *Journal of Experimental Botany*, erad136.



# Innovative Complex Coacervates of Gelatin and Sodium Carboxymethyl Cellulose for Cinnamaldehyde Delivery: Impact of Processing Conditions on Characteristics and Bioactivity

Mahran Abdulla<sup>1,2</sup>, Shuqin Xia<sup>1,\*</sup>

<sup>1</sup>School of Food Science and Technology, Collaborative Innovation Center of Food Safety and Quality Control, Jiangnan University, 1800 Lihu Road, Wuxi, Jiangsu 214122, P. R. China

<sup>2</sup>Food Science Department, Faculty of Agriculture, Cairo University, 12613 Giza, Egypt

\* Corresponding author

Received: 30 Oct 2023; Received in revised form: 02 Dec 2023; Accepted: 10 Dec 2023; Available online: 31 Dec 2023

©2023 The Author(s). Published by Infogain Publication. This is an open access article under the CC BY license

(<https://creativecommons.org/licenses/by/4.0/>).

**Abstract**— Cinnamaldehyde (CA) has a special flavor, and numerous bioactivities; nevertheless, it possesses a high level of volatility, low solubility in water, and limited stability. To address the shortcomings of CA and enhance its use in foods, CA-loaded microcapsules were created by complex coacervation. Gelatin (GL) and carboxymethyl cellulose (CMC) were used as the wall materials of CA. Ideal conditions for obtaining encapsulation efficiency and morphology were found for core/wall ratio 1:1 (w: w), and an emulsification speed 15,000 rpm. The optimized microcapsule formulation demonstrates an encapsulation efficacy of  $87.949 \pm 1.229$  % for CA with payload  $41.276 \pm 4.189$ % and a size of  $26.093 \pm 0.575$ µm. The examination of Fourier-transform infrared (FTIR) spectra of GL, CMC, GL-CMC complex coacervates and CA microcapsules exhibited an electrostatic attraction among GL and CMC molecules and the creation of hydrogen bonds among core (CA) and shell materials. When 1:1 core: wall ratio and 9000 rpm emulsification speed utilized in the microencapsulation of CA, the thermal stability significantly enhanced, possessed a slow-release property in ethanol 50%, and enhanced the antibacterial activity of CA.

**Keywords**— Complex coacervates, Cinnamaldehyde, Core/wall ratio, Emulsification, Encapsulation efficiency, Antimicrobial activity, Release properties.

## I. INTRODUCTION

Cinnamaldehyde (CA), the primary compound found in cinnamon oil obtained from cinnamon bark, is an aromatic aldehyde with low water solubility and has received approval from the Joint FAO/WHO Expert Committee on Food Additives (JECFA) for its use as a potential food-flavoring agent [1,2]. Furthermore, CA possesses garnered increased attention because of its inherent properties such as antibacterial, anticancer, antioxidant, insecticidal, and anti-inflammatory effects [3]. Despite these positives, there are significant challenges associated with its direct application, including low solubility in water, high volatility, susceptibility to harsh environmental conditions

(e.g., high temperatures, elevated ionic strength, and extreme pH), interaction with active components, and the potential to introduce an undesirable flavor that may impact the overall taste of foods [3,4]. To address these issues, various encapsulation methods have been explored to enhance its solubility in water and regulate its volatility, preserve its flavor, and enable sustained release over an extended period.

Microencapsulation involves enclosing various food components within a tiny protective shell or coating to safeguard them and enable their gradual release. This technology is extensively utilized to enhance the application of CA, which faces limitations. Among the

various techniques available, complex coacervation-based microencapsulation stands out due to its substantial capacity for loading, effective sustained release, and resistance to high temperatures, all achieved under mild conditions [5,6]. Complex coacervation hinges on the electrostatic attraction among biopolymers with opposite charges [7]. The formation of coacervates necessitates careful control of several process parameters, including pH, temperature, ionic strength, stirring speed, biopolymer ratios, molecular weight, and biopolymer concentration [8]. Typically, complex coacervation is performed using positively charged proteins and anionic polysaccharides.

Gelatin (GL) and sodium carboxymethyl cellulose (CMC) are two organic, safe, and environmentally degradable biopolymers that readily dissolve in water, extensively utilized in the pharmaceutical and food sectors [9]. GL, sourced from collagen, possesses excellent gelling, film-forming, and emulsifying properties. CMC, a cellulose derivative created by partially substituting cellulose hydroxyl groups at positions 2, 3, and 6 with carboxymethyl [10], is more commonly used due to its favorable qualities, including biocompatibility, biodegradability, and cost-effectiveness [11]. A study conducted by J. Zhang et al. [12], provided valuable insights and contribute to the creation of microcapsules via complex coacervation employing GL and CMC. These microcapsules have the potential to safeguard bioactive compounds that are sensitive to heat, as well as flavors and food ingredients such as zeaxanthin. Another study by Duhoranimana et al. [13], demonstrated that GL-CMC complex coacervates have the ability to be employed in microencapsulation, safeguard and transport bioactive components and food ingredients that are sensitive to heat. This study also highlighted the function of pH and the mixing ratio of GL to CMC in complex coacervation. Nevertheless, it was noted that high ionic strength and variations in pH can diminish or totally disrupt the electrostatic attraction among GL and CMC, affecting the rheological characteristics of the coacervates [14]. In complex coacervation, it is imperative to optimize the process to produce particles with desired characteristics. Factors such as emulsification speed and the core: wall ratio of microcapsules prepared through complex coacervation are pivotal, as they impact the ultimate attributes of microcapsules, including encapsulation efficiency, particle size, shape, and agglomeration rate [15]. These characteristics, in turn, influence release properties and antimicrobial effectiveness. Hence, this present study aims to investigate how processing conditions, such as emulsification speed and core: wall ratio, influence microcapsule size, shape, encapsulation efficiency, release properties, and antimicrobial activity.

Additionally, the study delves into the thermal stability of CA microcapsules through thermogravimetric analysis.

## II. MATERIALS AND METHODS

### 2.1. Materials

Gelatin (GL) (BLV 225, type B, isoelectric point ranging from 4.70 to 5.20) was sourced from Chengdu Classic Gelatin Co., Ltd. in Sichuan, China. FL9 Sodium carboxymethyl cellulose (CMC) (with a viscosity of 20.0 mPa s and a degree of substitution of 1) was acquired from Yixing Tongda Chemical Co., Ltd. in Jiangsu, China. Cinnamaldehyde (CA) (98%) was procured from Ji'an Jupeng Natural Flavor Oil Co., Ltd. located in Jilin, China. Hexane and Pure Ethanol Absolute were obtained from Sinopharm Chemical Reagent Co., Ltd. in Shanghai, China. Deionized water (Milli-Q) was employed in the preparation of all aqueous solutions.

### 2.2. Preparation of biopolymer solution

Solutions of GL/CMC were prepared at a predetermined mass concentration of 1% by weight. The procedure involved dissolving a specific quantity of GL and CMC in a 9:1 ratio in deionized water. This dissolution process took place with gentle stirring in a bath of water maintained at a temperature of 60°C for a period of 2 hours [16].

### 2.3. Preparation of cinnamaldehyde microcapsules

Microcapsules containing CA were created using a GL/CMC mixture with a ratio of 9:1 (w/w). CA was introduced into the previously prepared solution, where the wall material concentration was set at 1% (weight/volume). This was done while varying the core/wall ratios (1:1 and 2:1, w/w). Subsequently, the mixture was subjected to high-speed dispersion using a device that ran for 2 minutes at different speeds: 9000, 12000, and 15000 revolutions per minute (r/min). Following the emulsification step, the solutions were stirred gently at a temperature of 45°C for a duration of 30 minutes, maintaining an optimal pH of 4.5 with the addition of acetic acid at concentrations of 10%, 1%, and 0.1%, v/v. Afterward, the solution was cooled down using an ice bath. Once the temperature dropped below 15°C, it was maintained for 0.5 hours while stirring at a rate of 400 revolutions per minute (r/m) [17]. The subsequent steps involved allowing the system to settle overnight at 6°C, subsequently centrifugation at 2000 rpm for 4 minutes. The resulting material was then frozen and underwent the process of freeze-drying at  $55 \pm 7$  bar, with the condenser temperature maintained at -78°C, over a period of 48 hours using a Scientz-18N freeze dryer (Ningbo Scientz

Biotechnology Co. Ltd, China). The resulting CA microcapsule powder was stored in a desiccator.

#### 2.4. Morphology of suspension and dried microcapsules

Microcapsule suspensions were examined for their morphology under optical microscopy (BX51, Olympus Corporation, Japan) at a 50× magnification. To study the morphology of the dried microcapsules, a scanning electron microscope (SU8100, JEOL Ltd., Tokyo, Japan) was used. This analysis was performed at a voltage acceleration of 3 kV, and various magnifications were employed. For the scanning electron microscope examination, the microcapsules were initially evenly attached to a specimen holder through the application of double-sided tapes and subsequently applying a thin gold coating [18].

#### 2.5. Particle size

For the determination of the particle size of CA loaded microcapsules before the drying process, a laser particle size analyzer (S3500, Microtrac Inc., USA) was employed. This analyzer was equipped with a sample tank designed for liquid dispersion. Ultrapure water with a pH of 7.0 served as the testing medium [19,20].

#### 2.6. Determination of encapsulation efficiency, and payload

The determination of both free CA and total CA content was carried out in accordance with the method described by Liu et al. [21], using the organic solvent extraction technique. In this process, 0.1 gram of CA microcapsules were dispersed in a 10 mL n-hexane solution. To extract the surface oil, the mixture was oscillated for 30 seconds at ambient temperature and then allowed to settle. The amount of surface oil was determined by measuring the supernatant absorbance at 285 nm. The calibration curve for CA had a linear range of 0.0–8.0 µg/mL, with the standard curve represented by  $y = 0.165x - 0.0205$  ( $R^2 = 0.9992$ ), where  $y$  is the CA absorbance at 285 nm, and  $x$  is the free CA concentration in µg/mL. For the determination of total oil content, 0.1 grams of microcapsules were added to a 70 mL absolute ethanol solution and subjected to sonication (40°C, 20 kHz, 600 W) for 40 minutes, followed by centrifugation at  $12,000 \times g$  for 15 minutes at 25°C. The gathered precipitate underwent three washes with an ethanol solution, and the resulting supernatants from both stages were utilized to determine the total oil amount at 285 nm, following a linear range of CA from 0.0–8.0 µg/mL, with a measured standard curve of  $y = 0.1229x - 0.002$  ( $R^2 = 0.9992$ ), where  $y$  is the absorbance of CA at 285 nm, and  $x$  is the concentration (µg/mL) of free CA. The encapsulation efficiency and payload of microcapsules were computed by equations (1) and (2), respectively.

$$EE(\%) = (X1 - Xs) / X1 \times 100 \quad (1)$$

$$PL(\%) = X1 / X_m \times 100 \quad (2)$$

In these equations,  $X_1$  represents the total weight (g) of CA in the microcapsules,  $X_2$  is the mass (g) of CA initially loaded in the system,  $X_s$  is the mass (g) of oil on the surface of the microcapsules, and  $X_m$  corresponds to the weight of dried CA microcapsules.

#### 2.7. Thermal gravimetric analysis (TGA)

Thermal gravimetric analysis was conducted employing a thermal gravimetric analyzer (TGA/SDTA851e, Mettler-Toledo Corporation, Switzerland). Samples, including the coacervates, free CA and microcapsules each weighing 3–5 mg, were carefully measured on the TGA microbalance. They were then subjected to heating at a rate of 20°C per minute, ranging from 25 to 500°C. Nitrogen gas, flowing at a rate of 20 ml per minute, served as the heating medium. This analysis was conducted to assess the thermal characteristics of the sample powders [3].

#### 2.8. Fourier transform infrared spectroscopy (FTIR)

The FTIR (Fourier-transform infrared) spectra of various materials, including free CA, GL, CMC, complex coacervates, and dried microcapsules, were obtained at ambient temperature (25°C). This analysis was conducted using a Nicolet iS10 FTIR spectrophotometer from Thermo Electron Corp. in Madison, WI. The spectra were collected over a wavenumber range from 400 to 4000  $\text{cm}^{-1}$  with a resolution of 4  $\text{cm}^{-1}$ , and the total scan time for each sample was 32 scans. The samples were blended with potassium bromide (KBr) at a ratio (1:100). The resulting mixture was ground and then pressed onto a ZnSe plate. The sample spectrum was acquired with air spectrum subtraction. These procedures were in accordance with the methodology outlined by Q. Liu et al. [22].

#### 2.9. Determination of release properties

The release properties of CA in a 50% ethanol solution were conducted following the methodology described by Bustos C et al. [23], albeit with some adjustments. In this modified procedure, 10 mg of microcapsules or 4.3 mg of free CA were placed within a dialysis bag (cut off 14000 daltons, Sinopharm, Shanghai, China), and these bags were subsequently immersed in 100 ml of a solution consisting of 50% ethanol and 50% water. This 50% ethanol solution is a recognized standard simulant, referred to as simulant D2, utilized for migration studies as per CREU [24]. The samples were placed in an orbital shaking incubator, maintaining a temperature of 25°C and an agitation rate of 20 revolutions per minute in a dark environment throughout the entire testing duration. At predetermined time intervals, the absorbance of the solutions was assessed at 285 nm. After each

measurement, the samples were returned to the system to maintain consistent conditions throughout the experiment. The cumulative release of CA was calculated using equation (3).

$$\text{Cumulative release (\%)} = R1/R2 \times 100 \quad (3)$$

in this equation, R1 and R2 depict the masses of released CA and encapsulated CA, respectively.

### 2.10. Determination of antimicrobial ability

To investigate the antimicrobial properties of free and encapsulated CA, two common microbial strains, namely *Escherichia coli* (*E. coli*) and *Staphylococcus aureus* (*S. aureus*), were selected. These microbial strains were initially activated by being cultured overnight in Muller Hinton broth using an incubator set at 37°C. Subsequently, they were diluted to reach the colony count equivalent to a standardized inoculum (0.5 Mac-Farland) as per the methodology outlined by S. Zhang et al. [24] with some slight modifications. For the antimicrobial tests, CA, or CA microcapsules, along with 200 µL of the microbial suspension, were introduced into the cone-shaped flasks containing 100 mL of sterilized Muller Hinton broth. In these experiments, the concentration of CA employed was 0.02 mg/mL. Control samples were generated by adding 200 µL of microbial suspension into 100 mL of sterilized Muller Hinton broth in a separate cone-shaped flask. All the cone-shaped flasks were sealed using plastic film and positioned in a stable-temperature incubation shaker operating at 150 rpm and maintained at 37°C. The turbidity of each experimental group was measured at 600 nm every 2 hours to assess the growth condition of the bacteria under examination.

### 2.11. Statistical analysis

The findings are presented as the mean value ± standard deviation and were analyzed using one-way ANOVA. Statistical significance among mean values was evaluated using Duncan's multiple range tests with a confidence level of 95%. ( $p < 0.05$ ) using SPSS 26.0 software (SPSS Inc., Chicago, IL, USA).

## III. RESULTS AND DISCUSSION

### 3.1. Morphology and particle size of microcapsules

When the unit surface area was kept constant, the spherical shape exhibited a comparatively larger volume, providing increased capacity for encapsulating the core substance. Consequently, the spherical form was preferred in the process of microcapsule preparation. Optical microscopic images and particle size data, as shown in Fig. 1, indicated that all the microcapsules possessed a spherical shape. Lower emulsification speed promoted clustering and the

creation of larger multinuclear capsules, while higher homogenization speeds notably reduced the mean particle diameter and the extent of aggregation. This reduction can be attributed to the shearing force's capacity to break larger droplets into smaller ones and prevent collisions, as previous study [25,26]. Furthermore, an increase in the core-to-wall ratio led to a gradual increase in the mean particle size. This was because a greater quantity of CA became entrapped within the microcapsules, causing more mononuclear microcapsules to collide and accumulate into larger multinuclear microcapsules [27,28].

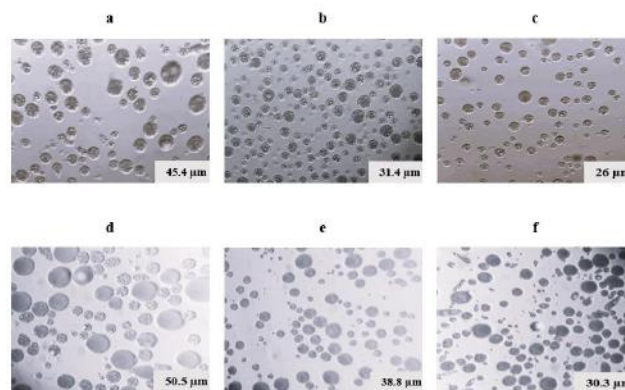


Fig. 1: Morphology of microcapsule suspensions (a, 9000 and 1:1; b, 12000 and 1:1; c, 15000 and 1:1; d, 9000 and 2:1; e, 12000 and 2:1; f, 15000 and 2:1).

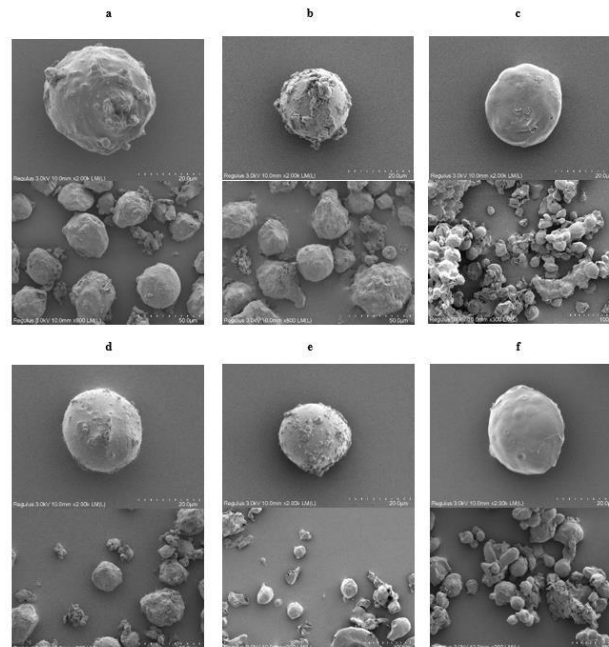


Fig. 2: Electron micrographs of dried microcapsules (a, 9000 and 1:1; b, 12000 and 1:1; c, 15000 and 1:1; d, 9000 and 2:1; e, 12000 and 2:1; f, 15000 and 2:1).

The microstructure of CA-loaded microcapsules was assessed using a scanning electron microscope (Fig. 2).



The images of the microcapsule particles illustrated the influence of homogenization speed on the microstructure and surface properties of the particles. As shown in Fig. 2a, 2b, 2d and 2e the microcapsules are almost spherical shape with rough and compact surface and some aggregation. However, as shown in Fig. 2c and 2f, Microcapsules created at an emulsification speed of 15,000 rpm exhibited a spherical shape with a compact and smoother surface, a higher degree aggregation. A compact wall structure was advantageous for enhancing the barrier properties of the CA-loaded microcapsules, ensuring effective protection and retention of CA. It's worth noting that a study conducted by Muhoza et al. [29], found that freeze-drying could significantly disrupt the microstructure of multinuclear microcapsules.

### 3.2. Efficacy of Cinnamaldehyde microcapsules Encapsulation and payload

The results pertaining to the efficiency of encapsulation (EE) and payload (PL) of CA microcapsules, which were created using the GL-CMC complex coacervate as a wall material, are summarized in Table 1. Our findings demonstrated that the highest EE and PL were achieved at higher emulsification speeds, it's important to note that elevated emulsification pressures generate emulsions with smaller droplet sizes and create new interfaces, which can lead to re-coalescence and an "over-processing" effect, as observed in the study by Jafari et al. [30]. Similar results were observed in a study by Esfahani et al. [31], where smaller particles and increased particle agglomeration were observed with higher emulsification speeds during the microencapsulation of fish oil, resulting in enhanced encapsulation efficiency. As indicated in Table 1, when the core-to-wall ratio rose from 1:1 to 2:1, there was a reduction in encapsulation efficiency. This reduction can be ascribed to the insufficient availability of wall materials to fully coat the entire core. Consequently, a higher concentration of unencapsulated core material remained, leading to losses during the encapsulation process. This finding aligns with the previous study [32,33].

Table 1. Encapsulation Efficiency, payload, and Particle size of Cinnamaldehyde microcapsules.

Sample	Encapsulation efficiency (%)	Payload (%)	Particle size (µm)
M1	86.166 ± 0.361 <sup>b</sup>	37.444 ± 0.978 <sup>c</sup>	45.414 ± 0.903 <sup>b</sup>
M2	87.036 ± 0.327 <sup>ab</sup>	38.929 ± 0.982 <sup>bc</sup>	31.463 ± 2.581 <sup>d</sup>
M3	87.949 ±	41.276 ±	26.093 ±

	1.229 <sup>a</sup>	4.189 <sup>ab</sup>	0.575 <sup>e</sup>
M4	79.314 ± 0.565 <sup>d</sup>	33.435 ± 0.913 <sup>d</sup>	50.492 ± 1.875 <sup>a</sup>
M5	84.115 ± 0.324 <sup>c</sup>	43.556 ± 0.889 <sup>a</sup>	38.863 ± 3.51 <sup>c</sup>
M6	83.457 ± 0.543 <sup>c</sup>	41.721 ± 1.368 <sup>ab</sup>	30.381 ± 0.411 <sup>d</sup>

M1: emulsification speed at 9000 and core-to-wall ratio 1:1, M2: emulsification speed at 12000 and core-to-wall ratio 1:1, M3: emulsification speed at 15000 and core-to-wall ratio 1:1, M4: emulsification speed at 9000 and core-to-wall ratio 2:1, M5: emulsification speed at 12000 and core-to-wall ratio 2:1, M6: emulsification speed at 15000 and core-to-wall ratio 2:1.

### 3.3. Thermal stability of CA and CA microcapsules

Analysis of thermal stability was carried out on CA, GL-CMC coacervates, and CA microcapsules, spanning a temperature range from 25 to 500°C, aiming to assess the heat resistance of both CA microcapsules and the GL-CMC complex coacervate matrix. The thermogravimetric (TGA) and differential thermogravimetric (DTG) profiles for CA, GL-CMC coacervates, and CA microcapsules are illustrated in Fig. 3. TGA data indicated that free CA experienced a mass loss of 3.3% at 100°C, primarily due to CA volatilization and water evaporation. At 195°C, both TGA and DTG curves exhibited a pronounced weight loss, reaching approximately 89%. A sharp weight mass loss of 89% occurred at 195 °C, indicating rapid volatilization of CA, with only 4.5% of its weight remaining at 500 °C. On the contrary, the GL-CMC complex coacervates displayed a more gradual weight loss, maintaining about 30% of their weight until 500°C, and a DTG minimum was noted at 334°C. This suggests that the shell materials demonstrated resistance to heat and displayed remarkable sustained release characteristics, as reported by Duhoranimana et al. [13]. Comparatively, the stability of microcapsules with core-to-wall ratios of 1:1 and 2:1 (w/w) was considerably greater than that of free CA. Additionally, the graph suggests that an increased core-to-wall ratio resulted in an elevated rate of thermal weight reduction at the same temperature, implying reduced embedding stability. This might be linked to the impact of the core-to-wall ratio on the formation of tight hydrogen bonds between the coacervates and core material, as discussed by Yu et al. [34]. Moreover, microcapsules created at an emulsification speed of 9,000 rpm with a core-to-wall ratio of 1:1 exhibited superior stability compared to other microcapsules, possibly due to the presence of large multinuclear capsules with thick

interfacial membranes, contributing to the stability of the core material and sustained release [35].

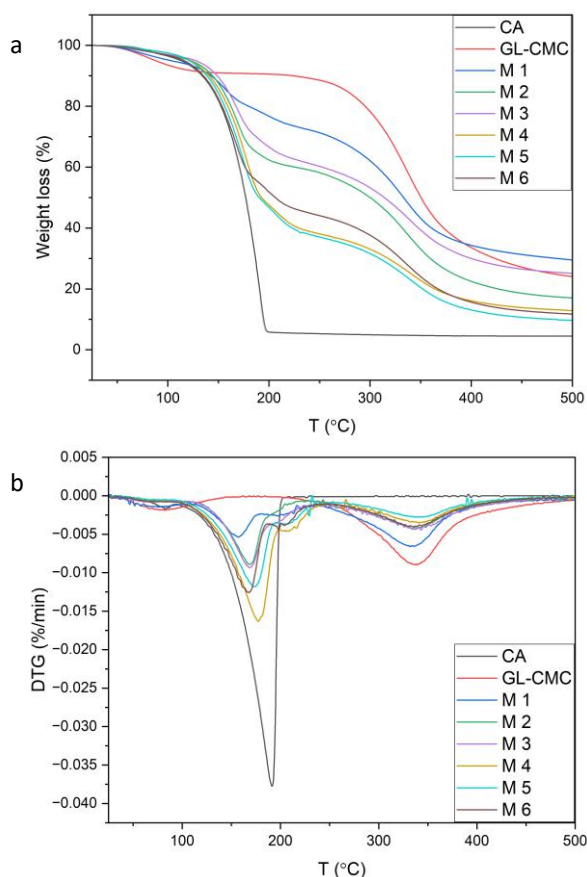


Fig. 3: The TGA (a) and DTG (b) curves of CA, GL-CMC coacervates and CA loaded microcapsules between the temperatures of 25 °C–500 °C.

The combined analysis of TGA and DTG curves demonstrated that the thermal breakdown of different microcapsules could be segmented into three stages. In the first stage, from 25 to 100°C, slight variations occurred, primarily because of water evaporation, resulting in a weight loss of approximately 5%. The second stage, around 200 °C, demonstrated a weight loss of 23%, 37%, 36%, 52%, 53%, and 50%, respectively, for the CA microcapsules. This was significantly higher compared to the almost flat thermal decomposition curve of the GL-CMC complex coacervate at this stage, indicating the liberation of surface core material and a portion of the internal core material. At 350°C, the weight loss increased to approximately 56%, 67%, 62%, 77%, 79%, and 76%, respectively, signifying further core material release. The third stage, from 350 to 500°C, showed a mass loss of 13% for the CA microcapsules, during which the microcapsule mass loss curve aligned with the complex coacervate mass loss curve, indicating the nearly complete evaporation of CA at this stage. Subsequently, this stage primarily

involved the breakdown of the wall substances, in accordance with previous report [36]. Our results were consistent with a research investigation on the microencapsulation of CA, where pectin and GL coacervates were employed [3].

### 3.4. FTIR features of GL/CMC coacervates and cinnamaldehyde microcapsules.

FTIR analysis was employed to investigate the interaction occurring between the wall materials (GL and CMC) and the core material. The FTIR spectra of GL, CMC, coacervates consisting of GL/CMC, and CA-loaded microcapsules are depicted in Fig. 4. In the FTIR spectrum of GL, a prominent peak was evident at 3436  $\text{cm}^{-1}$ , indicative of Hydrogen bonds formed within a molecule manifested as elongation oscillations of N–H bonds ( $\nu\text{N-H}$ ). A secondary peak at 2960  $\text{cm}^{-1}$  corresponded to the asymmetric stretching vibrations of C–H bonds ( $\nu\text{C-H}$ ) [37]. Notably, the amide bands displayed three distinct peaks. The peak observed at 1640  $\text{cm}^{-1}$  corresponded to the elongation vibrations of the carbonyl group ( $\nu\text{C=O}$ ) within the amide I structure [12]. At 1542  $\text{cm}^{-1}$ , a peak denoted the flexing oscillations of the N–H bond ( $\delta\text{N-H}$ ) in amide II, encompassing vibrations of –NH–R bonds at higher wavenumbers and –NH<sub>3</sub> bonds at lower wavenumbers. A weaker peak 1236  $\text{cm}^{-1}$  denoted the bending modes of the C–N bond ( $\delta\text{C-N}$ ) of amide III [38]. Furthermore, an intense absorption peak around 1450  $\text{cm}^{-1}$  suggested the presence of cis configuration in peptide bonds, likely due to proline or its hydroxylated form, hydroxyproline, within GL, in contrast to the trans configuration found in the majority of protein structures.

In the FTIR spectrum of CMC, a prominent peak at 3432  $\text{cm}^{-1}$  was identified, associated with intramolecular hydrogen bonding ( $\nu\text{O-H}$ ) within the cellulose structure. The secondary peak at 2919  $\text{cm}^{-1}$  was indicative of the methylene group in CMC. Prominent peaks at 1626  $\text{cm}^{-1}$  and 1423  $\text{cm}^{-1}$  were assigned to the symmetrical and asymmetrical elongation oscillations of ionized –COO– groups ( $\nu\text{-COO-}$ ), respectively [39]. Furthermore, a robust absorption at 1328  $\text{cm}^{-1}$  signified the flexing oscillations of –CH<sub>3</sub> bonds, and the peak at 1057  $\text{cm}^{-1}$  was associated with the elongation vibrations of C–O bonds ( $\nu\text{C-O}$ ) [38]. The FTIR spectra obtained from the GL-CMC complex coacervates were essentially a combination of the spectra of pure GL and CMC, with certain absorption peaks shifted positions. A shift towards higher wavenumbers, from 1542  $\text{cm}^{-1}$  to 1548  $\text{cm}^{-1}$ , indicated the disappearance of the –NH<sub>3</sub> vibration peak at the lower wavenumber. This shift left only the –NH–R vibration peak. Concurrently, the disappearance of the absorption peaks observed at 1626  $\text{cm}^{-1}$  and 1423  $\text{cm}^{-1}$ , which are associated with the elongation vibrations of –COO– groups in CMC. These

shifts in absorption peaks supported the notion of electrostatic interaction occurring between the  $-NH_3^+$  bond of GL and the  $-COO^-$  bond of CMC in the process of GL-CMC complex coacervate formation. Importantly, apart from electrostatic interactions, no additional chemical bonds participated in the process of GL-CMC complex coacervate formation, consistent with the findings of Azadirachta et al. [40]. Furthermore, the peaks associated with stretching vibrations of  $-OH$  and  $N-H$  in the GL-CMC complex coacervates transitioned from  $3432\text{ cm}^{-1}$  and  $3436\text{ cm}^{-1}$  to  $3424\text{ cm}^{-1}$ , respectively. potentially due to alterations in conformation and weak intermolecular interactions among the molecules of GL and CMC, aligning with findings by Lii et al. [41]. The  $C-H$  stretching vibration peaks also transitioned from  $2960\text{ cm}^{-1}$  and  $2919\text{ cm}^{-1}$  to  $2941\text{ cm}^{-1}$ , suggesting alterations in conformation occurring between GL and CMC molecules in the process of complex coacervate formation. The spectra of CA-loaded microcapsules exhibited remarkable spectral shifts, reflecting the interaction between CA and the shell materials. Fresh peaks with elevated intensity emerged at  $1680\text{ cm}^{-1}$  and  $1620\text{ cm}^{-1}$ , characteristic of  $C=O$  and aromatic vibrations in CA [42]. These findings are consistent with previous research on the characterization of CA-loaded microcapsules prepared with pectin and GL complex coacervates [3].

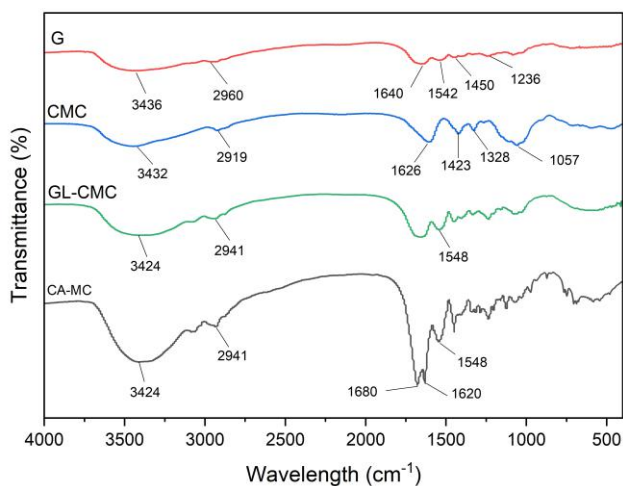


Fig. 4: FTIR spectra of G, CMC and GL-CMC and CA-Microcapsules (CA-MC).

### 3.5. release properties

The study investigated the release pattern of CA from microcapsule in a 50% ethanol solution simulating food conditions, aiming to assess the stability of these microcapsules within food matrix. The release patterns, depicted in Fig. 5. The dissolution profiles of free CA demonstrated a swift release, reaching 70.8% within 10

minutes and peaking at 82% within 20 minutes. In contrast, the cumulative release curves for CA microcapsules exhibited a notably slower rate of increase. Initially, a swift release (17-28%) occurred within the first 10 minutes, attributed to the surface-absorbed CA and void-released content [43], Subsequently, encapsulated CA within the microcapsules exhibited a gradual release, reaching maximum cumulative release (60-80%) around 150 minutes. Elevating the core-to-wall ratio from 1:1 to 2:1 heightened the cumulative release rate, indicative of reduced protective effects of the wall membrane due to enhanced loading capacity of microcapsules [44]. Consistent with (Khatibi et al. [45], our study observed that an elevated core: wall ratio led to increased cumulative release, akin to the behavior of *Zataria multiflora* Boiss essential oil. Additionally, augmenting homogenization speed amplified the cumulative release rate, in line with the findings of Huang et al. [46], who revealed that Larger multinuclear capsules exhibited enhanced CA retention due to a thicker interfacial membrane. Conversely, microcapsules with a smaller mean particle size exhibited notably lower retention rates. Briefly, microcapsules produced with a core-to-wall ratio of 1:1 and an emulsification speed of 9000 rpm exhibited a lower cumulative release of 60%.

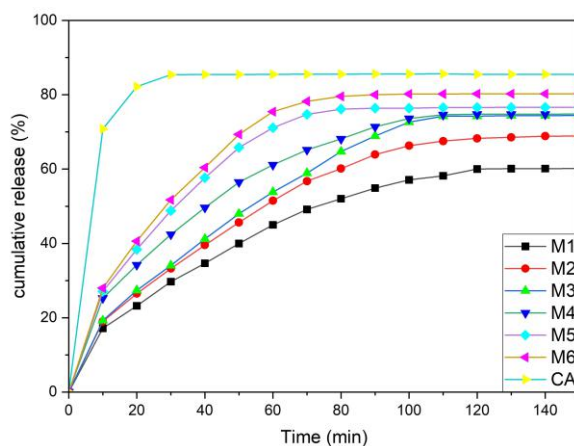


Fig. 5: Release profile of free and microencapsulated cinnamaldehyde in ethanol 50%.

### 3.6. The antibacterial activity

The antibacterial efficacy of both free CA and CA encapsulated within microcapsules was assessed through the examination of growth curves for the tested bacteria. Fig. 6a illustrates the growth phases (lag, exponential, and stabilization) of *S. aureus*. It was observed that the growth of *S. aureus* in both free and encapsulated CA was more constrained in comparison to the nutrient broth (control) throughout all phases, confirming the antibacterial efficacy of CA against *S. aureus* [47]. The growth rate of *S. aureus*

in encapsulated CA, particularly in microcapsule with a low release profile (M1), was slower than in free CA, suggesting a more robust antibacterial efficacy of encapsulated CA against *S. aureus*. This enhanced effect was attributed to the delayed-release property and improved dispersion of CA facilitated by microcapsules in water, thereby enhancing its efficacy in constraining the metabolism and growth of bacterial cells [48]. As time progresses, the growth curves of free and encapsulated CA gradually aligned, probably because the ongoing erosion of the microcapsule structure diminishes the slow-release characteristic and dispersion capability, thereby diminishing the antibacterial effectiveness of encapsulated CA. The growth curve of *E. coli* mirrored that of *S. aureus* (Fig. 6b). Notably, both free and encapsulated CA demonstrated greater effectiveness in inhibiting *E. coli* compared to *S. aureus*. It's worth noting that gram-positive bacteria, such as *S. aureus*, typically possess a thicker outer cell wall, which may contribute to higher resistance. In contrast, gram-negative bacteria like *E. coli* lack a thick cell wall, this structural distinction may suggest lower resistance in gram-negative bacteria to antibacterial agents [49]. The outcomes presented above underscored the potent antibacterial capability of CA, further augmented through microencapsulation.

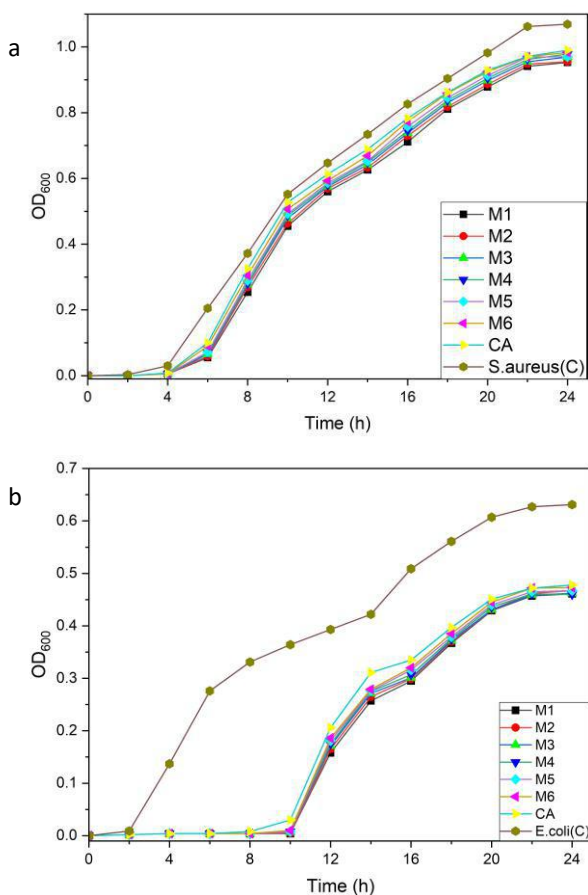


Fig. 6. The antibacterial efficacy of free and encapsulated cinnamaldehyde against *S. aureus* (a) and *E. coli* (b).

#### IV. CONCLUSION

To address the shortcomings of CA, such as limited stability and low solubility in water, in this study, GL and CMC complex coacervates were used as novel shell materials to microencapsulate CA. The CA-loaded complexes achieved optimal encapsulation efficiency ( $87.949 \pm 1.229$  %), morphology and particle size ( $26.093 \pm 0.575$   $\mu\text{m}$ ) with a core-to-wall ratio of 1:1, and emulsification speed of 15,000 rpm. The CA-loaded microcapsules had greater resistance to heat compared to free CA. The GL-CMC complex coacervate, as outer layer material, enhanced the sustained-release characteristics of CA. The antibacterial efficacy of CA was enhanced after encapsulation. This study offers valuable insights for formulating an optimal microcapsule carrier capable of delivering cinnamaldehyde and various flavors with considerable potential for applications in the food industry by using complex coacervates of CMC and gelatin under different processing conditions.

#### ACKNOWLEDGEMENTS

The authors greatly appreciate the joint support for study by the program of "Collaborative innovation center of food safety and quality control in Jiangsu Province".

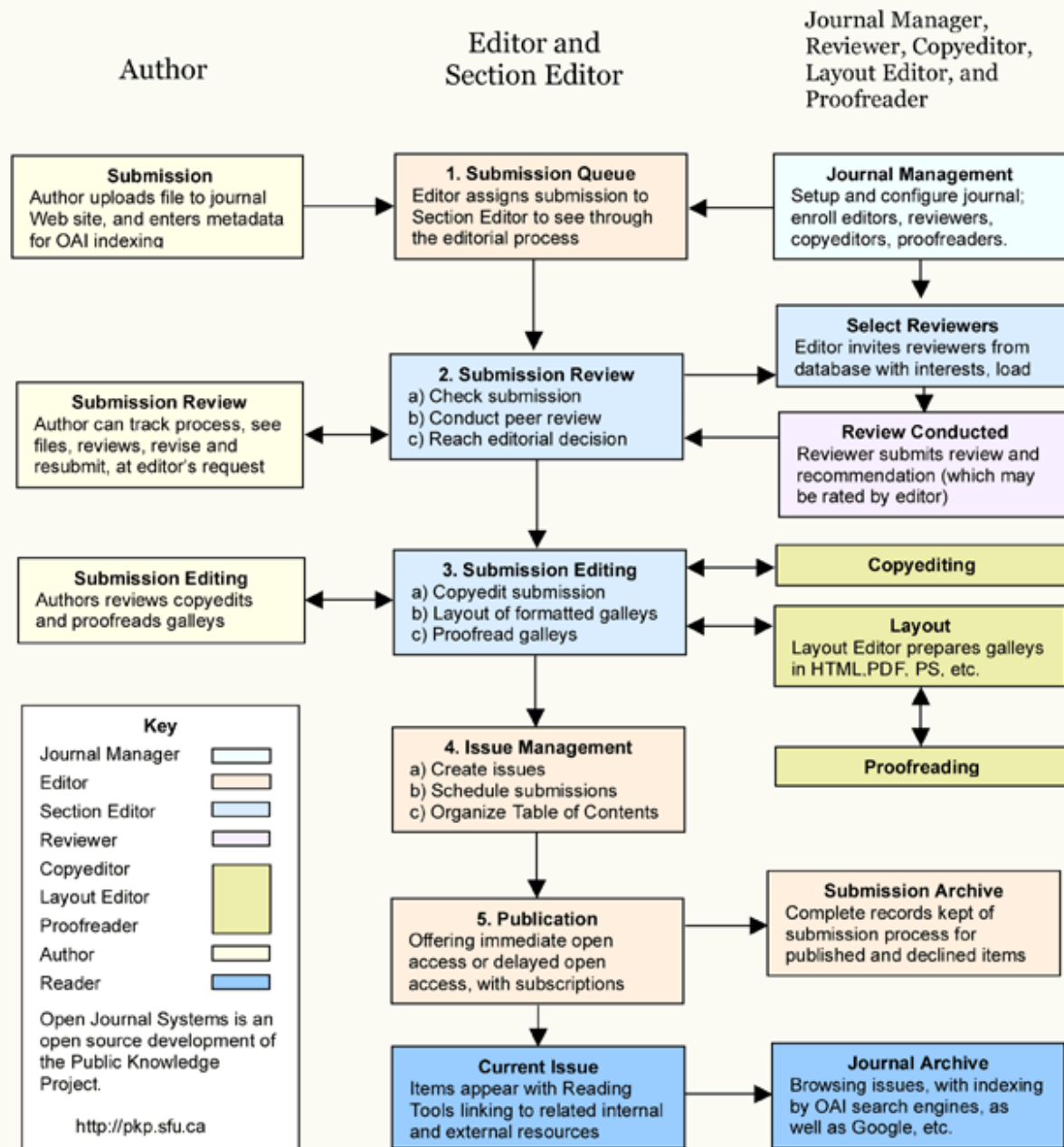
#### REFERENCES

- [1] E. Chen, S. Wu, D. J. McClements, B. Li, and Y. Li, "Influence of pH and cinnamaldehyde on the physical stability and lipolysis of whey protein isolate-stabilized emulsions," *Food Hydrocoll.*, vol. 69, pp. 103–110, 2017.
- [2] L. Lei, Z. He, H. Chen, D. J. McClements, B. Li, and Y. Li, "Microstructural, rheological, and antibacterial properties of cross-linked chitosan emulgels," *Rsc Adv.*, vol. 5, no. 121, pp. 100114–100122, 2015.
- [3] B. Muhoza, S. Xia, J. Cai, X. Zhang, E. Duhoranimana, and J. Su, "Gelatin and pectin complex coacervates as carriers for cinnamaldehyde: Effect of pectin esterification degree on coacervate formation, and enhanced thermal stability," *Food Hydrocoll.*, vol. 87, no. August 2018, pp. 712–722, 2019, doi: 10.1016/j.foodhyd.2018.08.051.
- [4] Y. Tian, Y. Zhu, M. Bashari, X. Hu, X. Xu, and Z. Jin, "Identification and releasing characteristics of high-amylose corn starch–cinnamaldehyde inclusion complex prepared using ultrasound treatment," *Carbohydr. Polym.*, vol. 91, no. 2, pp. 586–589, 2013.
- [5] Y. Lv, F. Yang, X. Li, X. Zhang, and S. Abbas, "Formation of heat-resistant nanocapsules of jasmine essential oil via gelatin/gum arabic based complex coacervation," *Food*

- Hydrocoll.*, vol. 35, pp. 305–314, 2014.
- [6] A. S. Prata and C. R. F. Grosso, “Production of microparticles with gelatin and chitosan,” *Carbohydr. Polym.*, vol. 116, pp. 292–299, 2015.
- [7] N. Devi, M. Sarmah, B. Khatun, and T. K. Maji, “Encapsulation of active ingredients in polysaccharide–protein complex coacervates,” *Adv. Colloid Interface Sci.*, vol. 239, pp. 136–145, 2017.
- [8] De Kruijff et al., “Complex coacervation of proteins and anionic polysaccharides,” *Curr. Opin. Colloid Interface Sci.*, vol. 9, no. 5, pp. 340–349, 2004.
- [9] Hazirah et al., “Effect of xanthan gum on the physical and mechanical properties of gelatin-carboxymethyl cellulose film blends,” *Food Packag. Shelf Life*, vol. 9, pp. 55–63, 2016.
- [10] Tong et al., “Preparation and properties of pullulan–alginate–carboxymethylcellulose blend films,” *Food Res. Int.*, vol. 41, no. 10, pp. 1007–1014, 2008.
- [11] Carpineti et al., “ $\beta$ -Lactoglobulin–carboxymethylcellulose core–shell microparticles: Construction, characterization and isolation,” *J. Food Eng.*, vol. 131, pp. 65–74, 2014.
- [12] J. Zhang et al., “Nanoencapsulation of zeaxanthin extracted from *Lycium barbarum* L. by complex coacervation with gelatin and CMC,” *Food Hydrocoll.*, vol. 112, no. December 2019, p. 106280, 2021, doi: 10.1016/j.foodhyd.2020.106280.
- [13] E. Duhoranimana et al., “Effect of sodium carboxymethyl cellulose on complex coacervates formation with gelatin: Coacervates characterization, stabilization and formation mechanism,” *Food Hydrocoll.*, vol. 69, pp. 111–120, 2017, doi: 10.1016/j.foodhyd.2017.01.035.
- [14] Muhoza et al., “Gelatin and high methyl pectin coacervates crosslinked with tannic acid: The characterization, rheological properties, and application for peppermint oil microencapsulation,” *Food Hydrocoll.*, vol. 97, no. June, p. 105174, 2019, doi: 10.1016/j.foodhyd.2019.105174.
- [15] J. C. Roy, S. Giraud, A. Ferri, R. Mossotti, J. Guan, and F. Salaün, “Influence of process parameters on microcapsule formation from chitosan—Type B gelatin complex coacervates,” *Carbohydr. Polym.*, vol. 198, pp. 281–293, 2018.
- [16] Liu et al., “Fabrication of low environment-sensitive nanoparticles for cinnamaldehyde encapsulation by heat-induced gelation method,” *Food Hydrocoll.*, vol. 105, no. February, p. 105789, 2020, doi: 10.1016/j.foodhyd.2020.105789.
- [17] E. Duhoranimana et al., “Thermodynamic characterization of Gelatin–Sodium carboxymethyl cellulose complex coacervation encapsulating Conjugated Linoleic Acid (CLA),” *Food Hydrocoll.*, vol. 80, pp. 149–159, 2018, doi: 10.1016/j.foodhyd.2018.02.011.
- [18] Xu et al., “Effect of Ultrasound Immersion Freezing on the Quality Attributes and Water Distributions of Wrapped Red Radish,” 2015, doi: 10.1007/s11947-015-1496-x.
- [19] L. Qiu, M. Zhang, B. Bhandari, Z. Fang, and Y. Liu, “Size reduction of raw material powder: The key factor to affect the properties of wasabi (*Eutrema yunnanense*) paste,” *Adv. Powder Technol.*, vol. 30, no. 8, pp. 1544–1550, 2019.
- [20] G. Wu, M. Zhang, Y. Wang, K. J. Mothibe, and W. Chen, “Production of silver carp bone powder using superfine grinding technology: Suitable production parameters and its properties,” *J. Food Eng.*, vol. 109, no. 4, pp. 730–735, 2012.
- [21] Liu et al., “Int J of Food Sci Tech - 2022 - Liu - Tannic acid modulated the wall compactness of cinnamaldehyde-loaded microcapsules and.pdf,” *Int. J. Food Sci. Technol.*, 2022.
- [22] Q. Liu et al., “Food Hydrocolloids Fabrication of low environment-sensitive nanoparticles for cinnamaldehyde encapsulation by heat-induced gelation method,” *Food Hydrocoll.*, vol. 105, no. October 2019, p. 105789, 2020, doi: 10.1016/j.foodhyd.2020.105789.
- [23] R. O. Bustos C, F. V. Alberti R, and S. B. Matiacevich, “Edible antimicrobial films based on microencapsulated lemongrass oil,” *J. Food Sci. Technol.*, vol. 53, no. 1, pp. 832–839, 2016, doi: 10.1007/s13197-015-2027-5.
- [24] S. Zhang, M. Zhang, Z. Fang, and Y. Liu, “Preparation and characterization of blended cloves/cinnamon essential oil nanoemulsions,” *LWT*, vol. 75, pp. 316–322, 2017, doi: https://doi.org/10.1016/j.lwt.2016.08.046.
- [25] T. Feng, C. Fan, X. Wang, X. Wang, S. Xia, and Q. Huang, “Food-grade Pickering emulsions and high internal phase Pickering emulsions encapsulating cinnamaldehyde based on pea protein-pectin-EGCG complexes for extrusion 3D printing,” *Food Hydrocoll.*, vol. 124, no. PA, p. 107265, 2022, doi: 10.1016/j.foodhyd.2021.107265.
- [26] Y. Liu and J. Jiang, “Preparation of  $\beta$ -ionone microcapsules by gelatin/pectin complex coacervation,” *Carbohydr. Polym.*, vol. 312, p. 120839, 2023, doi: https://doi.org/10.1016/j.carbpol.2023.120839.
- [27] Z. J. Dong, A. Touré, C. S. Jia, X. M. Zhang, and S. Y. Xu, “Effect of processing parameters on the formation of spherical multinuclear microcapsules encapsulating peppermint oil by coacervation,” *J. Microencapsul.*, vol. 24, no. 7, pp. 634–646, 2007, doi: 10.1080/02652040701500632.
- [28] S. Karagonlu, G. Başal, F. Ozyıldız, and A. Uzel, “Preparation of Thyme Oil Loaded Microcapsules for Textile Applications,” *Int. J. New Technol. Res.*, vol. 4, no. 3, 2018.
- [29] B. Muhoza, S. Xia, X. Wang, and X. Zhang, “The protection effect of trehalose on the multinuclear microcapsules based on gelatin and high methyl pectin coacervate during freeze-drying,” *Food Hydrocoll.*, vol. 105, no. December 2019, p. 105807, 2020, doi: 10.1016/j.foodhyd.2020.105807.
- [30] S. M. Jafari, E. Assadpoor, Y. He, and B. Bhandari, “Re-coalescence of emulsion droplets during high-energy emulsification,” *Food Hydrocoll.*, vol. 22, no. 7, pp. 1191–1202, 2008, doi: https://doi.org/10.1016/j.foodhyd.2007.09.006.

- [31] R. Esfahani, S. M. Jafari, A. Jafarpour, and D. Dehnad, "Loading of fish oil into nanocarriers prepared through gelatin-gum Arabic complexation," *Food Hydrocoll.*, vol. 90, no. December 2018, pp. 291–298, 2019, doi: 10.1016/j.foodhyd.2018.12.044.
- [32] Bastos et al., "core reference.pdf," 2020.
- [33] Y. P. Timilsena, R. Adhikari, C. J. Barrow, and B. Adhikari, "Microencapsulation of chia seed oil using chia seed protein isolate-chia seed gum complex coacervates," *Int. J. Biol. Macromol.*, vol. 91, pp. 347–357, 2016, doi: <https://doi.org/10.1016/j.ijbiomac.2016.05.058>.
- [34] J. Yu, Z. Jingjing, Z. Hongfei, and Z. Bolin, "Microencapsulation of *Elaeagnus mollis* oil to enhance the oxidation stability of polyunsaturated fatty acids: the interaction between fatty acids and wall materials," *Ital. J. Food Sci.*, vol. 32, no. 1, 2020.
- [35] Prata et al., "Influence of the oil phase on the microencapsulation by complex coacervation," *J. Am. Oil Chem. Soc.*, vol. 92, pp. 1063–1072, 2015.
- [36] T. Su, Q.-X. Wu, Y. Chen, J. Zhao, X.-D. Cheng, and J. Chen, "Fabrication of the polyphosphates patched cellulose sulfate-chitosan hydrochloride microcapsules and as vehicles for sustained drug release," *Int. J. Pharm.*, vol. 555, pp. 291–302, 2019, doi: <https://doi.org/10.1016/j.ijpharm.2018.11.058>.
- [37] E. Duhoranimana et al., "Effect of sodium carboxymethyl cellulose on complex coacervates formation with gelatin: Coacervates characterization, stabilization and formation mechanism," *Food Hydrocoll.*, vol. 69, pp. 111–120, 2017, doi: <https://doi.org/10.1016/j.foodhyd.2017.01.035>.
- [38] M. A. S. P. Nur Hazirah, M. I. N. Isa, and N. M. Sarbon, "Effect of xanthan gum on the physical and mechanical properties of gelatin-carboxymethyl cellulose film blends," *Food Packag. Shelf Life*, vol. 9, pp. 55–63, 2016, doi: <https://doi.org/10.1016/j.fpsl.2016.05.008>.
- [39] Singh et al., "Carboxymethyl cellulose-gelatin-silica nanohybrid: An efficient carrier matrix for alpha amylase," *Int. J. Biol. Macromol.*, vol. 67, pp. 439–445, 2014, doi: <https://doi.org/10.1016/j.ijbiomac.2014.03.051>.
- [40] N. Azadirachta, J. Seed, and O. Nso, "Study of Complex Coacervation of Gelatin A with Sodium Carboxymethyl Cellulose : Study of Complex Coacervation of Gelatin A with Sodium Carboxymethyl Cellulose : Microencapsulation of Neem ( *Azadirachta indica* A . Juss . ) Seed Oil ( NSO )," vol. 4037, 2011, doi: 10.1080/00914037.2011.553851.
- [41] C. Lii, P. Tomasik, H. Zaleska, S. Liaw, and V. M.-F. Lai, "Carboxymethyl cellulose-gelatin complexes," *Carbohydr. Polym.*, vol. 50, no. 1, pp. 19–26, 2002.
- [42] B. Muhoza, S. Xia, J. Cai, X. Zhang, E. Duhoranimana, and J. Su, "Gelatin and pectin complex coacervates as carriers for cinnamaldehyde: Effect of pectin esterification degree on coacervate formation, and enhanced thermal stability," *Food Hydrocoll.*, vol. 87, pp. 712–722, 2019.
- [43] Faisant et al., "Release (1).Pdf." 2003.
- [44] M. A. Bayomi, S. A. Al-Suwayeh, A. M. El-Helw, and A. F. Mesnad, "Preparation of casein-chitosan microspheres containing diltiazem hydrochloride by an aqueous coacervation technique," *Pharm. Acta Helv.*, vol. 73, no. 4, pp. 187–192, 1998.
- [45] S. A. Khatibi, A. Ehsani, M. Nemati, and A. Javadi, "Microencapsulation of *Zataria multiflora* Boiss. essential oil by complex coacervation using gelatin and gum arabic: Characterization, release profile, antimicrobial and antioxidant activities," *J. Food Process. Preserv.*, vol. 45, no. 10, 2021, doi: 10.1111/jfpp.15823.
- [46] Y. Huang, B. Sun, and B. Muhoza, "Influence of processing conditions on the physical properties, retention rate, and antimicrobial activity of cinnamaldehyde loaded in gelatin/pectin complex coacervates," *Food Biophys.*, vol. 17, no. 3, pp. 289–301, 2022, doi: 10.1007/s11483-022-09718-x.
- [47] Y. Zhang, X. Liu, Y. Wang, P. Jiang, and S. Y. Quek, "Antibacterial activity and mechanism of cinnamon essential oil against *Escherichia coli* and *Staphylococcus aureus*," *Food Control*, vol. 59, pp. 282–289, 2016, doi: 10.1016/j.foodcont.2015.05.032.
- [48] Y. Sun, M. Zhang, B. Bhandari, and B. Bai, "Nanoemulsion-based edible coatings loaded with fennel essential oil/cinnamaldehyde: Characterization, antimicrobial property and advantages in pork meat patties application," *Food Control*, vol. 127, p. 108151, 2021, doi: <https://doi.org/10.1016/j.foodcont.2021.108151>.
- [49] T. J. Silhavy, D. Kahne, and S. Walker, "The Bacterial Cell Envelope1 T. J. Silhavy, D. Kahne and S. Walker, .," *Cold Spring Harb Perspect Biol*, vol. 2, pp. 1–16, 2010, [Online]. Available: <https://www.ncbi.nlm.nih.gov/pmc/articles/PMC2857177/pdf/cshperspect-PRK-a000414.pdf>

## OJS Editorial and Publishing Process



~OJS Workflow~

## Important links:

### Paper Submission Link:

### OJS:

<https://ijeab.com/ojs/index.php/ijeab/about/submissions>

<https://ijeab.com/submit-paper/>

### Editorial Team:

<https://ijeab.com/editorial-board/>

### Peer Review Process:

<https://ijeab.com/peer-review-process/>

### Publication Ethics:

<https://ijeab.com/publication-policies-and-ethics/>

### Author Guidelines:

<https://ijeab.com/author-guidelines/>

### Join Us a Reviewer:

<https://ijeab.com/join-us/>

---

## Journal Indexed and Abstracted in:

- Qualis-CAPEs -Brazil
- Normatiza (Under Review)
- Bielefeld Academic Search Engine(BASE)
- Aalborg University Library (Denmark)
- WorldCat: The World's Largest Library Catalog
- Semantic Scholar
- J-Gate
- Open J-Gate
- CORE-The world's largest collection of open access research papers
- JURN
- Microsoft Academic Search
- Google Scholar
- Kopernio - powered by Web of Science
- Pol-Index
- PBN(Polish Scholarly Bibliography)Nauka Polaska
- Scilit, MDPI AG (Basel, Switzerland)
- Tyndale University College & Seminary
- indiana Library WorldCat
- CrossRef DOI-10.22161/ijeab
- Neliti - Indonesia's Research Repository
- Journal TOC
- Dimensions.ai: Re-imagining discovery and access to research
- Citeseerx
- Massachusetts Institute of Technology (USA)
- Simpson University (USA)
- University of Louisville (USA)
- Biola University (USA)
- IE Library (Spain)
- Mount Saint Vincent University Library ( Halifax, Nova Scotia Canada)
- University Of Arizona (USA)
- INDIANA UNIVERSITY- PURDUE UNIVERSITY INDIANAPOLIS (USA)
- Roderic Bowen Library and Archives (United Kingdom)
- University Library of Skövde (Sweden)
- Indiana University East (campuslibrary (USA))
- Tilburg University (The Netherlands)
- Williams College (USA)
- University of Connecticut (USA)
- Brandeis University (USA)
- Tufts University (USA)
- Boston University (USA)
- McGill University (Canada)
- Northeastern University (USA)
- BibSonomy-The blue social bookmark and publication sharing system
- Slide Share
- Academia
- Archive
- Scribd
- SJIF-InnoSpace
- ISSUU
- Research Bib
- DRJI
- journal-repository



Platform &  
workflow by  
**OJS / PKP**

Infogain Publication

International Journal of English, Literature and Social Science (IJELS)